UNIVERSITY OF CRETE
DEPARTMENT OF CHEMISTRY

IMT Lille Douai
& UNIVERSITY OF LILLE

Environmental Chemical Processes Laboratory, (E.C.P.L), University of Crete – Chemistry Department
&
Département Sciences de l'Atmosphère et Génie de l'Environnement (S.A.G.E), IMT Lille Douai

Doctoral Thesis

VOC source apportionment and emission inventory evaluation over the great Athens, comparison with other cities of the Mediterranean basin.

ANASTASIA PANOPOULOU

Thesis Supervisors: Nikolaos Mihalopoulos (University of Crete)
&
Nadine Locoge (IMT- Lille Douai)

HERAKLION 2019

PhD COMMITTEE

Nikolaos Mihalopoulos

Professor in University of Crete – Department of Chemistry (co-Director)

Nadine Locoge

Professor in IMT- Lille - Douai (co-Director)

Charbel Afif

Associated Professor in Saint Joseph University of Beirut – Faculty of Science

Valérie Gros

Research Director CNRS in the Laboratoire des Science du Climat et d'Environnement (LSCE)

Maria Kanakidou

Professor in University of Crete – Department of Chemistry

Eleni Liakakou

Associate Researcher in the Institute of Environmental Research and Sustainable Environment (IERSD) – National Observatory of Athens

Spyridon Pergantis

Professor in University of Crete – Department of Chemistry

Stéphane Sauvage

Associated Professor in IMT – Lille - Douai

Acknowledgments

C’est fini ! This is what I think when I write these lines, getting closer to the delivery of my PhD thesis. These three and a half years I worked hard to manage and finish the project I was assigned with satisfactory results and observations, to develop skills and to gain experience in order to move forward as an independent junior researcher. Thus, first of all, I would like to thank my two directors Nadine Locoge (IMT) and Nikos Mihalopoulos (UOC & IERSD), and my three supervisors Valérie Gros (LSCE), Eleni Liakakou (IERSD) and Stéphane Sauvage (IMT) (whom designed, organized and found funding for this work) for trusting me with the realization of the Athens VOC campaign and supporting me to walk through this path by becoming a better researcher and a better person. Specifically, I would like to thank Stéphane, Eleni and Valérie for the countless hours they devoted to me, explaining my questions, correcting my mistakes, discussing my troubles, making suggestions and expressing ideas that had a key role for the development of my scientific thinking and writing. And of course, Nadine and Nikos were always there to discuss with me and to guide me when I was in need, so for these and for their trust I will always be grateful.

Additionally, I would like to thank all those people who contributed in their way for the successful realization of the project: Starting from the Laboratoire des Science du Climat et d’ Environnement (LSCE), I would like to thank Bernard Bonsang, Dominique Baisnee and Roland Sarda-Esteve for their technical assistance on the field and remotely. From the Département des Science de l’Atmosphère & Génie de l’Environnement (SAGE) of IMT I would like to thank firstly Thierry Leonardis for his continuous technical assistance and guidance on field, remotely and after my arrival at Douai, and secondly Vincent Gaudion, Laurence Depelchin and Isabelle Fronval for their technical assistance and the treatment and analysis of my off-line samples which gained me some more time for data analysis. From the Department of Chemistry of UOC, I would like to thank prof. Maria Kanakidou and the secretary Vasilis Tsolis for their continuous assistance in the administrative part of my PhD, which was often tricky due to the international collaboration of the universities. I would like to thank the secretaries of SAGE (IMT) Veronique Frejek and Sadrine Taille for helping me with any administrative issues during my stay in Douai. From the IERSD of the National Observatory of Athens, I cannot forget all the people that helped with technical and other issues during the implementation of the field campaign. Finally, I would like to thank the two reviewers of my PhD thesis and the PhD committee for their time and their contribution.

Lastly, I want to thank my co-workers in Douai (Evi, Therese, Darya, Pablo, Manolis, Roger, Antoine, Cecile, Raphael, Cecilia, Lorene, Asma, Kenneth) that were always there for small talk, to share a meal and to give suggestions and explanations in my questions, which all made a nice working atmosphere. Therefore, I am more than grateful to my friends (especially to Vasiliki, Evi, Mado, Maria, Darya, Therese, Christos), my sister and my parents for their endless support, their understanding in difficult moments and for the strength they gave me to move forward and succeed!

Anastasia Panopoulou

Date of birth: 12/07/1991 / Gender: Female / Tel.: +30-6980811242

e-mail: panopoulou.anastasia1@gmail.com

webpage: https://www.linkedin.com/in/anastasia-panopoulou-6823a182/

CURRENT POSITION

July 2019 - present, Research Associate in Atmospheric Chemistry / PANhellenic infrastructure for Atmospheric Composition and climatE chAnge (PANACEA), University of Crete – Department of Chemistry (Heraklion, Greece)

June 2016 - present, PhD researcher in Atmospheric Chemistry / S.A.G.E Department, IMT – Lille – Douai (Ecole Mines – Télécom) & ECPL Laboratory, University of Crete, Department of Chemistry (co-tutorial thesis) / Greece (June 2016 – May 2017) & France (June 2017 to present)

PREVIOUS POSITIONS

2015-2017, Graduate Student Researcher / IERSD, National Observatory of Athens / Greece

2014-2014 (3 mo), Undergraduate Student Researcher / IERSD, National Observatory of Athens / Greece

2013-2013 (3 mo), Undergraduate Student Researcher / ECPL Laboratory, University of Crete, Department of Chemistry/ Greece

---

ACADEMIC STUDIES

2016-2019, PhD in Atmospheric Chemistry/ Co-tutorial thesis between IMT – Lille – Douai (Ecole Mines – Télécom) and University of Crete, Department of Chemistry / France and Greece

Dissertation title: « VOC source apportionment and emission inventory evaluation over the great Athens, comparison with other cities of the Mediterranean basin».

2014-2016, M.Sc in Environmental Chemistry / University of Crete, Department of Chemistry / Greece

Grade: 8.67 / 10
Graduation Thesis (Institute of Environmental Processes and Sustainable Development - IERSD, National Observatory of Athens): «Non-methane Hydrocarbons in the Greater Athens Area. Study of the time variation. Investigation of the contribution of the wood burning as a source».

2010-2014, B.Sc in Chemistry / University of Crete, Department of Chemistry / Greece

Grade: 8.19 / 10
Gratuation Thesis (Laboratory of Environmental Chemical Processes: Laboratory of Atmospheric Chemistry – ECPL, University of Crete, Department of

Chemistry): «Ionic Composition of Tropospheric Aerosols over Eastern Mediterranean: Seasonal Variation and Comparison between the results of different types of sampling filters».

EXPERSTISE

1. Measurements of Volatile Organic Compounds (VOC) in the atmosphere: field measurement campaigns, collection & analysis of air samples by Gas Chromatography (GC), analysis & interpretation of data using Microsoft Excel, IgorPro, EPA PMF, writing of reports & scientific articles
2. Measurements of Polycyclic Aromatic Hydrocarbons (PAHs) in the atmosphere: sample treatment and laboratory analysis of air samples by High-Performance Liquid Chromatography (HPLC), analysis & interpretation of data
3. Measurements of inorganic ions in the atmosphere: sample treatment and laboratory analysis of samples by Ion Chromatography (IC) for the identification and quantification of anions and cations, analysis & interpretation of data, report writing

RESEARCH AND PROJECTS

1. Participation in the PANACEA panhellenic project for the monitoring of VOC (Volatile Organic Compounds) in the atmosphere of Athens and the analysis and interpretation of the data (2019 - 2021)
2. Participation in the research projects of ACTRIS-II (Aerosol, Clouds and Trace Gases Research Infrastructure) and ChArMEx (Chemistry – Aerosol Mediterranean Experiment) for monitoring of VOC, for the better assessment of the local air quality and the identification and quantification of their emissions from sources (2016 - 2019).

SCIENTIFIC PUBLICATIONS

1. **A. Panopoulou** et al., 2017: Non Methane Hydrocarbons variability in Athens during winter-time: The role of traffic and heating", Atmos. Chem. Phys., 18, 16139-16154, 2018
DOI: https://doi.org/10.5194/acp-18-16139-2018

COMMUNICATION IN CONFERENCES

1. **Panopoulou A.**, Liakakou E., Gros V., Locoge N., Bonsang B., Mihalopoulos N., Sauvage S.,18- month time-resolved measurements of C2-C12 NMHCs to an urban background environment in Athens, Greece: Temporal variability and comparison with other studies, European Geosciences Union General Assembly – EGU 2016, Vienna, Austria, 07–12 April 2019, http://meetingorganizer.copernicus.org/EGU2019/EGU2019-8247.pdf
(oral presentation)

2. **Panopoulou A.,** Liakakou E., Psiloglou B., Gros V., Bonsang B., Sauvage S., Locoge N., Lianou M., Gerasopoulos E., Mihalopoulos N., Non Methane Hydrocarbons (NMHCs) at the centre of Athens: variability and relative contribution of traffic and wood burning, European Geosciences Union General Assembly – EGU 2016, Vienna, Austria, 17–22 April 2016, http://adsabs.harvard.edu/abs/2016EGUGA..18.9714P
(oral presentation by prof. Nikolaos Mihalopoulos)

COMMUNICATION IN WORKSHOPS	1. **Panopoulou A.,** Liakakou E., Gros V., Sauvage S., Kalogridis A.C., Bonsang B., Locoge N., Lianou M., Psiloglou B., Gerasopoulos E., Mihalopoulos N., Trends and sources of C2-C12 non- methane hydrocarbons (NMHCs) in the Great Athens Area, International workshop on Atmospheric Processes in the Mediterranean, Larnaca, Cyprus, 17 - 21 October 2016 **(poster presentation)**
ATTEDANCE IN CONFERENCES	1. 12° Cyprus – Greece Chemistry Conference, Thessaloniki, Greece, 8- 10 May 2015 2. 12° International Conference on Meteorology, Climate and Atmospheric Chemistry / COMECAP 2014, Heraklion Crete, Greece, 28 – 31 May 2014
OTHER SKILLS	1. **Languages:** Greek (native) English (Proficiency – Michigan C2) French (Basic – Delf B1) 2. **Personal:** Project Management, Teamwork, Creativity, Goal orientation, Communication, Commitment, Listening & Empathy
SUPERVISING AND TEACHING ACTIVITIES	**2015-2017:** Tutor / POUKAMISAS EDUCATIONAL GROUP / Athens, Greece **2015-2015 (6 mo):** Graduate Laboratory Supervisor / Laboratory of General Chemistry (Undergraduate Courses), University of Crete, Department of Chemistry / Heraklion, Greece

Abstract

VOC (Volatile Organic Compounds) are key constituents of atmospheric chemistry and pollution as precursors of harmful compounds like ground ozone and secondary organic aerosols, which in turn have a strong impact on local/regional air quality, climate, vegetation and human health. For that reason and in order to design and implement efficient air pollution control measures, there is a growing interest for their better characterization, as well as the identification, speciation and quantification of their respective sources.

Mediterranean basin is a complex environment, favoring the development of severe air pollution events. Despite that, there is a lack of VOC studies in the urban areas of the region, while the existing ones have shown significant uncertainties associated with compounds speciation and the contribution from the different emission sources. Considering this, Athens (Greece) is the ideal place for VOC measurements due to the lack of reported levels for NMHCs the last 15 years, the continuous exceedance of O_3 and aerosol concentrations and the increasing emissions from specific pollutant sources (e.g. wood burning for residential heating). In this work, we report the results of an 17-month field campaign for NMHCs in Athens (October 2015 – February 2017), under the frame of the international project ChArMEX (The Chemistry – Aerosol Mediterranean Experiment). This was supported by two one-month intensive observation periods (winter and summer) at the same station, and two additional near-source campaigns (tunnel and traffic station).

More than 40 VOC with 2 to 16 carbon atoms have been measured giving for the first time a detailed characterization of their temporal and spatial variability on an annual basis, especially for C2 – C3 NMHCs, followed by the determination of its driving parameters. The comparison with other VOC studies in cities worldwide highlighted the role of sources to the observed levels, with significant air pollution for Athens in winter. Furthermore, the analysis indicated that monoterpenes and isoprene, known compounds of biogenic origin, presented a complex variability probably influenced by emissions other than biogenic. The latter provides interesting insights for the assessment of their impact on air quality, as precursors of secondary pollutants. Moreover, the application of the receptor-oriented model Positive Matrix Factorization (PMF) allowed the identification of the main factors related to VOC sources and the quantification of their contribution. Traffic-related emissions and residential heating were determined as the major VOC sources in the city, whereas a second PMF simulation to the intensive observation period gave additional information about sources such as the fuel evaporation from stationary points.

Key words: VOC, Athens, monoterpenes, atmospheric pollution, PMF model, Mediterranean basin, ChArMEx project

Résumé

Les COV (Composés Organiques Volatils) jouent un rôle majeur dans la problématique de pollution atmosphérique, puisqu'ils interviennent en tant que précurseurs des composés secondaires comme l'ozone troposphérique (O_3) et l'Aérosols Organiques Secondaires (AOS) qui ont des impacts sur la santé et le climat. Afin de mettre en place des stratégies efficaces de réduction de la pollution de l'air, il est crucial de caractériser et quantifier la contribution des principales sources d'émission de COV.

Le basin Méditerranée constitue un environnement complexe, favorisant le développement des épisodes de pollution. Cependant, les mesures de COV dans les zones urbaines de la région restent limitées et les études existantes ont montré des incertitudes significatives quant à la contribution des différentes sources d'émission. Dans ce contexte, Athènes (Grèce) est un cas d'étude intéressant notamment pour les COV. Cette zone urbaine fait face à des dépassements des valeurs limites européennes en d'O_3 et d'AOS ainsi qu'à une augmentation des émissions de polluants pour des sources spécifiques (par exemple, le chauffage résidentiel au bois).

Les travaux présentés dans ce manuscrit portent sur l' étude des COV à Athènes, réalisée dans le cadre du projet international ChArMEX (The Chemistry - Aerosol Mediterranean Experiment). La méthodologie s'appuie sur une campagne de mesure de 17 mois (d'octobre 2015 à février 2017) sur un site représentatif proche du centre-ville, sur deux campagnes intensives d'un mois chacune réalisées à la même station ainsi que sur deux campagnes réalisées en champ proche des sources (en tunnel et en station trafic).

Plus de 40 COV de 2 à 16 atomes de carbone (C2 à C16) ont été mesurés, permettant la caractérisation détaillée de leur variabilité temporelle et spatiale sur une base annuelle, suivie de la détermination des facteurs d'influence. Les COV de C2 à C3 étaient mesurés pour la première fois à Athènes. La comparaison aux autres études de COV en zones urbaines a mis en évidence la typologie des sources ainsi que l'importance de la pollution atmosphérique en hiver à Athènes. Concernant les monoterpènes et l'isoprène, composés en général d'origine biogénique, l'analyse a mis en évidence des sources anthropiques dans cette atmosphère urbaine, ce qui fournit des informations intéressantes pour l'évaluation de leur impact sur la qualité de l'air en tant que précurseurs des polluants secondaires. L'application du modèle orienté récepteur « Positive Matrix Factorization » (PMF) sur la base de données annuelles, a permis d'identifier et quantifier les contributions des principaux facteurs associés aux sources de COV. Les émissions liées au transport routier et au chauffage résidentiel ont été déterminées comme les sources de COV dominantes. Une seconde analyse PMF sur la base de donnes des campagnes intensives a d'une part corroboré les résultats et, d'autre part, a conduit à l'identification de sources supplémentaires comme l'évaporation de carburants des points stationnaires.

Mots de clés : COV, Athènes, monoterpènes, pollution atmosphérique, modèle PMF, bassin Méditerranéen, Projet ChArMEx

Περίληψη

Παρά τις πρωτοβουλίες για τον περιορισμό και μείωση των ατμοσφαιρικών ρύπων, στη Μεσόγειο και τις πόλεις που την περιβάλλουν εξακολουθούν να καταγράφονται υπερβάσεις των προβλεπόμενων οριακών τιμών για την προστασία της υγείας. Παρόλα αυτά, οι μελέτες στα αστικά κέντρα της περιοχής για Πτητικούς Οργανικούς Υδρογονάνθρακες (Volatile Organic Compounds ή VOC), οι οποίοι είναι πρόδρομοι του τροποσφαιρικού όζοντος (O_3) και των αερολυμάτων, είναι περιορισμένες, ενώ ορισμένες υποδεικνύουν αβεβαιότητες στις παρατηρήσεις που προκύπτουν από συγκρίσεις με βάσεις δεδομένων εκπομπών, σχετιζόμενες με τη συνεισφορά των πηγών εκπομπής και το χημικό τους αποτύπωμα. Συνεπώς, η Αθήνα αποτελεί ιδανική τοποθεσία για μετρήσεις των ενώσεων αυτών, λόγω της μη-καταγραφής των επιπέδων τους τα τελευταία 15 χρόνια (πλην ελάχιστων εξαιρέσεων), της συνεχούς υπέρβασης των ορίων του O_3 και των αερολυμάτων, καθώς και της αύξησης των εκπομπών από μέχρι πρότινος ασθενείς πηγές ρύπων (π.χ. καύση ξύλου για οικιακή θέρμανση). Στην παρούσα εργασία παρουσιάζονται τα αποτελέσματα μιας 17μηνης καμπάνιας ατμοσφαιρικών μετρήσεων πεδίου για μη-Μεθανικούς Υδρογονάνθρακες (non-Methane Hydrocarbons ή NMHCs) στην Αθήνα (Οκτώβριος 2015 - Φεβρουάριος 2017), στο πλαίσιο του διεθνούς προγράμματος ChArMEX (The Chemistry - Aerosol Mediterranean Experiment). Παράλληλα, εκπονήθηκαν δύο εντατικές περίοδοι εποχικών μετρήσεων (χειμώνα και καλοκαίρι) στον ίδιο σταθμό και επιπλέον, δύο εκστρατείες συλλογής δειγμάτων αέρα σε γνωστές πηγές ρύπανσης (σήραγγα και αστικός σταθμός μετρήσεων).

Τα δεδομένα περισσότερων από 40 VOC με 2 έως 16 άτομα άνθρακα, που συλλέχθηκαν κατά τη διάρκεια της καμπάνιας, χρησιμοποιήθηκαν για τη μελέτη της ημερήσιας και εποχιακής διακύμανσης τους σε ετήσια βάση και των παραγόντων που την επηρεάζουν, ενώ τα επίπεδα C2 - C3 NMHCs στην Αθήνα παρουσιάζονται για πρώτη φορά. Η εποχικότητα παρουσιάζει σαφή διακύμανση, με μέγιστο το χειμώνα και ελάχιστο το καλοκαίρι για την πλειονότητα των ενώσεων, ενώ η ημερήσια διακύμανση επηρεάζεται από την ένταση των εκπομπών των πηγών, την ταχύτητα του ανέμου και το ύψος του στρώματος ανάμειξης. Η σύγκριση των αποτελεσμάτων αυτών με παρόμοιες έρευνες σε άλλες πόλεις ανέδειξαν το ρόλο των πηγών στα παρατηρούμενα επίπεδα, όπου για την Αθήνα αυτή η επίδραση είναι πιο έντονη τον χειμώνα. Επιπρόσθετα, τα μονοτερπένια και το ισοπρένιο, γνωστές ενώσεις βιογενούς προέλευσης, παρουσίασαν μία μοναδική μεταβλητότητα επηρεασμένη από ανθρωπογενείς εκπομπές, η οποία δεν λαμβάνεται υπόψη κατά την εκτίμηση της ποιότητας του αέρα. Τέλος, η χρήση του στατιστικού μοντέλου Positive Matrix Factorization (PMF) επέτρεψε τον προσδιορισμό των κύριων πηγών NMHCs στην Αθήνα και την εκτίμηση της συνεισφοράς τους στα επίπεδα των συγκεντρώσεων. Από αυτές, οι εκπομπές από την κίνηση οχημάτων και την οικιακή θέρμανση επικρατούν, ενώ μια δεύτερη PMF προσομοίωση στα δεδομένα της εποχικής εντατικής περιόδου παρατήρησης επιβεβαίωσε τα αποτελέσματα, δίνοντας επίσης πληροφορίες για πρόσθετες πηγές.

Λέξεις-κλειδιά: VOC, NMHCs, Αθήνα, μονοτερπένια, ατμοσφαιρική ρύπανση, PMF model, Μεσόγειος, ChArMEx

Table of contents

Abbreviations / Συντομογραφίες / Abréviations

VOC : Volatile Organic Compounds

NMHC : Non-methane Hydrocarbons

SOA: Secondary Organic Aerosols

PMF: Positive Matrix Factorization

ChArMEx project: Chemistry - Aerosol Mediterranean Experiment

MB: Mediterranean Basin

EMB: Eastern Mediterranean Basin

PTR-MS: Proton Transfer Reaction – Mass Spectrometry

OVOC: Oxygenated VOC

SA: Source apportionment

BVOC: Biogenic Volatile Organic Compounds

LPG: Liquified Petroleum Gas

POCP: Photochemical Ozone Creation Potential

OFP: Ozone Formation Potential

MIR: Maximum Incremental Reactivity

SOAFP: SOA Formation Potential

TVOC: Total VOC concentrations

HC: total NMHC concentrations

PBL: Planetary Boundary Layer

SoER: State of the Environment Report (for Greece)

BTEX: Benzene, Toluene, Ethylbenzene, Xylenes (m-, p-, o-)

TEX: Toluene, Ethylbenzene, Xylenes (m-, p-, o-)

GC: Gas Chromatograph

GC – FID: Gas Chromatograph equipped with Flame Ionization Detector

MOP: Main Observation Campaign

IOP: Intensive Observation Campaign

IVOC: Intermediate VOC

General Introduction

Earth's atmosphere is the gaseous body surrounding our planet. It is composed by a mixture of different gases, like nitrogen (~78%), oxygen (~21%), argon (~1%) and trace gases (<1%). In the atmosphere except for gases, solid particles or liquid droplets with diameters less than 100μm are suspended, namely aerosols. The interaction and exchange between the earth and the atmosphere change the composition of the atmospheric mixture. However, the last decades, this exchange is greatly affected by the increase of human activities that caused an increase of "anthropogenic" emissions of compounds in the air. Among the mentioned atmospheric species, trace gases play a crucial role in the altering of the atmospheric chemical reactions and the development of air pollution episodes, subsequently having a significant impact on climate change, air quality, ecosystems, vegetation and human health.

Nowadays, the effects of both the climate change and the deterioration of air quality on the quality of life (decrease of water reservoirs, increase of drought and temperature, decrease of crop yields, increase of floods, etc.) are among the main causes for the modern migration to urban locations or between countries. This phenomenon leads to the acceleration of climate change due to the increase of pollutants' emissions. It is a matter of fact that since 2013, air pollution is classified as carcinogenic for humans (IARC, 2013), while only in Europe it was responsible for more than 500.000 premature deaths in 2014 (EEA, Air Quality in Europe, report, N° 13/2017). Thus, the goal of scientific initiatives is the understanding of changes in atmospheric composition and the establishment of links to the air pollution development, in order to protect living organisms and the environment. In this context, observation campaigns are organized in selected sites worldwide for the monitoring of targeted air pollutants and if possible, their apportion to sources. In particular, Volatile Organic Compounds (VOC) raise concerns as they are precursors of important constituents of severe air pollution episodes, like tropospheric ozone and secondary organic aerosols (SOA).

Due to its location (intersection of three continentals: Europe, Africa and Asia) and climate (mild and rainy winters followed by hot and dry summers), the Mediterranean region is among the areas where climate change is expected to have a negative impact in the close future (Giorgi and Lionello, 2008; Sillmann et al., 2013). Furthermore, the development of air pollution episodes, such as photochemical smog (tropospheric ozone), are favoured, causing poor air quality in the area and therefore in the cities of the basin. It is a matter of fact that the concentrations of pollutants often exceed international and European standards (Kanakidou et al., 2011; Karanasiou and Mihalopoulos, 2013), while according to previously published studies, ozone concentrations can be almost a factor of 3 higher over the Mediterranean basin than the background of the entire hemisphere (Lelieveld et al., 2002).

For these reasons, the understanding and assessment of the air quality in the Mediterranean basin (MB) remain of scientific interest. Furthermore, more attention is paid in the Eastern Mediterranean Basin, in which high concentrations of trace gases and background tropospheric ozone are reported, in combination to the increasing population and the environmental issues (Cramer et al., 2018; Kanakidou et al., 2011; Lelieveld et al., 2002; Solomou et al., 2018). Nevertheless, estimates for 2050 show that premature immortality for Eastern Mediterranean region will account for 723.000 deaths (Lelieveld et al., 2015). Despite the aforementioned issues, the geographic distribution of the available studies on VOC concerning urban

environments of the EMB is limited and there is still a need of comprehensive analysis and source apportionment (Salameh et al., 2015, 2016). This highlights the importance for VOC studies in this area on their ambient levels, variability, driving parameters and sources, since they are precursors of tropospheric ozone and SOA, as it is already mentioned.

For Athens, the capital of Greece, the observations on the current air-quality reported by the available studies, indicate that although the levels of pollutants have decreased compared to the past, they still exceed European limits in frequent cases. Indeed, the most recent State of the Environment Report (SoER 2018, http://ekpaa.ypeka.gr/index.php/soer-2018) indicated that the O_3 annual mean level is still above the European legislation limit of 120 μg m^{-3}. However, the majority of VOC studies in Athens were conducted mainly in the 90s, and only one recent work reported the levels of ~11 VOC species (Kaltsonoudis et al., 2016) from two intensive campaigns (summer 2012 and winter 2013) by the means of a Proton Transfer Reaction – Mass Spectrometry (PTR-MS). The latter reported also a first attempt for source apportionment.

In order to fill the scientific gap of knowledge for VOC in the Eastern Mediterranean Basin and to better investigate their respective sources, the current thesis is dealing with VOC measurements in Athens (Greece), focusing on the factors controlling their variability, the main sources and their contribution. For that reason, C2 – C12 NMHCs were monitored for more than one year in a representative site in the centre of Athens, whereas information for additional VOC were obtained with parallel measurements in intensive observation campaigns. These datasets were used for the determination of the sources of VOC in Athens, with results to be further affirmed from the comparison to other pollutants (indicators of sources' emissions) and chemical profiles derived from measurements close to traffic-related sources.Thus, for the better presentation of the objectives, strategy, experimental set up and observations/results, the current work is organized in 6 chapters as follows:

1. **Chapter 1** presents an overview of the VOC in the troposphere, their sources and fate, followed by the status of the air quality in Mediterranean basin and Athens. The chapter ends with the main scientific questions that derived from this overview and the objectives/strategies of the PhD thesis.
2. In **Chapter 2** the experimental set-up is explained in detail.
3. In **Chapters 3, 4, 5** and **6** the results and observations from the analysis of the VOC datasets are presented, focused on the understanding of the parameters driving the variability, the possible impact to atmospheric chemistry and the respective sources.
4. Finally, the **last chapter** summarizes the main observations from the analysis of this work, concluding with the main scientific and future perspectives.

CHAPTER 1 – Volatile Organic Compounds (VOC) in Atmosphere: Focus on Mediterranean Basin

TABLE OF CONTENTS FOR CHAPTER 1

1. VOLATILE ORGANIC COMPOUNDS (VOC) IN THE ATMOSPHERE

1.1 VOC definition

Volatile organic compounds (VOC) are a very broad group of carbon-containing trace gases. The latter correspond to compounds with 1 to approximately 15 carbon atoms (Koppmann, et al., 2008 and references therein). In the Directive 1999/13/EC of the European Commission VOC are defined as any **organic compound having a vapor pressure equal or greater than 0.01 kPa at 293.15 K**, or simply as **volatile carbon compounds that participate significantly in atmospheric photochemical reactions** (EPA 2017; CEPA 2016). Methane (CH_4), carbon monoxide (CO) and carbon dioxide (CO_2) are excluded from this group because they are important greenhouse gases with low reactivity and high ambient concentrations (for instance, VOCs have concentrations of a few ppb, while CO_2 concentration for 2014 was 398 ppb – European Environmental Agency 2017).

Furthermore, VOCs are classified into several categories based on different criteria. One of their main categorizations depends on the chemical composition of the compounds. Non-Methane Hydrocarbons (NMHC) is a large group of VOCs that contain only carbon and hydrogen. They can be further distinguished according to the type of carbon bond (for example to alkanes, alkenes, alkynes etc.) and their carbon body structure (branched NMHC, aromatics, etc.). Oxygenated NMHCs are included in the group of oxygenated volatile organic compounds (OVOC). Beside oxygen, halogens are also found in the structure of volatile organic compounds. In this case the grouping depends on the halogen atom in the compound's chemical composition (as ClVOC for chlorinated VOCs) and they belong to halogenated hydrocarbons.

Another classification of VOCs is based on their degree of volatility. The latter is expressed for every compound by the **effective saturation mass concentration** (C_i^*), calculated from Eq I - 1 as follows (Shiraiwa and Seinfeld, 2012):

$$C_i^* = \frac{10^6 M_i p_i^\circ}{760 R T} \qquad \text{Eq. I - 1}$$

were M_i (g mol^{-1}) is the molecular weight of compound *i*, p_i° (Torr) is the saturation vapor pressure of pure compound *i*, R (m^3 atm mol^{-1} K^{-1}) is the gas constant and T (K) is the temperature.

Thus, from the above equation, organic compounds with $\mathbf{C^* > 10^6}$ μg m^{-3} are considered **volatile** (Robinson et al., 2007; de Gouw et al, 2011). Intermediate volatile organic compounds (**IVOC**) have a $\mathbf{C^*}$ between $\mathbf{10^3}$ and $\mathbf{10^6}$ **μg m^{-3}** (Tkacik et al., 2012), compounds with $\mathbf{C^*}$ between $\mathbf{10^{-3}}$ and $\mathbf{10^3}$ **μg m^{-3}** correspond to **semi-volatile organic compounds (SVOC)** (Donahue et al., 2006), while the rest are **non-volatile organic compounds.**

1.2 Sources of VOCs

Globally, there is a variety of VOC sources in the atmosphere. **Primary** emissions are of **anthropogenic** and **biogenic** origin, exhibiting different **strength** and **chemical composition** of emitted VOCs; in particular, biogenic emissions **exceed** anthropogenic, accounting for 90% of the global VOC respectively (Guenther et al., 1995; Kansal, 2009). Furthermore, these compounds can be formed in atmosphere from chemical reactions, which serves as a **secondary** source (for instance Atkinson, 2000).

As it described later in the chapter, VOCs take part in various atmospheric processes that can have a negative effect on air quality. Thus, it is important to **identify**, **quantify** and **categorize** their **sources** in order to establish control plans for their reduction. These can be determined using various **methods** and **tools**, and this procedure is named "**Source Apportionment or SA**". Due to the variety of approaches, the selection of the appropriate method takes into account firstly the **sampling location**, resulting in two categories of SA **models**: **source-** and **receptor- oriented models**. The former are useful for datasets obtained close to one specific source, whereas the latter are useful for sites representatives of the air pollution plumes around the entire study-area. Since there are various types of the aforementioned models, for the better choice are also considered the size and variability of the dataset, the climatology and topography of the sampling site, and the information for the major pollutant sources in the immediate vicinity. On the other hand, information for VOC sources and their contribution to selected areas or regions are also provided from **emission inventories** (**Sect. 1.2.3** of **this chapter**). A more detailed summary of the source apportionment approaches is given in **Sect. I – A1** of the **Annex I.**

Finally, in the following paragraphs, more details are given for the sources of VOCs, both per type (of source) and per group (of compounds).

1.2.1 Biogenic emissions

Previously it was shown that biogenic emissions are the main contributors of VOC in the atmosphere. The latter are therefore named BVOC (biogenic volatile organic compounds) for simplicity. According to studies, the major biogenic source is **terrestrial emissions** (vegetation and microbial activity) with a contribution of **98%**, with the rest of the sources being the ocean and soil (Bonsang et al., 1999; Koppman, et al., 2008; Schade & Goldstein, 2001; Kansal, 2009 et references therein). Furthermore, Guenther et al. (1995) estimated that **75%** of these BVOC are emitted from **trees**, while the rest **25%** is attributed to **shrub** and **crops** emissions (Guenther 1995). **Isoprene** is the most **abundant** BVOC, followed by **terpenoids** and **OVOCs** (Guenther 1995, Puxbaum 1997, Schade & Goldstein 2001, Koppmann 2008). Nevertheless, the type of the plant/tree affects the diversity of the emitted BVOCs. In particular, deciduous trees and shrubs emit mainly isoprene, in contrast to coniferous trees that emit terpenoids and OVOCs (Guenther 1995, Koppmann 2008, Kansal 2009).

Concerning terrestrial emissions, these are primarily dependent from **plant activity**, including the plant growth, the communication and competition to other species and its protection (Fuentes et al., 2000; Geron et al., 2000; Laothawornkitkul et al., 2009). Plant activity is

influenced by atmospheric dynamics both in **short-** and **long- term**. More specifically, **light** and **temperature**, and to a smaller scale **humidity**, are the main environmental factors which affect vegetation activity and thus emissions of BVOC (Fuentes et al., 2000; Geron et al., 2000; Guenther et al., 1995; Kesselmeier and Staudt, 1999; Tiiva et al., 2017). Based on these observations, a classification of BVOCs as light and or/ temperature dependent is attempted on several studies (i.e.Kesselmeier and Staudt, 1999). For example, it is reported that isoprene is both light and temperature dependent, while most of the monoterpenes and OVOC are mainly temperature dependent (Guenther et al., 1995; Kesselmeier and Staudt, 1999). As a result, the **seasonal variation** of BVOC levels is driven by atmospheric dynamics, presenting a maximum during summer, when high temperatures and increased sunlight prevail that favor biogenic activity, and a minimum during winter (Guenther et al., 1995; Liakakou et al., 2007; Seco et al., 2011). To summarize, biogenic emissions depend on climatology and the type of vegetation, thus they differ from a geographical region to another one.

1.2.2 Anthropogenic emissions

The **anthropogenic sources** of VOCs are numerous, including traffic- related emissions (stationary and mobile emissions), industrial emissions, solvent use, residential/commercial activities, agricultural emissions related to anthropogenic activity (livestock farms, deforestation etc) and waste management (Koppmann et al. 2008, Barletta et al., 2005). Since every village/city/region/country etc present different anthropogenic activity, there are studies that identify the pollutant sources in a selected area, quantifying also their VOC contribution. One example is given below for **Europe**, where the anthropogenic VOC sources have been identified, classified and quantified by the European Environmental Agency (EEA, 2017) (**Fig. I – 1**). In this case, almost 50% of the emissions originate from industrial processes, followed by residential/other emissions and agriculture emissions (16 & 15% respectively). Road transport emissions account only for the 9% of the VOC emissions, which is attributed to regulations and measures that were imposed on fuel composition for the improvement of the air quality (Huang et al., 2017).

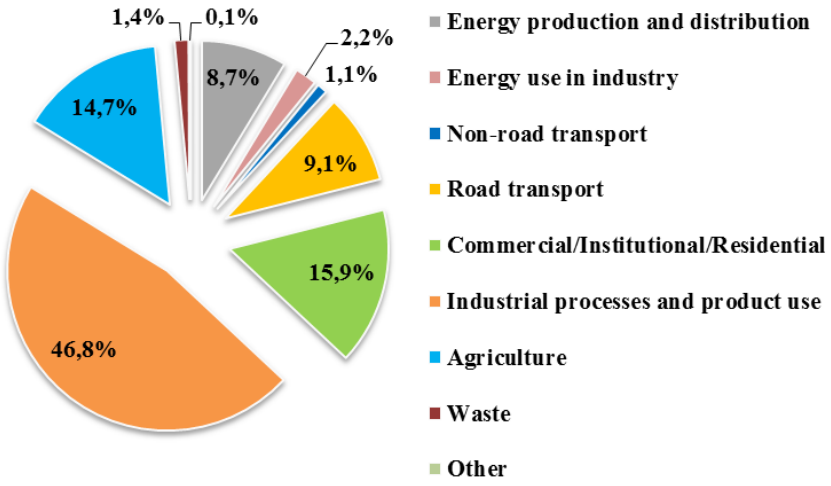

Figure I - 1: Emissions of NMVOC by sector group in Europe, EEA 2017

Every VOC source have its own **chemical composition** of emissions. The latter are established by near-source sampling campaigns or chamber experiments (for example in Watson et al., 2001). They can be used for the identification of sources and they provide useful information for the main emitted compounds from sources of interest, which can eventually facilitate the designing of control measures that target specific VOC. In the following paragraphs are given the chemical composition of some of the major VOC sources:

1. Based on **Figure I – 1**, the largest pool of VOC in Europe are **industrial processes**. Due to the large number of activities and materials in this sector, the chemical composition varies (Liu et al., 2008, Zheng et al., 2013). Among the predominant emitted species from petroleum refineries (diesel, gasoline, LPG production), petrochemical production and their evaporative emissions (Liu et al., 2008, Dumanoglu et al., 2014) are found aliphatic, aromatic and halogenated VOC (for example n-pentane, n-heptane, 1-pentene, 3-me-pentane, benzene, toluene, m/p xylenes, 1,2 dichloroethane, carbon tetrachloride).

2. **Road transport** emissions are linked to the type of fuel and its incomplete combustion, thus they consist from vehicle exhaust emissions, fugitive emissions from the vehicle's piping system, emissions from the various driving processes related also to the vehicle's condition/age (for example cold start emissions or refueling) (Montero et al., 2010). Gasoline and diesel are used the most as fuels, while biofuels, natural gas and LPG gain slowly part of the demand (TERM 001, EEA 2016). The chemical profile of **exhausts** from gasoline-powered and diesel vehicles presents ethylene, propene, benzene/toluene as the main emitted species (Liu et al., 2008; Baudic et al., 2016), followed by C5 - C6 alkanes. Higher VOC (>C10) are significant in the exhausts of diesel-powered vehicle exhausts, but not in the gasoline-powered exhausts.

3. **Fuel evaporation** emissions originate mainly from vehicles, storage facilities, fuel transportation and fuel distribution. Propane is the major VOC in the chemical profile of fuel evaporation in LPG-powered vehicles (Na et al., 2004; Liu et al., 2008). In the equivalent profile from oil-powered vehicles, a variety of VOCs is reported: C4-C7 alkanes/alkenes and aromatics (for example i/n – butanes, benzene and toluene) (Brown et al., 2007, Liu et al., 2008, Baudic et al., 2016).

4. **Residential emissions**, primarily for **heating** purposes, were recognized as important VOC sources only the recent years (Helen et al., 2008; Gustafson et al., 2007; Gaeggeler et al., 2008; Baudic et al., 2016; Kaltsonoudis et al., 2016). **Oil, wood, coal** and **natural gas** are the main burning fuels for residential heating. The major VOC originating from **wood burning** are ethylene, acetylene, benzene and various OVOCs, although strong emissions from ethane are also reported (Liu et al., 2008, Baudic et al., 2016). The same compounds dominate emissions from coal burning, with different contribution depending on the type of coal.

5. **Natural gas** is a "clean" fossil fuel used for industrial processes, power generation and residential heating and cooking (Dong et al., 2017; A.F. Campos et al., 2017). Emissions derive mainly from consumption related to combustion and leakages from the storage facilities and distribution network, thus ethane and propane are identified as the predominant VOC (Brown et al., 2008; Baudic et al., 2016).

1.2.3 Emission inventories: Another tool for VOC sources

Emission inventories are **datasets** that provide the **total amount** of pollutant/pollutants in the atmosphere at **different scales**: from local to global. These are used as input information in air pollution modelling and air quality monitoring and for air quality forecasting (Streets et al., 2003, Francois et al., 2005). It is a matter of fact that the estimations of the above modelling simulations are critical for **policy makers** when considering the implementation of new or improvement of the existing air quality abatement measures. Thus, the accuracy and representability of emission inventories is crucial for the delivery of representative outcomes. To better understand these datasets, a small summary of their built up and the estimation of their uncertainty is presented in **Sect. I – A2** of **Annex I**.

The uniqueness of each emission inventory is a result of 5 **main characteristics**:

- The source categories
- The studied pollutants
- The spatial distribution
- The temporal resolution
- And, the methodology for the compilation of the emission inventory.

Popular global emission inventories are EDGARv.4.3.1 (Emissions Database for Global Atmospheric Research) and MACCity (Monitoring Atmospheric Composition and Climate and megaCITY Zoom for the Environment). Continental inventories include the database of EMEP (Co-operative Programme for Monitoring and Evaluation of the Long-Range Transmission of Air pollutants in Europe) for Europe, SPECIATE4.4 for U.S.A, REAS (Regional Emission inventory in ASia) for Asia and L14-Africa for Africa. The majority of global and regional inventories report estimations only for anthropogenic air pollutants. Some of the few biogenic emission inventories are RETRO, GEIA (Global Emissions InitiAtive), POET and MEGAN-MACC. Numerous national and local inventories can be found in the literature: APEI (Air Pollutant Emission Inventory) for Canada, the emission inventory of CITEPA (Centre Interprofessionnel Technique d'Etudes de la Pollution Atmosphérique) for France and AIPARIF for Paris, for Lebanon in Waked et al (2012), for various locations of China in Zhao et al (2017) and for Greece the FEI-GREGAA (Flexible Emission Inventory for Greece and the Greater Athens Area) (Fameli & Assimakopoulos, 2016).

An important drawback of all the emission inventories are the reported large **uncertainties** per source. These originate from errors in input data, the different assumptions, the selected model and approach etc. As an example, European Environmental Agency in "Air pollutant emission inventory guidebook" (2016) estimates the uncertainty in emission factors for VOCs from 20% for solvent usage and waste management to 300% for natural emissions and other mobile

sources. One can easily understand that these high uncertainties are then induced into the air pollution prediction models, affecting significantly the accuracy of their estimations and creating conflicting results.

Overall, the **high uncertainties**, in combination with the **absence** of data from **field measurement** campaigns for VOC (Belis et al., 2014) can produce important **over- or under-estimates** of **emissions,** as well as **other implications** (Arriaga-Colina 2004; Gros et al., 2011; Borbon et al., 2013; Salameh et al., 2016,2017; and references therein):

- **Large discrepancies** are observed between VOC **observations** and **inventories,** for specific VOC and sectors.
- The **heterogeneity** of the VOC composition in observed anthropogenic emissions is **not presented** in global emission inventories.
- There is a **lack of information** in some areas that affect the predictions of models, like for example in Africa and Mediterranean (Salameh et al., 2017; Huang et al., 2017).

1.3 VOCs fate in the atmosphere

Once emitted in the atmosphere, VOCs undergo a variety of **processes** (chemical, physical, atmospheric horizontal and vertical transportation) that control their **atmospheric fate** and **lifetime**. Furthermore, through complex reaction pathways, VOCs participate in the **formation** of **tropospheric ozone (O_3)** and **secondary organic aerosols (SOA)**, which can cause adverse effects on vegetation, climate and health. Furthermore, the following paragraphs will deal with the oxidation of VOC by the main atmospheric oxidants, the main VOC sinks and the factors controlling their lifetime, their contribution to ozone and SOA formation and the effect of atmospheric dynamics.

1.3.1 Tropospheric chemistry of VOCs

Oxidation and **photolysis** are the principal reactions that chemically transform VOCs in the troposphere. The **OH radical**, **ozone** and the **nitric radical** are the main oxidants in the atmosphere (e.g. Atkinson, 2000), whereas chlorine radicals can contribute importantly to the atmospheric oxidation of VOC in coastal areas (Arsene et al., 2007; Hopkins et al., 2002). Nevertheless, the OH radicals are considered the most reactive towards VOCs (i.e. in Atkinson, 2000; Seinfeld and Pandis, 2016). Therefore, in the following paragraphs the tropospheric chemistry of VOC is analyzed more in detail, considering only the reactions that are significant in urban environments.

1.3.1 – 1 Photolysis of hydrocarbons

The term **"photolysis"** describes the **dissociation** of VOC due to **sunlight.** Although this chemical process has **minor role** to the depletion of the majority of compounds such as alkanes, alkenes and aromatics, for small aliphatic aldehydes and a,b-unsaturated carbonyl compounds is **significant,** antagonizing often the oxidation from the OH radical (Atkinson, 2000). A representative example is the behavior of **formaldehyde**, for which photolysis and the oxidation by the OH radical compete, resulting in lifetimes of 4 and 1.2 hours respectively (Atkinson 2000).

1.3.1 - 2 Main atmospheric oxidants

The OH radical

The OH radical has primary and secondary sources, with the former being the photolysis of atmospheric pollutants and the latter the recycling of the radicals in the reaction chains. Since the main source is associated to sunlight, OH radicals present their highest concentrations in summer and during day (i.e in Elshorbany et al., 2010; Liakakou et al., 2007 and references therein).

In non-polluted areas of the troposphere, like remote regions, photolysis of ozone in the presence of water vapor is a large source of OH radicals **(Fig. I - 2)** (Atkinson, 2000; J. Crutzen, 1995). As a result, two OH radicals can be produced from the destruction of an ozone molecule.

$$O_3 + h\nu \rightarrow O_2 + O(^1D) \qquad (\lambda \leqslant 335\ nm)$$

$$O(^1D) + H_2O \rightarrow 2OH$$

Figure I - 2: Main reaction chain for the production of OH radicals from the O_3 photolysis (Adjusted from Atkinson, 2000).

On the other hand, in polluted parts of the troposphere, the most significant sources of OH radicals are the photolysis of **nitrous acid** (HONO) and the photolysis of **formaldehyde** and other carbonyls in the presence of NO (**Fig. I - 3**). Moreover, **ozonolysis** of alkenes is also suggested as an OH source (i.e Elshorbany et al., 2009).

(a) $HONO + h\nu \rightarrow OH + NO$

(b) $HCHO + h\nu \rightarrow H + HCO\ (\lambda \leq 370nm) \rightarrow H_2 + CO$

$$H + O_2 \rightarrow HO_2$$

$$HCO + O_2 \rightarrow HO_2 + CO$$

$$HO_2 + NO \rightarrow OH + NO_2$$

Figure I - 3: (a) Production of OH radicals from the HONO photolysis (Adjusted from Atkinson; 2000) (a); and (b) Chain reactions for the formation of OH radical from the formaldehyde photolysis (Adjusted from Nan et al., 2017).

Furthermore, OH radicals can be recycled (secondary source) from the NOx and Ox recycling mechanisms, which are important only in NOx-limited and pristine air respectively (Lelieveld et al., 2016). Finally, important sinks of the radical are the implication to the VOC – NOx chemistry and the reaction with NO_2 (Atkinson, 2000; Elshorbany et al., 2009).

The NO_3 radical

The NO_3 is formed in the atmosphere from the reaction of **NO_2** and **O_3** (**Fig. I - 4**). It is present in measurable concentrations during **night**, since it **photolyzes quickly** in the morning to its primary constituents (**Fig. I - 5**).

$$NO + O_3 \rightarrow NO_2 + O_2$$
$$NO_2 + O_3 \rightarrow NO_3 + O_2$$

Figure I - 4: Production of NO_3 radicals at night (Adjusted from Atkinson, 2000).

$$NO_3 + h\nu \rightarrow NO + O_2$$
$$NO_3 + h\nu \rightarrow NO_2 + O(^3P)$$

Figure I - 5: Photolysis of NO_3 radicals (Adjusted from Atkinson, 2000).

The oxidation reactions from NO_3 influence the chemical fate of VOCs and NOx during **night,** which could possibly lead to a **nocturnal production** and atmospheric **cycling** of the OH, HO_2 and RO_2 radicals based on evidence (Brown and Stutz, 2012; Wayne et al., 1991). Moreover, organic nitrates and secondary organic aerosols can also be produced from the NO_3 reactions (Brown and Stutz, 2012).

Ozone (O_3)

Ozone is an abundant compound of the stratosphere. Low levels can be found also in the troposphere, for which their main origin is the stratosphere-troposphere exchange and the formation from precursors (i.e. Chameides et al., 1992). Its molecule consists from three oxygen atoms and presents two equivalent resonance structures, with delocalized π pair of electrons (**Fig. I – 6**). This grands ozone the ability to rapidly react with inorganic and organic compounds by subtracting hydrogen cations, leading to the formation of radical oxygen species (ROS), which are more oxidized, as it is shown in the following.

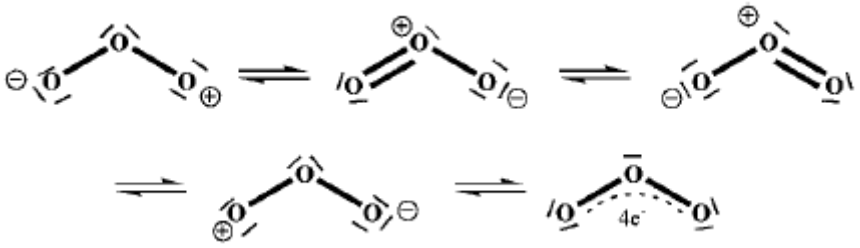

Figure I - 6: Ozone structure (Adjusted from Bocci et al., 2009).

1.3.1 – 3 Oxidation pathways of VOCs

As mentioned previously in the section, VOCs are **oxidized** in the atmosphere mainly from the **OH** radical during **daytime** and from the **NO_3** radical at **night**. **Cl** atoms can also oxidize some VOCs, however, they play a minor role in the global troposphere (Pechtl and von Glasow, 2007; Rudolph et al., 1997; Young et al., 2014).

In **Figure I – 7** is illustrated the general oxidation pathway of VOCs (Atkinson and Arey, 2003). The first step is the abstraction of an hydrogen atom from the oxidant, which leads to the formation of the alkyl radical (R°). The alkyl radicals are then reacting with O_2 forming peroxy

radicals (RO_2°). At this point, the reaction chain can either propagate or terminate. The continuation of the reactions with the hydroperoxyl radicals, nitrogen dioxide, nitrogen monoxide and other peroxy radicals leads to more substituted and oxidized products and the formation of secondary pollutants like tropospheric ozone and secondary organic aerosols (**Section 1.3.2**).

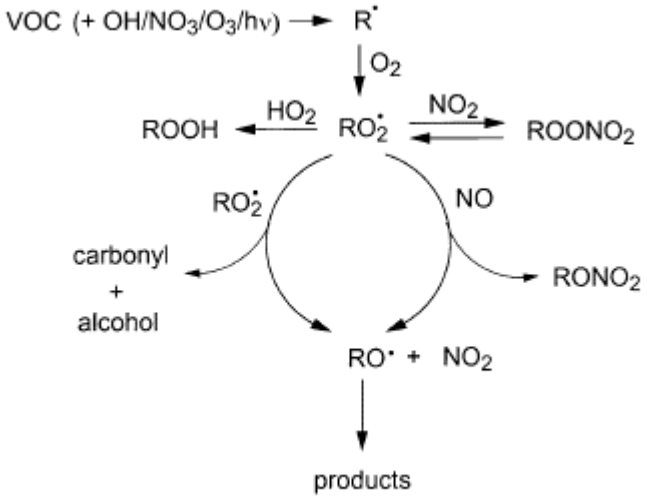

Figure I - 7: VOCs general oxidation process in the troposphere (scheme adjusted from Atkinson and Arey, 2003).

1.3.1 – 4 Ozonolysis of unsaturated hydrocarbons

The reaction of unsaturated hydrocarbons with tropospheric ozone is an additional transformation process for these compounds, creating a variety of OVOCs (Atkinson, 2000; Johnson and Marston, 2008). The first steps of **ozonolysis** (**Fig. I - 8**) include the formation of a **Criegee intermediate** that quickly decomposes through complex mechanisms, not-well understood yet (Atkinson, 2000; Hasson et al., 2001; Johnson and Marston, 2008).

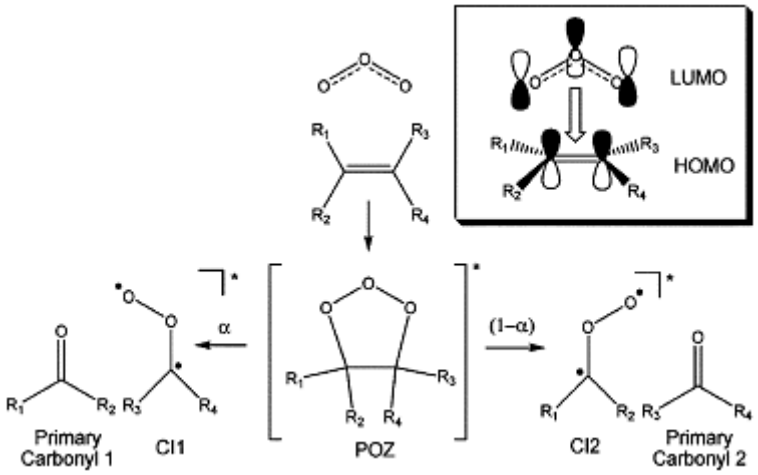

Figure I - 8: Formation of Criegee intermediate by ozonolysis of an alkene (Johnson and Marston, 2008).

Except of a major atmospheric **sink** of **hydrocarbons**, ozonolysis of unsaturated VOC can also produce **OH radicals** during **nighttime** and compounds that contribute to photochemical smog, such as **secondary organic aerosols** (Gutbrod et al., 1996; Koch et al., 2000; Johnson and Marston, 2008). For that reasons, until today the exact mechanism, kinetics, intermediates and products are under investigation, however, there are still a lot to be learned (Johnson and Marston, 2008; Giorio et al., 2017).

1.3.1 - 5 Secondary formation of VOC

In **Figure I – 8** it is apparent that the reaction of the peroxy radicals lead to the formation of additional VOC, such as **carbonyls** and **alcohols**. Few studies provide estimations for the contribution of this source (e.g. Altshuller, 1993; Borbon et al., 2004). For instance, for a rural site in France, at least 50% of the light aldehydes were attributed to secondary formation (Borbon et al., 2004), whereas Atkinson (2000) indicates that for compounds like **formaldehyde**, secondary formation is among its main sources.

1.3.1 - 6 VOC atmospheric sinks and lifetime

The reactions of VOC in the atmosphere, which were presented in **sections 1.3.1 – 1** and **1.3.1 – 3** are their main atmospheric sinks. In particular, the **oxidation** by the **OH radical** is the most important sink, driving the **lifetime** of VOC. **Photolysis** is an additional sink for certain VOC, like formaldehyde, intermediate or aliphatic VOC (Koppmann, 2008 and references). Furthermore, physical sinks like the wet (washing out) and dry deposition (surface uptake), sufficiently remove VOC, especially the more polar ones. Nevertheless, the chemical structure, the molecular weight, the solubility and the diffusion properties of VOC greatly influence the impact of their chemical and physical atmospheric sinks (Koppmann, 2008).

As it was previously mentioned, the lifetime of VOC in the atmosphere depends on their **removal processes**, which are oxidation, photolysis, wet and dry deposition. In general, the lifetime τ of an organic compound is defined as the time for its concentration to decrease to 1⁄e of its initial value. The overall **rate of removal** can be derived by summing the **reaction rates** of these processes (Eq. I – 2) (Seinfeld and Pandis, 2016):

$$1/\tau_{overall} = 1/\tau_{wetdep} + 1/\tau_{drydep} + 1/\tau_{phot} + 1/\tau_{OH} + 1/\tau_{O_3} + 1/\tau_{NO_3} + 1/\tau_{Cl} \quad \text{Eq. I - 2}$$

where $\tau = 1/\mu$ and μ is the reaction rate of the specific process. Therefore, for the compounds that react predominately with the OH radical, it is often practical to estimate their lifetimes using the more simplified Eq. I – 3, based only on this reaction and if the OH concentration is known.

$$\tau_{OH} = \frac{1}{k[OH]} \quad \text{Eq. I – 3}$$

where τ is the lifetime of the compound in respect to the oxidation by the OH radical, k is the reaction rate coefficient (k) and [OH] the concentration of the radical in molecules cm^{-3}.

Typical lifetimes of selected VOC are presented in **Table I - 1** (Atkinson, 2000). It is apparent that alkanes can residue in the atmosphere for long periods, while BVOCs and alkenes present

a very short lifetime. This difference in the lifetimes can be useful in the analysis and interpretation of results, as it will be discussed later in the thesis (**Chapter 4**).

Table I - 1: Calculated lifetimes of selected VOCs with respect to their reaction with the OH radical, the NO_3 radical, the O_3 radical and their photolysis (Atkinson, 2000)

		Lifetime due to			
Organic		**OH [a]**	**NO_3 [b]**	**O_3 [c]**	**Photolysis [d]**
Alkanes	*Propane*	10 days	7 years	>4500years	
	n-Butane	4.7 days	2.8 years	>4500 years	
	n-Octane	1.3 days	240days		
	i-Octane	3.2 days	1.4 years		
Alkenes	*Ethene*	1.4 day	225 day		
	Propene	5.3 hours	4.9 days	1.6 day	
	Trans-2-butene	2.2 hours	1.4 hours	2.1 hours	
	Isoprene	1.4 hour	50 minutes	1.3 day	
	α-Pinene	2.6 hour	5 minutes	4.6 hours	
	Limonene	50 minutes	3 minutes	2.0 hours	
Aromatics	*Benzene*	9.4 days	> 4 years	> 4.5 years	
	Toluene	1.9 days	1.9 years	> 4.5 years	
	m-Xylene	5.9 hours	200 days	> 4.5 years	
	1.2.4 Tri-me-benzene	4.3 hours	26 days	>4.5 years	
	Styrene	2.4 hours	3.7 hours	1.0 day	
Oxygenated	*Formaldehyde*	1.2 day	80 days	>4.5 years	4 hours
	Acetaldehyde	8.8 hours	17 days	> 4.5 years	6 days
	Glyoxal	1.1 day			5 hours

[a] For a 12-h daytime average OH radical concentration of 2.0x106 molecule cm-3
[b] For a 12-h night-time average NO3 radical concentration of 5x108 molecule cm-3.
[c] For a 24-h average O3 concentration of 7x1011 molecule cm-3
[d] For overhead sun.

1.3.2 VOC as precursors of atmospheric pollutants

1.3.2 – 1 Tropospheric Ozone formation

Tropospheric ozone constitutes **10%** of the total ozone planetary budget. It is a **greenhouse gas** and an **OH radical precursor**, whereas it is responsible for the photochemical smog (i.e. Chameides et al., 1992; Cooper et al., 2014). Furthermore, taking as an example Europe, episodes of increased ozone occurs over many cities and rural areas in summer, which are directly related to its local formation or its transport from distant sources. Apart from the air pollution, ozone is responsible for **adverse effects** on **ecosystems** and **health** after a long-term exposure (Turner et al., 2015).

As it was already mentioned, O_3 originates in the troposphere from **photochemical reactions** and the **downward transport** from the stratosphere. Major anthropogenic **precursors** of **ozone** are **VOC, NOx, CH_4** and **CO**, whose emissions influence greatly its production, while **chemical reactions** and **dry deposition** are the main **destruction pathways**.

In the presence of NOx, ozone is produced from the photolysis of NO_2, however it is immediately destroyed by the reaction to NO for the re-formation of NO_2 (**Figure I – 9**). Thus, from this reaction, the reactants and products are in equilibrium and no extra ozone is produced.

$$NO_2 + h\nu \rightarrow NO + O(^3P)$$

$$O(^3P) + O_2 + M \rightarrow O_3 + M \quad (M = \text{air})$$

$$NO + O_3 \rightarrow NO_2 + O_2$$

Figure I - 9: Production of O_3 in the atmosphere (Adjusted from Atkinson, 2000).

However, if in the reaction mix of **Figure I – 9** are added VOC, and more specifically the RO_2 and HO_2 radicals from their oxidation (**Figure I – 7** of **Sect. 1.3.1 – 2**), the reaction of the latter with NO produces NO_2, ending the equilibrium. Consequently, the depletion of NO by the additional reaction to VOCs, and the excess production of NO_2 contribute to tropospheric ozone formation (**Fig. I –10**):

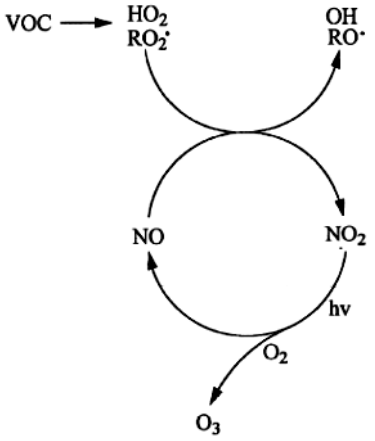

Figure I - 10: Ozone formation in the VOC – NO_x environment (adapted from Atkinson, 2000)

Because these reactions are sensitive, they can also serve for the destruction of tropospheric ozone. For example, high levels of nitric oxide scavenge ozone, like in the city centers where fresh emissions of traffic occur, while they produce additional NO_2 that reacts with VOC impeding ozone formation. Therefore, the photochemical formation or destruction of ozone is dependent from the **VOC/NOx ratio**. This is better illustrated by the **ozone isopleths** plots, like the ones presented in **Figure I - 11**. In the cities that NOx are high, the ratio tends to be VOC-limited, thus for the decrease of ozone any control measures should be imposed mainly on VOCs. On the contrary, for suburban and rural areas that receive aged air masses, ozone is increased due to the built-up from the photochemical formation during transport (longer exposure to sunlight); since VOC are considered stable in these areas, any **control of NOx** can sufficiently **reduce** the production of ozone (Finlayson-Pitts and Jr, 1993; Seinfeld and Pandis, 2016).

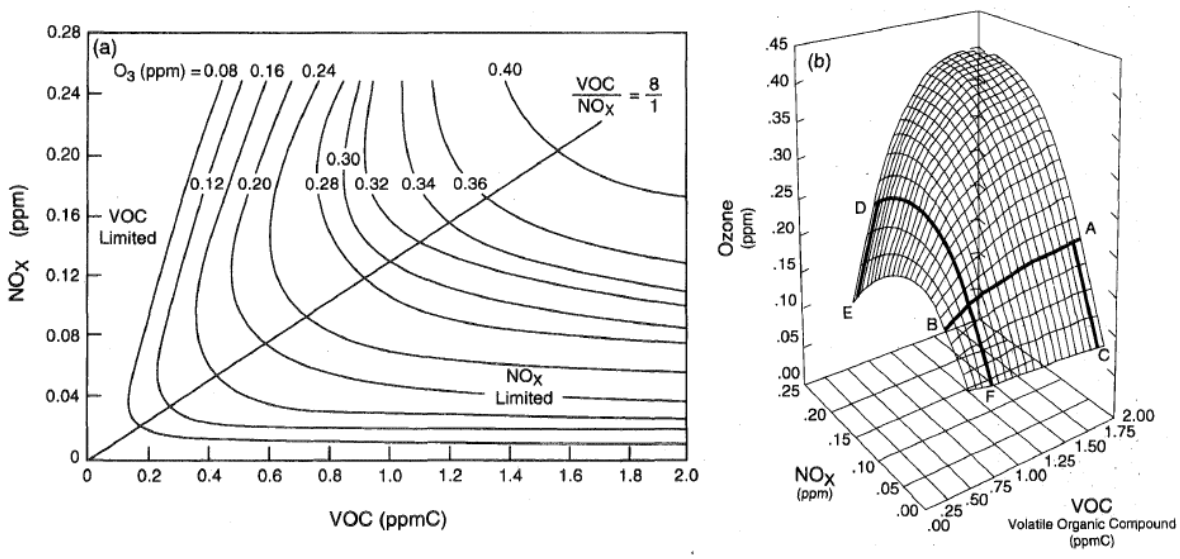

Figure I - 11: a) Typical ozone isopleths, generated from models based on initial mixtures of VOC and NOx in air, b) three-dimensional depiction of the ozone isopleth, generated from the same model as graph (a). The point D refers to a VOC-limited region, like highly polluted urban centres, while point A refers to the NOx limited region like downwind suburban and rural areas (Finlayson-Pitts and Jr, 1993).

Finally, due to the different chemistry and reaction of VOCs, their **ozone-generating** capacities vary. There are different concepts for the estimation of that in the literature, like the **POCP** (Photochemical Ozone Creation Potential) and the **OFP** (Ozone Formation Potential) using **MIR** (Maximum Incremental Reactivity). POCP was developed by Derwent et al. (1998) and it is defined as the change in mean ozone levels when a VOC compound is reduced relative to the change in mean ozone levels when ethene is reduced (reference compound). It is calculated for a certain area, time-frame and weather conditions, based also on the reaction to the OH radical. It has been used in studies (Andersson-Sköld and Holmberg, 2000; Lam et al., 2015; Wu et al., 2017), however, OFP is simpler to use. The incremental reactivity concept was developed by Carter (1994) and Carter et al. (1995), allowing the estimation of the OFP based on the molecules of ozone formed per NMHCs carbon atom added to a certain atmospheric reaction mixture of NMHCs and NOx. These maximum values are named MIR and they are reported in Carter (2009). As a result, the OFP of each NMHC can be calculated per sample by multiplying the concentration to the MIR value (Garg and Gupta, 2019; Tohid et al., 2019). In the literature, toluene, xylenes and BVOC are considered important ozone precursors giving high yields (Calfapietra et al., 2013; Tohid et al., 2019; Wu et al., 2017)

Implications of tropospheric ozone

Apart from the deterioration of the air quality, ozone is harmful to human health and ecosystems. Starting from the health issues, prolonged exposure to tropospheric O_3, especially during strong pollution episodes (for example photochemical smog) are the main cause of respiratory problems. In particular, since ozone is a gas, it easily penetrates the respiratory system and reaches the lungs, affecting negatively the interphase of the oxygen-carbon dioxide exchange in the blood and breath (Marchwinska-Wyrwal et al., 2011; Turner et al., 2015). This result in increased medication usage, hospital admissions and mortality. For that reason, the

European Environmental Agency has set an 8-hour threshold of 110 μg m^{-3} for the health protection, whereas WHO has set this threshold at 100 μg m^{-3} (https://www.who.int/news-room/fact-sheets/detail/ambient-(outdoor)-air-quality-and-health). It is a matter of fact that the European Environmental Agency report on Air Quality in Europe for 2014 (EEA report, N° 5/2014, 2014) indicates that the mortality rate due to ozone is probably higher than originally considered.

Moving on to the exposure of vegetation to tropospheric ozone, it is a result of its deposition on the earth's surface. Furthermore, ozone is absorbed by plants, leading to damages on their cells and impairing the growing and reproduction ability (Hatfield et al., 2011). For instance, Chuwah et al. (2015) estimated an increase of the local crop damage of up to 20% in 2050 for high ozone concentrations. Overall, the consequences include a possible alter of the ecosystem structure, reduction of biodiversity, forest growth and the agricultural crop yields. Considering all the above, European Environmental Agency has set a vegetation protection threshold of 65 μg m^{-3} mean value of 24 hours.

1.3.2 – 2 Formation of secondary organic aerosols (SOA)

The dispersion of gaseous and liquid particles in a gas is called **aerosol.** These particles can be emitted in the atmosphere **directly** from the sources or they can **be formed** in the atmosphere. For the latter, if their precursors are organic compounds, they are named **secondary organic aerosols (SOA).** SOA are produced from the **gas-to-particle partitioning** of VOC (Seinfeld and Pandis, 2016). More specifically, in **Figure I – 7** of **Sect. 1.3.1-3 (this chapter)** it is shown that the products of VOC oxidation are more oxidized, more substituted, more polar and with lower volatility like di- and poly-substituted alcohols, carbonyls and peroxynitrates. These compounds are less volatile (volatility decreases for more oxidized products), resulting to easier partioning between the gas and the particulate phase in already existing particles, or their condensation to form new nuclei. This process is simplified in **Figure I – 12**.

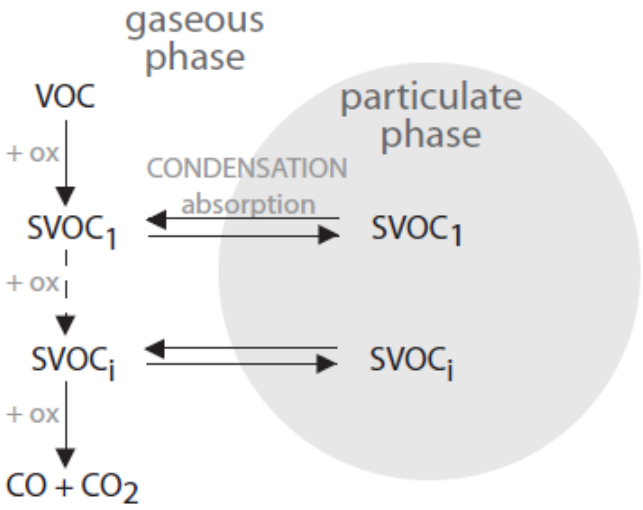

Figure I - 12: General scheme of SOA formation from VOCs oxidation in the atmosphere (adjusted from Camredon et al., 2007).

The **potential of SOA formation from VOCs** is dependent from certain factors (Kroll and Seinfeld, 2008; Seinfeld and Pandis, 2016):

- The **volatility** of the products from VOC oxidation.
- The **atmospheric abundance** of the precursor VOC. It is important for the precursor to be oxidized rapidly for the accumulation of its products, followed by their transition to particle if they reach the saturation mixing ratio.
- The **chemical reactivity** with other atmospheric components.

As a consequence, VOC have different **SOA formation potential (SOAFP)**. From studies in the literature (Koch et al., 2000; Wang et al., 2013; Wu et al., 2017; Zhang et al., 2018) it is known that **aromatics** (e.g. toluene) and **BVOC** (monoterpenes, isoprene) are among the main SOA precursors giving important yields of SOA. Nevertheless, SOAFP can be estimated either from **model simulation** (i.e. Wang et al., 2013) or from calculation using **equations** (i.e. Dominutti et al., 2018; Wu et al., 2017). For the latter are used the emission ratios of the VOCs to a reference compound (e.g. toluene) and a non-dimensional model-derived SOA formation potential, like the reported ones in Derwent et al. (2010).

Implications of SOA

SOA, as all aerosols, have **direct** and **indirect** impact on air quality and **climate**, whereas aerosols are also related to **health implications**. More specifically, SOA can **scatter** and **absorb** solar radiation (direct impact), whereas they act as **cloud condensation nuclei (CCN)**, creating droplets of **smaller radii**. The latter increases the number of droplets in the cloud, as well as their lifetime, which in turn scatter and absorb sunlight, while their smaller droplet size result in higher albeidos (indirect impact). As a consequence, SOA contribute to the **heating** or **cooling** of the atmosphere based on their **size** and **composition**, as well as their **albeido**. This is better depicted in **Figure I – 13**, in which it is apparent that the **overall contribution** of SOA to the radiative forcing is both positive and negative, in contrast to the total contribution of aerosols that is negative.

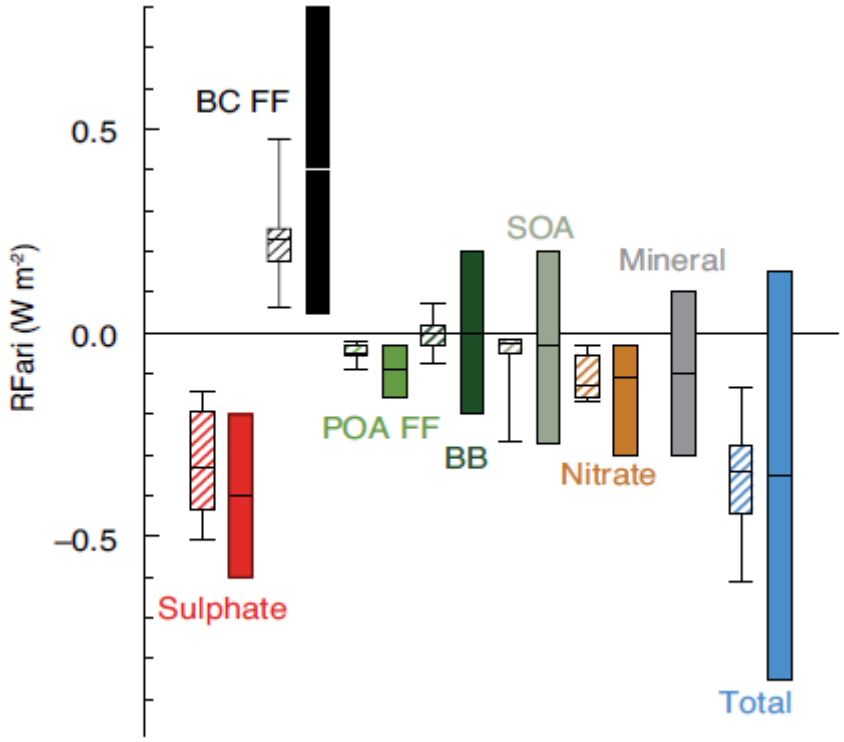

Figure I - 13: Annual radiative forcing due to aerosol–radiation interactions (RFari, in W m^{-2}) from different anthropogenic aerosol types. for the 1750–2010 period. BC FF is for black carbon from fossil fuel and biofuel, POA FF is for primary organic aerosol from fossil fuel and biofuel, BB is for biomass burning aerosols and SOA is for secondary organic aerosols (Adapted from Boucher et al., 2013).

For all the reasons above, the formation mechanism of SOA, their ambient levels and their impact to air quality are under investigation the latest years. It is a matter of fact that Tsigaridis and Kanakidou have predicted that the SOA yields will double by 2100 based only to the contribution of BVOC (Tsigaridis and Kanakidou, 2003, 2007). However, important uncertainties are reported to the model results due to the missing information for the VOC molecular composition of biogenic and anthropogenic emissions, as well as the SOA formation yields from their organic precursors (Camredon et al., 2007; Tsigaridis and Kanakidou, 2003, 2007; Yuan et al., 2013). This is apparent also in a new study (Zhang et al., 2018), in which it was shown that monoterpenes are the main precursors of SOA during summertime in a site at USA.

Concerning the health implications, SOA and aerosols in general, are responsible for **respiratory, cardiovascular and lung problems,** while they contribute to the reported **accelerated deaths** (EEA report, N° 13/2017, 2017). More specifically, they **penetrate the respiratory system** and they reach the lungs, from where they enter the circulatory system. However, the degree of penetration in the organism is depended from the size of their diameter. In addition, they are **carriers** of other harmful substances that are absorbed on the aerosols due to surface interactions (Marchwinska-Wyrwal et al., 2011; Pöschl and Shiraiwa, 2015), which also introduce in the system.

1.3.3 Effect of atmospheric dynamics on VOCs variability

In the previous sections was presented the atmospheric fate of VOCs in relation to their chemical transformation. However, their emissions are also influenced by atmospheric dynamics, which can accumulate or dilute them, while they transport them away from the sources vertically and horizontally. In this context, **meteorological factors** that influence often VOC variability are ambient temperature, solar radiation, wind velocity and wind direction. Moreover, atmospheric dynamics like the **atmospheric turbulences** (land-sea breeze, frontal air systems) and the **mixing layer height** should also be considered when VOC results are interpreted.

First of all**,** VOC can travel **along** the atmospheric **interfaces** where they are advected and diffused. For this process, **wind speed** and the local **topography** are the determining factors (Draxler and Taylor, 1982 and references therein). For instance, in urban environments, the dispersion of the pollutants is a complex interaction between atmospheric flow and flow around buildings, as it is depicted in **Fig. I – 14** (Tominaga and Stathopoulos, 2013; Vardoulakis et al., 2003).

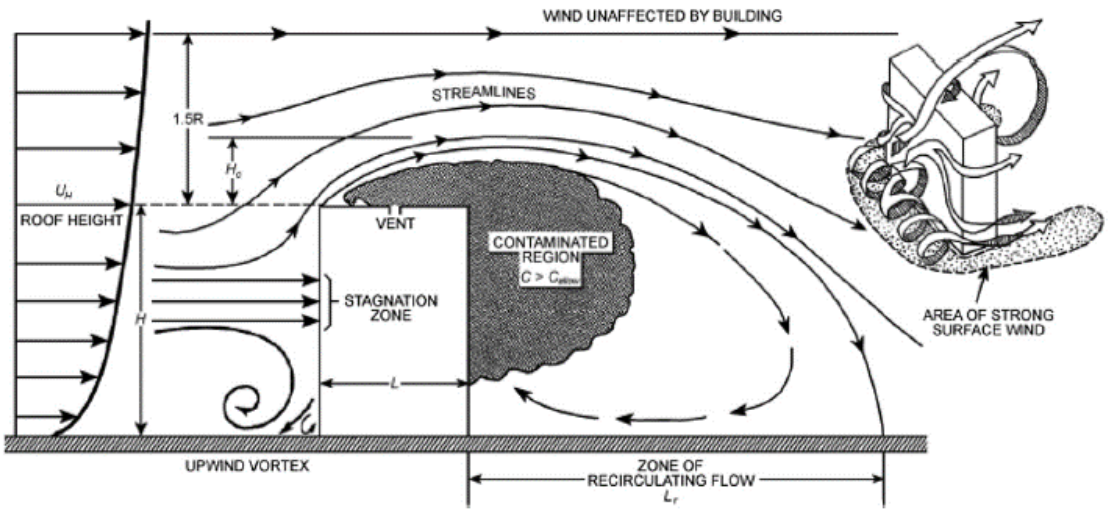

Figure I - 14: Schematic diagram of flow and contamination patterns around a rectangular building (Tominaga and Stathopoulos, 2013)

Furthermore, in local scales, **turbulences** like the land-sea breezes, are responsible for the circulation of VOCs between the sources and the close region, contributing often to air pollution episodes (Lalas et al., 1983). These turbulences are local wind system typically encountered along coastlines, which are driven by the difference between the heating or cooling of the water surface and the adjacent land surface (**Fig. I – 15**).

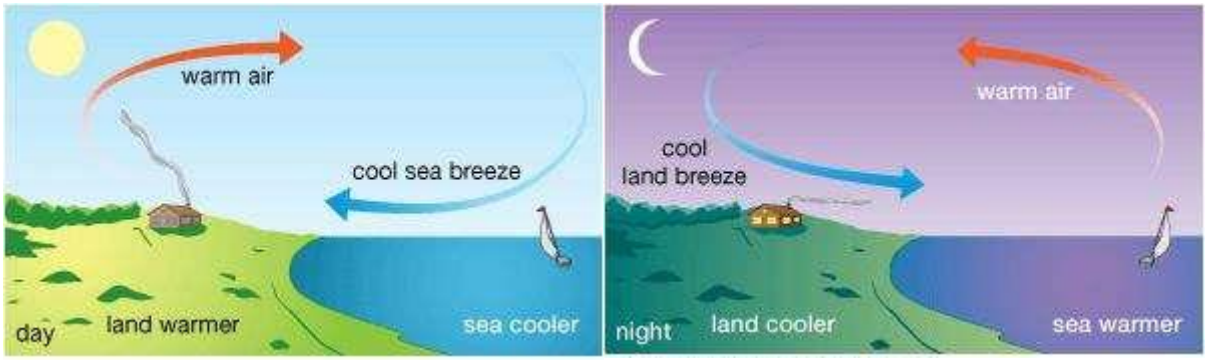

Figure I - 15: Typical sea-breeze (day) and land-breeze (night) circulations (Adjusted from Encyclopædia Britannica, Inc, 2014)

Another type of transport is the **vertical diffusion**. More specifically, VOCs move **upright** in the atmosphere or are **exchanged** between the layers of the atmosphere. This transportation is enhanced by the **atmospheric temperature gradient**, the **uplifting** by frontal systems (Purvis et al., 2003) and the turbulence of the Planetary Boundary Layer (PBL). Nevertheless, the knowledge of the PBL height and its seasonal and diurnal evolution is an important parameter for air quality analysis and the understanding of VOC dispersion. PBL is sensitive to the Earth's surface forcing (Stull, 2012), resulting in a distinct diurnal cycle that depends on both the synoptic and local weather conditions. In **Figure I – 16** is depicted the diurnal cycle of PBL in a clear convecting day (good weather). In general, and based on **Figure I – 16**, it is apparent that the PBL increases during day, as a result mainly of the increase of the surface temperature, whereas it decreases during night, following the decrease of the surface temperature.

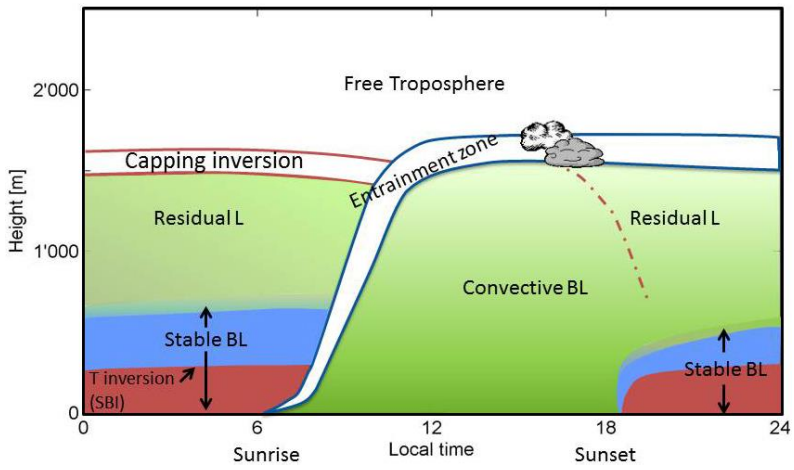

Figure I - 16: Diurnal cycle of the PBL height over land for a clear convective day (Collaud Coen et al., 2014).

At this point it should be mentioned that the **transportation time** of VOC can vary from **some hours** for regional scale advection, to **1 or 2 days** for vertical mixing out of the boundary later and to **4 – 6 years** for troposphere-stratosphere exchange (Seinfeld and Pandis, 2016). Consequently, **the lifetime** of the compound, along with the already mentioned atmospheric processes, **determine** its **transportation.** For that reason, increased concentrations of pollutants can be observed in remote or intercontinental regions, even though there are no local sources (i.e. Borbon et al., 2004). On the contrary, the transportation of pollutants is **not always**

free in the different atmospheric layers. In the boundary layer temperature inversion (0.5‑2 km), the tropopause (10‑15 km) and the intertropical conversion zone (ITCZ, 10◦S‑10◦N), the atmospheric mixing is physically impeded, resulting in strong gradients of organic compounds across these interfaces.

1.4 Additional information for VOC

1.4.1 Health effects

Short-term and **long-term exposure** to air pollution is associated with health implications. For the first case, which corresponds to an exposure of a few hours or days, **acute health effects** are observed. Moreover, the long-term exposure (over months or years) is linked with a **chronic health effect** and increased **morbidity** and **mortality**. In fact, from 2013 the International Agency for Research on Cancer (IARC) has classified air pollution as **carcinogenic to humans** (IARC, 2013). According to the European Environmental Agency (EEA) report on Air Quality in Europe (EEA report, N° 13/2017, 2017), almost **500000 premature deaths** of 2014 were attributed to air pollutants such as particulate matter, O_3 and NOx. However, VOCs in the ambient air are not a direct threat to human health, with the exception of **benzene** and **1.3 butadiene** that are classified as potentially carcinogen for human health (IARC, 2012). As a matter of fact, EU average annual limit of 5 μg m^{-3} or 1.5 ppb (Directive 2008/50/EC of the European Parliament). Nevertheless, it is important to remember that their secondary products (ozone and SOA) are causing important health implications, as it was seen in **Sects. 1.3.2 – 1** and **1.3.2 – 2**.

1.4.2 Action plans for VOC regulation

Following the recognition of VOCs as important atmospheric pollutants, **international protocols** have been enforced for the regulation of VOCs emissions in the atmosphere, as follows:

- 18/11/1991 – The VOCs Protocol. It was signed by 24 parties in Geneva. The main aim was the reduction of VOCs emissions, due to their contribution for the formation of ground-level ozone (Europe, 2004).

- 01/12/1999 - The Göteborg Protocol. Because the main aim was the reduction of Acidification, Eutrophication and Ground-level Ozone, it contains restrictions and target ceilings on several compounds including VOC. The latest revision of 2012 extends the application of national emission reduction commitments by 2020 and beyond.

European Union in particular, has also enforced **directives** targeted to the regulation of VOCs:

- 11/03/1999 – Directive n°1999/13/CE for the limitation of emissions of volatile organic compounds due to the use of organic solvents in certain activities and installations. Although it is no longer in force, it was the first detailed attempt for the control of VOC emissions from sources for the benefit of the health and the environment.

- 16/11/2000 – Directive n°2000/69/CE relating to limit values for benzene and carbon monoxide in ambient air. The annual limit of benzene was set at 5 μg m^{-3}, which had to be met by the participating countries by 2010. This limit is still in force under the directive n°2008/50/EC.

From the above information, the need for more VOC field measurements was highlighted, especially in urban areas where billions of people are gathered and their health, as well as the sustainable development, are threatened. This applies well in regions like Mediterranean basin, in which the lack of studies on specific air pollutants underestimate already the levels of key compounds (**Sect. 1.2.3**), in combination to the negative impact of climate change, as it presented in the next section.

2. AIR QUALITY OF THE EASTERN MEDITERRANEAN BASIN (EMB)

2.1 Air pollution and Urban agglomerations

The need of humans for **employment, higher income, better living conditions, security** and **contemporary health-care** lead millions of people to cities, creating large urban agglomerations or megacities (Baklanov et al., 2016). Although **megacities** are considered cities with more than 10 million habitants, the term is also widely used for **urban agglomerations with more than 5 million of people** (Molina and Molina, 2004). In reality, 54% of the population resides in urban environments, with 53% of them in Asia, 14% in Europe and Latin America & the Caribbean with 13% (UN, 2014).

The fast-growing urbanisation and the accumulation of the population in the megacities have a strong impact first locally to the **landscape** and **urban environment**. However, polluted air masses can transport from the city affecting the **air quality** on a **larger scale,** as well as the **global climate** (Baklanov et al., 2016). Megacities produce a huge amount of gaseous pollutants such **as particulate matter, greenhouse gases** (CO_2, CH_4), **NO_x, CO, VOC,** and **SO_x**. Therefore, based on observations close to megacities and model simulations, for example in Mexico City and Istanbul, the polluted plume can **transport many kilometres away from the city** affecting the surrounding region and extending the secondary production of pollutants like tropospheric ozone (Baklanov et al., 2016; Molina et al., 2010; Im and Kanakidou, 2012). Although, this is a global environmental issue, in this thesis the focus in on the Mediterranean Region.

2.2 The Mediterranean Region

Mediterranean Sea is located at the **intersection** of three **continentals**: Europe, Africa and Asia. It is semi-enclosed marginal sea with **only one opening to the ocean** through the narrow Strait of Gibraltar (Lascaratos et al., 1999). The Mediterranean **Basin** is the area surrounding the sea and it is separated to the **West, Central and East Mediterranean** (Karanasiou and Mihalopoulos, 2013) (**Fig. I - 17**). The climate is characterised by **mild and rainy winters** and

by **hot and dry summers**, in combination with **high solar radiation** and **cloud-free conditions** all year long (Kanakidou et al., 2011; Lelieveld et al., 2002). As a result of the climate and the location, the region is **sensitive to air pollution** (Im and Kanakidou, 2012; Monks et al., 2009) and **climate change** (Giorgi and Lionello, 2008; Lelieveld et al., 2012).

Figure I - 17: Mediterranean basin (photo from Google Maps).

Mediterranean Basin hosts a great number of **urban agglomerations**, with many of them being in the **Eastern part** (**Fig. I - 18**). Furthermore, **long-range transport of pollutants** from these cities is observed mainly in the **lower troposphere**, as reported by Lelieveld et al. (2002). More specifically, the **west** part of the Basin is influenced by **air masses from Western Europe** (for example Italy and France), whereas the **east** part from **Eastern European** air masses (for example from Poland and Greece). On the other hand, in the **free troposphere** are combined plumes from **Asia and North America** and in the **upper troposphere Asian monsoons** carry loads of pollutants from the **East.**

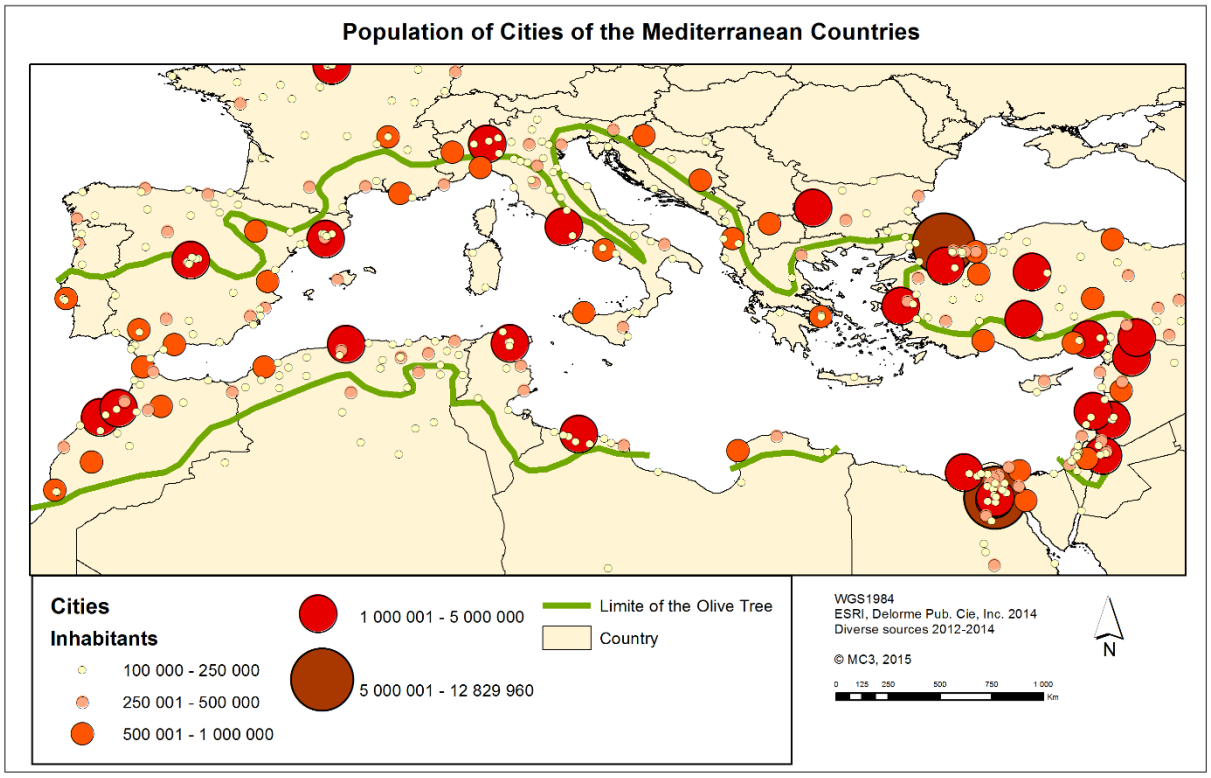

Figure I - 18: Megacities and urban agglomerations around Mediterranean basin (photo adjusted from Mediterranean cities and Climate Change – MC3, 2016)

One of the main air quality issues reported for the region (for urban and remote areas) is severe episodes of **photochemical smog**, meaning elevated concentrations of tropospheric ozone, especially in summer. In particular, Lelieveld et al. (2002) found that ozone concentrations can be almost a factor of 3 higher over the Mediterranean than the background of the entire hemisphere. In addition, the existence of important natural sources of particulates like the sea, the desert and the forests (apparent in Figure **I – 17**), air pollution events are also associated with increasing levels of **aerosols** (Kanakidou et al., 2011; Lelieveld et al., 2002). It is a matter of fact that this region has the **highest Aerosol Optical Depth (AOD)** in the world (Hatzianastassiou et al., 2009).

As it was mentioned previously, air masses from urban agglomerations carry pollutants, from which VOC and NOx are **precursors** of tropospheric ozone and SOA. Furthermore, many studies have shown that long-range transport of these precursors and their transformation during transport contribute the most to ground ozone and SOA (Derstroff et al., 2017; Finardi et al., 2018; Im and Kanakidou, 2012; Kanakidou et al., 2011; Solomou et al., 2018). It is a matter of fact that in a **remote site** of Eastern Mediterranean elevated concentrations of peroxyacetyl nitrate or **PAN** and **ground ozone** (indicator of anthropogenic impact on photochemical smog) were observed, which were associated with precursors that reached the area with **aged air-masses** (Rappenglück et al., 2003).

Recent studies have shown that **climate change** will have a **negative impact** on the Mediterranean region in the close future, with increase of the **warming** (25% higher than the global rates) and drought, increase of sea's temperature and the number of heatwaves, and

decrease of rainfall (Giorgi and Lionello, 2008; Sillmann et al., 2013). This mixture, apart from the strong **negative effect** on water, ecosystem, food, health, security and the **sustainable development** of the MB in general, will influence greatly the air pollution episodes (Cramer et al., 2018; Finardi et al., 2018). More specifically, in an exceptionally warm summer in Europe, characterized as prototype of the air quality in a warmer climate (Vautard et al., 2007), the increase of the heat in parallel to the decline of rainfall were identified as the **driving parameters** for this unique (for that decade) air quality situation. These caused the persistence of anticyclonic conditions over Mediterranean and the prevailing of stagnant conditions, leading to a significant increase of heat and pollutants, which are then trapped and re-circulated in continental-sea circulation systems, increasing the background levels of ozone and SOA. Moreover, the estimations of the previous studies showed that reduction to the ozone precursors locally and globally can have an important effect on tropospheric ozone levels and related episodes (Finardi et al., 2018; Vautard et al., 2007). Lastly, it is worthwhile mentioned that this summer prototype of the future air quality was the inspiration of a recent scientific initiative in Mediterranean, the ChArMEx project that we will see in the next paragraph.

For all the above reasons, the understanding and assessment of the air quality in MB has gathered the scientific interest for decades. Furthermore, scientific initiatives were organised, whose **objectives** can be summarised as follows: (1) the **monitoring** of pollutants for the observation of their temporal and spatial **variability**; (2) the **influence** of **meteorology** and **dynamics** on the observed variability and the **transport** of pollutants; (3) the **source allocation** of the pollutants; (4) the **assessment** of the influence of the monitored compounds on **air pollution** and **air quality**; and (5) the use of **model simulations** for the air quality forecasting and climate change prediction. For these reasons, short- or long-term measurement campaigns were organised with advanced instrumentation in selected sites of the MB, using field measurements, aircraft and/or satellites observations.

Some **examples** of such **initiatives** are:

- The Mediterranean Campaign of Photochemical Tracers – Transport and Evolution (**MEDCAPHOT-TRACE**) organised at Athens (Greece) in 1994-1995 with the participation of 16 international scientific groups (Ziomas, 1998; Ziomas et al., 1998).

- The Photochemical Activity and solar Ultraviolet Radiation – **PAUR** (1996-1998) and Photochemical Activity and solar Ultraviolet Radiation Modulation Factors-**PAUR II** (1998-2000) funded by European Union, focused on the photochemistry of Eastern Mediterranean (Zerefos et al., 2001).

- The Chemistry-Aerosol Mediterranean Experiment (**ChArMEx**) that was part of MISTRALS (Mediterranean Integrated Studies At Local And Regional Scales) international project. In general, it is a search program that aims at the better understanding of the air quality and tropospheric chemistry in Mediterranean, which in turn would help for a more efficient estimation of the future impacts on the region. Furthermore, it has many sub-projects that focus on air quality, regional climate, and

biogeochemistry, and their future evolution. In this context, advanced methods and instrumentation are used, combined with field, aircraft and satellite observations.

Nevertheless, the role of VOCs in the current and future air quality of the MB was apparent in this paragraph, highlighting the need for studies on their ambient levels, variability, driving parameters and sources. This will increase the robustness of the model estimations and forecasting, which in turn will facilitate the policy making of air pollution abatement measures. In the following section the focus is on the Eastern Mediterranean Basin, in which high concentrations of trace gases and background tropospheric ozone are reported, in combination to the increasing population and the environmental issues (Cramer et al., 2018; Kanakidou et al., 2011; Lelieveld et al., 2002; Solomou et al., 2018). In addition, the climate of the region resembles the predicted conditions of the future air quality in Europe under the warmer climate scenario, thus it constitutes an interesting area for scientific expertise.

2.3 Eastern Mediterranean Basin

Figure I – 19 presents the Eastern Mediterranean Basin (**EMB**), including some of the surrounding **megacities** and **large urban agglomerations** such as Istanbul (Turkey), Cairo (Egypt), Athens (Greece), Beirut (Lebanon) and Tel Aviv (Israel). The cities marked with stars were chosen based on the availability of research works on air pollutants. Common characteristic of these urban areas (and other cities that are not marked in the map) is the **poor air quality** due to the high concentrations of pollutants that often **exceed international** and **European standards** (Kanakidou et al., 2011; Karanasiou and Mihalopoulos, 2013). Therefore, the report of World Health Organisation for 2014 (WHO, Regional Committee 61, 2014) attributes 400000 premature deaths to Eastern Mediterranean (with a focus on the Middle East – North Africa part), directly linked to outdoor air pollution. This number is smaller than the corresponding one for Europe in 2015 specifically (535000 premature deaths attributed to air pollution; EEA, N° 13/2017, 2017), however, estimates for 2050 showed that premature immortality for Eastern Mediterranean will be the third highest (723000 deaths) after Western Pacific and Southeast Asia (2470000 and 2070000 deaths respectively) (Lelieveld et al., 2015).

Figure I - 19: Urban agglomerations in EMB: 1) Athens, Greece; 2) Istanbul, Turkey; 3) Izmir, Turkey; 4) Beirut, Lebanon; 5) Tel Aviv, Israel; 6) Cairo, Egypt (photo adjusted from Google maps).

Furthermore, the deterioration of the local air quality is complemented by the **long-range transport of pollutants** between cities and close continentals (Solomou et al., 2018). For instance, Kanakidou et al., (2011) simulated air mass back-trajectories showing that polluted masses from Athens and Istanbul have 10 to 30% probability to reach southern areas of EMB, in contrast to Cairo that is only 1 to 3% (**Fig. I – 20**). Another example is found in the study of Koçak et al., (2011), in which model simulations showed that air masses from Istanbul can travel over Aegean and Greece and even reach Libya and Egypt during summer, whereas Wagner et al., (2000) have investigated the long-range transport of pollutants from northern and central EMB cities to Israeli coasts.

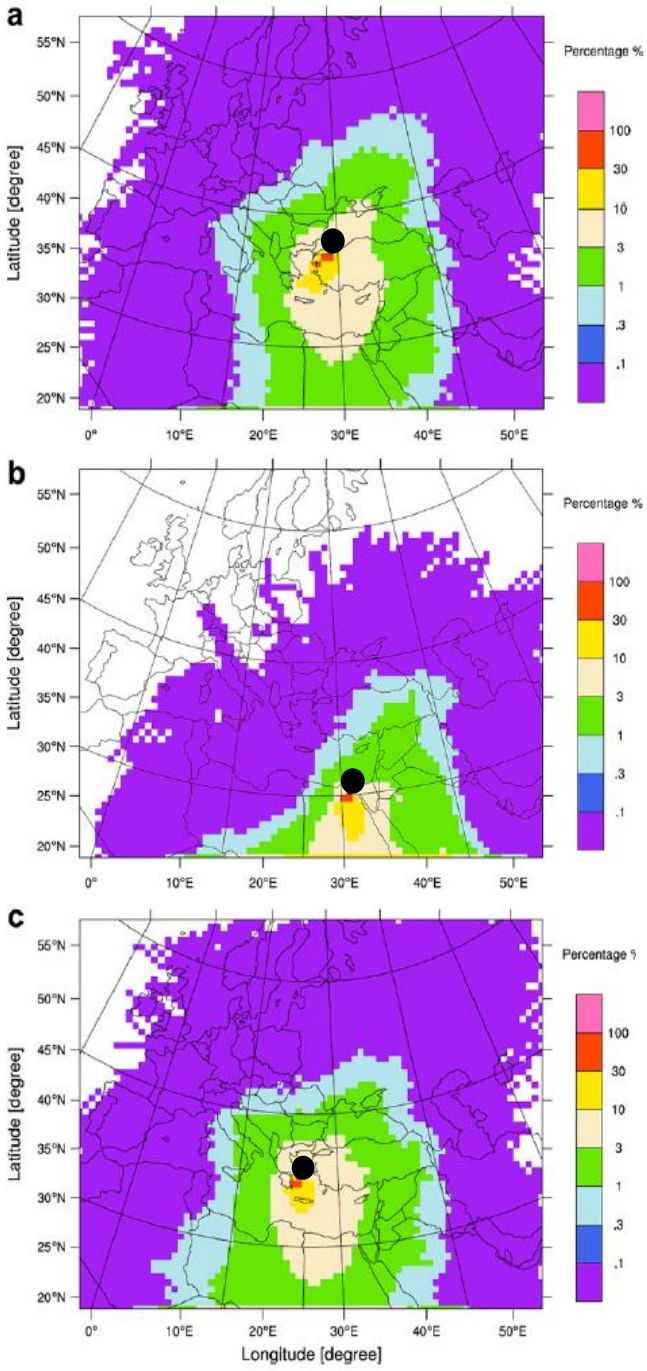

Figure I - 20: Map for the probability of arrival of trajectories starting from (a) Istanbul, (b) Cairo and (c) Athens. The black points indicate the city of Istanbul, Cairo and Athens respectively (adjusted from Kanakidou et al., 2011).

Despite the known air quality issues, the "geographic distribution" of the available studies on air pollutants in the EMB (and especially for urban environments) is uneven, in addition to the lack of comprehensive analysis. The existing ones are mainly focused on **particulate matter** and some indicators (**NO_x, CO, SO_2**), while VOC measurements and their apportionment to sources are even less and, in most cases, not recent or provide limited information. This absence of information for some regions can be partly justified due to the difficulties in the realization

of experimental campaigns due to geopolitical issues and constrains, and the closeness of cities (Sarnat et al., 2010). In the next paragraphs, an overview of the existing studies on VOCs at the EMB is given:

- ***Egypt:*** Only one study reports VOC measurements for Egypt, and more specifically for the Greater Cairo Area (Khoder, 2007). In this work, short-term measurements of VOC >C5 were conducted in 3 locations (one traffic site, one urban site and one rural site) indicating higher levels for all sites in comparison with other megacities worldwide (like Hong Kong in China, Manila in Philippines and Rome in Italy) and EMB cities such as Athens (Greece) and Beirut (Lebanon) (Rappenglück et al., 1998, 1999; Salameh et al., 2015). Moreover, information about VOCs for this country cannot be found elsewhere since there are no national or local VOC emission inventories.
- ***Israel, Palestine & Jordan:*** For these countries there are not any VOC studies in the literature. Nonetheless, for Israel, there is one national emission inventory of pollutants with data until 1998, also reporting estimations for some VOC (Weinroth et al., 2006).
- ***Lebanon:*** In the literature there are detailed and recent VOC measurements in Beirut that examine the seasonality of VOC levels and identify their sources and contribution (Salameh et al., 2014, 2015, 2016). In general, the reported levels are two times higher compared to other megacities of the North Hemisphere (like Paris in France and Los Angeles in USA). Furthermore, the main VOC sources are mobile traffic and gasoline evaporation. Information about VOCs are also provided by a national emission inventory for anthropogenic and biogenic sources (Waked et al., 2012).
- ***Turkey:*** As it is already mentioned before, due to the bad air quality of the Turkish cities, efforts for the documentation of the VOC levels and apportion to their sources have been made (Kuntasal et al., 2013). Most of the studies were conducted in **Izmir**, due to the petroleum refinery, petrochemical industry and commercial port of the city (Elbir et al., 2007; Muezzinoglu et al., 2001). The general conclusion was that the BTX levels are higher in comparison to other cities worldwide and the main source is motor vehicle emissions. On the contrary, very high VOC loads are reported for locations close to heavily industrialized areas of the region (Cetin et al., 2003; Civan et al., 2015; Dumanoglu et al., 2014). VOC levels in **Ankara** are comparable (Lille, France; London, UK) or lower (Athens, Greece; Hong Kong, China) to other urban centres, with traffic emissions being the primary source (Kuntasal et al., 2013; Yurdakul et al., 2013). In **Bursa**, a recent study (with C_2 - C_{12} VOC) revealed VOC concentrations similar or lower to Ankara for most compounds, originating from various sources apart from traffic emissions (Yurdakul et al., 2017). For **Istanbul** only one study exists for VOCs (Demir et al., 2011). The measurements were conducted to a suburban station, with the collection of 141 daily samples and additionally, 90 and 51 day and night samples, from March to May 2011. They found low ambient VOC levels, with the emissions mainly from industrial activities in the close vicinity. An important **drawback** for most of the previous works is that the results are based on **very few samples, plus only heavy VOCs are measured** (from 5 carbon atoms and above). As a result, in some cases, like Istanbul, additional VOC measurements and analysis are needed in order to understand the air quality better. Data for VOC and their sources can be also obtained from emission

inventories for various Turkish cities (Alyuz and Alp, 2014; Markakis et al., 2012 and references therein), although most of them report estimations of TVOC (total VOC concentrations) or HC (total NMHC concentrations). In particular, emission inventories with emission estimations for individual VOC are given by Markakis et al., (2012).

- ***Cyprus:*** As part of the **ChArMEx** project, VOC field campaigns were organized at a background station of Cyprus (Debevec et al., 2017, 2018). The published works provided information for the **VOC variability**, their **sources** (biogenic and anthropogenic) and their contribution to the **formation of new particles**. Especially for the latter, the work of Debevec et al. (2018) is among the few existing ones in the literature considering the important influence of BVOC to that. Nevertheless, the influence from **continental air masses**, which could enhance VOC levels depending on their origin, was highlighted.

Among the Mediterranean countries, Greece presents an important amount of published works on the origin and evolution of air pollution episodes and pollutants' variability. Greek cities suffer from poor air quality, due to the frequent air pollution episodes related to natural and anthropogenic emissions of pollutants, the Mediterranean climate and the complex topography (Kanakidou et al., 2011; Karanasiou and Mihalopoulos, 2013; Diapouli et al., 2017). For these and other reasons, Athens was chosen for the conduct of the current thesis, which was mainly funded by the ChArMEx project. Thus, the following section deals with the air quality in city, with a special attention to the existing VOC studies in Athens.

2.4 Air quality in Athens

Located in the Eastern Mediterranean basin, Athens is the **4th** largest **urban agglomeration** of the EMB after Istanbul (Turkey), Cairo and Alexandria (Egypt) (Brinkhoff, 2015), with more than **4 million population**. The Mediterranean **climate** and its **location** inside a semi-closed cycle of **mountains** with one opening to the **sea,** favours the **development** of severe **air pollution** episodes such as photochemical smog, winter night smog and dust events (Cvitas et al., 1985; Fourtziou et al., 2017; Gratsea et al., 2017; Kalabokas et al., 1999; Karanasiou and Mihalopoulos, 2013; Lalas et al., 1983; Paraskevopoulou et al., 2014; Theodosi et al., 2011). Apart from the local deterioration of the air quality, it was observed that **polluted air masses** originating from Athens **transport** many kilometres away, affecting greatly other areas in the Mediterranean basin (Im and Kanakidou, 2012; Kanakidou et al., 2011; Rappenglück et al., 2003). As a result, this is an ideal location for the air quality assessment and the characterisation of VOC in the atmosphere.

2.4.1 Athens topography, climate and dynamics

The city of Athens is located in a **basin**, on the west coast of the Attica peninsula (central south-east Greece). The basin covers an area of 450 Km^2 that it is defined by four surrounding **mountains**, Parnitha (1400m at N/NW), Penteli (1000m at N/NE), Hymettos (900m at E) and Egaleo (450m at W) (**Fig. I – 21**). Except of these mountains, the area is partitioned by smaller **hills** like Philopapou, Pnika and Lycabettus. At the south is found the gulf of Saronicos that connects the city to the sea. The **climate** of Athens is hot and dry in summer but wet and mild

in winter, while the prevailing **wind circulation** develops along the **axis** of the basin, between the mountain openings and the sea (Katsoulis, 1996; Ziomas et al., 1995).

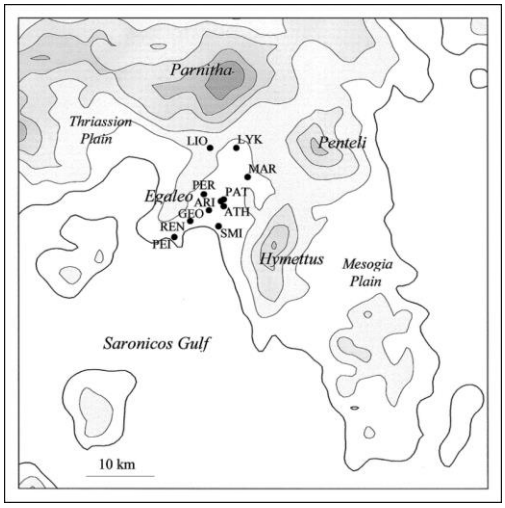

Figure I - 21: Typical map of the Greater Athens Area, including the Thriassion and Mesogea plan, the city center, the Mountains and Saronicos Gulf (adjusted from Kassomenos et al., 2003).

The complicated **topography**, in combination to the **microscale** and **mesoscale climatology** affect greatly the **air quality** of Athens. The presence or not of high- and low-pressure systems, the weather conditions, the anabatic/katabatic wind flow, the development of local wind cells, the temperature inversions, wind speed and wind direction, as well as the emission strengths of sources can influence the development of air pollution episodes.

Although every season presents different meteorological characteristics (i.e. high and low temperatures/solar radiation respectively, etc), the **pollution** events are **driven** from four common factors: **(1)** the presence of **anticyclonic weather** in stable atmospheric conditions; **(2)** a **swallow** surface temperature **inversion** for many consecutive days; **(3) low wind speed**; and **(4)** increased **emissions** from the sources.

Starting from the first factor, stationary anticyclonic conditions are usually formed when a **high-pressure system** passes over Greece, which produces light winds. This situation favors the development of a **temperature inversion** close to the surface (1200m mean value height; Katsoulis, 1988) in the night as a result of the land nocturnal cooling. The latter, in combination to other local circulation systems (e.g. katabatic air flows, sea-land breeze) and stable atmospheric conditions (cloudless skies) causes a **stratification** of the lower troposphere by air masses of different origin and photochemical age. These layers inhibit the vertical mixing of the pollutants, **trapping** them **under** the inversion. The nocturnal inversion systems are often dissolved the first morning hours due to the surface heating by solar radiation, thus having a minor impact (Katsoulis, 1988a, 1988b, 1996; Lalas et al., 1983). Finally, the surface inversion systems end when a cold front pass over or strong northerly winds persist, or due to the increase of the pressure gradient (under specific conditions) (Katsoulis, 1988). Furthermore, the entrapment is also favored by the height of the **planetary boundary layer (PBL)** (Gratsea et al., 2017; Kallos et al., 1993; Lalas et al., 1983 and references therein), which is **higher** during

day favoring the better vertical mixing and dilution of pollutants, whereas it is **lower** during **night**, allowing the accumulation of pollutants into the swallower inversion layer. In particular for Athens, a distinct seasonal and diurnal variability is reported with **higher heights in summer** and in **daytime**, and more specifically (Alexiou et al., 2018): (a) The mean daily PBL height is 1.8 times higher than the mean night height, taking into account all months, and (b) In summer, the difference between the mean daily and the mean night PBL height is a factor of 2, while in winter it is approximately 1.6 To summarize, the PBL height in summer is higher than winter (for both daytime and nighttime) and also the difference between the daily and night PBL height in summer is higher than winter.

The **previous conditions** are applied more in **winter** than summer. More specifically, **summer** air pollution events are usually associated with the **local circulation systems** that are enhanced from the weakening of the background synoptic winds. These circulation systems are mainly the sea/land breeze and anabatic/katabatic flows. The **sea/land breeze** plays an important role to the air quality of Athens in summer (occurring almost 50% of the days), since it promotes strong **pollution events** (Lalas et al., 1983). Three sea-land breeze **cells** are identified in Athens. The **strongest** one is developing from **Saronicos Gulf** towards Athens, and the two others from **Thriassion plan (South)** and **Mesogea (East)** towards Athens. An **anti-clockwise rotation** is observed for the sea breeze. During night, the land breeze originating from northerly directions, together with the katabatic air flows, transport the pollutants from the city to the sea, followed by their recirculation towards the city with the next sea breeze; the latter originates from **S/SW** direction with a depth of 400 – 800 m and occurs during day (Katsoulis, 1988a, 1996; Lalas et al., 1983). As a result, pollutants that were transported from the city over the sea flow back to Athens, where they are **trapped** into the mountainous barrier resulting in their **accumulation**. In addition, since solar radiation in summer is strong, the pollutants can be chemically transformed during their transportation, while they contribute to the formation of ground ozone (photochemical smog) (Katsoulis, 1996). Finally, **clean tropospheric atmosphere** is observed when strong northerly winds persist (in summer are named “Etesians”) that ventilate the basin (Katsoulis, 1988a, 1988b, 1996; Lalas et al., 1983)

2.4.2 Air pollution measurements in Athens

Due to the frequent exceedance of ozone and particulate matter (PM) levels that characterize air pollution events in Athens, the first studies assessing air quality were published over 40 years ago and they were dedicated to the examination and description of the microscale, mesoscale and synoptic climate conditions that influence the formation of these pollution episodes (Kallos et al., 1993; Katsoulis, 1996; Klemm et al., 1998; Lalas et al., 1983; Ziomas et al., 1995). Except of tropospheric **ozone** and **aerosols**, among the studied pollutants in Athens are found black carbon **(BC),** carbon monoxide **(CO),** nitrogen oxides **(NO, NO_2, NO_x),** peroxyacyl nitrates **(PAN),** volatile organic compounds **(VOC)** and other (Diapouli et al., 2017a, 2017b; Eleftheriadis et al., 1998; Glavas and Moschonas, 2001; Gratsea et al., 2017; Grivas et al., 2004, 2012; Kalabokas et al., 1999; Kaltsonoudis et al., 2016; Karanasiou and Mihalopoulos, 2013; Paraskevopoulou et al., 2014, 2015; Petrakis et al., 2003; Rappenglück et al., 1998; Stavroulas et al., 2019; Theodosi et al., 2011, 2018; Vasilakos et al., 2007 and references therein).

Since the primary concern of the past years was photochemical smog (O_3), and in studies it was shown that ozone levels could increase following the increase of its precursors, many campaigns were organized in Athens targeting NO_x and VOC (later in the section). Although NO_x levels are reported since 1981 (Lalas et al., 1983), it was not before 1993 that the **first** short-term **VOC measurements** in Athens were conducted, followed by other studies mainly in the 90s (Bakeas and Siskos, 2002; Giakoumi et al., 2009; Kourtidis et al., 1999; Moschonas et al., 2001; Moschonas and Glavas, 1996; Pateraki et al., 2008; Rappenglück et al., 1998, 1999). The majority of these works report the ambient levels of VOC, their temporal evolution and the effect of various parameters, as well as their contribution to ozone formation. However, as it will be shown in the next section, their complete seasonal variation was never examined, nor they were allocated in sources. Nevertheless, the evolution of tropospheric ozone in the ambient air of the city is always under investigation due to the frequent exceedances that still occur (State of the Environment Report - SoER 2018, http://ekpaa.ypeka.gr/index.php/soer-2018)

Finally, the observations and conclusions that derive from the air pollution measurements in Athens, are summarized as follows:

1. *From the past until today, the **levels** of pollutants **decrease***. Kalabokas et al. (1999) presented multi-year trends (11 years of measurements) of CO, NO_x and SO_2 in various stations in Athens, reporting the important decrease of their levels after 1990 as a result of the **pollution abatement actions**, like the old car replacement program, the introduction of catalytic systems at the vehicles exhausts, the circulation rearrangements at the city centre, the metro line extension etc (Kalabokas et al., 1999; Katsoulis et al., 1996). SO_2 was reduced already from 1977 due to the prohibition of heavy oil for residential heating and the reduction of the sulphur content in diesel oil. The decrease continued the following years and it is observed also in recent studies; however, after 2009, the decrease of the concentrations can be attributed also to the economic recession in Greece, which lead firstly to the increase of the price of all types of fuels and consequently brought a decrease of traffic emissions, and secondly, to the cessation of industrial activities (~30% for Athens) (Gratsea et al., 2017; Karanasiou and Mihalopoulos, 2013; Paraskevopoulou et al., 2015; Theodosi et al., 2011, 2018; Vrekoussis et al., 2013). For example, Vrekoussis et al. (2013) showed an accelerated decrease of NO_2 and SO_2 for the period 2008 – 2011 by 7.5 and 3.5 times respectively, due to the aforementioned recession. Nevertheless, the decrease of pollutants since 1988 is illustrated in **Figure I – 22** for CO, NO, and NO_2, although differences related to the acquisition of the data are not considered.

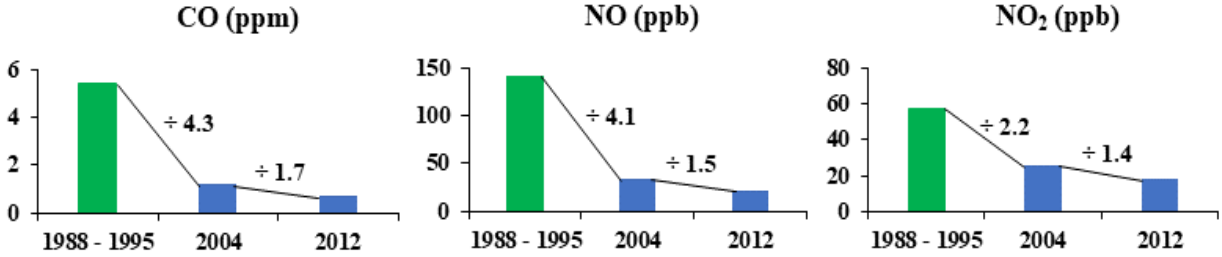

Figure I - 22: Annual mean values of CO, NO and NO_2 for Athens for the years 1988 –

1995 (Patission station, green bar; adjusted from Kalabokas et al., 1999), 2004 and 2012 (blue bars; adjusted from Vrekoussis et al., 2013 for Athens).

2. *Pollutants' **levels** often **exceed European limits***. Lalas et al., (1982) report hourly levels of surface ozone more than 147 μg m^{-3} every day for summer of 1980, which is close to the value of 160 μg m^{-3} (maximum value: 220 μg m^{-3}) in Katsoulis (1996) for the years 1984 – 1993. Even today that the pollutants' levels decrease, the ozone and PM concentrations often exceed the European legislation limits (120 and 50 μg m^{-3} respectively), as it is depicted in **Figure I - 23** from the current State of the Environment for background stations participating at the national monitoring network (SoER 2018, http://ekpaa.ypeka.gr/index.php/soer-2018). This is also corroborated by the most recent European air quality report (EEA Report, N° 12/2018). In the same context, Theodosi et al. (2011) and Grivas et al. (2012) present PM10 values higher that the European legislated annual average and the 24h value. Moreover, Petrakis et al. (2003) report a 4-month average concentration of benzene of 10 μg m^{-3} for summer 2000, which was two times higher than the European annual target and also it was expected to increase greatly in winter.

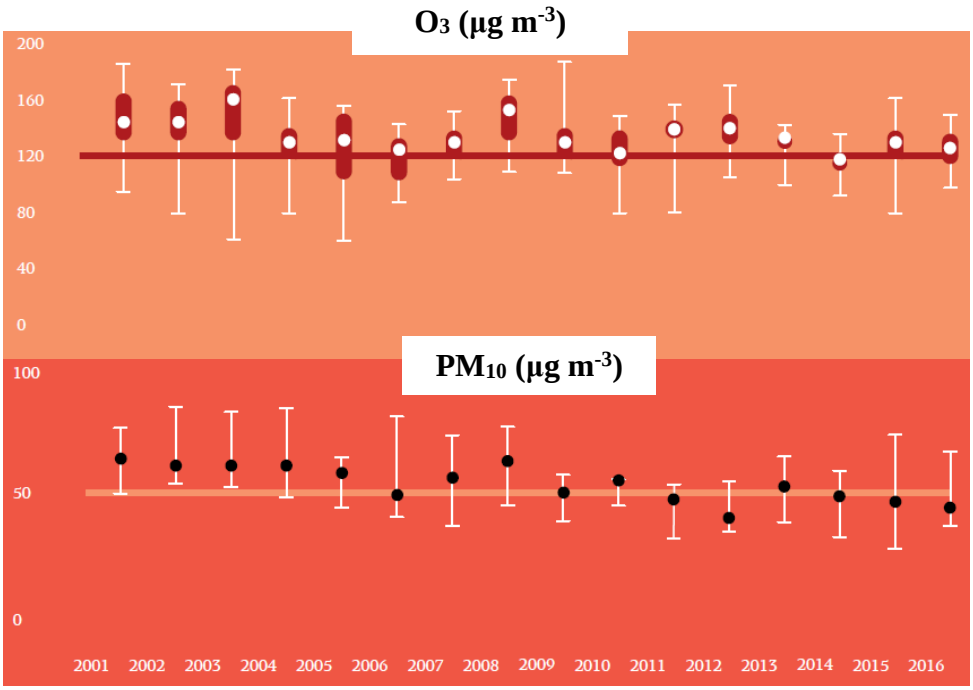

Figure I - 23: Median, interquartile range and min-max values for the 93.2 percentile of maximum daily 8-h mean O3 concentration values (upper graph), and median and min-max values for the 90.4 percentile of daily mean PM10 values (lower graph). Adapted from the SoER, 2018.

3. ***Low** wind **speed** and the **PBL** height favour the accumulation of pollutants.* Katsoulis (1996) examined the effect of microscale conditions to pollutant levels, showing that wind speed is the main factor controlling the observed variability, while the effect of sources is apparent for specific classification of the data. This is pointed out also in other studies (i.e. Fourtziou et al., 2017; Gratsea et al., 2017).

4. ***Higher*** *levels are observed in* ***winter*** *compared to summer, except from the levels of ground ozone*. This trend is shown for CO, NO_x, NO, PM_{10} and $PM_{2.5}$ in many studies (i.e.Gratsea et al., 2017; Katsoulis, 1996; Paraskevopoulou et al., 2015) and it is attributed to stronger emissions from sources during winter, as well as the favourable meteorological conditions. Moreover, it is worth mentioned that Gratsea et al. (2017) report increased levels of CO during winter night pollution events (**Fig. I - 24**) that are reaching the levels of 2000, in contrast to the morning concentrations that continue to decrease. These are associated to the increased wood burning for residential heating (Athanasopoulou et al., 2017), since the increase of the oil price made citizens to choose wood stoves and fireplaces as means for heating due to the smaller price of wood logs. This is observed in other cities of Greece as well (Dimitriou and Kassomenos, 2018; Saffari et al., 2013) and for other compounds like EC (Theodosi et al., 2018). In addition, Stavroulas et al. (2019) showed that organics are the largest fraction of aerosols in both winter and summer, with 50% of their winter levels originating from domestic heating emissions. Finally, Kaltsonoudis et al. (2016) report a decrease of the winter mean concentrations of VOCs from 11 – 34% if winter smog events are excluded from the dataset, highlighting the important contribution of this source.

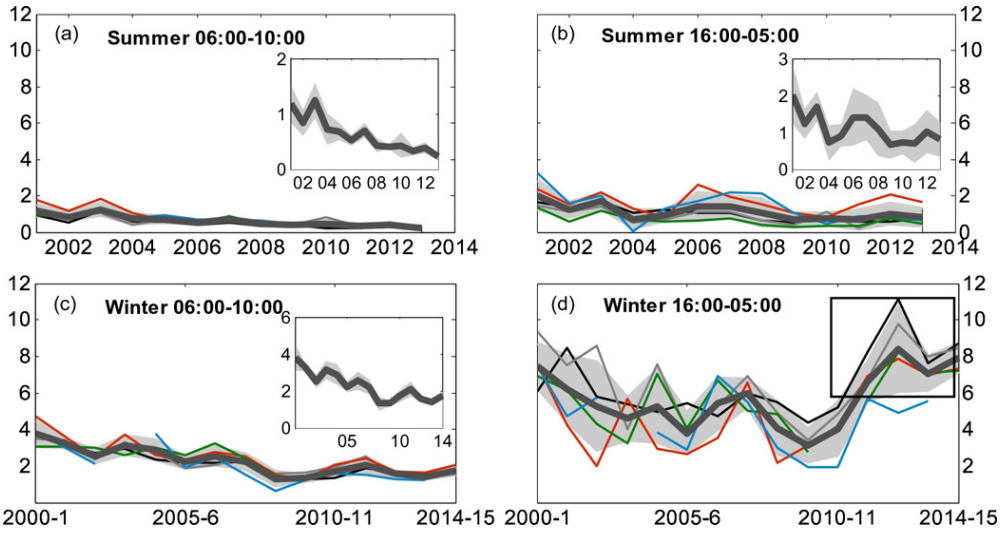

5.

Figure I - 24: Mean integrals of the morning and evening CO peaks for summer (top panels) and winter months (bottom panels) calculated for five monitoring stations in Athens. The time scale is different for summer and winter. The dark grey curve corresponds to the mean value of all five stations and the grey shaded area represents the standard deviation (1σ). In the internal panels the mean value is reproduced in different scale to highlight the existing trend over time (Adapted from Gratsea et al., 2017).

6. ***Traffic***, ***industrial*** *and* ***domestic heating emissions*** *are the main pollutant* ***sources*** *in Athens*. In the past, industrial emissions accounted for the 2/3 of SO_2 and all particulate emissions, while traffic emissions for the 3/4 of NO_x and almost all CO (Kalabokas et al., 1999). However, due to the implementation of air pollution abatement measures, as well as the industrial activity recline, emissions related to traffic and residential heating are the two main sources of pollutants in Athens (Fourtziou et al., 2017; Gratsea et al., 2017; Kaltsonoudis et al., 2016; Theodosi et al., 2018).

From the previous overview are missing the VOC studies in Athens. Since these are the compounds of interest in the current thesis, the next section presents in chronological order the scientific initiatives and studies on VOC, to better understand the evolution of their objectives and perspectives.

2.4.3 Overview of VOC measurements in Athens

1991 – 2000

Moschonas and Glavas, (1996) were the first team to measure and report VOC levels in Athens. Their experiments were conducted in the city center, giving the levels of 57 **C3 – C10 VOC** from five sampling periods in **summer** 1993 and **spring** 1994 (sampling only during morning), providing also some insights on their potential sources. A few months later, the first quasi-continuous measurements of 46 **C4 – C12 VOC** with the means of a **GC – FID** analyzer were performed under the frame of MECAPHOT-TRACE for one month in **September** 1994 (Rappenglück et al., 1998) in a traffic and a suburban station. Except of investigating VOCs impact on the photochemical smog evolution episodes, they also examined the factors affecting the observed temporal variability, including some discussion for the potential sources. A continuation of this project followed from October 1995 to September 1996, with the off-line sampling of 15 VOCs to three different stations inside Athens (Bakeas and Siskos, 2002). Since the purpose of this campaign was to **evaluate** the **photochemical pollution**, the sampling frequency varied from one hourly sample per day to one sample per week depending on the station, resulting in approximately 300 samples. Under the frame of PAUR, Rappenglück et al. (1999) implemented a second VOC campaign in Athens to a rural station in summer 1996, for a period of 15 days. They provided the levels and **temporal variability** of 49 compounds, from which 13 species are considered of biogenic origin; these are the first reported concentrations of this group of VOC. Moschonas et al. (2001) performed a one-day sampling campaign in June 1997, determining the noon concentrations of 29 NMHCs in the center of Athens and estimating their emission rates. Finally, 4-month time-resolved summer concentrations of benzene, toluene and xylenes (BTX), measured by a **DOAS** system in a semi-urban station close to the city-center, are reported by Petrakis et al. (2003) for 2000.

2001 – 2010

From 2001 and after, only **two VOC studies** were conducted in Athens, both monitoring only benzene, toluene and xylenes (**BTX**). First, Giakoumi et al. (2009) conducted BTX off-line measurements in 2004 at two locations in Athens (a traffic and a suburban station), which comprised from three sampling campaigns over a period of eight months (**warm seasons**), examining the **temporal variability** of the species in function of specific **meteorological conditions** (i. e. during sea-breeze). Afterwards, Pateraki et al. (2008) also determined the BTX levels in an urban and a suburban station (the latter was the same as in Giakoumi et al., 2009), with the implementation of two off-line sampling campaigns in winter and summer 2005.

2011 – Today

It was not before 2012 that a new VOC campaign was implemented in Athens: Kaltsonoudis et al. (2016) conducted two intensive campaigns in **summer 2012** and **winter 2013** at a suburban and an urban background station respectively, by the means of a Proton Transfer Reaction – Mass Spectrometry (**PTR-MS**). Their examination showed firstly an important **decrease** to the VOC ambient **levels**, and secondly, the effect of **smog episodes** on the concentrations in winter months. Similar observations for this trend are also reported by Psiloglou et al. (2017), which compared benzene and toluene levels from 2014 – 2015 to previous values from 2009, both monitored by a **DOAS** system in a suburban station. Furthermore, Kaltsonoudis et al. (2016) made a first attempt for the **source allocation** of the measured VOCs, however, the limited VOC suite did not allow a more source-specific VOC identification.

Emission inventories for Athens

A small number of **emission inventories** exist in the literature for Athens and Greece (i.e. Bossioli et al., 2002; Dimitropoulou et al., 2018; Fameli and Assimakopoulos, 2015, 2016; Kourtidis et al., 1999; Markakis et al., 2010), with some of them being traffic emission inventories (Fameli and Assimakopoulos, 2015; Kourtidis et al., 1999). Recently, a new emission inventory for BVOC emissions over Greece was published (3 groups: isoprene, monoterpenes and OVOC) covering the year of 2016 (Dimitropoulou et al., 2018). However, it is important to mention that only one emission inventory appears to include or have been validated or constrained by actual VOC measurements (Kourtidis et al., 1999). Finally, the lack of national and official emission inventories was also indicated in the latest National Emission Ceilings Directive from the European Environmental Agency (NEC; Directive 2016/2284)

As a summary, in this section it is apparent that the seasonal variability of VOCs on an annual basis was never reported for Athens, whereas the information for light NMHCs are limited or completely absent (like for C2 NMHCs). Additionally, the available reported studies on VOC date back almost twenty years, with the exception of Kaltsonoudis et al. (2016). The latter, in combination to the limited information for their current sources and their intensity highlight the scientific gap for these compounds in Athens, which is crucial considering the continuous exceedances of their secondary pollutants (O_3 and SOA).

3. Objectives and Strategy of the PhD Thesis

In the previous sections, the need for the continuation of the assessment of the air quality in Mediterranean basin and especially in the EMB and its urban centres, was highlighted, ultimately for the better understanding of the future air quality in Europe. More specifically, research works focused on VOCs and their sources are of great importance since they are important precursors of ground ozone and SOA, with demonstrated impact on climate change. In particular, it is worthwhile mentioned that the predicted future ground ozone levels appear sensitive to precursor emissions. Thus, the obtained information on VOCs from field measurements serve many purposes in local to global scale:

a) They provide **insights** for the **variability** of VOC, their **implication** in local and regional atmospheric chemistry and burden, their **interactions**, the influence from atmospheric dynamics and their **origin**
b) In urban environments, the mixture of sources and pollutants is complex, thus VOC field measurements assist the **determination** of the **contribution** of all significant **sources**
c) The combination of VOC datasets with other pollutants can help the better understanding of the **formation processes** of **secondary compounds** and the chemical **reactions**
d) Especially in **Athens**, the characterization of the VOC variability is important since it is currently **limited** (or completely absent in some cases). This will assist the **assessment** of air quality and the better understanding of **O_3 exceedances** and **SOA levels**, as well as the **impact** of VOC on air quality during **winter** smog events
e) In national scale, the **policy makers** can establish more targeted air pollution **abatement measures** on the pollutants in question and their secondary products (O_3 and SOA) by knowing their levels and sources
f) In **European** and **global** scale, the observations from the VOC field measurements could **constrain** existing **emission inventories** or future **model simulations**, increasing the **accuracy** of model predictions. This in turn could help policy makers to plan and implement better adapted strategies for the **improvement** of the air quality, based on real-life conditions (Abbass et al., 2017)
g) At the end, all these previous purposes aim at the **protection** of **human health**, of the **environment** and **ecosystem** that is achieved by the **sustainable development**, which in turn is linked to the efficiency of the previously mentioned air quality improvement strategies.

Therefore, all the aforementioned needs and future perspectives, as well as the choice of Athens for VOC measurements in the EMB, set the **framework** of the current PhD thesis, based on the two big questions originating from the scientific gap:

What are the VOC levels in Athens, and which are the factors controlling their variability?

What are the main sources and their relative contribution on VOC levels?

In a summary, the objectives are:

1. The investigation of the **temporal variation** of VOC concentrations in Athens (Greece) by conducting **high resolution measurements.**
2. The **comparison** of VOC levels in Athens with other **Mediterranean cities**, for the better understanding or the current air quality and the factors affecting it.
3. The **identification** and **quantification** of VOC **sources**.
4. The **establishment** of **sources' fingerprints** with field **measurements**.
5. The **comparison** of the results to **estimations of emission inventories**.

Accordingly, the **strategy** can be summarized as follows and includes:

- ✓ **C_2 – C_{12}** VOCs continuous measurements in Athens (Greece) from **15 October 2015 to 28 February 2017**, at an **urban background station**. A **high temporal resolution** is ensured by a cycle analysis of **30min**.
- ✓ **3 intensive campaigns** (winter, summer and traffic station) with **additional sampling methods** and **different instrumentation** of analysis (canisters, charcoal and DNPH cartridges) that allow the examination of the seasonality of more VOC species and the specification of the various sources' emission profiles.
- ✓ **Collection of samples** close to **sources** with **off-line sampling** methods**,** for the detection of more VOC species.
- ✓ **PMF source apportionment**, for the identification and quantification of VOC sources.
- ✓ **Comparison** of the **results** with **similar works** for other **Mediterranean cities**.

Following the presentation of the theoretical background and the establishment of the state of the art that concluded with the objectives and the strategy of the current thesis (**Chapter 1**), the outline of the next chapters is the following: a) **Chapter 2** explains in detail the experimental set-up for the implementation of the Athens VOC campaign, the different campaigns, the data treatment and validation of the results; b) **Chapter 3** presents the 1st publication of results from the campaign, aiming to gain a first insight of the VOC variability in winter, which was never examined, and the main VOC sources; c) **Chapter 4** focuses on the characterization of the variability of VOCs from all the datasets of the campaign and the investigation of its driving parameters; d) **Chapter 5** focuses on the variability of monoterpenes and isoprene and their origin; e) In **Chapter 6** the analysis of the observations via the source apportionment of VOCs using the PMF method is presented. The results are then compared to similar works in other cities (Paris and Beirut), as well as to preliminary results from a PMF simulation on the additional VOC dataset from the Athens campaign; and f) The dissertation ends by the **Conclusions and Perspectives** section, where a summary of the observations and results of the PhD thesis will be presented, followed by the new scientific questions and the future perspectives.

CHAPTER 2 – Materials and Methods

TABLE OF CONTENTS FOR CHAPTER 2

The current chapter describes the experimental strategy that was deployed for the field campaign in Athens, in order to obtain high-resolution VOCs measurements and further determine the chemical profiles of the individual emission sources. The 1st part of this chapter provides information relative to the monitoring sites, the compounds of interest and the equipment utilized, whereas the 2nd part focuses on the description of the measurement methods, the associated quality assurance and the data validation process.

1. Experimental strategy

The first step for the design of the field campaign is the selection of the sampling site. To serve our goals (**Sect. 3** of **Chapter I**), this site should be a receptor of the air pollution from the city, thus the Thissio Monitoring Station of the National Observatory of Athens was selected (**Fig. II – 1**). The station is operated by the Institute of Environmental Research and Sustainable Development (IERSD). It is located in the **historical center** of Athens, on top of a **hill** (Lofos Nimfon, NOA, 37.97° N, 23.72° E, 105 m a.s.l and ~50 m above the mean city level), surrounded by a small park of coniferous trees, a pedestrian zone, a residential area and by the Filopappou (108 m a.s.l) and Acropolis Hills (150 m a.s.l), which are located 500 m and 800 m away respectively. Furthermore, this site is characterized as **urban background** (Paraskevopoulou et al, 2015; Gratsea et al., 2017), i.e. representative of the air quality over Athens. In addition, the population around the site is sparse, thus the impact of local emissions is expected to be weak. Furthermore, **Figure II – 1** illustrates the location of the station on the top of hill and the building where the equipment was installed.

Figure II - 1: From up to down: Location of Athens (2nd panel), Thissio station (3rd panel) and the building hosting the equipment (4th panel).

The selection of the urban background monitoring station of Thissio in Athens, in combination with the need for VOC monitoring raised by the issues analyzed in Chapter 1, was the basis of the experimental protocol that has been applied. The design and implementation of a series of sampling campaigns targets firstly to monitor a broad variety of VOC and secondly to obtain high resolution data series. In particular, one major campaign of more than one-year duration (referred hereafter as Main Observations Campaign – MOP) and two seasonal intensive campaigns (Intensive Observation Campaigns – IOP) were conducted at the urban background site. Two short-term additional campaigns close to major VOC sources (Near-source Campaigns) were also implemented.

Since two of the main objectives of this work are the **chemical speciation** of specific sources and the **source allocation** (**Section 3** of **Chapter 1**), a great variety of compounds was selected including tracers of possible sources:

- **Alkanes C_2 – C_9**. These compounds are emitted from various sources including traffic related processes, fuel evaporation, biomass burning (domestic, agricultural or natural), oil and natural gas exploitation and solvent usage (Abeleira et al., 2017; Dominutti et al., 2016; Dalsøren et al., 2018; Gilman et al., 2013; Kalabokas et al., 2001; Schauer et al., 2001 and references therein).
- **Alkenes C_2 – C_3**. These compounds are products of incomplete combustion and thus associated to traffic emissions (fuel combustion for transportation) or domestic heating and any other kind of combustion (Gilman et al., 2013; Koppmann, 2008; Salameh et al., 2014; Schauer et al., 2001)
- **Alkynes.** Acetylene is the only compound monitored from this group. Like alkenes, it is also emitted as a product of incomplete combustion (Salameh et al., 2015; Schauer et al., 2001).
- **Aromatic hydrocarbons.** Major sources of these compounds are vehicle exhaust, fuel evaporation and spillage, industrial emissions and solvent usage. Following the application of the European directives for the reduction of the atmospheric levels of benzene (maximum content of 1% for benzene in petrol fuels – Directive 98/70/EC), nowadays it is emitted mainly by wood burning for residential heating than by traffic (Borbon et al., 2017; Gelencsér et al., 1997).
- **Biogenic hydrocarbons (BVOC).** Isoprene and terpenes are well-known compounds of this category. They are mainly emitted from vegetation, although there is evidence of anthropogenic sources (Geron et al., 2000; Guenther et al., 1995; Hellén et al., 2012; Liakakou et al., 2007; Rouvière et al., 2006).
- **Oxygenated volatile organic compounds (OVOC).** Aldehydes, ketones, alcohols and organic acids belong to this category. They can be emitted from both natural and anthropogenic sources, whereas they can also be secondarily formed in the atmosphere. OVOCs are thus considered as key products of the VOC oxidation and could also contribute on the oxidation capacity of the lower troposphere (Mellouki et al., 2015; Zhu et al., 2018).
- **Intermediate volatile organic compounds (IVOC).** C11 – C16 alkanes are of atmospheric importance, due to their high SOA formation rate (Aumont et al., 2012).

Traffic, cooking and biomass burning are among their main emission sources (Salameh et al., 2015, Zhao et al., 2014).

1.1 Main and intensive campaigns

Apart from the wide range of VOC, a sufficient number of high-resolution samples were acquired in order to accurately deconvolute and apportion the sources. For these reasons, the "VOC Athens campaign" is composed of one main campaign (**MOP**) and two seasonal intensive campaigns (in winter and summer - **IOP**). The targeted compounds of the MOP are the **C2-C12 NMHCs**, using two **automatic gas chromatographs** equipped with a flame ionization detector (**GC – FID**, Chromatotec, Saint Antoine, France). These analyzers collect and analyze air samples on-line (continuously) under a 30-min sequence. More specifically, the "**airmoVOC C2 – C6**" GC – FID was operating from 15th of October 2015 to 28th of February 2017 (18-months) and the "**airmoVOC C6 – C12**" Chromatrap GC – FID from 1st of February 2016 to 28th of February 2017 (13 months) for the determination of C2 – C6 and C6 – C12 NMHCs respectively.

Additional VOC, including OVOC and IVOC, as well as more alkanes, alkenes and aromatics were measured during the two short-term-campaigns **(IOPs)**, which were implemented in **winter** and **summer 2016**. The scope of these campaigns was to obtain a more detailed dataset to be related to the sources. For that purpose, additional **measurement methods** were deployed. More specifically, VOCs were monitored by off-line sampling of air in adsorbent tubes that was followed by their posteriori analysis at the laboratory, whereas a PTR-MS (Proton Mass Transfer - Mass Spectrometer, Ionicon Analytic, Austria) was used for the on-line measurements of VOC including OVOC. However, the results of the PTR-MS and the OVOC dataset from the summer IOP will not discussed further in this manuscript, as the instrument (PTR-MS) and (still on-going) data analysis were under the responsibility of a post-doctoral researcher, whereas the summer IOP OVOC dataset will be used for their inter-comparison. A description of the intensive campaigns is given in the following paragraphs.

Table II – 1 summarizes the period and duration of every sampling campaign during the Athens VOC experiment, whereas **Table II – 2** presents the technical summary of the campaigns, including information for the target compounds, the sampling method and the instrumentation used. In addition, in **Table II – A1** of the Annex the target compounds per sampling campaign are presented. In this point, it is important to mention that the operation of the GC analyzers and the treatment of MOP, IOPs and near-source campaign datasets were under my sole responsibility.

Table II - 1: Time coverage of the VOC measurement campaigns in Athens. For the MOP campaigns, the operational period (%) is indicated at the right (considering the maximum potential)

Athens VOC campaign	2015			2016												2017		
	10	11	12	1	2	3	4	5	6	7	8	9	10	11	12	1	2	
MOP (C2 - C6 NMHCs)																		≈ 81%
MOP (C6 - C12 NMHCs)																		≈ 93%
IOPs																		
Near-source campaign 1 (Tunnel)																		
Near-source campaign 2 (Traffic station)																		

Table II - 2: Summary of the sampling campaigns, the instrumentation and the target compounds

	Duration	Sampling method	Analysis instrument	Sampling & analysis time	Target VOC
MOP (C2 – C6 NMHCs)	17 months (16/10/2015 – 28/02/2017)	On-line sampling	GC -FID	Continuous, 30 minutes	Alkanes, Alkenes, Alkyne, Isoprene, Benzene
MOP (C6 – C12 NMHCs)	13 months (20/01/2016 – 28/02/2017)	On-line sampling	GC -FID	Continuous, 30 minutes	Alkanes, Aromatics, Monoterpenes
Winter IOP	14 days (28/01/2016 – 10/02/2016)	Off-line sampling with Charcoal cartridges	GC -FID (analysis in Douai, France)	3 hours	Alkanes, Alkenes, aromatics, OVOC, IVOC, monoterpenes
Summer IOP	20 days (02/09/2016 – 23/02/2016)	Off-line sampling with Charcoal & DNPH cartridges	GC -FID (analysis in Douai, France)	3 hours	Alkanes, Alkenes, aromatics, OVOC, IVOC, monoterpenes

1.2 Tunnel and Patission campaign

To obtain the VOC chemical fingerprint of emissions related to traffic, two short-term near sources campaigns were organized; the first in a tunnel on the Athenian peripheral and the second in a traffic monitoring station (Patission Station) close to the city centre. The tunnel is located approximately 10 Km northward of the Thissio station, whereas Patission station is 3 Km away in the same direction (**Fig. II - 2**).

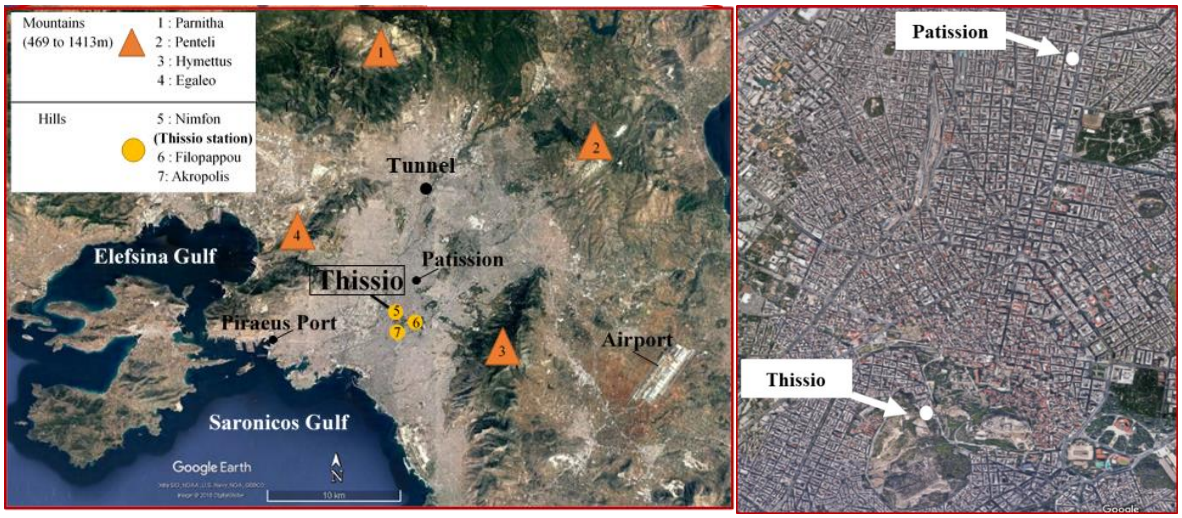

Figure II - 2: (left) The location of Thissio (urban background) and Patission (traffic) monitoring stations as well as the tunnel for the VOC tunnel campaign; (right) Zoom on Thissio and Patission stations to better depict their position on the city plane. (The map and city plane are adapted from Google Maps).

For the first campaign a tunnel on the peripheral highway of Athens (namely Attiki Odos) of 200 m length and 3 lanes per direction was chosen, with no specific restrictions for heavy duty vehicles. The off-line measurements took place on 12 May 2016 from 12:00 LT to 12:45 LT (LT = UTC+2) at the middle of the tunnel, to limit the influence of ambient air from outside. **Figure II – 3** presents the instrumental set-up deployed in the tunnel.

Figure II - 3: Experimental set-up in the tunnel during the VOC tunnel campaign of Athens in May 2016.

For the second campaign, the Patission monitoring station of the Air Quality agency of Athens, located at the homonym street canyon in downtown Athens (37.99°N, 23.73°E), was selected. This canyon-street is an ideal site for the investigation of the Athenian traffic fingerprint, since

it is characterized by increased flux of vehicles with frequent traffic jams (**Figure II – 4**). The VOC measurements were conducted from 22 to 24 February 2017 with off-line sampling on canisters and cartridges, while the sampling line was placed on the 5th floor of the building.

Figure II - 4: Location of Patission Traffic station.

In **Table II – 3** technical information of the two campaigns, including the target compounds, the sampling method and the instrumentation used is summarized.

Table II - 3: Summary of the sampling campaigns, the instrumentation and the target compounds

Near-source campaign 1: Tunnel sampling	1 day (12/5/2016)	Off-line sampling (Canisters, Charcoal & DNPH cartridges)	Analysis: GC- FID at Thissio for canisters & GC -FID at Douai (France) for the cartridges	3 – 10 minutes, 9 samples (3 canisters, 4 charcoal, 2 DNPH)	Targeted VOC: alkanes, alkenes, aromatics, monoterpenes, isoprene, OVOC, IVOC
Near-source campaign 2: Patission Traffic station	3 days (22/02/2017 – 24/02/2017)	Off-line sampling (Canisters, Charcoal & DNPH cartridges)	Analysis: GC- FID at Thissio for canisters & GC -FID at Douai (France) for the cartridges	10 minutes (canisters) and 1 to 3 hours for cartridges (14 canisters & 54 cartridges (27 of each)	

2. Instrumentation for VOC measurements

2.1 NMHC Analyzers: Automatic GC–FIDs

For the measurement of NMHCs with 2 to 12 carbon atoms (C2-C6), two compact automatic gas chromatographs equipped with a flame ionization detector (FID) (**airmoVOC C2 – C6 and airmoVOC C6 – C12**, Chromatotec, Saint Antoine, France) were installed at the Thissio station. The sampling system of these analyzers is **automatic**, meaning that air samples are collected and analyzed on-line, based on the settings provided by its operating software, without manual injection by the user. The **analysis cycle** includes **4** steps, which are repeated every 30 minutes: **(1)** The sampling and preconcentration of the NMHCs ; **(2)** The injection of the sample to the chromatographic column; **(3)** The chromatographic separation of the compounds by the column; and **(4)** The detection of the compounds. At the end of the analysis, the software

generates a chromatogram for each sample, which is processed later on by the user for the extraction of the final data. These steps have different order and duration for every analyzer, thus in **Figure II – 5** the sampling and analysis program of every analyzer is presented.

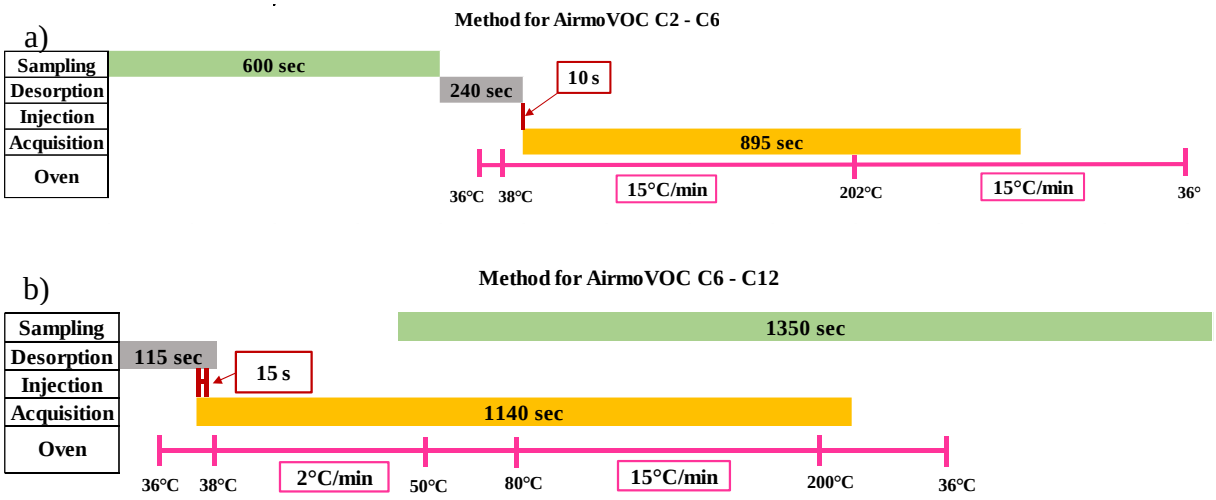

Figure II - 5: Sampling and analysis program of the a) airmoVOC C2 – C6 and b) airmoVOC C6 – C12 for the Athens MOP.

Furthermore, **Figure II – 6** presents the general scheme of the two GCs with all the different mechanical parts that are involved in the sampling and analysis of the air samples. The green (**Fig. II – 6a**) and blue (**Fig. II – 6b**) lines indicate the air flow after the introduction of the sample to the GCs, whereas the red lines correspond to the air flow after the desorption of the compounds from the trap.

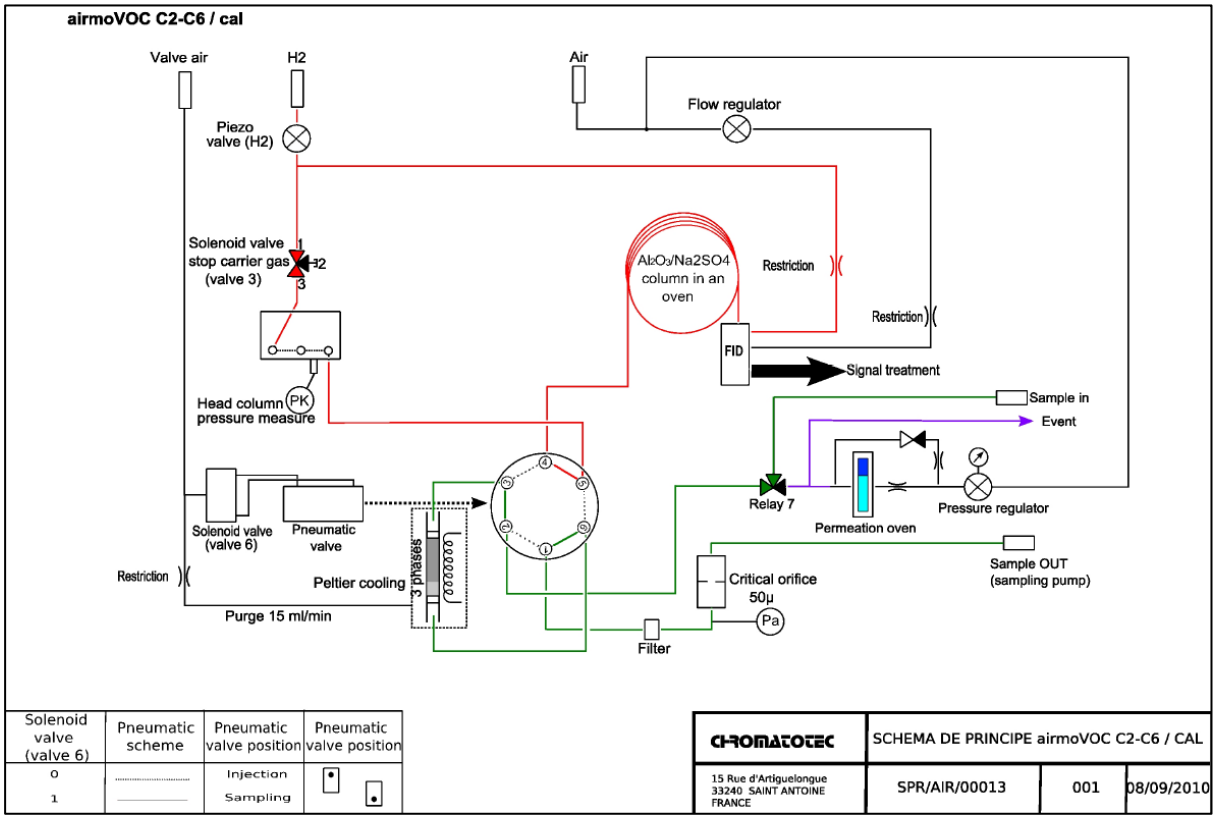

b)

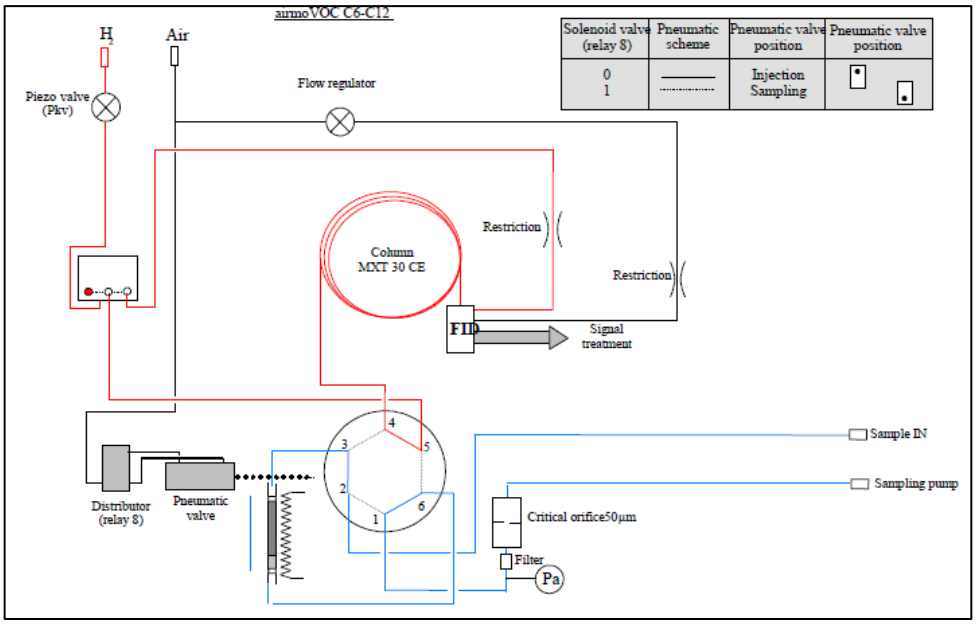

Figure II - 6: General scheme of the a) AirmoVOC C2 – C6 and b) AirmoVOC C6 – C12 for the sampling and analysis of ambient air (**Copyright**: CHROMATO-SUD, 2004, France).

Starting from the operational parameters, 2 types of gases are needed for the performance of the instruments: 1) Hydrogen (≥ 99,999% of purity) as carrier gas and as carburant for the FID detector and 2) Zero-air – VOCs free (≥ 99,999% of purity) as a fuel for the FID detector. AirmoVOC C2 – C6 uses in addition nitrogen (of purity ≥ 99,99%) for the sample drying system and the operation of the pneumatic valve, with a gas flow of 80 ml m^{-1} at the start of the campaign and around 200 ml m^{-1} at the end of the campaign. The change of the flow of nitrogen was required in order to increase the drying efficiency of the sample, which was the origin of analytical issues that will be described in the next paragraphs (**Sect. 2.2.1**). Nevertheless, the change of nitrogen did not affect the identification of the compounds, as it is verified by the calibration samples (**Sect. 2.2.1, Figure II – 8**).

Ambient air is introduced at ambient pressure by means of an external pump via a 6-m stainless-steel line of 0.315 cm diameter. The flowrate was measured at 19 ml min^{-1} and 45 ml min^{-1} for the GC C2 – C6 and C6- C12 respectively, giving a residence time of less than 150 seconds. The sampling time for this campaign was set at 22.5 minutes for the GC C6 – C12 and for the GC C2 – C6 at 10 minutes from 16/10/2015 to 15/07/2016 and was set down to 6 minutes for March 2016 and from 16/07/2016 to 28/02/2017. The decrease of the sampling time was imposed by the higher concentrations often encountered in winter 2016, especially for butanes and pentanes. A porous filter of 4 µm size was placed at the sampling inlets of both instruments (placed next to each other on the same height) to avoid any particles that can damage the instrument or hinder the analysis of the targeted compounds. At the end of the line the air sample is carried inside the instrument towards a trap, to pre-concentrate the VOCs before their injection to the separation column. However, this procedure and the rest of the analysis method is different for the two analyzers thus the main points will be summarized as follows:

Preconcentration of the NMHCs before the injection:

AirmoVOC C2 – C6

1) A Nafion dryer is placed before the trap to reduce the water content of the sample. The operation of this dryer is explained in the next paragraph (**Sect. 2.1 – 1**).
2) The dried sample is then carried towards a trap cooled at -8°C with a Peltier system, to pre-concentrate the VOCs before their injection to the separation column. The latter step is important because C2 – C6 NMHCs are very volatile (boiling point < 30°C), thus their trapping is favored by the cold environment that is created by the Peltier system (temperature set to -8°C).
3) The pre-concentration tube is 8-cm long and of 2.25 mm diameter. It is filled with 3 different types of absorbents that are separated by a metallic net: Carboxen 1000 (carbon molecular sieve 50 mg) for the C2 – C4 NMHCs, Carbopack B (black graphitized carbon, 10 mg) for the C4 – C6 NMHCs, and Carbotrap C (black graphitized carbon, 10 mg) for the heavier NMHCs. When the sample enters the trap, it interacts firstly with Carbopack, then with Carbotrap and lastly with Carboxen, while the temperature of the system is kept stable at -8°C.

AirmoVOC C6 – C12

1) The sample is introduced directly to the pre-concentration trap (8-cm long, 2.25 mm diameter). There is not a Nafion dryer, nor a Peltier cooling system, thus nitrogen gas is not needed in this analyzer.
2) The pre-concentration trap is operating in ambient air temperature.
3) The absorbent of the trap is the Carbopack C (black graphitized carbon) (10mg), for the entrapment of NMHCs with more than 5 carbon atoms.

Desorption of the sample and injection:

In both instruments, the trapping of NMHCs follows a rapid thermo-desorption, which is achieved by the increase of the trap temperature in a few seconds. Then, the NMHCs are instantaneously reversely flashed from the trap into the column in order to reduce the possible retention of the heavier compounds from the absorbents. The characteristics of every analyzer for this phase are presented below:

AirmoVOC C2 – C6

1) The rapid thermo-desorption is achieved by increasing the trap temperature to 220°C and the whole procedure lasts 4 minutes (**Figure II – 5a**).
2) The NMHCs are flashed from the trap crossing firstly the Carboxen material, in order to reduce the possible retention of the heavier compounds from the absorbents.
3) The injection of the sample to the analytical column is 10 s.

AirmoVOC C6 – C12

1) For the thermo-desorption the trap temperature increases to 380^{o}C and the procedure lasts 2 minutes.
2) The injection of the sample to the analytical column is 10 s.

Chromatographic separation:
In this stage, the compounds are separated based on their molecular mass and their interactions with the stationary phase of the column. The elution is assisted by a column temperature program. Both the column and the program are different for the two GCs, as listed below:

AirmoVOC C2 – C6

1) A capillary analytical column (Al_2O_3/Na_2SO_4) with a length of 25m long and a diameter of 0.53 mm is used.
2) The column temperature program that is followed is presented in **Figure II – 5a**; in a summary, it starts at 36°C for two minutes, then going up to 38°C in 60 s, followed by a gradual increase to 202°C (rate: 15°C/min) until one minute before the acquisition. The temperature remains steady and starts decreasing to 36°C (rate: 15°C/min) 5 minutes before the end of the acquisition.

AirmoVOC C6 – C12

1) The capillary analytical column is a metal MTX30CE (30 m x 0.28 mm diameter and 1 mm film thickness).
2) The temperature gradient of the oven is depicted in **Figure II – 5b**. The starting temperature of the oven is set at 36°C. 30 seconds after the start of the desorption increases up to 38°C in 60 s, followed by a gradual increase to 50°C (rate: 2°C/min) for 6 minutes, then it reaches 80°C in 3 minutes (rate: 10°C/min) and 200°C in 8 minutes. Then, the temperature remains stable for 3 minutes, followed by a gradual decrease to 36°C (rate: 15°C/min) until the next cycle of analysis.

At the end of the column, the eluted compounds successively reach the FID detector. The hydrocarbons are burnt and decomposed from the high temperature (170°C), producing ions. The latter are collected on a metal electrode connected to a high DC voltage. This creates an electric current that is proportional to the mass of the VOC arriving to the detector. The electric signal is then digitalized and transferred to the central processing unit (CPU) of the GC computer. All the parameters generated by the acquisition of the sample (data, chromatograms, etc) are then transferred through a RS – 232 portal to the software VistaCHROM allowing the plot and process of chromatograms.

In **Table II – 4** the operational parameters of the two analyzers are summarized.

Table II - 4: Operation parameters of the airmoVOC C2 – C6 and airmoVOC C6 – C12.

	Unit	C2 – C6	C6 – C12
Carrier gas flow (H_2)	ml min^{-1}	7 - 8	3 - 4
FID H_2 flow	ml min^{-1}	23 (2 Bar)	27 (2 Bar)
FID Zero air flow	ml min^{-1}	180 (3 Bar)	180 (3 Bar)
N_2 flow (Nafion & valve)	ml min^{-1}	75 (3 bar) until November 2016, 200 (3 bar) until February 2017	-
Room temperature	°C	+10 - +35	+10 - +35
FID temperature	°C	170	170
Sampling time (ambient air & calibration)	min	10 or 6	22.5
Analysis time of every cycle	min	30	30
Trap temperature	°C	-8 °C (Peltier effect)	Ambient temperature
Thermo - desorption temperature of the trap	°C	220	380
Thermo - desorption time	min	4	2
Injection time	sec	10	10
Oven program	°C	38 → 202 → 36	38 → 50 → 80 → 200 → 36
FID temperature	°C	170	170
Analysis time of every cycle	min	30	30

2.1 - 1 GC – FID C2 – C6: Nafion dryer contribution on the sample drying process and Peltier system

The necessity of the drying lies on the absorbents that are used for the pre-concentration of the sample that are sensitive to humidity (Ras et al., 2009).

The Nafion dryer is a semi-permeable membrane tube. More specifically, it is consisted from two tubes made from the material nafion, which are one inside the other. The chemical structure of nafion is depicted in **Fig. II – 7**; in general, it is an tetrafluoroethylene-perfluoro-3,6-dioxa-4-methyl-7-octenesulfonic acid copolymer or simply a Teflon polymer with branches that ending in the sulfonic group of $–SO_3H$. The acidic properties of this group grant the material the ability to remove the humidity from a sample by retain water.

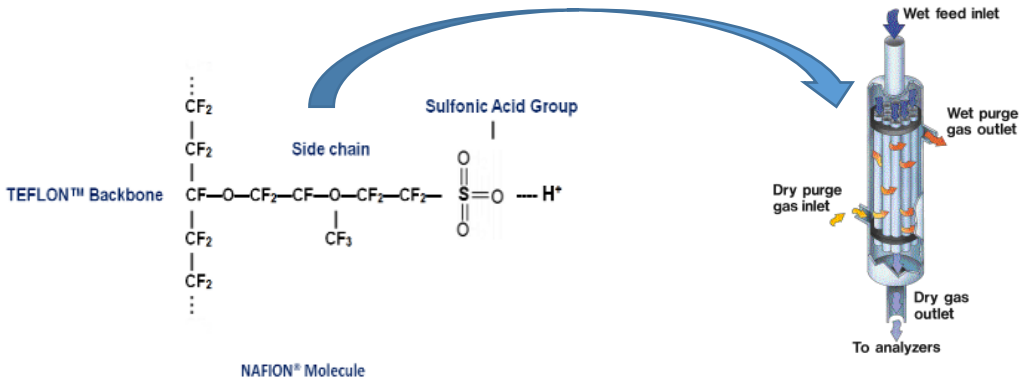

Figure II - 7: Nafion chemical structure (image from http://www.nafionstore.com/pg/19-Nafion-_US.aspx) and the Nafion – permapure - tube (image from https://www.inacom.nl/gasdrogers-nafion-permeabel.html)

The drying operation is the following: the air sample is passing through the inner tube while an inert gas is flowing at the opposite direction in the outer tube. The "drying" gas should have less water content than the air sample in order to have a drying effect; for instance, nitrogen was chosen (99.99% purity) for the Athens VOC campaign. The sulfonic groups of the Nafion retain only the water molecules, whereas they are not interacting with the sample's components. From then, the retained water is transferred through chemical exchanges deeper in the Nafion membrane, since the water content is less there. This exchange continues until the water molecules reach the outer part of the tube, from where they evaporate back in the atmosphere by the "dry" gas. The drying operation is repeated non-stop during the entire campaign.

At the outlet of the nafion dryer, the dry sample is carried into the trap that is placed inside a Peltier Cooling system. The system consists from a thermo-electric device in which is placed a glass tube for the pre-concentration of the sample. Thermo-electric coolers operate according to the Peltier effect; when a DC electric current flows through the device, heat is removed from one junction and goes to the other, resulting in a cooling and a heating effect respectively. The hotter junction is attached to a heat sink so that it remains at ambient temperature, while the cooler junction can reach below room temperature. In our case the Peltier system was set to -8°C.

2.2 Quality control and post processes

2.2.1 Calibration of the analyzers and control charts

Two NPL (National Physical Laboratory) NMHC standard gas mixtures were used during the Athens MOP campaign. The 1st NPL (D64 1636) contained 30 NMHCs of ~4 ppb concentration each and was used for 5 months (January – May 2016). The 2nd NPL (D09 0597) contained 32 NMHCs of ~2 ppb concentration each. Both standard mixtures were certified by the National Reference Laboratory of the United Kingdom and their composition is presented in **Table II – A2** of the **Annex II**. The simultaneous calibrations of both chromatographs were performed almost every 15 days and each calibration cycle was composed from 4 to 5 measurements of the calibration standard.

For the determination of the **stability** of the two analyzers during the campaign, **control charts** were created. More specifically, the mean value of the coefficients derived from the 1st calibration of the campaign was used as a reference for the calculation of the relative difference of every coefficient obtained in the following calibrations during the campaign. The relative difference is plotted against the calibration date. By considering the stable NPL composition, records out of the ± 20 % limit denote stability issues of the GC, otherwise no changes on the calibration outcomes are expected.

The control charts of **acetylene** and **i-butane** as well as of **toluene** and **1.2.4 TMB** representatives for the C2 – C6 and C6 - C12 NMHCs respectively are presented in **Figures II – 8** and **II – 9.** Even though two different standard mixtures were used, the derived coefficients did not present any difference and therefore these points are not highlighted. The calibrations of the GC C2 – C6, which correspond to the two different sampling times of the campaign, are marked with black (for the 10 min sampling) and orange (for the 6 min sampling).

In **Figure II – 8** for the NMHCs of GC C2 – C6, an **increasing trend** of the relative difference occurs from the 1st calibration until the end of August 2016, which reflects the **decrease** of the response **coefficients**. This issue had a higher **impact** on the more volatile compounds such as **ethane, ethylene, propene** and **acetylene**, whereas the **heavier NMHCs** like i-butane and pentanes were less affected. Furthermore, this decrease was accompanied by a **noisy baseline** for many chromatograms. An excess of **humidity** in the sample was identified as the major cause, due to an **inefficient** Nafion dryer (**Sect. 2.1**of **this chapter**). Apart from that, the humidity also caused the **deterioration of the trap**, leading to its replacement at the end of August 2016. After the change, the coefficients of all the compounds **recovered** to stable levels comparable to the 1st calibrations or even higher. The effectiveness of the trap replacement is verified by the comparison with the Paris calibration prior the transport of the GC to Greece, revealing comparable relative differences of the coefficients that are maintained until the end of the MOP. Overall, it is quite difficult to have a unique response coefficient representative for the total period of the C2 – C6 NMHCs measurements. Therefore, **2** or **3 different response coefficients** were calculated **per compound,** based on the individual control chart trends.

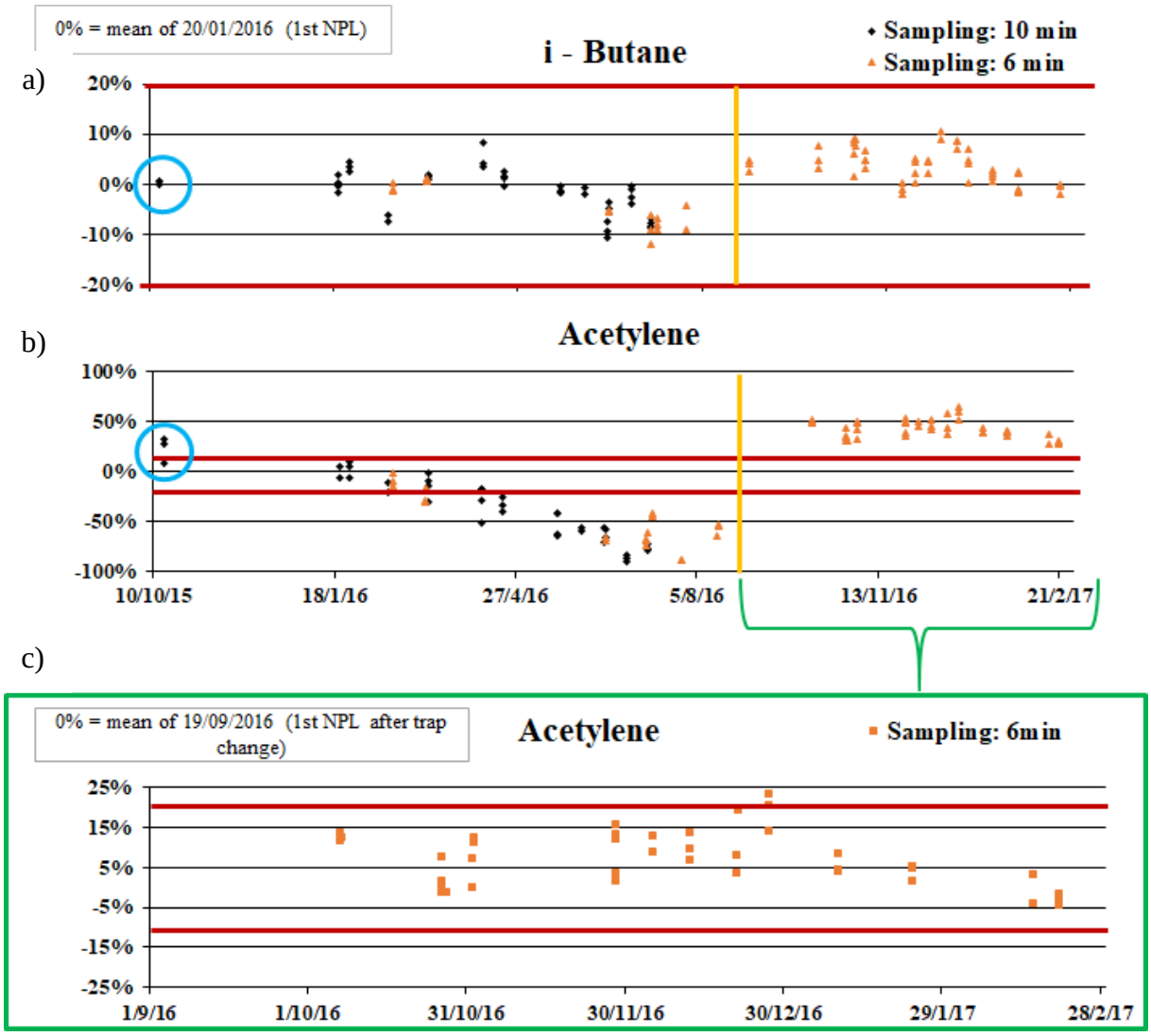

Figure II - 8: Control charts of a) i-butane, b) acetylene before the change of the trap and c) acetylene after the change of the trap focused on the period from the change of trap and after. The date of the calibration used as reference +/- 20% (red lines) is indicated in the box on the top left of every chart. The blue circle indicates the calibration in Paris, before the transport of the equipment to Greece, and the yellow vertical line marks the date of the trap change

Concerning the control charts of the response coefficient for toluene and 1.2.4 TMB (**Fig. II – 9**), discrepancies of **20 – 40%** are observed from the 1st calibration (20/01/2016) until 09/03/2016. This difference was not associated with changes on the chromatograms or with any interference. However, on 11/03/2016, the analyzer presented an instability which gradually shifted the retention times, before going back to the previous values without any external intervention. Moreover, since there was no apparent cause and in order to address this issue, two response coefficients were calculated and used for the C6 – C12 NMHCs, one for the period from 20/01/2016 to 11/03/2016, and a second one from 12/03/2016 until the end of the campaign. Moreover, it is important to note that the heavier compounds presented higher variability of their response coefficients compared to the others, however, remaining within ± 20%, except of a few points (e.g. 1.2.4 TMB in **Fig. II – 9**).

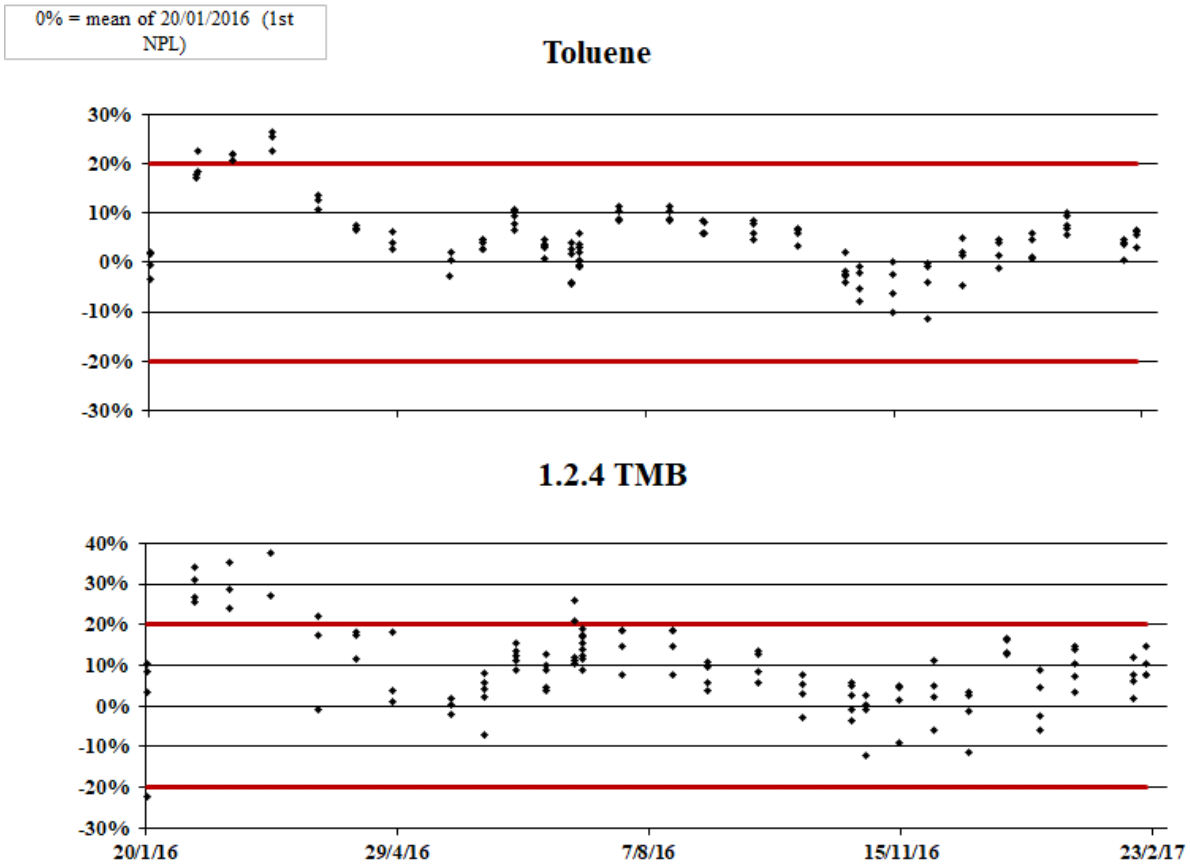

Figure II - 9: Control charts of the response coefficient for toluene and 1.2.4 TMB for the total period of measurements. The date of the calibration used as a reference for the calculation of the limit of ±20% (red lines) is indicated in the box on the top left of every chart.

Finally, zero-air samples were analyzed during the campaign whenever it was possible, serving as blank samples but only for examining if there is a strong contamination that could affect the analysis of a compound (**Sect. II – A1** of the **Annex II**).

2.2.2 Post process of the chromatograms

For every analyzed sample, the software Vistachrom (installed in both GCs) generates a chromatogram that is treated by the program "PeakViewer" (an extension of Vistachrom). Firstly, the chromatogram is qualitatively analyzed for the identification of the compounds, and secondly, a quantitative analysis for the calculation of the concentrations of the VOC is performed.

Qualitative analysis

The identification of the peaks of the chromatograms is performed automatically by the program "PeakViewer" with the use of an identification table, based on the retention time of the compounds in the calibration samples. Examples of such reference chromatograms are presented in **Figure II - 10** for the GC C2 – C6 and C6 – C12. For all the compounds, the retention time window was set at ±5s around the reference retention time. Moreover, the

identification table was often checked and adapted based on the calibration chromatograms of that period.

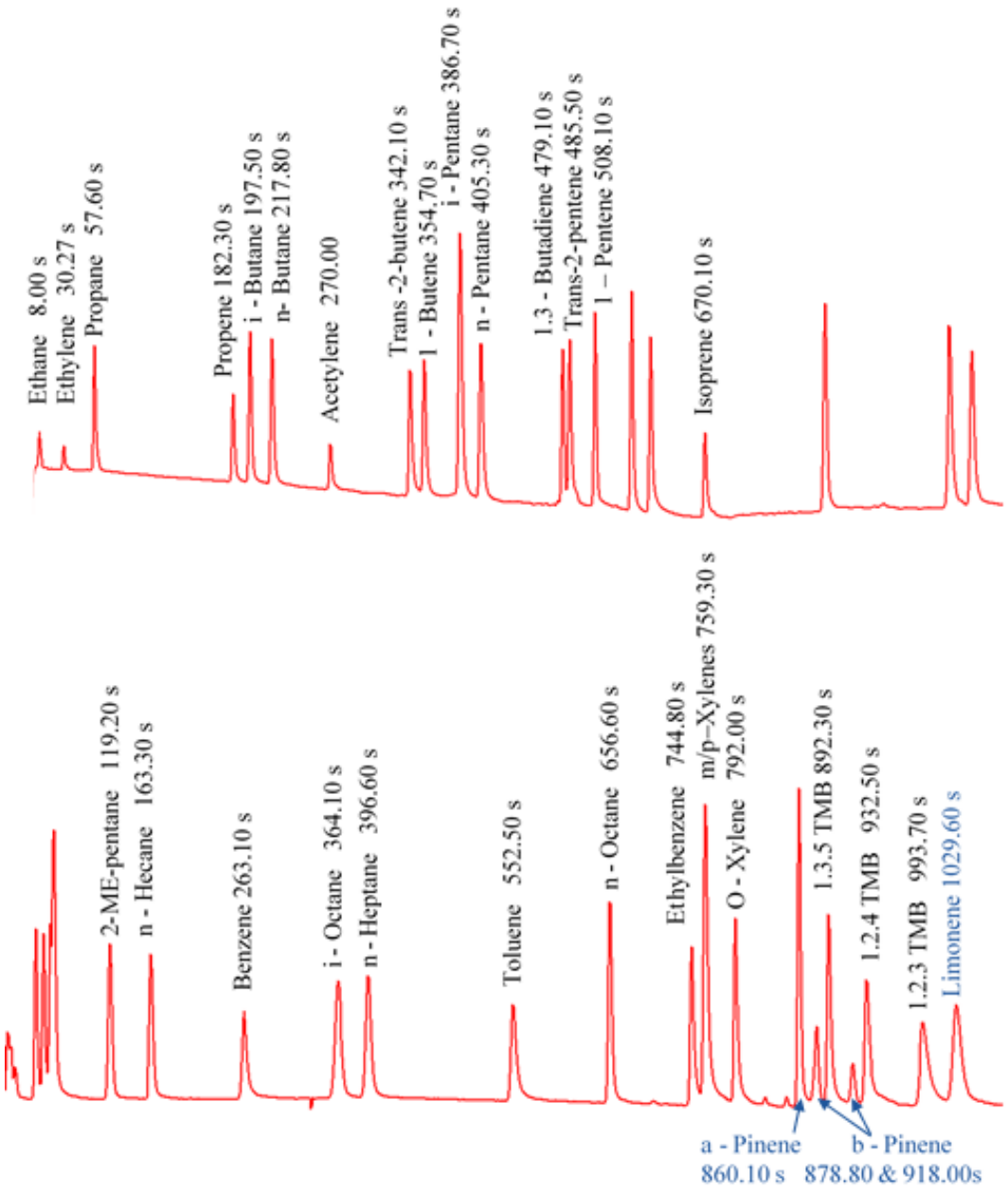

Figure II - 10: Example of a chromatogram obtained from a NPL sample. Identification of the target compounds of the GC C2 – C6 (upper graph) and of GC C6 – C12 (lower graph). In the lower graph the blue compounds were included only in the 2ppb NPL that was used after 20/05/2016.

Quantitative analysis

In order to calculate the concentration, the response coefficient k has to be determined for each compound according to Eq. II – 1:

$$k_i = \frac{A_{i\,NPL}}{[NMHC]_{i\,NPL}} \qquad \text{Eq. II - 1}$$

where $A_{i\ NPL}$ is the peak area of the compound *i* detected in an NPL sample and $[NMHC]_{i\ NPL}$ is the certified concentration of the compound *i* (ppb) in the NPL.

Then, the concentration of each NMHC is calculated following Eq. II – 2:

$$[NMHC_i] = \frac{A_{i\ amb\ air}}{K_i} \qquad \text{Eq. II - 2}$$

where $[NMHC_i]$ is the concentration (in ppb) of the compound *i* in the chromatogram of one sample, $A_{i\ amb\ air}$ (in UA , unit of the area) is the peak area of the compound *i* detected in the specific sample, and K_i is the response coefficient of the compound *i* (in UA ppb^{-1}).

At this point it is important to mention that for the discussion of the results in the following chapters, the concentrations of the NMHCs were averaged to 1-hour and the 30-min data were used only for the source allocation.

2.2.3 Limit of Detection (LoD)

The Limit of Detection (LoD) is the **lowest concentration** of a compound that can be detected in a sample. The Eq II – 3 is applied on the baseline results as follow:

$$LoD_i = 3\frac{H_{BN}}{H_i}\ x\ \frac{A_i}{k_i} \qquad \text{Eq. II - 3}$$

where LoD_i is the detection limit of the compound *i* in ppb, H_{BN} and H_i are the height of the noise in the baseline and the height of the peak of the compound *i* (in UA s^{-1}) respectively in the selected sample, A_i is the area of the compound *i* detected in the selected sample and k_i is the response coefficient of the compound *i* during the sampling period of the selected sample. The LoDs calculated for our systems are presented in **Table II – 5** demonstrating detectable levels of 0.02 to 0.05 ppb for both systems.

Table II - 5: LoD of the C2 – C6 and C6 – C12 NMHCs.

GC C2 – C6	LoD (ppb)	GC C6 – C12	LoD (ppb)
Ethane	0.05	**2–me–Pentane**	0.04
Ethylene	0.04	**n - Hexane**	0.04
Propane	0.04	**Benzene**	0.04
Propene	0.04	**i - Octane**	0.03
i - Butane	0.02	**n - Heptane**	0.03
n - Butane	0.03	**Toluene**	0.03
Acetylene	0.03	**n - Octane**	0.03
Trans – 2 – butene	0.02	**Ethylbenzene**	0.03
1 - Butene	0.02	**m- /p-Xylenes**	0.03
i - Pentane	0.03	**o-Xylene**	0.03
n - Pentane	0.03	**Nonane**	0.03
Isoprene	0.04	**1.3.5 TMB**	0.02
		1.2.4 TMB	0.03
		1.2.3 TMB	0.03
		α-Pinene	0.03
		Limonene	0.02

2.2.4 Uncertainty of the concentration

The concentrations of the compounds are associated with an uncertainty, which reflects random and systematical errors in the measurement method. The procedure of determination starts by estimating the uncertainty of each component used in the Eqs. II – 1 and II – 2 and then calculating the final uncertainty by propagating the errors. The steps of this procedure are explained in detail in **Sect. II – A2** of the **Annex II**.

The total absolute uncertainty of the concentration of the compound *i* in a sample ($u\,(C_i)$) is calculated by Eq. II – 4, based on the propagation of uncertainties (assuming that the standard uncertainties of each factor are not correlated):

$$u^2(y) = \sum_{i=1}^{n} \left[\frac{\partial f}{\partial x_i}\right]^2 * u^2(x_i) \qquad \text{Eq. II - 4}$$

Where y is a function of x_n parameters that are considered independent like the $y = f(x_1, x_2, \dots, x_i, \dots., x_n)$, and $u^2(x_i)$ is the variance associated with the sample x_i of the compound *i*.

By combining the relative uncertainties presented in **Sect. II – A2** of the **Annex II**, we obtain the equation for the total uncertainty ($u\,(C_i)$) in the concentration of the compound *i* (Eq. II - 5):

$$u\,(C_{ij}) = \sqrt{\left(\frac{u_{int}^2(A_{i\,NPL})}{A_{i\,NPL\,norm}^2} + \frac{u_{repro}^2\,(A_{i\,NPL})}{A_{i\,NPL}^2} + \frac{u_{NPL}^2\,(C_i)}{C_{i\,NPL}^2}\right)} * C_{ij} \qquad \text{Eq. II - 5}$$

Where $u_{int}(A_{i\,NPL})$, $u_{repro}\,(A_{i\,NPL})$ and $u_{NPL}\,(C_i)$ are the absolute uncertainties due to the integration of the peaks in the chromatograms, the reproducibility of the calibrations and the NMHC concentrations in the NPL standards (**Eqs. II – A1, II – A2 and II – A3, Sect. II – A1, Annex II**), $A_{i\,NPL\,norm}$ is the mean peak area (derived from normal integration; refer to explanation of the **Eq. II – A1, Annex II**) of the samples used for the calculation of the $u_{int}(A_{i\,NPL})$, $A_{i\,NPL}$ is the mean of the peak areas of the compound *i* that were used for the calculation of the $u_{repro}\,(A_{i\,NPL})$, $C_{i\,NPL}$the concentration of the compound *i* in the NPL standard and C_i is the concentration of the compound *i* in the sample *j*.

Furthermore, for the concentrations of the compounds between the ½ LoD and the LoD, the relative uncertainty is calculated from Eq. II – 6:

$$u\,(C_{ij}) = \frac{5}{6} * LoD \qquad \text{Eq. II - 6}$$

Finally, in order to have a 95% confidence in the concentrations, the absolute total uncertainty $u\,(C_i)$ is enlarged by a coefficient (k = 2).

In **Table II – 6** the mean values of the concentration and the corresponding enlarged uncertainty (U) for the C2 – C12 NMHC for their common period of 13 months (1/02/2016 – 28/02/2017), summer 2016 and winter 2017 are given. The values are expressed in μg m^{-3} since this unit is

better for the positive matrix factorization (the statistical tool for the source apportionment) input matrix (for the mixing ratio).

It is apparent that for the majority of the compounds the uncertainty of the concentration in winter 2017 is lower than for summer 2016, which is related to the higher levels that were recorded in the cold seasons, as well as the good stability of the instruments. Moreover, it should be mentioned that for compounds with an important number of concentrations close to the LoD (like 1.2.3 TMB, isoprene, limonene etc), the value of U is high, due to the higher uncertainty of these concentrations.

Table II - 6: Mean concentrations and mean enlarged uncertainty (U) of the NMHCs of the MOP for the common period of measurements (01/02/2016 – 28/02/2017), summer 2016 and winter 2017.

NMHC (μg m^{-3})	13-months		Summer 2016		Winter 2017	
	Concentration (mean)	Uncertainty (mean)	Concentration (mean)	Uncertainty (mean)	Concentration (mean)	Uncertainty (mean)
Ethane	4.49	0.35	2.70	0.42	5.21	0.32
Ethylene	3.23	0.24	1.85	0.33	4.11	0.09
Propane	3.62	0.10	1.99	0.13	4.75	0.07
Propene	1.42	0.27	0.52	0.52	2.03	0.12
i - Butane	3.13	0.09	1.56	0.12	3.86	0.08
n - Butane	4.09	0.10	2.41	0.09	5.01	0.11
Acetylene	5.18	0.40			4.87	0.16
Trans-2-butene	0.60	0.38	0.22	0.62	0.72	0.27
1-Butene	0.65	0.39	0.24	0.75	0.82	0.26
i - Pentane	7.66	0.08	6.20	0.07	7.91	0.06
n - Pentane	1.82	0.10	1.45	0.11	1.76	0.10
Isoprene	0.15	1.52	0.36	1.28	0.12	1.49
2-me-pentane	3.80	0.12	2.90	0.11	3.83	0.12
n - Hexane	1.16	0.35	0.81	0.44	1.16	0.29
Benzene	1.74	0.25	0.85	0.28	2.62	0.21
i - Octane	0.41	1.08	0.22	1.21	0.47	1.14
n-Heptane	0.44	0.84	0.26	1.07	0.50	0.79
Toluene	6.98	0.21	4.54	0.20	7.55	0.21
n - Octane	0.47	0.84	0.30	0.97	0.52	0.86
Ethylbenzene	1.33	0.39	0.81	0.44	1.46	0.43
mp-Xylene	8.38	0.30	5.10	0.31	9.20	0.34
o-Xylene	1.38	0.41	0.81	0.47	1.52	0.44
Nonane	0.31	0.70	0.25	0.74	0.31	0.75
a-Pinene	0.72	0.42	0.71	0.29	0.71	0.59
1.3.5-TMB	0.31	1.32	0.15	1.46	0.36	1.34
1.2.4-TMB	1.40	0.69	0.86	0.74	1.64	0.75
1.2.3-TMB	0.26	1.31	0.21	1.33	0.27	1.35
Limonene	0.33	1.34	0.15	1.29	0.48	1.35

2.3 Off – line VOC measurements

Additional VOCs were measured during the IOP with off - line measurement methods, i.e. an in-situ sampling method followed by an analysis of the samples later on in the laboratory (**Sects. 1.1** and **1.2** of **this Chapter**). For our case, an auto-sampler and sampling tubes of charcoal cartridges were used, collecting more than **200 air samples** during the various campaigns in Athens in different locations. Cartridges are sampling tubes which are coated or filled with selected absorbents for VOC sampling and entrapment. Because of the different physico – chemical properties of targeted VOC, the **charcoal ones** were used for the C6 – C11 oxygenated VOC, substituted aromatic VOC and C10 – C16 alkanes.

For the off – line sampling of the ambient air an auto – sampler ACROSS from TERA Environnement (France) which can be operated by the user's PC through the software ACROSS, was used. In **Figure II – 11** the scheme of the sampler is presented: four independent channels (A, B, C, D) of 6 ports are used for the sampling on the tubes, with the A and B port-groups for the charcoal cartridges. Each of these 6-port groups are connected to individual mass flow controllers (MFC), in order to set a stable sampling volume depending on the cartridge type and the measurement needs. In particular, the MFCs of the A and B groups allow a flow around 200 ml min^{-1}, An ozone scrubber is used to prevent ozonolysis of unsaturated compounds as well as any interference for the targeted carbonyls (Helmig et al., 1997, Detournay et al., 2011; Dettmer and Engewald, 2003; Kleindienst et al., 1998). In our case a MnO_2 scrubber offers the best compromise for the measurement method. A porous filter of 2μm was placed in the inlet for the retention of the particles.

The operation parameters of the sampling method are determined through the program ACROSS from which can be set the number of samples, their name, the sampling flow, the starting date and duration of sampling, as well as the time interval between two samplings. At the end of the sampling of each ramp, the program generates a file with all the above information and the total sampling volume of every cartridge.

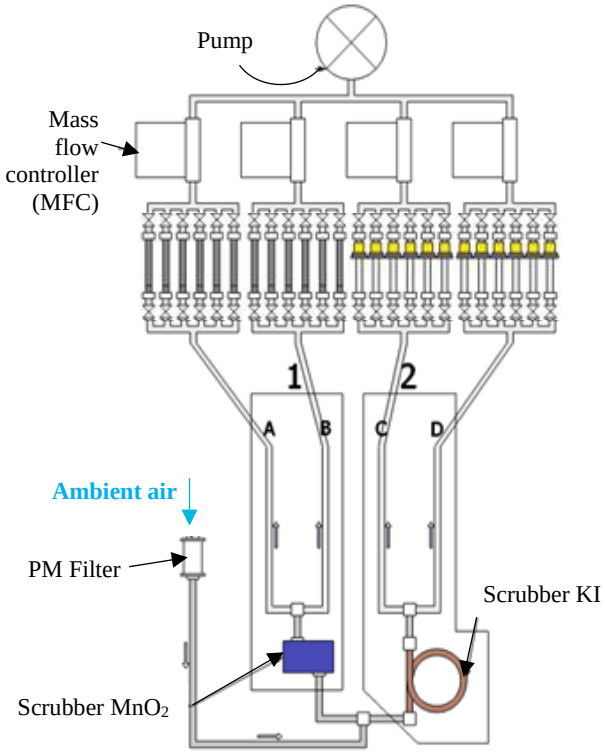

Figure II - 11: The scheme of the auto-sampler ACROSS/TERA.

In the intensive campaigns at Thissio station, the sampler was placed beside to the GCs C2 – C6 and C6 – C12, with its sampling line at the same height than the GCs lines.

In addition, air samples were collected with canisters and analyzed afterwards at the Thissio station by the two GC – FID by configuring them for off-line operation. All the above methods are described in detail in the following paragraphs.

2.3.1 Sampling and analysis of VOC in Charcoal cartridges

The charcoal cartridges were chosen based on the **methodology** developed by **Detournay et al**. (2011) for the off – line sampling of VOC**,** justifying that the best absorbent for the target compounds is a **combination** of **Carbotrap** and **Carbopack** (also mentioned in **Sect. 2.1** of **this chapter**). These two absorbents are black graphitized carbon and they are commercialized by SIGMA ALDRICH.

The sampling time on the cartridges had a duration of 180 min (3 h). The long duration of sampling is required due to the low ambient concentrations that the targeted compounds are expected to have, thus they need to be adsorbed in ahigh enough amount (Detournay et al., 2011). The flow rate for charcoal cartridges was set to 200 mL m^{-1} resulting in a sample volume of ~35 L. At the beginning of the campaigns and at random times during them, the sampling lines were purged by ambient air for 5 - 10 minutes. In addition, blank samples were taken, in order to check any contamination during the sampling, the storage and the transportation of the cartridges. After the sampling, the cartridges were stored in a cool place and were analyzed within three months.

The same parameters were applied as well to the intensive campaign of Patission station (February 2017) and for the 4 tunnel samples (May 2016), with the exception of the sampling time. More specifically, because in Patission traffic campaign were expected higher levels of concentration depending on the time of the day, the sampling duration was 60 minutes for the traffic rush hours (06:00 – 10:00 LT), 120 minutes for the noon to afternoon hours (11:00 – 18:00 LT) and 180 minutes for the night hours (19:00 – 05:00 LT). For the tunnel samples, the sampling duration was 30 minutes (12:00 – 12:30 LT and 12:30 – 13:00 LT).

2.3.1 – 1 Laboratory analysis of charcoal cartridges

The cartridges were transported and analyzed in the Laboratory of Volatile Organic Compounds in IMT Lille Douai (Douai, France). For their analysis a GC – FID (Clarus 680, Perkin – Elmer, USA) coupled with a thermo-desorption system or ATD (TurboMatrix 650 "Automatic Thermal Desorption", Perkin – Elmer, USA), was used. The analytical procedure is composed of 4 steps: the transfer of VOCs from the cartridge to the thermo-desorption system, the chromatographic analysis and the identification of the compounds by the GC – FID and finally, the qualitative and quantitative analysis.

Transfer of VOCs from the cartridges to the ATD system

For this first step, the system is purged for 1 min for the removal of interfering substances like water and CO_2. Afterwards, the cartridge is heated at 350 °C for 15 min and with an inverse, to the sampling, flow of Helium (carrier gas). VOCs are desorbed and transferred to the pre-concentration trap (heated in lower temperature than the thermo-desorption) with duration of 15 min for the effective entrapment of the VOC. In addition, the used absorbent for the trap for this project is Carbopack B (**Sect. 2.1** of **this chapter**). The initial temperature of the trap is set at 10°C, however, for the rapid desorption of the compounds towards the column, the temperature is rising with a rate of 40°C s^{-1} until it reaches 350°C. Then, the VOC are transferred to the column by a He flow rate of 50 ml min^{-1} through a heated line of 210°C temperature, while a split ratio of 1/5 is applied at the exit of the trap.

Chromatographic separation and identification

The principles of the VOC chromatographic analysis and identification from a GC – FID system were described in the previous section (**Sect. 2.1** of **this chapter**). Nevertheless, the chromatographic column and the temperature program of the oven are different in this GC – FID compared to the ones used at Thissio station. More specifically, the capillary column is a CP-Sil-5CB (100% dimethypolysiloxane, 1 μm film thickness). The oven follows a 141 min temperature gradient program that starts with a temperature of 36°C for 13 min. Then, the temperature rises to 135 °C with a rate of 1°C min^{-1} followed by a second rise of 5°C min^{-1} until 250°C, remaining then stable for 5 min. During these 141 min, the VOC are eluted from the column and are transferred to the FID detector. The total cycle of analysis has a duration of 160 min.

Qualitative analysis

For the identification of the compounds in the chromatograms, the retention times of reference samples were used. These could be gas mixture standards (like a NPL gas cylinder) or liquid standards of specific VOC that are not included in the gas standards. The latter are prepared based on gravimetric analysis: the liquid solution of known concentration for a specific VOC is diluted in methanol, and then it is vaporized and transferred rapidly in a charcoal cartridge. For that procedure, the vaporization of the solution needs a temperature of 200°C and it is transferred through a heated line of deactivated silica (at 200°C) with a Helium flow (carrier gas) of less than 15 ml min^{-1} (fixed injection pressure of 6 bar). Finally, the cartridge is analyzed under the same conditions as any sample. An example of the identification of the peaks of an ambient air chromatogram during the winter campaign of 2016 in Thissio is presented in **Figure II – 12**. Most of the samples from the "Athens VOC campaigns" have been analyzed by the engineers of the Department of Atmospheric Science and Environmental Engineering of IMT Lille Douai (Douai, France).

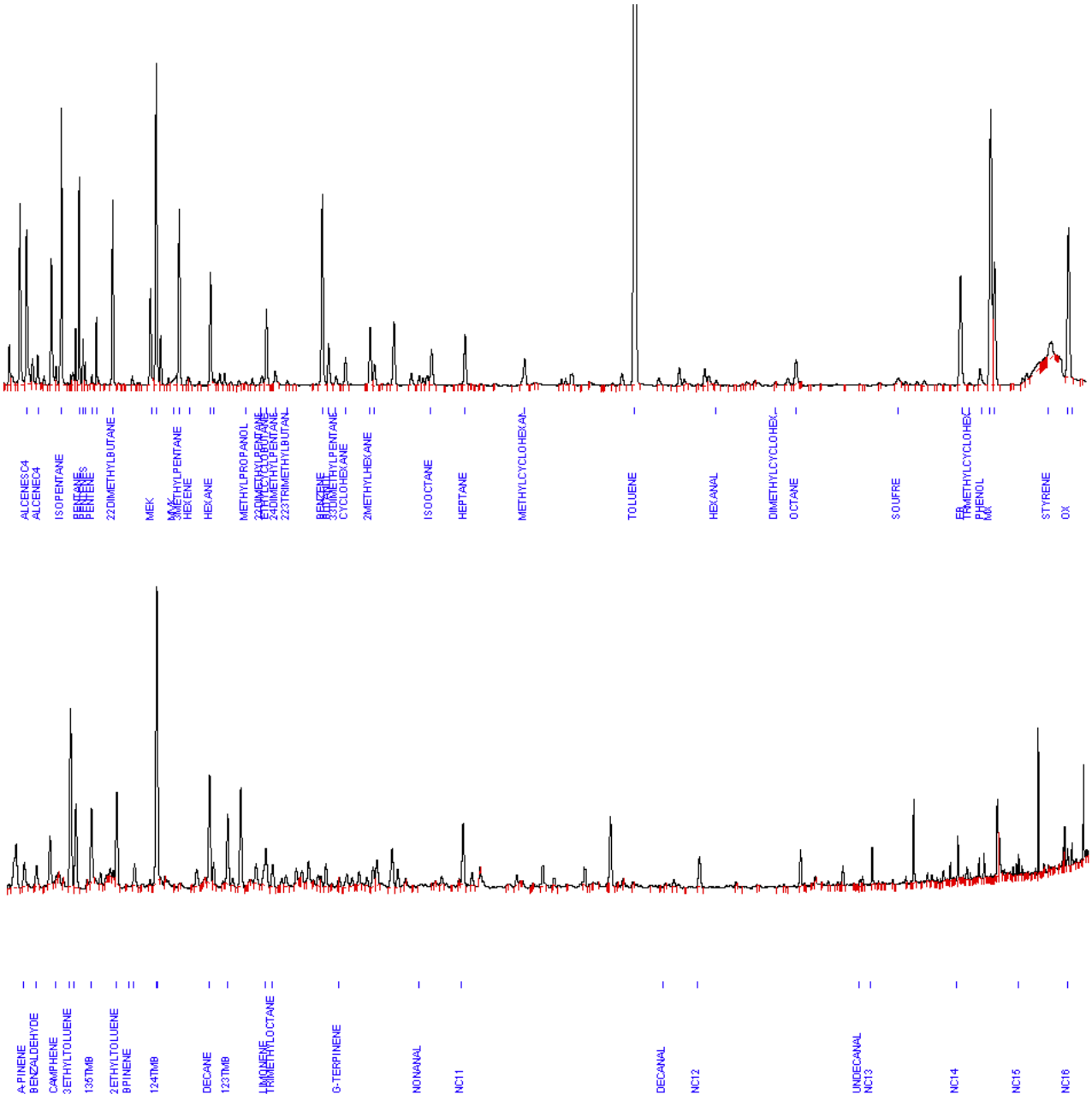

Figure II - 12: Chromatogram of an ambient air sample (in two parts due to size restrictions) from the winter campaign of 2016 in Thissio.

Quantitative analysis

The concentrations of the VOC in the cartridges are calculated by Eq. II – 7 in μg m^{-3}:

$$[VOC]_i = \frac{A_{i\,amb\,air} - A_{i\,blanc}}{k_i * V_{sample}} \qquad \text{Eq. II - 7}$$

Where $[VOC]_i$ is the concentration of the compound i (in μg m^{-3}), $A_{i\,amb\,air}$ and $A_{i\,blanc}$ (in UA) are the peak areas of the compound i in the specific cartridge sample and the blank samples respectively, k_i is the response coefficient of the compound i (UA ng^{-1}) and V_{sample} (in L) is the total volume of air collected through the cartridge.

For the comparison of these results with the ones measured by the GCs, the concentrations of the VOC of the cartridges $[VOC]_i$ were also converted in ppb, with the use of their molar mass (Eq. II – 8):

$$[VOC]_i\ (ppb) = [VOC]_i \frac{24}{M} \qquad \text{Eq. II - 8}$$

Where $[VOC]_i$ is concentration of the compound i in μg m^{-3} and M_i is the molar mass of the compound i (in g.mol^{-1}).

During the analysis of the samples of the intensive campaigns a limited number of standards were acquired for the verification of the analytical performance of the analyzer. Thus, the response coefficients k used in the Eq. II – 8 are calculated from past calibrations of the instrument. Nevertheless, response coefficients were also calculated for the current standards, which are then compared to the used (previous) response coefficients. The comparison indicated a difference less than ±20% for all the campaigns, except of α-pinene that is -36%. As an example, in **Figure II – 13** the comparison of the coefficients of the common compounds for the summer IOP 2016 is presented.

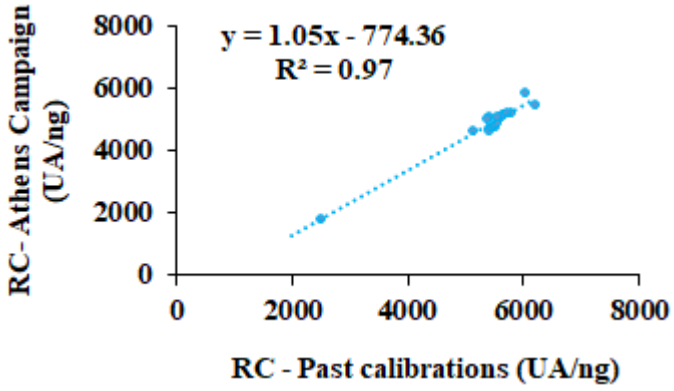

Figure II - 13: Regression between the response coefficients (RC) from the standards of the summer IOP 2016 and from past calibrations.

2.3.2 Off-line sampling in canisters

The canisters used in our campaign for the VOC off-line sampling were Entech's Silonite (Silonite™ VS Summa) of 6L. They have an internal Silonite™ coating that provides a high-quality, long-term sample storage solution. These canisters are certified to meet the technical specifications required for EPA methods TO-14a and TO-15.

Before sampling, the canisters were cleaned by repeated cycles of zero-air filling and evacuation of at least three times. In the last cycle, the canister was filled with zero air to be then analyzed by the GC-FID system to verify the efficiency of the cleaning procedure. They were finally evacuated a few days prior to the sampling at the site, resulting in under-pressurized canisters.

For the sampling of ambient air, the valve of the canister was opened slightly to achieve low air flow sampling during 3 to 4 minutes. For the Patission intensive campaign, another sampling method was used, which involved the installation of a portable mass flow meter at the sampling port of the canister, permitting the set-up of a certain flow rate and fixed sampling duration from 3 to 10 minutes (Sauvage et al., 2009).

At the end of every sampling campaign, the canisters were transported back to Thissio station for their analysis with the GCs within 20 days, as described in **Sect 2.1 (this chapter)**. Before the analysis, canisters were pressurized by adding a known amount of zero-air resulting in a sample dilution by a factor of two.

2.4 Inter-comparison of sampling methods

The parallel sampling of VOC with different methods in every campaign (seasonal and Patission) facilitated the inter-comparison of the levels of the common species for the verification of the robustness of the results. The results are presented for each campaign in the following paragraphs.

2.4.1 Inter–comparison of the results of the winter IOP 2016

During the winter IOP of 2016, on-line and off-line measurements with the GC – FIDs and charcoal cartridges were conducted in parallel respectively. For this comparison, the common species of the two techniques are used. From **Sect 2.1 (this chapter)** it is known that the on-line measurements of the GC – FIDs were performed every 30 minutes and for the off-line measurements (cartridges) every 3h. Due to the difference in sampling time, each cartridge sample corresponds to 6 GC integrated samples. The inter-comparison showed an excellent linear relationship for the majority of the common compounds and with a slope between 0.8 and 1.2, as it is depicted in **Figure II – 14** for benzene and toluene (**Figure II – A1** of the **Annex II** for the rest). These compounds are used as reference, since they are indicators of the stability and optimal performances of the instruments. An exception is 2-me-pentane, for which the slope is 1.45, indicating higher recorded concentrations from the GC – FID, which are justified by the co-elution of this compound with another not-identified one.

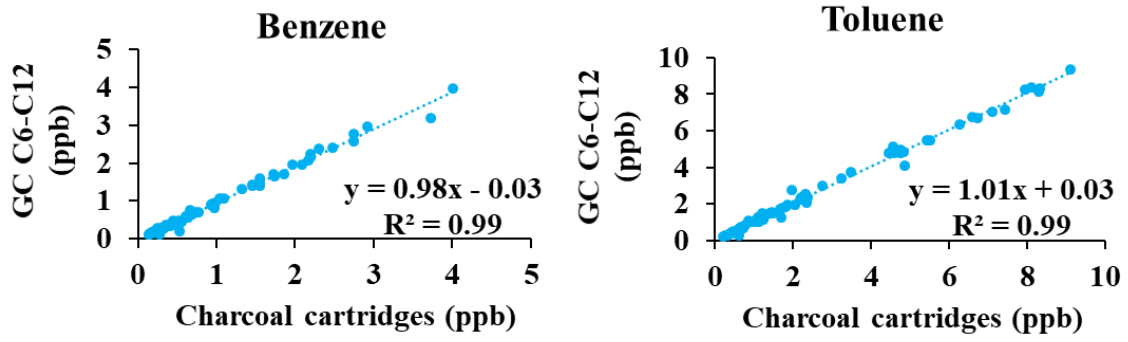

Figure II - 14: Relationship between benzene and toluene from the GC – FID C6 - C12 and the off-line method using charcoal cartridges, for the period of the winter IOP 2016 (28/01 – 10/02/2016).

2.4.2 Inter–comparison of the results of the summer IOP 2016

In **Figure II – 15** the correlation of benzene and toluene from the GC – FID on-line measurements and the charcoal cartridges is depicted (**Figure II – A2** of the **Annex II** for the rest). Although in this case the relative difference of the levels is ~±20%, the majority of the compounds demonstrate slopes between 0.97 (toluene) and 1.49 (1.2.3 TMB) with $R^2 > 0.90$, despite the lower concentrations observed in summer compared to the ones in winter 2016. However, it is important to note that for some compounds like n-Octane, the levels measured by the GC C6 – C12 analyzer are two times higher than the concentrations from charcoal cartridges. Due to the discrepancies, possibly attributed to integration procedure or the storage handling, the cartridges results were excluded, keeping only the online GC results.

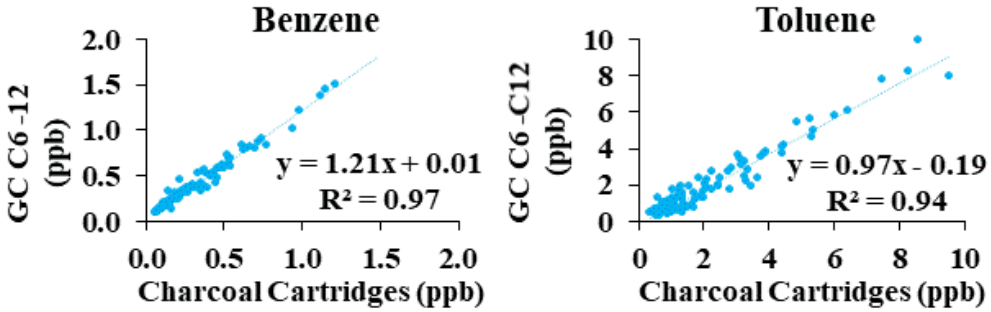

Figure II - 15: Relationship of benzene and toluene from the GC – FID C6 - C12 and the charcoal cartridges, for the period of the summer IOP 2016 (2/09 – 23/09/2016).

2.4.3 Inter–comparison of the results of the Traffic Near Source Campaign 2017

The Patission intensive campaign took place in a traffic monitoring station on the homonym street (**Sect. 1.2** of **this chapter**), with the use of off-line sampling methods for VOC, i.e. canisters, charcoal and DNPH cartridges. The sampling time of canisters was 10 min and for the cartridges 1h. In addition, the canisters were analyzed within 2 days after the sampling from the GC – FIDs in Thissio station, whereas the cartridges were analyzed within 2 months in Douai (France) (**Sect. 2.3** of **this chapter**). The time-window between sampling and analysis was set from stability experiments for other campaigns with similar characteristics and instrumentation, since such experiments were not conducted during this campaign. Thus, it is important to compare the common species in order to verify that the differences in sampling methods, storage, transportation and handling are not impacting the results.

The similarities of the two techniques with regard to the levels of benzene and toluene are presented in **Figure II - 16**, whereas the rest of the compounds in common are illustrated in **Figure II – A3 (Annex II)**. The comparison indicated that despite the different sampling time and handling of the two types of samples, the results are almost similar for the majority of the compounds with slopes between 0.96 and 1.39 ($R^2 > 0.80$), indicating thus the suitability of the methods and the stability of the compounds during storage. In this case, n-octane is also an exception presenting a slope of 1.82.

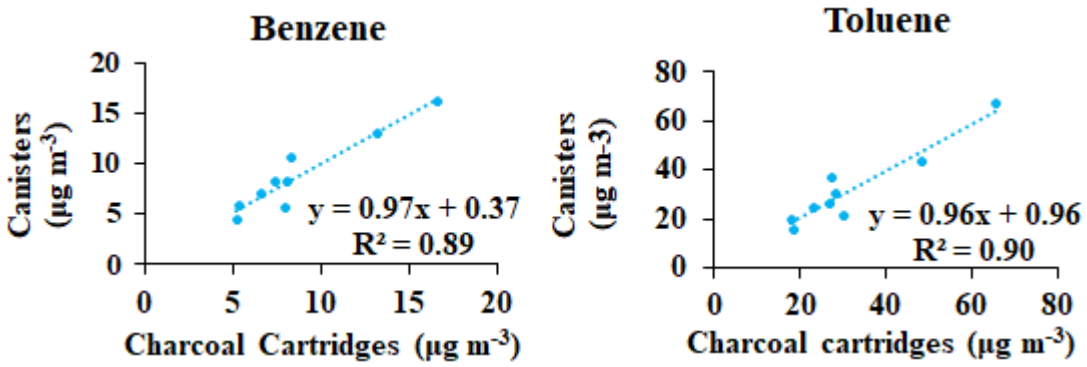

Figure II - 16: Relationship of benzene and toluene from canisters and charcoal cartridges, for the period of the near-source campaign in Patission station in 2017 (22/02 – 24/02/2017).

2.5 Robustness of monoterpene results

A-pinene and limonene, known for their biogenic origin, are having high reactivity making their monitoring quite challenging due to fast chemistry. The first step to assure the validity of the measurements is the verification of their retention time, followed by the inter-comparison of the concentrations derived from on-line and off-line sampling methods. The mean retention time of α-pinene and limonene in the calibration samples (STD), in the ambient air levels and a "Retention time" experiment that was conducted at the Laboratory of Volatile Organic Compounds in IMT Lille Douai (Douai, France) are compared in **Figure II – 17**, along with toluene as a reference for the stability and performance index of the method. The respective results for 1.2.4 TMB are additionally depicted due to vicinity of its retention time relative to the terpenes. The comparison showed that in all cases the retention time of the compounds is similar, with a relative standard difference less than 1%, except of limonene that is 17%. The latter might be explained by the elution of the compound, which occurs at the end of the temperature gradient program (**Fig. II – 5, Sect. 2.1** of **this chapter**), resulting in a small instability of the chromatographic separation.

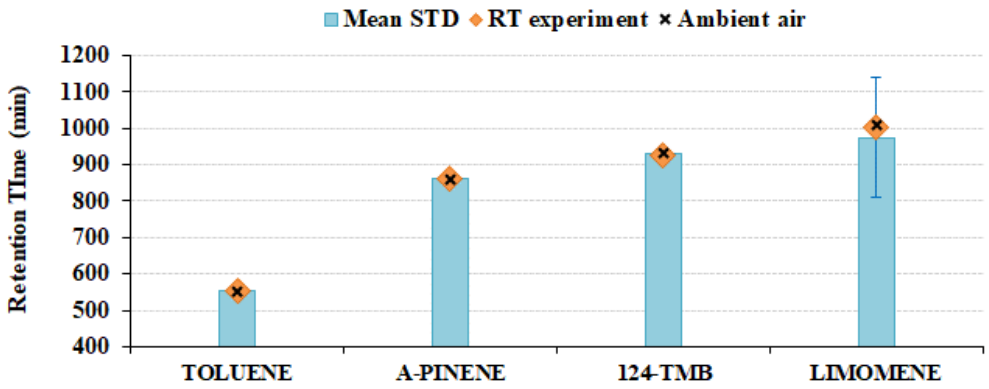

Figure II - 17: Mean retention time of toluene, α-pinene, limonene, and 1.2.4-TMB in the calibration samples, ambient air samples and the "Retention time" experiment. The error bars (apparent only for limonene) correspond to the standard deviation of the retention time in the calibration samples.

Furthermore, the inter-comparison of the levels of α-pinene and limonene from the on-line sampling with the GC – FID C6 – C12 and the off-line sampling with charcoal cartridges in winter IOP is presented in **Figure II – 18**. Limonene's off-line and on-line data are well correlated with a slope of 0.88 and a correlation coefficient of 0.94 highlighting their similar variability and the robustness of the results. For α-pinene, the scatterplot is broader presenting a slope of 0.77 with a correlation coefficient of 0.64. These values indicate that the on-line measurements often result to higher concentrations and not always in agreement. It is already known that the trapping and analysis of terpenes is not easy due to their isomerization during storage, analysis and other processes related to heat. This affects mainly α-pinene over limonene (Larsen et al., 1997; McGraw et al., 1999, and references therein). In addition, the peak of α-pinene is very close to the one of benzaldehyde in the off-line chromatograms, which might affect the integration of α-pinene. These two parameters might be the factors for the observed behavior of α-pinene. Nevertheless, these results are satisfactory.

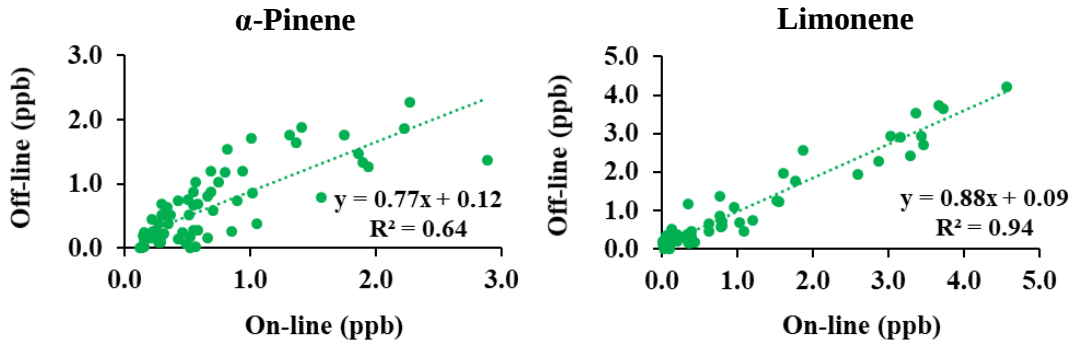

Figure II - 18: Relationship of α-pinene and limonene from the off-line measurements on cartridges and on-line measurements by the GC -FID for the winter IOP (1/02/2016 – 10/02/2016).

The inter-comparison for the summer IOP did not present similar results. In **Sect. 2.4.2** we saw slightly elevated levels of the on-line measured concentrations compared to the off-line which might be associated to bad storage of the cartridges, as well as integration issues due to the low detected levels. This issue affected mainly α-pinene, whereas for limonene we obtained a very good correlation coefficient (R^2: 0.93) but a slope lower than one (graphs not shown).

2.6 Ancillary measurements

Apart from the VOC measurements, a variety of high-resolution equipment was also operated in Thissio Station, providing additional information for the synergistic investigation of the compounds of interest. The equipment covering gaseous and particulates species, as well as other parameters, is as follows:

1. A CO and a NOx (NOx = NO and NO_2) Automatic Analyzers (Horiba Ltd., 360 series) of one-minute resolution.
2. An ozone analyzer (Thermo 49i) of one-minute resolution.
3. A seven wavelength Dual Spot Aethalometer (Magee Scientific AE33) that separates the fossil fuel and wood burning BC components (BC_{ff} and BC_{wb} respectively).

4. The NOA Meteorological Station that provides hourly averaged data for atmospheric temperature, relative humidity, wind speed and direction.

2.7 Conclusions

Following the determination of the objectives of the project in Chapter 1, this chapter described the strategy and the organization of the 17-months "Athens VOC campaign", which is comprised by one main campaign with time-resolved measurements of C2 – C12 NMHCs (MOP) and intensive campaigns in winter and summer (IOP). The latter was implemented by the application of additional off-line techniques for the determination of a variety of VOC, including oxygenated and intermediate volatile organic compounds. Furthermore, near-source campaigns were conducted, by collecting samples close to targeted emission sources to obtain their chemical fingerprint.

During the MOP, C2 – C6 NMHC were monitored from October 2016 to February 2017 and C6 – C12 NMHCs from February 2016 to February 2017 by means of two autonomous, on-line GC – FIDs. This allowed a great time coverage of measurements (~81% and ~93% for the C2 – C6 and C6 – C12 analyzers) with high-resolution (30-min quasi-continuous sampling), which in turn will permit the investigation of the temporal and spatial variability of the compounds of interest and their allocation to sources. Furthermore, it is worthwhile noting that a VOC dataset of that extended size and resolution (more than 19500 and 17500 30-min samples for C2 – C6 and C6 – C12 NMHCs respectively) was never reported previously for the Athens environment showing its importance. On the other hand, the data treatment was quite challenging. For example, the C2 – C6 analyzer suffered from stability issues related to humidity for many months, which were reflected on the dataset. The resolution of this issue required also the establishment of a robust approach for the calculation of the concentrations of these compounds for this period (**Sect. 2.2.1**). Nevertheless, as it was shown in the chapter, the previous efforts resulted in a robust dataset which will be examined in the following chapters.

For the winter and summer IOPs of 2016, the deployment of off-line sampling methods (cartridges) allowed the identification and quantification of additional VOC species, with a very low detection limit (0.01 $\mu g\ m^{-3}$). These two seasonal datasets provide further information for the in-depth investigation of the seasonal profiles of VOC and their incorporation to the MOP dataset might contribute to the better source allocation of the VOC in Athens by increasing the input information for the source apportionment. In the same context, the near-source campaigns in the tunnel and to Patission monitoring station allowed the determination of the chemical profile of the traffic source, which also will be used later for the validation and interpretation of the source apportionment results.

Finally, the implementation of all the above on-line and off-line sampling methods enabled the verification of the robustness of the results of the campaigns by the inter-comparison of the datasets. The common species of the MOP and the winter IOP are in a very good agreement. Similar is also the NMHCs comparison from the near-source campaign in Patission station. On the contrary, the MOP and the summer IOP showed slopes between 1.20 and 1.60 for the

majority of the compounds, indicating higher concentrations of the NMHCs from the MOP (on-line sampling method). This might be attributed to the storage conditions of the cartridges and/or integration issues due to the low levels in this season. Last but not least, a special focus was given to the validation of the concentrations of α-pinene and limonene, which required additional experiments and inter-comparison between data. Thus, having acquired all the above VOC and ancillary datasets from Thissio Station, the analysis and the discussion on the outcomes follows in the next chapters.

CHAPTER 3 – Non-methane hydrocarbon variability in Athens during wintertime: the role of traffic and heating

TABLE OF CONTENTS FOR CHAPTER 3

1.Introduction

In **Section 2.4** of **Chapter 1** it was demonstrated that the air quality in Athens has changed during the last decade. Despite the decrease of the atmospheric levels of pollutants like CO, NO and NO_2 that was attributed to the reduction of emissions, nowadays, the contribution of individual emission sources has been modified by enhancing some types of pollution events induced by socioeconomic factors. Such an example is the winter night-time smog events which are associated with domestic heating practices forced by the financial recession in the country. The occurrence and persistence of these events are of concern for the air quality in Athens. Diapouli et al., 2017a, 2017b; Fourtziou et al., 2017; Gratsea et al., 2017; Paraskevopoulou et al., 2014, 2015; Stavroulas et al., 2019; Theodosi et al., 2018 (and references therein) have already investigated the role of residential wood burning emissions to the production and variability of pollutants in the Attica basin. Regarding the VOCs, the only recently published work by Kaltsonoudis et al. (2016), reports an enhancement of the night-time concentrations during smog events attributed to domestic heating.

Therefore, the need for the monitoring of VOCs is reinforced by two facts: (1) nowadays there is only one study in Athens that reports the winter levels of aromatic and oxygenated VOC (Kaltsonoudis et al., 2016), whereas no information about the light NMHCs is available for the area and (2) at the time of this work, the information for the chemical characterization of the VOC profile from wood burning emissions remains limited worldwide and challenging (i. e. Baudic et al., 2016; Gaeggeler et al., 2008; Gustafson et al., 2007; Hellén et al., 2008; Liu et al., 2008; Rouvière et al., 2006).

A first dataset of C2 – C6 compounds has been obtained during the first winter-time of the Athens MOP. The dataset includes light alkanes, alkenes, acetylene and benzene that are classified among the wood burning tracers (e. g in Barrefors and Petersson, 1995; Baudic et al., 2016; Schauer et al., 2001) and isoprene as well. Thus, a first study of VOC levels and variability in winter allowed to highlight the influence of domestic heating emissions. The originality of the results combines two facts. At first, they are the first reported levels of C2 – C6 NMHC since the last VOC research study in Athens 20 years ago and then, they constitute the first ever recorder winter levels for these compounds. These results lead to a peer-review article with the following objectives: (a) the examination of the temporal variability of the studied VOC; (b) the determination of the effect of atmospheric dynamics; (c) the assessment of the influence of the main VOC sources in Athens; and (d) the evaluation of the current air quality in Athens concerning VOC levels, especially for light compounds that were almost never reported **(Chapter 1, Sect. 2.4.3).** The aforementioned article was published in November 2018 in the ChArMEx special issue of the "Atmospheric Chemistry and Physics" journal (Panopoulou et al., ACP-18-16139-2018) and is presented below.

2.Non-methane hydrocarbon variability in Athens during wintertime: the role of traffic and heating

Atmos. Chem. Phys., 18, 16139–16154, 2018
https://doi.org/10.5194/acp-18-16139-2018

Atmospheric Chemistry and Physics
Open Access
EGU

Non-methane hydrocarbon variability in Athens during wintertime: the role of traffic and heating

Anastasia Panopoulou[1,2,4], Eleni Liakakou[2], Valérie Gros[3], Stéphane Sauvage[4], Nadine Locoge[4], Bernard Bonsang[3], Basil E. Psiloglou[2], Evangelos Gerasopoulos[2], and Nikolaos Mihalopoulos[1,2]

[1]Environmental Chemical Processes Laboratory (ECPL), Department of Chemistry, University of Crete, 71003 Heraklion, Crete, Greece
[2]National Observatory of Athens, Institute for Environmental Research and Sustainable Development, 15236 P. Penteli, Athens, Greece
[3]LSCE, Laboratoire des Sciences du Climat et de l'Environnement, Unité mixte CNRS-CEA-UVSQ, CEA/Orme des Merisiers, 91191 Gif-sur-Yvette Cedex, France
[4]IMT Lille Douai, Univ. Lille, SAGE – Département Sciences de l'Atmosphère et Génie de l'Environnement, 59000 Lille, France

Correspondence: Eleni Liakakou (liakakou@noa.gr)

Received: 8 October 2017 – Discussion started: 22 November 2017
Revised: 28 August 2018 – Accepted: 1 October 2018 – Published: 9 November 2018

Abstract. Non-methane hydrocarbons (NMHCs) play an important role in atmospheric chemistry, contributing to ozone and secondary organic aerosol formation. They can also serve as tracers for various emission sources such as traffic, solvents, heating and vegetation. The current work presents, for the first time to our knowledge, time-resolved data of NMHCs, from two to six carbon atoms, for a period of 5 months (mid-October 2015 to mid-February 2016) in the "greater Athens area" (GAA), Greece. The measured NMHC levels are among the highest reported in the literature for the Mediterranean area during winter months, and the majority of the compounds demonstrate a remarkable day-to-day variability. Their levels increase by up to factor of 4 from autumn (October–November) to winter (December–February). Microscale meteorological conditions, especially wind speed in combination with the planetary boundary layer (PBL) height, seem to contribute significantly to the variability of NMHC levels, with an increase of up to a factor of 10 under low wind speed ($< 3\,m\,s^{-1}$) conditions; this reflects the impact of local sources rather than long-range transport. All NMHCs demonstrated a pronounced bimodal, diurnal pattern with a morning peak followed by a second peak before midnight. The amplitude of both peaks gradually increased towards winter, in comparison to autumn, by a factor of 3 to 6 and closely followed that of carbon monoxide (CO), which indicates a contribution from sources other than traffic, e.g., domestic heating (fuel or wood burning). By comparing the NMHC diurnal variability with that of black carbon (BC), its fractions associated with wood burning (BC_{wb}) and fossil fuel combustion (BC_{ff}), and with source profiles we conclude that the morning peak is attributed to traffic while the night peak is mainly attributed to heating. With respect to the night peak, the selected tracers and source profiles clearly indicate a contribution from both traffic and domestic heating (fossil fuel and wood burning). NMHCs slopes versus BC_{wb} are similar when compared with those versus BC_{ff} (slight difference for ethylene), which indicates that NMHCs are most likely equally produced by wood and oil fossil fuel burning.

1 Introduction

Non-methane hydrocarbons (NMHCs) are key atmospheric constituents for atmospheric chemistry. In the presence of NO_x, their oxidation leads to the formation of tropospheric ozone and other species, such as peroxy radicals (RO_2) and peroxy acetyl nitrate (PAN), which affect the oxidative capacity of the atmosphere (Atkinson, 2000 and references therein). NMHC oxidation contributes to the formation of secondary organic aerosols (SOA), which in turn affect light

Published by Copernicus Publications on behalf of the European Geosciences Union.

scattering, visibility and cloud condensation nuclei formation (Tsigaridis and Kanakidou, 2003; Seinfeld and Pandis, 2016 and references therein). In urban areas NMHCs mainly originate from anthropogenic sources such as traffic, solvent use, residential heating, natural gas use and industrial activity, but they can also be emitted from natural sources such as vegetation (Guenther et al., 1995; Barletta et al., 2005; Kansal, 2009; Sauvage et al., 2009; Salameh et al., 2015; Baudic et al., 2016; Jaimes-Palomera et al., 2016). Besides their key role as a precursor for secondary pollutants, NMHCs are of interest due to their association with human health issues (EEA report no. 28/2016, 2016). Since 2013, atmospheric substances have been classified into four major groups by the International Agency for Research on Cancer (WHO-IARC, 2013) with respect to their carcinogenicity to humans, with benzene and 1,3-butadiene among those NMHCs classified as potential carcinogens (IARC, 2012).

Athens, the capital of Greece with almost 5 million inhabitants, is frequently subject to intense air pollution episodes, which lead to exceedances of the EU air quality limits. The driving processes and atmospheric dynamics of these episodes have been scrutinized over the last few decades (Cvitas et al., 1985; Lalas et al., 1982, 1983, 1987; Mantis et al., 1992; Nester, 1995; Melas et al., 1998; Ziomas et al., 1995; Kanakidou et al., 2011). However, measurements of pollution precursors are mostly limited to ozone and nitrogen oxides. The few existing, non-continuous NMHC measurements in Athens were carried out using canisters or sorbent tubes and were only performed over short periods of time (days) during summer or autumn (Moschonas and Glavas, 1996; Klemm et al., 1998; Moschonas et al., 2001; Giakoumi et al., 2009). Continuous measurements of NMHCs in Athens were carried out for a period of 1 month during summer 20 years ago at three locations, two suburban and one urban, and reported almost 50 C4–C12 compounds (Rappenglück et al., 1998, 1999). More recently continuous measurements of NMHCs were carried out by Kaltsonoudis et al. (2016), for 1 month in winter 2013 at an urban location (Thissio) and 1 month in summer 2012 at a suburban location (A. Paraskevi), and reported 11 oxygenated organic gaseous compounds and C5–C8 NMHCs. Meanwhile, significant changes in pollutant sources have occurred in Athens over the last 20 years, which have led to significant decreases in the annual concentrations of major pollutants such as CO, SO_2 and NO_x (Gratsea et al., 2017; Kalabokas et al., 1999). As this trend has been attributed to the car fleet renewal, fuel improvement, the metro line extension and industrial emission controls, a related decrease in NMHC levels originating from traffic and industrial emissions is also expected. However, since 2012, a new wintertime source of pollution has emerged in Greece in the form of uncontrolled wood burning for domestic heating (Saffari et al., 2013; Paraskevopoulou et al., 2015; Kaltsonoudis et al., 2016; Fourtziou et al., 2017; Gratsea et al., 2017). This is an important source of various pollutants such as particulate matter (PM), polycyclic aromatic hydrocarbons (PAHs), black carbon (BC) and CO (Gratsea et al., 2017; Hellén et al., 2008; Paraskevopoulou et al., 2015; Schauer et al., 2001, and references therein), and it can represent up to 50 % of the mass of volatile organic compounds (VOCs) during winter as found in Paris by Baudic et al. (2016). Studies regarding the characterization of VOC emissions from domestic wood burning based on emissions close to sources, in ambient air or in chambers have been published; however, differences have been observed in the emission rates or the emission profiles, which are attributed to the type of wood, stove, fire lighting material and the burning stages (Barrefors and Petersson, 1995; Baudic et al., 2016; Evtyugina et al., 2014; Gaeggeler et al., 2008; Gustafson et al., 2007; Hellén et al., 2008; Liu et al., 2008; Schauer et al., 2001 and references therein). Moreover, very few studies report light NMHC measurements from domestic wood burning (Barrefors and Petersson, 1995; Baudic et al., 2016; Liu et al., 2008; Schauer et al., 2001), and the studies that do exist present significant discrepancies. For example, the higher contribution of benzene relative to acetylene in the residential wood burning profile reported by Baudic et al. (2016) was different to the profile presented by Liu et al. (2008). In addition, in their recent work, Kaltsonoudis et al. (2016) reported the important contribution of wood burning to the winter nighttime concentrations of aromatics and oxygenated VOCs. The above clearly demonstrates the increasing need for intensive measurements of NMHCs in Athens, which in turn will allow for the impact of future changes (fuel composition changes or other control strategies) on atmospheric composition to be assessed. In other words, there is the need to establish a "current baseline" for the atmospheric composition in Athens in terms of NMHC levels.

The current study presents, time-resolved data of 11 selected (from 15 determined) C2–C6 NMHCs, over a time span of several months (October 2015 to mid-February 2016) in the greater Athens area (GAA). In addition, time-resolved data of toluene, ethylbenzene, *m*-/*p*-xylenes and *o*-xylene are used, which were simultaneously monitored from mid-January to mid-February 2016. The emphasis of this work is on (1) the determination of the ambient levels of C2–C6 NMHCs during autumn and winter, 20 years after the first summertime measurements were carried out – these are the first ever known continuous measurements of NMHCs (especially C2–C3 NMHCs) in Athens; (2) the study of the NMHC temporal characteristics and the determination of the factors controlling their variability; and (3) the investigation of the impact of traffic and residential heating on NMHC levels which are among the most important sources of air pollution in Athens, especially during the "economic crisis" period that was characterized by an important decline of industrial activity (Vrekoussis et al., 2013).

2 Experimental

2.1 Sampling site

Measurements were conducted from 16 October 2015 to 15 February 2016, at the urban background station of the National Observatory of Athens (NOA, 37.97° N, 23.72° E, 105 m a.s.l and about 50 m above the mean city level) at Thissio; this site is considered to be a receptor of pollution plumes of different origins (Paraskevopoulou et al., 2015). The station is located in the historical center of Athens, on top of a hill (Lofos Nimfon), and is surrounded by a pedestrian zone, a residential area and the Filopappou (108 m a.s.l) and Acropolis hills (150 m a.s.l), which are located 500 and 800 m away, respectively (Fig. 1). More information about the morphology, meteorology and dominant transport patterns in Athens can be found in Kanakidou et al. (2011), Melas et al. (1998) and references therein.

2.2 Online NMHC measurements

Two portable gas chromatographs equipped with respective flame ionization detectors (GC-FID; Chromatotec, Saint Antoine, France) were used for NMHC measurements in Athens. Specifically, airmoVOC C2–C6 (during the whole period, from October 2015 to February 2016) and airmoVOC C6–C12 Chromatrap GC (from mid-January until mid-February 2016) analyzers were used for the determination of C2–C6 and C6–C12 NMHCs, respectively. These instruments collected ambient air through collocated inlets on the rooftop of the station, 4 m above ground. The C2–C6 NMHC analyzer was set to sample ambient air on a 10 min basis followed by an analysis time of 20 min, while the C6–C12 NMHC analyzer sampled on a 20 min basis with an analysis time of 20 min and a total cycle time of 30 min (sampling and analysis). Therefore, the synchronized monitoring was performed with an overall 30 min time resolution, for both analyzers.

For the airmoVOC C2–C6 analyzer, 189 mL of air was drawn through a 0.315 cm diameter, 6 m-long stainless-steel line with a filter pore size of 4 µm at the sampling inlet, and a flow rate of 18.9 mL min^{-1}. Once sampled, ambient air was passed through a Nafion dryer (activated by gas nitrogen) to reduce the water content. Hydrocarbons were then preconcentrated at −9 °C (Peltier cooling system) on a 2.25 mm internal diameter, 8 cm-long glass trap containing the following adsorbents: Carboxen 1000 (50 mg), Carbopack B (10 mg) and Carbotrap C (10 mg) all from Supelco Analytical, Bellefonte, PA, USA. Next, the trap was heated rapidly to 220 °C for 4 min and the pre-concentrated VOCs were thermally desorbed onto a PLOT column (Restek Corp., Bellefonte, PA, USA, Al_2O_3/Na_2SO_4; 25 m × 0.53 mm, 10 mm film thickness). One minute prior to the analysis, the oven temperature was raised from 36 to 38 °C, followed by a constant heating rate of 15 °C min^{-1} that reached 200 °C by the end of the analysis. Details regarding the equipment technique and performance, as well as the estimation of the uncertainty, are provided by Gros et al. (2011). The detection limit is in the range of 0.02 ppb (propene, *n*-pentane) to 0.05 ppb (propane), while for ethane and ethylene it is 0.1 ppb.

The airmoVOC C6–C12 analyzer collected 900 mL of air through a 0.315 cm diameter, 6 m-long stainless-steel line with a filter pore size of 4 µm at the sampling inlet, and a flow rate of 45 mL min^{-1}. The hydrocarbons were preconcentrated at ambient temperature on a glass trap containing the adsorbent Carbotrap C. The trap was then heated to 380 °C over 2 min to desorb the pre-concentrated VOCs into a separation column (MXT30CE; 30 m × 0.28 mm, 1 mm film thickness). With 1 min delay, the oven temperature was raised from 36 to 50 °C at a rate of 2 °C min^{-1}, followed by a second heating of 10 °C min^{-1} up to 80 °C. Finally, at a constant heating rate of 15 °C min^{-1} the temperature reached 200 °C and remained there until the end of the analysis. In the present work, toluene, ethylbenzene, *m-/p*-xylenes and *o*-xylene (TEX) will be used from the GC C6–C12 data series. The uncertainty of the instrument is less than 20 %, and the detection limit of the BTEX is 0.03 ppb.

Simultaneous calibrations and identification of the compounds were performed by a certified National Physical Laboratory (NPL) standard NMHC mixture (∼ 4 ppb) containing ethane, ethylene, propane, propene, *i*-butane, *n*-butane, acetylene, *i*-pentane, *n*-pentane, isoprene, benzene and 15 additional hydrocarbons.

2.3 Auxiliary measurements

Real-time monitoring of carbon monoxide (CO), black carbon (BC) and nitrogen oxides (NO_x = NO and NO_2) was also conducted during the study period. For CO and NO_x measurements, Horiba 360 series gas analyzers with a 1 min resolution were used and were calibrated with certified standards. A seven-wavelength AE33 Aethalometer (1 min resolution; Magee Scientific) was operated for the measurement of BC, and its fractions associated with fossil fuel and wood burning (BC_{ff} and BC_{wb}, respectively) were derived automatically by the instrument software. Meteorological data were provided by the NOA meteorological station at Thissio.

2.4 Street canyon measurements

To identify the NMHC fingerprint of traffic emissions, NMHC measurements were conducted at a monitoring station belonging to the air quality agency of Athens from the 22 to 24 February 2017. The station is located in a street canyon in downtown Athens which is subject to heavy traffic and frequent traffic jams (Patission street; 37.99° N, 23.73° E). Samples were collected every hour during the morning rush hour from 06:55 to 10:15 LT (LT = UTC+2), in 6 L stainless steel–silonite canisters. The sampling method for ambient air

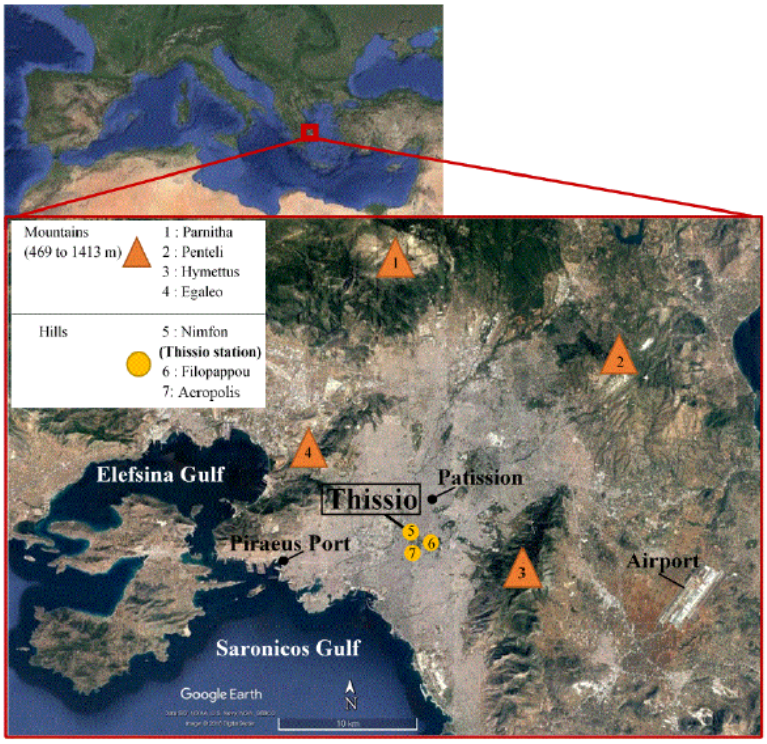

Figure 1. Map of the greater Athens area. The four mountains listed in the legend define the borders of the study area.

is described in detail elsewhere (Sauvage et al., 2009). Before the analysis, the cylinders were pressurized by adding a known amount of zero air which resulted in the sample being diluted by a factor of 2. Afterwards each canister was connected to the GC-FID system using a Teflon polytetrafluoroethylene sampling line and analyzed using the method described in Sect. 2.2. Before sampling, the canisters were cleaned by filling them up with zero air and re-evacuating them, which was done at least three times. The content of the cylinders was then analyzed using the GC-FID system to verify the efficiency of the cleaning procedure. The canisters were evacuated a few days prior to the analysis and were analyzed a maximum of 1 day after sampling.

3 Results and discussion

3.1 Temporal variability of NMHCs

Figure 2 presents the temporal variability of selected NMHCs for five major groups of compounds: ethane and *n*-butane (for saturated hydrocarbons), propene and ethylene (for alkenes), acetylene (for alkynes), benzene and toluene (for aromatics) and isoprene (for potential biogenic compounds). Other measured NMHCs are presented in Fig. S1 in the Supplement. During the study period, the data availability (in comparison with the maximum potential data availability) for all C2–C6 NMHCs was higher than 87 %. Most of the data for isoprene were below the limit of detection due to the low vegetation activity during this period of the year (Fuentes et al., 2000; Guenther et al., 1995). Moreover, the significant nighttime levels (above 300 ppt in some cases) could be indicative of non-vegetation sources, like traffic or domestic wood burning (Borbon et al., 2001, 2003; Gaeggeler et al., 2008; Kaltsonoudis et al., 2016). However, due to the low data coverage it is not possible to determine an accurate diurnal variability for this compound.

The majority of the compounds showed a remarkable day-to-day variability throughout the study period with levels increasing by up to factor of 4, from autumn (October–November) towards winter (December–February; Figs. 2 and S1). The highest values observed for ethane and ethylene mostly ranged between 26 and 23 ppb, and were encountered in wintertime. For these compounds, the lowest values were above 0.3 ppb for the whole period. During the intensive 4-month measurement period, toluene exceeded 10 ppb, while benzene was below 6 ppb. Benzene is the only NMHC included in the European air quality standards due to its possible adverse human health effects (IARC, 2012).

In Table 1, the mean values of the measurements of this study are compared with those reported in the existing liter-

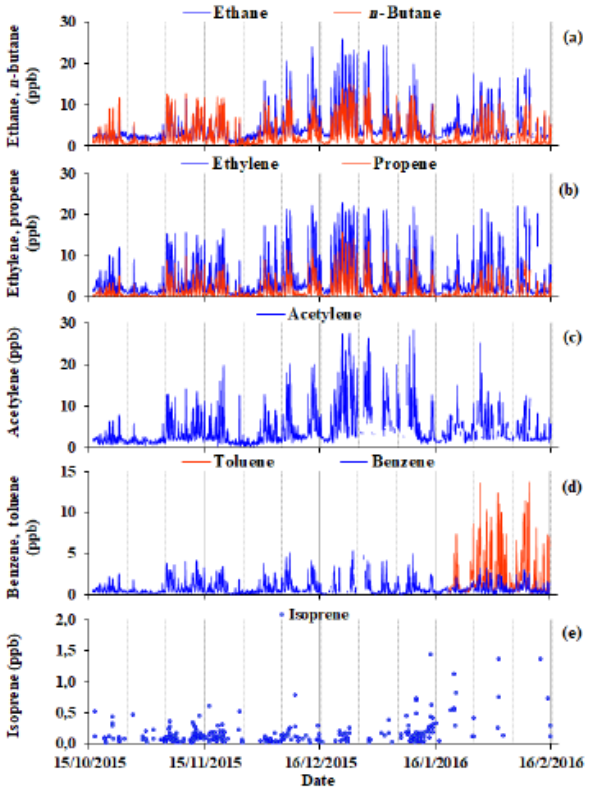

Figure 2. Temporal variability of (**a**) ethane and *n*-butane, (**b**) ethylene and propene, (**c**) acetylene, (**d**) benzene and toluene and (**e**) isoprene, based on hourly averaged levels for the period from 16 October 2015 to 15 February 2016, at the NOA urban background site in Thissio, downtown Athens.

ature for Athens and other selected areas. The comparison with published data for the GAA, indicates an apparent decrease by a factor of 2 to 6 for the majority of the species lying above C4 (taking the case of "Ancient Agora" urban area in the close vicinity of the Thissio station as a reference). This decreasing trend is in agreement with the decrease in primary pollutants, such as CO, SO_2, already reported by Kalabokas et al. (1999) and Gratsea et al. (2017), due to the air quality measures taken by the Greek government and the economic recession (since 2012). Apart from changes in emission sources and source strength over the last 20 years, differences in sampling period (summer versus winter) and analytical resolution (samples collected in the morning compared to continuously averaged levels) should be considered, which renders the direct comparison between present and past measurements quite difficult regarding the overall evaluation of the NMHC decrease. However, in order to better investigate this observed decreasing trend and compare these results with past measurements, enhancement ratios (ppb/ppb) have been calculated for *i*-pentane, benzene, toluene, ethylbenzene and *o*-xylene to NO_x (sum of NO and NO_2), following the approach of Kourtidis et al. (1999); this was undertaken using the measurements performed in the street canyon (Patission) and presented in Table 2. In short, the enhancement ratios are the slopes of the x–y plots of the selected NMHC (in ppb) to NO_x (or CO, both in ppb), for which morning concentrations (07:00 to 10:00 LT) at wind speeds lower than 2 m s^{-1} from the SSW–SW (206 to 237°) were used. The NO_x and CO data for the Patission site are provided by the Hellenic Ministry of Environment & Energy, Department of Air Quality. Additionally, the same enhancement ratios were calculated for Thissio station for concentrations associated with wind speeds lower than 2 m s^{-1} (no distinction regarding wind direction), which maximized the local influence. Since the enhancement ratios are calculated during the traffic rush hours, it is assumed that they are only representative of traffic emissions. Both Thissio station and Patission street canyon demonstrate similar enhancement ratios with differences in the order of 15 %–30 % and 20 %–35 % relative to NO_x and CO, respectively, and large differences compared to previously reported values. Enhancement ratios for *i*-pentane, toluene, ethylbenzene and *o*-xylene to NO_x for the same station (Patission) show values which are lower by a factor of 6±1 compared to those reported in Kourtidis et al. (1999), whereas a factor of 12 decrease is observed for benzene. The same stands for the present enhancement ratios of the selected NMHCs to CO with a decrease of 2 to 5 times compared to previously reported values. The lower enhancement ratios reveal the strong impact of the air quality measures regarding VOC emissions, while the high difference in the benzene enhancement ratio is a direct outcome of Directive 2000/69/CE (now Directive 2008/50/EC) of the European Union for the reduction of this compound, especially in fuels.

Beirut, located in the eastern Mediterranean Basin (approximately 200 km SE of Greece, 230 m a.s.l.), has a population of 2 million inhabitants and a typical Mediterranean climate with mild winters and hot summers (Salameh et al., 2015). Bilbao, in comparison, is an urban and industrial city with 400 000 inhabitants in northern Spain, located along a river delta in a SE–NW direction, with two mountain ranges in parallel to the river (Ibarra-Berastegi et al., 2008). Due to their location, both cities experience intense sea breeze cycles. The NMHC levels observed in Athens are higher by a factor of approximately 2 for ethylene, propene, acetylene and pentanes compared to these two cities and up to 3.5 for isopentane in comparison to Bilbao. Exceptions to this trend are propane, butanes and toluene for Beirut and *n*-butane, benzene and toluene for Bilbao, which are comparable to Athens. NMHC levels are also compared with those obtained in Paris, a European megacity with more than 10 million inhabitants that experiences relatively mild winters and warm summers. Again, the observed levels in Athens are significantly higher (almost 2 to 8 times) compared to those reported for Paris (Baudic et al., 2016), with the most impor-

Table 1. Comparison of mean NMHC levels between this study and previously published works in Athens, Greece, and other Mediterranean or European sites. Information regarding the analysis or sampling techniques and data resolution are included when available. The number of measurements[a] made for each compound determined in the current samples is included below the table.

Studies	Rappenglück et al. (1998)		Rappenglück et al. (1999)	Moschonas and Glavas (1996)	Kaltsonoudis et al. (2016)		Baudic et al. (2016)	Salameh et al. (2015)	Durana et al. (2006)	Current work			
Analysis details	GC - FID Every 20 min		GC - FID Every 20 min	GC - MS 60 min (morning sampling, 12 canisters)	PTR-MS Every 10 s/24 h		GC - FID	GC - FID	GC - FID	GC- FID Every 30 min			
NMHCs	20 August – 20 September 1994, Athens, Greece		30 May – 16 June 1996, Athens, Greece	June 1993, May and July 1994, Athens, Greece	3–26 July 2012 (Demokritos) & 9 January – 6 February 2013 (Thissio)		16 October – 22 November 2010 Paris, France	28 January – 12 February 2012 Beirut, Lebanon	April–October 1998–2001 February–July 2004 Bilbao, Spain[b]	16 October 2015–15 February 2016, Athens, Greece			
	Patision (urban)	Demokritos (suburban)	Tatoi (suburban)	Ancient Agora (urban)	Demokritos (suburban)	Thissio (urban background)	Les Halles station (urban background)	Saint Joseph University (suburban)	Bilbao (urban center)	Thissio (urban background)			
										Mean	Median	Min	Max
	ppbv		ppbv	ppbv	ppb		ppb	ppb	ppbv	ppb			
Ethane							3.8	2.8	2.5–3.5	4.5	3.1	0.6	25.9
Ethylene							1.3	2.1	2–2.3	4.1	2.2	0.3	22.9
Propane				1.2			1.6	3.0	1.7–2.5	3.1	1.8	0.2	17.8
Propene				3.9			0.4	0.6	0.7–0.9	1.5	0.6	0.02	15.7
i-Butane				1.1			0.9	1.9	0.7–2	2.3	1.1	0.1	14.9
n-Butane	12.4 (with 1-butene)	1.6	0.19 (with 1-butene)	2.1			1.5	3.6	1.8–2.6	2.6	1.3	0.1	15.2
Acetylene							0.5	2.2	1.5–2.7	4.2	2.4	0.1	28.5
i-Pentane	26.3	3.2	0.93	11.7			0.7	2.4	1–1.7	4.7	2.6	0.2	23.8
n-Pentane	14.2 (with 2-methyl-1-butene)	1.7	0.27 (with 2-methyl-1-butene)	4.2			0.3	0.5	0.4–0.7	1.1	0.6	0.1	9.3
Isoprene			3.18(with *trans*-2-pentene & *cis*-2-pentene)		0.7	1.1	0.1	0.1		0.2	0.1	0.01	1.4
Benzene	11.7	2.5	2.12	5.0	0.2	1.0	0.4	0.5	0.5–1	0.8	0.5	0.02	5.3
Toluene	21.2	6.7	1.15	14.3	0.8	2.3	0.8	2.2	2–2.6	2.2[d]	1.0[d]	0.1[d]	13.7[d]
Ethylbenzene	4.0	1.3	0.20	2.7				0.3	0.6–0.8	0.4[d]	0.2[d]	0.03[d]	2.7[d]
m-/*p*- Xylenes	11.3[c]	3.2[c]	0.63[c]	12.1				0.4	2.0–2.4	1.2[d]	0.5[d]	0.03[d]	8.3[d]
o - Xylene	5.5	1.5	0.3	3.7				0.3	0.4–0.5	0.4[d]	0.2[d]	0.03[d]	3.1[d]

[a] ethane $N = 2848$, ethylene $N = 2859$, propane $N = 2861$, propene $N = 2842$, *i*-Butane $N = 2876$, *n*-butane $N = 2879$, acetylene $N = 2565$, *i*-pentane $N = 2874$, *n*-pentane $N = 2859$, isoprene $N = 264$, benzene $N = 2683$, toluene $N = 637$. [b] Range estimated from Fig. 1, included in Durana et al. (2006). [c] Sum of the reported mean value for *m*-xylene and *p*-xylene. [d] Only from 21 January to 15 February 2016.

tant differences concerning acetylene and *i*-pentane (which are factors of 8.4 and 6.7 higher in Athens, respectively, Table 1).

According to Fig. 2, a common pattern for all NMHC concentrations is their gradual increase from October to December, which reflects the transition from a warmer period to a colder one. This is better illustrated in Fig. 3, which depicts the monthly median concentration for every NMHC presented in Fig. 2. The increase in NMHC levels during the cold period could be explained by the respective increase in their lifetime due to less photochemistry and the contributions from additional sources, such as heating. However, the role of atmospheric dynamics should not be neglected, as the decrease in the height of the planetary boundary layer (PBL) could also trigger the observed wintertime enhancement of NMHC levels. Nevertheless, according to Alexiou et al. (2018) the mean wintertime decrease of the PBL compared to autumn is in the range of 20 % for both day and night periods; thus, the PBL height is likely not the only factor determining the enhancement of the NMHC levels observed during wintertime. Furthermore, according to Kassomenos et al. (1995) the day–night difference of the PBL is more pronounced during summer. Thus, the nighttime accumulation of pollutants during winter relative to summer essentially highlights the impact of additional emission sources. Meteorological conditions such as wind speed and direction also have to be considered, and their respective role will be discussed in the following.

3.2 Diurnal variability of NMHCs

During the whole monitoring period, all hydrocarbons demonstrated a pronounced bimodal diurnal pattern (Figs. 4 and S2). A morning peak was observed that lasted from 07:00 to 10:00 LT, followed by a second peak before midnight. The amplitude of both peaks gradually increases from October to wintertime by a factor of 3 to 6 and closely follows that of carbon monoxide (CO), BC and its fractions associated with wood burning (BC_{wb}) and fossil fuel combustion (BC_{ff}) (Fig. 4). As was noted in Gratsea et al. (2017), the morning maximum of CO is attributed to morning traffic, while the winter nighttime increase is attributed to additional sources such as domestic heating (fossil fuel or wood burning). Al-

Table 2. Enhancement ratios of NMHC to NO_x (ppb/ppb) and to CO (ppb/ppb), calculated from the present dataset for Thissio station and the street canyon measurements (Patission station) for the traffic rush hour periods. The enhancement ratios presented in the third and sixth column are reported in Kourtidis et al. (1999) and were calculated for the same station in the street canyon.

Ratios of NMHCs to:	NO_x (ppb / ppb)			CO (ppb / ppb)		
	Thissio station (urban background)	Patission station (traffic)	Patission station (traffic), 1994*	Thissio station (urban background)	Patission station (traffic)	Patission station (traffic), 1994
	21 January–15 February 2016	23–24 February 2017	20 August–20 September 1994	21 January–15 February 2016	23–24 February 2017	20 August–20 September 1994
i-Pentane	0.0639	0.0490	0.2468	0.0072	0.0058	0.0098
Benzene	0.0095	0.0083	0.1042	0.0012	0.0009	0.00414
Toluene	0.0417	0.0320	0.1799	0.0056	0.0034	0.00715
Ethylbenzene	0.0073	0.0053	0.0338			
o-Xylene	0.0082	0.0059	0.0471			

* The NMHC-to-NO_x enhancement ratios of Kourtidis et al. (1999) given in w/w (weight/weight) were converted into ppb/ppb by dividing them by the ratio of the molecular weight of the NMHC to the molecular weight of NO_x (equal to 31.6 according to Kourtidis et al., 1999).

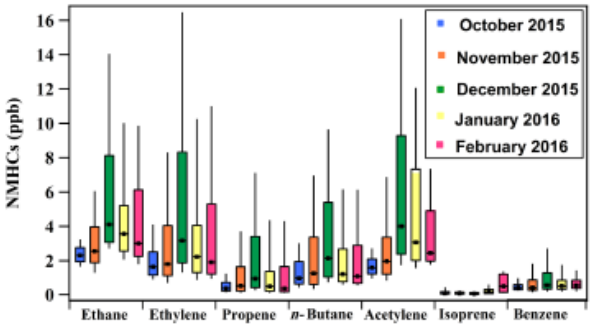

Figure 3. Monthly box plots for ethane, ethylene, propene, *n*-butane, acetylene, isoprene and benzene. The black dots represent the median values and the boxes shows the interquartile range. The bottom and the top of the boxes depict the first and third quartiles (i.e., Q1 and Q3). The whiskers correspond to the first and the ninth deciles (i.e., D1 and D9).

though the amplitude of both CO peaks (morning and night) is similar (with the exception of December), the duration of the night peak is at least a factor of 2 larger, which could imply that heating impacts the air quality during wintertime. Moreover, nighttime emissions occur in a shallower boundary layer relative to midday emissions, resulting in the accumulation of pollutants (Alexiou et al., 2018). These observations are indicative of the contribution of traffic and heating to NMHC levels. By comparing the NMHC diurnal variability with that of BC, as well as its fractions associated with wood burning (BC_{wb}) and fossil fuel combustion (BC_{ff}), it is deduced that the morning peak can mainly be attributed to traffic, and the late evening peak to traffic and heating from the combined use of heavy oil and wood burning.

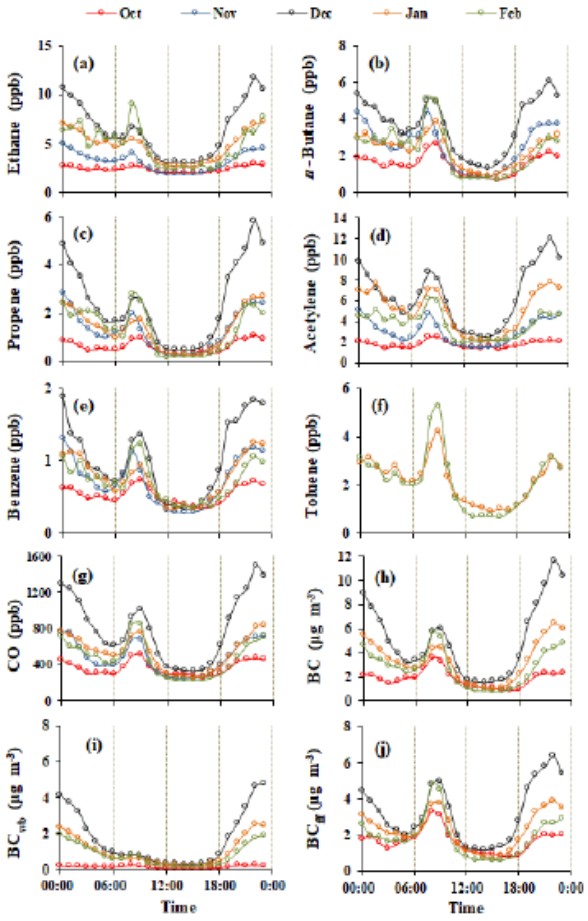

Figure 4. Monthly diurnal variability of (**a**) ethane, (**b**) *n*-butane, (**c**) propene, (**d**) acetylene, (**e**) benzene, (**f**) toluene, (**g**) CO, (**h**) BC, (**i**) BC_{wb} and (**j**) BC_{ff} based on hourly averaged values.

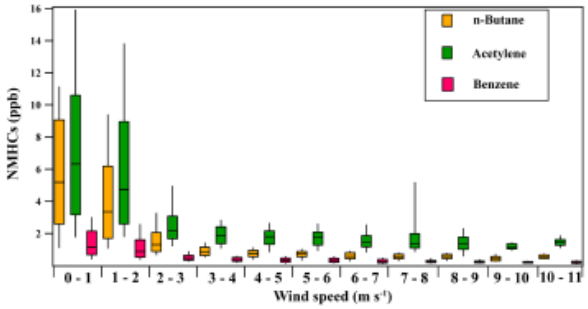

Figure 5. Box plots for (**a**) *n*-butane, (**b**) acetylene and (**c**) benzene relative to wind speed for the period from 16 October 2015 to 15 February 2016. The black lines represent the median value and the boxes show the interquartile range. The bottoms and the tops of the boxes depict the respective first and third quartiles (i.e., Q1 and Q3). The whiskers correspond to the first and the ninth deciles (i.e., D1 and D9). The range of each wind speed bin is depicted on the *x* axis.

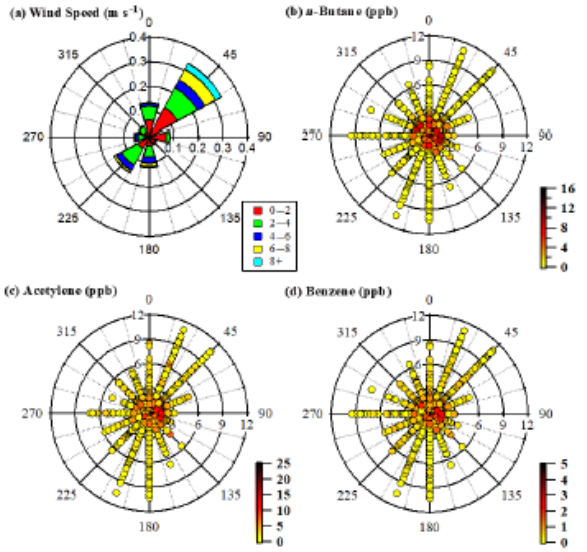

Figure 6. Wind rose (**a**) and concentration roses of (**b**) *n*-butane, (**c**) acetylene and (**d**) benzene for the period from 16 October 2015 to 15 February 2016.

3.3 The role of meteorology on NMHC levels

Once emitted in the atmosphere, NMHCs mainly react with OH and NO_3 radicals during daytime and nighttime, respectively, and with ozone throughout the day (Crutzen, 1995; Atkinson, 2000); the role of Cl can also not be omitted, especially for coastal areas (Arsene et al., 2007). Still, in addition to chemistry, many other factors, such as the strength of the emission sources and the atmospheric dynamics (meteorology and boundary layer evolution), determine NMHC abundance and diurnal variability. To investigate the role of wind speed and wind direction, the dependence of *n*-butane, acetylene and benzene, selected as representative of alkanes, alkynes and aromatics, against wind speed and direction, is depicted in Figs. 5 and 6 respectively (Fig. S3 and S4 include the rest of the compounds). For all of the NMHCs studied, the highest concentration occurred at low wind speed conditions ($< 3\,\mathrm{m\,s^{-1}}$) which reflects the critical role of local sources versus long-range transport. On a monthly basis, the NMHC dependence on wind speed remained the same for the total period examined (Fig. S5).

To investigate the impact of wind direction on NMHC levels, Fig. 6 presents the distribution of the wind sector frequency of occurrence during the sampling period and that of wind speed per sector. In addition, the variability of *n*-butane, acetylene and benzene levels as a function of wind direction is also depicted. Enhanced levels of NMHCs are found under the influence of air masses from all directions, especially at low wind speeds. During the sampling period, the NE sector, associated with relative strong winds ($u > 3\,\mathrm{m\,s^{-1}}$), was the most frequent sector, resulting in moderate levels of NMHCs. Overall, a similar distribution was found for all NMHCs, indicating moderate to higher values in the N–NE–E–SE sector, and lower levels in the NW–W–SW sector, the latter associated with high wind speeds. The influence of the N–SE sector on the enhanced NMHCs levels is probably related to the northern suburbs of the GAA, which are characterized by an increased number of fireplaces and higher living standards that allow for the combined use of heating oil in central heating systems and wood in fireplaces and/or woodstoves. The impact of the N–ESE sector on NMHC levels can be also seen when comparing the concentrations of the morning (07:00–09:00) and night (21:00–23:00) peaks in October and December (Fig. S6). The probability of wind from the N–ESE is similar for both months, but significantly higher concentrations are observed at nighttime in December due to low wind speeds ($< 2\,\mathrm{m\,s^{-1}}$) from the N–NE sector.

The ambient temperature is another parameter which can influence NMHC levels, as high temperatures favor the evaporation of low volatility hydrocarbons and also trigger the production of biogenic compounds, whereas lower temperatures can potentially trigger the emission of NMHCs from increased heating demand, in addition to other tracers (Athanasopoulou et al., 2017). The average monthly temperatures varied from 18 °C in October and November to 10–13 °C in December and late winter. By examining NMHCs against temperature (Fig. S7), a clear tendency is not evident, although the highest levels are observed at lower temperatures.

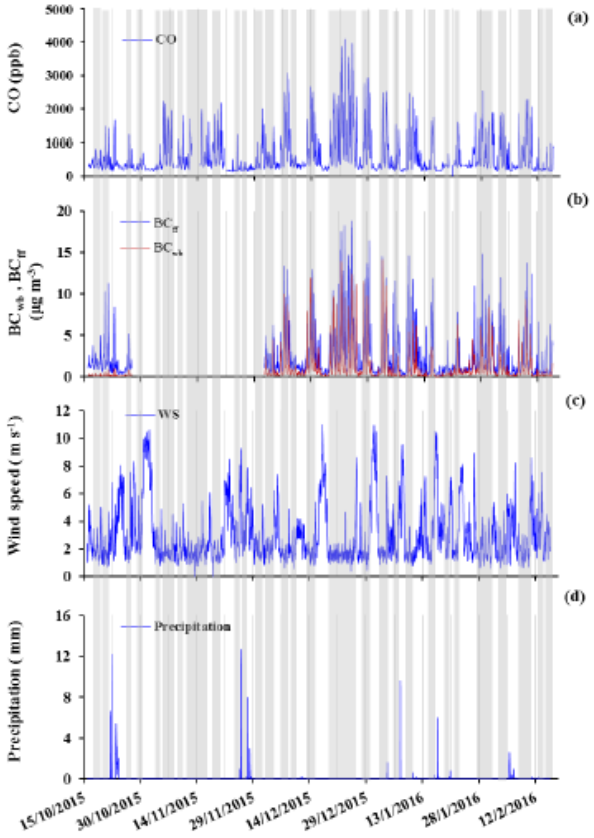

Figure 7. Temporal variability of (**a**) CO, (**b**) BC_{wb} and BC_{ff} fractions, (**c**) wind speed and (**d**) precipitation for the experimental period. Grey frames correspond to smog periods (SPs), while the remaining frames represent non-smog periods (nSPs).

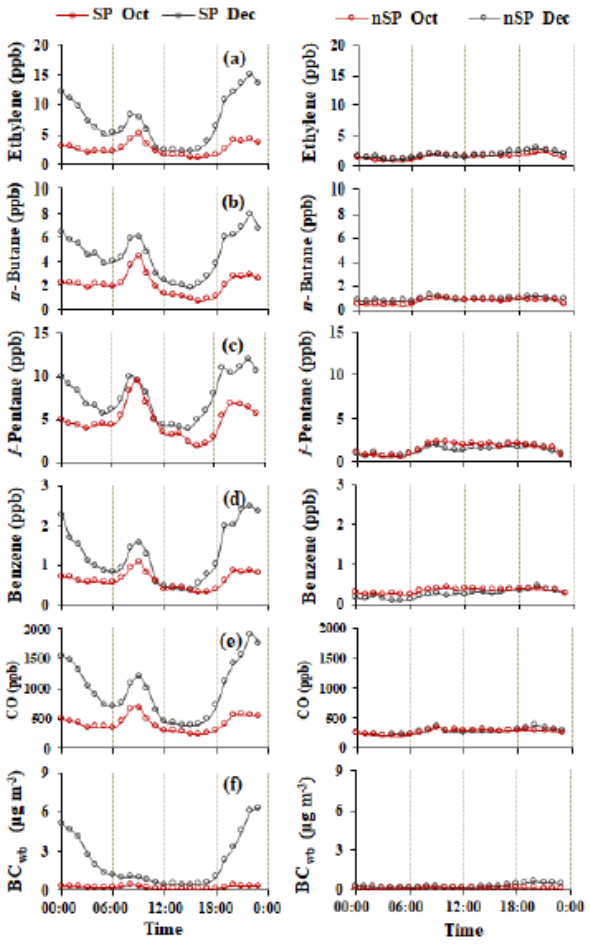

Figure 8. Diurnal patterns of (**a**) ethylene, (**b**) *n*-butane, (**c**) *i*-pentane, (**d**) benzene, (**e**) CO and (**f**) BC_{wb} during the SPs (left column) and nSPs (right column) identified during October 2015 (red) and December 2015 (black), respectively. Note: SP are defined by wind speeds lower than $3\,m\,s^{-1}$ and the absence of rainfall, while nSP are defined by winds speeds higher than $3\,m\,s^{-1}$.

3.4 Identification of NMHC emission sources with emphasis on traffic and heating

3.4.1 Interspecies correlation

Table 3 shows the interspecies correlation of NMHCs for the total measurement period. All NMHCs were well correlated ($R^2 > 0.81$), with the exception of isoprene which as previously noted, only had few data above the limit of detection and was therefore excluded from Table 3. The excellent correlation of toluene with ethylbenzene, *m-/p*-xylenes and *o*-xylene (R^2 from 0.92 to 0.93) during the common measurement period (from mid-January until mid-February 2016) should also be noted, as it highlights their common origin. The strong correlation of NMHCs with combustion tracers, such as CO, NO and BC, could also indicate common emission sources and variability. The deconvolution of BC into its fossil fuel and biomass burning fractions enables further classification of NMHCs into groups that could possibly be emitted by these two distinct sources. The stronger correlation ($R^2 > 0.84$) of the hydrocarbons with BC_{ff} compared to BC_{wb} ($R^2 > 0.64$) could imply stronger emission of NMHCs from fossil fuel combustion processes relative to wood burning. Finally, no change in the correlation coefficients is observed when datasets are separated into daytime (06:00–18:00) and nighttime (18:00–06:00) intervals. However, the above analysis could only give a rough idea regarding the sources impacting NMHCs levels. A more precise picture could emerge via a comparison with source profiles, and a discussion on this topic follows in the paragraph below.

3.4.2 Impact of various sources on NMHC levels

To identify periods with differentiated impacts from different pollution sources (with an emphasis on traffic and heat-

Table 3. Correlation coefficients (R^2) of NMHCs and major gaseous pollutants for the total period of measurements (all significant at $p < 0.01$).

	Ethane	Ethylene	Propane	Propene	*i*-Butane	*n*-Butane	Acetylene	*i*-Pentane	*n*-Pentane	Benzene	BC	BC_{wb}	BC_{ff}	CO
Ethane														
Ethylene	0.94													
Propane	0.92	0.94												
Propene	0.94	0.97	0.96											
i-Butane	0.82	0.90	0.95	0.92										
n-Butane	0.84	0.91	0.97	0.92	0.99									
Acetylene	0.89	0.91	0.90	0.91	0.88	0.88								
i-Pentane	0.73	0.85	0.88	0.85	0.96	0.95	0.81							
n-Pentane	0.74	0.85	0.90	0.88	0.97	0.96	0.84	0.96						
Benzene	0.87	0.95	0.93	0.96	0.91	0.92	0.89	0.87	0.89					
BC	0.93	0.95	0.92	0.96	0.88	0.89	0.90	0.84	0.85	0.93				
BC_{wb}	0.91	0.87	0.81	0.89	0.70	0.72	0.77	0.65	0.64	0.83	0.91			
BC_{ff}	0.84	0.90	0.89	0.90	0.91	0.91	0.89	0.89	0.90	0.89	0.95	0.75		
CO	0.91	0.95	0.94	0.96	0.92	0.93	0.92	0.87	0.89	0.95	0.97	0.87	0.93	
NO	0.86	0.90	0.90	0.90	0.90	0.91	0.89	0.90	0.88	0.89	0.91	0.76	0.92	0.94

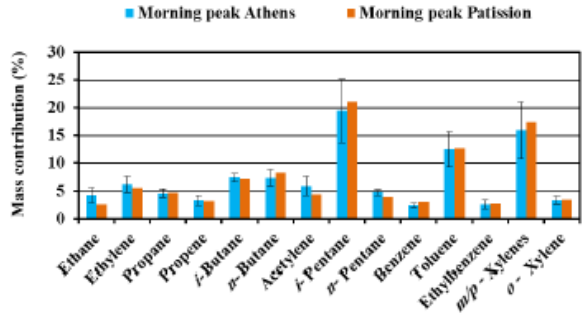

Figure 9. % Mass contribution of the measured NMHCs during the morning peak (07:00–10:00 LT), median values in Thissio and mean values at Patission monitoring station.

ing), the methodology described by Fourtziou et al. (2017) was applied. The criteria for this separation were that the wind speed did / did not exceed a threshold value of 3 m s^{-1} (light breeze conditions) and precipitation was present / absent (on / off criterion). The role of wind speed was clearly visible in Sect. 3.3 (Fig. 5). Based on these criteria, the first group (non-shaded in Fig. 7) which corresponded to higher wind speeds and thus the more efficient dispersion of emitted pollutants (ventilation) as well as incidents of rain was denominated non-smog periods (nSPs). The second group (shaded area in Fig. 7) referred to lower wind speeds, favoring the accumulation of high pollution loads within the mixing layer, and is henceforth referred to as smog periods (SPs). The frequency of SPs and nSPs was 65 % and 35 %, respectively. Note that the word "smog" is used as a synonym to highlight cases of relatively high air pollution, as also indicated by the high levels of CO and BC encountered during the SPs (Fig. 7).

The diurnal variability of all compounds was investigated separately for two distinct months, October and December, representative periods of non-heating and heating activities, respectively (Figs. 8 and S8). Note that SPs represent 55 % of the time considered in October and 73 % in December. According to previous findings (Paraskevopoulou et al., 2015; Kaltsonoudis et al., 2016; Fourtziou et al., 2017; Gratsea et al., 2017) wood burning for domestic heating has gained a marked role as a wintertime emission source in Greece over the last few years. Since wood burning is reported as emission source of specific organic compounds such as ethane, ethylene, acetylene, benzene, methanol, acetaldehyde and acetonitrile (Baudic et al., 2016; Gaeggeler et al., 2008; Gustafson et al., 2007; Hellén et al., 2008; Kaltsonoudis et al., 2016), it can be safely considered as a possible factor contributing to the wintertime increase of NMHC levels in the GAA. Thus, the two selected months are expected to have different source profiles. October, without or very limited heating demand, was used as a reference period, while December in south-central Greece is traditionally the beginning of the heating period. The low values of BC_{wb} recorded in October, even during the SPs, support the methodology chosen for the separation (Fig. 8).

The levels of all measured NMHCs were significantly higher in December than in October for the SPs (Figs. 8 and S8). The most striking difference is related to the nighttime peak, while during the midday period the difference is minimal. For all compounds examined in this work, the nighttime peak in December (SP) was 2 to 6 times higher compared with that in October (SP) with the highest differences found for ethane, ethylene, propene and acetylene. Conversely, the December to October ratio during the midday period ranged between 2.6 (for propene and acetylene) and 0.9 (for benzene). It is worth noting the levels of NMHCs during the traffic related morning peak. Although higher mean levels were observed in December, the amplitude of the morning peak is similar in both of the months examined, representing no important change in the traffic source between the heating and non-heating periods. In contrast, during the nSPs in October

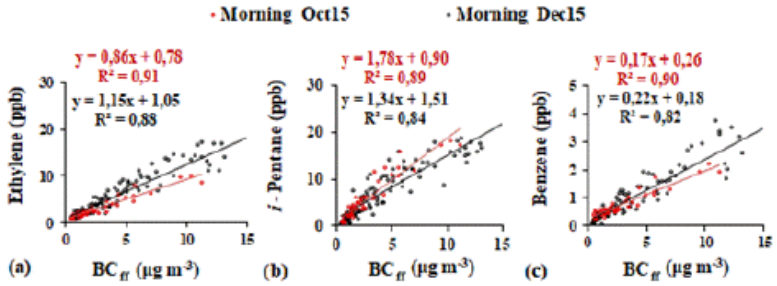

Figure 10. Regressions between ethylene, *i*-pentane and benzene versus BC_{ff} (a)–(c) for the morning periods (07:00–10:00 LT) in October and December 2015.

and December NMHC levels were equal (Figs. 8 and S8). Furthermore, the concentrations of all compounds during nSPs were very low – even lower than the minimum values observed at midday during the SPs of the same months. Accordingly, the diurnal variability of all investigated NMHCs was less pronounced compared to the SPs with a slight increase during the night in December, which could be attributed to a background contribution from heating sources. In Sect. 3.4.3 the origin of the morning and nighttime peaks related to NMHCs will be further investigated.

3.4.3 Impact of sources on morning and night peaks of NMHCs

Morning peak

As discussed in Sect. 3.2, the morning NMHC peak (07:00–10:00 LT) was mainly attributed to traffic. Fig. 9 presents the profile of this peak (percent mass contribution of the measured NMHCs), during January and February SP days when toluene, ethylbenzene, *m*-/*p*-xylenes and *o*-xylene data were also available. Additionally, in the same figure the morning profile obtained during the 2-day measurement campaign conducted in the street canyon in central Athens (Patission monitoring station) is also reported. Details regarding the calculations of the morning profile for the two sites are provided in Sect. S2. The Patission profile reflects all types of traffic-related emissions due to the combination of the high number of vehicles and buses driving on this street, the frequent traffic jam conditions, the variety of fuel types (gas, oil, diesel, natural gas), vehicles ages, maintenance etc.

The two morning profiles, although performed at sites with different traffic impacts, agree quite well ($R^2 > 0.98$). *Iso*-pentane, toluene and *m*-/*p*-xylenes are the three main compounds that contribute to the morning profiles, accounting for about 50 % of the total measured NMHCs at both locations, followed by *n*- and *i*-butane and ethylene, which account for almost 21 %. Differences between the two morning profiles regarding these five main species are weak (less than a factor of 1.2). However, the morning profile at Thissio is the mean of a whole month compared to the 2-day campaign at Patission which could explain the small differences between the two profiles. In addition, a comparison with a tunnel study in Athens is made in the Supplement (Sect. S2a.), in which similarities are seen for most of the main compounds (*i*-pentane, *m*-/*p*-xylenes, ethylbenzene, *o*-xylene, benzene, *n*-pentane, *i*-butane, propene and ethane), with the exception of acetylene and toluene that are a factor of 4 and 1.5 lower, respectively. The similarity between the Thissio and Patission morning profiles and their difference from the Athens tunnel profile probably indicates the importance of the fuel type used. The latter is also observed in recent works (Ait-Helal et al., 2015; Q. Zhang et al., 2018; Y. Zhang et al., 2018), where important differences have been reported between tunnel measurements, and have been attributed to various car-fleet typologies (type of vehicles and fuels). In our case there is a possibility that the car fleet in the tunnel is not representative of the GAA, as the existing tolls reduce the use of the tunnel due to financial constrictions. Furthermore, measurements are performed during the noon period when the traffic density is relatively low compared to the morning peak. In any case, the prevalence of *i*-pentane and toluene in all profiles indicates the continuing dominance of gasoline powered cars and evaporative losses. The importance of evaporative losses can

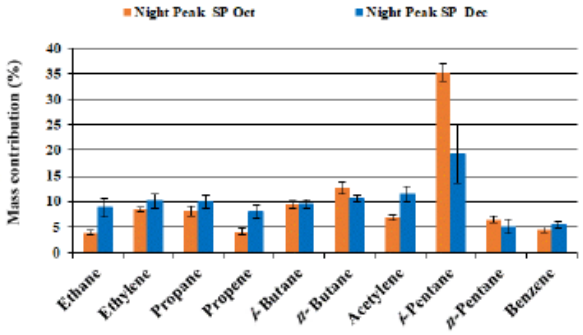

Figure 11. The percent mass contribution of the measured NMHCs during the nighttime enhancement period (18:00–05:00 LT) for the SP in October (orange) and the SP in December (black).

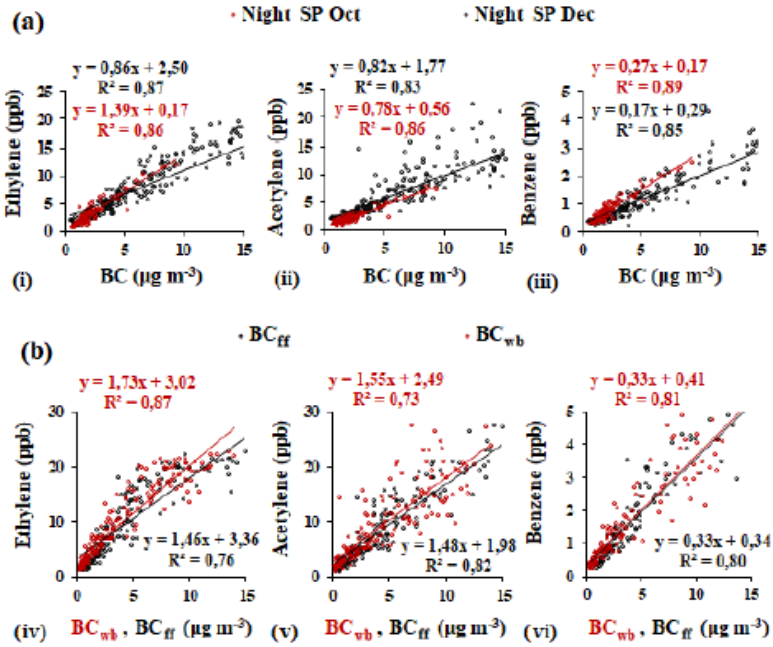

Figure 12. Regressions between ethylene, acetylene and benzene (**a**) against BC (i–iii) for the nighttime (18:00–05:00 LT) SPs in October and December 2015 and (**b**) against BC_{wb} (red) and BC_{ff} (black) for the nighttime (22:00–04:00 LT) SP in December 2015.

be seen in Figs. S11 and S12 where the ratios of butanes and pentanes-to-(C2–C5) alkanes (percent) versus the temperature are examined, respectively. Taking the positive dependence of the two ratios into account, especially that of pentanes, to temperature, we can assume that fuel evaporative losses are also an important source of NMHCs. These observations are in agreement with the general behavior of the temperature dependency reported in Kourtidis et al. (1999) (Fig. S13 and Sect. S3), who performed an investigation on the dependence of the fractionation of NMHCs in evaporative emissions on temperature in Athens. Although the periods examined differ regarding ambient temperature (winter is colder than autumn), the exponential curve fitting of both datasets was similar. In addition, the abovementioned results could indicate why the Athens tunnel results from May differ from Patission and Thissio winter morning profiles. Moreover, the higher values of propane and butanes that are depicted in the morning peaks at the urban sites relative to the tunnel measurement, reflect the increased number of LPG powered vehicles in Athens in addition to natural gas-powered buses (Fameli and Assimakopoulos, 2016). This is further highlighted when the monthly variation of *i*-butane relative to *n*-butane is examined (Fig. S14). The two compounds have a linear relationship with no significant temporal differences in the slopes between the various months. Furthermore, the regression is similar to that derived from the Patission measurements, which enhances our assumption that butanes emissions are traffic related. Moreover, the relation between the high levels of C2–C4 alkanes and the number of LPG-powered cars has also been highlighted in other tunnel studies (Ait-Helal et al., 2015; Q. Zhang et al., 2018).

To obtain a better idea of the variability of the traffic source during the study period, the variability of selected NMHCs (ethylene, *i*-pentane and benzene) relative to BC_{ff} (the latter used as traffic source tracer) was also plotted for October and December (Fig. 10). Significant correlations were revealed with slopes remaining almost stable (within 30 %) during both months. This indicates similar emission ratios throughout the study period, and most likely an equal contribution from traffic.

Nighttime enhancement period

During nighttime both BC_{ff} and BC_{wb} were maximized (e.g., Figs. 4 and 8), denoting a significant contribution from both fossil fuel and wood burning (the contribution of the latter was more evident during winter). Figure 11 presents the NMHC profile of the nighttime enhancement period for October and December SP nights (details for the calculations are given in Sect. S4 in the Supplement). As previously discussed, traffic is expected to be the main source of NMHCs during nighttime in October, whereas heating competes with traffic during December. When these two profiles are compared (Fig. 11), a statistically significant difference at $p < 0.01$ confidence is obvious, with a smaller contribution from *i*-pentane (traffic source contributor) during December. In addition, enhanced contributions from C2 NMHCs (ethane,

ethylene and acetylene) are apparent in December compared with October. These C2 hydrocarbons were reported as important contributors to the wood burning source profile by Baudic et al. (2016) in Paris. Preliminary data from a fireplace experiment (not part of this work) also confirm these findings; these data are also in line with our results reported in Fig. 8 that indicate an impact from wood burning during nighttime in the winter months.

Figure 12a (i–iii) presents the relation of ethylene, acetylene and benzene, the main contributors of the wood burning profile (Baudic et al., 2016), to BC during the nighttime (18:00–05:00 LT) SPs in October and December. During both months, significant correlations were revealed for all examined NMHCs and the slopes remained relatively stable, indicating almost equivalent emission ratios from both traffic and heating sources. To better tackle a possible difference in NMHC emissions from traffic and residential heating, these NMHCs were also plotted against BC_{wb} and BC_{ff} during the SPs in December, from 22:00 to 04:00 LT, i.e., the time frame when traffic is quite limited (Fig. 12b, iv–vi). The NMHC slopes versus BC_{wb} are similar when compared to those versus BC_{ff} (slight difference for ethylene), with a contribution of BC_{wb} and BC_{ff} to BC of 43 % (±10 %) and 55 % (±11 %), respectively, indicating that the NMHCs studied are probably equally produced by wood and fossil fuel burning.

4 Conclusions

For the first time to our knowledge, time-resolved measurements of 11 non-methane hydrocarbons with two to six carbon atoms (C2–C6 NMHCs) were conducted for several months (mid-October 2015 to mid-February 2016) in the greater Athens area (GAA) by means of an automatic chromatograph, in parallel with the monitoring of major pollutants and meteorological parameters. The temporal variability of the NMHCs presented an increasing trend from October to December, due to changes in the type and strength of sources, and atmospheric dynamics. In comparison with other works, higher concentrations are reported for the majority of the NMHCs, which indicates an air quality issue in Athens. With the exception of isoprene, all NMHCs presented a bimodal diurnal pattern with a morning and a broader nighttime maxima, whereas lower concentrations were observed early in the afternoon. Typical indicators of combustion processes such as CO and BC, with the latter further deconvoluted into BC_{ff} and BC_{wb}, presented similar seasonal and diurnal variability relative to the NMHCs, providing the opportunity to investigate their possible emission sources. Thus, the morning maximum, which follows the BC_{ff} tendency, was attributed to traffic, while the second peak during nighttime which reached a maximum in December and coincided with those of BC_{wb} and BC_{ff} was mainly attributed to heating by both fossil fuel and wood burning.

For a better understanding of the impact of sources on NMHC levels, the study period was further separated into smog periods (SPs) and non-smog periods (nSPs), based on the absence of rainfall and low wind speeds. October and December were chosen for further comparison due to the different temperature conditions and possible sources, taking the previously reported increased wintertime heating demand into account (Athanasopoulou et al., 2017). The comparison of the morning maximum of the NMHC profile during SP days with those obtained in a street canyon in Athens (Patission) further confirms the role of traffic regarding the observed morning NMHC peak. The October and December NMHC SP nighttime profiles depicted differences that are mainly attributed to heating. However, NMHC slopes versus BC_{wb} are similar when compared with those versus BC_{ff} (slight difference for ethylene), indicating that NMHCs are probably equally produced by wood and oil fossil fuel burning. An extended dataset of NMHCs and other organic tracers (future long-term measurements) is needed to apportion different sources types on a seasonal basis and quantify their impact on the NMHC levels.

Data availability. All the data presented in this paper are available upon request. For further information, please contact Eleni Liakakou (liakakou@noa.gr).

Supplement. The supplement related to this article is available online at: https://doi.org/10.5194/acp-18-16139-2018-supplement.

Author contributions. AP operated the instrument, collected and analyzed samples, processed the dataset and drafted the article. EL contributed to sample collection and provided auxilliary data. BEP provided data for the variables presented in this work. SS, VG, BB, NL, EL, NM and EG designed the study and performed critical revisions of the article including the final approval of the version to be published.

Competing interests. The authors declare that they have no conflict of interest.

Special issue statement. This article is part of the special issue "CHemistry and AeRosols Mediterranean EXperiments (ChArMEx) (ACP/AMT inter-journal SI)". It is not associated with a conference.

Acknowledgements. Support from CEA, CNRS and the Charmex program is acknowledged. This study also received financial support from the European community through the Aerosols, Clouds, and Trace gases Research InfraStructure Network (ACTRIS) Research Infrastructure Action under the 7th Framework Programme (grant agreement no. 262254). We thank François Dulac and

Eric Hamonou for the successful management of the Charmex program, Dominique Baisnée and Thierry Leonardis for technical support with the gas chromatographs, and the editor and the two anonymous reviewers for their comments which greatly improved the submitted version of the paper. The authors also acknowledge the Hellenic Ministry of Environment & Energy, Department of Air Quality for access at Patission station and the use of their database for the purposes of the short intensive campaign. Attiki Odos is also acknowledged for providing access to the tunnel.

Edited by: Matthias Beekmann
Reviewed by: two anonymous referees

References

Ait-Helal, W., Beeldens, A., Boonen, E., Borbon, A., Boréave, A., Cazaunau, M., Chen, H., Daële, V., Dupart, Y., Gaimoz, C., Gallus, M., George, C., Grand, N., Grosselin, B., Herrmann, H., Ifang, S., Kurtenbach, R., Maille, M., Marjanovic, I., Mellouki, A., Miet, K., Mothes, F., Poulain, L., Rabe, R., Zapf, P., Kleffmann, J., and Doussin, J.-F.: On-road measurements of NMVOCs and NO_x: Determination of light-duty vehicles emission factors from tunnel studies in Brussels city center, Atmos. Environ., 122, 799–807, https://doi.org/10.1016/j.atmosenv.2015.09.066, 2015.

Alexiou, D., Kokkalis, P., Papayannis, A., Rocadenbosch, F., Argyrouli, A., Tsaknakis, G., and Tzanis, C. G.: Planetary boundary layer height variability over Athens, Greece, based on the synergy of Raman and Radiosonde data: Application of the Kalman filter and other techniques, EPJ Web of Conferences, 176, 06007, https://doi.org/10.1051/epjconf/201817606007, 2018.

Arsene, C., Bougiatioti, A., Kanakidou, M., Bonsang, B., and Mihalopoulos, N.: Tropospheric OH and Cl levels deduced from non-methane hydrocarbon measurements in a marine site, Atmos. Chem. Phys., 7, 4661–4673, https://doi.org/10.5194/acp-7-4661-2007, 2007.

Athanasopoulou, E., Speyer, O., Brunner, D., Vogel, H., Vogel, B., Mihalopoulos, N., and Gerasopoulos, E.: Changes in domestic heating fuel use in Greece: effects on atmospheric chemistry and radiation, Atmos. Chem. Phys., 17, 10597–10618, https://doi.org/10.5194/acp-17-10597-2017, 2017.

Atkinson, R.: Atmospheric chemistry of VOCs and NO_x, Atmos. Environ., 34, 2063–2101, https://doi.org/10.1016/S1352-2310(99)00460-4, 2000.

Barrefors, G. and Petersson, G.: Volatile hydrocarbons from domestic wood burning, Chemosphere, 30, 1551–1556, https://doi.org/10.1016/0045-6535(95)00048-D, 1995.

Barletta, B., Meinardi, S., Sherwood Rowland, F., Chan, C.-Y., Wang, X., Zou, S., Yin Chan, L., and Blake, D. R.: Volatile organic compounds in 43 Chinese cities, Atmos. Environ., 39, 5979–5990, https://doi.org/10.1016/j.atmosenv.2005.06.029, 2005.

Baudic, A., Gros, V., Sauvage, S., Locoge, N., Sanchez, O., Sarda-Estève, R., Kalogridis, C., Petit, J.-E., Bonnaire, N., Baisnée, D., Favez, O., Albinet, A., Sciare, J., and Bonsang, B.: Seasonal variability and source apportionment of volatile organic compounds (VOCs) in the Paris megacity (France), Atmos. Chem. Phys., 16, 11961–11989, https://doi.org/10.5194/acp-16-11961-2016, 2016.

Borbon, A., Fontaine, H., Veillerot, M., Locoge, N., Galloo, J. C., and Guillermo, R.: An investigation into the traffic-related fraction of isoprene at an urban location, Atmos. Environ., 35, 3749–3760, https://doi.org/10.1016/S1352-2310(01)00170-4, 2001.

Borbon, A., Fontaine, H., Locoge, N., Veillerot, M., and Galloo, J. C.: Developing receptor-oriented methods for non-methane hydrocarbon characterisation in urban air – Part I: source identification, Atmos. Environ., 37, 4051–4064, https://doi.org/10.1016/S1352-2310(03)00525-9, 2003.

Crutzen, P. J.: Ozone in the troposphere, Composition, chemistry, and climate of the atmosphere, in: Composition, Chemistry, and Climate of the Atmosphere, edited by: Singh, H. B., Van Nostrand Reinhold Publ., New York, 349–393, 1995.

Cvitas, T., Gusten, H., Heinrich, G., Klasinc, L., Lalas, D., and Petrakis, M.: Characteristics of summer air pollution during the summer in Athens, Greece, Staub Reinhalt Luft, 45, 297–301, 1985.

Directive 2000/69/EC of 16 November relating to limit values for benzene and carbon monoxide in ambient air, 2000.

Directive 2008/50/EC of the European Parliament and of the Council of 21 May on ambient air quality and cleaner air for Europe, 2008.

Durana, N., Navazo, M., Gómez, M. C., Alonso, L., García, J. A., Ilardia, J. L., Gangoiti, G., and Iza, J.: Long term hourly measurement of 62 non-methane hydrocarbons in an urban area: Main results and contribution of non-traffic sources, Atmos. Environ., 40, 2860–2872, https://doi.org/10.1016/j.atmosenv.2006.01.005, 2006.

European Environmental Agency (EEA): Air quality in Europe – 2016 report (No. 28), available at: https://www.eea.europa.eu/publications/air-quality-in-europe-2016 (last access: 2 October 2017), 2016.

Evtyugina, M., Alves, C., Calvo, A., Nunes, T., Tarelho, L., Duarte, M., Prozil, S. O., Evtuguin, D. V., and Pio, C.: VOC emissions from residential combustion of Southern and mid-European woods, Atmos. Environ., 83, 90–98, https://doi.org/10.1016/j.atmosenv.2013.10.050, 2014.

Fameli, K.-M. and Assimakopoulos, V. D.: The new open Flexible Emission Inventory for Greece and the Greater Athens Area (FEI-GREGAA): Account of pollutant sources and their importance from 2006 to 2012, Atmos. Environ., 137, 17–37, 2016.

Fourtziou, L., Liakakou, E., Stavroulas, I., Theodosi, C., Zarmpas, P., Psiloglou, B., Sciare, J., Maggos, T., Bairachtari, K., Bougiatioti, A., Gerasopoulos, E., Sarda-Estève, R., Bonnaire, N., and Mihalopoulos, N.: Multi-tracer approach to characterize domestic wood burning in Athens (Greece) during wintertime, Atmos. Environ., 148, 89–101, https://doi.org/10.1016/j.atmosenv.2016.10.011, 2017.

Fuentes, J. D., Gu, L., Lerdau, M., Atkinson, R., Baldocchi, D., Bottenheim, J., Ciccioli, P., Lamb, B., Geron, C., and Guenther, A.: Biogenic hydrocarbons in the atmospheric boundary layer: a review, B. Am. Meteorol. Soc., 81, 1537–1575, 2000.

Gaeggeler, K., Prevot, A. S. H., Dommen, J., Legreid, G., Reimann, S., and Baltensperger, U.: Residential wood burning in an Alpine valley as a source for oxygenated volatile organic compounds, hydrocarbons and organic acids, Atmos. Environ., 42, 8278–8287, https://doi.org/10.1016/j.atmosenv.2008.07.038, 2008.

Giakoumi, A., Maggos, T., Michopoulos, J., Helmis, C., and Vasilakos, C.: $PM_{2.5}$ and volatile organic compounds (VOCs) in ambient air: a focus on the effect of meteorology, Environ. Monit. Assess., 152, 83, https://doi.org/10.1007/s10661-008-0298-2, 2009.

Gratsea, M., Liakakou, E., Mihalopoulos, N., Adamopoulos, A., Tsilibari, E., and Gerasopoulos, E.: The combined effect of reduced fossil fuel consumption and increasing biomass combustion on Athens' air quality, as inferred from long term CO measurements, Sci. Total Environ., 592, 115–123, https://doi.org/10.1016/j.scitotenv.2017.03.045, 2017.

Gros, V., Gaimoz, C., Herrmann, F., Custer, T., Williams, J., Bonsang, B., Sauvage, S., Locoge, N., d'Argouges, O., Sarda-Estève, R., and Sciare, J.: Volatile organic compounds sources in Paris in spring 2007, Part I: qualitative analysis, Environ. Chem., 8, 74–90, https://doi.org/10.1071/EN10068, 2011.

Guenther, A., Hewitt, C. N., Erickson, D., Fall, R., Geron, C., Graedel, T., Harley, P., Klinger, L., Lerdau, M., Mckay, W. A., Pierce, T., Scholes, B., Steinbrecher, R., Tallamraju, R., Taylor, J., and Zimmerman, P.: A global model of natural volatile organic compound emissions, J. Geophys. Res.-Atmos., 100, 8873–8892, https://doi.org/10.1029/94JD02950, 1995.

Gustafson, P., Barregard, L., Strandberg, B., and Sällsten, G.: The impact of domestic wood burning on personal, indoor and outdoor levels of 1,3-butadiene, benzene, formaldehyde and acetaldehyde, J. Environ. Monit., 9, 23–32, https://doi.org/10.1039/B614142K, 2007.

Hellén, H., Hakola, H., Haaparanta, S., Pietarila, H., and Kauhaniemi, M.: Influence of residential wood combustion on local air quality, Sci. Total Environ., 393, 283–290, https://doi.org/10.1016/j.scitotenv.2008.01.019, 2008.

IARC: Chemical Agents and Related Occupations, Monographs on the Evaluation of Carcinogenic Risks to Humans, 100, 249–285, 309–333, available at: http://monographs.iarc.fr/ENG/Monographs/vol100F/mono100F.pdf (last access: 5 October 2017), 2012.

Ibarra-Berastegi, G., Elias, A., Barona, A., Saenz, J., Ezcurra, A., and Diaz de Argandoña, J.: From diagnosis to prognosis for forecasting air pollution using neural networks: Air pollution monitoring in Bilbao, Environ. Model. Softw., 23, 622–637, https://doi.org/10.1016/j.envsoft.2007.09.003, 2008.

Jaimes-Palomera, M., Retama, A., Elias-Castro, G., Neria-Hernández, A., Rivera-Hernández, O., and Velasco, E.: Non-methane hydrocarbons in the atmosphere of Mexico City: Results of the 2012 ozone-season campaign, Atmos. Environ., 132, 258–275, https://doi.org/10.1016/j.atmosenv.2016.02.047, 2016.

Kalabokas, P., Viras, L., and Repapis, C.: Analysis of the 11-year record (1987–1997) of air pollution measurements in Athens, Greece, Part I: Primary air pollutants, Glob. Nest Int. J., 1, 157–168, 1999.

Kaltsonoudis, C., Kostenidou, E., Florou, K., Psichoudaki, M., and Pandis, S. N.: Temporal variability and sources of VOCs in urban areas of the eastern Mediterranean, Atmos. Chem. Phys., 16, 14825–14842, https://doi.org/10.5194/acp-16-14825-2016, 2016.

Kanakidou, M., Mihalopoulos, N., Kindap, T., Im, U., Vrekoussis, M., Gerasopoulos, E., Dermitzaki, E., Unal, A., Koçak, M., Markakis, K., Melas, D., Kouvarakis, G., Youssef, A. F., Richter, A., Hatzianastassiou, N., Hilboll, A., Ebojie, F., Wittrock, F., von Savigny, C., Burrows, J. P., Ladstaetter-Weissenmayer, A., and Moubasher, H.: Megacities as hot spots of air pollution in the East Mediterranean, Atmos. Environ., 45, 1223–1235, https://doi.org/10.1016/j.atmosenv.2010.11.048, 2011.

Kansal, A.: Sources and reactivity of NMHCs and VOCs in the atmosphere: A review, J. Hazard. Mater., 166, 17–26, https://doi.org/10.1016/j.jhazmat.2008.11.048, 2009.

Kassomenos, P., Kotroni, V., and Kallos, G.: Analysis of climatological 710 and air quality observations from Greater Athens Area, Atmos. Environ., 29, 3671–3688, https://doi.org/10.1016/1352-2310(94)00358-R, 1995.

Klemm, O., Ziomas, I. C., Balis, D., Suppan, P., Slemr, J., Romero, R., and Vyras, L. G.: A summer air-pollution study in Athens, Greece, Atmos. Environ., 32, 2071–2087, https://doi.org/10.1016/S1352-2310(97)00424-X, 1998.

Kourtidis, K. A., Ziomas, I. C., Rappenglueck, B., Proyou, A., and Balis, D.: Evaporative traffic hydrocarbon emissions, traffic CO and speciated HC traffic emissions from the city of Athens, Atmos. Environ., 33, 3831–3842, https://doi.org/10.1016/S1352-2310(98)00395-1, 1999.

Lalas, D. P., Veirs, V. R., Karras, G., and Kallos, G.: An analysis of the SO2 concentration levels in Athens, Greece, Atmos. Environ., 16, 531–544, https://doi.org/10.1016/0004-6981(82)90162-7, 1982.

Lalas, D. P., Asimakopoulos, D. N., Deligiorgi, D. G., and Helmis, C. G.: Sea-breeze circulation and photochemical pollution in Athens, Greece, Atmos. Environ., 17, 1621–1632, https://doi.org/10.1016/0004-6981(83)90171-3, 1983.

Lalas, D. P., Tombrou-Tsella, M., Petrakis, M., Asimakopoulos, D. N., and Helmis, C.: An experimental study of the horizontal and vertical distribution of ozone over Athens, Atmos/ Environ., 21, 2681–2693, https://doi.org/10.1016/0004-6981(87)90200-9, 1987.

Liu, Y., Shao, M., Lu, S., Chang, C.-C., Wang, J.-L., and Chen, G.: Volatile Organic Compound (VOC) measurements in the Pearl River Delta (PRD) region, China, Atmos. Chem. Phys., 8, 1531–1545, https://doi.org/10.5194/acp-8-1531-2008, 2008.

Mantis, H. T., Repapis, C. C., Zerefos, C. S., and Ziomas, J. C.: Assessment of the Potential for Photochemical Air Pollution in Athens: A Comparison of Emissions and Air-Pollutant Levels in Athens with Those in Los Angeles, J. Appl. Meteorol., 31, 1467–1476, https://doi.org/10.1175/1520-0450(1992)031<1467:AOTPFP>2.0.CO;2, 1992.

Melas, D., Ziomas, I., Klemm, O., and Zerefos, C. S.: Anatomy of the sea-breeze circulation in Athens area under weak large-scale ambient winds, Atmos. Environ., 32, 2223–2237, https://doi.org/10.1016/S1352-2310(97)00420-2, 1998.

Moschonas, N. and Glavas, S.: C3-C10 hydrocarbons in the atmosphere of Athens, Greece, Atmos. Environ., 30, 2769–2772, https://doi.org/10.1016/1352-2310(95)00488-2, 1996.

Moschonas, N., Glavas, S., and Kouimtzis, T.: C3 to C9 hydrocarbon measurements in the two largest cities of Greece, Athens and Thessaloniki, Calculation of hydrocarbon emissions by species, Derivation of hydroxyl radical concentrations, Sci. Total Environ., 271, 117–133, https://doi.org/10.1016/S0048-9697(00)00838-X, 2001.

Nester, K.: Influence of sea breeze flows on air pollution over the attica peninsula, Atmos. Environ., 29, 3655–3670, https://doi.org/10.1016/1352-2310(95)98468-N, 1995.

Paraskevopoulou, D., Liakakou, E., Gerasopoulos, E., and Mihalopoulos, N.: Sources of atmospheric aerosol from long-term measurements (5 years) of chemical composition in Athens, Greece, Sci. Total Environ., 527 (Supplement C), 165–178, https://doi.org/10.1016/j.scitotenv.2015.04.022, 2015.

Rappenglück, B., Fabian, P., Kalabokas, P., Viras, L. G., and Ziomas, I. C.: Quasi-continuous measurements of non-methane hydrocarbons (NMHC) in the Greater Athens area during medcaphot-trace, Atmos. Environ., 32, 2103–2121, https://doi.org/10.1016/S1352-2310(97)00430-5, 1998.

Rappenglück, B., Kourtidis, K., Melas, D., and Fabian, P.: Observations of biogenic and anthropogenic NMHC in the greater Athens area during the PAUR campaign, Phys. Chem. Earth Pt. B, 24, 717–724, https://doi.org/10.1016/S1464-1909(99)00071-4, 1999.

Saffari, A., Daher, N., Samara, C., Voutsa, D., Kouras, A., Manoli, E., Karagkiozidou, O., Vlachokostas, C., Moussiopoulos, N., Shafer, M. M., Schauer, J. J., and Sioutas, C.: Increased Biomass Burning Due to the Economic Crisis in Greece and Its Adverse Impact on Wintertime Air Quality in Thessaloniki, Environ. Sci. Technol., 47, 13313–13320, https://doi.org/10.1021/es403847h, 2013.

Salameh, T., Sauvage, S., Afif, C., Borbon, A., Léonardis, T., Brioude, J., Waked, A., and Locoge, N.: Exploring the seasonal NMHC distribution in an urban area of the Middle East during ECOCEM campaigns: very high loadings dominated by local emissions and dynamics, Environ. Chem., 12, 316–328, https://doi.org/10.1071/EN14154, 2015.

Sauvage, S., Plaisance, H., Locoge, N., Wroblewski, A., Coddeville, P., and Galloo, J. C.: Long term measurement and source apportionment of non-methane hydrocarbons in three French rural areas, Atmos. Environ., 43, 2430–2441, https://doi.org/10.1016/j.atmosenv.2009.02.001, 2009.

Schauer, J. J., Kleeman, M. J., Cass, G. R., and Simoneit, B. R. T.: Measurement of Emissions from Air Pollution Sources. 3. C1−C29 Organic Compounds from Fireplace Combustion of Wood, Environ. Sci. Technol., 35, 1716–1728, https://doi.org/10.1021/es001331e, 2001.

Seinfeld, J. H. and Pandis, S. N.: Atmospheric Chemistry and Physics: From Air Pollution to Climate Change, John Wiley & Sons, Hoboken, New Jersey, 2016.

Tsigaridis, K. and Kanakidou, M.: Global modelling of secondary organic aerosol in the troposphere: a sensitivity analysis, Atmos. Chem. Phys., 3, 1849–1869, https://doi.org/10.5194/acp-3-1849-2003, 2003.

Vrekoussis, M., Richter, A., Hilboll, A., Burrows, J. P., Gerasopoulos, E., Lelieveld, J., Barrie, L., Zerefos, C., and Mihalopoulos, N.: Economic crisis detected from space: Air quality observations over Athens/Greece, Geophys. Res. Lett., 40, 458–463, https://doi.org/10.1002/grl.50118, 2013.

WHO-IARC: Outdoor air pollution a leading environmental cause of cancer deaths, Press Release no221, 2013.

Zhang, Q., Wu, L., Fang, X., Liu, M., Zhang, J., Shao, M., Lu, S., and Mao, H.: Emission factors of volatile organic compounds (VOCs) based on the detailed vehicle classification in a tunnel study, Sci. Total Environ., 624, 878–886, https://doi.org/10.1016/j.scitotenv.2017.12.171, 2018.

Zhang, Y., Yang, W., Simpson, I., Huang, X., Yu, J., Huang, Z., Wang, Z., Zhang, Z., Liu, D., Huang, Z., Wang, Y., Pei, C., Shao, M., Blake, D. R., Zheng, J., Huang, Z., and Wang, X.: Decadal changes in emissions of volatile organic compounds (VOCs) from on-road vehicles with intensified automobile pollution control: Case study in a busy urban tunnel in south China, Environ. Pollut., 233, 806–819, https://doi.org/10.1016/j.envpol.2017.10.133, 2018.

Ziomas, I. C., Suppan, P., Rappengluck, B., Balis, D., Tzoumaka, P., Melas, D., Papayiannis, D., Fabian, P., and Zerefos, C. S.: A contribution to the study of photochemical smog in the greater Athens area, Beitr. Phys. Atmosph., 68, 191–204, 1995.

3.Conclusions

As stated in the conclusion of the article, a careful examination of the temporal, seasonal and diurnal variation of 11 NMHCs in Athens during the winter season has been performed. C2 NMHCs (ethane and ethylene) exhibited the highest concentrations (> 22 ppb and with mean values of 4.5 and 4.1 ppb respectively) and these are the first ever reported values of these compounds for the urban Athens area. The comparison of NMHCs between this work and past published studies for Athens showed a decrease of the NMHCs levels for a factor of 2 (i-butane) to 6 (benzene), which was also further affirmed by the comparison of published enhancement ratios to NOx and CO that have decreased. The temporal variability of the NMHCs presented an increasing trend from October (autumn, warm season) to December (winter, cold season). The factors affecting the observed levels have been examined, showing that low wind speed and a swallow boundary layer were the main parameters among atmospheric dynamics favoring the accumulation of NMHC in the air. In addition, the separation of the dataset to specific periods of pollution or not (namely "SP" smog and "nSP" non-smog periods) highlighted the effect of sources. This is supported also by the similar bimodal diurnal pattern that is consistent with the variability of other pollutants/tracers (CO, BC_{ff} and BC_{wb}).

Furthermore, the influence of sources emissions was evaluated from the development of the chemical profile of the morning peak and night-time enhancement period for Thissio. The morning chemical profile presented i-pentane, toluene and xylenes as the dominant compounds and it was in agreement with the profile that was derived from the data of the near-source campaign in Patission station, indicating an influence mainly from traffic. Isopentane was also the dominant NMHC in the night chemical profile; however, its contribution was significantly decreased from October to December, indicating a change in the composition of the night sources emissions. Nevertheless, the observations highlighted the strong impact of traffic and residential heating to NMHCs levels, which are now considered as the most important sources of VOC in winter.

This study introduced insights on the temporal variability and sources of the VOCs during the winter season. The next step is to examine the VOC variability over a full year in order to document and understand the seasonal variations on both VOCs levels and sources. The scope of the study will be extended to a longer dataset including also heavier VOCs (C6 - C12). The results of the entire campaign will provide the seasonal variability of these compounds, which was never reported in the literature. Moreover, the examination of the influence of atmospheric dynamics on a seasonal basis could further support the findings of the first article and provide new information for a better understanding of the driving processes of the VOC variability. This is the objective of the next chapter (**Chapter 4**).

Finally, since the scope of the article was not the source allocation of the emissions and taking into account the rather low variability in the dataset, it was neither possible to completely separate and quantify the contribution of the two main VOC sources nor to determine new ones. For that reason, the number and type of sources, as well as their contribution to the observed concentrations are evaluated in **Chapter 6**, by using a source-receptor statistical tool namely Positive Matrix Factorization (PMF) that was applied to the whole dataset.

CHAPTER 4 – Volatile Organic Compounds (VOC) in Athens during the 13-month monitoring period: Temporal variability and driving factors

TABLE OF CONTENTS FOR CHAPTER 4

Introduction

According to the published article presented in the previous chapter (**Chapter 3**) the concentrations of the studied **NMHCs** in Athens have **decreased** relative to the past (based on the observations of i-pentane, benzene and toluene), but at the same time, they are also higher than the reported values in other studies elsewhere (for the majority of the compounds). Nevertheless, these observations depict only the **cold season** and were limited to a few NMHCs/tracers compared to the variety of the target compounds of the MOP (Main Observation Period). What are the **levels** and **variability** of NMHCs in the other seasons and what are the effects of atmospheric processes and sources on these observations? These are the new questions that arose, by further considering the seasonal variability of meteorological parameters such as the temperature and the solar radiation, which can also have an impact on the NMHCs emission sources. Thus, the descriptive analysis of the MOP extended dataset is important for the understanding of the NMHC variability over a longer period in respect to the driving parameters, which in turn will contribute to their source allocation in the following chapter. In addition, the assessment of NMHC concentrations on the air quality will be evaluated on a yearly and seasonal basis through the comparison to other studies in urban areas.

Following the previous need, the **objectives** of the first part of this chapter are: **(1)** to report the levels of all the VOC that were monitored during the MOP (**Chapter 2**), and the next 13 months of measurements (February 2016 to February 2017) that were not documented in the published article; **(2)** to examine the seasonal and spatial variability, which, to our knowledge, was never reported for Athens in annual basis; **(3)** to investigate the effect of atmospheric dynamics on the observed concentrations; and **(4)** to compare our levels with the results of other studies. Therefore, the above examination feeds the discussion with robust results, while the understanding of the variability and its driving factors will help the source allocation that will follow in a next chapter.

In the same context and to facilitate the source apportionment, two seasonal intensive sampling campaigns in Thissio (Intensive Observation Period or IOP) were organised and conducted in winter and summer 2016 (**Chapter 2**). Briefly, these campaigns introduced information for additional VOC including heavier alkanes and intermediate VOC (IVOC), which can be used as tracers of targeted emission sources. Thus, the second part of this chapter deals with the **presentation** and **analysis** of the obtained **IOPs** datasets, with the same data treatment and analysis that was done for the NMHCs of the MOP: the levels of the new species are reported for both seasons, followed by the examination of their temporal and spatial variability, along with the possible factors that affects it.

1. C2 – C12 VOCs from the MOP

1.1 NMHCs levels

During the MOP that lasted in total 17-months (**Chapter 2**), 12 alkanes, 4 alkenes, 9 aromatics and 3 biogenic compounds were identified and quantified. Acetylene was also measured, but

the identification problems that were discussed in **Sect. 2.2.1** of **Chapter 2**, allowed the retrieval of only 61% of its data, mainly from winter 2016, spring 2016 and winter 2017. Furthermore, from **March 2016** to **February 2017** (common period of operation of the two GCs), **alkanes** averagely accounted for almost **50%** of the total NMHC concentration, followed by aromatics, alkenes and biogenic VOC (BVOC) with ~35%, ~7.5% and ~2% respectively (**Figure IV - 1**), however, the contribution varies depending on the season. For example, BVOC (sum of isoprene, α-pinene and limonene) contribute two times more in the total NMHC concentrations in summer than the other seasons, whereas alkenes contribution is two folded in winter relative to summer.

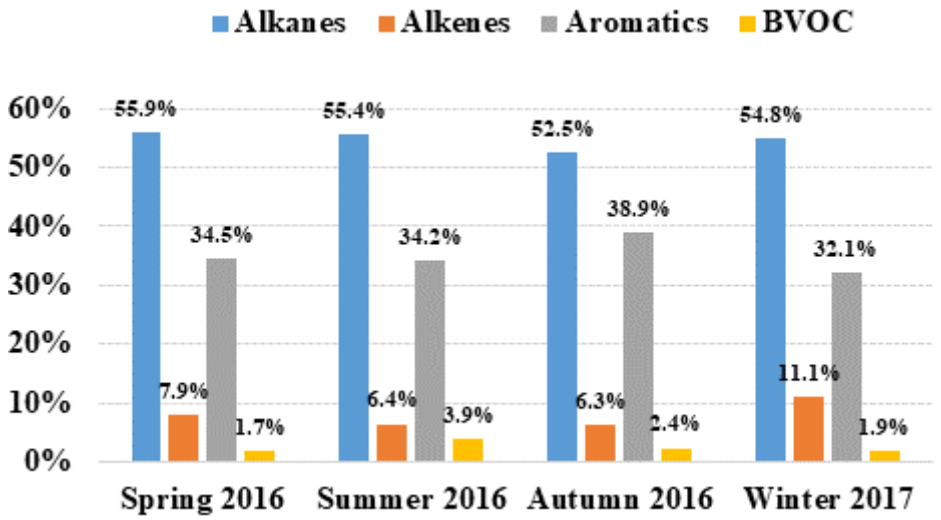

Figure IV - 1: Seasonal contribution of alkanes, alkenes, aromatics and BVOC to the total NMHC from 1 March 2016 to 28 February 2017. Note that for Autumn 2016 the periods when the GC C2 – C6 was not measuring, are not taken into account for the contribution.

The concentrations (and relevant statistical information) of the NMHCs from the MOP are listed in **Table IV – 1**. Among alkanes and alkenes, i-pentane and ethylene exhibit the highest mean concentration (9.5 μg m^{-3} and 3.7 μg m^{-3} respectively), with values during the campaign ranging from the limit of detection to 74 μg m^{-3} and 38 μg m^{-3} respectively. For aromatics, toluene and m-/p- xylenes prevail, with mean values of 6.6 μg m^{-3} and 4.2 μg m^{-3} respectively. **Benzene**, which is the only NMHC included in the European air quality standards due to its carcinogenicity to humans (IARC, 2012), presented a mean value of 1.9 μg m^{-3} for the whole campaign and an annual mean of **1.7 μg m^{-3}**(January to December 2016 2017; 92% data coverage over the maximum potential) which is **below** the **EU threshold** of 5 μg m^{-3}. Nevertheless, it is worthwhile noting that in **winter**, benzene concentrations are often higher than **10 μg m^{-3}**, with the highest recorded value being 31.1 μg m^{-3}. Among monoterpenes, α-pinene presented the highest mean concentration (0.7 μg m^{-3}), with levels ranging from 0.08 μg m^{-3} to 8.7 μg m^{-3}, whereas isoprene's mean value was 0.2 μg m^{-3}. Finally, concerning acetylene (not presented in Table IV - 1), a mean value for the whole campaign is not representative (due to the absence of data for an entire season), however, the mean concentrations in winter 2016 and 2017 are 6.3 ±5.1 μg m^{-3} (max value: 30.9 μg m^{-3}) and 4.8 ±4.5 μg m^{-3} (max value: 36.3 μg m^{-3}) respectively, denoting similar levels in winter for these two years.

Table IV - 1: Concentrations of NMHCs measured in the MOP, from 16 October 2015 to 28 February 2017. The compounds in *italics* were monitored from February 2016 to February 2017 from the GC C6 – C12.

NMHCs ($\mu g\ m^{-3}$)	Mean	Median	STD	Min	Max	Summer 2016 (mean±STD)	Winter 2017 (mean±STD)	(%) Data coverage
Ethane	4.80	3.52	4.16	0.08	34.32	2.68 (1.43)	5.18 (4.85)	74%
Ethylene	3.64	1.96	4.52	0.07	38.39	1.83 (1.88)	4.04 (4.97)	71%
Propane	4.17	2.40	4.74	0.04	36.79	1.98 (2.37)	4.71 (4.75)	74%
Propene	1.77	0.66	2.97	0.03	27.59	0.52 (0.70)	2.00 (3.15)	71%
i-Butane	3.80	1.76	5.01	0.04	42.23	1.55 (2.06)	3.81 (5.05)	75%
n-Butane	4.70	2.34	5.79	0.04	49.77	2.39 (3.1)	4.94 (6.28)	75%
Trans-2-butene	0.84	0.29	1.35	0.03	13.00	0.22 (0.36)	0.71 (1.13)	65%
1-Butene	0.85	0.35	1.32	0.03	12.98	0.24 (0.36)	0.80 (1.24)	66%
i-Pentane*	9.47	4.87	11.05	0.04	74.39	6.23 (5.89)	7.81 (10.43)	77%
n-Pentane	2.23	1.16	2.79	0.04	27.96	1.44 (1.69)	1.74 (2.2)	77%
Isoprene	0.16	0.06	0.31	0.04	4.06	0.48 (0.56)	0.12 (0.18)	80%
2-me-pentane	3.78	2.07	4.52	0.08	46.50	2.90 (2.60)	3.83 (5.37)	93%
n-Hexane	1.16	0.51	1.52	0.07	13.95	0.81 (1.09)	1.17 (1.66)	93%
Benzene	1.91	1.14	2.34	0.05	31.14	0.85 (0.76)	2.63 (3.36)	92%
i-Octane	0.41	0.08	0.78	0.07	10.52	0.22 (0.34)	0.47 (1.04)	93%
n-Heptane	0.44	0.18	0.63	0.07	7.04	0.26 (0.34)	0.51 (0.79)	93%
Toluene	6.98	3.41	9.09	0.06	97.78	4.54 (5.08)	7.57 (10.78)	93%
n-Octane	0.47	0.16	0.70	0.07	9.20	0.30 (0.42)	0.52 (0.85)	93%
Ethylbenzene	1.33	0.67	1.75	0.07	19.11	0.81 (0.89)	1.46 (2.15)	93%
m-/p- Xylenes	4.20	2.05	5.60	0.13	61.25	2.56 (2.80)	4.62 (6.87)	93%
o - Xylene	1.38	0.65	1.97	0.06	21.64	0.81 (0.95)	1.52 (2.41)	93%
Nonane	0.31	0.15	0.36	0.06	3.59	0.25 (0.28)	0.31 (0.41)	93%
1.3.5 TMB	0.31	0.05	0.61	0.05	6.70	0.15 (0.29)	0.36 (0.77)	93%
1.2.4 TMB	1.40	0.63	2.13	0.07	24.78	0.86 (1.11)	1.65 (2.80)	93%
1.2.3 TMB	0.26	0.08	0.48	0.07	5.43	0.21 (0.37)	0.27 (0.55)	94%
α-Pinene	0.70	0.44	0.83	0.08	8.86	0.70 (0.66)	0.67 (0.91)	88%
Limonene	0.33	0.07	0.78	0.07	9.86	0.15 (0.31)	0.48 (1.06)	93%

*Co-elutes with cis-2-butene

Figure IV – 2 presents the mean monthly variation of selected C2 – C12 NMHCs, covering the total period of measurements, while in **Figure A1** of **Annex IV** the temporal variability of the rest of the compounds is presented. The selected species are considered representative of the homologues VOC classes (alkanes, alkenes, aromatics, biogenic VOC), with correlation coefficients higher than 0.69 (**Table V -A1** of **Annex IV**), except ethane's relationship to heavier alkanes ($R^2 < 0.69$). More specifically, **alkanes** are represented by **ethane** and **n-butane**, **alkenes** by **propene**, **aromatics** by **benzene** and **toluene** (as tracers of different sources; i.e. in Panopoulou et al., 2018 and Borbon et al., 2018), and **BVOC** by **isoprene**. The seasonal variability for all the compounds apart from isoprene, α-pinene and limonene, exhibits a distinct cycle with **high** concentrations in **winter** and **lower** in **summer**, whereas in spring and autumn the levels vary in between. More specifically, the C2 – C6 NMHCs concentrations increase from autumn 2015 to winter 2016, then they slowly decrease from spring to summer 2016 followed by a gradual increase to autumn 2016 and winter 2017. The same seasonal cycle is also observed for the C6 – C12 NMHCs. Furthermore, the duration of the campaign allowed

the examination of the inter-annual variability; the transition from autumn to winter follows the same pattern for both years (2016 and 2017), although in autumn 2016 the concentrations are similar (i. e. n-butane) or higher (i. e. toluene) to winter 2017, whereas NMHCs levels in winter 2016 are usually higher than winter 2017. Nevertheless, it is worth noting the important **day-to-day variability** that is observed in **Figure IV - A1**. In the following paragraphs, the selected NMHCs will be used for the analysis and discussion, to facilitate the understanding of the findings. However, **isoprene**, ***α*-pinene** and **limonene** will be **presented separately** due to the differences in their variability compared to the other NMHCs (**Table IV - 1** and **Figure IV - A1** of the **Annex IV**), and their origin would be further investigated.

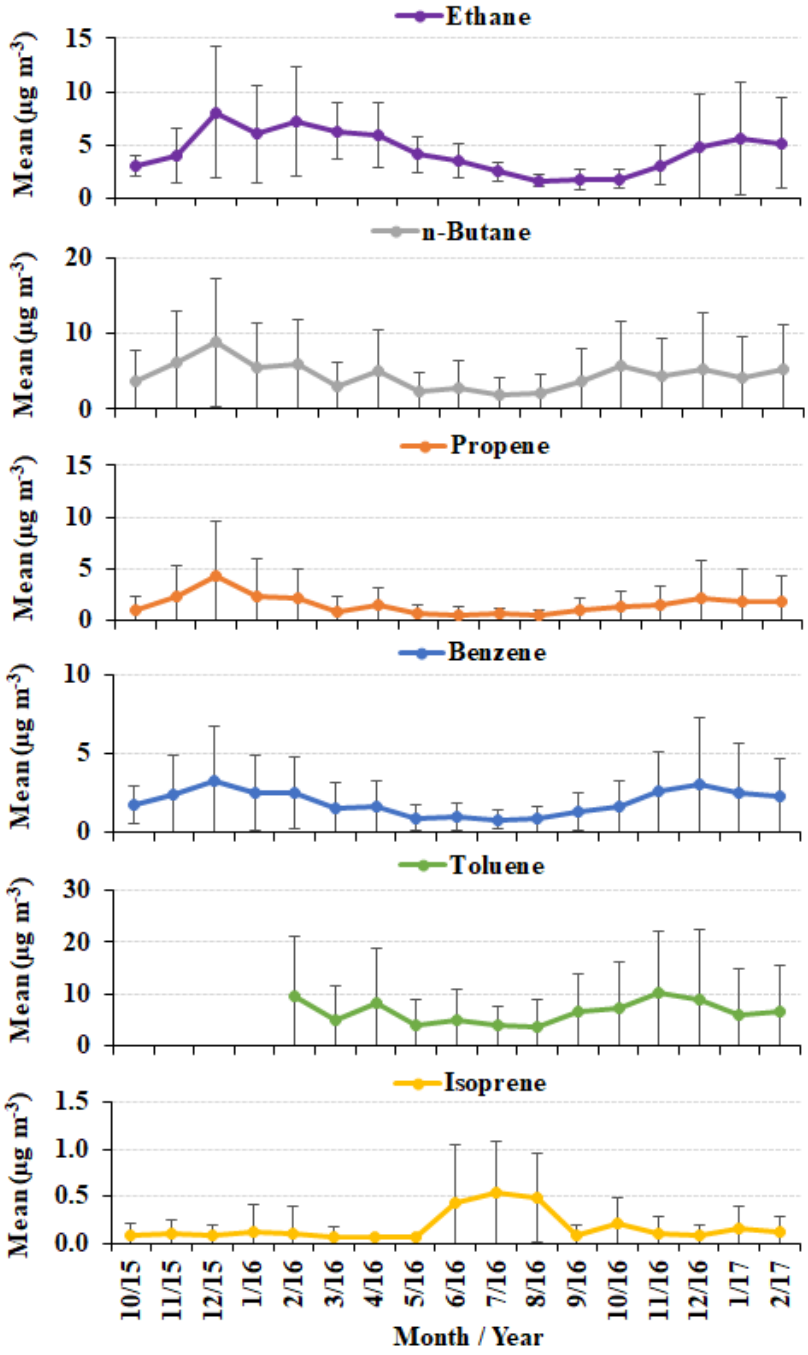

Figure IV - 2: Monthly variability of the mean levels for selected NMHCs over the period from October 2015 to February 2017.

1.2 Seasonal diurnal variability

In **Figure IV – 3** the seasonal diurnal variability of ethane, n-butane, propene, benzene and toluene (reference compounds; **Sect. 1.1** of **this chapter**) is presented and the rest of the compounds are depicted in **Figure IV – A2** of the **Annex IV**. NMHCs exhibit a **bimodal diel cycle** regardless the season, with a **morning maximum** at 6:00 – 10:00 LT, followed by a noon to early **afternoon plateau shaped minimum** and a **night-time enhancement period** after 20:00 LT. According to **Figures IV - 3** and **IV - A2** the following observations are derived:

(1) The duration of the night-time enhancement period is longer for heavier compounds like C7 – C9 alkanes and TMBs, compared to lighter ones like butanes;

(2) For C6 – C9 alkanes and aromatics, the mean hourly concentrations are on the same levels for every season except of summer that are lower;

(3) For C2 – C5 alkanes and alkenes, the morning peak is higher by 1.3 and 1.7 times (i. e. for propane and n-pentane respectively) and the night enhancement period levels increase by 2 times (i. e. for trans-2-butene and i-pentane) in winter.

(4) Ethane's levels increase dramatically from autumn 2016 to winter 2017 (factors of 2 to 3.5 depending on the hour) compared to the other NMHCs, suggesting additional emissions of this compound in winter (cold season), probably related to wood burning for residential heating (**Chapter 3**).

(5) The levels in autumn 2016 are comparable to winter 2017 for the majority of the species.

(6) The amplitude of the morning and night levels vary depending on the season. In particular, the night-time concentrations increase during the transition from summer to winter, tending to exceed over the morning levels (**Figures IV – 3** and **IV - A2** of the **AnnexIV**). It is worth noting that in winter 2017, the morning maximum was 2 (i. e toluene and n-butane) to 3.5 (i.e benzene) times higher than summer, whereas the night maximum increases considerably for the majority of NMHCs (2 to 9 times) and especially for propene and benzene (factors of 7 and 5 respectively).

In **Chapter 3** it was shown that the observed seasonal variability in autumn 2015 and winter 2016 was influenced by the combination of two parameters: **(1) atmospheric dynamics** and **(2) emission from sources**. More specifically, in winter, the **lower** height of the Planetary Boundary Layer (**PBL**), the frequent occurrence of **stagnant conditions** (low wind speeds and absence of rainfall), as well as the **stronger emissions** of NMHCs from sources, result in **high** ambient **levels** of pollutants. On the contrary, in **summer** the **opposite conditions** are expected: (1) NMHCs emissions reduce as a result of the lower anthropogenic activity in the city due to the vacation period, (2) the height of PBL is higher than winter both during day and night allowing a better vertical mixing of pollutants (Alexiou et al., 2018), (3) the occurrence of "Etesians" cause the ventilation of the Athenian basin (Cvitas et al., 1985; Katsoulis, 1996; Lalas et al., 1983), and (4) photochemistry is more intense in this season, favoring the oxidation of the NMHCs and therefore the decrease of their levels. Thus, due to the different atmospheric

conditions that are observed depending on the season, in the following paragraphs we examine the influence of atmospheric dynamics (photochemical removal, PBL height, meteorological parameters) , as well as the impact of emissions from sources based on the relationship of VOC to other pollutants.

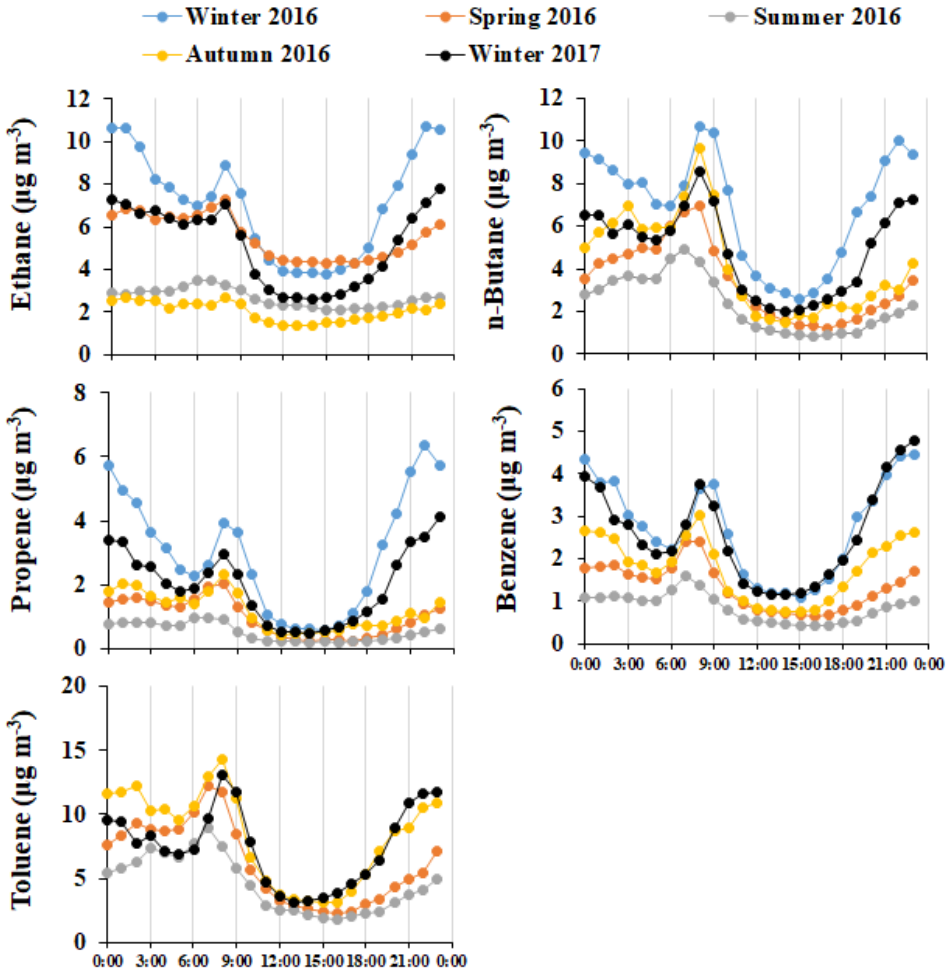

Figure IV - 3: Seasonal diurnal variability of selected NMHCs for the period 1 December 2015 to 28 February 2017, and for toluene from 1 March 2016 to 28 February 2017, in order to cover complete seasons.

1.3 Factors affecting the temporal variability

Once emitted in the atmosphere, NMHCs undergo various processes resulting in their chemical transformation or vertical/horizontal dispersion (**Chapter 1**, **Sect. 1.3**). In this context, the possible photochemical depletion of the VOC levels will be firstly examined, then the effect of the height of the planetary boundary layer will be considered, followed by the examination of their relationship to wind velocity, wind direction and temperature. In the last paragraph of this section, the influence of the emission from sources will be investigated through the linear regression with other pollutants.

1.3.1 The effect of photochemistry

The reactivity of the compounds can be expressed in terms of their atmospheric lifetime, in function of their principal oxidation pathway (**Chapter 1**, **Sect. 1.3**). With regard to the reaction with the OH radicals (and a specific atmospheric mean level for them; Atkinson, 2000), alkanes have a lifetime of some days (e .g. propane and n-octane with a lifetime of 10 to 1.3 days respectively), which characterize them as less reactive compared to alkenes that present a lifetime of some hours (e. g. ethylene and propene with a lifetime of 36 to 5.3 hours). Aromatics on the other hand present diverse reactivities; benzene has a lifetime of 10 days and m-xylene only 6 hours (Atkinson, 2000). However, unsaturated compounds like trans-2-butene and terpenes, react rapidly also with O_3 (throughout the day) and NO_3 radical during night, resulting in comparable or lower lifetimes with the reaction to the OH radical (e.g. for isoprene,1.5 hours and 50 minutes for the reaction to OH and NO_3 radicals respectively). Thus, for the correct assessment of the photochemical depletion and the atmospheric oxidation in general, especially for the very reactive compounds, the lifetimes of NMHCs in respect to the main atmospheric oxidants should be evaluated by using their current levels in Athens. However, this is not possible in our case since there are no reported concentrations for the OH and the NO_3 radicals.

Nevertheless, the approach of Salameh et al. (2015) is applied to estimate roughly the possible influence of the reaction to the OH radical (main reaction pathway for the majority of the compounds); this uses linear regressions between NMHCs that are having contrasted lifetimes, allowing an estimation of its impact that is expected to be higher in summer. In this approach, atmospheric dilution and mixing are not considered as they are similar for both compounds. The possible effect will be reflected on the slope of their linear regression as a result of the different reactivity of the selected compounds (Gelencsér et al., 1997). In our case, three reactive compounds, ethylene, 1.2.4 TMB and m-/p- xylenes are examined against two less reactive species, benzene (**Fig. IV – 4a,b**) and n-butane **(Fig. IV – 4c**), for day (09:00 – 17:00 LT) and night (21:00 – 05:00 LT). In particular, ethylene, 1.2.4 TMB and m-/p- xylenes have a lifetime of ~1.5 day, 6 hours and 4 hours respectively (Atkinson, 2000), whereas benzene and n-butane have a lifetime of ~9.5 days and 4.7 days respectively (Atkinson, 2000). Additionally, summer and winter day- and night-time data are plotted in Figure **IV - 4,** assuming that during night the reaction to the OH radical is insignificant (low levels due to the absence of insolation) and the composition of emissions remains the same. The daytime and nighttime scatterplots of ethylene (**Fig. IV – 4a**) agree very well for both summer and winter, whereas for m- / p- xylenes and 1.2.4 TMB **(Figs. IV – 4b,c**) a decrease of 1.1 and 1.5 times of the slope for the day-time points is observed in summer. This indicates a comparable effect for the daytime and nighttime oxidation for the less reactive compounds, and an increase of the daytime impact for the most reactive compounds (like 1.2.4 TMB).

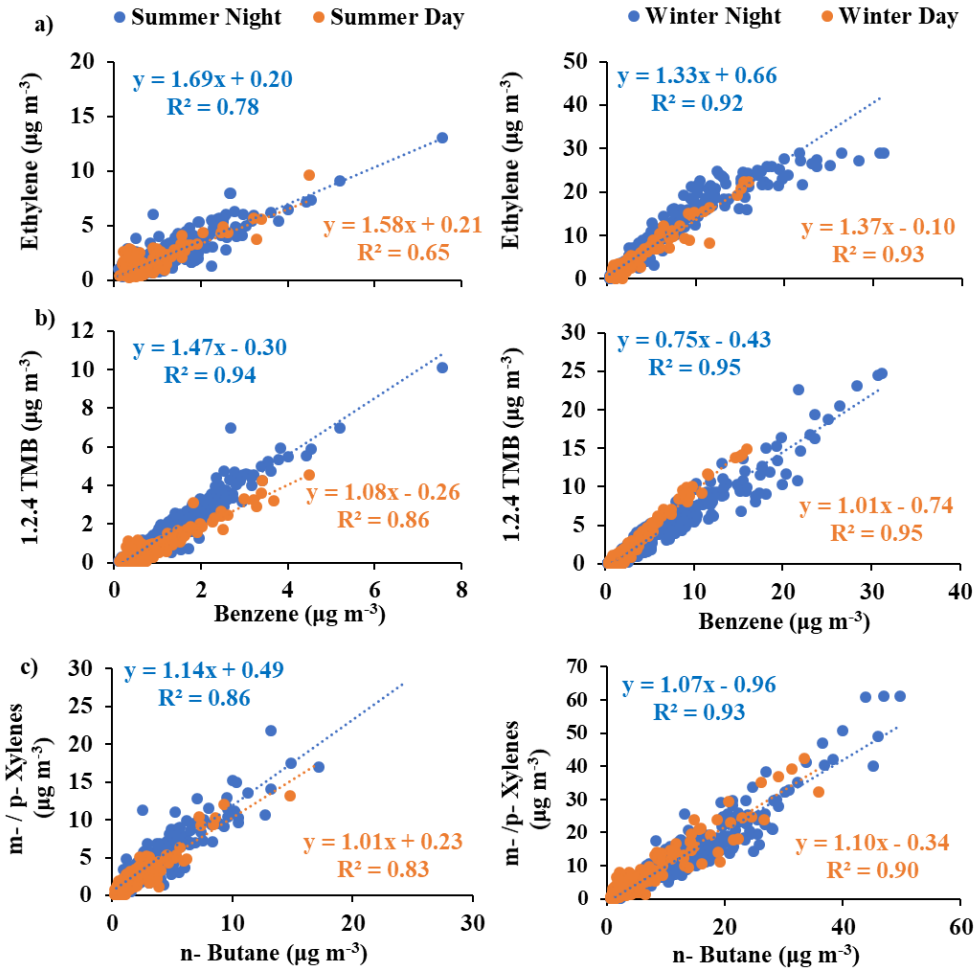

Figure IV - 4: Scatterplots of selected NMHCs to benzene (a,b) and n-butane (c) for the night-time (21:00 – 05:00 LT) and day-time (09:00 – 17:00 LT) concentrations in summer 2016 (1st column) and winter 2017 (2nd column). Note that for the same set of compounds, the x and y axis are different for summer and winter.

1.3.2 The influence of the PBL height

Among atmospheric dynamics, the boundary layer evolution determines the pollutants abundance and diurnal variability. Briefly, the PBL height is influenced by temperature, solar radiation and wind speed, exhibiting its highest height in summer (2090 m for July) and its lowest one in winter (982 m in December) (Alexiou et al., 2018). During our campaign there were no parallel measurements for the PBL determination, however Alexiou et al., (2018) measured it for 5 years using a lidar system, reporting a mean annual height of ~1617±324 m and ~892±130 m for the day and night respectively. The swallower PBL during night favors the accumulation of pollutants, whereas the daily growth allows their dispersion, as a result of the better ventilation of the basin. The diurnal variability of NMHCs is opposite to the evolution of the PBL in general terms, as it can be seen in **Figures IV – 3** and **Figure IV - A2 (Annex IV)**, however the important increase of the night winter levels compared to summer (**Sect. 1.2 of this chapter**) cannot be attributed only to the decrease of the PBL, which was also observed in Panopoulou et al. (2018). For the better understanding of the latter, the winter concentrations

were normalized relative to the mixing layer height (MLH), by using model-estimated hourly MLH values at 1o x 1o resolution. These were obtained over the station's area for the study period by using the HYSPLIT (HYbrid Single-Particle Lagrangian Integrated Trajectory) model (Draxler and Rolph, 2016) turbulent kinetic energy (TKE) profile method (Dumka et al., 2018, 2019). Specifically, the winter mean hourly values of the reference compounds are multiplied by the ratio of the seasonal-mean MLH at each hour with the minimum hourly seasonal-mean MLH, occurring during the early morning hours based on the proposed method of Bansal et al. (2019) (**Fig. IV - 5**). Unfortunately, this method is applied only in winter because atmospheric oxidation of NMHCs is not considered in the previous calculation, whereas it is considered less important in winter. In **Figure IV – 5** is apparent that both measured and normalized concentrations of NMHCs have rather similar diurnal cycles, whereas the MLH effect becomes evident only during the daytime. This indicates that during night the increased VOC and BC levels are exclusively attributed to sources than to MLH variability.

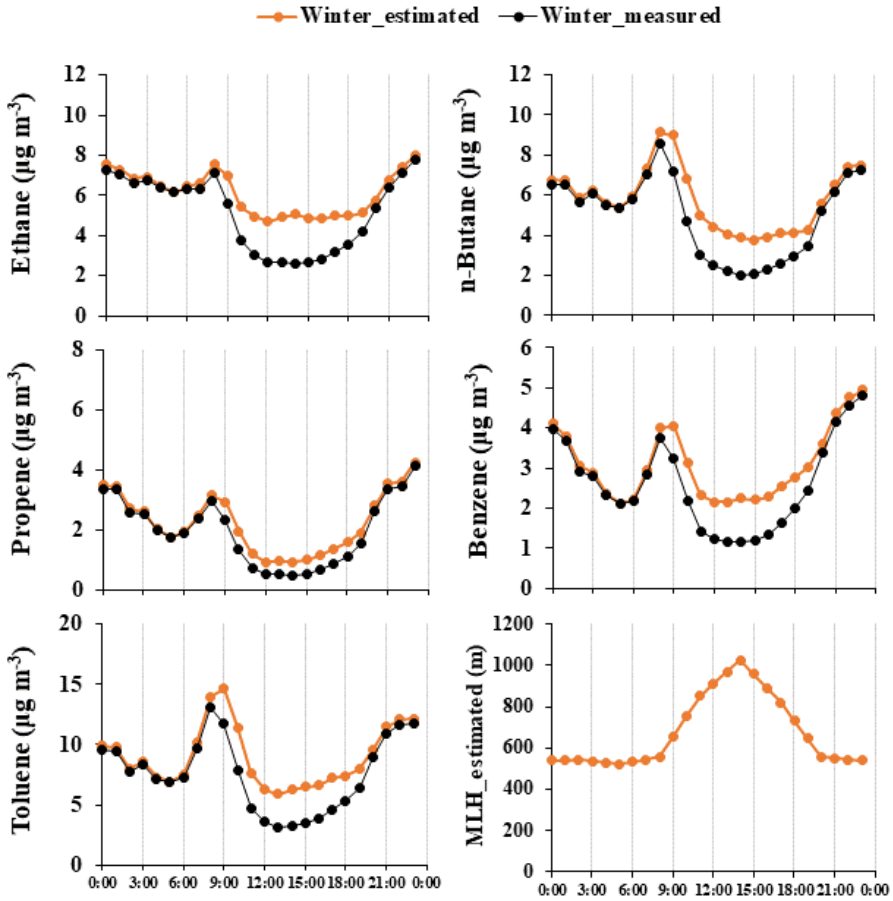

Figure IV - 5: Mean diurnal variation of the selected NMHCs, as well as their MLH-normalized values in winter 2017. The last figure includes the seasonal-mean diurnal cycle of the MLH (m) obtained from HYSPLIT

1.3.3 The influence of meteorology on the levels

Figure IV – 6 presents the monthly variability of solar radiation, ambient temperature, relative humidity and wind speed for the total period of measurements. However, only the period from **winter 2016** to **winter 2017** will be examined in detail in the discussion, since the temporal

trend in autumn 2015 and winter 2016 was already presented in **Chapter 3** (Panopoulou et al., 2018). Briefly, ambient temperature and relative humidity decrease from autumn 2015 to winter 2016, with the latter remaining stable throughout winter 2016. On the contrary, wind speed and solar radiation do not present significant changes.

Starting from solar radiation (**Fig. IV – 6a**), the lowest levels are encountered in cold months and especially in winter (mean value: 86.3 ±144.2 W m^{-2}), followed by a gradual increase towards summer that the highest values are recorded (mean value: 336.1 ±377.6 W m^{-2}). Furthermore, ambient temperature (**Fig. IV – 6b**) follows the variability of solar radiation, with increasing values from winter 2016 (mean value: 12.1±4.2°C) towards summer (mean value: 28.5 ±4.0°C) when it reaches its highest values in accordance to the higher solar intensity; finally the levels decrease again from autumn (mean value: 19.7 ±5.2°C) to winter (mean value: 9.2 ±3.9°C). Moreover, the trend of solar radiation and temperature drives also the seasonal variability of relative humidity that is the exact opposite, with the lowest values in summer (~ 42.8 ±12.1%) and the highest in winter (~ 62.0 ±12.7 %). On the other hand, although the mean levels of wind speed are similar for almost all seasons, an increase is observed in summer.

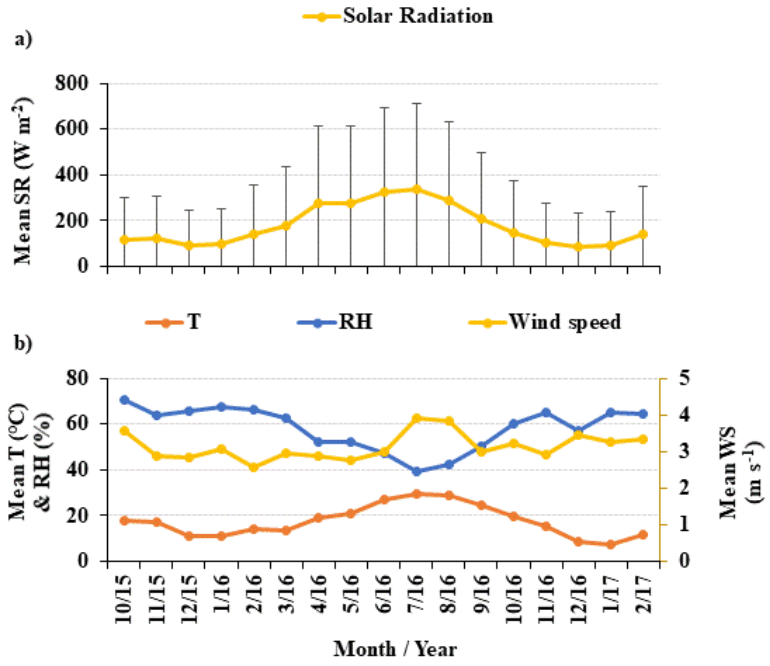

Figure IV - 6: (a) Mean monthly variability of solar radiation; The bars indicate the standard deviation; (b) Mean monthly variability of temperature, relative humidity and wind speed for the period of 16 October 2015 to 28 February 2017.

The role of temperature (**Fig. IV - 7**), wind speed (**Fig. IV - 7**) and wind direction (**Figs. IV – 8, 9**) to the NMHCs concentration trend is investigated for every season for the selected compounds and in **Figure IV - A3** and **A4** for the rest of the VOC. The highest concentrations are associated with wind speed less than 3 m s^{-1}, indicating the influence of emissions from sources close to the station (**Fig IV – 7, 1st row**). During the campaign, winds from the NE direction and in general the N to E sector occurred more frequently, followed by the winds from

SSW direction and the S to W sector (**Fig. IV – 8a**), which is the typical wind circulation as reported in other studies (**Sect. 2.4**, **Chapter 1**). Moreover, air masses from N to E directions, often associated with high velocity, prevail in every season except of spring 2016, in which winds from the S – W sector exhibit the highest occurrence (**Figs IV – 8b - f**). Therefore, the comparison of the wind roses of winter 2016 and winter 2017 (**Figs IV – 8b, f**) showed that NE winds of high speed occurred more often in winter 2017 than in winter 2016; these air masses favor the ventilation of the basin (**Sect 2.4.1** of **Chapter 1**), justifying partly the lower concentrations of some compounds in winter 2017 compared to winter 2016.

The geographical location of the air masses can influence the observed concentrations of NMHCs, due to their enrichment from emissions of sources along their trajectory to the monitoring station, in addition to their depletion due to photochemical reactions (aging of the mass) and the atmospheric dilution (Ashbaugh et al., 1985; Debevec et al., 2017). Consequently, after the examination of the wind roses, the possible influence of wind direction on NMHCs levels is investigated from the pollution roses of the representative compounds for the whole period of measurements (**Figure IV – 9**). An enhancement of the levels is observed for wind speed under 3m s^{-1} (also observed previously in Figure **IV –7**), which is unrelated to wind direction. In addition, the lowest values that are recorded for wind speed higher than 3m s^{-1} they are related to NE, S and W directions, which are among the most frequent air origins.

Concerning the rest of the meteorological parameters, relative humidity is not having an influence on VOC levels (graphs not shown here). Furthermore, NMHCs exhibit non-uniform relation to ambient temperature (**Fig IV – 7**, **2nd row**). For C2 – C5 alkanes, high concentrations are associated with temperatures between 5°C and 15°C (± 5°C) with the exception of summer that increased levels are found close to 30°C (± 5°C). The latter is more evident for butanes and pentanes. For aromatics and C6 – C9 alkanes, the scatterplots show that for every season except of summer, increased levels are observed around the mean ambient temperature of the season (± 5°C of the mean value); in summer, high levels are found close to 22°C (± 5°C). Nevertheless, it is worth noting that in winter, high concentrations are found for low ambient temperatures (< 10°C). The above observations indicate two different relationships to ambient temperature. In summer, the high temperatures probably increase the evaporation of some compounds, as it is seen for example in light alkanes. On the contrary, in winter, based on the volatility of the studied NMHCs (**Chapter 1**, **Sect. 1.1**), lower concentrations were expected especially for cold temperatures (< 10°C). Thus, the high winter levels for low temperatures are probably associated to additional winter emissions from sources. This is corroborated also by the observations of Panopoulou et al. (2018).

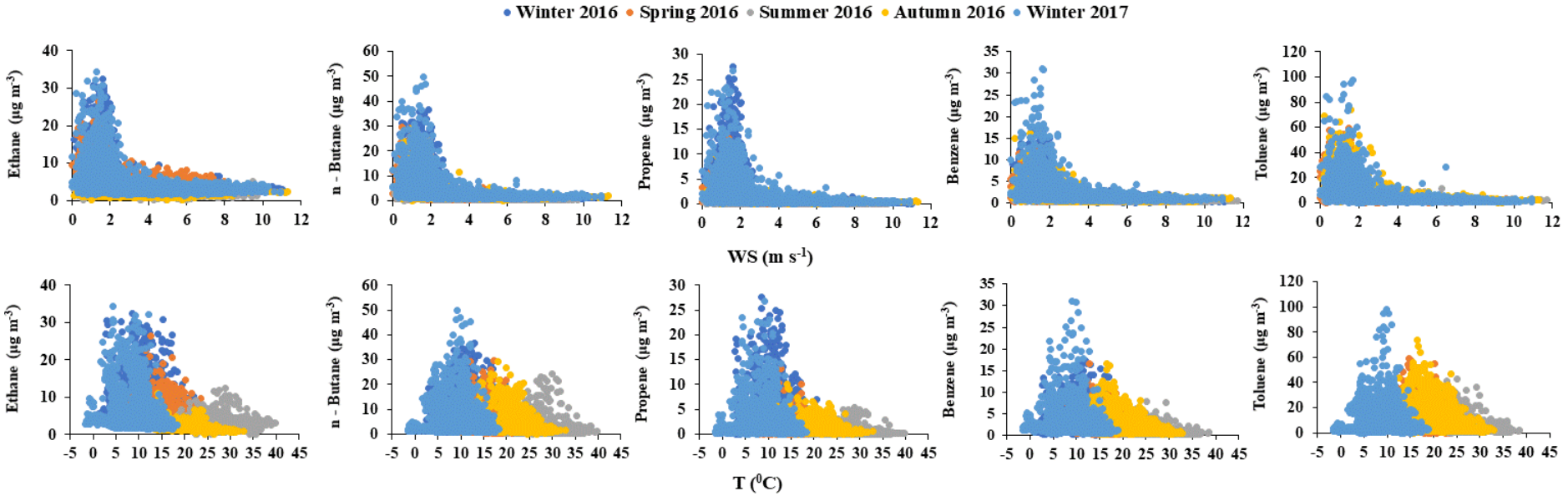

Figure IV - 7: Relationship of selected NMHCs to wind speed (1st row) and ambient temperature (2nd row) for every season, from 1 December 2015 to 28 February 2017 for the C2 – C6 compounds and from 1 March 2016 to 28 February 2017 for the C6 – C12 compounds.

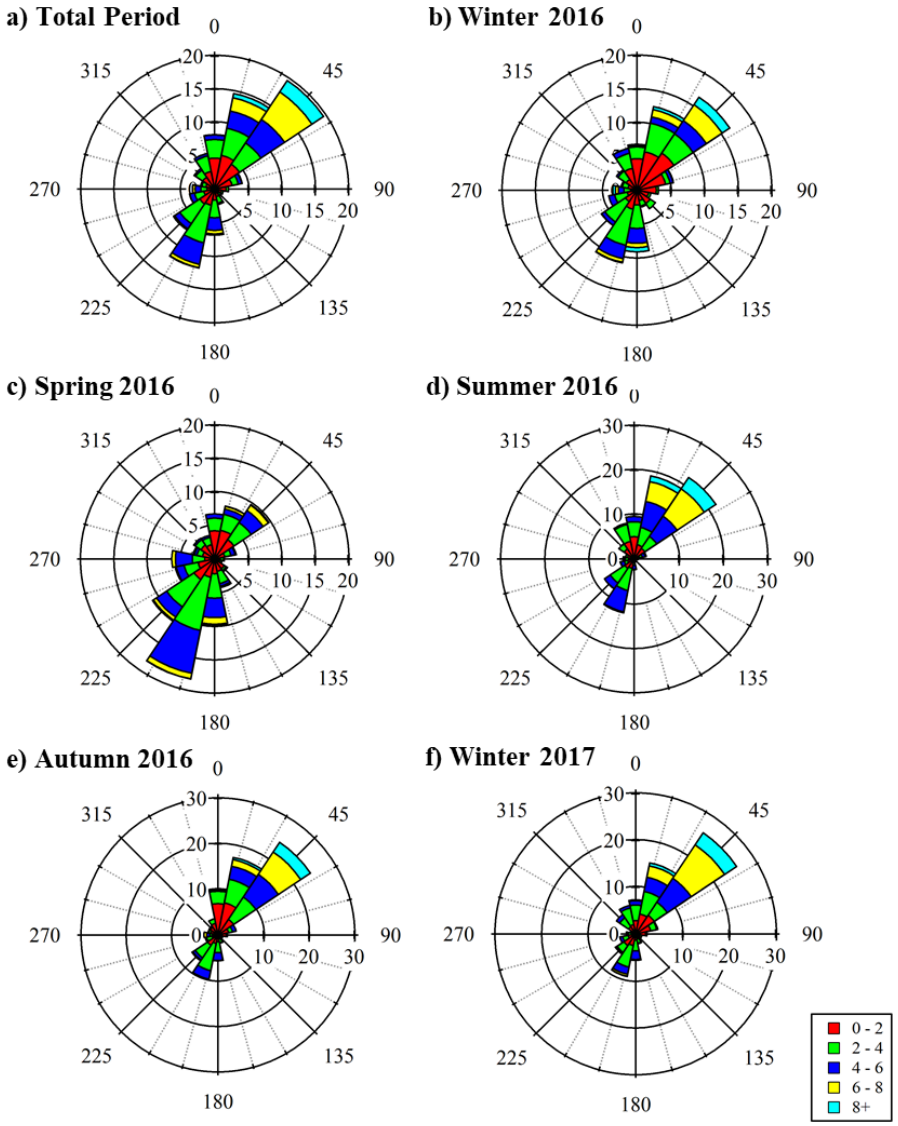

Figure IV - 8: Wind roses of (a) the total period of measurements (16 October 2015 – 28 February 2017); (b) winter 2016; (c) spring 2016; (d) summer 2016; (e) autumn 2016 and (f) winter 2017

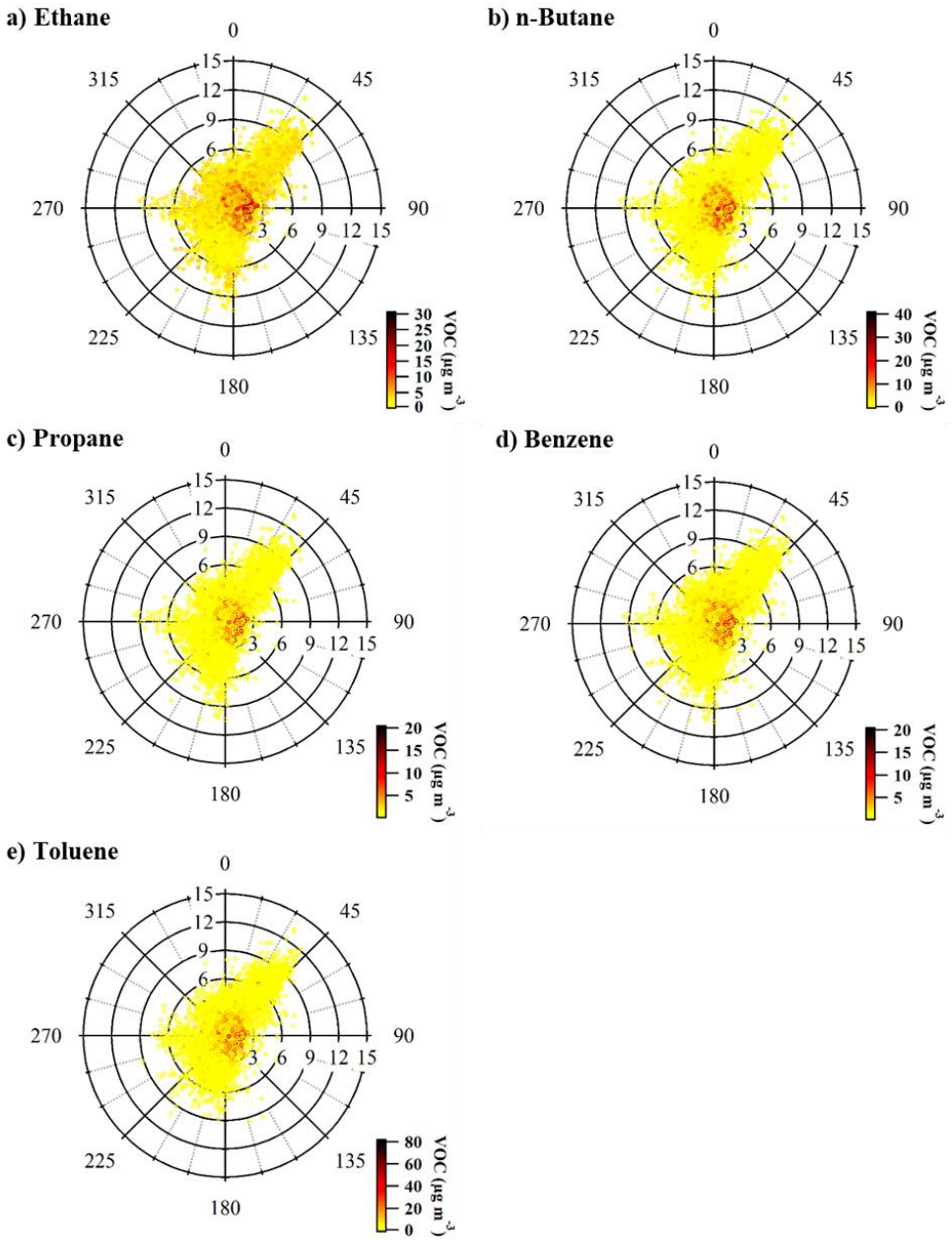

Figure IV - 9: Pollution roses of (a) ethane; (b) n-butane; (c) propene and (d) benzene from 16 October 2015 to 28 February 2017; and (e) toluene from 1 February 2016 to 28 February 2017.

1.3.4 Effect of emissions from major pollution sources

In parallel to the Athens VOC campaign, additional pollutants were monitored in Thissio station, as it is mentioned in **Sect. 2.6** of **Chapter 2**. From these, NO_x, CO, BC, BC_{ff} and BC_{wb} are chosen for the further analysis, as tracers of the main anthropogenic sources of pollutants in Athens, which are traffic and residential heating (Gratsea et al., 2016; Kaltsonoudis et al., 2016; Panopoulou et al., 2018). In **Table IV - A2** of **Annex IV** the concentration and statistics of these compounds are given and in **Figure IV – 10** their seasonal diurnal variability is presented. In general, the mean levels of the selected pollutants are higher in winter and lower in summer, whereas in spring and autumn the concentrations are in between. Remarkably, the

levels in winter 2016 are higher than winter 2017, as it is also observed for the examined NMHCs in **Sect. 1.2** (**this chapter**).

The diurnal variability of NO_x, CO, BC, and BC_{ff} presents a bimodal pattern regardless of the season, with a morning maximum at 06:00 – 10:00 LT and a night-time enhancement period starting at 18:00 LT (**Fig. IV – 10**). On the other hand, a diurnal variability of BC_{wb} is notable only in autumn and winter, exhibiting a night maximum at 23:00 – 00:00 LT, followed by the gradual decrease of the levels until the appearance of a low secondary morning peak. Furthermore, the amplitude of the maxima changes depending on the season. For NO_x and CO both the morning maximum and the night-time enhancement period are 3 and 2 times higher in winter than summer respectively. In addition, compared to summer, BC exhibits a remarkable elevation during winter nights (taking as reference winter 2017), due to the increase of BC_{wb} by a factor of 12, in contrast to BC_{ff} that increases only by a factor of 3. The latter is the result of the impact of wood burning for residential heating on BC_{wb} ambient concentrations as it is shown elsewhere (Gratsea et al., 2017). Moreover, the morning levels of BC_{wb} also increase towards winter 2017 by a factor 2, compared to both summer and autumn 2016.

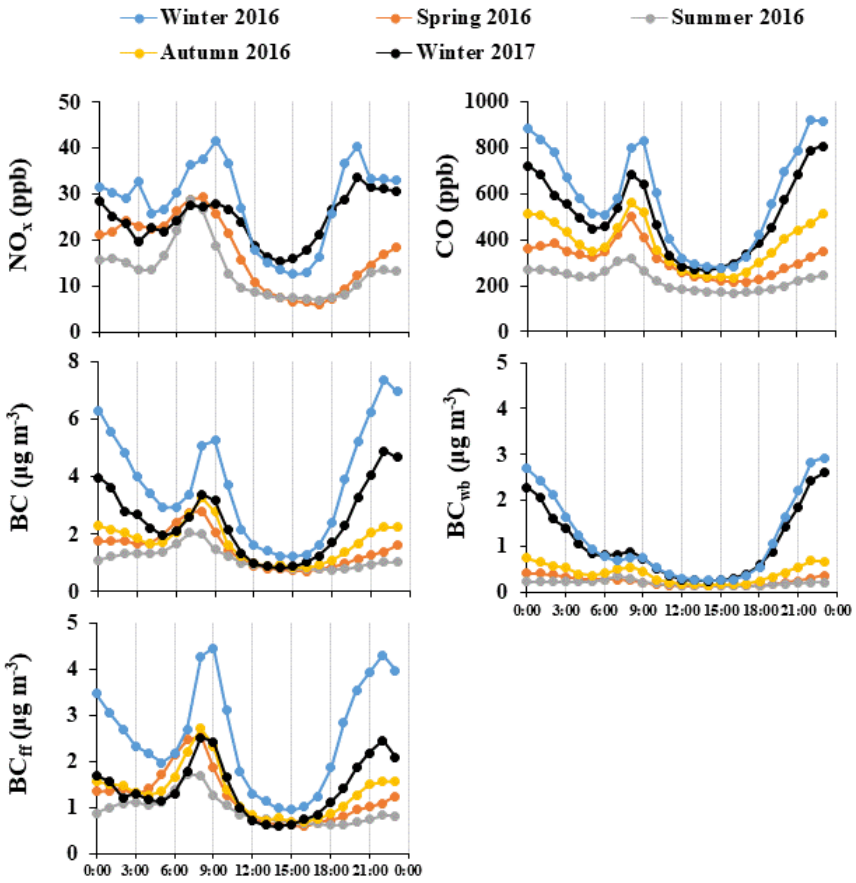

Figure IV - 10: Seasonal diurnal variability of NO_x, CO, BC, BC_{wb} and BC_{ff} from 1 December 2015 to 28 February 2017 in order to cover complete seasons. Note that for NOx autumn is not included due to the low data coverage (<30%).

It is apparent that the anthropogenic NMHCs and NO_x, CO and BC exhibit a similar seasonal diurnal profile considering both the trend and the intensity of the levels. This indicates common

sources for these compounds and generally a similar influence from atmospheric dynamics. This is also observed in Panopoulou et al. (2018; **Chapter 3**) for autumn 2015 and winter 2016.

Finally, the latter is further affirmed from the interspecies correlation, presented in **Table IV - A3** of the **Annex IV**. The majority of VOC are correlated ($R^2 > 0.57$) to BC, BC_{ff} and CO. NO_x (R^2: 0.36 – 0.8) are correlated with $R^2 > 75$ with C4– C5 alkanes and aromatics, but only with 1.2.4 from the TMBs. BC_{wb} presents a very good relationship with propene (R^2: 0.78), and good relationships (R^2: 0.61 – 0.69) with the rest of C2 – C3 alkanes and alkenes, 1-butene and benzene. In addition, more and better correlations are observed for winter (2017) than summer (2016) (Tables not shown). Nevertheless, the determination of typical source profiles and the corresponding contribution to NMHC levels and seasonal variability is conducted in the following chapter.

1.4 Comparison with other studies

After the examination of the temporal and spatial variability of the VOC in Athens and the identification of its main drivers, this last section is dealing with the assessment of these levels compared to other cities, particularly the few ones existing in the Mediterranean region but also with some cities worldwide A first comparison of the NMHCs levels of our campaign was conducted in the frame of the 1st article (Panopoulou et el., 2018; **Chapter 3**) only to Beirut (Salameh et al., 2015) due to the variety of the reported compounds. Concentrations of benzene, toluene and xylenes were also available for Cairo (Khoder, 2007) and Barcelona (Seco et al., 2013), however the comparison to the current NMHC levels was not possible because TEX levels were not included in the 1st article, in addition to the great uncertainty it would have as a result of the different sampling periods. Nevertheless, the comparison showed that the winter levels in Athens were higher compared to the studied cities, thus further comparison is needed in order to expand or not this observation to the other seasons as well.

In this section, the annual mean, summertime (2016) and wintertime (2017) mean of all the compounds from the main campaign are compared with other international published works in **Table IV - 2** and **Figure IV - 11**. The selected studies were conducted **after 2010**, in order to take into account the **reduction** of VOC atmospheric levels as a result of the **air pollution control strategies** implemented by each country (i. e. in Fanizza et al., 2011 and Dominutti et al., 2016). Differences on climatological characteristics, population and industrialization are met between these areas. Rome and Beirut, the capitals of Italy and Lebanon located in the Western and Eastern Mediterranean basin respectively, with 4 and 2 million population each, have a typical Mediterranean climate with mild winters and hot summers (Fanizza et al., 2014; Salameh et al., 2015). In Northwestern Europe, Paris is one of its megacities, with a temperate climate characterized by mild winters and warm summers, although often influenced by oceanic air masses (Baudic et al., 2016). São Paulo, located in the southern Brazil under the Tropic of Capricorn, is its most populous state with more than 90% of its 31.5 million inhabitants living in an urban environment. Due to its location, it has a characteristic climate with dry winters and hot summers (Alvares et al., 2013). Finally, in Asia, Tianjin is the third largest megacity of China, with a 14 million population and a fast-growing industrial activity (Liu et al., 2016). Its

climate is continental, with cold and dry winters, whereas the summers are hot and rainy due to the monsoon winds.

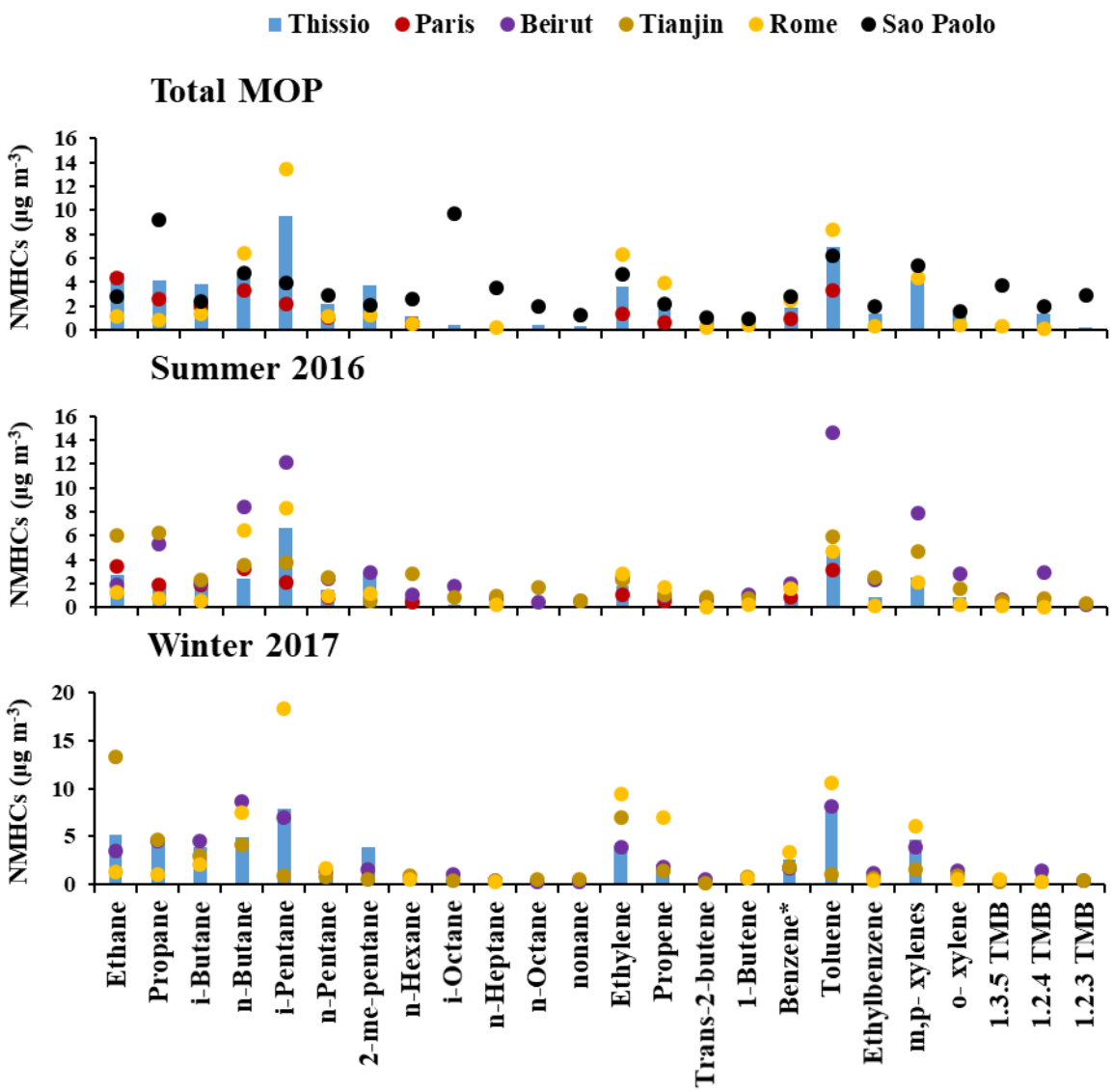

Figure IV - 11: Comparison of the mean concentrations for the MOP, summer 2016 and winter 2017 between Thissio and other cities worldwide (also in Table IV - 2).

Starting from the alkanes, the winter concentrations for the majority of the compounds (with 2017 as reference) measured in this study were within the range of the values reported in Beirut and Tianjin, however there are some exceptions. During winter, n-butane and i-octane in Beirut are 2 times higher, due to fuel storage facilities outside the city (Salameh et al., 2015), whereas 2-me-pentane, n-hexane and n-octane are a factor of 2 higher in Athens. Additionally, i-pentane, 2-me-pentane and n-pentane are 8, 7 and 2 times higher in Athens relatively to Tianjin. On the other hand, the opposite is observed for summer, with alkanes' concentrations to be higher than a factor of 1.5 for the majority of the compounds in Beirut compared to Athens, whereas in Tianjin they are 2 to 5 times higher than Athens, apart from pentanes. Furthermore, higher winter and summer mean concentrations are observed in Athens compared to Rome, with n-butane and i-pentane to be the only exceptions (factor of 1.5 higher in Rome for both seasons).

Moreover, as it was already reported in Panopoulou et al., (2018), the mean levels of alkanes in Athens are 1.5 (n-butane) to 7.7 (n-hexane) times higher compared to Paris, a trend also observed in summer but with lower difference (1.5 to 3.5 times higher for n-butane and i-pentane respectively). Lastly, the comparison to Sao Paulo shows that propane and C8 – C9 alkanes are a factor of 2 (propane) to 23 (i-octane) higher in Sao Paulo, whereas ethane, i-butane and i-pentane are up to 2.5 higher in Athens.

Concerning alkenes, the winter concentrations are comparable only to Beirut, in contrast to summer, when they are up to 2 times higher in Beirut. Furthermore, the winter levels of ethylene and propene are 2 to 3.5 times higher in Rome, whereas in Tianjin only ethylene is 2 times higher; for summer, alkenes' mean levels are higher within a factor of 1.2 to 3.8, except of 1-butene and trans-2-butene. Moreover, the mean concentrations of alkenes are similar to Sao Paulo, but 2 times higher compared to Paris.

Moving on to aromatics, the winter levels are comparable to Beirut, except of benzene that is 1.5 times higher in Athens. In summer, the opposite is observed, thus benzene, toluene and m-/p- xylenes are 2 to 3 times higher in Beirut. Furthermore, all aromatics except of TMBs are 1.5 (i.e benzene) to 7 (i.e toluene) times higher in Athens compared to Tianjin in contrast to summer that the levels are higher for Tianjin. Compared to Rome, the winter and summer levels of benzene and toluene are by a factor of 2 lower in Athens, whereas the rest are higher 1.5 to almost 4 times, except of m-/p- xylenes. Additionally, benzene mean levels are similar to Paris, whereas toluene is higher by a factor of 2. Finally, benzene and ethylbenzene are almost a factor of 2 higher in Sao Paulo considering the mean for the total period.

The large variations in the concentrations reported in the different cities could be attributed first of all to the different sampling periods, the instrumentation resolution, the spatial differences at the sampling locations and the effect of atmospheric dynamics. However, the **type** and **strength** of the pollution emissions **sources** could also drive the observed levels of VOCs. In general terms, considering the whole period, the maximum mean levels are shared between the examined cities, denoting the possible influence from different sources. Furthermore, the air quality in Athens with respect to NMHCs is **worse** relatively to the other cities during **winter**, with regulating factors the prevailing stagnant conditions, and the enhancement of emissions from sources like traffic and residential heating according to Panopoulou et al (2018). However, in **summer**, heavier alkanes (C8 – C9), alkenes and aromatics are **significantly lower** than other cities and this could **not** be attributed **only** to the effect of **dynamics** (e. g. photochemical reactions). For example, in Beirut and Tianjin, the increased mean concentrations of these compounds can be attributed to fuel or solvent evaporation that is favored by the higher temperatures. In addition, the great variability of the VOCs levels relatively to the rest of the cities, with mean levels comparable or not, points out the importance of sources like traffic and the type of fuel used (i. e. gasoline or LPG; Panopoulou et al., 2018) and/or residential heating, which need to be determined in order to assess the current air quality in Athens, as well as to be considered in the future comparisons to other cities.

Table IV - 2: Comparison of mean VOC levels for the total period of measurements, summer 2016 and winter 2017 between this study and other international cities. Information regarding the sampling frequency and duration and the type of sampling station are included when available. The compounds in *italics* were measured from February 2016 to February 2017 by the GC-FID C6 – C12. The numbers in brackets indicate the standard deviation.

	Thissio, Greece **Continuous (18 mo)** Urban background			**Beirut, Lebanon[1]** **Continuous (2m)** Urban background		**Paris, France[2]** **Continuous (9 mo)** Urban background		**Rome, Italy[3]** **Continuous (1 y)** Urban center			**Sao Paolo, Brazil[4]** **Continuous (1 y)** Urban background	**Tianjin, China[5]** **Continuous (1 y)** Urban center	
	Mean	**Summer 2016**	**Winter 2017**	**Feb 2012**	**July 2011**	**Mean**	**Summer 2010**	**Mean**	**Winter 2011**	**Summer 2011**	**Mean (2013)**	**Winter 2015**	**Summer 2015**
Ethane	4.8	2.68 (1.43)	5.18 (4.85)	3.48	1.94	4.31	3.49	1.19	1.30	1.28	2.85	13.31	6.05
Propane	4.17	1.98 (2.37)	4.71 (4.75)	4.55	5.32	2.63	1.92	0.81	1.06	0.70	9.20	4.69	6.23
***i*-Butane**	3.8	1.55 (2.06)	3.81 (5.05)	4.53	2.1	1.94	1.84	1.33	2.11	0.57	2.37	2.90	2.32
***n*-Butane**	4.7	2.39 (3.1)	4.94 (6.28)	8.59	8.37	3.31	3.28	6.46	7.48	6.49	4.76	4.08	3.50
i*-Pentane	9.47	6.23 (5.89)	7.81 (10.43)	6.95	12.09	2.24	2.12	13.48	18.40	8.29	3.90	0.90	3.78
***n*-Pentane**	2.23	1.44 (1.69)	1.74 (2.2)	1.46	2.39	1.01	0.86	1.21	1.62	0.97	2.94	0.75	2.46
2-me-pentane	3.78	2.90 (2.60)	3.83 (5.37)	1.53	2.91			1.23		1.16	2.11	0.54	0.54
n-Hexane	1.16	0.81 (1.09)	1.17 (1.66)	0.6	1.03	0.49	0.40	0.56	0.53		2.62	0.86	2.80
i-Octane	0.41	0.22 (0.34)	0.47 (1.04)	0.98	1.83						9.74	0.33	0.81
n-Heptane	0.44	0.26 (0.34)	0.51 (0.79)	0.4	0.73			0.2	0.2	0.2	3.54	0.38	1.00
n-Octane	0.47	0.30 (0.42)	0.52 (0.85)	0.22	0.4						1.95	0.48	1.66
nonane	0.31	0.25 (0.28)	0.31 (0.41)	0.26	0.54						1.23	0.53	0.59
Ethylene	3.64	1.83 (1.88)	4.04 (4.97)	3.86	2.4	1.35	1.03	6.29	9.42	2.77	4.63	6.93	2.29
Propene	1.77	0.52 (0.70)	2.00 (3.15)	1.73	0.99	0.62	0.53	3.97	6.97	1.63	2.21	1.35	1.02
Trans-2-butene	0.84	0.22 (0.36)	0.71 (1.13)	0.51	0.64			0.18		0.05	1.03	0.14	0.84
1-Butene	0.85	0.24 (0.36)	0.80 (1.24)	0.67	1.03			0.41	0.64	0.25	1.00	0.82	0.77
Benzene**	1.91	0.85 (0.76)	2.63 (3.36)	1.72	2	0.99	0.82	2.46	3.29	1.53	2.86	1.76	26.85
Toluene	6.98	4.54 (5.08)	7.57 (10.78)	8.09	14.6	3.33	3.18	8.40	10.58	4.71	6.21	1.04	5.90
Ethylbenzene	1.33	0.81 (0.89)	1.46 (2.15)	1.14	2.29			0.3	0.43	0.17	1.94	0.66	2.47
m-/p-Xylenes	4.20	2.56 (2.80)	4.62 (6.87)	3.87	7.89			4.38	6.03	2.08	5.39	1.59	4.68
o- Xylene	1.38	0.81 (0.95)	1.52 (2.41)	1.35	2.78			0.43	0.56	0.26	1.55	0.88	1.59
1.3.5 TMB	0.31	0.15 (0.29)	0.36 (0.77)	0.31	0.69			0.29	0.44	0.15	3.75	0.25	0.50
1.2.4 TMB	1.4	0.86 (1.11)	1.65 (2.80)	1.38	2.93			0.15	0.25	0.05	1.95	0.20	0.80
1.2.3 TMB	0.26	0.21 (0.37)	0.27 (0.55)	0.32	0.27						2.95	0.35	0.35

[1]Salameh et al. (2015) [2]Baudic et al. (2016) [3]Fanizza et al. (2014) [4]Dominutti et al. (2016) [5]Liu et al. (2016) *Co-elutes with cis-2-butene **Monitored from February 2016 until February 2017 by the GC C6 – C12

2. C6 – C16 VOCs from the IOP

2.1 VOC variability

The target species of the IOP included **C5 – C16 VOC** from various classes. The new compounds in the dataset were 9 alkanes (including cyclohexane), 1 alkene (hexene), 4 aromatic [styrene, (3-, 4-, 2-) ethyltoluenes], 6 IVOC (up to n-hexadecane) and 2 BVOC (camphene and g-terpinene), which are listed in **Table V - A4** of the **Annex IV**. Because the measurements were conducted in February and September as representatives of the winter and summer seasons respectively, to facilitate the discussion from hereafter the results of the measurements for each month will be referred to as "winter" and "summer" respectively. From **Table IV - A4** it is apparent that C6 – C10 **alkanes**, **hexene**, **styrene** and **aromatics** present their **highest levels** in **winter** than summer. However, for g-terpinene and IVOC we observe similar mean seasonal concentrations, whereas n-hexadecane is two times higher in summer than winter.

Furthermore, the existence of two seasonal datasets from the IOP (February for winter and September for summer) allows the examination of the "seasonal" diurnal cycle of the additional compounds. **Benzene** and **toluene**, which were also measured in the IOPs, will be used as a **reference** for the discussion, as two compounds with different sources (e. g. wood burning for residential heating versus traffic; Borbon et al., 2018). The comparison of the diel cycles to the ones of benzene and toluene will highlight the similarities and discrepancies to the seasonal diurnal variability of the VOC from the MOP, since the inter-comparison of the levels of the different measurement methods already showed that the datasets agree well (**Chapter 2, Sect. 2.4**).

In **Figure IV – 12** the seasonal diurnal cycles of benzene, toluene, 3-me-pentane, hexene, decane, n-tetradecane (nC14), n-pentadecane (nC15) and n-hexadecane (nC16) are presented, whereas the rest of the compounds from the IOP are presented in **Figure IV - A5** of the **Annex IV**. Starting from benzene and toluene in **winter,** a **bimodal pattern** with **morning** and **night maxima** are observed: for **benzene**, the **night maximum** is **higher** than the **morning one**, in contrast to **toluene** that the **two maxima** have the **same intensity**. In **summer**, both compounds present a **night-time enhancement period** (starting after 18:00 LT) that **persist until morning**, followed by a decrease after 09:00 LT. However, for benzene, the mean 3-hour levels can be lower than winter up to a factor of 2, while for toluene the mean 3-hour levels are almost similar to winter apart from the maxima. These observations are **in agreement** with the diurnal cycles presented in **Sect. 1.2** and **Fig. IV – 3** for these compounds, considering also that the cycles of **Figure IV – 11** derive from measurements that lasted only a few days in each season with 3h intervals.

The compounds of the IOP exhibit a seasonal diurnal profile similar to the one of benzene (i.e. hexene and styrene) and toluene (i.e. branched alkanes and aromatics), with the amplitude of the night enhancement period over the morning maximum to be dependent from the season or

the compound. Nevertheless, the results showed a **common seasonal diurnal profile** for the majority of the VOCs from the **MOP** and **IOPs**.

Furthermore, **light IVOCs (C10 – C12)** follow the **variability** of **toluene**, with similar levels **regardless** of the **season**. On the contrary, although **C13 - C16 IVOC** exhibit a **summer** diurnal cycle with a **night-time enhancement period** after midnight, the **winter** diurnal cycles are **contrasted**. Specifically, the levels of n-tridecane and n-tetradecane start to increase after 06:00 LT and reach a maximum at 12:00 LT, which is then followed by a slow decrease of the levels until midnight. N-pentadecane on the other hand, presents a day-time enhancement of the levels from 9:00 LT that persists until midnight with a night peak at 21:00 LT. Finally, n-hexadecane exhibits an obvious diurnal cycle only in summer with a night-time enhancement period starting at 18:00 LT and persisting until 9:00LT in the morning.

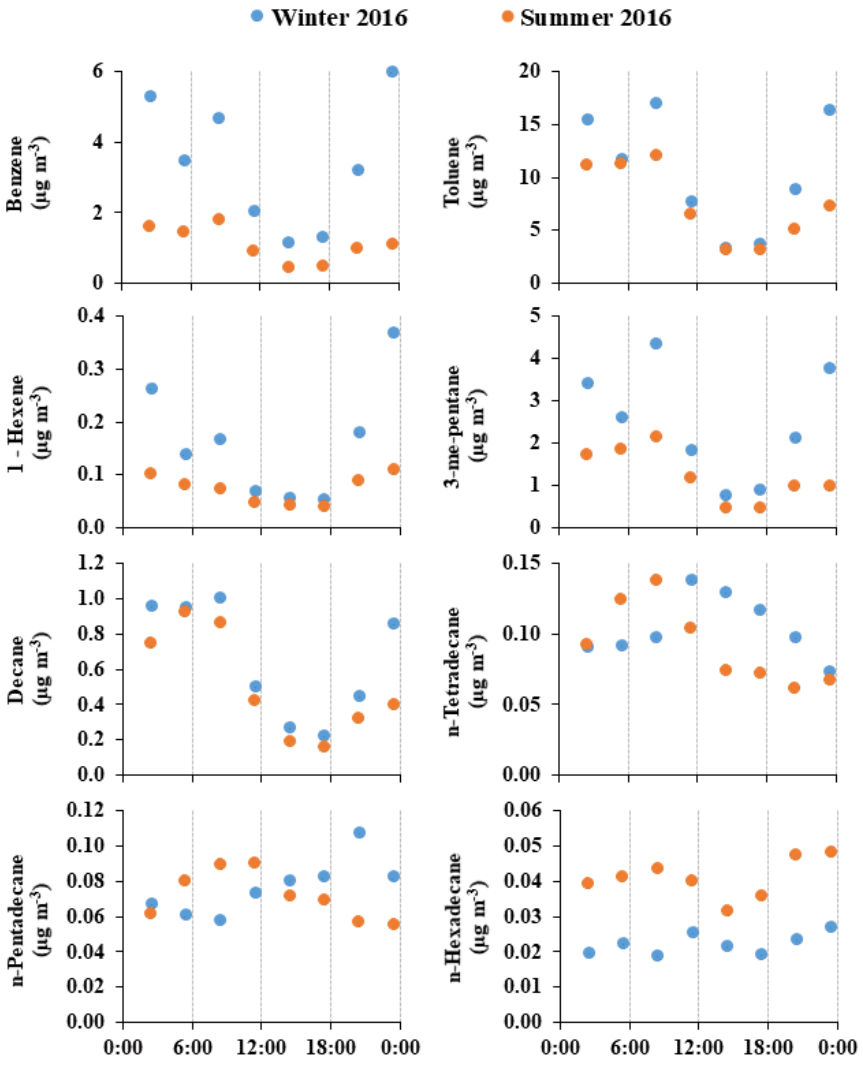

Figure IV - 12: Seasonal diurnal variability of selected NMHCs from the IOPs of winter and summer 2016.

2.2 The influence of meteorology

In **Sect. 1.3.3 (this chapter)** it was shown that wind speed and temperature are the main meteorological parameters affecting the atmospheric levels of the NMHCs from the MOP. The VOCs of the IOPs are affected similarly by the aforementioned meteorological parameters (graphs not shown) with the exception of IVOC, for which their relationship to wind speed and temperature will be examined separately Moreover, the role of the height of the planetary boundary layer will not be discussed here, because a similar effect is expected for all the compounds (**Sect. 1.3.2**).

Figure IV – 13 presents the relationship to wind speed of **decane** and **tetradecane** as representatives of light IVOC (C10 – C12) and heavy IVOC (C13 – C16) respectively, color-coded to wind direction. For the rest of the IVOC these relationships are presented in **Figure IV - A6** of the **Annex IV**. It is apparent that the relationship to wind speed become **less dependent** with **increasing number** of **carbon** atoms. In this context, tetradecane, pentadecane and hexadecane are independent from wind speed (and wind direction), with this behavior to be associated probably to their **physico-chemical properties** than to the impact of anthropogenic sources. Specifically, because the saturation concentration of IVOC is between 10^3 μg m^{-3} and 10^6 μg m^{-3}, while the rest of the studied compounds that are considered volatile have saturation concentration $>10^6$ μg m^{-3} (Robinson et al., 2007), they are important **precursors** of **secondary aerosols**. Thus, **partitioning** between the gaseous and the particulate phase can be an additional "**source**" or "**sink**" of IVOC in the atmosphere, with this being more **dependent to temperature** than wind speed and direction.

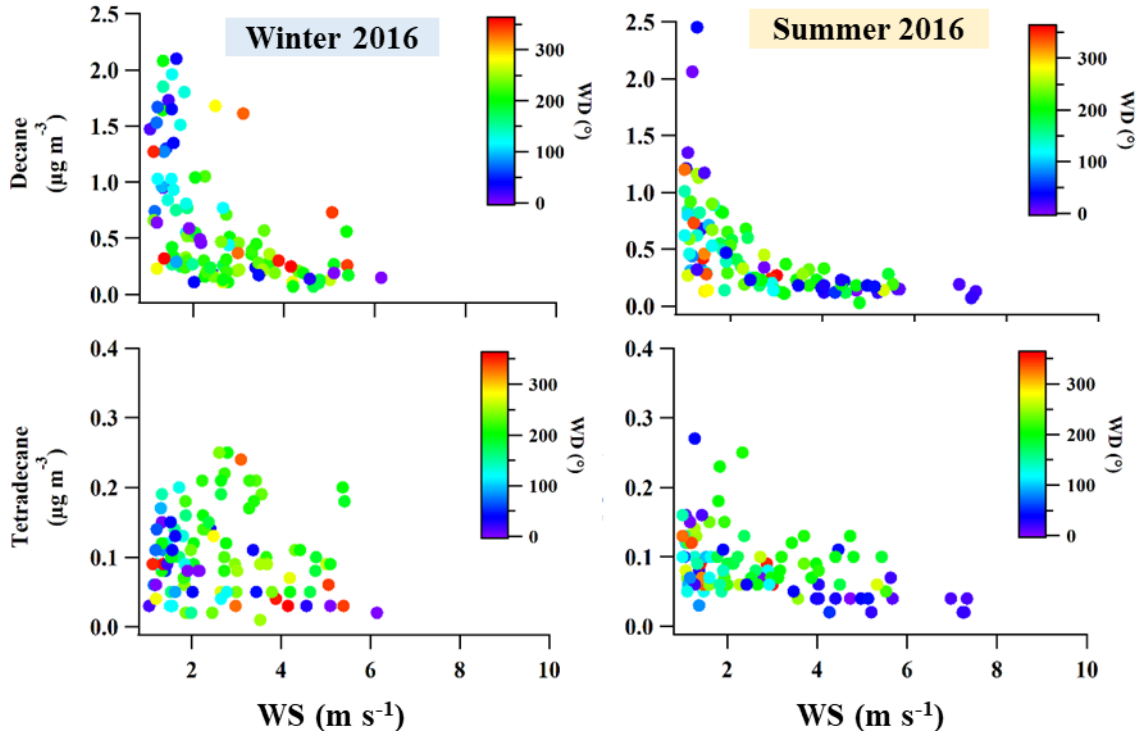

Figure IV - 13: Relationship of selected IVOC (in μg m^{-3}) from the IOPs of winter and summer 2016 to wind speed. The color-code denotes wind direction (degrees). Note that the compounds' names are not shown for the summer relationships.

Following the previous observation, the relationship of the selected IVOC to temperature is examined for every season in **Figure IV – 14**, whereas the rest of the IVOC are presented in **Figure IV - A7** of **Annex IV**. Remarkably**,** the levels of tetradecane seem to **increase** with the **increase** of the ambient **temperature** in **winter**, whereas in summer high levels are recorded independently from the temperature. This trend is not observed for decane.

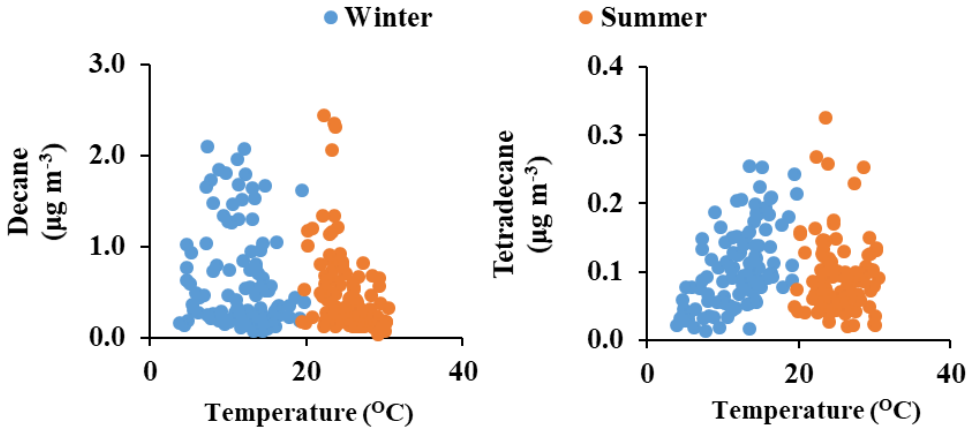

Figure IV - 14: Relationship of IVOC from the IOPs (winter and summer 2016) to temperature.

The unique behavior of heavy IVOC (C13 – C16) related to wind speed and to temperature indicate the possible influence of other processes like the **gas-to-particle partitioning** that it was mentioned before. To test this, the relationship of IVOC (C11 – C16) to decane is examined in **Figure IV – 15** for winter and summer, applying a color-code for ambient temperature. Decane, the lightest of the IVOC, presented a temporal variability close to the majority of the studied compounds (Sects. 2.2 and 2.3), thus any differences to the relationship can be attributed mainly to different "sources". In **Figure IV – 15** it is apparent that in winter, the aforementioned relationship is influenced by temperature with increasing number of carbon atoms. Precisely, although undecane and dodecane exhibit a linear relationship to decane, for the rest of the compounds (C13 - C15) the datapoints corresponding to higher temperatures for the season (> 15°C) present a differentiated trend, which is more apparent in tridecane than tetradecane and pentadecane. The levels of hexadecane are close to the limit of detection, thus conclusions for its temperature dependence are not robust enough. In summer, light IVOC (nC11 – nC14) present a linear relationship to decane, whereas only in pentadecane some datapoints that correspond to high ambient temperature fall higher in the scatterplot.

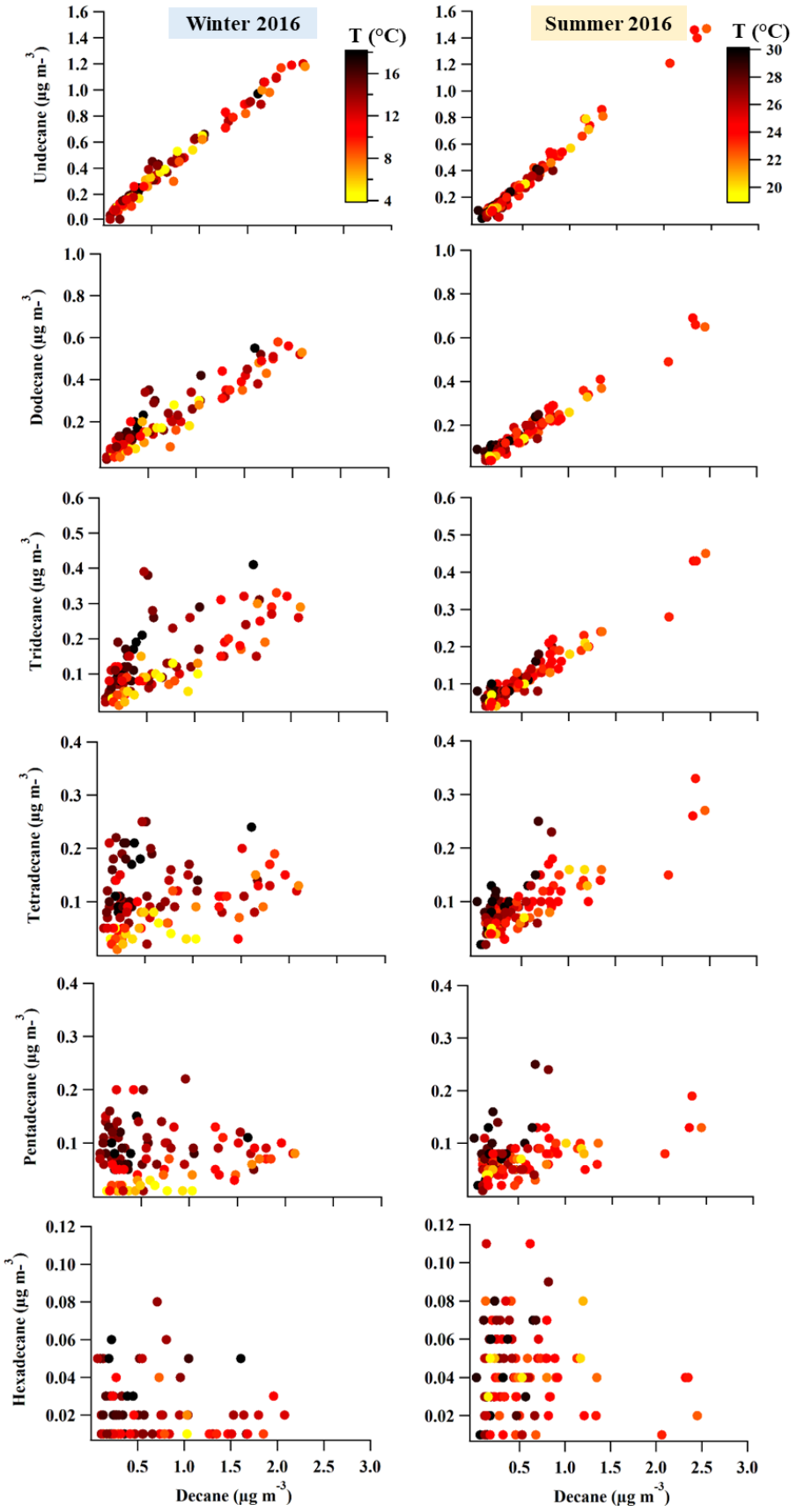

Figure IV - 15: Relationship of IVOC (C11 – C16) to decane for winter (left column) and summer (right column) 2016. The color-coding denotes ambient temperature.

Consequently, the above analysis indicated that the **increase** of **temperature** in **winter** might **trigger** more **emissions** of **heavy IVOC** (C13 – C15) than decane, because if sources' emissions were the only factor affecting the levels, then similar relationship to decane would be expected in both seasons. These additional sources of heavy IVOC could be associated to the **gas-to-particle partitioning,** which is favored under low temperatures, resulting to the reverse of the condition when ambient temperature increases. Furthermore, in **Figure IV – 16**, the temporal variability of decane and tetradecane (as reference for the behavior of light and heavy IVOC respectively) is presented along with ambient temperature in winter and summer. It is apparent that tetradecane's concentrations increase with the increase of temperature in both seasons, whereas this is not observed for decane (especially in winter). Thus, the previous observation gives insight into the behavior and temporal variability of IVOC in ambient air, since these compounds are **rarely studied** (Ait-Helal et al., 2014; Aumont et al., 2012; Li et al., 2019). Recent works have shown their important contribution to the formation of secondary organic aerosols (Aumont et al., 2012; Lu et al., 2018), however they are often neglected in model studies and emission inventories, which might be one of the reasons for the reported high uncertainties in the sources, formation and fate of organic aerosols in the atmosphere (Tsigaridis and Kanakidou, 2007).

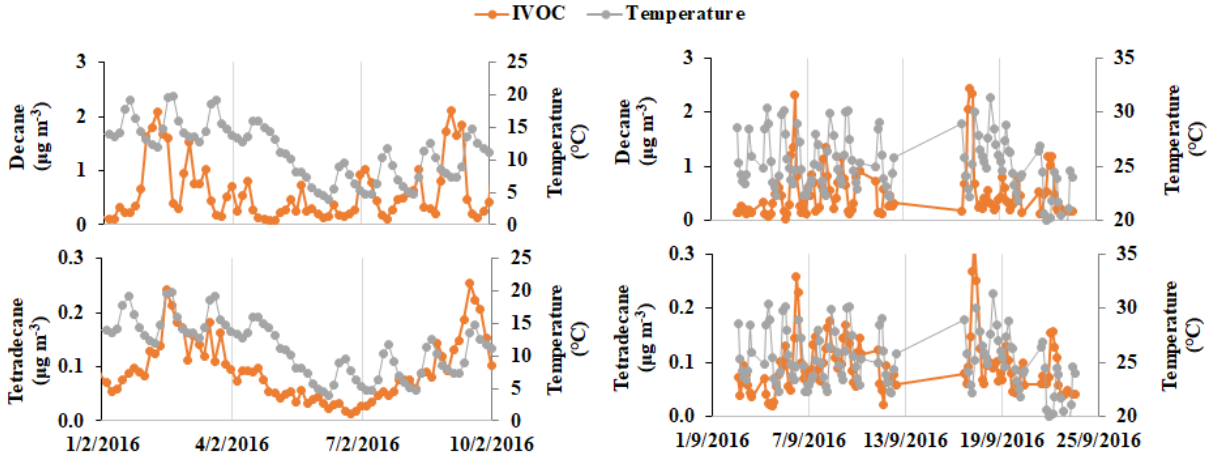

Figure IV - 16: Temporal variability of decane, tetradecane and temperature in the winter (left) and summer (right) IOP.

2.3 Relationship to other pollutants/Effect of sources

In this last section of the chapter, the relationship of the VOCs from the IOPs to NO, CO, BC, BC_{wb} and BC_{ff} is investigated by examining their correlation. The relationship coefficients are presented in **Tables IV - 3** and **IV - 4** for winter and summer IOPs.

Compared to summer, the correlation coefficients in winter between the VOC are slightly better for the majority of the compounds and more relationships are observed for the saturated and unsaturated compounds (like hexene and styrene). Exceptions are IVOC, camphene and g-terpinene that exhibit more and better relationships in summer (for IVOC, R^2 ranges from 0.5 to 0.91), although pentadecane and hexadecane don't correlate with any VOC regardless of the season.

Concerning the relationship to other pollutants, VOC are mainly correlated to NO and CO in winter (For NO: R^2 from 0.52 for dodecane to 0.79 for 2.4-dime-pentane; for CO: R^2 from 0.53 for g-Terpinene to 0.78 for cyclohexane), whereas in summer almost the same number of correlations are observed with slightly different correlation coefficients. BC_{wb} presents more relationships to ethyltoluenes, branched alkanes and IVOC (R^2: 0.55 to 0.72) in summer, whereas in winter it correlates only with styrene, hexene and 3.3-dime-pentane. Finally, decane and undecane are the only IVOC that correlate to other pollutants in winter, and more specifically with NO, CO, BC and BC_{ff} (R^2: 0.54 to 0.68), whereas dodecane correlates only with NO (R^2 from 0.52). In summer however, the IVOC with 10 to 13 carbon atoms correlate to all the pollutants (NO CO, BC, BC_{wb} and BC_{ff} with R^2 from 0.55 to 0.81), while tetradecane correlates with BC and BC_{ff} (R^2 0.68 to 0.72 respectively).

In a summary, the good interspecies correlation observed in both seasons for the majority of the compounds, indicate that most of the additional **VOC** have **common origin** and **similar atmospheric fate**, whereas the observed discrepancies highlight the influence of the different **emissions** from sources and/or the effect of atmospheric dynamics. Nevertheless, the observations follow closely the ones of the VOC from the MOP, apart from IVOC that exhibit different behavior, which is a completely new element.

Table IV - 3: Interspecies correlation between the additional VOC of the intensive campaign and selected pollutant/tracers for winter 2016. All compounds have the same resolution of 3 hours. The concentrations are in μg m^{-3} except of NO, NO_2 and CO that they are in ppb. The blue bold and italics indicate R^2: 0.5 – 0.79 and red bold and italics indicate R^2 >0.79.

Winter 2016	3-me-pentane	Hexene	2.2-dime-pentane	2.4-dime-pentane	2.2.3-trime-butane	3.3-dime-pentane	Cyclohexane	2-me-hexane	2.3-dime-pentane	Styrene	3-ethyltoluene	4-ethyltoluene	2-ethyltoluene	Camphene	g-Terpinene	Decane	nC11	nC12	nC13	nC14	nC15	nC16
3-me-pentane	1.00																					
Hexene	0.58	1.00																				
2.2-dime-pentane	0.49	0.33	1.00																			
2.4-dime-pentane	0.96	0.64	0.54	1.00																		
2.2.3-trime-butane	0.82	0.67	0.42	0.85	1.00																	
3.3-dime-pentane	0.73	0.78	0.76	0.79	0.86	1.00																
Cyclohexane	0.83	0.48	0.44	0.83	0.65	0.64	1.00															
2-me-hexane	0.99	0.61	0.50	0.98	0.86	0.77	0.86	1.00														
2.3-dime-pentane	0.99	0.59	0.51	0.98	0.84	0.78	0.87	1.00	1.00													
Styrene	0.81	0.70	0.44	0.86	0.84	0.85	0.75	0.85	0.85	1.00												
3-ethyltoluene	0.98	0.63	0.49	0.98	0.85	0.78	0.85	0.99	0.99	0.86	1.00											
4-ethyltoluene	0.98	0.62	0.49	0.97	0.86	0.78	0.85	1.00	1.00	0.86	1.00	1.00										
2-ethyltoluene	0.98	0.62	0.49	0.97	0.87	0.79	0.86	0.99	0.99	0.89	0.99	1.00	1.00									
Camphene	0.54	0.51	0.27	0.59	0.63	0.67	0.40	0.59	0.58	0.72	0.61	0.61	0.63	1.00								
g-Terpinene	0.55	0.30	0.53	0.54	0.43	0.34	0.58	0.54	0.54	0.47	0.53	0.53	0.53	0.14	1.00							
Decane	0.88	0.51	0.44	0.88	0.83	0.73	0.78	0.91	0.91	0.85	0.90	0.91	0.93	0.68	0.46	1.00						
nC11	0.88	0.50	0.44	0.87	0.82	0.71	0.78	0.90	0.91	0.82	0.90	0.91	0.93	0.66	0.49	0.99	1.00					
nC12	0.80	0.38	0.41	0.75	0.72	0.60	0.67	0.81	0.81	0.70	0.80	0.82	0.83	0.59	0.46	0.89	0.94	1.00				
nC13	0.43	0.13	0.24	0.37	0.37	0.30	0.32	0.43	0.43	0.34	0.41	0.43	0.43	0.33	0.27	0.50	0.57	0.78	1.00			
nC14	0.06	0.00	0.07	0.03	0.02	0.01	0.02	0.05	0.05	0.02	0.04	0.05	0.04	0.02	0.07	0.05	0.07	0.17	0.48	1.00		
nC15	0.02	0.00	0.02	0.01	0.00	0.00	0.00	0.01	0.01	0.00	0.01	0.01	0.00	0.00	0.04	0.00	0.00	0.01	0.03	0.34	1.00	
nC16	0.01	0.02	0.00	0.02	0.01	0.03	0.04	0.01	0.01	0.03	0.02	0.02	0.02	0.02	0.00	0.02	0.02	0.01	0.01	0.01	0.08	1.00
NO	0.74	0.58	0.38	0.79	0.63	0.60	0.81	0.77	0.78	0.73	0.78	0.77	0.78	0.40	0.59	0.68	0.66	0.52	0.19	0.00	0.00	0.07
CO	0.72	0.71	0.35	0.77	0.65	0.68	0.78	0.75	0.76	0.77	0.77	0.76	0.77	0.40	0.53	0.66	0.63	0.48	0.17	0.00	0.00	0.10
BC	0.63	0.67	0.32	0.69	0.57	0.65	0.70	0.67	0.67	0.72	0.68	0.67	0.68	0.36	0.48	0.57	0.54	0.40	0.13	0.00	0.00	0.10
BC_{wb}	0.36	0.70	0.20	0.43	0.40	0.57	0.41	0.40	0.40	0.57	0.42	0.41	0.42	0.29	0.22	0.34	0.31	0.19	0.04	0.00	0.00	0.10
BC_{ff}	0.73	0.52	0.35	0.76	0.58	0.58	0.80	0.75	0.76	0.68	0.76	0.75	0.75	0.34	0.59	0.64	0.63	0.49	0.19	0.01	0.00	0.08

Table IV - 4: Interspecies correlation between the additional VOC of the intensive campaign and selected pollutant/tracers for summer 2016. All compounds have the same resolution of 3 hours. The concentrations are in μg m^{-3} except of NO, NO_2 and CO that they are in ppb. The blue bold and italics indicate R^2: 0.5 – 0.79 and red bold and italics indicate R^2 >0.79.

Summer 2016	3-me-pentane	Hexene	2.2-dime-pentane	2.4-dime-pentane	2.2.3-trime-butane	3.3-dime-pentane	Cyclohexane	2-me-hexane	2.3-dime-pentane	Styrene	3-ethyltoluene	4-ethyltoluene	2-ethyltoluene	Camphene	g-Terpinene	Decane	nC11	nC12	nC13	nC14	nC15	nC16
3-me-pentane	1.00																					
Hexene	0.40	1.00																				
2.2-dime-pentane	*0.72*	0.49	1.00																			
2.4-dime-pentane	***0.89***	0.50	*0.74*	1.00																		
2.2.3-trime-butane	*0.59*	0.41	*0.55*	*0.76*	1.00																	
3.3-dime-pentane	***0.81***	0.47	*0.73*	***0.86***	*0.76*	1.00																
Cyclohexane	*0.64*	0.49	*0.60*	*0.65*	0.48	*0.59*	1.00															
2-me-hexane	***0.91***	0.48	*0.70*	***0.95***	*0.74*	***0.88***	*0.65*	1.00														
2.3-dime-pentane	***0.91***	0.50	*0.71*	***0.97***	*0.73*	***0.87***	*0.67*	***0.99***	1.00													
Styrene	0.39	0.25	0.32	*0.52*	*0.54*	0.48	0.18	0.47	0.47	1.00												
3-ethyltoluene	***0.86***	*0.60*	*0.69*	***0.94***	*0.73*	***0.82***	*0.68*	***0.92***	***0.93***	*0.53*	1.00											
4-ethyltoluene	***0.85***	*0.59*	*0.69*	***0.93***	*0.72*	***0.82***	*0.67*	***0.90***	***0.92***	*0.54*	***0.98***	1.00										
2-ethyltoluene	***0.87***	*0.57*	*0.69*	***0.94***	*0.75*	***0.83***	*0.68*	***0.92***	***0.93***	*0.55*	***0.99***	***0.96***	1.00									
Camphene	*0.56*	0.26	0.42	*0.57*	0.49	*0.50*	0.39	*0.55*	*0.56*	0.44	*0.59*	*0.59*	*0.63*	1.00								
g-Terpinene	*0.76*	0.36	*0.59*	***0.85***	***0.79***	*0.78*	*0.52*	***0.81***	***0.82***	*0.58*	***0.85***	***0.85***	***0.89***	*0.62*	1.00							
Decane	***0.82***	0.43	*0.65*	***0.86***	*0.74*	*0.79*	*0.62*	***0.84***	***0.85***	*0.57*	***0.89***	***0.89***	***0.93***	*0.72*	***0.88***	1.00						
nC11	***0.81***	0.43	*0.64*	***0.87***	*0.76*	*0.78*	*0.63*	***0.84***	***0.85***	*0.56*	***0.89***	***0.89***	***0.94***	*0.71*	***0.90***	***0.99***	1.00					
nC12	*0.74*	0.29	*0.50*	*0.67*	0.49	*0.59*	0.50	*0.63*	*0.65*	0.42	*0.72*	*0.72*	*0.78*	*0.64*	*0.75*	***0.84***	***0.84***	1.00				
nC13	*0.75*	0.29	*0.54*	*0.78*	*0.68*	*0.71*	0.47	*0.76*	*0.76*	*0.51*	*0.78*	*0.78*	***0.83***	*0.63*	***0.86***	***0.91***	***0.91***	***0.84***	1.00			
nC14	*0.52*	0.11	0.33	*0.53*	*0.54*	*0.52*	0.20	*0.51*	*0.51*	0.42	0.48	0.48	*0.54*	0.46	*0.67*	*0.62*	*0.63*	*0.65*	*0.78*	1.00		
nC15	0.17	0.01	0.09	0.15	0.19	0.19	0.02	0.15	0.14	0.12	0.11	0.12	0.14	0.15	0.24	0.18	0.18	0.22	0.31	*0.69*	1.00	
nC16	0.00	0.00	0.00	0.00	0.01	0.01	0.01	0.00	0.00	0.00	0.00	0.00	0.00	0.00	0.02	0.00	0.00	0.00	0.01	0.08	0.26	1.00
NO	*0.76*	0.35	*0.51*	***0.83***	*0.55*	*0.69*	0.45	***0.79***	*0.79*	*0.68*	***0.82***	***0.81***	***0.83***	*0.68*	*0.78*	***0.83***	***0.81***	*0.74*	*0.70*	0.47	0.13	0.01
CO	*0.73*	*0.69*	*0.68*	***0.81***	*0.61*	*0.70*	*0.66*	*0.74*	*0.77*	0.40	***0.87***	***0.86***	***0.85***	0.48	*0.69*	*0.74*	*0.73*	*0.62*	*0.60*	0.34	0.06	0.00
BC	***0.80***	0.36	*0.56*	***0.80***	*0.66*	*0.71*	0.49	*0.77*	*0.78*	0.50	***0.80***	*0.79*	***0.82***	*0.56*	***0.83***	***0.80***	***0.81***	***0.79***	***0.80***	*0.68*	0.28	0.01
BC_{wb}	*0.64*	0.48	0.48	*0.65*	0.45	*0.52*	0.47	*0.60*	*0.61*	0.33	*0.72*	*0.70*	*0.71*	0.39	*0.58*	*0.62*	*0.62*	*0.62*	*0.55*	0.35	0.07	0.00
BC_{ff}	*0.79*	0.31	*0.54*	*0.77*	*0.66*	*0.70*	0.46	*0.76*	*0.76*	*0.50*	*0.75*	*0.75*	*0.79*	*0.56*	***0.83***	*0.79*	***0.79***	*0.78*	***0.81***	*0.72*	0.32	0.02

2.4 Comparison to other studies

Finally, the last part of this section focuses on the comparison of the results of the IOPs with other studies. Specifically, in **Figure IV – 17** and **Table IV - 5**, the mean seasonal concentrations are compared to studies from Beirut and Tianjin (same to **Table IV - 2**, **Sect. 1.4** of **this chapter**) and to Paris (Ait-Helal et al., 2014). Since special attention is given for IVOC, the comparison of their levels will be conducted separately in the next paragraph. For the rest of the compounds, starting from winter, the mean concentrations of C6 – C9 alkanes are in accordance with the Beirut measurements but lower compared to Tianjin, except of 3-me-pentane that is 2.5 and 4.5 times higher in Thissio than the other two cities respectively. Concerning the unsaturated compounds, they can be either within range (i.e. hexene compared to Beirut), lower (i.e. styrene compared to Tianjin) or higher (e.g. ethyltoluenes compared to both cities). In addition, styrene is a factor of 2 and 11 lower in winter and summer compared to Tianjin, whereas is 3 times higher in winter and 2 times lower in summer compared to Beirut; in summer the observed levels in Thissio are generally a factor of 2 lower from Beirut for 3 –, 4 – ethyltoluenes and for 4 – and 2 – ethyltoluenes from Tianjin. On the contrary, in summer, the mean levels are either within range (i.e. C7 poly-substituted alkanes) or lower (i.e. cyclohexane compared to Tianjin and 2-me-hexane compared to Beirut).

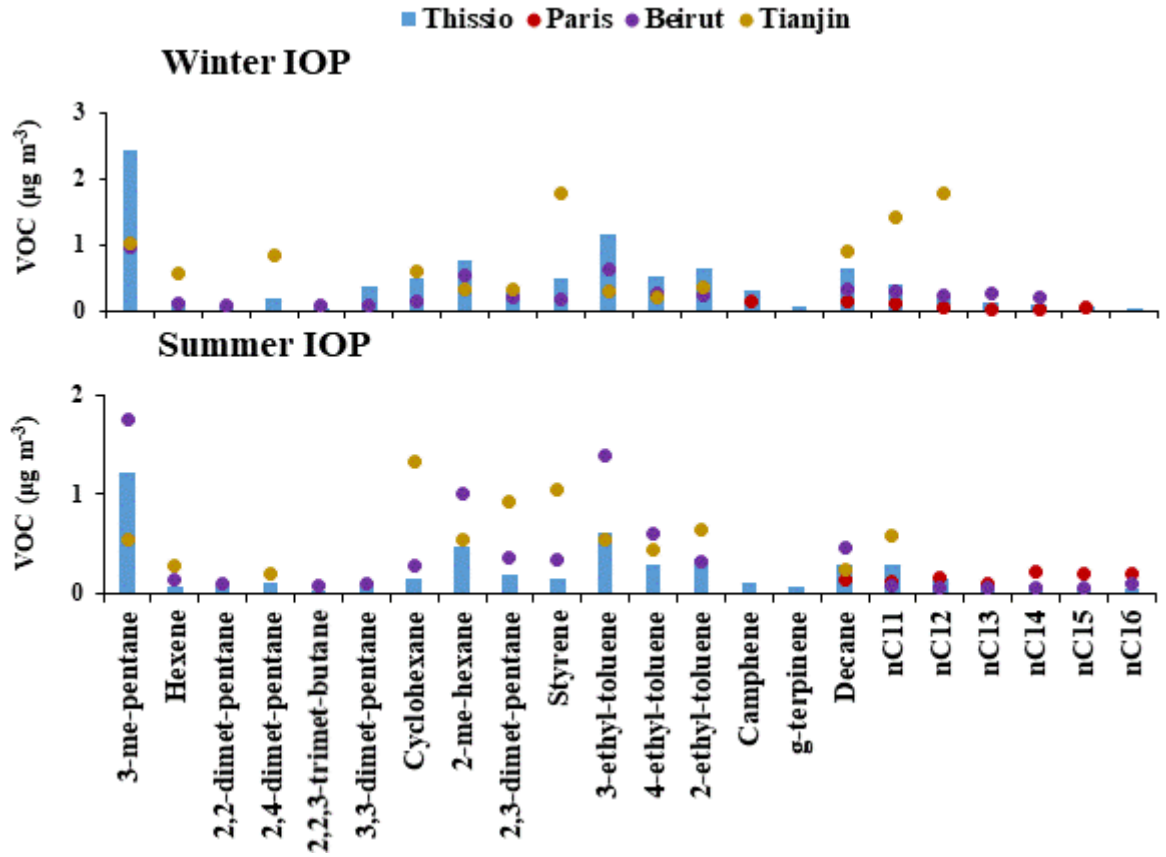

Figure IV - 17: Mean winter (upper) and summer (lower) values for Thissio, Paris, Beirut and Tianjin (reported also in Table IV - 5).

Finally, decane and IVOC (C11 – C16 n-alkanes) present different behavior. Firstly, decane in winter is two to five times higher compared to Beirut, Tianjin and Paris; in summer, it is higher

only compared to Paris (factor of 2), whereas it is more than 50% lower compared to Beirut and Tianjin. In addition, in winter, undecane and dodecane are a factor of 4 higher compared to Paris, within range compared to Beirut and lower than Tianjin (more than 80% for n-dodecane); in summer, both compounds are 3 and 4 times higher than Beirut respectively, whereas undecane is 2 times higher than Paris and 5 times lower than Tianjin, and n-dodecane a factor of 11 higher in Tianjin. Moreover, n-tridecane and n-tetradecane can be compared only to Beirut and Paris. In winter, both compounds are a factor of 2 lower than the mean reported values for Beirut, but in summer it is observed the exact opposite. Compared to Paris, the compounds are 8 and 6 times higher in winter respectively, however the mean concentration of n-tridecane in summer is similar to Paris, whereas n-tetradecane is more than a factor of 2 lower. Lastly, n-pentadecane and n-hexadecane are 3 and 5 times higher in Paris than Thissio for summer respectively, whereas in winter only n-pentadecane was detected in Paris with a mean value 2 times lower compared to Thissio. Nevertheless, compared to Beirut in summer, n-pentadecane is similar between the two cities, while n-hexadecane is a factor of 2 lower in Thissio. Unfortunately, a comparison to winter is not possible since these compounds were not quantified in Beirut.

The previous comparison showed that the majority of the compounds in Thissio, except of IVOC, exhibit **higher** mean **winter levels** than the **other studies**, but usually **lower** in **summer**. This is in line with the observations of the MOP, indicating that winter emissions from sources (apart from atmospheric dynamics) are having an important impact on the concentrations. Concerning IVOC, their winter mean concentrations are higher compared to Paris and Beirut (for the latter n-pentadecane and n-hexadecane were below detection limit), but lower to Tianjin. In summer however, we observed differences depending on the compound. Furthermore, in Paris the variability of IVOC (with higher mean values in summer than winter) was attributed to different emission from sources than the partitioning between gas and particle phase, whereas in Beirut the variability (with higher levels in winter and lower in summer) seems to be controlled by both the strength of sources and atmospheric dynamics (e. g. mild temperatures in winter and high photochemistry in summer). Although the characteristics of the seasonal variability in Thissio seems to be in-between the reported ones for Paris and Beirut, the mean levels observed in Thissio are in general higher for both seasons.

Table IV - 5: Comparison of mean VOC levels between the measurements from the IOP of winter and summer 2016 and other international cities. Information regarding the type of sampling station is included. The numbers in brackets indicate the standard deviation.

μg m^{-3}	Thissio Urban back/nd		Paris, France[1] Suburban		Beirut, Lebanon[2] Urban back/nd		Tianjin, China[3] Urban Center	
	Winter 2016	Summer 2016	Winter 2010	Summer 2009	Winter 2012	Summer 2011	Winter 2015	Summer 2015
3-me-pentane	2.43 (2.28)	1.22 (1.05)			0.95	1.76	1.01	0.54
Hexene	0.16 (0.18)	0.07 (0.05)			0.12	0.14	0.56	0.28
2,2-dimet-pentane	0.10 (0.11)	0.07 (0.06)			0.09	0.09		
2,4-dimet-pentane	0.19 (0.20)	0.10 (0.11)					0.84	0.21
2,2,3-trimet-butane	0.05 (0.03)	0.02 (0.02)			0.08	0.08		
3,3-dimet-pentane	0.38 (0.15)	0.07 (0.05)			0.08	0.09		
Cyclohexane	0.49 (0.39)	0.14 (0.09)			0.13	0.28	0.60	1.33
2-me-hexane	0.76 (0.72)	0.48 (0.45)			0.54	1.01	0.33	0.54
2,3-dimet-pentane	0.27 (0.26)	0.19 (0.18)			0.2	0.36	0.33	0.92
Styrene	0.49 (0.52)	0.15 (0.18)			0.17	0.34	1.78	1.04
3-ethyl-toluene	1.16 (1.12)	0.61 (0.56)			0.63	1.39	0.30	0.55
4-ethyl-toluene	0.53 (0.50)	0.29 (0.26)			0.25	0.60	0.20	0.45
2-ethyl-toluene	0.64 (0.60)	0.35 (0.31)			0.23	0.32	0.35	0.65
Camphene	0.30 (0.43)	0.10 (0.10)	0.13					
g-terpinene	0.06 (0.05)	0.06 (0.06)						
Decane	0.65 (0.53)	0.29 (0.28)	0.13	0.14	0.33	0.47	0.89	0.24
nC11	0.39 (0.33)	0.30 (0.28)	0.10	0.12	0.3	0.07	1.43	0.59
nC12	0.20 (0.15)	0.15 (0.13)	0.05	0.16	0.23	0.06	1.77	2.20
nC13	0.13 (0.09)	0.11 (0.08)	0.02	0.10	0.26	0.06		
nC14	0.10 (0.06)	0.09 (0.05)	0.02	0.22	0.19	0.06		
nC15	0.08 (0.05)	0.07 (0.04)	0.04	0.20		0.06		
nC16	0.02 (0.02)	0.04 (0.02)		0.21		0.09		

[1]Ait-Helal et al. (2014) [2]Salameh et al. (2015) [3] Liu et al. (2016)

3. Conclusions

Following the conclusions of **Chapter 3**, the need for the examination of the MOP and IOPs datasets was highlighted, in order to observe the variability of the NMHCs over a long period and determine the driving factors for the different seasons. Ultimately, these results will assist the source apportionment of the NMHCs in the following chapter.

In this context, the analysis of the first part of this chapter focused on the last 13 months of the MOP that were not presented in chapter 3 (1st article) and it showed, first of all that, that alkanes are the dominant group in every season (~50%), with levels reaching up to 74 μg m^{-3} for i-pentane (mean value: 9.2 μg m^{-3}), followed by aromatics and alkenes. The levels exhibit a distinct seasonality (higher in winter, lower in summer) and a pronounced diurnal variability (morning maximum and nighttime enhancement period) which is explained by the different influence of atmospheric dynamics and sources emissions. In particular, the height of the PBL, wind speed and temperature

are the main atmospheric parameters that affect the aforementioned variability, whereas the intensity of the sources is dependent from the season.

Since the impact of VOC sources is always of interest in the current thesis, in this chapter this was investigated for the whole MOP through the relationship of the NMHCs with the other pollutants/tracers. The correlation of the majority of the compounds to NOx, CO and BC is in agreement with the observations from **Chapter 3**, denoting their common origin. Nevertheless, sources emissions seem to be one of the main reasons for the differences between our results and observations from other cities worldwide, which in addition highlighted the important air pollution in winter, in contrast to the summer levels that are significantly lower.

In general, the results of the MOP are in line with the observations and conclusions of the 1st article (**Chapter 3**), although new insights are gained for the temporal variability and its driving factors. To examine the seasonal variability of additional VOC and to assist the source allocation in the next chapter, the concentrations of the VOCs from the IOPs were determined and the factors affecting them were examined in the second part of the chapter. The additional compounds exhibited a seasonal and diurnal profile close to the observed one of the NMHCs from the MOP, which was explained by a similar influence of atmospheric dynamics and sources emissions.

IVOC are the only group that presents significant exceptions; similar mean levels are encountered in winter and summer but with contrasted seasonal diurnal cycles. Moreover, it should be noted the temperature dependence of their concentrations which increase with increasing number of carbon atoms. Since these compounds are rarely investigated in the available studies, while they are important precursors of secondary organic aerosols, this dataset could be used in the future for the examination of their contribution to the organic aerosol matter in the atmosphere of Athens.

To sum up, the analysis of the datasets of the MOP and IOPs provided robust information for the temporal variability of NMHCs in Athens and its driving factors. During the discussion, the impact of sources was denoted, especially from the higher levels (and corresponding air pollution) in winter compared to summer. Since all the elements are now gathered, in **chapter 6** are determined the sources of NMHCs in Athens and their seasonal contribution is quantified. Can we finally separate and quantify the emissions from traffic and wood burning for residential heating?

CHAPTER 5 – Yearlong measurements of Monoterpenes and Isoprene in a Mediterranean city (Athens): Natural vs anthropogenic origin.

TABLE OF CONTENTS FOR CHAPTER 5

1.Introduction

Monoterpenes and **isoprene** were excluded from the analysis of chapter 4, since the first results indicated that separate analysis is required. These compounds are known for their **biogenic origin**, thus higher levels were expected in summer, when high temperatures and increased solar intensity prevail; these conditions trigger biogenic activity and thus the increase of natural emissions (Fuentes et al., 2000). However, when the summer and winter mean levels were presented in **Table IV – 1** of **Chapter 4**, it was apparent that only **isoprene** exhibited the **highest** mean levels in **summer** (0.48 ±0.56 μg m^{-3} over 0.12 ±0.18 μg m^{-3} in winter), whereas **α-pinene** has **similar** mean **summer** and **winter** levels (0.70 ±0.66 μg m^{-3} and 0.67 ±0.91 μg m^{-3} respectively) and **limonene** has higher levels in **winter** (0.48 ±1.06 μg m^{-3} over 0.15 ±0.31 μg m^{-3} in summer). Since in winter, biogenic activity decreases following the decrease of temperature and solar insolation, the important levels of α-pinene and limonene suggest **additional emissions** in the **cold season**. These are probably of **anthropogenic origin**, which is corroborated by the fact that isoprene is emitted also from vehicle exhausts (Borbon et al., 2001; Wagner and Kuttler, 2014). In this context, the literature research regarding monoterpene levels in urban environments and their respective sources is limited (i.e. Hellén et al., 2012). However, the aforementioned studies clearly indicate an important influence from anthropogenic sources like emissions from **wood burning** for domestic heating.

During MOP, monoterpenes and isoprene were monitored for more than 12 months. This allowed the detailed examination of their variability and the driving factors. In addition, the ancillary data for CO and BC, tracers of different combustion processes, which are available from Thissio station, assisted the investigation of the anthropogenic sources of these compounds. Consequently, and to provide robust information for these rarely reported compounds in cities, the above examination resulted in a **manuscript** that it will be submitted to Atmospheric Environment for publication. The manuscript is presented below.

2. Yearlong measurements of Monoterpenes and Isoprene in a Mediterranean city (Athens): Natural vs anthropogenic origin

Anastasia Panopoulou[1,2], Liakakou Eleni[3], Stéphane Sauvage[2], Valérie Gros[4], Nadine Locoge[2], Bernard Bonsang[4], E. Gerasopoulos[3], Nikolaos Mihalopoulos[1,3]

[1]University of Crete, Department of Chemistry, Environmental Chemical Processes Laboratory (ECPL), 71003 Heraklion, Crete, Greece
[2]IMT Lille Douai, Univ. Lille, SAGE – Département Sciences de l'Atmosphère et Génie de l'Environnement, 59000 Lille, France
[3]National Observatory of Athens, Institute for Environmental Research and Sustainable Development, 15236 P. Penteli, Athens, Greece
[4]LSCE, Laboratoire des Sciences du Climat et de l'Environnement, Unité mixte CNRS-CEA-UVSQ, CEA/Orme des Merisiers, 91191 Gif-sur-Yvette Cedex, France

1. Introduction

Monoterpenes and isoprene are the most important biogenic volatile organic compounds (BVOCs) which, due to their high reactivity, are contributing significantly, to the formation of secondary organic aerosol (SOA) and tropospheric ozone (Atkinson, 2000; Camredon et al., 2007; Carlton et al., 2009; Guenther et al., 1995). These compounds are known for their impact on climate, vegetation and human health (Fehsenfeld et al., 1992; Laothawornkitkul et al., 2009; Tsigaridis and Kanakidou, 2007; Turner et al., 2015). The emission of isoprene and monoterpenes from vegetation is closely linked to their synthetic processes and the storage capability in plants (Kesselmeier and Staudt, 1999; Laothawornkitkul et al., 2009). In particular, the isoprene photosynthetic formation depends on the ambient temperature and the solar radiation and appears to have a stress protecting role on the leaves. On the other hand, monoterpenes are usually stored in large pools in the plants, and their emission is not always linked to meteorological conditions (Geron et al., 2000; Hakola et al., 2009; Kesselmeier and Staudt, 1999).

Although the biogenic origin of isoprene and monoterpenes is well established, recent studies conducted in various areas around the world reported an additional anthropogenic origin for these compounds. Indeed Borbon et al. (2001) and Wagner and Kuttler (2014) reported isoprene to be partially linked to traffic emissions, while Dai et al. (2010), by conducting laboratory experiments, identified α-pinene and β-pinene in the exhaust of different types of cars in China, which were correlated to combustion products like alkenes. Simpson et al. (2010) reported important concentrations of α-pinene and β-pinene over oil and mining facilities in Alberta (Canada) which were well correlated with tracers of industrial emissions but not with isoprene. Finally, Pallozzi et al. (2018) during a chamber experiment provided emission data for isoprene and monoterpenes from the combustion of two types of typical Mediterranean trees (pine and oak). They showed that limonene is emitted during all burning phases from both types of trees, while α-pinene and β-pinene

are emitted mainly from pine with varying concentrations depending on the type of burning tissue (needles, branch etc).

Despite the reported emissions of BVOCs from human activities only few works investigated BVOCs variability and levels in urban areas (e.g Bonn et al., 2018). In addition, recent published studies demonstrate large discrepancies in the estimated levels, sources and fate of isoprene and monoterpenes to SOA formation (Gilman et al., 2015; Wang et al., 2013; Zhang et al., 2018). Moreover, the anthropogenic component of isoprene and monoterpenes is not considered in emission inventories and air quality models.

In the Mediterranean area, although few works report levels of isoprene and monoterpenes in rural or urban areas, most of them have been conducted during 1-2 months in summer or winter (e.g Harrison et al., 2001; Kaltsonoudis et al., 2016; Moschonas and Glavas, 2000; Rappenglück et al., 1999; Seco et al., 2013) and only Liakakou et al. (2007) reported year round measurements of isoprene at a remote location in Finokalia, Crete. Therefore, there is a clear need for measurements of BVOCs during different seasons, especially in urban locations, to understand their sources, as well as their role in oxidation capacity of the atmosphere and SOA formation.

This work reports results from a 13-months (2/2016-2/2017) campaign in Athens, where monoterpenes (α-pinene and limonene) and isoprene were monitored, among other species. The scope of the current study is: (a) to provide for the first time to our knowledge information for the ambient levels of monoterpenes and isoprene in an urban area of the Mediterranean basin over a complete year; (b) to examine BVOCs temporal variability and investigate the factors controlling their levels with focus on meteorology (c) to identify their sources, natural vs anthropogenic; and (d) to estimate their contribution to ozone and SOA formation.

2. Methodology

2.1 Sampling site

The VOC measurements were conducted at the Thissio urban background monitoring station of the National Observatory of Athens (NOA, 37.97° N, 23.72° E, 105 m a.s.l) located close to the historical center of the city. The station is situated on top of one of the three hills in the area (Lofos Nimfon), and it is surrounded by a pedestrian zone and a residential area. More details are provided in Panopoulou et al., (2018). C2 – C12 NMHCs measurements (including isoprene and monoterpenes) were conducted for 13 months, from 1 February 2016 to 28 February 2017.

2.2 On line NMHC measurements

Two gas chromatographs equipped with flame ionization detector (GC – FID), the "airmoVOC C_2 – C_6" and the "airmoVOC C_6 – C_{12}" Chromatrap GC (Chromatotec, Saint Antoine, France) were

used for the determination of $C_2 – C_6$ and $C_6 – C_{12}$ NMHCs respectively (Panopoulou et al., 2018). The two synchronized analyzers were collecting ambient air through collocated inlets at the rooftop of the station, 4 m above ground. A total sampling and analysis cycle of 30 minutes was set for both analyzers and the results were averaged to hourly values. A thorough description and technical information of the "airmoVOC $C_2 – C_6$" and "airmoVOC $C_6 – C_{12}$" analyzers, can be found in Gros et al. (2011) and Xiang et al. (2012) respectively.

During the campaign, two gas standards, certified by NPL (National Physical Laboratory, Teddington, Middlesex, UK) were used on a 2 weeks basis for the verification of the compounds' retention times and the calibration of the two analyzers. From the beginning of the campaign until April 2016 the 1st NPL containing 4 ppb of 30 $C_2 – C_{10}$ VOCs and for the rest of the campaign the 2nd NPL of almost 2 ppb of 32 $C_2 – C_{10}$ VOC were utilized. Although different calibration mixtures were used, no change was observed to the calculated response coefficients. The detection limits (LoD) have been determined at 0.125 μg m^{-3}, 0.114 μg m^{-3} and 0.135 μg m^{-3} for isoprene, α-pinene and limonene respectively. Regarding the $C_6 – C_{12}$ measurements, toluene is used, as representative constituent of the anthropogenic VOCs (Panopoulou et al., 2018), with a limit of detection at 0.112 μg m^{-3}.

2.3 Ancillary measurements

Real time monitoring of carbon monoxide (CO) and nitrogen oxides (NO_x = NO and NO_2) was conducted during the reported period by using Horiba 360 Series Gas Analyzers, calibrated with certified standards. For ozone's real-time measurements was used a Thermo 49i ozone analyzer of one minute resolution. A seven-wavelength dual spot aethalometer (Magee Scientific AE33) of one minute resolution was operated for the monitoring of black carbon (BC) and its fractions associated with fossil fuel and wood burning (BC_{ff} and BC_{wb}, respectively). Data for the meteorological parameters were provided by NOA's meteorological station at Thissio premises. Hourly mixing-layer height (MLH) values at 1º x 1º resolution were obtained over the station's area during the whole study period by using the HYSPLIT (HYbrid Single-Particle Lagrangian Integrated Trajectory) model (Draxler and Rolph, 2016) turbulent kinetic energy (TKE) profile method (Dumka et al., 2018, 2019).

3. Results and discussion

3.1 Monoterpene and isoprene levels: Seasonal variability.

The results of the isoprene, α-pinene and limonene measurements are presented in Table 1. Table S1 provides further information including also the ancillary parameters. A-pinene exhibited the highest levels with a mean value of 0.70 μg m^{-3} and concentrations ranging from 0.08 μg m^{-3} to 8.86

μg m^{-3}, whereas limonene and isoprene follow with mean levels of 0.33 μg m^{-3} (0.07 – 9.86 μg m^{-3}) and 0.19 μg m^{-3} (0.06 – 3.88 μg m^{-3}) respectively. The mean monthly and hourly variability of isoprene and monoterpenes is presented in Figures 1 and S1 respectively. Isoprene's concentration is higher in summer, when biogenic emissions are stronger due to the higher ambient temperature and solar radiation (Guenther et al., 1995) and lower for the rest of the year. As it was already mentioned, α-pinene and limonene are usually related to emissions from vegetation, thus a similar variability to isoprene was expected (Kesselmeier and Staudt, 1999; Laothawornkitkul et al., 2009). Nevertheless, monoterpenes exhibit a more complex seasonal cycle with pronounced variability in winter and maximum during the coldest months. Furthermore, the mean spring and summer levels of limonene are insignificant relatively to the α-pinene.

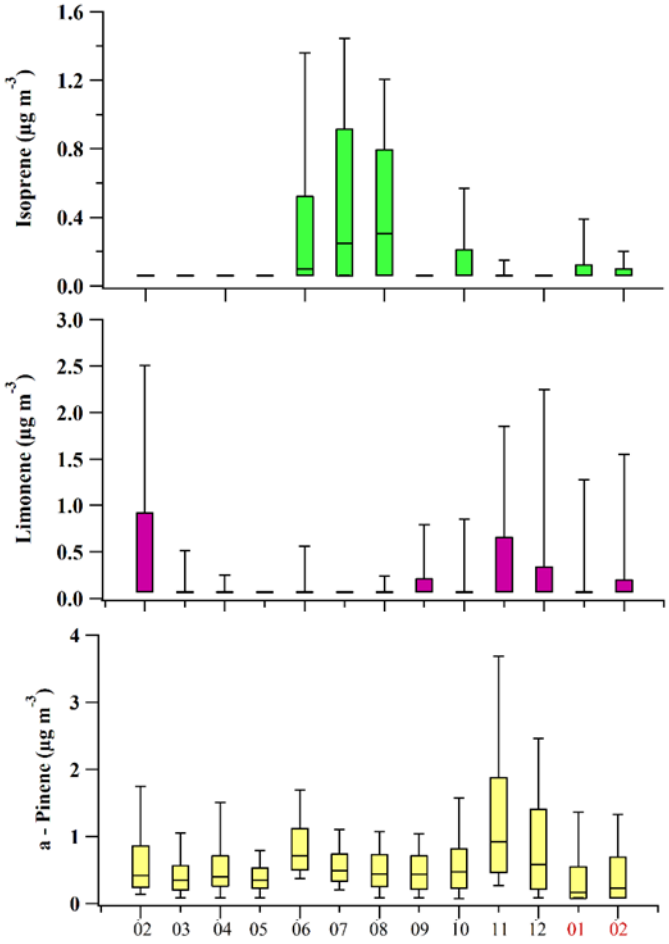

Figure 1. Monthly boxplots of biogenic VOCs for the period 01 February 2016 to 28 February 2017. The x-axis color indication reflects the year: black for 2016 and red for 2017.

In Athens, limonene levels reported for a rural background site in summer by Rappenglück et al. (1999) were found higher by a factor of 5 compared to the current one. Table 1 compares our measurements with the studies conducted in Athens and residential areas worldwide. A-pinene and

limonene winter mean values at an urban site in the French Alpine Valley (Chamonix) were found higher by a factor of 2 and 17 respectively compared to Thissio (Rouvière et al., 2006). Furthermore, the comparison with another French urban background site (Paris) revealed higher levels of α-pinene and limonene in Thissio, by a factor of 6 and 5 for winter and ~3 and ~2 in summer respectively for each compound, whereas isoprene was within the range for winter and by factor of 3 lower in summer (Ait-Helal et al., 2014). Isoprene's, α-pinene's and limonene's mean winter concentrations were higher in Thissio than in an urban area of Helsinki (Finland) by factors of 6, 7 and 9 respectively, whereas in summer α-pinene and limonene are two-folded (Hellén et al., 2012). Finally, α-pinene is 7 times higher compared to an urban site of Beijing, whereas isoprene is lower by a factor of 9 (Cheng et al., 2018). The comparison highlights that in urban centers monoterpenes and isoprene exhibit significant concentrations even in winter. In few locations, including Athens, wintertime levels of α-pinene and limonene are comparable or even higher than in summer, which suggests the impact of an anthropogenic source.

Table 1: Comparison of isoprene, α-pinene and limonene levels (in μg m^{-3}) in Thissio with already published data. The standard deviation is given in the brackets. Information regarding the sampling frequency, duration and the type of sampling station is also included.

	Thissio, Greece*			**Chamonix France[1]**	**Paris, France[2]**		**Helsinki, Finland[3]**		**Beijing, China[4]**
	Continuous (18 m)			Every 2h (7 d)	Continuous (2 m)		Continuous (~1 y)		Continuous (1 y)
	Urban back/nd			Urban back/nd	Urban back/nd		Urban Back/nd		Urban back/nd
	Annual mean	**Summer 2016**	**Winter 2017**	**Mean Winter 2003**	**Mean Summer 2009**	**Mean Winter 2010**	**Mean 1/2011**	**Mean 7/2011**	**Mean 2014-2015**
Isoprene	0.19 (0.35)	0.48 (0.56)	0.12 (0.18)		1.01	0.20	0.02	0.31	1.66
α-Pinene	0.70 (0.83)	0.70 (0.66)	0.67 (0.91)	1.48	0.27	0.11	0.1	0.32	0.10
Limonene	0.33 (0.78)	0.15 (0.31)	0.48 (1.06)	7.18	0.09	0.09	0.05	0.06	

[1]Rouvière et al. (2006); [2]Ait-Helal et al. (2014); [3]Héllen et al. (2013); [4]Cheng et al. (2018) *Current study

3.2 Monoterpene and isoprene levels: Diurnal variability.

The diurnal variability of monoterpenes and isoprene is illustrated in Figure 2 on a seasonal basis. The winter of 2016 which covers only 1 month of measurements (February 2016) is not considered. Monoterpenes' diel cycle is generally characterized by low levels during the day with a clear night-time to early morning increase. In spring and summer, the night-time enhancement period starts before midnight and the levels gradually increase till a morning maximum at 08:00 LT. In autumn and winter, the trend is similar, however the night-time enhancement period starts around 19:00 LT,

which is more pronounced comparable to the morning peak and it is maintained for a longer period (12h vs 8 in spring and summer). Regardless the season, the morning maximum of α-pinene and limonene is followed by a rapid decrease and the levels remain close to LoD for the rest of the day. Nevertheless, α-pinene noon levels during the warm periods are more than two times higher relative to the winter one. The nighttime enhancement of these compounds is in agreement with other works reported in the literature (Ghirardo et al., 2016; Seco et al., 2013). The comparison of the two winters for α-pinene and limonene (Figure 2 for the full season and Figure S2 for February 2016) showed the same variability for α-pinene and slightly higher mean hourly values and standard deviation for limonene for February 2016. Concerning isoprene, the diurnal variability is differentiated in summer relatively to autumn and winter and follows the cycle reported in the literature with a clear day maximum. In spring of 2016 no isoprene is depicted due to the limited data above LoD. In summer, isoprene increased from 07:00 LT to 12:00 LT, followed by a gradual decrease from 15:00 LT to 20:00 LT, maintained below LoD during night. In autumn and winter, a morning maximum from 07:00 to 10:00 LT is observed.

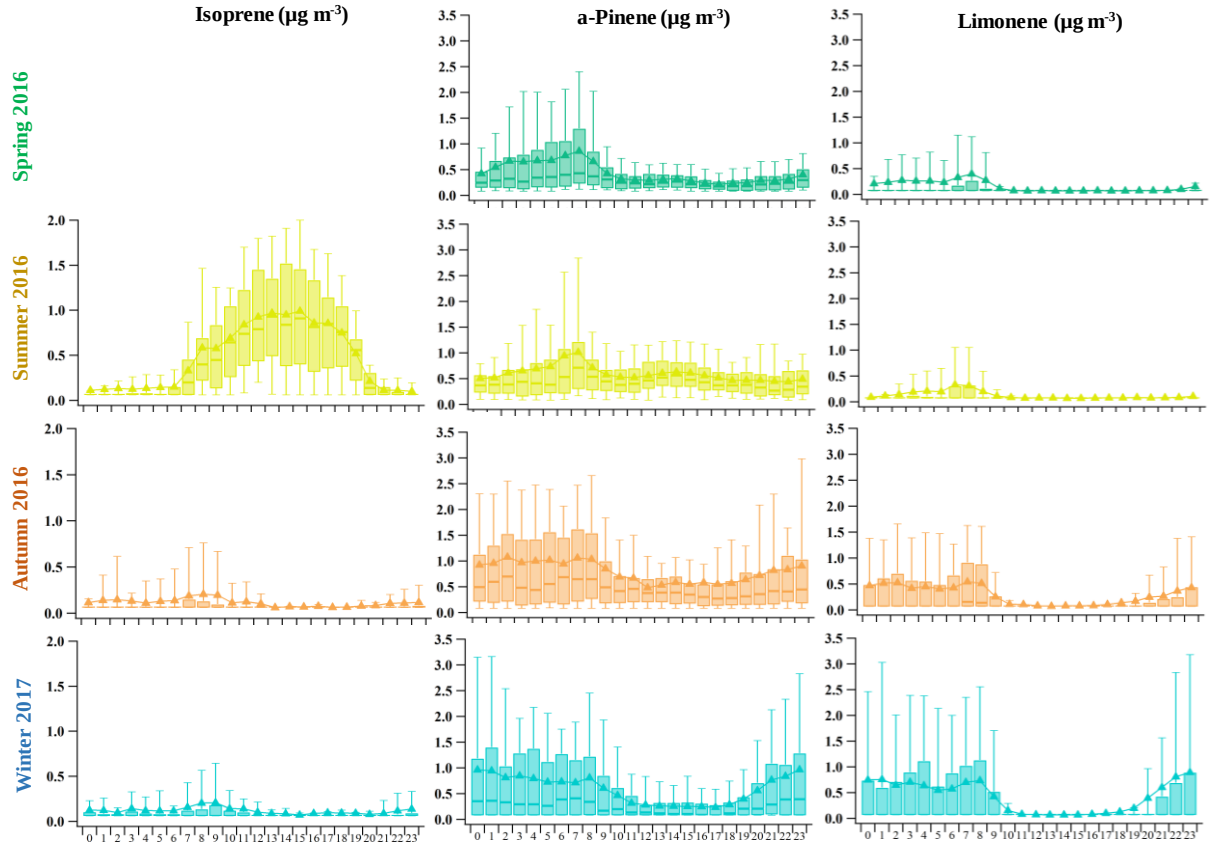

Figure 2. Seasonal diurnal variability of isoprene, α-pinene, and limonene. The seasons are marked with different colors.

To better understand the origin of the above reported diurnal variability of terpenes, the seasonal diurnal variability of NO, CO, BC_{wb} and BC_{ff}, known as tracers of combustion processes (Diapouli

et al., 2017; Gratsea et al., 2017) is depicted in Figure S3. NO, CO and BC_{ff} exhibit a bimodal diel pattern regardless the season, with a morning maximum and a night-time enhancement period. On the contrary, BC_{wb} diurnal variability is notable only in autumn and winter, exhibiting a night maximum at 23:00 – 00:00 LT, followed by the gradual decrease till the appearance of a lower secondary morning peak. For all primary pollutants and BVOCs, the morning peak occurs at 08:00 and the night-time enhancement starts permanently at 19:00. The ratio of the night to the morning maximum is 2 and 3.5 times higher in winter than in summer for α-pinene and limonene respectively. Simultaneously for BC_{ff} the same amplitude is also increased by a factor of 3 during winter-time, whereas for BC_{wb} by almost a factor of 12. The latter is the result of the impact of wood burning for residential heating as it is has been also shown elsewhere (Gratsea et al., 2017). Finally, CO is 2 times higher in winter than in summer for both the morning maximum and the night-time enhancement period. Isoprene, α-pinene and limonene seem thus to follow a diurnal variation similar to anthropogenic compounds, especially in autumn and winter. Similar observations have been reported by other studies on monoterpenes conducted in urban areas (Hellen et al., 2012, Katsonoudis et al., 2016).

3.3 Role of dynamics and meteorology

Once emitted in the atmosphere, VOCs undergo various processes resulting in their chemical transformation or vertical/horizontal dispersion. The boundary layer evolution could drive the VOCs abundance and diurnal variability. The swallower mixing layer height (MLH) during night favors the accumulation of pollutants, whereas the daily growth allows the better ventilation of the basin and the dispersion of pollutants. It is already shown in Panopoulou et al. (2018) that in winter, the lower height of the MLH, the frequent occurrence of stagnant conditions (low wind speeds and absence of rainfall), as well as the higher emissions of VOC from sources related to heating, result in high ambient levels of pollutants. In summer however, the opposite conditions are expected. First of all, anthropogenic VOC emissions are reduced as a result of the lower activity in the city (e.g. holidays) and the absence of heating. The intense photochemistry also contributes to the VOC depletion. Furthermore, the height of the MLH in summer is higher than winter for both day and night, allowing the better vertical mixing of pollutants (Alexiou et al., 2018), in addition to the occurrence of “Etesians” which favor the ventilation of the Attica basin (Cvitas et al., 1985; Katsoulis, 1996; Lalas et al., 1983). For these reasons the measured VOC levels were re-evaluated relative to the MLH effect, by normalizing VOC values to MLH (multiplication with the ratio of the seasonal-mean MLH at each hour with the minimum hourly seasonal-mean MLH, occurring during the early morning hours) (Bansal et al., 2019). In winter (Figure 3), both measured and normalized VOC and BC, the latest used as a tracer of human activities, present rather similar diurnal cycles

and the MLH effect becomes evident only during the daytime. This indicates that during night the increased VOC and BC levels are exclusively attributed to sources than to MLH variability. During summer, the extremely lower measured VOC during daytime compared to night-time (Figure S4) is mostly attributed to dilution into a deeper boundary layer, without ignoring the role of photochemistry and emissions.

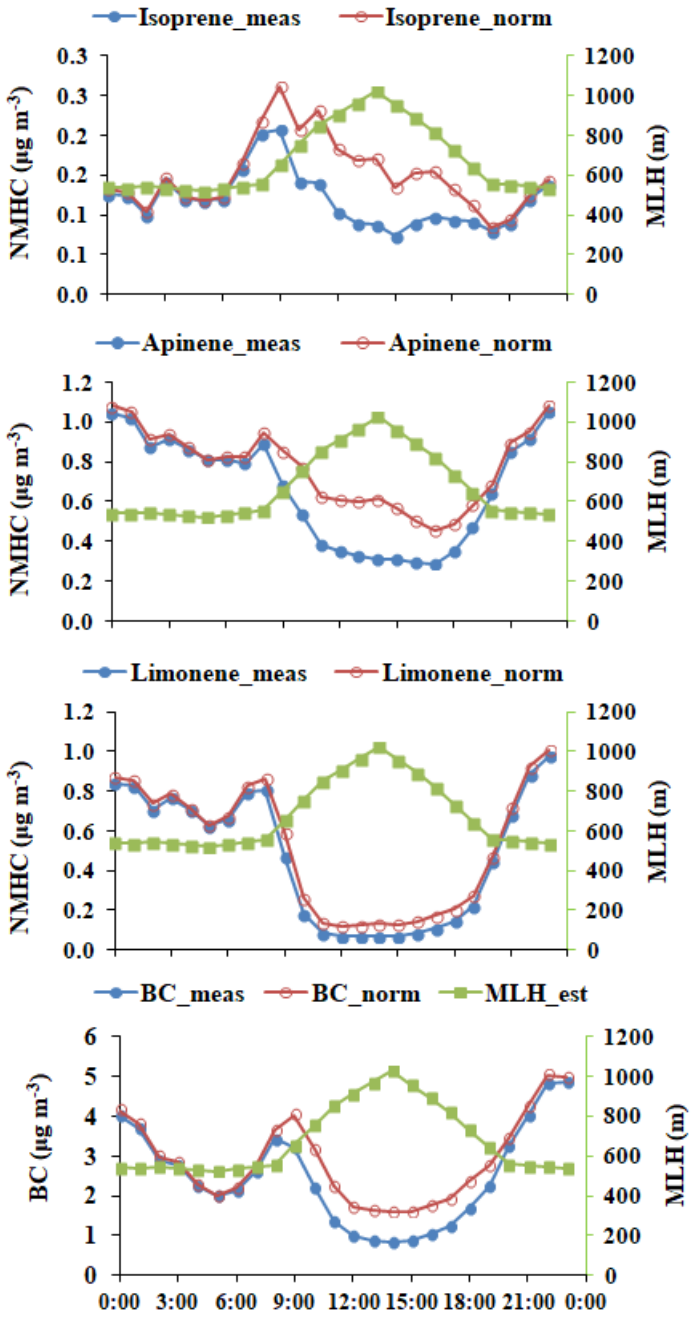

Figure 3. Mean diurnal variation of isoprene, α-pinene, limonene and BC, as well as their MLH-normalized values in winter. Each figure includes the seasonal-mean diurnal cycle of the MLH (m) obtained from HYSPLIT.

Since monoterpenes and isoprene are considered as species of biogenic origin, their emissions from vegetation are controlled by meteorological parameters such as the ambient temperature, relative humidity and solar radiation (Debevec et al., 2018; Guenther et al., 1995). It is known that the low wind speed prohibits the dispersion of compounds thus leading to elevated levels as already reported by e.g Fourtziou et al. (2017) and Panopoulou et al. (2018). The monthly variability of the aforementioned meteorological parameters is presented in Figure S5. As expected, the ambient temperature increases from winter (mean value: 12.1 ±4.2°C) towards summer (mean value: 28.5 ±4.0°C), followed by a gradual decrease from autumn (mean value: 19.7 ±5.2°C) to the next winter (mean value: 9.2 ±3.9°C). This trend affects greatly the seasonal variability of relative humidity that is the exact opposite, with the lowest values in summer (~ 42.8 ±12.1%) and the highest in winter (~ 62.0 ±12.7 %). On the other hand, there is not a distinguishable seasonal variability for wind speed, however, the highest median values and variability are observed in summer. The role of wind speed and temperature on monoterpenes and isoprene levels is then investigated on a seasonal basis and the results are depicted in Figures 4 and 5. The highest concentrations of all the studied compounds are associated to wind speed lower than 3 m s^{-1} (Fig. 4), indicating influence from local emissions. Exceptions are observed mainly for isoprene in summer where the summer concentrations are independent on wind speed. This indicates two different mechanisms of isoprene emissions in summer and winter.

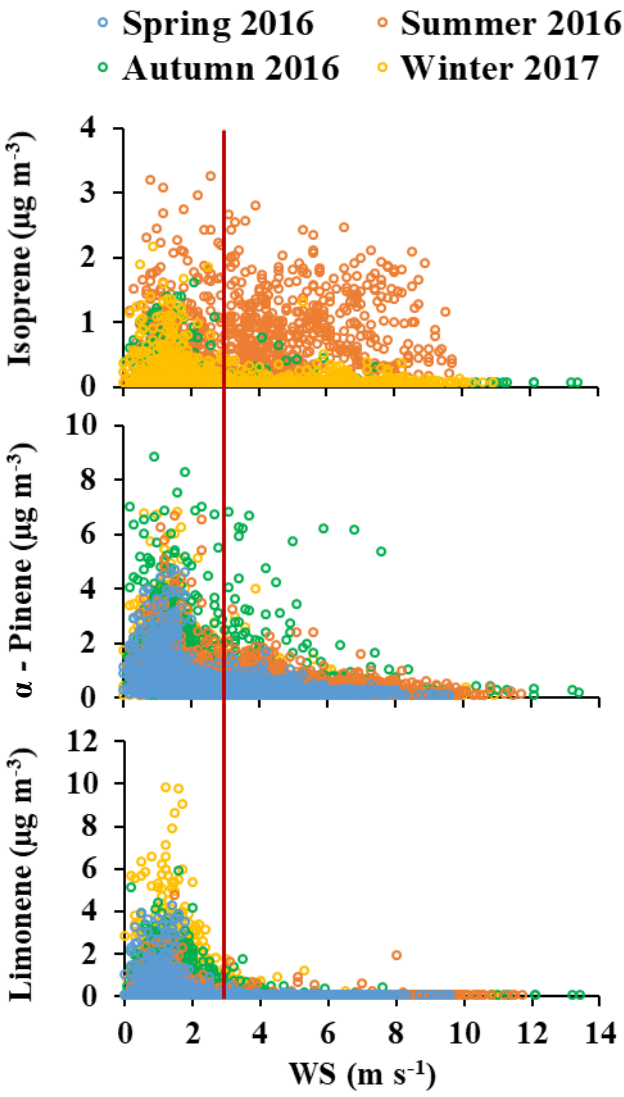

Figure 4. Seasonal variability of monoterpenes and isoprene relative to wind speed. The red line indicates the WS threshold of 3 m s^{-1}.

Furthermore, the group of some autumn α-pinene samples that appears to be excluded by the general wind speed related pattern is attributed to emissions after a rain event which facilitates the release of biogenic compounds from trees. Indeed, monoterpenes can be released from vegetation during or after rainfall events, due to the stress caused to the plants (Lamb et al., 1985; Debevec et al., 2018; Bouvier-Brown et al., 2009). In this work, the behavior of monoterpenes during and after the rainfall throughout the period of measurements was examined for rain events occurring under wind speed < 3 m s^{-1} (stagnant conditions). For comparison purposes, toluene was also used as reference of anthropogenic sources. The detailed analysis of the rain events is mainly based on observations during- and post-rain, with temperature and relative humidity conditions linked to the levels of monoterpenes before, during and after the precipitation as expressed by the enhancement ratios ($ER = \frac{VOC_{during\ or\ after\ the\ rain\ event}}{VOC_{before\ or\ during\ the\ reain\ event}}$). During rain events, the decrease of temperature for more than

3°C, accompanied by an increase of relative humidity from lower than 55% to higher than 65% seem to influence the biogenic emissions, which is independent of the precipitation height. For these cases, the ER could be even fourfold, whereas toluene levels remained almost the same (ER of ~1). For rain events occurring during the morning or night maximum, the naturally induced emissions could be masked by the enhanced anthropogenic local emissions and ER for terpenes not different to 1 were observed. Thus, in the following discussion and to avoid a sporadic influence of strong biogenic emissions, days with rain events (7% of the monitoring period) are excluded from further analysis.

Finally, α-pinene, limonene and isoprene present a non-uniform relation to ambient temperature (Fig. 5a and b). For isoprene, with the exception of winter, an almost exponential increase is observed with temperature. During winter a unimodal distribution is observed with higher levels being associated to low (<10^{o}C) temperatures and with no difference between night and day. Although the increase of isoprene with temperature has already been reported in the literature, the high isoprene values associated to low temperatures in winter indicate a non-biogenic origin. For terpenes, again with the exception of winter, a decrease with temperature is observed, which could be attributed to photochemistry, whereas the enhanced levels during cold conditions indicate a non-biogenic source. The increased night-time levels of terpenes under low temperatures and wind speed (T< 10°C and WS < 3 m s^{-1}), point also towards emissions of these compounds from sources other than biogenic.

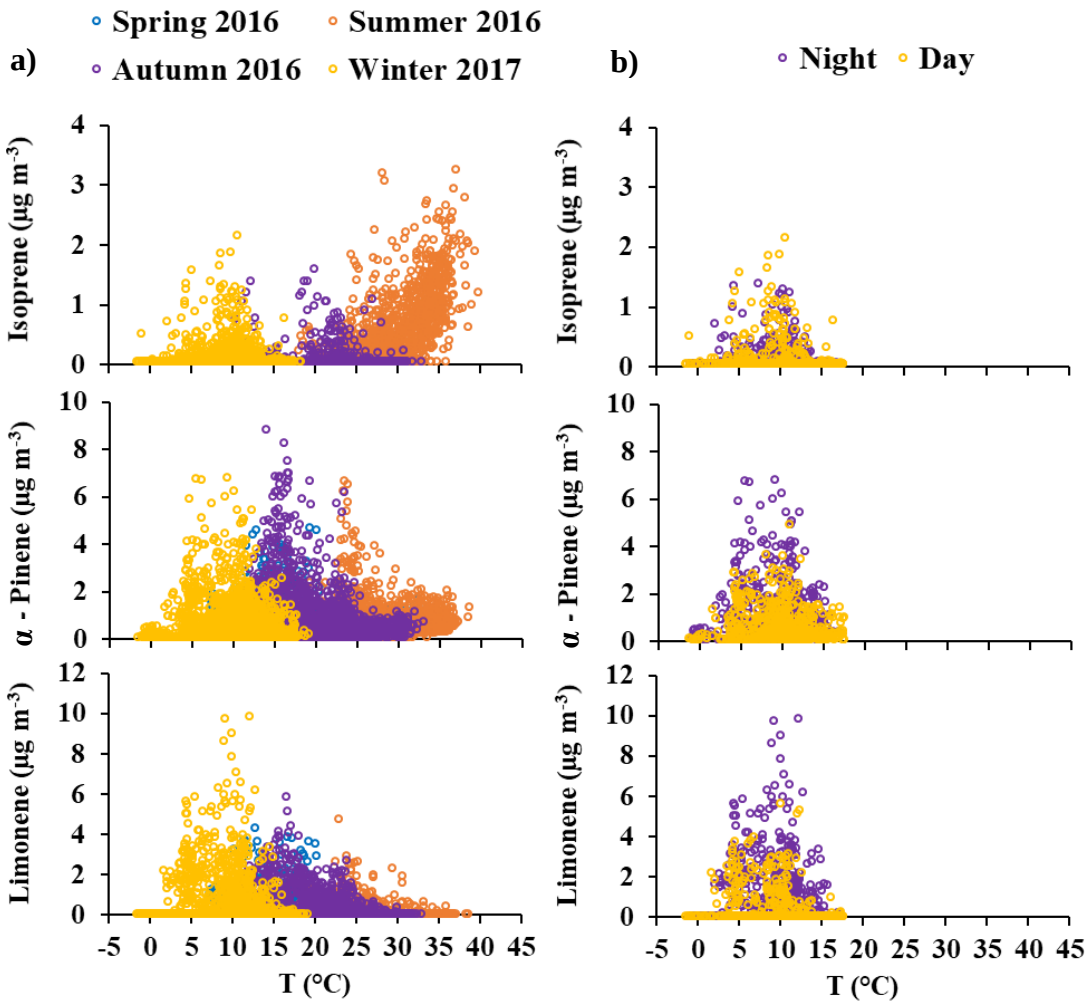

Figure 5. Scatterplots of isoprene, α-pinene and limonene with temperature (a) in seasonal basis and (b) during winter day-time (06:00 - 17:00 LT) and night-time (18:00 – 05:00 LT) concentrations for WS less than 3 m s^{-1}.

3.4 Biogenic versus anthropogenic emissions of terpenes and isoprene in Athens

Table S2 presents the interspecies correlations of α-pinene, limonene, isoprene and major primary pollutants including toluene used as a tracer for VOCs emitted by anthropogenic activities. Overall, the correlation of monoterpenes to the combustion tracers are found to be dependent on season; in summer, when biogenic activity is expected to be more intense, the relationships are very low but statistical significant at 95%, whereas in winter both species significantly correlate with each other and with the tracers. Specifically, during summer quite low correlation coefficients (R^2<0.50) were observed for limonene versus α-pinene, while limonene is correlated to BC, NO and CO (R^2: 0.51 – 0.61). On the contrary during winter, α-pinene and limonene correlate well with each other (R^2 = 0.81) as well as with the combustion related compounds (R^2>0.55). Isoprene is not correlated with any of these tracers in any season. Note than limonene is also highly correlated to toluene, BC, BC_{wb}, BC_{ff} and CO (R^2: 0.74, 0.71, 0.62, 0.51 and 0.51 respectively) when the whole dataset is considered,

whereas α-pinene and isoprene not. By further correlating the diurnal patterns of VOCs presented in Figure 2, indications for common emission sources exist for the terpenes throughout the year. On the other hand, isoprene follows a different diurnal pattern (Figure S6).

To further examine the possible anthropogenic origin of monoterpenes the relationship against toluene was examined on a seasonal basis for the time-frame 06:00 – 09:00 LT, i.e period with important traffic impact (Panopoulou et al., 2018) and by excluding the rainy days (Fig. 6). Both monoterpenes present a relationship to toluene, with statistically significant correlation coefficients for all seasons indicating emissions from traffic. Furthermore, the slope of α-pinene to toluene is almost a factor of 2 higher in summer than in winter, probably due to additional biogenic emissions of α-pinene in summer. On the other hand, the slope of limonene to toluene is slightly higher in winter compared to summer indicating more emissions for that season, in addition to traffic, most probably heating based on the significant correlation with BC_{wb} (Table S2).

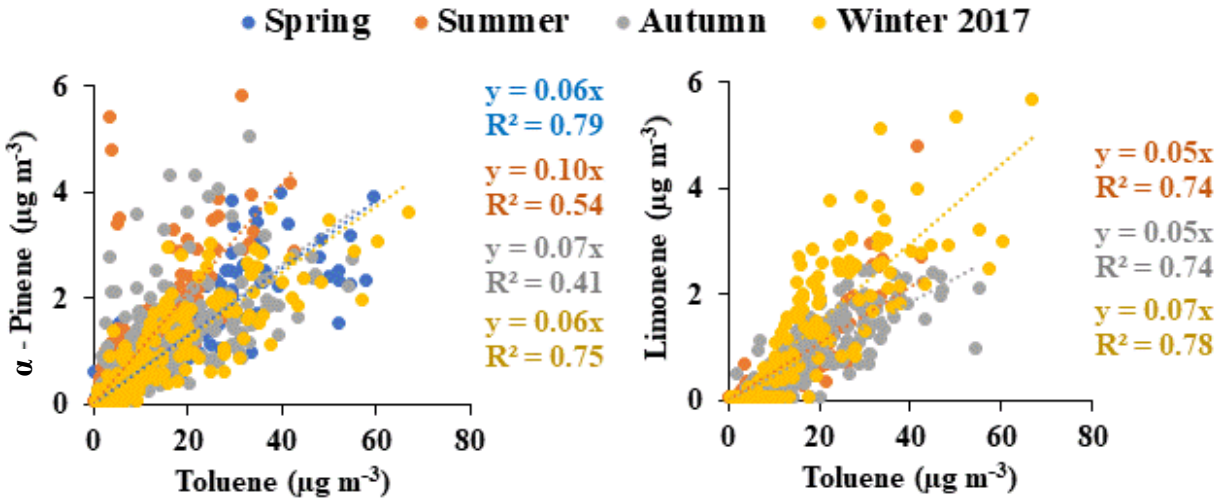

Figure 6: Seasonal scatterplots of α-pinene and limonene to toluene for the daytime (06:00 – 09:00 LT) time frame. The scatterplot of limonene in spring 2016 is excluded due to the great number of values equal to ½ LoD.

Since in winter we expect an insignificant biogenic activity, we focus at that season to better understand the origin of high levels of terpenes and isoprene during that period (Figures 2 and 5). Consequently, their morning (06:00 – 09:00 LT) and night (21:00 – 02:00 LT) maxima were related to toluene, CO, BC_{ff} and BC_{wb} (Figure 7). Monoterpenes and toluene are significantly correlated during both day and night, corroborating the assumption of their common anthropogenic origin. In addition, the slopes were slightly higher during night compared to daytime, indicative of a source in addition to traffic. The slopes of α-pinene and limonene to CO were almost identical for both day and night, supporting the assumption of fuel combustion as a source of monoterpenes. The latter is further supported by the increased monoterpenes emission under low temperatures during night (Fig.

4), as well as by their correlation to BC_{wb} and BC_{ff} especially at night (R^2 between 0.65 and 0.79). Furthermore, the higher morning slope for the relationship to BC_{wb} could be attributed to the lower morning levels of BC_{wb} compared to night-time (Figure S3 of the supplement). Concerning isoprene, significant correlation was observed only with CO during morning (Figure 7b). The higher morning slope compared to night, could indicate stronger impact of the not complete heating processes leading to higher CO emissions relative to traffic. Moreover, the stronger correlation to BC_{wb} fraction in the night depicts the role of wood burning for residential heating on the levels. All the above relations clearly suggest that vehicle and heating have an effect on monoterpenes and isoprene depending on the fuel type (oil or wood).

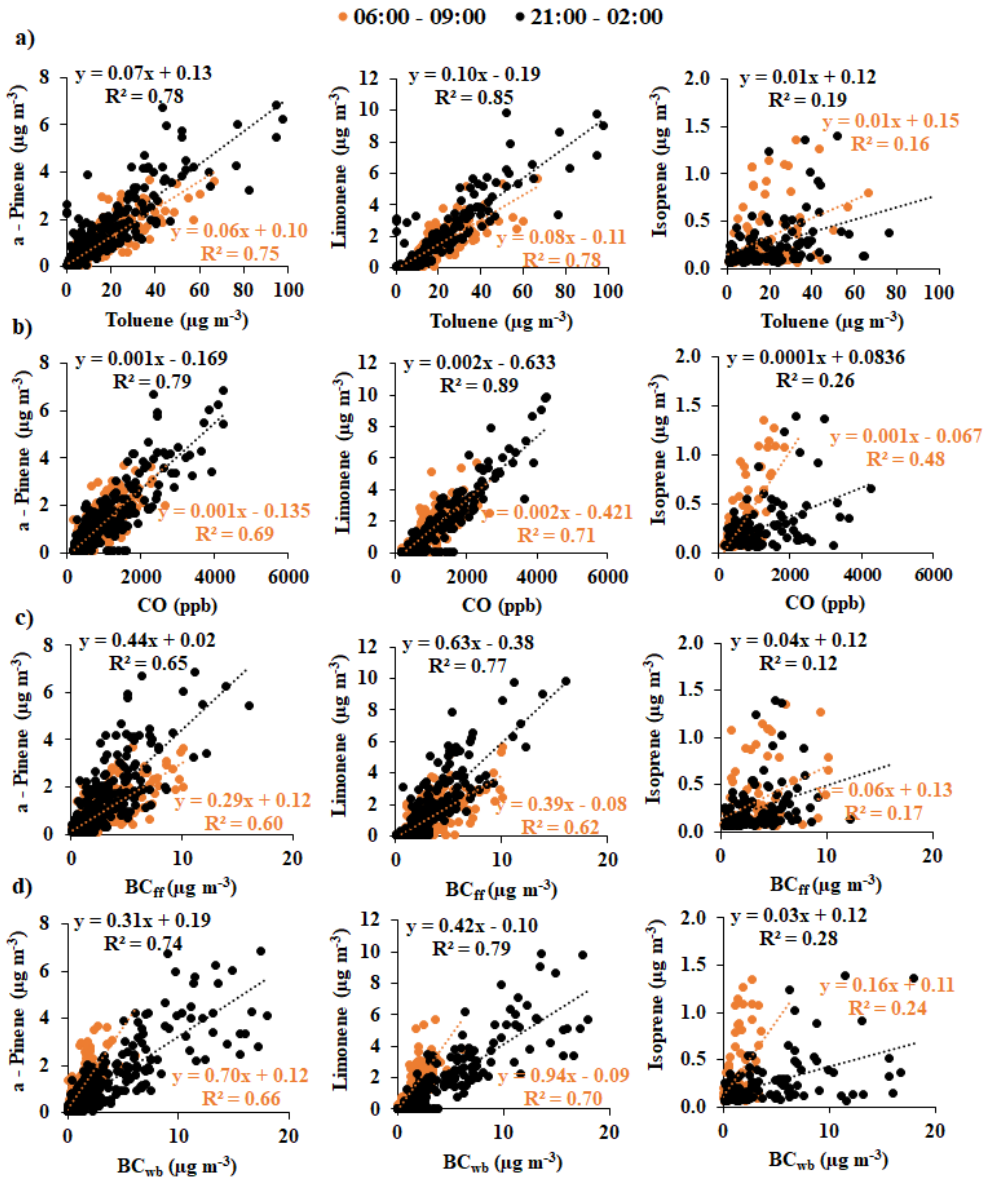

Figure 7: Scatterplots of α-pinene, limonene and isoprene to (a) toluene, (b) CO, (c) BC_{ff} and (d) BC_{wb} during day and night (6:00-9:00 and 21:00-02:00 respectively) in winter 2017.

An estimation of the anthropogenic and biogenic fraction of monoterpenes is attempted, based on an adapted method from Brito et al. (2015). This approach uses the VOC-to-CO night ratios (20:00 – 06:00 LT) to calculate the anthropogenic fraction (AF), since at this time-frame any biogenic contribution related to photosynthesis is absent. In our case we used toluene as a tracer of anthropogenic activities as a significant background contribution for CO could impact the results. Consequently, the VOC-to-Toluene ratios were calculated for summer and winter, in order to evaluate the different anthropogenic sources (traffic vs traffic plus residential heating respectively). This method was applied only to α-pinene which presents significant amount of levels above LoD throughout the year.

The primary anthropogenic component of monoterpenes was thus calculated for every sample in winter and summer using the following equation:

$$AF_i = ER_{ij} \times [\text{Toluene}] \quad \text{Eq. 1}$$

Where AF is the primary anthropogenic factor of a given VOC *i* and ER_{ij} is the emission ratio to toluene of the compound *i.* The period 18:00 – 05:00 LT was used for the calculation of the ER and the results are presented in Table S3.

The biogenic contribution was then calculated as the difference between the AF and the measured levels of α-pinene using Eq. 2:

$$BFi = [VOC_i] - AFi \quad \text{Eq. 2}$$

Where BFi is the biogenic fraction of the concentration of a compound *i*, $[VOC_i]$ is the concentration of the compound *i* and AF the anthropogenic fraction from Eq. 1. Finally when the actual concentrations of the α-pinene were equal to ½ LoD the contribution of both AF and BF was set as 0.

The mean VOC concentration and the seasonal contributions of AF and BF for α-pinene are depicted in Figure 8. AF dominates in both seasons, although in summer the BF contribution is also important and accounts for almost 40% of the measured levels.

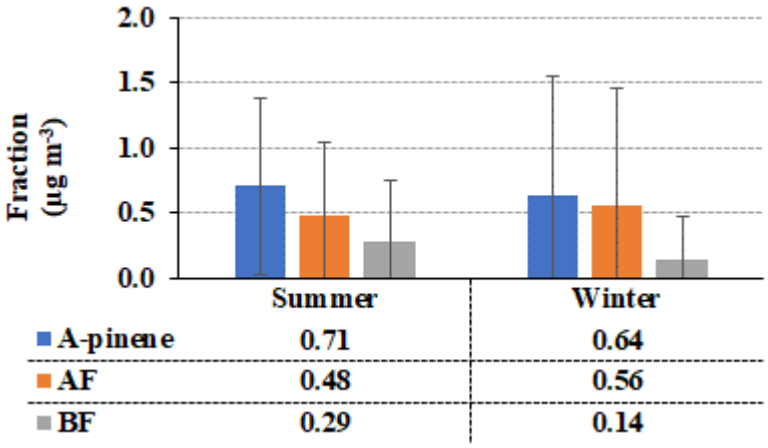

Figure 8: Mean seasonal concentrations of α–pinene and its anthropogenic (AF: orange) and biogenic fractions (BF: grey). The bars indicate the standard deviation. Days with rain events are excluded.

3.5 Ozone and secondary organic aerosol formation potential

The ozone formation potential (OFP) from the oxidation of the measured terpenes and isoprene could be estimated by taking into account the concentration of monoterpenes and their reactivity as expressed by the maximum incremental reactivity (MIR). OFP is calculated as the amount of ozone formed (in gram) per gram of VOC added to initiate the VOC–NOx reaction (Carter, 1994, 2009) according to Equation 3:

$$OFP_i = \sum_{i=1}^{n} C_i \; x \; MIR_i \qquad \text{Eq. 3}$$

Where C_i (µg m^{-3}) is the mass concentration of the compound *i* and MIR_i the maximum incremental reactivity (MIR) of the compound I, taken from Carter (2009) and provided in Table S3.

The seasonal relative contribution (%) of monoterpenes and isoprene to the OFP is depicted in Fig. 9a, presenting high contribution in summer (35%) and almost a factor of 2 lower values in spring (15%). According to Figure 9b, the dominant contributor to ozone formation regardless the season is α-pinene (by producing on average 2.9 µg m^{-3} of O_3), whereas limonene participates significantly on the OFP mainly during winter and isoprene is important mainly during summer yielding into averagely 5 µg m^{-3} of ozone. To better evaluate the role of monoterpenes and isoprene on observed ozone levels, OFP deduced form the above calculations was compared to the sum of measured O_3 + NO_x, hereafter called oxidants. Almost 7% and 6% of the observed oxidants levels during summer and winter, or in other words 9 and 6 µg m^{-3} respectively, is attributed to the total reactivity of isoprene and monoterpenes.

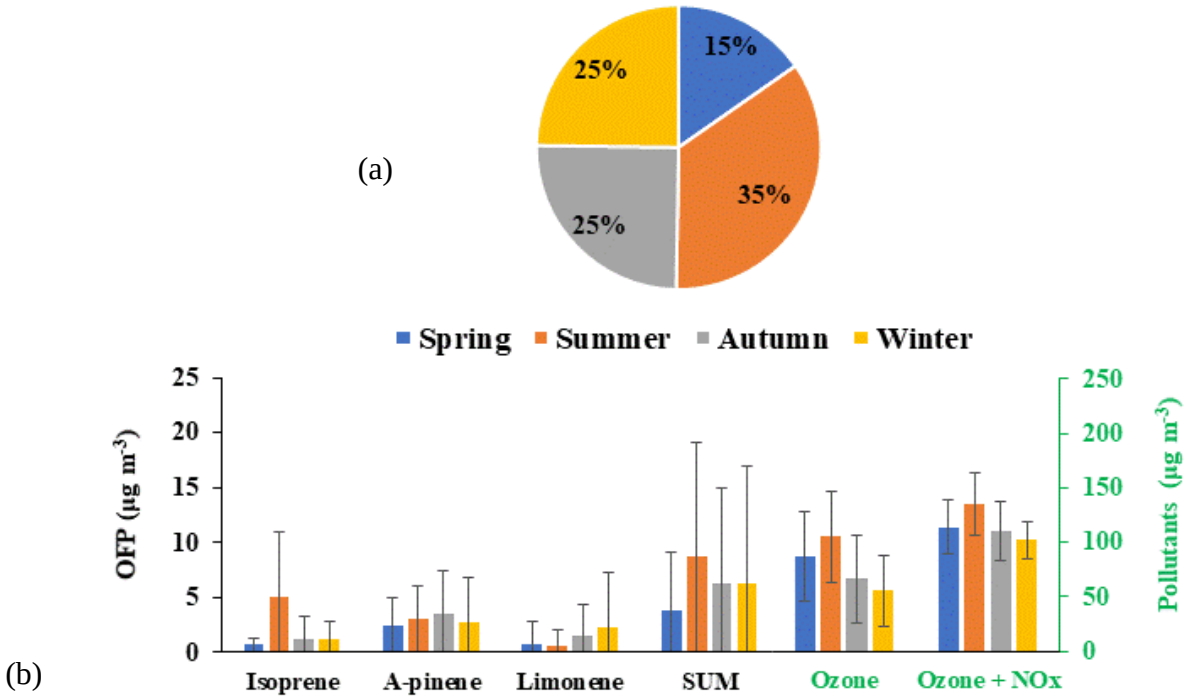

Figure 9: (a) Seasonal contribution of isoprene and monoterpenes to the OFP and (b) deconvolution of contributions relative to the observed levels of O_3 and oxidants (as sum of O_3 and NO_x).

For the secondary organic aerosol formation potential (SOAFP) the emission ratios of the monoterpenes to a reference compound are considered. In our case toluene was used as a reference with $SOAP_{Toluene}$=100. Isoprene is excluded due to the absence of correlation with toluene. The model-derived SOAFP reflects the simulated mass of aerosol formed per mass of VOC reacted and was estimated based on the following equation:

$$SOAFP_i = ER_i \; x \; SOAP_i \qquad \text{Eq. 4}$$

where ER is the emission ratio to toluene for the compound *i* and SOAP is the model-derived SOA potential (no units) taken from Derwent et al. (2010) and provided in Table S3.

SOAFP is estimated for every season for the day-time (06:00 – 17:00 LT) and night-time levels (18:00 – 05:00 LT), by calculating the corresponding emission ratios to toluene (Table S3). According to Figure 10, α-pinene contributes with about 2 µg m^{-3} during summer and 1.2 µg m^{-3} for the rest of the year. The contribution of limonene increases from summer to winter, with maximum SOAFP of approximately 1.5 µg m^{-3} in winter nights. Limonene's SOAFP in spring was excluded due to the great number of concentrations close to the LoD. The importance of the terpenes' contribution on SOA is exploited in Figure 10 by the comparison with the non-refractory PM_1 fractions of organic aerosols derived from Stavroulas et al., 2019 and especially the sum of semi-volatile oxygenated organic aerosol (SV-OOA) and hydrocarbon-like organic aerosol (HOA). During summer both SVOOA and HOA levels could be fully explained by the monoterpenes'

reactivity (sum of α-pinene and limonene). The same stands for the winter day time, whereas the 40% contribution of monoterpenes to SOAFP during night (i.e 2.8 μg m^{-3} from 7.0 μg m^{-3}) reflects the existence of other wood burning emitted compounds. The hypothesis of the winter-time production of organic aerosol by the monoterpenes can also be supported from the common variability of their diurnal patterns (R^2=0.68; Figure S7).

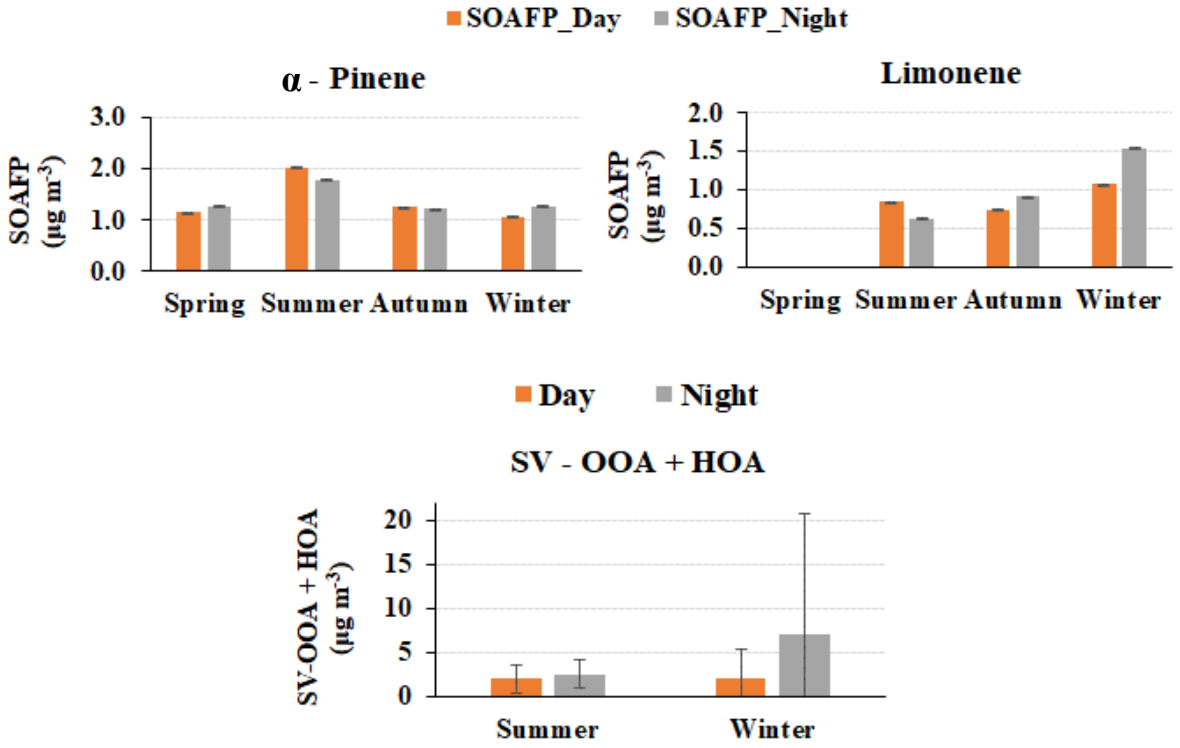

Figure 10: Seasonal SOAFP of α-pinene and limonene during the day-time (06:00 – 17:00 LT) and night-time 18:00 – 05:00 LT) periods. The levels of semi-volatile and hydrocarbon-like organic aerosols (SV-OOA and HOA respectively) are also depicted for the respective time frames.

3. Conclusions

As it was mentioned in the introduction of the chapter, α-pinene and limonene exhibit significant mean levels in winter (0.67 ±0.91 μg m^{-3} and 0.48 ±1.06 μg m^{-3} respectively), whereas isoprene's is also present but with a lower mean value of 0.12 ±0.18 μg m^{-3}, denoting an influence probably from anthropogenic emissions. The examination of their variability for 13 months presented in this manuscript -to be submitted for publication-, gave important insights for the verification of the previous basic assumption. Whereas isoprene's seasonal variability follows biogenic activity, with the highest values in summer and a decreased (but not absent) variability in the cold period, the seasonal variability of monoterpenes is more unusual. Indeed, α-pinene and limonene showed an unexpected maximum during the coldest months, and only the former presents significant levels in spring and summer. Furthermore, the diel cycle of monoterpenes is characterized by low levels during the day with a night-time to early morning increase, which is more pronounced in autumn and winter and lasting also longer. Nevertheless, it is worthwhile mentioning the levels of α-pinene at noon during summer, which are two times higher relative to the winter ones. On the other hand,

the seasonal diurnal variability of isoprene is different for the warm and cold period, with a daytime maximum in summer (following the increase of temperature and insolation that triggers biogenic emissions) and a morning maximum from 07:00 to 10:00 LT in autumn and winter.

Concerning the influence of atmospheric dynamics on the observed variability of monoterpenes (wind speed, wind direction, temperature, relative humidity, precipitation, solar intensity), there are no observations that could justify an influence from biogenic activity, with the exception of some sporadic data related to precipitation for α-pinene. Specifically, an enhancement of the levels is observed for low wind speed (except of isoprene in summer) under stagnant conditions (low mixing layer), highlighting an effect from local emissions. Moreover, high concentrations are related also to low temperatures in (<10°C) in winter, denoting an influence from residential heating emissions.

Following the above observations, the influence of anthropogenic sources was investigated by the relationship of monoterpenes and isoprene to other pollutants (toluene, CO, BC_{wb}, BC_{ff}) in selected time-frames. These showed correlations for all seasons with statistically significant correlation coefficients, verifying the contribution of emissions that originate from traffic (in all seasons) and wood burning related to residential heating in winter. Furthermore, since for monoterpenes the biogenic influence is hidden by the anthropogenic emissions, the estimation of the biogenic and anthropogenic contribution in α-pinene's levels was estimated using the approach of Brito et al., (2016). This approach showed that indeed even in summer, the anthropogenic contribution surpasses the biogenic one. Interestingly, the biogenic fraction of α-pinene follows the variability of isoprene in summer, corroborating its origin from vegetation.

Finally, since monoterpenes and isoprene are very reactive species, their ozone and SOA formation potential were estimated. Specifically, in summer and winter, 9 and 6 μg m^{-3} respectively or 7% and 6% of the reported concentrations of oxidants (sum of O_3 + NO_x) is attributed to the reactivity of both isoprene and monoterpenes. Furthermore, the reactivity of α-pinene and limonene in summer and winter day-time fully explain the SVOAA and HOA levels, whereas they contribute 40% to SOA in winter nights. Therefore, these results highlight the key role of these compounds in the formation of important secondary pollutants that are responsible for the most severe air pollution episodes (e.g. photochemical smog).

Having seen in **chapters 3, 4** and **5** the important influence of the emission sources on VOC variability in Athens, a source allocation is conducted in the next and final chapter of the current thesis, using a statistical tool (Positive Matrix Factorization or PMF).

CHAPTER 6 –Sources of VOCs in Athens.

TABLE OF CONTENTS FOR CHAPTER 6

Introduction

In the previous chapters it was shown that emissions from sources have a strong impact on the variability of all types of VOC. This is more apparent in winter, when high concentrations of compounds are observed in comparison to the other seasons, as well as to other studies worldwide (**Chapters 3** and **4**). Furthermore, in **Chapter 3**, traffic and residential heating are identified as the main VOC sources in Athens for the cold period, however it was not possible to quantify their contribution, nor identify other sources. Nevertheless, the same anthropogenic sources were found to contribute significantly also to monoterpene levels, a trend that is rarely investigated in the existing VOC studies (**Chapter 5**). Going back to Athens, the only existing study on VOC sources was performed using mainly aromatics and OVOCs (Kaltsonoudis et al., 2016), thus the results were not representative of all VOCs classes, denoting the need of a new approach that takes into account lighter compounds from other VOC classes (alkanes, alkenes etc). In the same context, in **Chapter 1** it was shown that more studies dedicated to the source allocation of VOC emissions are needed in the urban areas of the Mediterranean region, firstly due to their limited number and secondly due to the high uncertainties that are observed between their results and observations from emission inventories (i.e. Salameh et al., 2017). Consequently, since one of the main objectives of the current thesis is the source allocation of the VOC emissions in Athens, in this chapter we expect: (1) to understand better the type of sources of these compounds in this capital city of the Mediterranean region, and (2) to give robust results and conclusions for the sources of monoterpenes (**Chapter 5**).

In general, "source apportionment**"** is the procedure followed for the allocation of pollutants to their respective sources, using various tools and approaches that include statistical analysis, model simulation and other (Belis et al., 2014; Hopke, 2016). These were already described in **Sect. I – A1** of the **Annex I**. Thus, this chapter focuses on the source allocation of VOCs, which is applied separately to the two obtained datasets (MOP and IOPs, or Main and Intensive Observation Period). This will allow firstly the comparison of both PMF results in terms of sources' number and type, and secondly a discussion of the identified sources in comparison with other studies in the literature. What are the VOC sources in Athens?

1. PMF source apportionment on the MOP dataset

Since for the current thesis, the selected sampling station was urban background (**Chapter 2**), the receptor-oriented models can be applied to the VOC dataset (**Sect I – A1** of **Annex I**). In addition, there was only little prior information for the number of pollutant sources in Athens due to the absence of this type of studies (**Chapters 1** and **3**), whereas only the chemical profile of the traffic sources was established (**Chapter 2** and **3**). Thus, the most appropriate tool for the source apportionment of the compounds of the MOP is PMF. In the next paragraphs are explained in detail the preparation for the PMF analysis, the choice of the optimal solution and the results.

1.1 PMF model description

Positive Matrix Factorization (or PMF) is a multivariate factor analysis tool for the quantification and the identification of the sources of atmospheric pollutants (**Sect I – A1** of **Annex I**). It has being used for the VOC source allocation in several studies already, in urban and other locations (e.g.

Baudic et al., 2016 – Paris, France; Salameh et al., 2016 – Beirut, Lebanon; Kaltsonoudis et al., 2016 – Athens and Patras, Greece; Brown et al., 2007 – Los Angeles, California; Bari and Kindzierski, 2018 – Alberta, Canada; Guo et al., 2011 – suburban area in the PRD region, China; Sauvage et al., 2009 – rural area in France; Yang et al., 2018 – rural area in Beijing, China; Abeleira et al., 2017 – semirural area in Colorado, America). For the current thesis, the PMF v.5 software developed by EPA (Environmental Protection Agency) was used. The mathematical theory of PMF is described in detail in Paatero and Tapper, (1994) and Paatero, (1997).

In general, the PMF statistical method uses a weighted least square fit that decomposes a matrix of a speciated dataset into two matrices, namely factor contributions and factor profiles. The main principles are summarized in Eq. VI - 1:

$$X = F\ G\ x\ E \qquad \text{Eq. VI - 1}$$

where X is the input dataset matrix (for example, the observed concentrations at a receptor site) of certain dimension (*m* compounds x *n* samples), G is the source contribution matrix (i.e the mass contribution of one source to one sample), F is the source's profile matrix (meaning the species mass fraction from the source) and E is the residual matrix that is associated to the concentration of the species in every sample. Along with the dataset matrix, an uncertainty (of the concentrations) matrix, with the same dimensions as the input data matrix (*m* compounds x *n* samples), is also needed, since the PMF tool weights is based on the Signal to Noise (S/N) ratios of each variable. Lastly, the results have a non-negative constrain, meaning that no sample can have significantly negative sources' contribution.

1.1 - 1 Dataset and uncertainty matrix

The input dataset matrix used for the PMF statistical analysis contains the 30-min concentrations (in μg m^{-3}) of the NMHC monitored in the MOP (**Chapter 2**). Acetylene, isoprene and terpenes were excluded. In particular, as it was mentioned in **Sect. 1.1** of **Chapter 4,** the data coverage of acetylene is not satisfactory, whereas the concentrations of isoprene are most of the time below the LoD. In addition, α-pinene and limonene were excluded by this PMF because they present a complex share of emissions between anthropogenic and biogenic sources (**Chapter 5**), which could make the interpretation of the resulted factors difficult, thus these compounds are included only in the IOPs PMF (later in the chapter). Moreover, prior to the analysis, the data points were treated as follows:

$$x_{ij}\begin{cases} x_{ij} & ,\ x_{ij} > {LoD_j}/{2} \\ {LoD_j}/{2} & ,\ x_{ij} \le {LoD_j}/{2} \\ N/A & ,\ x_{ij} missing \end{cases}$$

Unfortunately, due to technical issues in the GC C2 – C6 that hindered the identification and quantification of some compounds, the proportion of missing values is high. More specifically, the missing values for the C2 – C6 compounds vary between 30% (i-pentane) – 50% (butenes), with the highest number of missing points in autumn (>30% over the maximum potential of the season and for continuous periods). On the other hand, for the C6 – C12 compounds the missing points are less than 10% and they mainly consist in calibrations samples. Consequently, concerning the C2 – C6 NMHCs dataset, since the missing values correspond to different compounds in every sample and

additionally, to consecutive samples for a long period, as well as the moderate representativity of autumn, indicate that the substitution of these points by their geometrical means (conducted in other studies like in Baudic et al., 2016) is not possible. However, the remaining matrix has large dimensions (24 compounds x 8278 samples), thus a robust PMF statistical analysis is expected (Norris et al., 2014).

For the uncertainty matrix, the uncertainty of the concentration of the NMHCs was calculated taking into account all possible errors, as it is already described in Sect. **2.2.6** of **Chapter 2**. In a summary, the individual uncertainty applied in our approach is described as follows:

$$u_{ij}\begin{cases} u_{ij} & , \quad x_{ij} > LoD_j \\ 5/6\, LoD_j & , \quad LoD_j/2 \le x_{ij} \le LoD_j \\ N/A & , \quad x_{ij} missing \end{cases}$$

Lastly, the compounds are categorized based on their signal-to-noise ratio (S/N) before the application of the method. Paatero and Hopke (2003) firstly introduced this term, which considers the variability of the concentration and the uncertainty. The ratio indicates whether the variability in the measurements is real or within the noise of the data, since only concentrations above their species uncertainty contribute to the signal portion. Similarly, compounds with the majority of their concentrations below the uncertainty or with a large number of observations with high uncertainty are characterized by a low S/N ratio. Usually, for S/N ratio less than 0.2, the species are categorized as "bad" and they are excluded; for an S/N ratio between 0.2 and 2, the species are considered as "weak", thus their uncertainty is tripled; finally, the compounds with S/N greater than 2 are considered "strong" and their uncertainty remains unchanged. In our case, most of the species have a S/N ratio higher than 2. 1.3.5 TMB and 1.2.3 TMB were characterized as "bad". Isooctane and 1.2.4 TMB were species with S/N > 1.6, but since they are good tracers of sources related to fuels, they were kept as strong. Finally, because trans-2-butene and 1-butene were the compounds with the highest number of missing points (48% and 47% respectively) they were also characterized as bad in order to increase the number of modelled data from 38% to 44%. The NMHCs of the input matrix, their S/N ratio and their characterization is presented in **Table VI – A1** of the **Annex VI**.

1.1 - 2 Determination of the optimal solution

For the determination of the optimal solution, PMF simulations were performed with 4 to 8 factors. For all the simulations were performed 50 runs, in order to obtain the most robust solution. The diagnostic parameters include the value of R^2, which is the correlation coefficient of the measured sum of VOC per sample to the modelled sum of VOC per sample, IM (maximum individual column mean) and IS (maximum individual column standard deviation), which were defined by Lee et al. (1999), as well the $Q_{true}/Q_{expected}$ value. For the latter, a value close to 1 indicates that the data of the uncertainty input matrix are well estimated, thus the reproduced datapoints are within the estimated error value. These parameters are then plotted against the number of factors (from 4 to 8). The number of factors (p) that is chosen, normally corresponds to a significant change of Q, IM, and IS (**Fig. VI - 1**).

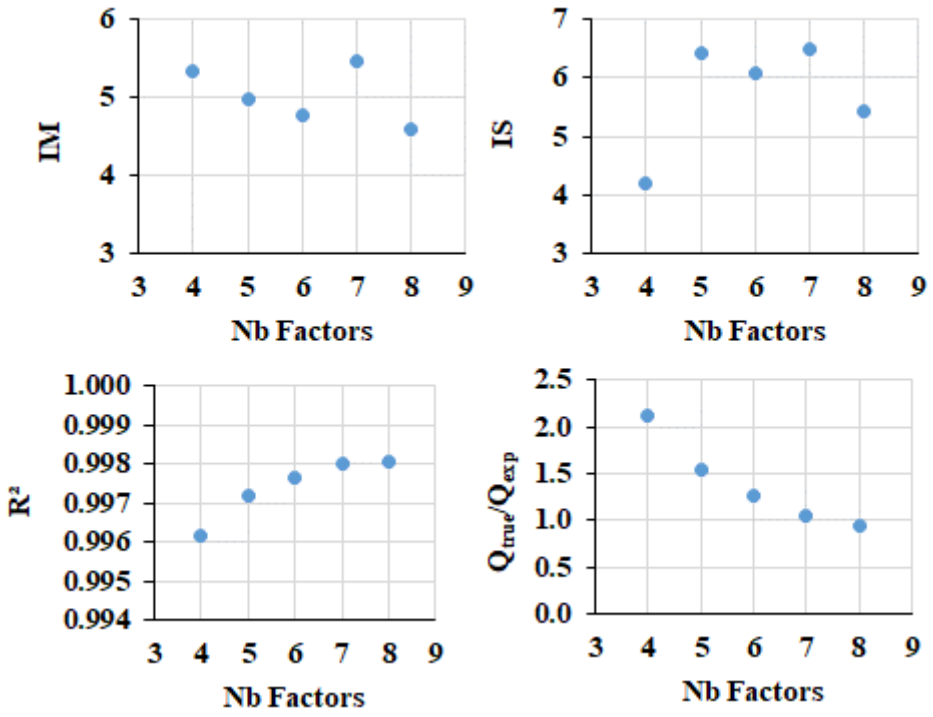

Figure VI - 1: IM, IS and R^2 in function of the number of factors.

In **Figure VI - 1**, we observe firstly a slight decrease of the IM parameter from the 4-factor solution to a 6-factors solution, which is not accompanied by a decrease of the IS. On the contrary IS increases with increasing number of factors. The R^2 is already very good (> 0.995). The optimal solution seems to be between a 4- and 6-factor solution. Furthermore, the Q_{true}/Q_{exp} values decrease with increasing number of factors reaching ~1 for the 8-factor solution, with the most important decrease to be from the 4-factor solution to the 5-factor solution. This happens because when new factors are added, the variability in the factor profiles increases. However, the decrease is not significant after the 5-factor solution indicating that the variability of the dataset is predicted well even from this run despite the addition of factors (Paatero and Tapper, 1993). Finally, by examining the profiles and temporal variation of each factor for every PMF simulation for 4 to 8 factors it is apparent that opting for p > 6 did not provide any additional physical meaningfulness to existing profiles, whereas by choosing p=5 instead of p=4, two factors of different profiles are gained (Factors 1 and 4 for the 5-factor solution)(**Figure V1 - A1** of the **Annex VI**). This phenomenon is known as splitting (Ulbrich et al., 2009) and it serves as an additional criterion while narrowing down on a PMF solution. Thus, the final solution is the 5-factor one.

1.1 - 3 Robustness of PMF results

In this paragraph are reported the technical and mathematical indicators of the 5-factor solution for the assessment of its robustness and quality. Firstly, the ratio between Q_{robust} and Q_{true} is 0.93 which is close to 1.0, indicating that the modeled results were not biased by peak events. Furthermore, 98.5% of the scaled residuals were within ±3σ. In addition, the very good R^2 (0.997) shows that all variance in the total concentration of the 20 VOCs can be explained by the PMF model. The same is observed for all the chemical species that displayed good correlation coefficients (R^2 > 0.75) between predicted and observed concentrations. The slopes between the modeled and measured NMHC concentrations were higher than 0.85 for all the compounds, except of ethane and i-octane

that were 0.70 and 0.72 respectively. The smaller slope of ethane reflect the insufficient modelling of its concentrations the period prior to the trap change (**Chapter 2**, **Sect. 2.2.1**), whereas for i-octane it is associated to its greater number of concentrations close to the LoD, which could affect the simulation of these compounds by the PMF. Overall, the statistical parameters indicate that the 5-factor PMF solution is robust and can explain greatly the variation of the NMHC measured concentrations. Finally, the mathematical diagnostics for the final solution are presented in **Table VI – 1**.

Table VI - 1: Mathematical diagnostics for the final solution of the MOP PMF.

(m) species	25
(n) samples (without excluded)	8278
(p) Factors	5
Number of species characterized as bad	4
Number of species indicated as "weak"	1 (Total Variable)
Runs	100
Number of random seed	23
$Q_{(robust)}$	177224
$Q_{(true)}$	189934
Q(T)/Qexp	1.53
$NMHC_{modeled}$ vs. $NMHC_{measured}$ (R^2)	0.997
Number of species with $R^2 > 0.75$ (modeled vs. measured)	19
Fpeak	-0.5
$dQ_{(robust)}$ of Fpeak	4 (0.0%)

1.1 - 4 Estimation of model prediction uncertainties

PMF output uncertainties can be estimated using the error estimation options starting with DISP (dQ-controlled DISPlacement of factor elements) and processing to BS (classical BootStrap). These two uncertainty methods are designed to provide key information on the stability and the precision of the chosen PMF solution (Paatero et al., 2014).

The DISP (base model displacement error estimation) assesses the rotational ambiguity of the PMF solution by exploring intervals (minimum and maximum) of source profile values. During the DISP, a minimum Q value is calculated, based on the adjustment up and down in factor profile values, and compared with the unadjusted solution Q value. The difference between the initial Q value and the modified Q value (the so-called dQ) should be lower than dQ max value, for which four levels (values of 4, 8, 15 and 25) were taken into account. For each dQ max value, 120 intervals were estimated. The DISP analysis results are considered validated: no error could be detected, and no drop of Q was observed.

The BS is also used to evaluate the reproducibility of the PMF solution. A further description on the bootstrapping technique is presented in Norris et al. (2014) and in Paatero et al. (2014). A base model bootstrap method was carried out, executing 100 iterations, using a random seed (number 65), a block size of 6406 samples (calculated according to the methodology of Politis and White, 2004) and a minimum Pearson correlation coefficient (R value) of 0.6. All factors were well reproduced through this technique over at least 97% of runs, thus indicating that BS uncertainties can be interpreted, and the number of factors may be appropriate.

Finally, the rotational ambiguity of this 5-factor PMF configuration was also investigated using the Fpeak parameter. Different Fpeak values from -2.5 to 2.5 were used to generate a more realistic PMF solution. The results from the non-zero Fpeak values were generally consistent with the runs associated with the zero Fpeak value (base model run), thus illustrating a low rotational ambiguity of the final PMF solution.

1.2. PMF results of the MOP

1.2 - 1 Fugitive emissions from ONG/LPG exploitation and distribution

As shown in **Figure VI - 2**, C2 – C9 alkanes and propene are the dominant compounds in the speciation profile of Factor 3. 40% of propane and butanes are explained by this factor, along with >20% of propene, n-pentane and nonane. In published works, propane and butanes are associated to LPG usage (Abeleira et al., 2015; Yao et al., 2019; Lai et al., 2009; Yang et al., 2005), whereas ethane and propane are present to chemical profiles related to natural gas emissions (Baudic et al., 2016; Salameh et al., 2016). Furthermore, LPG emissions can have two origins: (a) LPG vehicle exhausts, and (b) fugitive emissions from oil/natural gas and LPG (ONG/LPG) distribution and exploitation. Thus, the temporal variability of the contribution of the factor and the relationship to other pollutants will clarify the source.

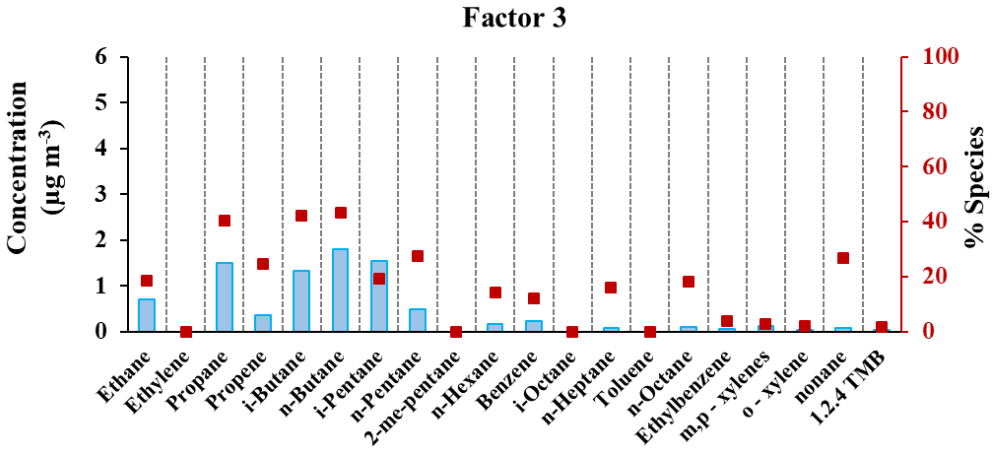

Figure VI - 2: Modelled contribution (µg m^{-3}) of each species to the Factor 3 (light blue bars) and relative contribution of the factor to each species (red squares).

According to Lai et al. (2009), who used VOC ratios for the characterization of their sources, one of the main characteristics of VOC emissions from LPG vehicle exhaust is that the emitted compounds (propane, i-/ n-butane) have similar temporal variation to NO (typical traffic exhaust marker). In addition, they correlate well with other tracers of incomplete combustion (like propene or CO), indicating a common origin namely car exhaust (Lai et al., 2009). This is further confirmed by the

PMF profile of LPG exhaust presented by Yao et al. (2019), in which small quantities of ethylene, benzene, toluene and CO are also present.

On the other hand, fugitive emissions from oil and natural gas/ LPG (ONG/LPG) exploitation and distribution are more constant and with no apparent diurnal variation, based on the observations reported by Yang et al. (2005). Because they don't originate from processes that involve incomplete combustion, there is no correlation of these emissions to combustion or traffic tracers (for example NO and CO). In addition, in the speciation profile of this source presented in Abeleira et al., (2015), important contribution of C6 – C8 alkanes is also reported, with a possible origin the flashing of oil and condensate tanks (Abeleira et al., 2015).

In **Figure VI – 3a** is presented the temporal variability of Factor 3. The highest contribution is observed in winter (12.0 ± 12.5 μg m^{-3}) and the lowest in summer (4.4 ± 8.0 μg m^{-3}). The seasonal diurnal variability of the factor is the same for all seasons, with a night-time enhancement period from midnight until 08:00 LT, followed by a decrease of the levels that remain low and stable for the rest of the day (**Fig. VI – 4a**). In addition, the mean hourly contribution is similar for all seasons, apart from summer when they are lower. Interestingly, the diurnal cycle is different than the one of NO (as tracer of traffic emissions), indicating that the factor is not related to traffic emissions but to fugitive emissions as it was described before (**Fig. VI – 4**). Moreover, the diel cycle of factor 3 shows its possible influence from the PBL height; during day, the increased vertical mixing and dilution processes favor the dispersion of pollutants whereas at night, the lower mixing layer favors their accumulation (**Chapters 3** and **4**). In addition, the higher levels in all seasons except of summer could be attributed to the lower effect from photochemistry, in addition to the lower mixing layer compared to summer (Alexiou et al., 2018). All the above point towards a rather stable source such as the fugitive emissions from stationary points (like the storage and distribution facilities). Consequently, this factor is identified as fugitive emissions from ONG/LPG distribution and exploitation. Nevertheless, it is worth noting that Abeleira et al, (2015) observed a similar diel pattern for this source both in spring and summer (**Fig. VI – A2 of Annex VI**).

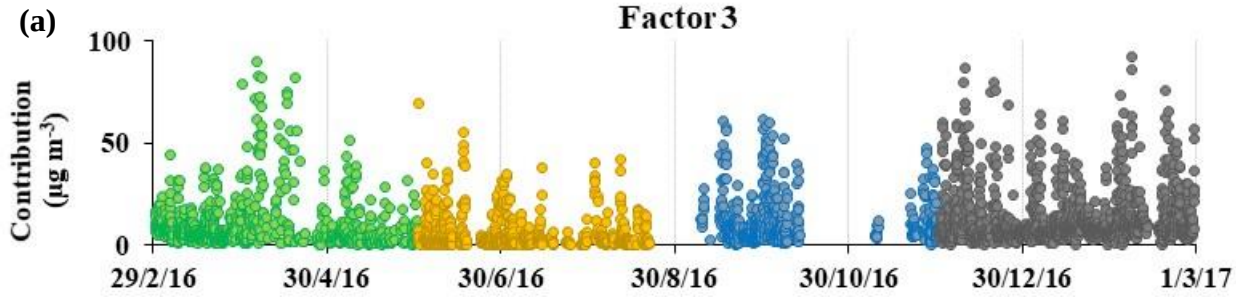

(b)

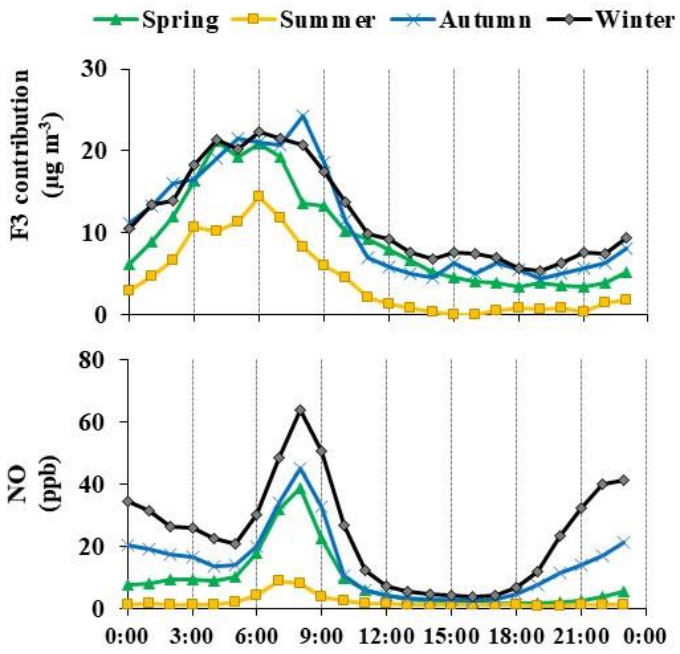

Figure VI - 3: a) Temporal variation of Factor 3. The seasons are marked with different colors: spring – green, summer – yellow, autumn- blue and winter – grey, b) Diurnal variability of Factor 3 contribution (ONG/LPG exploitation and distribution) and NO for every season.

The relationship of factor 3 to wind speed and temperature is examined for every season in **Fig. VI – 4**. High contribution of the factor is observed for low wind speed (<3 m s^{-1}), while it seems independent of the temperature.

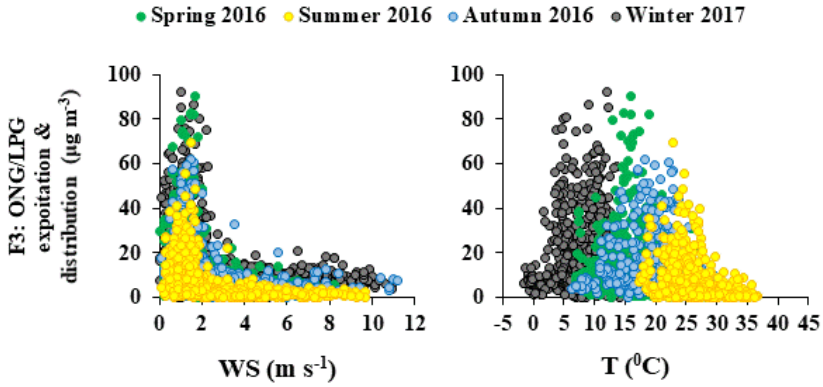

Figure VI - 4: Factor 3 contribution versus wind speed (left) and versus temperature (right) color-codded by the seasons.

Finally, for the better investigation of the origin of the emissions related to this factor, NWR and CPF graphs are presented in **Figures VI – 5a, b**. More specifically, NWR are called the graphs produced by the non-parametric wind regression (NWR) model developed by Henry et al., (2009), which couples pollution data with data for wind speed and direction. The graphs were created by the ZeFir software (Petit et al., 2017). Furthermore, the CPF graphs examine the geographical origin of high level of pollutants (per wind sector) using a conditional probability function. The method for the estimation of the values for the CPF graphs is explained in **Sect. VI-A3** of the **Annex VI**.

In **Figure VI - 5** are presented the NWR and the CPF graph for the factor (WS > 3m s^{-1}). The factor is influenced by local air masses (< 2 m s^{-1} that is equal to ~7 Km s^{-1}) from all directions, with the highest contribution being from N – E – S direction and in particular from the E. Nevertheless, an estimated contribution of less than ~10 μg m^{-3} is observed from the SW to N direction regardless the wind speed, denoting the possible contribution of fugitive emissions from the ONG facilities in West Attica (**Figure VI – A4a** of the **Annex VI**). On the other hand, extreme events of high contribution and associated to wind velocity higher than 3m s^{-1} are observed from the NNE sector (~50%) (**Fig. VI – 5b**), pointing towards the LNG 1st priority consumption center located > 25Km at N – NE of the GAA (**Fig. VI – A4b** of the **Annex VI**).

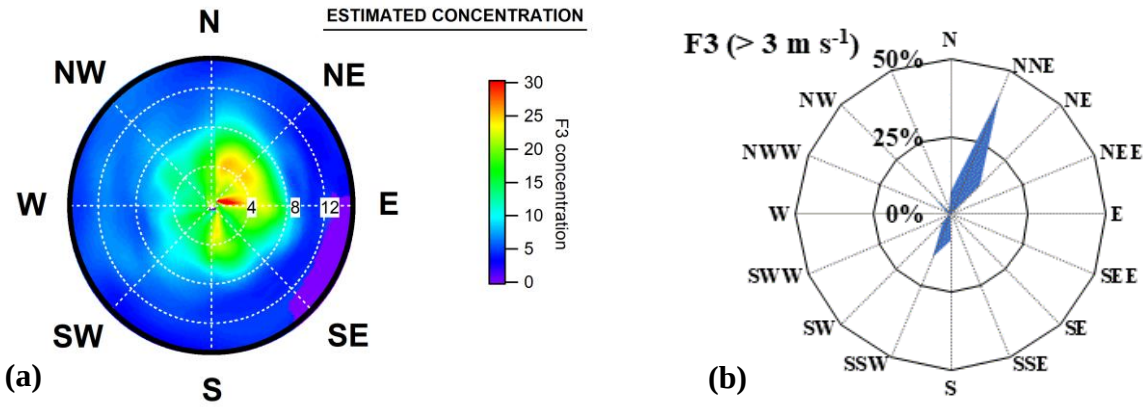

Figure VI - 5: (a) NWR graph for Factor 3 – Fugitive emissions from ONG/LPG exploitation and distribution for the studied period. The contribution is in μg m^{-3} and the wind speed (radius) in Km h^{-1}; (b) CPF graph (above the 75th centile) for Factor 3, for wind speed > 3 m s^{-1}.

1.2 - 2 Wood – burning / Background factor

The chemical profile of Factor 1, shown in **Figure VI - 6**, is characterized by C2 – C3 alkanes, alkenes and benzene. More than 70% of ethane and 40% of ethylene are explained by this factor, as well as >33% of benzene and propane and 25% of toluene. The strong dominance of C2 NMHCs and benzene allows the identification of the factor primarily as "wood burning". More specifically, studies for the characterization of VOC emissions from domestic wood burning based on emissions close to sources, in ambient air or in chambers report important contribution from these compounds (Barrefors and Petersson, 1995; Baudic et al., 2016; Liu et al., 2008; Schauer et al., 2001, Hellén et al., 2008, Sauvage et al., 2009, Wang et al., 2014) with the differences in the emission rates or the emission profiles to be attributed to the type of wood, stove, lightening material and the burning stages (Barrefors and Petersson, 1995; Evtyugina et al., 2014 and references therein). Since 2012, the decline of the greek economy and the subsequent increase of the price of oil lead the citizens to turn their consumption towards wood burning for residential heating (Dimitriou and Kassomenos, 2018; Fameli and Assimakopoulos, 2016; Gerasopoulos et al., 2017; Gratsea et al., 2017; Saffari et al., 2013). Furthermore, studies in Athens after this period have shown an increase of various combustion related compounds like PM, BC and CO, as well as some VOC (Diapouli et al., 2017; Fourtziou et al., 2017; Gratsea et al., 2017; Kaltsonoudis et al., 2016; Paraskevopoulou et al., 2015).

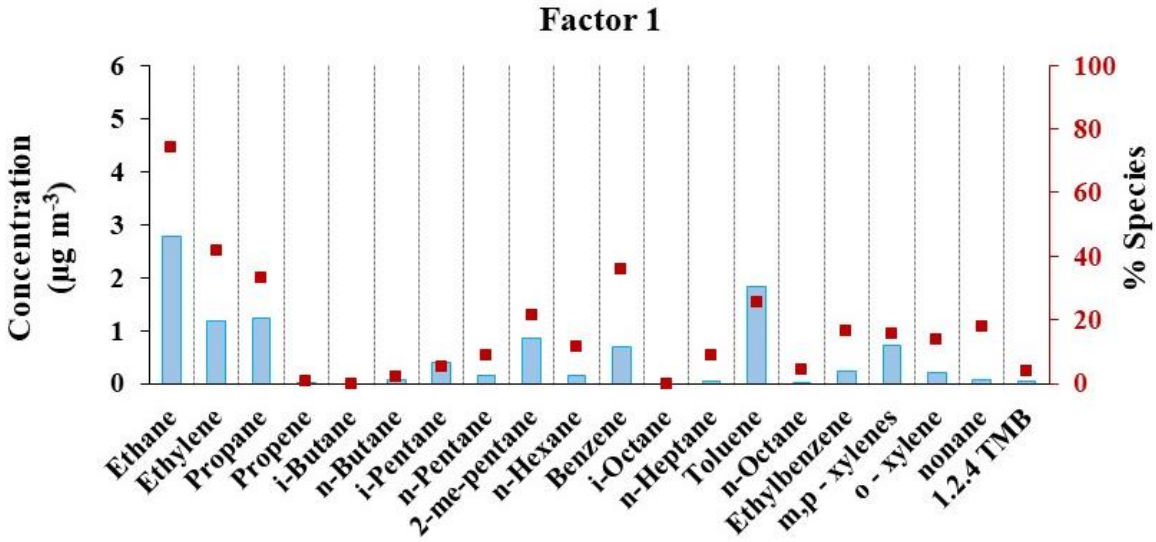

Figure VI - 6: Modelled contribution (µg m^{-3}) of each species to the Factor 1(light blue bars) and relative contribution of the factor to each species (red squares)

This factor contribution to NMHCs levels displays a distinct annual cycle (**Fig. VI-7**), with higher contribution in winter (mean: 14.0 ± 10.3 µg m^{-3}) and almost three times lower contribution in autumn (mean: 6.9 ± 3.2 µg m^{-3}). In **Figure VI - 8** is presented the seasonal diurnal variation of the factor along with BC_{wb} and CO for comparison. The cycle is characterized by a night maximum at midnight and a morning peak of lower amplitude in spring and winter 2017, whereas in summer and autumn, the hourly mean contribution remains stable throughout the day. In addition, the persistent night-time enhancement of the contribution during winter nights follows the trend of CO and BC_{wb} (the latter in winter). This is in line with recent studies in Athens that have shown increasing emissions of these pollutants during cold winter nights and stagnant conditions (low wind speed and absence of rainfall) (Gratsea et al., 2017; Fourtziou et al., 2017).

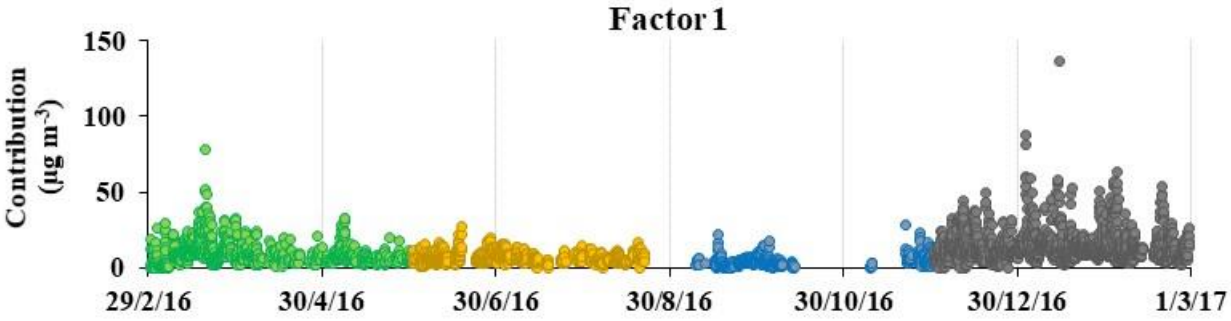

Figure VI - 7: Temporal variation of contribution of Factor 1 – Wood-burning/background. The seasons are marked with different colors: spring – green, summer – yellow, autumn- blue and winter – grey

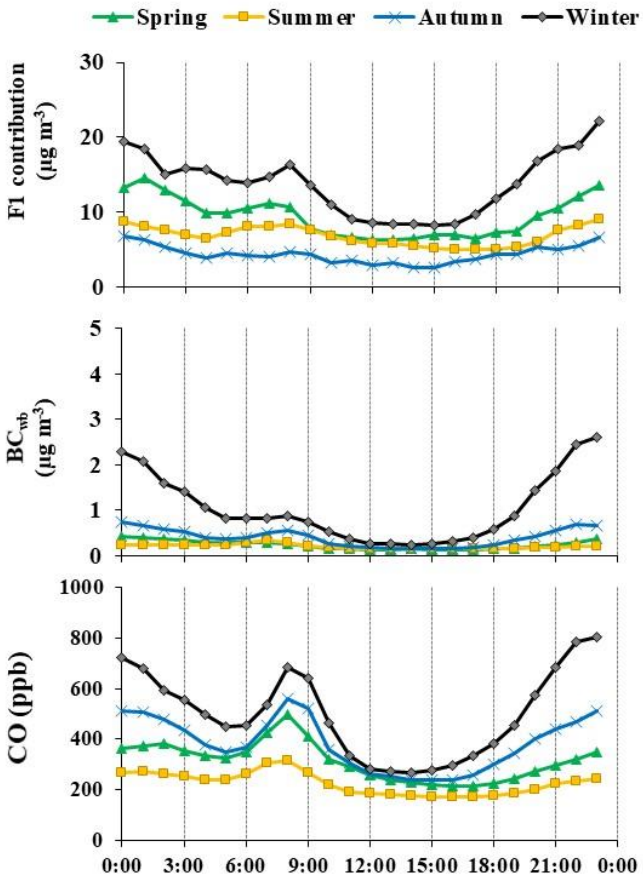

Figure VI - 8: Seasonal diurnal variability of Factor 1 (Wood-burning / Background), BC_{wb} and CO.

However, it is interesting to note that although the levels of BC_{wb} decrease from winter towards summer reaching values close to zero, the contribution of Factor 1 to VOCs decreases only two times (by comparing the night-time levels of the seasons of **Fig. VI - 8**). This is explained by the chemical profile of the factor, which includes species with long lifetimes. More specifically, ethane and propane (and even benzene) have lifetime of 48 to 10 days respectively (Atkinson, 2000), thus they are often associated with aged air masses, probably due to regional background transport (Salameh et al., 2016; Sauvage et al., 2009, and refences therein). On the other hand, ethane and propane are also included in the emission profile of natural gas leakages (**Sect. 1.2 – 1** of **this chapter**; Baudic et al., 2016; Salameh et al.,2016). Studies have shown that natural gas emissions are dependent from the amount of the gas consumption, thus higher contribution is expected in winter due to the increased demand (Na et Kim, 2001) notably for domestic heating (IEA report for Greece, 2017) leading to a co-variation of natural gas demand for heating and wood burning.

Wood-burning for residential heating occurs in the cold seasons like winter, later autumn and early spring (Athanasopoulou et al., 2017; Diapouli et al., 2017; Gratsea et al., 2017) and it is more apparent during night when people are staying at home. The relationship of the factor contribution to wind velocity and temperature shows that the highest values are observed for low temperatures (<12°C) and low wind velocity, highlighting the influence of wood burning from domestic heating. (**Fig. V – 9**). This is also corroborated by the variability of the factor (**Fig. VI – 7** and **VI – 8**). Furthermore, although the highest contribution is observed for low wind speed (< 3 m s^{-1}), the decrease of the values with increasing wind velocity is not very steep, denoting the possible

influence of emissions further from the station. This is in line with the background emissions that contribute to the factor and it is also apparent in the NWR graph of the factor (**Figure VI – 10a**). Of course, the role of the height of the PBL in the night-time enhancement should not be omitted, however its effect on VOC and pollutants' levels was already discussed in **Chapters 3** and **4**.

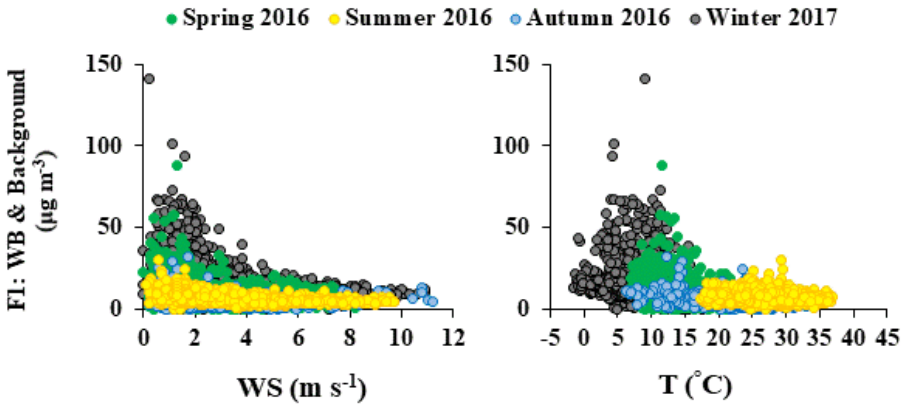

Figure VI - 9: Factor 1 versus wind speed (left) and versus temperature (right) color-coded by the season.

Finally, the CPF graph (**Fig. VI – 10b**) shows that 50% of the factor contribution above the threshold is associated to wind speed > 3m s^{-1} and originates from the North sector (50% from NNE), where the wealthy suburbs of the greater Athens area are located. In Panopoulou et al. (2018; **Chapter 3**) it was indicated that the higher living standards in these suburbs allow the combined use of oil and wood burning for heating, thus increased emissions related to wood burning are expected from this direction, corroborating the observations of the CPF graph of the factor.

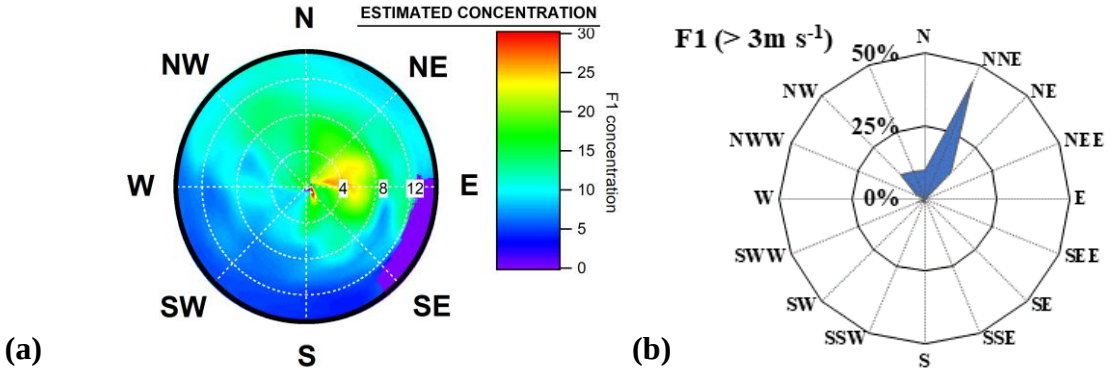

Figure VI - 10: (a) NWR graph for Factor 1– Wood burning/ Background for the studied period; (b) CPF graph (above the 75th centile) for Factor 3, for wind speed > 3 m s^{-1}.

1.2 - 3 Fuel combustion (related to traffic and heating)

Propene (74%), ethylene (44%), benzene (29%) and m-/ p- xylenes (14%) are the main compounds in the chemical profile of Factor 4 (**Fig. VI - 11**). The strong contribution of alkenes, which are known as combustion tracers often found in the chemical profile of motor vehicle exhaust emissions (Lai et al., 2009; Na et Kim, 2001; Salameh et al., 2016), allow the characterization of the factor firstly as "Combustion". Furthermore butanes, i-pentane and m- / p- xylenes are found in the

emissions of vehicle exhausts from gasoline, diesel or LPG burning as fuels (Salameh et al., 2016; Liu et al., 2008; Yao et al., 2019).

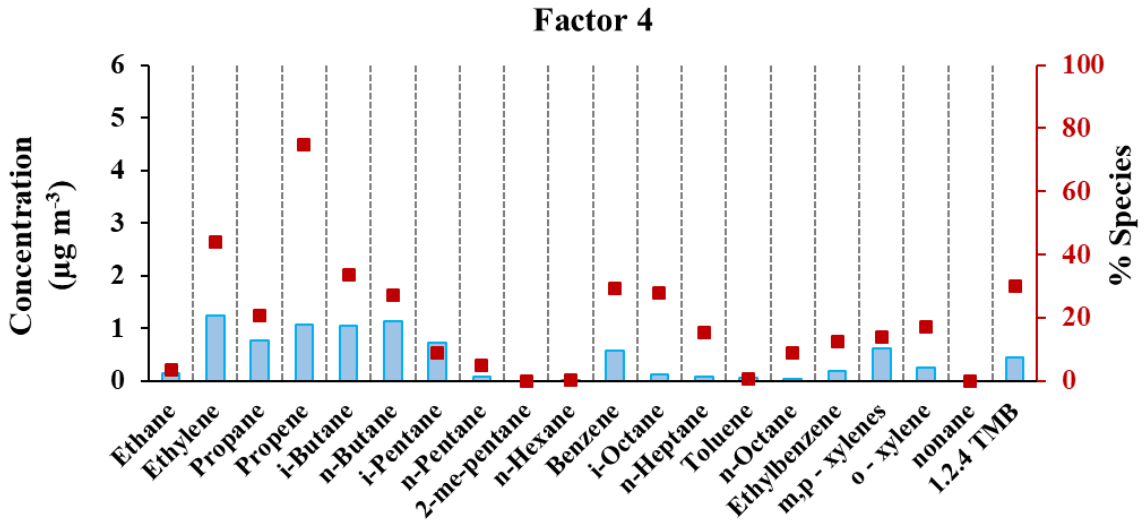

Figure VI - 11: Modelled contribution (µg m^{-3}) of each species to the Factor 4 (light blue bars) and relative contribution of the factor to each species (red squares).

The temporal variability of factor's contribution presents a distinct seasonal variation with higher contribution in winter (14.5 ±25.4 µg m^{-3}) and almost a factor of eight lower concentrations in summer (1.8 ± 2.7 µg m^{-3}; **Fig. VI – 12a**). The seasonal diurnal cycle of the factor is characterized by a morning maximum which is observed in all seasons. In addition, a night-time enhancement period is observed in winter, with higher amplitude than the morning maximum and levels up to a factor of three higher than autumn and spring (**Fig. VI - 12b**). The trend appears to follow closely the variability of BC and CO (**Fig. V – 12c**), which are combustion tracers as we have already seen. This factor can be attributed to fuel combustion. The increase of the contribution in winter and the important decrease during summer means that it can be related to both traffic and residential heating in winter whereas only traffic-related emissions occur in summer. If we consider the impact of dynamics, photochemical depletion appears to have the strongest effect, which is more important in summer than winter. This is corroborated by the significantly lower contribution of the factor in summer, as well as the dominance of propene in the factor's chemical profile, which is among the reactive NMHCs.

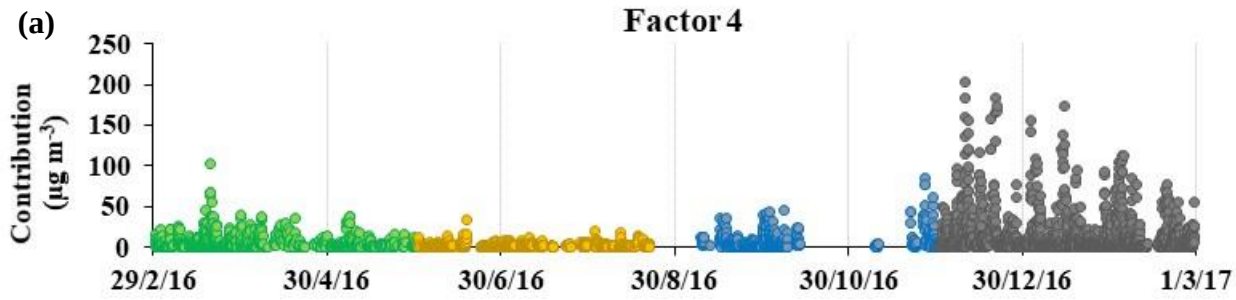

(b)

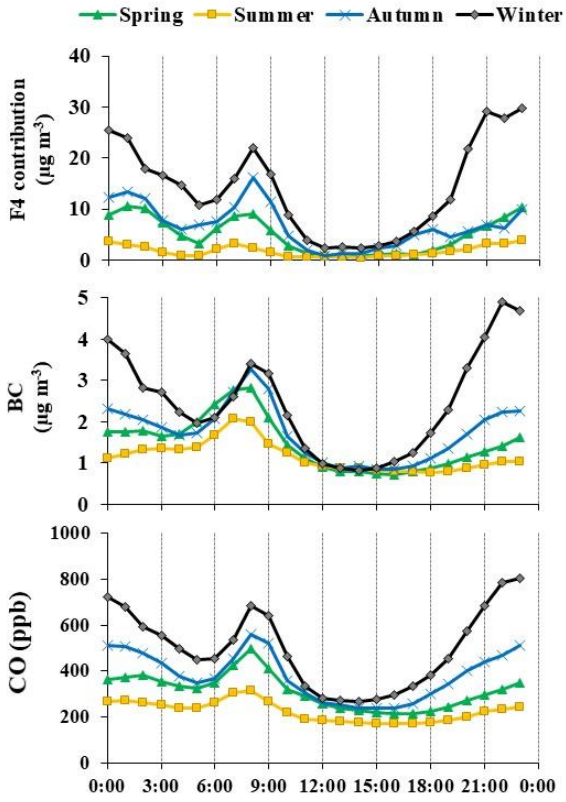

Figure VI - 12: a) Temporal variation of Factor 4. The seasons are marked with different colors: spring – green, summer – yellow, autumn- blue and winter – grey; b) Seasonal diurnal variability of Factor 4, BC and CO.

The role of wind velocity and temperature to the contribution of factor 4 is examined for every season in **Figure VI – 13**. This factor seems to be influenced mainly by local sources, due to the increase of its contribution for low wind velocity (<3m s^{-1}). In addition, the highest contribution occurs for temperatures < 12°C, which is in line with the seasonality of the factor (**Fig. VI – 13b**).

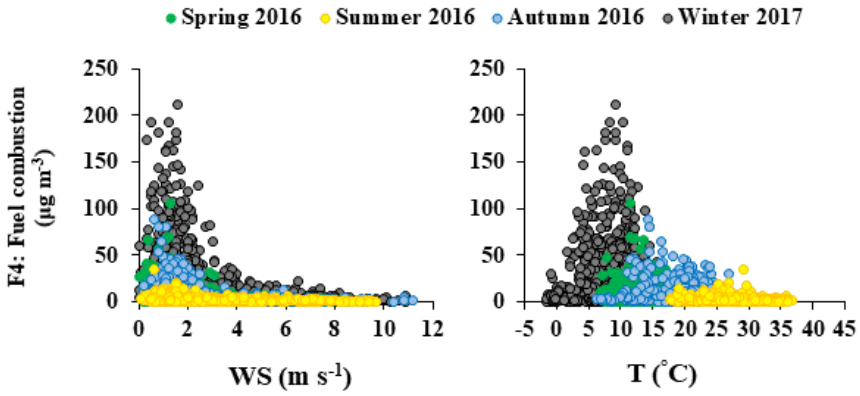

Figure VI - 13: Factor 4 contribution versus wind speed (left) and versus temperature (right) color-codded by the season.

In **Figure VI – 14a** the NWR graph of Factor 4 is presented. It is apparent that the contribution is influenced mainly by local winds (< 2 m s^{-1} that is equal to ~7 Km s^{-1}) from N to SE direction, with the highest values to be associated with NE to SE air masses. These reflect fresh air masses from

traffic emissions in the vicinity of the measurement site as it is denoted by the NWR graph of NO (**Fig. VI – 14b**) (Alvarez et al., 2008).

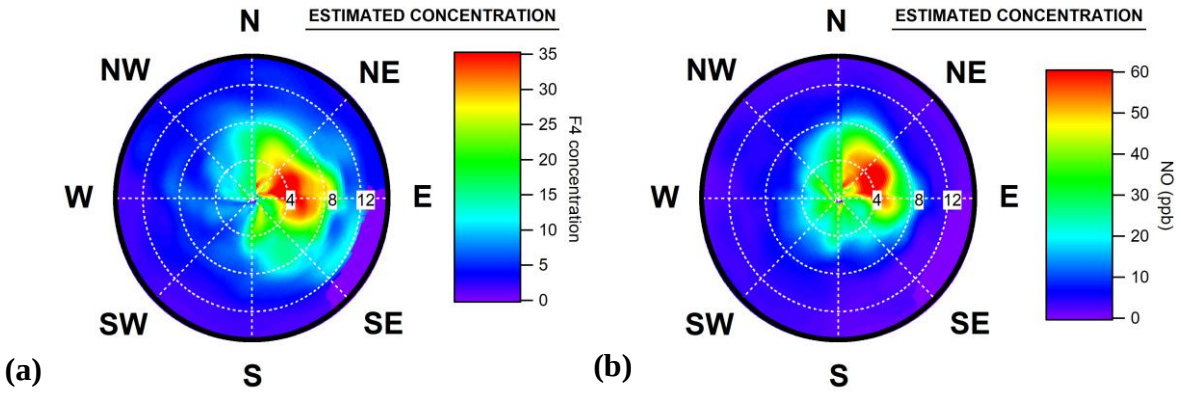

Figure VI - 14: (a) NWR graph for Factor 4. The contribution is in μg m^{-3} and the wind speed (radius) in Km h^{-1}; (b) NWR graph for NO (ppb) for the studied period. The wind speed (radius) is in Km h^{-1}

1.2 - 4 Vehicle exhaust

The profile of factor 5 has significant loadings of aromatics, explaining more than 60% of their variance, with the exception of benzene (**Fig. VI - 15**). Profiles with high load of aromatics are often associated with solvent usage (Baudic et al., 2016 and references therein); however, the dominance of toluene and m-/p- xylenes, in combination to the presence of 2-me-pentane corresponds rather to traffic (Salameh et al., 2016) and motor vehicle exhaust (Baudic et al., 2016; Sauvage et al., 2009; Brown et al., 2007; Liu et al., 2008). The smaller contribution of benzene compared to the other aromatics is in line with the Directive 98/70/EC of the European Union for the reduction of benzene to fuels and solvents (Panopoulou et al., 2018). In order to apportion correctly the factor to a source, it is important to examine its temporal variation and its relationship with other pollutant tracers.

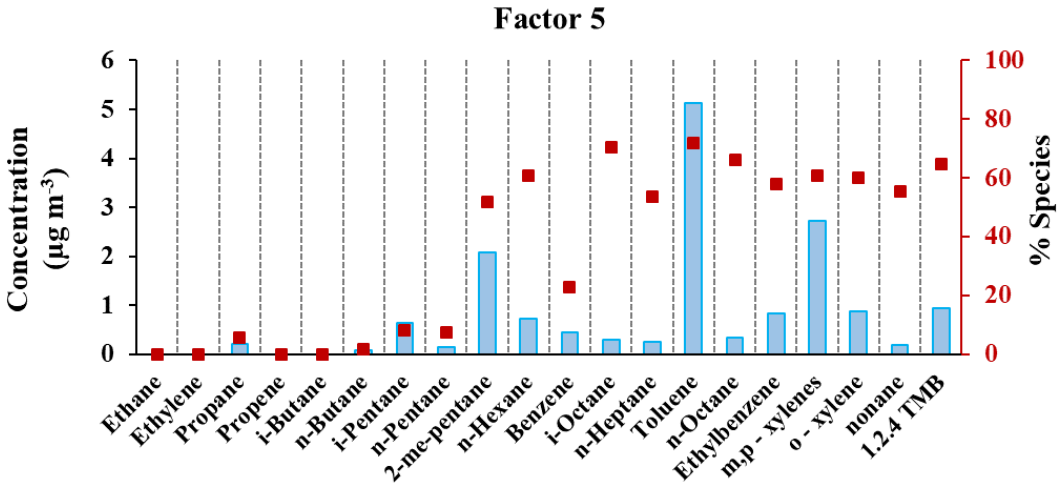

Figure VI - 15: Modelled contribution (μg m^{-3}) of each species to the Factor 5 (light blue bars) and relative contribution of the factor to each species (red squares).

Figure VI - 16a presents the seasonal variability of factor 5 and in Figure **VI – 16b** the diurnal cycle for the period, including also NOx. The contribution is higher in autumn (23.5 ± 28.4 μg m^{-3}) and the lowest in summer (11.4 ± 14.0 μg m^{-3}). The diurnal pattern of the source follows closely the one

of NOx, with a morning maximum, followed by an important decrease of the levels (factor of 8 decrease considering the morning peak and the afternoon minimum) and then the levels increase again after 19:00 LT until midnight. This similarity with NOx levels indicates their common origin which is traffic related. In particular, the morning peak is completely influenced by traffic (**Chapters 3** and **4**), whereas the night peak is also affected by traffic emissions, as well as the decrease of the PBL height that favors the accumulation of pollutants. Since night traffic ends before midnight, the levels persist during night but without enhancement, due to the stagnant conditions. Furthermore, this factor could not be related to fuel evaporation due to the important decrease of the contribution during day, when the highest temperatures are recorded. Moreover, it should be mentioned that the above pattern is followed in every season but with different levels (**Fig VI – A5** of the **Annex VI**). All the above observations indicate that the factor is related to emissions from vehicle exhaust.

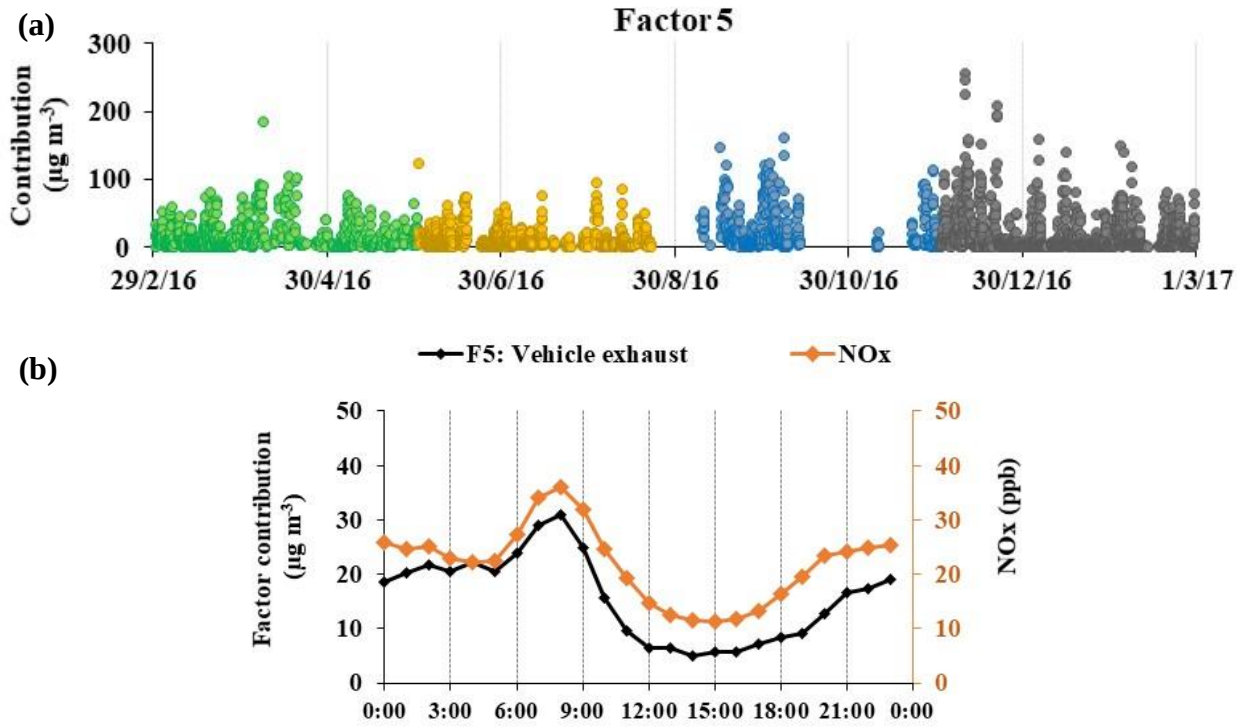

Figure VI - 16: (a) Temporal variation of Factor 5 – Vehicle exhaust. The seasons are marked with different colours: spring – green, summer – yellow, autumn- blue and winter – grey; (b) Diurnal variation of Factor 5 and NOx for the studied period.

The relationship of factor 5 to wind speed and temperature is illustrated in **Figure VI – 17**. The enhancement of the contribution is related to low wind speed (< 3 m s^{-1}) but is independent from temperature, although in winter higher contribution is observed even for temperatures <12°C. This denotes that the source behind the factor is local and in general, not driven by temperature.

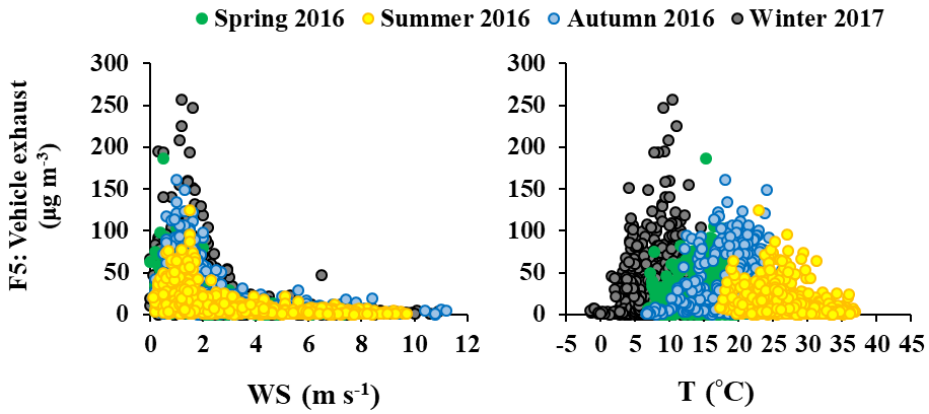

Figure VI - 17: Factor 5 contribution versus wind speed (left) and versus temperature (right) color-codded by the seasons.

The possible influence of wind direction to the factor is examined by the NWR graph (**Fig.VI – 18a**). Factor 5 is influenced by air masses similarly to Factor 4 (**Fig. VI – 18a**), with the highest contribution associated to local winds (< 2 m s^{-1} that is equal to 8 Km s^{-1}) from N to SE direction. Furthermore, the CPF graph (WS > 3 m s^{-1}) indicates that 25% of the highest values are found under the N - NNE direction, whereas another 20% from the SSW direction.

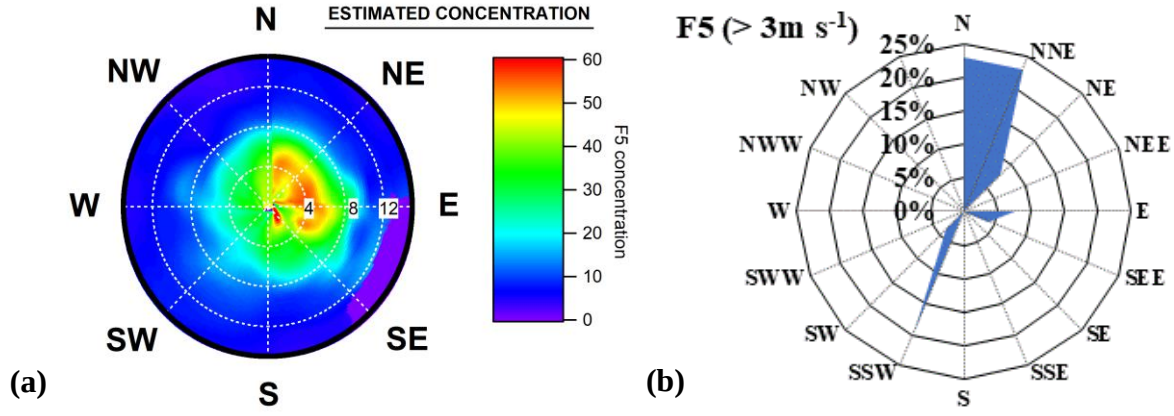

Figure VI - 18: a) NWR graph for Factor 5 – Vehicle exhaust distribution for the studied period. The contribution is in μg m^{-3} and the wind speed (radius) in Km h^{-1} ; (b) CPF graph (above the 75th centile) for Factor 5, for wind speed > 3 m s^{-1} .

Finally, it is important to understand the reason behind the high contribution of aromatics for this factor. The T/B ratio (calculated by the mean contribution to the factor in μg m^{-3} converted to ppb/ppb) is 9.9, which is way higher than the reported values for urban background stations (for instance in Yurdakul et al., 2017). This suggests that there might be additional "sources" that contribute significantly to the aromatic fraction of factor 5. One assumption is that these are emissions from motorcycle exhausts. Emission fingerprints and emission factors of various types of vehicles indicate that motorcycles are important contributors of aromatics through their exhaust emissions due to the incomplete combustion of fuel from their engines, the absence of a catalyst at the tailpipe end, and/or their poor maintenance and age (Platt et al., 2014; Tsai et al., 2017; Montero et al., 2010). A recent study (Salameh et al., 2019) revealed that two-wheelers are the cause for the higher aromatic concentrations observed in a traffic station in Paris, whereas 30% of the two-wheelers are circulating regardless the meteorological conditions. In the Greater Athens Area for

2017, motorcycles accounted for the 18.7% of the total number of motor vehicles, from which 99.6% is for private use (**Fig. VI - 19**) (data from the Hellenic Statistical Authority). Therefore, we can assume that motorcycle vehicle emissions stand for a significant part of the emissions related to this factor.

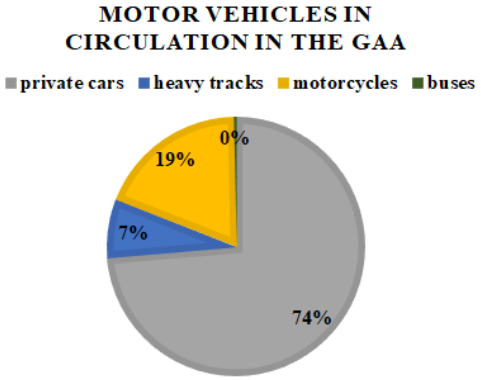

Figure VI - 19: Percentage of the different types of motor vehicles in circulation in the GAA (data from the Hellenic Statistical Authority, https://www.statistics.gr/en/statistics/-/publication/SME18/-).

1.2 -5 Fuel evaporation (related to traffic)

In the speciation profile of Factor 2 (**Fig. VI - 20**) the major species are pentanes (i- / n-) (58.8% and 51.5% respectively), butanes (i- / n-) and 2-me pentane (>20% each). The presence of pentanes and butanes in the profile strongly indicates that the factor is related to fuel evaporation (Liu et al., 2008; Salameh et al., 2015; Baudic et al., 2016). Furthermore, in Chapter 3 (Panopoulou et al., 2018) was shown the temperature dependence of the isomeric ratio of butanes and pentanes with increasing temperature, relating them to fuel evaporation. Thus, this factor has been identified primarily as fuel evaporation.

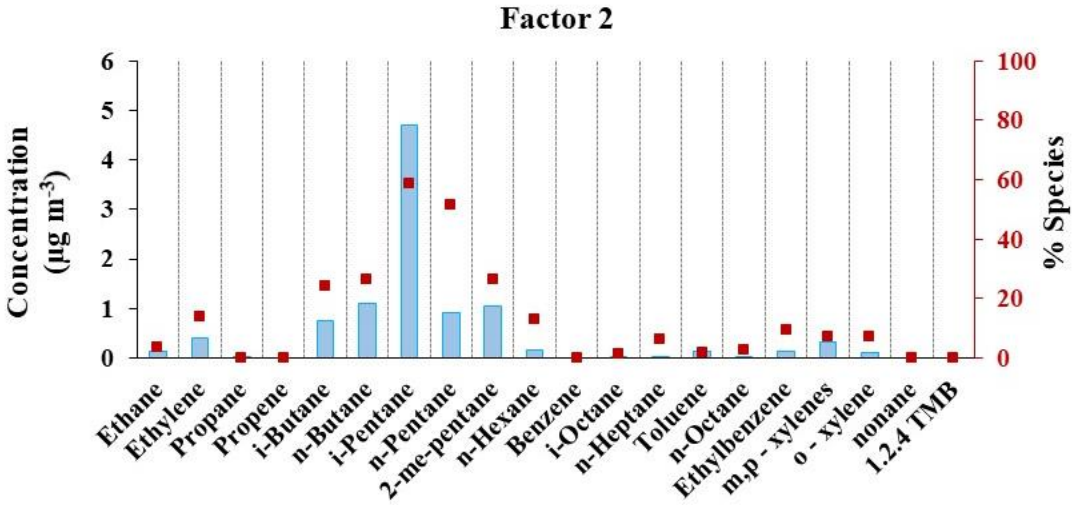

Figure VI - 20:. Modelled contribution (µg m^{-3}) of each species to the Factor 2 (light blue bars) and relative contribution of the factor to each species (red squares).

Figure VI - 21a presents the seasonal variability of the factor contribution, which is quite similar whatever the season: autumn (13.6 ± 15.4 μg m^{-3}) > summer (11.0 ± 9.2 μg m^{-3}) > spring (10.7 ± 12.0 μg m^{-3}) > winter (9.8 ± 15.6 μg m^{-3}). For the better understanding of the variability, the seasonal diurnal cycles are presented in **Figure VI - 21b**. The diurnal pattern is characterized by a morning maximum (when the traffic density is high), with the amplitude being dependent on the season. Furthermore, a small enhancement of the levels is observed in the night, which could be linked to the swallower mixing layer. This pattern resembles the one of NO (**Fig. VI – 21b**), whereas the diurnal cycle of the studied period is identical to the one of BC_{ff} (**Fig. VI – A6** of the **Annex VI**). The above clearly affirming the relationship of this source to traffic and especially evaporation form the vehicle.

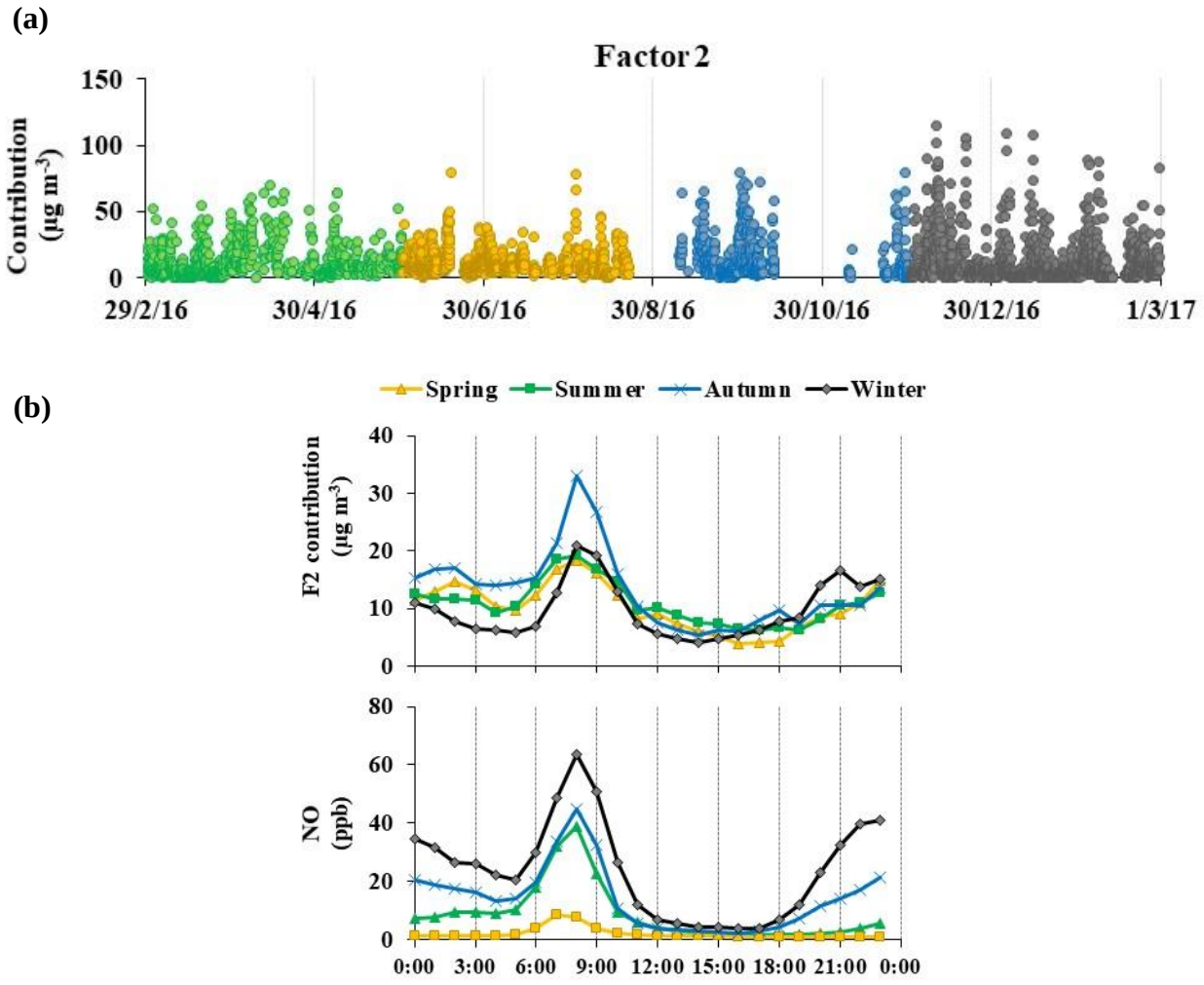

Figure VI - 21: (a) Temporal variation of Factor 2. The seasons are marked with different colours: spring – green, summer – yellow, autumn- blue and winter – grey. (b) Seasonal diurnal variability of Factor 2 and NO.

Concerning the relationship to temperature (**Fig. VI – 22**), although the factor is related to fuel evaporation during traffic, the contribution seems independent from temperature for all seasons, whereas in winter the highest values are associated to temperatures even <12°C. In addition, the highest contribution is related to low wind speed, indicating that the emissions are local, like it was observed for all the discussed factors (**Fig. VI – 22**).

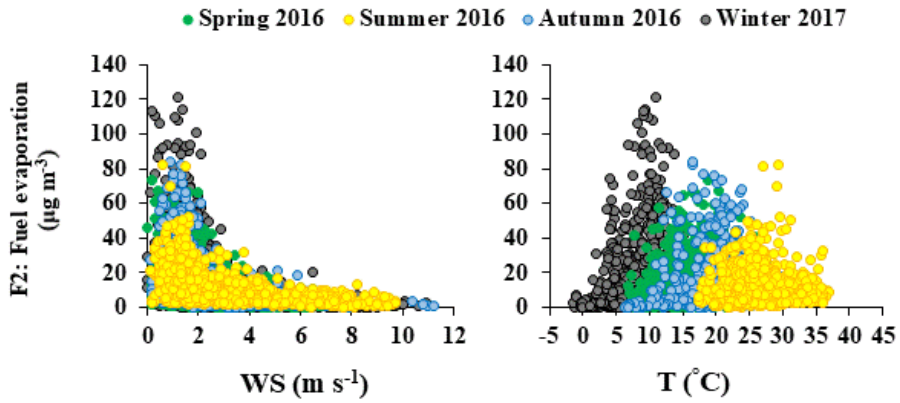

Figure VI - 22: Factor 5 contribution versus wind speed (left) and versus temperature (right) color-codded by the seasons.

Lastly, the NWR graph of Factor 2 shows a contribution for wind speed less than 10 Km h^{-1} regardless of the origin (**Fig. VI – 23a**), with an enhancement for winds of NE to SE direction, which is consistent with the NWR graphs of the traffic related factors (**Figs VI - 14a** and **18a**). Moreover, an estimated contribution of 10 μg m^{-3} is associated with the SW and E to SE direction, which is consistent with the observations from the NWR graph of the "Gasoline Vehicle Exhaust" factor (**Fig. VI – 18a**). Finally, the 40% and 30% of the values above the 75th centile for wind speed > 3m s^{-1} are associated with the N - NE and S - SW sectors respectively (**Fig. VI – 23b**), which are along the main wind circulation pathway in Athens (**Sect. 2.4.1**, **chapter 1**).

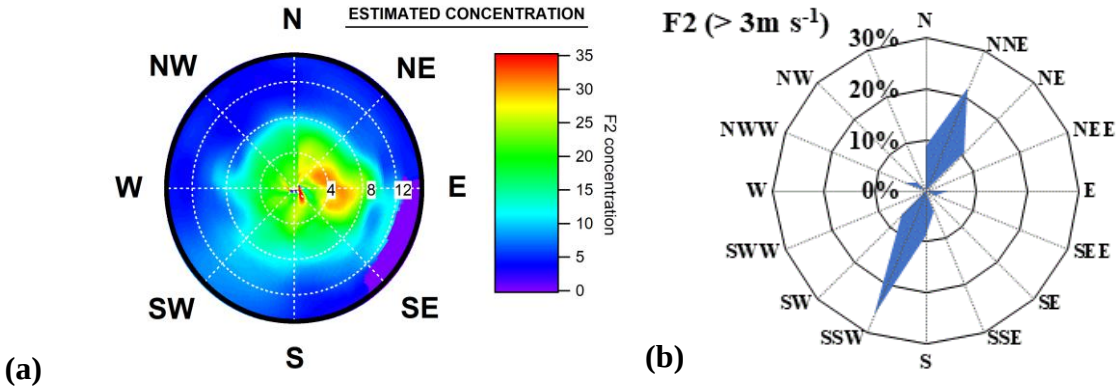

Figure VI - 23: a) NWR graph for Factor 2 for the studied period. The contribution is in μg m^{-3} and the wind speed (radius) in Km h^{-1}(b) CPF graph (above the 75th centile) for Factor 2, for wind speed > 3 m s^{-1} .

1.2.1 Factors' contribution to the NMHCs total ambient levels.

To summarize, the PMF simulation for the MOP gave 5-factors related to sources, from which four factors were traffic and combustion related. In **Figure VI – 24** are presented the relative contributions (%) of the 5 factors to the NMHCs (total). Vehicle exhaust accounts for 28% of the NMHCs emissions during the studied period, whereas the rest of the sources contribute 16% to 20%. This indicates that traffic-related sources are responsible for the 64% of the reported NMHCs concentrations (sum of Factors "Fuel Evaporation", "Fuel Combustion" and "Vehicle Exhaust"), although this percentage is a little overestimated since it includes also a portion of fuel combustion related to residential heating. Nevertheless, traffic is the main source of NMHCs in Athens.

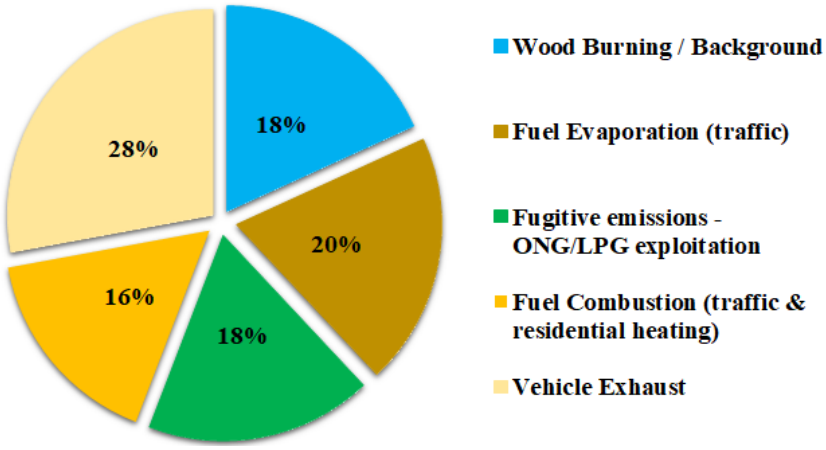

Figure VI - 24: Pie chart of the Total NMHCs contribution (%) of the factors modelled by the PMF for the MOP.

2. Discussion on the MOP PMF results

2.1 Comparison to other factors

In the previous section we saw that the PMF solution separates 3 different factors related to traffic emissions (Fuel combustion related to traffic and heating, vehicle exhaust and fuel evaporation) and 2 factors related to combustion (Fuel combustion related to traffic and heating and wood burning / background). As a result, in the next paragraphs their relevance is examined by the comparison of their mass contribution (%) profiles to other available profiles.

The first profiles to be examined are the traffic related. Thus, the contributions of factors 2, 4 and 5 (fuel evaporation, fuel combustion and vehicle exhaust respectively) to the NMHCs are combined and normalized by the sum of NMHCs in the factors (methodology described in Panopoulou et al., 2018; Chapter 3). This created a "new" chemical profile representative of traffic for Thissio (hereafter "Traffic emissions" profile; **Fig. VI – 25**). In the same graph is plotted the mass contribution (%) of the NMHCs to the morning peak observed in Patission station, which was established by the near-source campaign in Patission Monitoring station (**Chapter 2**, **Sect. 1.2** and **Chapter 3**). The two profiles agree very well (R^2: 0.91). The dominant species in both sites are i-pentane (> 15%), toluene (>10%) and m- /p- xylenes (~10%), which are the typical tracers of motor vehicle exhaust, as reported by other studies (Baudic et al., 2016; Brown et al., 2007; Sauvage et al., 2009 and references therein). Consequently, this comparison verified the robustness of the identification of the factors 2,4 and 5 and their representativity of the traffic emissions in the GAA. The only significant difference is observed for ethane, which is higher in Patission morning profile than in the "Traffic emissions" profile (although low in contribution). The main reason is the underestimation of ethane from the PMF simulation to these factors and its apportion mainly to the wood-burning / background factor (74%) (**Sect 1.2 – 2** of **this chapter**).

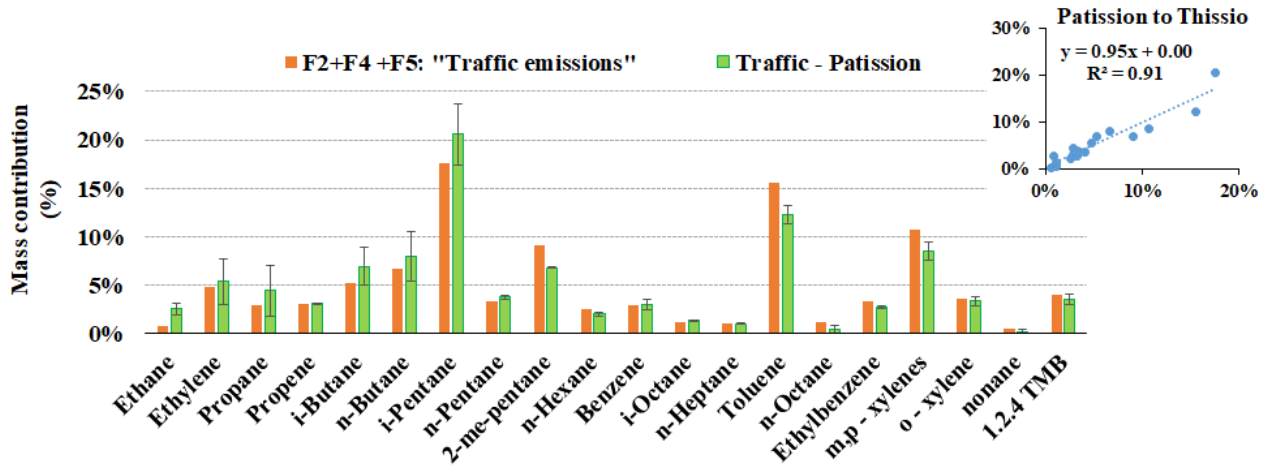

Figure VI - 25: Mass contribution (%) of NMHC in the profiles of Factor 2+4+5: «Traffic emissions» and the traffic profile from Patission station. The right upper graph is the x-y relationship of the species mass contribution (%) of the two profiles.

Furthermore, the "Traffic emissions" profile is compared to two other profiles from data reported in the literature (**Fig VI - 26**). More specifically, the profile is compared to a "Traffic" profile derived from the PMF results of the VOC measurements in Beirut (courtesy of Thérèse Salameh; Salameh et al., 2015), and to the Motor Vehicle Exhaust profile (MVE) from the PMF results of the VOC measurements in Paris (values taken from Fig. 8 in Baudic et al., 2016). The mass contribution (%) was re-calculated for every profile, considering only common species. Salameh et al. (2015) identified 3 factors related to traffic in both summer and winter PMF simulations, thus a combination of all was proven more suitable for the current comparison (more details in **Annex VI**, **Sect VI – A2**). In the same context, the "Evaporative emissions" factor from Baudic et al. (2016) was not taken into account, although it is partly influenced by traffic.

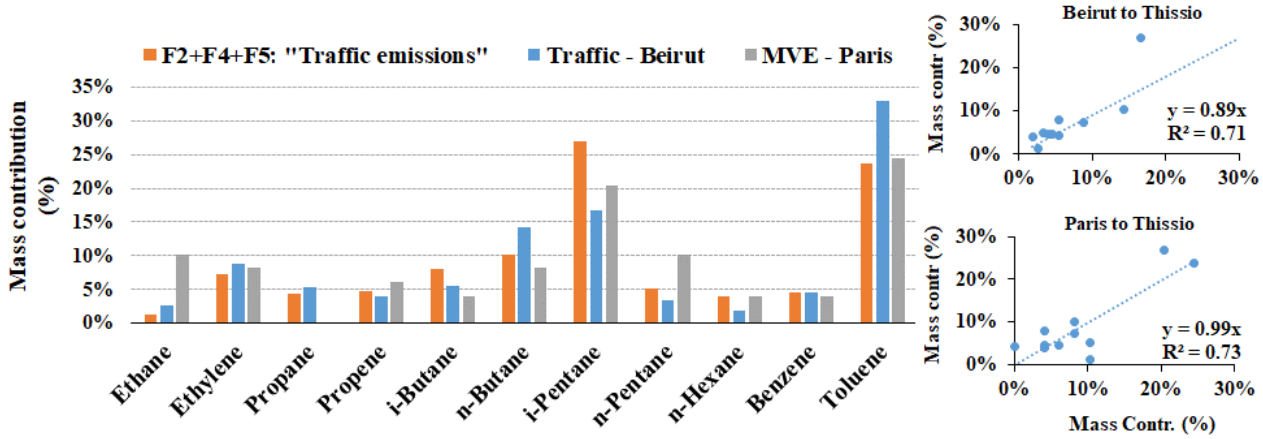

Figure VI - 26: Mass contribution (%) of NMHC in the profiles of Factors 2+4+5 « Traffic emissions », in the combined « Traffic » profile derived from Salameh et al. (2015) and in the Motor Vehicle Exhaust profile from Baudic et al. (2016**).**

The "Traffic emissions" profile of Thissio agrees quite well with the "Traffic" profile of Beirut (R^2: 0.71) and the Motor Vehicle Exhaust profile of Paris (R^2: 0.73). Differences between the traffic profile of Thissio (Athens) and Beirut are found mainly for isopentane and toluene. These compounds are typical markers of gasoline evaporation and motor vehicle exhaust, thus the differences could be attributed to the different gasoline composition in the two countries

(unfortunately, there is no information about the gasoline composition in Greece), as well as discrepancies in the traffic fleet composition (e.g. different proportion of the two-wheelers) and the temporal variability of the sources (average of winter and summer contribution versus yearly contribution). Concerning the comparison to the MVE profile, differences are observed for ethane, propane, i-butane and pentanes (i- / n-). As we have already discussed, ethane is probably underestimated to all the traffic factors, due to its higher apportion to the wood-burning/background factor. At the same time, ethane is considered as overestimated in the MVE profile in Paris, as it was reported by Baudic et al. (2016). Furthermore, it is apparent in **Figure VI - 26** that propane is not present in the MVE profile of Paris, whereas the contribution of butanes is lower compared to the other profiles. This is attributed to their apportion from the PMF of Baudic et al. (2016) to the evaporative sources factor, which is not considered in the MVE profile of **Figure VI - 26** (Baudic et al., 2016; Salameh et al., 2015).

The next comparison is between Factor 1–Wood burning/background and the Wood-burning profile of Baudic et al., (2016). The mass contribution (%) of the NMHCs in the profiles is recalculated taking into account only the common compounds, following the same procedure as described previously (**Fig. VI – 27**). The two profiles agree very well (R^2: 0.89), with differences mainly for propene and butanes, since it is known that ethane is overestimated in this factor. More specifically, our PMF analysis apportioned the majority of butanes (~25%) to Factor 2 which is related to fuel evaporation (**Sect. 1.2 - 4**), whereas propene (74%) is apportioned to Factor 4 (Fuel combustion related to traffic and heating). On the other hand, butanes could be overestimated in the PMF analysis of Paris, since in the reported source profile of the fireplace experiment in Paris, butanes present very low mass contribution (Baudic et al., 2016), which is corroborated by other studies (Barrefors and Petersson, 1995; Schauer et al., 2001). Nevertheless, the similarities of the two profiles verify the identification of our factor and its relationship to wood burning emissions.

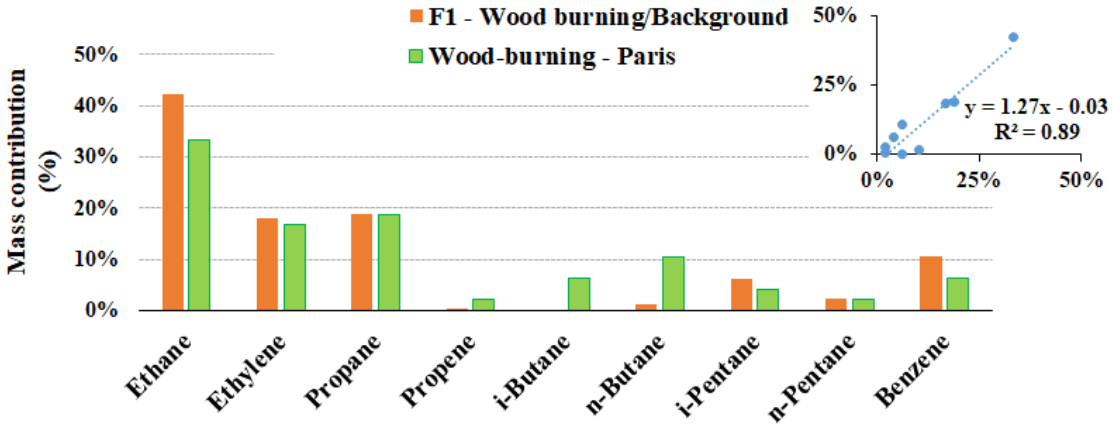

Figure VI - 27: Mass contribution (%) of NMHC in the profile of F1 – Wood burning/Background and the Wood-burning profile of Baudic et al. (2016)

2.2 PMF overview

The PMF simulation for the MOP gave 5-factors related to sources, from which four factors were traffic and combustion related (**Fig. VI - 24**). In **Figure VI – 28** the relative contributions of the factors are examined separately for summer 2016 and winter 2017. More specifically, "Vehicle Exhaust" and "Fuel Evaporation (traffic)" contributes more to the total NMHCs in summer (32%

and 31% respectively) than winter (23% and 15% respectively),. The rest of the factors contribute more in winter than summer. The seasonality of the factors and the driving parameters were already discussed in **Sects 1.2 – 1** to **1.2 – 5.**

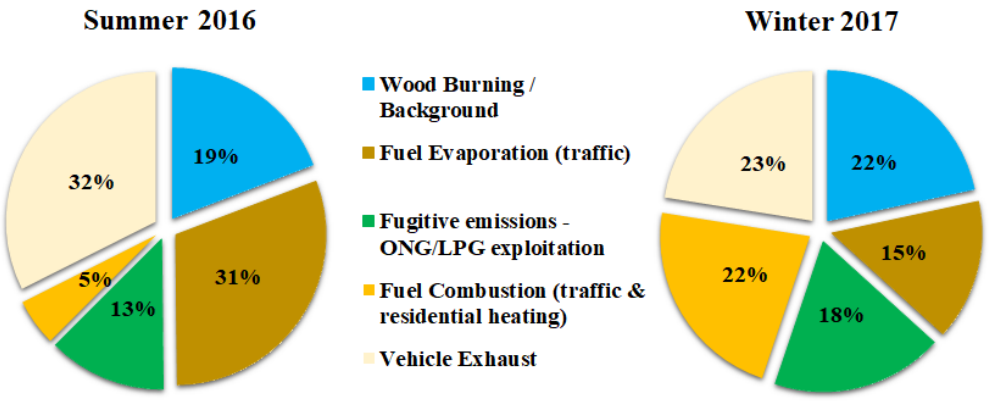

Figure VI - 28: Pie chart of the Total VOC contribution (%) of the factors; on the left for summer 2016 and on the right for winter 2017

In addition, the contribution to the total NMHCs of some factors is compared to the reported values of the PMF results for Paris (Baudic et al., 2016) and Beirut (Salameh et al., 2016). Starting from Paris and the traffic-related factors, it is apparent that in Athens (64%; Fig. VI - 24) contribute two times more than Paris (29%: sum of motor vehicle exhaust and evaporative sources contribution, accounting for 19% and 10% respectively). On the other hand, the contribution of wood-burning emissions is similar between Athens (18%) and Paris (19%). The rest of the factors from the Athens and Paris PMF analysis cannot be compared since the different variety of NMHCs that were used in the Paris PMF (e.g. oxygenated VOCs, isoprene) helped the identification of other types of sources like solvents usage and biogenic emissions. These observations highlight the importance of traffic as the main VOC source in Athens. This is further justified by the fact that Athens is an urban agglomeration of approximately 3 million citizens that own for private use ~3.5 million cars and motorcycles, meaning almost 1 vehicle per person. This ratio is two times higher than the reported one for the entire Greece and for France (Eurostat, 2018).

Furthermore, the comparison of the factor contribution to TVOC between other cities of Eastern Mediterranean basin is only possible with Beirut (Salameh et al., 2016) due to the absence of relevant studies in the area (**Sect. 2.3** of **Chapter 1**). For Beirut, six VOC sources were identified in winter and five VOC sources in summer. Traffic contributes 51% in winter and 74% in summer of the total NMHCs concentration in Beirut, if we aggregate the combustion and evaporation sources related to traffic for every season, which are similar to the contribution of traffic emissions in Athens for the same seasons (60% in winter and 68% in summer, **Fig. VI - 28**). The strong influence of the emissions from the transport sector to the NMHCs in Beirut were pointed out in other studies as well (Waked and Afif, 2012) and it was attributed to the high ratio of car per person (0.4), the age of the vehicles and the absence of catalytic systems for emission control, the high traffic density in some road segments. Concerning the rest of the sources, the "Gas Leakage" contribution in winter (10%) in Beirut is a little lower than the contribution of "Fugitive Emissions of ONG/LPG exploitation & distribution" (18% for winter, **Fig.VI - 28**) in Athens, although the diurnal pattern of the two sources is different (higher contribution during day for Beirut, the opposite for Athens, see also **Fig. VI - 3**).

To summarize, the observations from the **Sects. 2.1** and **2.2** (**this chapter**) indicate that VOC emissions from the transportation sector are important in the Eastern Mediterranean Basin than in Northern Europe. Possible reasons are related to the different climate, as well as the socio-economic situation of the two regions, that may affect the successful implementation of air quality measures. Nevertheless, more studies on VOCs and their sources are needed in the Mediterranean region in order to feed the discussion with robust data and probably create or update emission inventories, which are missing for Athens and Greece. These will help the delivery of better estimations for the evolution of the air pollution, which in turn could assist policy makers to implement more targeted measures for the improvement of the air quality.

3. PMF simulation of the IOPs

The existence of two VOC datasets from the winter and summer IOPs, which include 22 additional alkanes, aromatics, IVOC etc (**Sect. 1.2, Chapter 4**) triggered the idea to their PMF simulation, to examine the consistency of the results with the MOP PMF simulation. However, this PMF modelling is not easy due to various limitations that are imposed by the number of samples and the different measurement methods. Because the data preparation and the choice of the optimal solution follow the same basic principles as the presented ones for the MOP (**Sect. 1.1** of **this chapter**), they are explained in detail in **Sect. VI – A3** of the **Annex VI**. In addition, the VOCs of the input matrix, their S/N ratio and their characterization is presented in Table VI – A2 of the Annex VI. In summary, the examination of the statistical parameters showed that a 7-factor solution is the optimal one, which is further affirmed by the error estimation (DISP and BS). In **Table VI – 2** the mathematical parameters of the final solution are presented.

Table VI - 2: Mathematical diagnostics for the final solution of IOPs PMF

(m) species	47
(n) samples	153
(p) Factors	7
Runs	100
Number of species characterized as weak	2
Number of species characterized as bad	4
Number of random seed	3
$Q_{(robust)}$	8734
$Q_{(true)}$	9284
Q(T)/Qexp	1.89
$NMHC_{modeled}$ vs. $NMHC_{measured}$ (R^2)	0.993
Number of species with $R^2 > 0.75$ (modeled vs. measured)	42
Fpeak	-0.5

$dQ_{(robust)}$ of Fpeak	113.7 (1.28%)
BS mapping	73%

3.1 IOPs PMF results

In this section, the factors and their identification from the IOP PMF simulation are presented. In order to facilitate the reading, the identification starts with the factors presenting common species and variability to the MOP factors, by keeping the same names. These are presented in detail in **Sect. VI – A4** of the **Annex VI**, thus in this section only a brief summary is reported. Furthermore, the 2 additional factors will be more investigated. Therefore, since the IOP was conducted in different seasons (winter and summer) but only for 15 days of a selected month (February and September), for the further analysis we consider February as representative of winter and September of summer. After the identification of the factors, the discussion focuses on the differences between the MOP and IOP results.

3.1 – 1: Wood burning

The chemical profile of Factor I6 (**Sect. VI – A4.1, Annex VI**) is characterized by C2 – C3 alkanes and alkenes (48% to 21%), benzene (26%), hexene (35%) and cyclohexane (25%). This profile has many dominant compounds similar to Factor 1 "Wood-burning/Background" of the MOP, thus it is characterized as "Wood-Burning". It presents the highest concentrations in winter (February), whereas the diurnal cycle follows closely the one of BC_{wb} in both seasons. The identification is further corroborated by the relationship of the factor contribution to temperature, with higher values towards lower temperatures.

3.1 – 2: Fuel combustion (related to traffic and heating)

This factor's profile is characterized by alkenes like trans-2-butene (76%), 1-butene (63%) and styrene (63%), however, the highest concentrations are observed for i-pentane, C2 – C4 alkanes and alkenes (**Sect. VI – A4.2, Annex VI**). The profile resembles the one of Factor 4 from the MOP, so it is identified as "Fuel combustion related to traffic and heating". The contribution of the factor is high in winter (mean: 36.6 μg m^{-3}) but very low in summer (mean: 1.4 μg m^{-3}), with photochemical depletion in summer and the increase of sources' emissions in winter to be the main drivers of these observations (considering also the effect of atmospheric dilution). Furthermore, a diurnal variability is apparent only in winter, presenting a bimodal pattern with a morning and night maxima that follow closely the trend of BC_{ff} and NO.

3.1 – 3 Vehicle exhaust

The chemical profile of the related factor explains more than 20% aromatics and substituted alkanes, while the highest concentrations are observed for toluene, m-/p- xylenes, 2-me-pentane and i-pentane (**Sect. VI – A4.3, Annex VI**). These compounds are found in the profiles of vehicle exhausts however, the important contribution of BTEX and aromatics is often associated to solvent usage also (Baudic et al., 2016; Liu et al., 2008; Song et al., 2019; Yao et al., 2019). Furthermore, the presence of decane, undecane, alkenes and BTEX, indicates emissions from diesel and gasoline vehicle exhausts, as well as motorcycles (Guha et al., 2015; Hong-li et al., 2017; Liu et al., 2008; Salameh et al., 2019). Consequently, the factor is identified as "Vehicle exhausts". Furthermore, the

contribution is higher in winter (mean: 20.7 μg m^{-3}) and two times lower in summer, whereas the diurnal variability follows the one of CO. In addition, the factor correlates very well with CO, NO, NO_x, BC_{ff} and the previously described factor "Fuel combustion (related to traffic and heating)" (R^2 0.66 to 0.76).

3.1 – 4 Fuel evaporation (related to traffic)

Pentanes (~40%), butanes (~30%), propane (~23%) and toluene (~18%) are the main species of the speciation profile of Factor I2 (**Sect. VI – A4.4**). These compounds are highly volatile, so they are found often in the profiles of fuel evaporation emissions (Liu et al., 2008; Salameh et al., 2015; Baudic et al., 2016). Moreover, pentanes and butanes were also the principal compounds of the homonymous Factor 2 of the MOP PMF (**Sect. 1.2 – 5 of this Chapter**), which corroborates the identification of the factor as "Fuel evaporation (related to traffic)". The factor contributes more in summer than winter (mean values: 20.5 μg m^{-3} and 11.4 μg m^{-3} respectively). In addition, the diurnal variability follows the one of BC_{ff} in winter.

3.1 – 5 Fugitive emissions of ONG exploitation

More than 20% of branched alkanes, aromatics and C10 – C13 IVOC (58% of dodecane) are explained in the chemical profile of Factor I3 (**Sect. VI – A4.5**). In addition, ethane, propane, n-butane and 3-me-pentane have the highest concentrations in the profile. This combination of compounds has been attributed to fugitive emissions from petroleum and ONG exploitation in facilities (Abeleira et al., 2017; Guha et al., 2015). Thus, the factor is identified as "Fugitive emissions of ONG exploitation". The contribution of the factor is similar in both seasons denoting a stable source, while the seasonal diurnal variability is characterized by a night-time enhancement period.

*3.1 – 6: **New Factor** - Fuel Evaporation (stationary)*

The speciation profile of Factor I1 explains toluene and m-/p- xylenes, as well as more than 20% of aromatics, C5 – C9 alkanes and substituted alkanes and IVOC (**Fig. VI - 29**). From the previous discussion it is known that toluene and m-/p- xylenes are related to fuel combustion and evaporation, thus they are found in the chemical profiles of these emissions. Furthermore, in the speciation profile of Factor I1 there are no alkenes, indicating that the emissions are not related or occur simultaneously to combustion. Thus, the factor is identified as fuel evaporation (stationary).

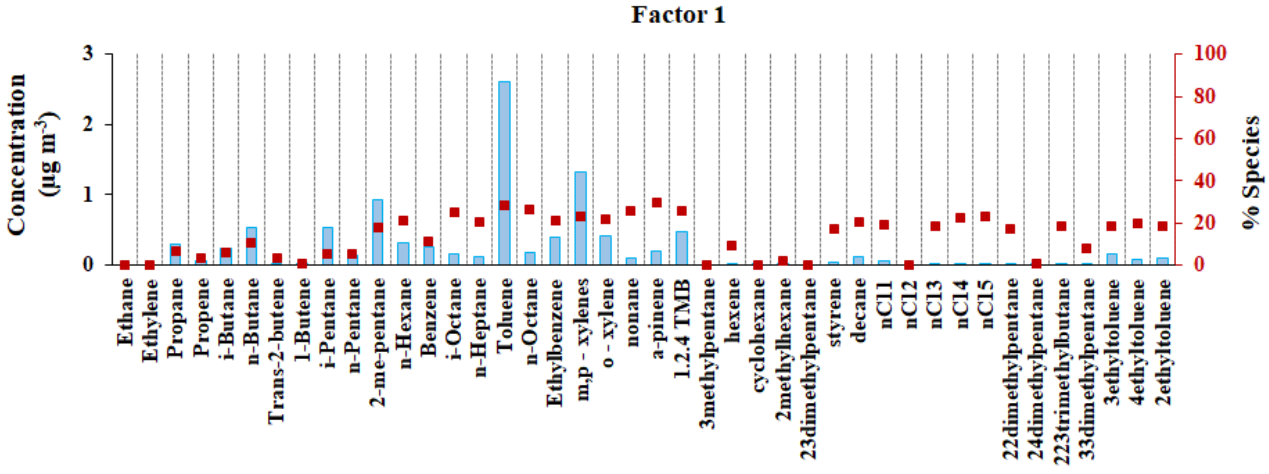

Figure VI - 29: Modelled contribution (μg m^{-3}) of each species to the Factor I1 (light blue bars) and relative contribution of the factor to each species (red squares).

Two differences are observed between this factor and Factor 2 "Fuel evaporation related to traffic" of MOP: the diurnal variability and the relationship to temperature. Starting from the former, the contribution of the factor is higher during night in both February and September, with a more persistent night-time enhancement in summer (**Fig. VI – 30c**). This cycle seems to follow the evolution of the mixing layer height, since during night the PBL decreases favoring the accumulation of pollutants. Furthermore, the contribution in September is higher than February (12.8 ± 15.8 μg m^{-3} and 8.5 ± 9.1 μg m^{-3} respectively; **Fig. VI – 30a,b**), although the highest values appear to be sporadic in both seasons. In addition, ambient temperature is higher in September than February and this enhances evaporation, as it is depicted in **Figure VI – 30d**; during the day fuels from stationary points evaporate, leading to their accumulation in the night. Moreover, in the literature is reported an enhancement of aromatics in the composition of gasoline in summer (i.e. Borbon et al., 2003), which corroborates the higher contribution in September.

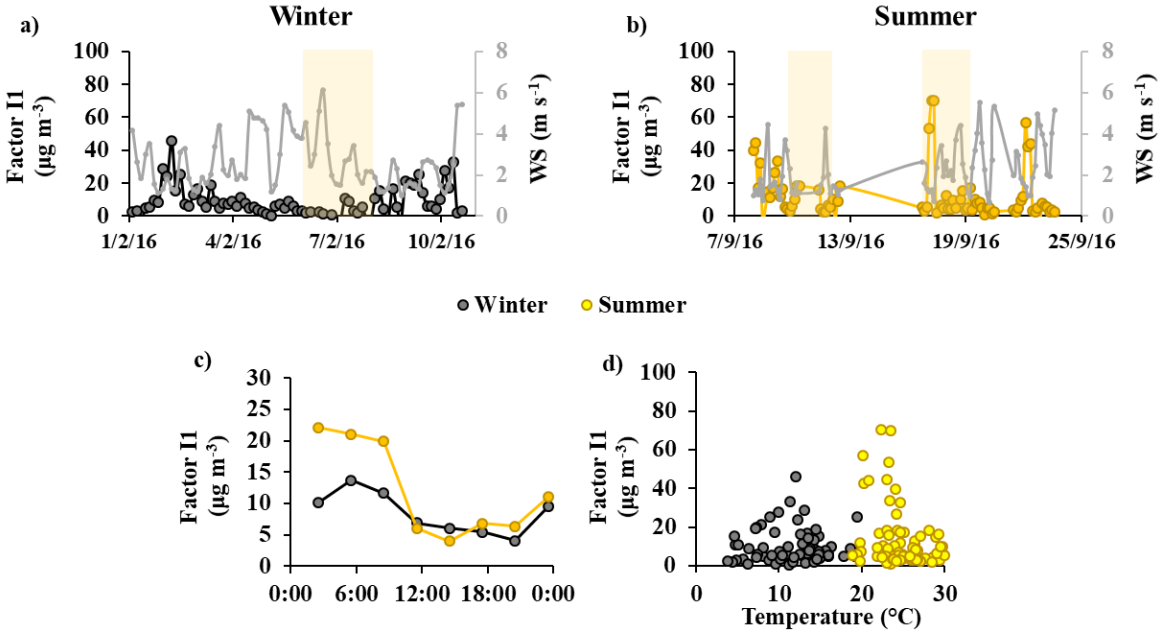

Figure VI - 30: Temporal variability of Factor I1 and wind speed in a) February (winter) and b) September (summer) 2016; c) Diurnal variability of Factor 1 and d) Relationship of Factor I1 to temperature, for February (winter) and September (summer).

3.1 – 7 ***New Factor:*** *Temperature-related factors*

The speciation profile of Factor 7 explains C14 – C15 IVOC (>55%), but i-pentane presents the highest concentration (**Fig. VI – 31**). In **Chapter 4** it was shown that these compounds are influenced greatly from temperature, whereas they seem to have other sources than decane. This is also reflected in the profile of the factor that explains only 3% of decane. Consequently, it is primarily identified as "Temperature-related factors". Other PMF studies deal with only light IVOC (< C12), thus comparison of this speciation profile to other in the literature is not possible.

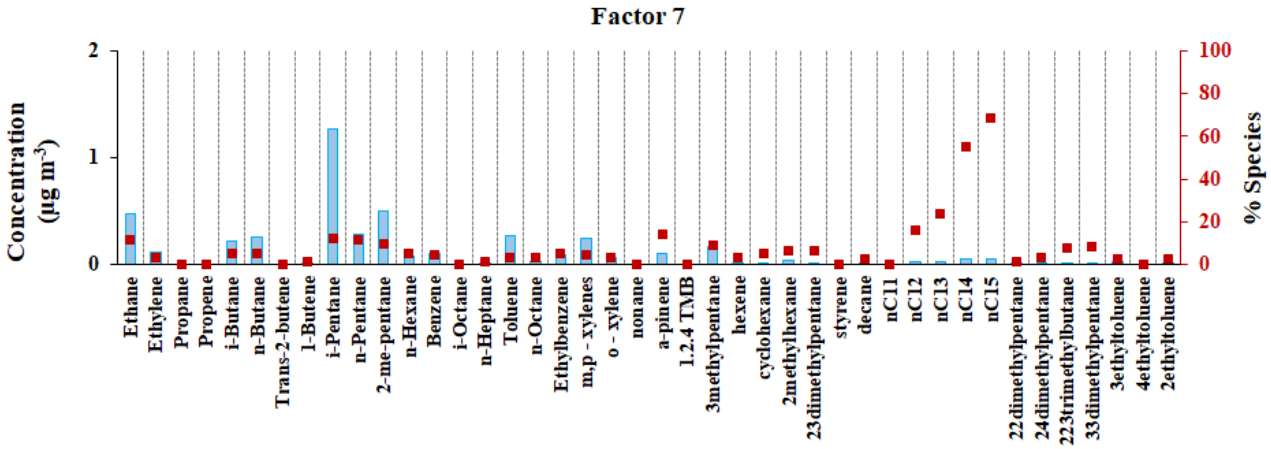

Figure VI - 31: Modelled contribution (µg m^{-3}) of each species to the Factor I7 (light blue bars) and relative contribution of the factor to each species (red squares).

Figures VI – 32a,b present the temporal variability of Factor I7 and ambient temperature, while the diurnal variability is presented in **Figure VI – 32c.** The contribution of this factor is similar for both months (3.8 ± 3.5 µg m^{-3} and 4.1 ± 2.5 µg m^{-3} for February and September respectively; **Fig. VI – 32a,b**) and it is clearly driven by ambient temperature. The latter is also illustrated in **Figure VI – 32d**, where it is apparent that the contribution of the factor increases with the increase of temperature. Furthermore, the diurnal variability is characterized by elevated contribution during the day starting from 12:00 LT in February and 06:00 LT in September, followed by a slow decrease at 15:00 LT until night **(Fig. VI – 32c**), which is opposite to the evolution of the PBL height. In addition, the contribution is independent from wind speed (graph not shown). The above observations clearly indicate that this factor reflects "sources" or atmospheric processes that are triggered solely from temperature, like the gas-to-particle partitioning and the evaporation of compounds. The former is further corroborated by the fact that in winter the contribution increases at midday when the highest temperatures occur, whereas in summer that the ambient temperature is already high (>20°C), the increase is apparent even from the first hours of the morning. Nevertheless, this trend follows the one of the heavy IVOC (dominant compounds in the chemical profile of the factor), as it was discussed in **Sects. 2.1** and **2.2** of **Chapter 4**.

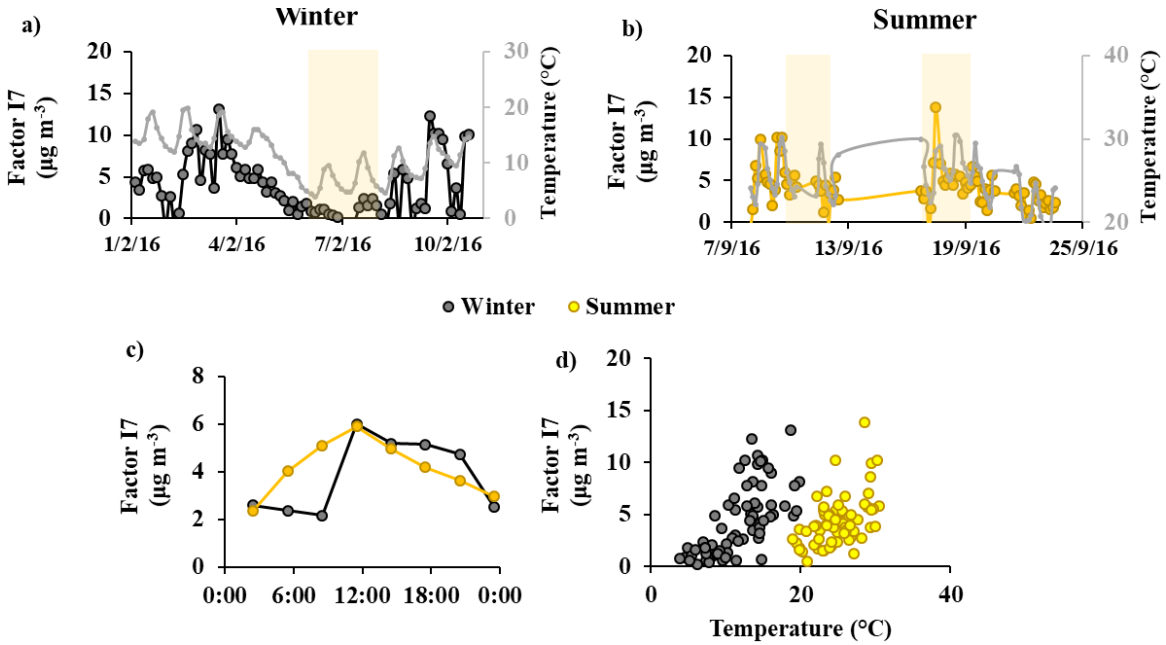

Figure VI - 32: Temporal variability of Factor I7 and wind speed in a) February (winter) and b) September (summer) 2016; c) Diurnal variability of Factor 3 and d) relationship of Factor I7 to temperature for February (winter) and September (summer). The yellow frames indicate weekends. Please note the different y-axis for temperature in Figure (b).

3.2 Inter-comparison of common factor profiles

Before the PMF overview, an inter-comparison of common factor profiles is conducted to verify the consistency and liability of the IOP PMF results. More specifically, the chemical profiles of Factors 2,4 and 5 ("Fuel evaporation related to traffic", "Vehicle exhaust" and "Fuel Combustion related to traffic and heating") are combined following the same method described in **Sect. 2.1** (**this chapter**), creating the "Traffic emissions IOP" profile. Furthermore, for this profile are used the common species of the MOP and IOP. The "Traffic emissions" profiles of the MOP and IOP are presented in **Figure VI – 33**. In the same graph is also illustrated the traffic profile that derived from the near-source measurements in Patission (**Section 2.1**, **this chapter**). It is apparent that the traffic profile of Patission and the "Traffic emissions" profile of the IOP have an excellent correlation (R^2: 0.99) and a slope equal to 1, denoting the correct and representative simulation of the traffic-related emissions in the IOP from the PMF. This is also depicted in the very good correlation (R^2: 0.92) of the "Traffic emissions" profiles of the MOP and IOP, with the few discrepancies being the slight underestimation of ethane and propane, and the overestimation of toluene and m-/p- xylenes from the MOP PMF. The underestimation of ethane was already pointed out in **Sect 2.1** (**this chapter**), whereas it could also be deducted that the **increase** of the **number** of **factors** helped the **better separation** of the **traffic-related factors**.

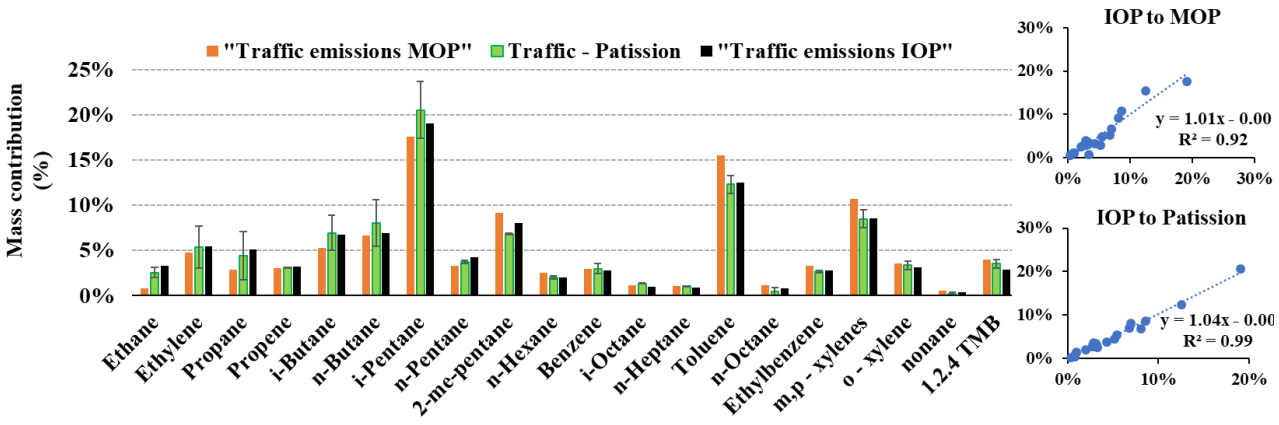

Figure VI - 33: Relative mass contribution (%) for combined Factors I2+I4+I5: «Traffic emissions IOP», the traffic profile from the MOP ("Traffic emissions MOP") and the traffic profile from Patission station. The right upper graph is the x-y relationship of the mass contribution (%) of the MOP and IOP traffic profiles and the right lower graph of IOP and Patission traffic profiles.

Finally, the profile of Factor I6 "Wood-Burning" is compared to the one from the MOP and the reported profile of Baudic et al., (2016), following the same method as in **Sect. 2.2** (**this chapter**). The three profiles are depicted in **Figure VI – 34**. The "Wood burning" profile of the IOP is better correlated (R^2: 0.89) to the wood burning profile of Paris (Baudic et al., 2016) than the "Wood burning" of the MOP (R^2: 0.72), compared to which the mass contribution is higher, resulting in a slope lower than 1 (0.62). This indicates significant discrepancies in the MOP and IOPs "Wood burning" profiles, which are found for propene, butanes and i-pentane. These compounds in the IOPs are attributed mainly to the traffic factors (>60%), however, they contribute also in this factor. This was not the case in the "Wood burning/Background" profile of the MOP, although it is known from the literature that wood burning emits light alkanes (Barrefors and Petersson, 1995; Evtyugina et al., 2014). In addition, the IOPs PMF attributed 50% of i-pentane to Factor I2 (Fuel evaporation related to traffic) and smaller amounts to other traffic and combustion factors, probably underestimating the contribution in wood-burning emissions. Thus, it can be assumed that the smaller number of samples with the additional monitored compounds and the sampling period with clear presence (February) and absence (September) of wood burning helped the better resolution of the chemical profile of this source, if we consider that the wood-burning factor of the MOP includes also background emissions.

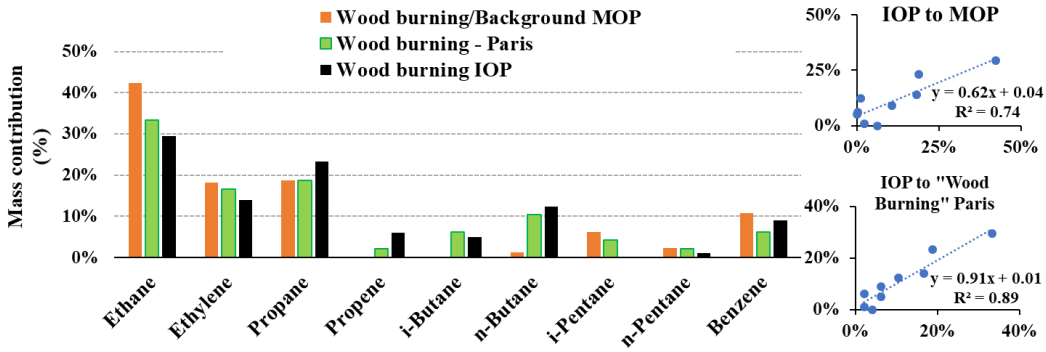

Figure VI - 34: Mass contribution (%) of NMHC in the profile of Factor I6 – "Wood burning IOP", "Wood burning MOP" and the Wood-burning profile of Baudic et al. (2016). The right upper graph is the x-y relationship of the mass contribution (%) of the IOP and MOP "Wood burning" profiles and the right lower graph of "Wood burning" of the IOP and the Wood burning profile of Baudic et al. (2016).

3.3 Discussion

3.3.1 PMF overview: Comparison to the MOP results

As it was presented in the previous paragraphs, the IOPs PMF simulation identified and quantified 7 factors related to sources, namely "Wood burning", "Fuel combustion related to traffic and heating", "Vehicle exhaust", "Fuel evaporation related to traffic", "Stationary Fuel evaporation", "Fugitive emissions from ONG exploitation" and "Temperature-related factors". In **Figure VI – 35** is presented the relative contribution of each factor to the total VOC concentration (TVOC) for the IOPs.

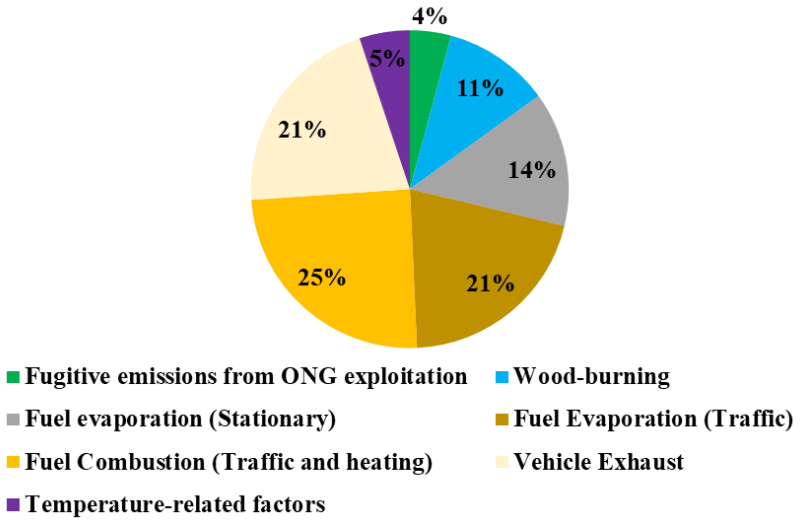

Figure VI - 35: Pie chart of the Total VOC contribution (%) of the factors modelled by the PMF for the MOP.

From the 7 separated factors, 3 of them ("Fuel evaporation related to traffic", "Vehicle exhaust" and "Fuel Combustion related to traffic and heating") explain ~20% of the TVOC each, Factors I1 ("Fuel Evaporation (Stationary)") and I6 ("Wood-burning") explain >10% of TVOC, while the last 2 Factors ("Fugitive emissions from ONG exploitation" and "Temperature-related factors") contribute < 5% each. Among them, 5 factors presented similarities to the MOP factors and they were identified accordingly, while Factor 1 "Fuel Evaporation (stationary)" (14%) and Factor 7 "Temperature-related factors" (5%) were 2 newly separated factors. Although the "Temperature-related factors" have little contribute to the VOC atmospheric budget, they are of interest due to the presence of IVOC. From **Chapter 4** it is known that these compounds are strong SOA precursors and their variability was clearly driven by temperature. This was also apparent to the variability of Factor I7 ("Temperature-related factors") (**Fig. VI - 32**).

Furthermore, the IOPs PMF identified the traffic-related factors ("Fuel evaporation related to traffic", "Vehicle exhaust" and "Fuel Combustion related to traffic and heating") as the main NMHCs emitters, attributing 65% of the TVOC denoting the importance of this source. In addition, the contribution (to TVOC) of the common factors of the IOP and the MOP PMF is illustrated in **Figure VI – 36**, for which the IOPs factors' contribution was re-calculated considering only the common factors to the MOP.

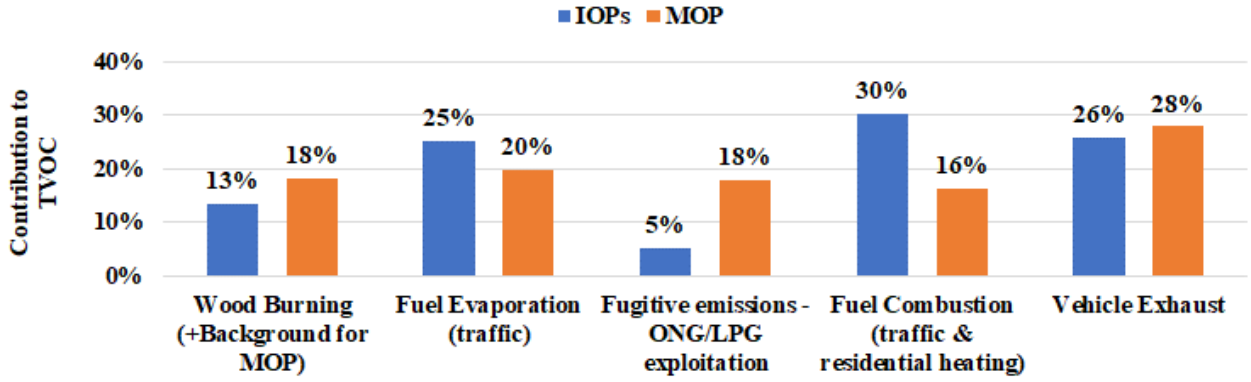

Figure VI - 36: Relative contribution to the TVOC (%) of the common factors between the IOPs (February and September 2016) and MOP PMF simulations (February 2016 to February 2017)

Among the common factors of the IOPs and MOP, "Wood-Burning", "Fuel evaporation related to traffic" and "Vehicle Exhaust" present similar contribution to the total VOC concentrations in both PMF simulations (±6%). Major differences are found for "Fugitive Emissions from ONG exploitation" and "Fuel combustion (traffic and residential heating)" that are estimated 3 times lower and 2 times higher respectively by the IOP PMF. For the latter, the higher estimation is related to the shorter period of sampling, since in the IOP only some days of two months are considered over a year of measurements for the MOP in which the factor contribution was very low for the entire summer and autumn (**Fig. VI – 12a**). Furthermore, for the former difference, it appears that the IOP PMF attributes higher relative contribution to the new factor namely "Fuel Evaporation (stationary)" (Factor I1) to the detriment of "Fugitive emissions from ONG exploitation". Both factors are related to evaporative sources, however, the shorter sampling period and the introduction of more compounds, like aromatics and branched alkanes that could originate from similar sources (i.e. in Liu et al., 2008) might have influenced the PMF simulation. Nevertheless, the results of the IOPs PMF could be considered satisfactory, given that the major VOC souses in Athens (traffic and residential heating) were apportioned similarly (±6%), as well as presenting close chemical profiles.

3.3.2 Anthropogenic sources of monoterpenes: The case of α-pinene

In **Chapter 5** it was shown that monoterpenes have an anthropogenic origin in Athens, the emissions of which are more important than the biogenic sources even in summer and autumn. The latter was also reported in Hellén et al. (2012) especially for the cold months. Furthermore, few studies report monoterpene levels in the atmosphere of urban centers, whereas even less include monoterpenes in their source apportionment simulations (i.e. Bari and Kindzierski, 2018; Guha et al., 2015; Hellén et al., 2012; Kaltsonoudis et al., 2016). Monoterpenes were excluded from the MOP PMF but they were included in the IOPs PMF dataset. In the end, only α-pinene was kept, since limonene had a low S/N ratio (**Sect. VI - A3** of the **Annex VI**). In **Figure VI – 37** is presented the apportion of α-pinene (%) to each factor.

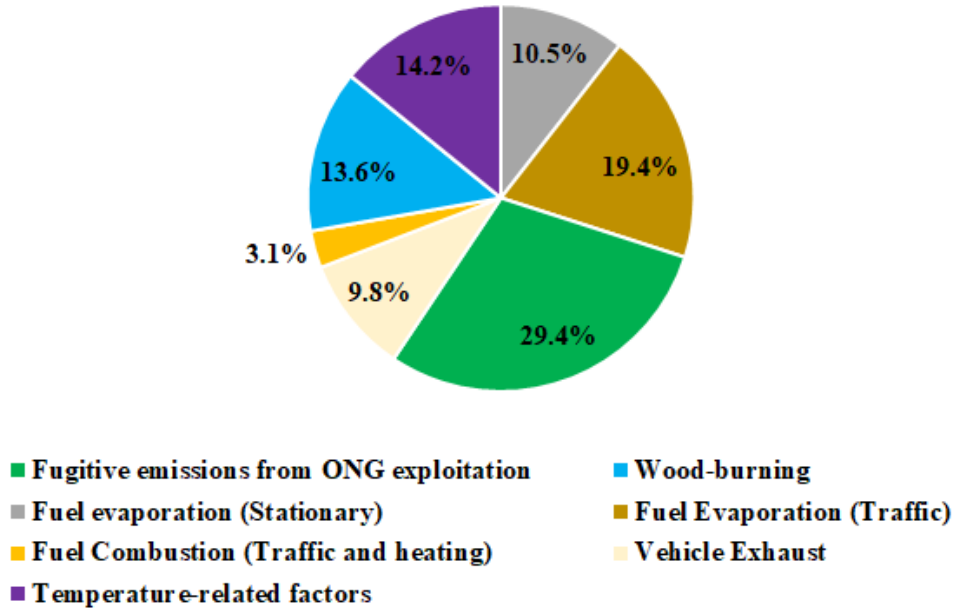

Figure VI - 37: Apportion of α-pinene (%) to factors of the IOP PMF.

Although all factors contribute to α-pinene, "Fugitive emissions from ONG exploitation"" contributes the most (29%), followed by "Fuel Evaporation (traffic)" (20%). The rest of the factors contribute 10 to 14% of α-pinene, whereas "Fuel combustion related to traffic and heating" contributes the lowest (3%). From the above results are derived the following conclusions:

a) A-pinene is not emitted from combustion of fossil fuels (or emits in very low levels), in contrast to the combustion of wood. It is known from the literature that monoterpenes are emitted from wood processing industries (McGraw et al., 1999), whereas their emission from wood burning for residential heating was reported in Hellén et al. (2012) and Kaltsonoudis et al. (2016). Especially the latter study apportioned 36% of monoterpenes in the wood burning factor for their winter PMF simulation.

b) The majority of α-pinene (29%) was attributed to an evaporative source ("Fugitive emissions from ONG exploitation"). As it was seen in **Sect. 3.1 – 6 (this chapter)**, the chemical profile of this source explains mainly branched alkanes, aromatics and C10 – C13 IVOC, with the highest contribution to the concentrations of light alkanes. Thus, the exact origin could be fugitive emissions from liquid fuels from tanks, tailpipes, gasoline stations, industrial emissions etc. However, α-pinene emissions seem to be linked to oil facilities. In the literature, one study conducted close to oil sand mining facilities reported increased levels of α-pinene and β-pinene close to the facility, which could not be explained by local vegetation (Simpson et al., 2010). In another study conducted in an urban area close to these oil mining facilities, the PMF simulation apportioned α-pinene to oil-sand fugitive emissions and petroleum processing among other factors (Bari and Kindzierski, 2018). However, the information regarding the possible connection of α-pinene emissions to oil mining and processing facilities is poor and further investigation is needed.

c) The traffic related-factors explain 33% of α-pinene. In Hellén et al. (2012), traffic was identified as the main source of monoterpenes and isoprene in Helsinki in winter and spring,

whereas Kaltsonoudis et al. (2016) apportioned 33% of monoterpenes to the traffic factor in winter. A-pinene was also identified at the exhaust's emissions of various cars in chamber experiments conducted by Dai et al. (2010).

d) The "Temperature-related factors" explain 14% of α-pinene. In **Sect. 3.1 – 7** (**this chapter**) it was shown that the variability of this factor is driven by ambient temperature, thus the contribution increases during day. The apportion of α-pinene to this factor might reflect the biogenic emissions of α-pinene which are usually masked by the anthropogenic emissions, as it was seen in **Chapter 5**. Nevertheless, both Hellén et al. (2012) and Kaltsonoudis et al. (2016) report that although in winter the sources of monoterpenes are human-related, in summer, the major source is biogenic emissions.

To sum up, the above examination showed that the main anthropogenic sources of α-pinene in Athens are fugitive emissions from ONG exploitation, wood burning for residential heating and traffic. However, it also showed the limited information regarding the sources and ambient levels of this compound in urban environments. Since monoterpenes are both important ozone and SOA precursors that are underestimated in the input datasets of model simulations for future projections (Wang et al., 2013; Zhang et al., 2018), the importance of VOC measurements including monoterpenes is highlighted.

4. Conclusions

In this chapter the **source allocation** of the **VOCs** from the **MOP** and **IOPs** was presented and discussed, which was one of the **main objectives** of the current thesis. The overview of the source apportionment approaches in **Annex I** showed that the Positive Matrix Factorization method was the most appropriate one for the MOP and IOPs datasets considering the type of sampling station and the available information on sources. In this context, the chapter was separated in two major sections: the MOP and IOPs PMF simulations.

Starting from the MOP dataset, the PMF simulation included 24 major NMHCs that were selected based on the S/N ratio and the data availability. Five factors related to sources were resolved from the MOP PMF, namely "Fuel evaporation related to traffic", "Fugitive emissions from ONG/LPG exploitation and distribution", "Vehicle exhaust", "Fuel combustion related to traffic and heating" and "Wood burning/Background". From these, the traffic-related sources are the main NMHC emitters in Athens contributing 64% to the TVOC. All the factors present distinct seasonal variability: the combustion related sources contribute more in winter whereas the evaporative ones more in summer. Only "Fugitive emissions from ONG exploitation and distribution" present similar contribution for every season apart from summer. Moreover, the comparison of the factor speciation profiles (% mass contribution of NMHCs) to profiles from the other studies and the near-source campaign in Patission station showed many similarities, denoting the good attribution of the factors to sources. However, the comparison of the factor contribution showed more similarities to Beirut than Paris, indicating that some sources (e.g. traffic-related) are more intense in cities of Mediterranean basin than cities at a Northern latitude (taking as reference Paris).

The IOPs PMF simulation identified and quantified seven factors related to sources from which "Fuel evaporation (Stationary)" and "Temperature-related factors" were completely new, contributing 19% to the total VOC. Furthermore, the traffic related factors were also identified as the main VOC sources in Athens, attributing 65% of the total VOCs. In addition, the introduction of α-pinene to the IOPs PMF dataset permitted the identification of its anthropogenic sources, with "Fugitive emissions from ONG exploitation", "Wood-burning" and traffic related sources ("Fuel evaporation related to traffic", "Vehicle exhaust" and "Fuel Combustion (traffic and heating)") being the main ones, explaining 75% of α-pinene. Furthermore, 14% of α-pinene was attributed to the "Temperature-related factors", which might reflect the biogenic contribution.

Furthermore, the similarities and differences that are observed in the IOPs and MOP PMF results highlight the important role of the resolution of the PMF dataset and the variety of species. Firstly it was shown that by using data from the same dataset, even if they are of different time resolution, for a short period, or they are accompanied by additional compounds, PMF is able to simulate the same major sources and generate close chemical profiles regarding the contribution of the dominant species. Furthermore, by adding more compounds like IVOC, branched alkanes and aromatics, which have different life-time and chemistry, two more VOC factors related to sources in Athens were identified, from which one chemical profile was never reported ("Temperature-related factors"), whereas profiles like for the traffic-related sources were better resolved. The above observations denote the possibility to include at least the majority of the monitored compounds in a study, however, such detailed sources profiles, in terms of variety of compounds, are not reported in the literature making the comparison to other works difficult. Nevertheless, it is important to note that important classes of VOCs were missing from the PMF, like OVOC and BVOC, making impossible the estimation of sources rich in OVOCs or biogenic sources.

In addition, the combination of the two datasets from the IOP (winter and summer; different atmospheric dynamics and intensity of sources emissions) is of importance for the representativity of the study which is confirmed by the closeness of the MOP and IOPs PMF results. Moreover, the shorter observation period of the IOPs dataset was one of the main reasons for the over/under-estimation of the contribution of some factors, such as the "Fuel combustion related to traffic". This is the major drawback for using this type of datasets; the contribution of some factors might not be well reflected, like for active sources in specific seasons (e.g. biogenic emissions), or for sources impacted by atmospheric chemistry (like "Fuel combustion related to traffic") or for sources that are enhanced/reduced in specific periods due to change of needs (like traffic emissions in summer vacations). Thus, high-resolved VOC datasets of several months are encouraged, especially for regions with diverse VOC sources. Robust conclusions can be derived from short-term intensive VOC studies, because they allow the monitoring of more species by deploying instruments of higher performance and demanding handling, which in turn assist the identification of additional sources or the better deconvolution of co-linear sources (e.g. traffic and domestic heating).

CONCLUSIONS & PERSPECTIVES

General Conclusions

The high concentrations of O_3 and aerosols in the Eastern Mediterranean, in combination to the foreseen climate change, highlight the need for the assessment of pollutant precursors' variability and their sources, such as the VOC. In this context, Athens is an area of interest for VOC measurements for the following reasons: a) Despite the reported decrease of the levels of atmospheric pollutants, O_3 and PM (particular matter) often exceed the European legislation limits; b) Information for VOCs is limited and dates back 15 years, the levels of C2 NMHCs were never reported and the seasonal variability was never examined in an annual basis, with the majority of the published data obtained from summer-time measurements; c) The VOC source apportionment was never addressed in detail; and d) current studies have shown that during winter night-time smog events, the concentrations of particulate and major gaseous pollutants increase significantly, reaching levels similar to 2000, whereas the impact on VOC is not known. Thus, the objectives of the current work were (1) to investigate the temporal variation of VOC concentrations in Athens (Greece), with high resolution measurements, (2) to determine the driving factors of the observed variability, (3) to assess the relative contribution of VOC to the air quality in Athens by the comparison to other cities at Mediterranean, European and international level; (4) to establish sources' fingerprints with field measurements, (5) to identify and quantify VOC sources in Athens, and (6) to compare our results to estimations of emission inventories.

In this context, one main observation campaign (MOP) was carried out at Thissio station (urban background) from October 2015 to February 2017 for the monitoring of C2 – C12 NMHCs, under the frame of ChArMEx project. Furthermore, two intensive observation campaigns (IOP) were also performed in parallel to the MOP in winter and summer 2016 for the monitoring of additional compounds, as well as two near-source campaigns for the determination of the traffic emission profile. Moreover, data for ancillary pollutants like CO, BC and NOx and meteorological parameters are also available from Thissio station.

For the MOP campaign, 27 C2 – C12 NMHCs (e.g. alkanes, alkenes, aromatics etc) were monitored by two automatic on-line GC – FID systems resulting to data with coverage from 65% to 94%. For the monitoring of the additional 22 C6 – C16 VOC (e.g. branched alkanes, IVOC etc) in the IOPs, off-line sampling methods on sorbent tubes and posteriori laboratory analysis were deployed, resulting in more than 100 samples per tube type and per campaign. Furthermore, for the near-source campaigns only off-line sampling was conducted close to traffic sites (tunnel and traffic monitoring station). Finally, the existence of the previous datasets allowed the inter-comparison of the on-line and off-line sampling methods for the compounds in common, giving satisfactory results. The analysis of the MOP and IOP datasets resulted in the following main observations:

1. Temporal variability of C2 – C12 NMHCs

NMHCs levels, except of monoterpenes and isoprene (presented below), present a distinct seasonal variability with increasing concentrations from autumn to winter when the highest concentrations occur, followed by a gradual decrease until summer, meeting their lowest levels. Among the monitored compounds, alkanes contribute > 50% to the total VOC concentrations, however, i-pentane and toluene exhibit the highest mean values (9.5 and 7 respectively). Benzene's annual mean concentration for 2016 was 1.7 $\mu g\ m^{-3}$ (92% data coverage over the maximum potential), which is below the EU threshold of 5 $\mu g\ m^{-3}$. Furthermore, the seasonal diurnal variability of the

NMHCs exhibits a bimodal pattern with a morning and a night maximum separated by a late afternoon minimum regardless of the season. In addition, the amplitude of the maxima changes depending on the season, with the night-time enhancement period to increase significantly relative to the morning maximum in winter (factors of 2 to 7, for i-pentane and propene respectively). Moreover, the diurnal trend follows closely the reported one for pollutants like CO, BC and NO, which are known tracers of combustion and traffic emissions, indicating their possible common origin.

2. Factors affecting the NMHCs variability

Atmospheric dynamics and emission from sources are the main drivers of the observed NMHCs variability. Starting from the atmospheric dynamics, low wind speed (< 3 m s^{-1}) favors the enhancement of the concentrations, denoting the influence from local emissions than long-distant ones. Furthermore, the enhancement is more apparent for emissions occurring under a swallow mixing layer, like for example during night under stagnant conditions. Concerning the relationship of VOC to temperature, two trends are observed: increased concentrations are associated to high temperatures, which is in line with their volatility. However, the concentrations increase also under low temperatures in winter, indicating an effect from emissions from sources related to the cold weather in winter (e.g. residential heating). Finally, photochemical depletion has a slight influence only for the most reactive compounds (like 1.2.4 TMB with a lifetime of 4 hours).

The previous observations showed that the enhancement of the levels is a synergy between atmospheric parameters (like wind speed) and emissions from sources, with the latter playing the most important role. This is corroborated by the similar seasonal diurnal trend of the NMHCs and pollutants/indicators of combustion processes (like domestic heating) and traffic-related emissions such as CO, BC and NO, as well as by their good correlation coefficients. Nevertheless, in Panopoulou et al. (2018), the separation of the C2 – C6 NMHCs dataset (autumn 2015 and winter 2016) to smog and non-smog periods (wind speed did / did not exceed 3 m s^{-1} and precipitation as on/off criterion) showed that the night-time enhancement period (taking midnight as reference) increases 2 (i-pentane) to 6 (propene) times in December than October, highlighting emissions from additional sources in winter that occur under stagnant conditions (low wind speed and low mixing layer).

3. Comparison to other studies

In Panopoulou et al. (2018), the comparison of the C2 – C6 NMHCs levels (autumn 2015 and winter 2016) to other works showed that most of the compounds had higher mean levels compared to other cities in Europe and Mediterranean. Furthermore, the comparison of the mean concentrations of the C2 – C12 NMHCs of the MOP, summer 2016 and winter 2017 to worldwide distributed cities indicated that (a) the mean levels for the MOP in winter can be indeed higher compared to other cities but this depends on the compound and (b) the mean levels in summer are in general lower than the other cities. This difference for the winter and summer comparison, as well as the distribution of the maximum mean values between the studied cities denotes that sources' emissions probably drive the observed levels.

4. Variability of the VOC from the IOPs

The examination of the variability of the 22 additional C6 – C16 VOC (3 hours resolution) showed similar seasonal and diurnal profiles to the NMHCs from the MOP in February and September (as

reference to winter and summer respectively), with higher concentrations in winter than summer (e.g. 3-me-pentane with 2.43 ±2.28 μg m^{-3} and 1.22 ±1.05 μg m^{-3} in February and September respectively). In addition, the diurnal cycle exhibits a bimodal pattern with a morning maximum and a night-time enhancement period, although for some compounds the night-time elevated levels persist till morning (e.g. hexene). Furthermore, the observed variability is also explained by a similar influence of atmospheric dynamics and sources emissions.

The only exceptions to the above trend are the C11 – C16 VOC (or intermediate VOC – IVOC). These compounds are precursors of secondary organic aerosols due to their gas-to particle partitioning properties. Particularly, their mean concentrations in winter and summer are almost similar, like for tridecane (0.13 ±0.09 μg m^{-3} in February and 0.11 ±0.08 μg m^{-3} in September). Although C10 – C12 IVOC exhibit similar diel cycles to the rest of VOC, the heavier IVOC (C13 – C16) present contrasted cycles in winter and summer. More specifically, the concentrations increase during day in winter, whereas they increase after midnight in summer. In addition, the increase/decrease of their levels is independent from wind speed, whereas they increase with temperature. This relationship to atmospheric dynamics indicates that their levels in the atmosphere are driven mainly by their physico-chemical properties which are also responsible for their gas to particle partitioning.

5. Monoterpenes and isoprene's variability

The unusual variability of isoprene and monoterpenes justifies their examination separately from the other NMHCs. These compounds are typically considered of biogenic origin, thus higher levels are expected in summer than winter, since the increased temperatures and solar intensity triggers the biogenic activity. Remarkably, although isoprene has the highest mean concentration in summer (0.48 ±0.56 μg m^{-3}), for α-pinene we observe similar mean winter (0.67 ±0.91 μg m^{-3}) and summer (0.70 ±0.66 μg m^{-3}) values, whereas limonene is higher in winter (0.48 ±1.06 μg m^{-3}) than summer (0.15 ±0.31 μg m^{-3}). This suggest additional emissions than biogenic, probably of anthropogenic origin. This is corroborated by the seasonal diurnal cycles which exhibit a night-time enhancement period persisting until morning, when a maximum is also observed. Isoprene on the contrary was increased during day for the summer period. Overall, the examination of the influence of atmospheric dynamics (wind speed, wind direction, temperature, relative humidity, precipitation, solar intensity) did not show a dependence that could justify emissions from biogenic activity for monoterpenes, with the exception of some sporadic data of α-pinene related to precipitation. Specifically, the enhancement of the levels is favored by low wind speed, denoting local emissions, whereas high levels are encountered also in temperatures <10°C in winter, highlighting the assumption of the anthropogenic contribution. The latter was investigated firstly by the relationship of monoterpenes and isoprene to other pollutants (toluene, CO, BC_{wb}, BC_{ff}) in selected time-frames representatives of the anthropogenic activities. The compounds presented a linear relationship with statistically significant correlation coefficients for all seasons indicating the contribution of emissions from traffic, and in winter from both traffic and residential heating. Finally, the anthropogenic and biogenic contribution to α-pinene is estimated following the approach of Brito et al., (2016), showing higher contribution of anthropogenic emissions over biogenic even in summer, corroborating the above observations.

6. Monoterpenes' and isoprene's ozone and secondary organic aerosol formation potential (OFP and SOAFP)

Monoterpenes and isoprene are among the reactive VOC with lifetimes less than 4 hours in respect to the OH radical. Thus, an estimation of their OFP showed that α-pinene produces annually an average of 2.5 μg m^{-3} O_3, whereas limonene participates significantly on the OFP mainly during winter. In addition, isoprene contributes 5 μg m^{-3} of ozone during summer. Based on the above calculations, the sum of monoterpenes and isoprene contribute up to 6% of the oxidants (sum of O_3 and NO_x) observed in winter and summer.

The SOAFP was estimated for monoterpenes only; isoprene was excluded due to the applied methodology limitations. A-pinene contributes about 2 μg m^{-3} during summer and 1.2 μg m^{-3} for the rest of the year, whereas limonene contributes 1.5 μg m^{-3} in winter nights (maximum observed SOA). The importance of the terpenes' contribution on SOA was further verified by the comparison to the sum of semi-volatile oxygenated organic aerosol (SV-OOA) and hydrocarbon-like organic aerosol (HOA) (Stavroulas et al., 2019). Specifically, SVOOA and HOA levels could be fully explained by the monoterpenes' reactivity (sum of α-pinene and limonene) in summer and in winter daytime, whereas for winter nights they contribute 40% to SOAFP.

7. Sources of NMHCs in the atmosphere of Athens

The two VOC datasets from the MOP and IOPs campaigns were subjected in two separate PMF simulations. The MOP PMF simulation resulted in five factors related to sources: "Fuel evaporation related to traffic", "Fugitive emissions from ONG/LPG exploitation and distribution", "Vehicle Exhaust", "Fuel combustion related to traffic and heating" and "Wood burning/Background". Furthermore, the traffic-related sources (sum of "Fuel evaporation related to traffic", "Vehicle Exhaust" and «Fuel combustion related to traffic and heating") are the main NMHC sources in Athens contributing 64% to the TVOC. All the factors, except of the "Fugitive emissions from ONG exploitation and distribution", present distinct seasonal variability: the combustion related sources contribute more in winter whereas the evaporative ones more in summer. Moreover, the comparison of the PMF results to Paris and Beirut showed that the emissions from the traffic sector are two times higher in Athens than Paris (29%), but similar to Beirut (51% in winter and 74% in summer in Beirut over 60% in winter and 68% in summer in Athens), denoting their importance in the cities of the EMB, in contrast to the Central/North/Western Europe. On the other hand, the Athens "Wood burning/Background" contribution to the total VOC is similar to Paris (18% and 19% respectively). Concerning the IOPs PMF, seven factors were identified and quantified related to: "Stationary Fuel evaporation", "Fuel evaporation related to traffic", "Fugitive emissions from ONG exploitation", "Vehicle exhaust", "Fuel combustion related to traffic and heating", "Wood burning" and "Temperature-related factors". Five of them were identified similarly to the MOP factors, thus only two were completely new contributing ~19% to the total VOC. The traffic-related factors dominated also in this simulation, contributing 65% to the total VOCs. "Wood-burning" contributed lower (11%) in the TVOC of the IOPs than in the MOP (18%). Moreover, by including α-pinene to the IOPs PMF simulation, it was possible to determine its anthropogenic sources. Specifically, "Fugitive emissions from ONG exploitation", "Wood-burning" and traffic related sources explain 75% of α-pinene, whereas 14% was also attributed to the "Temperature-related factors", which might reflect the biogenic contribution.

To summarize, during my work for this PhD, I managed to handle 2 GC instruments (and additional sampling during intensive campaigns) and to obtain a unique dataset allowing the successful characterization of the C2 – C12 NMHC variability in the atmosphere of Athens for 17-months and to allocate these observations to sources given the variety of compounds and despite the technical

issues that occurred. The examination allowed the documentation for the first time of C2 NMHCs levels in four seasons, as well as the observation of the seasonal variability of the monitored VOCs in an annual basis. Furthermore, the driving factors of the observed variability were demonstrated, showing that low wind speed favor the accumulation of NMHCs in the atmosphere, especially under stagnant conditions (low height of the mixing layer), denoting the influence of local emission from sources. In this context, traffic emissions are the main source of NMHCs in Athens, followed by wood-burning for residential heating. The existence of two seasonal datasets (IOPs) with 22 additional VOC (poly-substituted alkanes, IVOC and aromatics), allowed the performance of a second PMF simulation that on one hand gave 5 factors similar to the MOP factors (with different contribution to the TVOC compared to the MOP PMF factors), validating the PMF results of the MOP. On the other hand, the estimation of the contribution to the VOC levels was different for some factors in comparison to the MOP PMF results, indicating an impact from the smaller resolution of the IOPs dataset. Moreover, it is important to mention the two observations of this campaign, which are rarely or not at all mentioned in the literature: a) the anthropogenic sources of monoterpenes and isoprene in urban environments and b) the examination of the IVOC and their use in PMF simulations.

Scientific Perspectives

Following the above observations and conclusions, the new scientific perspectives and questions are presented below:

1. Robustness of short-term seasonal VOC field campaigns for source apportionment

The results from the MOP and IOPs PMF simulations showed the positive and negative aspects of using shorter observation periods. In our case, it is assumed that the sampling in two contrasted seasons for the IOP (winter and summer; different atmospheric dynamics and intensity of sources emissions) and with additional instrumentation of higher performance, helped the PMF tool to generate chemical profiles of factors similar to the ones from the annual MOP, to deconvolute co-linear sources and to determine additional factors related to sources. On the other hand, the drawbacks for using short-term datasets in the PMF is that sources active in specific seasons (like residential heating) might be over/underestimated or not determined at all. Consequently, these type of short-period VOC campaigns could add value to a long-term monitoring period or they could be employed for a low-cost strategy to address sources and processes (however with a limited time-representability).

2. Urgent need for the characterization of monoterpenes in the urban atmosphere

Monoterpenes and isoprene, due to their high reactivity, contribute more to ozone and SOA formation than other VOC. Nevertheless, the information regarding their levels and sources in urban environments is limited. This might be attributed partly to their instability (thermo-degradation) during analysis that made their determination difficult. However, in this study it was shown that some representative monoterpenes can be successfully separated, identified and quantified by the on-line GC – FID system, which makes possible their monitoring in future VOC field measurements. Furthermore, it was shown that monoterpenes (and isoprene) can have anthropogenic sources in the urban environments, but the information regarding these emissions are sparse. Given the

aforementioned contribution to O_3 and SOA (which are key constituents of the air pollution episodes in cities with known adverse effects on climate change, human health, environment etc), there is still a need to fully understand their formation processes for better mitigation.

3. Need for the characterization of IVOC in the urban atmosphere

Like monoterpenes, IVOC are also important precursors of SOA, because their lower volatility (between volatile and semi-volatile organic compounds) favors their gas-to-particle partitioning depending on the temperature. In this work it was possible to identify and quantify C10 – C16 IVOC using off-line sampling on sorbent tubes. Although their SOAFP potential was not estimated in this framework, they were used in the IOPs PMF simulation and attributed separately (> 20% of the C12 – C16 IVOC) to a temperature related factor. This factor might include evaporative sources, but it might as well reflect partitioning of IVOC from particle to gas which could be an additional secondary "source" or "sink" of VOCs in the atmosphere. To our knowledge, heavy IVOC were never used in the PMF simulations of published works, thus our approach creates the following questions: a) is it useful to use IVOC in the PMF simulation to obtain factors related to processes (than sources) like the particle-to-gas partitioning?; b) Could the observations of this work validate the modelling and predictions of Chemical & Transport Models (CTM) concerning the gas-to-particle partitioning? Nevertheless, it should be kept in mind that the above observations on one hand give important insights, but on the other hand they are based on a limited IVOC dataset. Thus, for the better estimation of the gas-to-particle partitioning, information for other compounds is needed in parallel, like for example for semi-volatile VOCs, OVOC and highly oxidized VOC.

4. Need for the characterization of OVOC in the atmosphere of Athens

One limitation of the current project was the non-exploitation of the OVOC data. This class of compounds constitutes a large fraction of the VOC in the atmosphere. For example, in Kaltsonoudis et al. (2016), the monitored OVOC presented the highest mean values in summer, and among the highest mean values in winter. Since these compounds have primary but also secondary sources, while there are indicators of sources like solvent usage, their absence from the analysis lead to less information on atmospheric processes (i.e. secondary formation, SOA formation), whereas additional sources or sources that co-variate were not separated (e.g. solvents usage). Thus, measurements of these compounds should be included in the future VOC monitoring projects as well.

5. Need for the characterization of the oxidants' levels in Athens

Although for the majority of the studied VOC the reaction to the OH radical is the main oxidation pathway, this is not the case for the reactive compounds (like terpenes) that react rapidly with the other oxidants like O_3 and the NO_3 radical during the night. A better knowledge of the oxidant capacity would allow a better estimation of the photochemical decay of VOCs and a more accurate source apportionment for the more reactive compounds. This information needs advanced instruments which could complete the set-up of intensive campaigns.

6. Are VOC measurements in a background station in Athens enough?

In the current work, C2 – C12 NMHCs were determined for more than 12 months. The reported levels and subsequent source apportionment filled the scientific gap of these compounds in Athens, but the continuous evolution of pollutants sources indicate that VOC studies should be reinforced for the better assessment of the air quality. Furthermore, the recent Annual Report on Air Quality for the year 2018 from the Ministry of Environment and Energy (edition in Greek; http://www.ypeka.gr/LinkClick.aspx?fileticket=FJbhHPSTih4%3d&tabid=490&language=el-GR) indicated that in Patission traffic station, benzene levels exceed the European threshold (5 μg m^{-3}), with an annual mean of 5.9 μg m^{-3} but a data coverage of only 50%. Thus, although this seems alarming, the data coverage is not satisfactory for the delivery of safe conclusions based on the European standards. Consequently, this highlights the need for the implementation of monthly-term VOC campaigns in other sites inside the city, close to major sources (like on-road traffic emissions) and in areas like the city center that most of the population gathers. In addition, the following question arises: although the urban background NMHCs measurements showed an annual benzene level lower than the threshold, could this be representative of other sites close to major sources like roads? Since the majority of the population in cities lives close to the city center that is characterized by increased traffic, is the current information on VOC enough for their protection? This urges the design of VOC field campaigns simultaneously in specific sites (like traffic stations) and urban background stations.

7. Constrain of emission inventories

One of the main motivations of this work was to use the results for the constrain of existing emission inventories. This was motivated by the work of Salameh et al. (2016, 2017) in which it was shown that NMVOC emissions for the transportation sector were underestimated by a factor of 10 from global emission inventories, whereas the chemical composition of anthropogenic emissions estimated from emission inventories presented important discrepancies (i.e. for the aromatics) between cities of the Middle East. Although it became impossible to actually constrain an emission inventory during the time-frame of this PhD, the observations from the MOP and IOP datasets gave important information that should be taken into account by developersto update and constrain existing national and international inventories. In particular, monoterpenes and IVOC are not characterized often in the urban environment, whereas the anthropogenic sources of monoterpenes are not considered in emission inventories. Thus, it is of great importance to introduce these compounds in emission inventories for the better and more accurate evaluation of the air quality and the prediction of the future evolution of air pollution and its impacts.

BIBLIOGRAPHY

Abeleira, A., Pollack, I. B., Sive, B., Zhou, Y., Fischer, E. V. and Farmer, D. K.: Source characterization of volatile organic compounds in the Colorado Northern Front Range Metropolitan Area during spring and summer 2015, J. Geophys. Res. Atmospheres, 122(6), 3595–3613, doi:10.1002/2016JD026227, 2017.

ACTRIS – II : https://www.actris.eu/About/ACTRIS/WhatisACTRIS.aspx

ACTRIS Measurement Guidelines VOC. WP4 – NA4: Trace gases networking: Volatile organic carbon and nitrogen oxides Deliverable D4.9: Final SOPs for VOC measurements, 2014.

Adam, T. and Zimmermann, R.: Determination of single photon ionization cross sections for quantitative analysis of complex organic mixtures, Anal. Bioanal. Chem., 389(6), 1941–1951, doi:10.1007/s00216-007-1571-x, 2007.

Adam, T. W., Astorga, C., Clairotte, M., Duane, M., Elsasser, M., Krasenbrink, A., Larsen, B. R., Manfredi, U., Martini, G., Montero, L., Sklorz, M., Zimmermann, R. and Perujo, A.: Chemical analysis and ozone formation potential of exhaust from dual-fuel (liquefied petroleum gas/gasoline) light duty vehicles, Atmos. Environ., 45(17), 2842–2848, doi:10.1016/j.atmosenv.2011.03.002, 2011.

Afif, C., Dutot, A. L., Jambert, C., Abboud, M., Adjizian-Gérard, J., Farah, W., Perros, P. E. and Rizk, T.: Statistical approach for the characterization of NO<Subscript>2</Subscript> concentrations in Beirut, Air Qual. Atmosphere Health, 2(2), 57–67, doi:10.1007/s11869-009-0034-2, 2009.

Ahmed, S. O., Mazloum, R. and Abou-Ali, H.: Spatiotemporal interpolation of air pollutants in the Greater Cairo and the Delta, Egypt, Environ. Res., 160, 27–34, doi:10.1016/j.envres.2017.09.005, 2018.

Ait-Helal, W., Beeldens, A., Boonen, E., Borbon, A., Boréave, A., Cazaunau, M., Chen, H., Daële, V., Dupart, Y., Gaimoz, C., Gallus, M., George, C., Grand, N., Grosselin, B., Herrmann, H., Ifang, S., Kurtenbach, R., Maille, M., Marjanovic, I., Mellouki, A., Miet, K., Mothes, F., Poulain, L., Rabe, R., Zapf, P., Kleffmann, J. and Doussin, J.-F.: On-road measurements of NMVOCs and NOx: Determination of light-duty vehicles emission factors from tunnel studies in Brussels city center, Atmos. Environ., 122, 799–807, doi:10.1016/j.atmosenv.2015.09.066, 2015.

Ait-Helal, W., Borbon, A., Sauvage, S., de Gouw, J. A., Colomb, A., Gros, V., Freutel, F., Crippa, M., Afif, C., Baltensperger, U., Beekmann, M., Doussin, J.-F., Durand-Jolibois, R., Fronval, I., Grand, N., Leonardis, T., Lopez, M., Michoud, V., Miet, K., Perrier, S., Prévôt, A. S. H., Schneider, J., Siour, G., Zapf, P. and Locoge, N.: Volatile and intermediate volatility organic compounds in suburban Paris: variability, origin and importance for SOA formation, Atmospheric Chem. Phys., 14(19), 10439–10464, doi: https://doi.org/10.5194/acp-14-10439-2014 , 2014.

Alexiou, D., Kokkalis, P., Papayannis, A., Rocadenbosch, F., Argyrouli, A., Tsaknakis, G., and Tzanis, C. G.: Planetary boundary layer height variability over Athens, Greece, based on the synergy of Raman and Radiosonde data: Application of the Kalman filter and other techniques, EPJWeb of Conferences, 176, 06007, https://doi.org/10.1051/epjconf/201817606007, 2018.

Alfoldy, B., Mahfouz, M. M. K., Yigiterhan, O., Safi, M. A., Elnaiem, A. E. and Giamberini, S.: BTEX, nitrogen oxides, ammonia and ozone concentrations at traffic influenced and background urban sites in an arid environment, Atmospheric Pollut. Res., doi:10.1016/j.apr.2018.08.009, 2018.

Altshuller, A. P.: Production of aldehydes as primary emissions and from secondary atmospheric reactions of alkenes and alkanes during the night and early morning hours, Atmospheric Environ. Part Gen. Top., 27(1), 21–32, doi:10.1016/0960-1686(93)90067-9, 1993.

Alvares, C. A., Stape, J. L., Sentelhas, P. C., de Moraes Gonçalves, J. L. and Sparovek, G.: Köppen's climate classification map for Brazil, Meteorol. Z., 22(6), 711–728, doi:10.1127/0941-2948/2013/0507, 2013.

Alvarez, R., Weilenmann, M. and Favez, J.-Y.: Evidence of increased mass fraction of NO2 within real-world NOx emissions of modern light vehicles - derived from a reliable online measuring method, Atmos. Environ., 42(19), 4699–4707, doi:10.1016/j.atmosenv.2008.01.046, 2008.

Alyuz, U. and Alp, K.: Emission inventory of primary air pollutants in 2010 from industrial processes in Turkey, Sci. Total Environ., 488–489, 369–381, doi:10.1016/j.scitotenv.2014.01.123, 2014.

Andersson-Sköld, Y. and Holmberg, L.: Photochemical ozone creation potentials (POCP) and replacement of solvents in Europe, Atmos. Environ., 34(19), 3159–3169, doi:10.1016/S1352-2310(99)00391-X, 2000.

Arriaga-Colina, J. L., West, J. J., Sosa, G., Escalona, S. S., Ordúñez, R. M. and Cervantes, A. D. M.: Measurements of VOCs in Mexico City (1992–2001) and evaluation of VOCs and CO in the emissions inventory, Atmos. Environ., 38(16), 2523–2533, doi:10.1016/j.atmosenv.2004.01.033, 2004.

Arsene, C., Bougiatioti, A., Kanakidou, M., Bonsang, B., and Mihalopoulos, N.: Tropospheric OH and Cl levels deduced from non-methane hydrocarbon measurements in a marine site, Atmos. Chem. Phys., 7, 4661–4673, https://doi.org/10.5194/acp-7-4661-2007 , 2007.

Ashbaugh, L. L., Malm, W. C. and Sadeh, W. Z.: A residence time probability analysis of sulfur concentrations at grand Canyon National Park, Atmospheric Environ. 1967, 19(8), 1263–1270, doi:10.1016/0004-6981(85)90256-2, 1985.

Athanasopoulou, E., Speyer, O., Brunner, D., Vogel, H., Vogel, B., Mihalopoulos, N. and Gerasopoulos, E.: Changes in domestic heating fuel use in Greece: effects on atmospheric chemistry and radiation, Atmospheric Chem. Phys., 17(17), 10597–10618, doi: https://doi.org/10.5194/acp-17-10597-2017 , 2017.

Athanasopoulou, E., Speyer, O., Brunner, D., Vogel, H., Vogel, B., Mihalopoulos, N., and Gerasopoulos, E.: Changes in domestic heating fuel use in Greece: effects on atmospheric chemistry and radiation, Atmos. Chem. Phys., 17, 10597–10618, https://doi.org/10.5194/acp-17-10597-2017 , 2017.

Atkinson, R. and Arey, J.: Atmospheric Degradation of Volatile Organic Compounds, Chem. Rev., 103(12), 4605–4638, doi:10.1021/cr0206420, 2003.

Atkinson, R. and Aschmann, S. M.: Rate constants for the gas-phase reactions of the OH radical with a series of aromatic hydrocarbons at 296 ± 2 K, Int. J. Chem. Kinet., 21(5), 355–365, doi:10.1002/kin.550210506, 1989.

Atkinson, R., Aschmann, S. M., Winer, A. M. and Pitts, J. N.: Rate constants for the reaction of OH radicals with a series of alkanes and alkenes at 299 ± 2 K, Int. J. Chem. Kinet., 14(5), 507–516, doi:10.1002/kin.550140508, 1982.

Atkinson, R.: Atmospheric chemistry of VOCs and NOx , Atmos. Environ., 34, 2063–2101, https://doi.org/10.1016/S1352-2310(99)00460-4, 2000.

Aumont, B., Valorso, R., Mouchel-Vallon, C., Camredon, M., Lee-Taylor, J. and Madronich, S.: Modeling SOA formation from the oxidation of intermediate volatility n-alkanes, Atmospheric Chem. Phys., 12(16), 7577–7589, 2012.

Badol, C., Locoge, N. and Galloo, J.-C.: Using a source-receptor approach to characterise VOC behaviour in a French urban area influenced by industrial emissions: Part II: Source contribution assessment using the Chemical Mass Balance (CMB) model, Sci. Total Environ., 389(2), 429–440, doi:10.1016/j.scitotenv.2007.09.002, 2008.

Bakeas, E. B. and Siskos, P. A.: Volatile hydrocarbons in the atmosphere of Athens, Greece, Environ. Sci. Pollut. Res., 9(4), 234–240, doi:10.1007/BF02987497, 2002.

Baker, A. K., Beyersdorf, A. J., Doezema, L. A., Katzenstein, A., Meinardi, S., Simpson, I. J., Blake, D. R. and Sherwood Rowland, F.: Measurements of nonmethane hydrocarbons in 28 United States cities, Atmos. Environ., 42(1), 170–182, doi:10.1016/j.atmosenv.2007.09.007, 2008.

Baklanov, A., Molina, L. T. and Gauss, M.: Megacities, air quality and climate, Atmos. Environ., 126(Supplement C), 235–249, doi:10.1016/j.atmosenv.2015.11.059, 2016.

Bansal, O., Singh, A., & Singh, D. (2019). Characteristics of Black Carbon aerosols over Patiala Northwestern part of the IGP: Source apportionment using cluster and CWT analysis. Atmos. Pollut. Res., 10, 244-256.

Bari, Md. A. and Kindzierski, W. B.: Ambient volatile organic compounds (VOCs) in Calgary, Alberta: Sources and screening health risk assessment, Sci. Total Environ., 631–632, 627–640, doi:10.1016/j.scitotenv.2018.03.023, 2018.

Barletta, B., Meinardi, S., Sherwood Rowland, F., Chan, C.-Y., Wang, X., Zou, S., Yin Chan, L., and Blake, D. R.: Volatile organic compounds in 43 Chinese cities, Atmos. Environ., 39, 5979–5990, https://doi.org/10.1016/j.atmosenv.2005.06.029, 2005.

Barrefors, G. and Petersson, G.: Volatile hydrocarbons from domestic wood burning, Chemosphere, 30, 1551–1556, https://doi.org/10.1016/0045-6535(95)00048-D , 1995.

Baudic, A., Gros, V., Sauvage, S., Locoge, N., Sanchez, O., Sarda- Estève, R., Kalogridis, C., Petit, J.-E., Bonnaire, N., Baisnée, D., Favez, O., Albinet, A., Sciare, J., and Bonsang, B.: Seasonal variability and source apportionment of volatile organic compounds (VOCs) in the Paris megacity (France), Atmos. Chem. Phys., 16, 11961–11989, https://doi.org/10.5194/acp-16-11961-2016 , 2016.

Belis, C. A., Larsen, B. R., Amato, F., El Haddad, I., Favez, O., Harrison, R. M., Hopke, P. K., Nava, S., Paatero, P. and Prévôt, A.: Air Pollution Source Apportionment, 2014.

Bocci, V., Borrelli, E., Travagli, V. and Zanardi, I.: The ozone paradox: Ozone is a strong oxidant as well as a medical drug, Med. Res. Rev., 29(4), 646–682, doi:10.1002/med.20150, 2009.

Bonn, B., von Schneidemesser, E., Butler, T., Churkina, G., Ehlers, C., Grote, R., Klemp, D., Nothard, R., Schäfer, K., von Stülpnagel, A., Kerschbaumer, A., Yousefpour, R., Fountoukis, C. and Lawrence, M. G.: Impact of vegetative emissions on urban ozone and biogenic secondary organic aerosol: Box model study for Berlin, Germany, J. Clean. Prod., 176, 827–841, doi:10.1016/j.jclepro.2017.12.164, 2018.

Bonsang, B. and Boissard, C.: Chapter 6 - Global Distribution of Reactive Hydrocarbons in the Atmosphere, in Reactive Hydrocarbons in the Atmosphere, edited by C. N. Hewitt, pp. 209–265, Academic Press, San Diego., 1999.

Borbon, A., Boynard, A., Salameh, T., Baudic, A., Gros, V., Gauduin, J., Perrussel, O. and Pallares, C.: Is Traffic Still an Important Emitter of Monoaromatic Organic Compounds in European Urban Areas?, Environ. Sci. Technol., doi:10.1021/acs.est.7b01408, 2017.

Borbon, A., Coddeville, P., Locoge, N. and Galloo, J.-C.: Characterising sources and sinks of rural VOC in eastern France, Chemosphere, 57(8), 931–942, doi:10.1016/j.chemosphere.2004.07.034, 2004.

Borbon, A., Fontaine, H., Locoge, N., Veillerot, M. and Galloo, J.: Developing receptor-oriented methods for non-methane hydrocarbon characterisation in urban air. Part II: source apportionment, Atmos. Environ., 37(29), 4065–4076, 2003.

Borbon, A., Fontaine, H., Locoge, N., Veillerot, M., and Galloo, J. C.: Developing receptor-oriented methods for nonmethane hydrocarbon characterisation in urban air – Part I: source identification, Atmos. Environ., 37, 4051–4064, https://doi.org/10.1016/S1352-2310(03)00525-9, 2003.

Borbon, A., Fontaine, H., Veillerot, M., Locoge, N., Galloo, J. C., and Guillermo, R.: An investigation into the traffic-related fraction of isoprene at an urban location, Atmos. Environ., 35, 3749–3760, https://doi.org/10.1016/S1352-2310(01)00170-4, 2001.

Borbon, A., Fontaine, H., Veillerot, M., Locoge, N., Galloo, J. C. and Guillermo, R.: An investigation into the traffic-related fraction of isoprene at an urban location, Atmos. Environ., 35(22), 3749–3760, doi:10.1016/S1352-2310(01)00170-4, 2001.

Borbon, A., Gilman, J. B., Kuster, W. C., Grand, N., Chevaillier, S., Colomb, A., Dolgorouky, C., Gros, V., Lopez, M., Sarda-Esteve, R., Holloway, J., Stutz, J., Petetin, H., McKeen, S., Beekmann, M., Warneke, C., Parrish, D. D. and Gouw, J. A. de: Emission ratios of anthropogenic volatile organic compounds in northern mid-latitude megacities: Observations versus emission inventories in Los Angeles and Paris, J. Geophys. Res. Atmospheres, 2041–2057, doi:10.1002/jgrd.50059@10.1002/(ISSN)2169-8996.CALNEX1, 2018.

Bossioli, E., Tombrou, M. and Pilinis, C.: Adapting the Speciation of the VOCs Emission Inventory in the Greater Athens Area, Water Air Soil Pollut. Focus, 2(5–6), 141–153, doi:10.1023/A:1021302427057, 2002.

Boucher, O., Randall, D., Artaxo, P., Bretherton, C., Feingold, G., Forster, P., Kerminen, V.-M., Kondo, Y., Liao, H. and Lohmann, U.: Clouds and aerosols, in Climate change 2013: the physical science basis. Contribution of Working Group I to the Fifth Assessment Report of the Intergovernmental Panel on Climate Change, pp. 571–657, Cambridge University Press., 2013.

Bourtsoukidis, E., Ernle, L., Crowley, J. N., Lelieveld, J., Paris, J.-D., Pozzer, A., Walter, D. and Williams, J.: Non-methane hydrocarbon (C2–C8) sources and sinks around the Arabian Peninsula, Atmospheric Chem. Phys., 19(10), 7209–7232, doi: https://doi.org/10.5194/acp-19-7209-2019 , 2019.

Bouvier-Brown, N., Goldstein, A., Gilman, J., Kuster, W. and De Gouw, J.: In-situ ambient quantification of monoterpenes, sesquiterpenes, and related oxygenated compounds during BEARPEX 2007: implications for gas-and particle-phase chemistry, Atmospheric Chem. Phys., 9(15), 5505–5518, 2009.

Brinkhoff, T.: The Principal Agglomerations of the World, http://www.citypopulation.de/world/Agglomerations.html , 2015.

Brito, J., Wurm, F., Yáñez-Serrano, A. M., de Assunção, J. V., Godoy, J. M. and Artaxo, P.: Vehicular Emission Ratios of VOCs in a Megacity Impacted by Extensive Ethanol Use: Results of Ambient Measurements in São Paulo, Brazil, Environ. Sci. Technol., 49(19), 11381–11387, doi:10.1021/acs.est.5b03281, 2015.

Brown, S. G., Frankel, A. and Hafner, H. R.: Source apportionment of VOCs in the Los Angeles area using positive matrix factorization, Atmos. Environ., 41(2), 227–237, doi:10.1016/j.atmosenv.2006.08.021, 2007.

Brown, S. S. and Stutz, J.: Nighttime radical observations and chemistry, Chem. Soc. Rev., 41(19), 6405–6447, doi:10.1039/C2CS35181A, 2012.

Calfapietra, C., Fares, S., Manes, F., Morani, A., Sgrigna, G. and Loreto, F.: Role of Biogenic Volatile Organic Compounds (BVOC) emitted by urban trees on ozone concentration in cities: A review, Environ. Pollut., 183, 71–80, doi:10.1016/j.envpol.2013.03.012, 2013.

Campos, A. F., da Silva, N. F., Pereira, M. G. and Vasconcelos Freitas, M. A.: A review of Brazilian natural gas industry: Challenges and strategies, Renew. Sustain. Energy Rev., 75, 1207–1216, doi:10.1016/j.rser.2016.11.104, 2017.

Camredon, M., Aumont, B., Lee-Taylor, J. and Madronich, S.: The SOA/VOC/NOx system: an explicit model of secondary organic aerosol formation, Atmos Chem Phys, 7(21), 5599–5610, doi:10.5194/acp-7-5599-2007, 2007.

Carlton, A., Wiedinmyer, C. and Kroll, J.: A review of Secondary Organic Aerosol (SOA) formation from isoprene, Atmospheric Chem. Phys., 9(14), 4987–5005, 2009.

Carter, W. P. L., Pierce, J. A., Luo, D. and Malkina, I. L.: Environmental chamber study of maximum incremental reactivities of volatile organic compounds, Atmos. Environ., 29(18), 2499–2511, doi:10.1016/1352-2310(95)00149-S, 1995.

Carter, W. P.: Calculation of reactivity scales using an updated carbon bond IV mechanism, Systems Applications International., 1994.

Carter, W. P.: Updated maximum incremental reactivity scale and hydrocarbon bin reactivities for regulatory applications, Calif. Air Resour. Board Contract, 07–339, 2009.

Cetin, E., Odabasi, M. and Seyfioglu, R.: Ambient volatile organic compound (VOC) concentrations around a petrochemical complex and a petroleum refinery, Sci. Total Environ., 312(1), 103–112, doi:10.1016/S0048-9697(03)00197-9, 2003.

Chameides, W. L., Fehsenfeld, F., Rodgers, M. O., Cardelino, C., Martinez, J., Parrish, D., Lonneman, W., Lawson, D. R., Rasmussen, R. A., Zimmerman, P., Greenberg, J., Mlddleton, P. and Wang, T.: Ozone precursor relationships in the ambient atmosphere, J. Geophys. Res. Atmospheres, 97(D5), 6037–6055, doi:10.1029/91JD03014, 1992.

CHARMEX project: http://charmex.lsce.ipsl.fr/index.php/what-is-charmex-mainmenu-35.html

Cheng, X., Li, H., Zhang, Y., Li, Y., Zhang, W., Wang, X., Bi, F., Zhang, H., Gao, J., Chai, F., Lun, X., Chen, Y., Gao, J. and Lv, J.: Atmospheric isoprene and monoterpenes in a typical urban area of Beijing: Pollution characterization, chemical reactivity and source identification, J. Environ. Sci., 71, 150–167, doi:10.1016/j.jes.2017.12.017, 2018.

Chuwah, C., van Noije, T., van Vuuren, D. P., Stehfest, E. and Hazeleger, W.: Global impacts of surface ozone changes on crop yields and land use, Atmos. Environ., 106, 11–23, doi:10.1016/j.atmosenv.2015.01.062, 2015.

Civan, M. Y., Elbir, T., Seyfioglu, R., Kuntasal, Ö. O., Bayram, A., Doğan, G., Yurdakul, S., Andiç, Ö., Müezzinoğlu, A., Sofuoglu, S. C., Pekey, H., Pekey, B., Bozlaker, A., Odabasi, M. and Tuncel, G.: Spatial and temporal variations in atmospheric VOCs, NO2, SO2, and O3 concentrations at a heavily industrialized region in Western Turkey, and assessment of the carcinogenic risk levels of benzene, Atmos. Environ., 103(Supplement C), 102–113, doi:10.1016/j.atmosenv.2014.12.031, 2015.

Collaud Coen, M., Praz, C., Haefele, A., Ruffieux, D., Kaufmann, P. and Calpini, B.: Determination and climatology of the planetary boundary layer height above the Swiss plateau by in situ and remote sensing measurements as well as by the COSMO-2 model, Atmos Chem Phys, 14(23), 13205–13221, doi:10.5194/acp-14-13205-2014, 2014.

Cooper, O. R., Parrish, D. D., Ziemke, J., Balashov, N. V., Cupeiro, M., Galbally, I. E., Gilge, S., Horowitz, L., Jensen, N. R., Lamarque, J.-F., Naik, V., Oltmans, S. J., Schwab, J., Shindell, D. T., Thompson, A. M., Thouret, V., Wang, Y. and Zbinden, R. M.: Global distribution and trends of tropospheric ozone: An observation-based review, Elem Sci Anth, 2(0), doi:10.12952/journal.elementa.000029, 2014.

Cramer, W., Guiot, J., Fader, M., Garrabou, J., Gattuso, J.-P., Iglesias, A., Lange, M. A., Lionello, P., Llasat, M. C., Paz, S., Penuelas, J., Snoussi, M., Toreti, A., Tsimplis, M. N. and Xoplaki, E.: Climate change and interconnected risks to sustainable development in the Mediterranean, Nat. Clim. Change, 8(11), 972–980, doi:10.1038/s41558-018-0299-2, 2018.

Crutzen, P. J.: Introductory lecture. Overview of tropospheric chemistry: developments during the past quarter century and a look ahead, Faraday Discuss., 100(0), 1–21, doi:10.1039/FD9950000001, 1995.

Crutzen, P. J.: Ozone in the troposphere, Composition, chemistry, and climate of the atmosphere, in: Composition, Chemistry, and Climate of the Atmosphere, edited by: Singh, H. B., Van Nostrand Reinhold Publ., New York, 349–393, 1995.

Cvitas, T., Gusten, H., Heinrich, G., Klasinc, L., Lalas, D., and Petrakis,M.: Characteristics of summer air pollution during the summer in Athens, Greece, Staub Reinhalt Luft, 45, 297–301,1985.

Dai, T., Wang, W., Ren, L., Chen, J. and Liu, H.: Emissions of non-methane hydrocarbons from cars in China, Sci. China Chem., 53(1), 263–272, doi:10.1007/s11426-010-0002-6, 2010.

Dalsøren, S. B., Myhre, G., Hodnebrog, Ø., Myhre, C. L., Stohl, A., Pisso, I., Schwietzke, S., Höglund-Isaksson, L., Helmig, D., Reimann, S., Sauvage, S., Schmidbauer, N., Read, K. A., Carpenter, L. J., Lewis, A. C., Punjabi, S. and Wallasch, M.: Discrepancy between simulated and observed ethane and propane levels explained by underestimated fossil emissions, Nat. Geosci., 11(3), 178–184, doi:10.1038/s41561-018-0073-0, 2018.

Dayan, U. and Levy, I.: Relationship between synoptic-scale atmospheric circulation and ozone concentrations over Israel, J. Geophys. Res. Atmospheres, 107(D24), 4813, doi:10.1029/2002JD002147, 2002.

Dayan, U. and Levy, I.: The Influence of Meteorological Conditions and Atmospheric Circulation Types on PM10 and Visibility in Tel Aviv, J. Appl. Meteorol., 44(5), 606–619, doi:10.1175/JAM2232.1, 2005.

Debevec, C., Sauvage, S., Gros, V., Sciare, J., Pikridas, M., Stavroulas, I., Salameh, T., Leonardis, T., Gaudion, V. and Depelchin, L.: Origin and variability in volatile organic compounds observed at an Eastern Mediterranean background site (Cyprus), Atmospheric Chem. Phys., 17(18), 11355, 2017.

Debevec, C., Sauvage, S., Gros, V., Sellegri, K., Sciare, J., Pikridas, M., Stavroulas, I., Leonardis, T., Gaudion, V. and Depelchin, L.: Driving parameters of biogenic volatile organic compounds and consequences on new particle formation observed at an eastern Mediterranean background site, Atmospheric Chem. Phys., 18(19), 14297–14325, 2018.

Demir, S., Saral, A., Isik, D., Akyildiz, A., Kuzu, S. L., Mert, S., Demir, G. and Goncaloglu, B. I.: Characterization of ambient volatile organic compounds and their diurnal variations in istanbul, Turkey, Fresenius Environ. Bull., 20(11), 2951–2958, 2011.

Derstroff, B., Hüser, I., Bourtsoukidis, E., Crowley, J. N., Fischer, H., Gromov, S., Harder, H., Janssen, R. H., Kesselmeier, J. and Lelieveld, J.: Volatile organic compounds (VOCs) in photochemically aged air from the Eastern and Western Mediterranean, Atmospheric Chem. Phys., 17(15), 9547–9566, 2017.

Derwent, R. G., Jenkin, M. E., Saunders, S. M. and Pilling, M. J.: Photochemical ozone creation potentials for organic compounds in northwest Europe calculated with a master chemical mechanism, Atmos. Environ., 32(14), 2429–2441, doi:10.1016/S1352-2310(98)00053-3, 1998.

Derwent, R. G., Jenkin, M. E., Utembe, S. R., Shallcross, D. E., Murrells, T. P. and Passant, N. R.: Secondary organic aerosol formation from a large number of reactive man-made organic compounds, Sci. Total Environ., 408(16), 3374–3381, doi:10.1016/j.scitotenv.2010.04.013, 2010.

Detournay, A., Sauvage, S., Locoge, N., Gaudion, V., Leonardis, T., Fronval, I., Kaluzny, P. and Galloo, J.-C.: Development of a sampling method for the simultaneous monitoring of straight-chain alkanes, straight-chain saturated carbonyl compounds and monoterpenes in remote areas, J. Environ. Monit., 13(4), 983–990, doi:10.1039/C0EM00354A, 2011.

Dettmer, K. and Engewald, W.: Ambient air analysis of volatile organic compounds using adsorptive enrichment, Chromatographia, 57(1), S339–S347, doi:10.1007/BF02492126, 2003.

Diapouli, E., Kalogridis, A.-C., Markantonaki, C., Vratolis, S., Fetfatzis, P., Colombi, C. and Eleftheriadis, K.: Annual Variability of Black Carbon Concentrations Originating from Biomass and Fossil Fuel Combustion for the Suburban Aerosol in Athens, Greece, Atmosphere, 8(12), 234, doi:10.3390/atmos8120234, 2017a.

Diapouli, E., Manousakas, M., Vratolis, S., Vasilatou, V., Maggos, T., Saraga, D., Grigoratos, T., Argyropoulos, G., Voutsa, D., Samara, C. and Eleftheriadis, K.: Evolution of air pollution source contributions over one decade, derived by PM10 and PM2.5 source apportionment in two metropolitan urban areas in Greece, Atmos. Environ., 164, 416–430, doi:10.1016/j.atmosenv.2017.06.016, 2017b.

Dimitriou, K. and Kassomenos, P.: A meteorological analysis of PM10 episodes at a high altitude city and a low altitude city in central Greece – The impact of wood burning heating devices, Atmospheric Res., 214, 329–337, doi:10.1016/j.atmosres.2018.08.014, 2018.

Dimitropoulou, E., Assimakopoulos, V. D., Fameli, K. M., Flocas, H. A., Kosmopoulos, P., Kazadzis, S., Lagouvardos, K. and Bossioli, E.: Estimating the Biogenic Non-Methane Hydrocarbon Emissions over Greece, Atmosphere, 9(1), 14, doi:10.3390/atmos9010014, 2018.

Directive 1999/13/EC of 11 March 1999 on the limitation of emissions of volatile organic compounds due to the use of organic solvents in certain activities and installations, Official Journal L 085 , 29/03/1999 P. 0001 – 0022, https://eur-lex.europa.eu/legal-content/EN/TXT/?uri=celex%3A31999L0013

Directive 2000/69/EC of 16 November 2000 relating to limit values for benzene and carbon monoxide in ambient air, Official Journal L 313, 13/12/2000 P. 0012 - 0021

Directive 2008/50/EC of the European Parliament and of the Council of 21 May 2008 on ambient air quality and cleaner air for Europe

Directive 98/70/EC of the European Parliament and of the Council of 13 October 1998 relating to the quality of petrol and diesel fuels and amending Directive 93/12/EEC https://www.eea.europa.eu/policy-documents/directive-98-70-ec-quality

Dominutti, P. A., Nogueira, T., Borbon, A., Andrade, M. de F. and Fornaro, A.: One-year of NMHCs hourly observations in São Paulo megacity: meteorological and traffic emissions effects in a large ethanol burning context, Atmos. Environ., 142, 371–382, doi:10.1016/j.atmosenv.2016.08.008, 2016.

Dominutti, P., Keita, S., Bahino, J., Colomb, A., Liousse, C., Yoboué, V., Galy-Lacaux, C., Bouvier, L., Sauvage, S. and Borbon, A.: Anthropogenic VOC in Abidjan, southern West Africa: from source quantification to atmospheric impacts, Atmospheric Chem. Phys. Discuss., 1–39, doi:https://doi.org/10.5194/acp-2018-1263, 2018.

Donahue, N. M., Robinson, A. L., Stanier, C. O. and Pandis, S. N.: Coupled Partitioning, Dilution, and Chemical Aging of Semivolatile Organics, Environ. Sci. Technol., 40(8), 2635–2643, doi:10.1021/es052297c, 2006.

Dong, X., Pi, G., Ma, Z. and Dong, C.: The reform of the natural gas industry in the PR of China, Renew. Sustain. Energy Rev., 73, 582–593, doi:10.1016/j.rser.2017.01.157, 2017.

Draxler, R. R. and Taylor, A. D.: Horizontal Dispersion Parameters for Long-Range Transport Modeling, J. Appl. Meteorol., 21(3), 367–372, doi:10.1175/1520-0450(1982)021<0367:HDPFLR>2.0.CO;2, 1982.

Draxler, R.R., & Rolph, G.D. : HYSPLIT (HYbrid Single-particle Lagrangian Integrated Trajectory) Model Access via NOAA ARL READY. NOAA Air Resources Laboratory, Silver Spring, MD Website. http://ready.arl.noaa.gov/HYSPLIT.php , 2016

Dumanoglu, Y., Kara, M., Altiok, H., Odabasi, M., Elbir, T. and Bayram, A.: Spatial and seasonal variation and source apportionment of volatile organic compounds (VOCs) in a heavily industrialized region, Atmos. Environ., 98, 168–178, doi:10.1016/j.atmosenv.2014.08.048, 2014.

Dumka, U.C., Kaskaoutis, D.G., Devara, P.C.S., Kumar, R., Kumar, S., Tiwari, S., Gerasopoulos, E., & Mihalopoulos, N. (2019). Year-long variability of the fossil fuel and wood burning black carbon components at a rural site in southern Delhi outskirts. Atmos. Res., 216, 11–25.

Dumka, U.C., Kaskaoutis, D.G., Tiwari, S., Safai, P.D., Attri, S.D., Soni, V.K., Singh, N., & Mihalopoulos, N. (2018). Assessment of biomass burning and fossil fuel contribution to black carbon concentrations in Delhi during winter. Atmos. Environ., 194, 93–109.

Durana, N., Navazo, M., Gómez, M. C., Alonso, L., García, J. A.,Ilardia, J. L., Gangoiti, G., and Iza, J.: Long term hourly measurement of 62 non-methane hydrocarbons in an urban area: Main results and contribution of non-traffic sources, Atmos. Environ., 40, 2860–2872, https://doi.org/10.1016/j.atmosenv.2006.01.005, 2006.

Elbir, T., Cetin, B., Cetin, E., Bayram, A. and Odabasi, M.: Characterization of Volatile Organic Compounds (VOCs) and Their Sources in the Air of Izmir, Turkey, Environ. Monit. Assess., 133(1–3), 149–160, doi:10.1007/s10661-006-9568-z, 2007.

Eleftheriadis, K., Balis, D., Ziomas, I. C., ColBeck, I. and Manalis, N.: Atmospheric aerosol and gaseous species in Athens, Greece, Atmos. Environ., 32(12), 2183–2191, 1998.

Elshorbany, Y. F., Kleffmann, J., Kurtenbach, R., Lissi, E., Rubio, M., Villena, G., Gramsch, E., Rickard, A. R., Pilling, M. J. and Wiesen, P.: Seasonal dependence of the oxidation capacity of the city of Santiago de Chile, Atmos. Environ., 44(40), 5383–5394, doi:10.1016/j.atmosenv.2009.08.036, 2010.

Elshorbany, Y. F., Kurtenbach, R., Wiesen, P., Lissi, E., Rubio, M., Villena, G., Gramsch, E., Rickard, A. R., Pilling, M. J. and Kleffmann, J.: Oxidation capacity of the city air of Santiago, Chile, Atmos Chem Phys, 9(6), 2257–2273, doi:10.5194/acp-9-2257-2009, 2009.

EMEP/EEA 2016 : EMEP/EEA air pollutant emission inventory guidebook 2016, report N° 21/2016

Environmental European Agency (EEA): Air Quality in Europe, N° 12/2018, 2018. https://www.eea.europa.eu/publications/air-quality-in-europe-2018

Environmental European Agency, (EEA): Air Quality in Europe, N° 13/2017, 2017 https://www.eea.europa.eu//publications/air-quality-in-europe-2017

Environmental European Agency, (EEA): Air Quality in Europe, N° 5/2014, 2014 https://www.eea.europa.eu/publications/air-quality-in-europe-2014

EPA 2017, “Technical overview of Volatile Organic Compounds”: https://www.epa.gov/indoor-air-quality-iaq/technical-overview-volatile-organic-compounds#3

EPA-CMB v8.2, Environmental Protection Agency of United States of America (EPA), 2005: https://www.epa.gov/scram/chemical-mass-balance-cmb-model

Europe, U. N. E. C. for: Handbook for the 1979 Convention on Long-range Transboundary Air Pollution and Its Protocols, United Nations Publications., 2004.

European Environmental Agency (EEA): Air quality in Europe– 2016 report (No. 28), available at: https://www.eea.europa.eu/publications/air-quality-in-europe-2016 (last access: 2 October 2017), 2016.

European Environmental Agency (EEA): Emissions of main air pollutants, 2017. https://www.eea.europa.eu/data-and-maps/daviz/share-of-eea-33-emissions-3#tab-based-on-data

European Environmental Agency (EEA): Trends in atmospheric concentrations of CO2, CH4 and N2O, 2017. https://www.eea.europa.eu/data-and-maps/daviz/atmospheric-concentration-of-carbon-dioxide-3

Eurostat : https://ec.europa.eu/eurostat/statistics-explained/index.php/Passenger_cars_in_the_EU, 2018

Evtyugina, M., Alves, C., Calvo, A., Nunes, T., Tarelho, L., Duarte, M., Prozil, S. O., Evtuguin, D. V., and Pio,C.: VOC emissions from residential combustion of Southern and mid-European woods, Atmos. Environ., 83, 90–98, https://doi.org/10.1016/j.atmosenv.2013.10.050, 2014.

Fameli, K. and Assimakopoulos, V.: Development of a road transport emission inventory for Greece and the Greater Athens Area: Effects of important parameters, Sci. Total Environ., 505, 770–786, 2015.

Fameli, K.-M. and Assimakopoulos, V. D.: The new open Flexible Emission Inventory for Greece and the Greater Athens Area (FEI-GREGAA): Account of pollutant sources and their importance from 2006 to 2012, Atmos. Environ., 137, 17–37, 2016.

Fanizza, C., Incoronato, F., Baiguera, S., Schiro, R. and Brocco, D.: Volatile organic compound levels at one site in Rome urban air, Atmospheric Pollut. Res., 5(2), 303–314, doi:10.5094/APR.2014.036, 2014.

Favez, O., Cachier, H., Sciare, J., Alfaro, S. C., El-Araby, T. M., Harhash, M. A. and Abdelwahab, M. M.: Seasonality of major aerosol species and their transformations in Cairo megacity, Atmos. Environ., 42(7), 1503–1516, doi:10.1016/j.atmosenv.2007.10.081, 2008.

Fehsenfeld, F., Calvert, J., Fall, R., Goldan, P., Guenther, A. B., Hewitt, C. N., Lamb, B., Liu, S., Trainer, M., Westberg, H. and Zimmerman, P.: Emissions of volatile organic compounds from vegetation and the implications for atmospheric chemistry, Glob. Biogeochem. Cycles, 6(4), 389–430, doi:10.1029/92GB02125, 1992.

Finardi, S., Agrillo, G., Baraldi, R., Calori, G., Carlucci, P., Ciccioli, P., D'Allura, A., Gasbarra, D., Gioli, B., Magliulo, V., Radice, P., Toscano, P. and Zaldei, A.: Atmospheric Dynamics and Ozone Cycle during Sea Breeze in a Mediterranean Complex Urbanized Coastal Site, J. Appl. Meteorol. Climatol., 57(5), 1083–1099, doi:10.1175/JAMC-D-17-0117.1, 2018.

Finlayson-Pitts, B. J. and Jr, J. N. P.: Atmospheric Chemistry of Tropospheric Ozone Formation: Scientific and Regulatory Implications, Air Waste, 43(8), 1091–1100, doi:10.1080/1073161X.1993.10467187, 1993.

Fourtziou, L., Liakakou, E., Stavroulas, I., Theodosi, C., Zarmpas, P., Psiloglou, B., Sciare, J., Maggos, T., Bairachtari, K., Bougiatioti, A., Gerasopoulos, E., Sarda-Estève, R., Bonnaire, N. and Mihalopoulos, N.: Multi-tracer approach to characterize domestic wood burning in Athens (Greece) during wintertime, Atmos. Environ., 148(Supplement C), 89–101, doi:10.1016/j.atmosenv.2016.10.011, 2017.

François, S., Grondin, E., Fayet, S. and Ponche, J.-L.: The establishment of the atmospheric emission inventories of the ESCOMPTE program, Atmospheric Res., 74(1), 5–35, doi:10.1016/j.atmosres.2004.10.002, 2005.

Frey, H. C.: Quantification of uncertainty in emission factors and inventories., 2007: https://www.researchgate.net/publication/228618100_Quantification_of_Uncertainty_in_Emission_Factors_and_Inventories

Fuentes, J. D., Gu, L., Lerdau, M., Atkinson, R., Baldocchi, D., Bottenheim, J., Ciccioli, P., Lamb, B., Geron, C. and Guenther, A.: Biogenic hydrocarbons in the atmospheric boundary layer: a review, Bull. Am. Meteorol. Soc., 81(7), 1537–1575, 2000.

Gaeggeler, K., Prevot, A. S. H., Dommen, J., Legreid, G., Reimann, S., and Baltensperger, U.: Residential wood burning in an Alpine valley as a source for oxygenated volatile organic compounds, hydrocarbons and organic acids, Atmos. Environ., 42, 8278–8287, https://doi.org/10.1016/j.atmosenv.2008.07.038 , 2008.

Gaimoz, C., Sauvage, S., Gros, V., Herrmann, F., Williams, J., Locoge, N., Perrussel, O., Bonsang, B., d'Argouges, O., Sarda-Estève, R. and Sciare, J.: Volatile organic compounds sources in Paris in spring 2007. Part II: source apportionment using positive matrix factorisation, Environ. Chem., 8(1), 91–103, doi:10.1071/EN10067, 2011.

Garg, A. and Gupta, N. C.: A comprehensive study on spatio-temporal distribution, health risk assessment and ozone formation potential of BTEX emissions in ambient air of Delhi, India, Sci. Total Environ., 659, 1090–1099, doi:10.1016/j.scitotenv.2018.12.426, 2019.

Gelencsér, A., Siszler, K. and Hlavay, J.: Toluene−Benzene Concentration Ratio as a Tool for Characterizing the Distance from Vehicular Emission Sources, Environ. Sci. Technol., 31(10), 2869–2872, doi:10.1021/es970004c, 1997.

Gerasopoulos, E., Gratsea, M., Liakakou, E., Lianou, M., Psiloglou, B., Kappos, N., Kambezidis, H. and Mihalopoulos, N.: An Overview of Biomass Burning Impacts on Athens Air Quality and Analysis of Its Increasing Significance, in Perspectives on Atmospheric Sciences, pp. 1111–1116, Springer., 2017.

Geron, C., Rasmussen, R., R. Arnts, R. and Guenther, A.: A review and synthesis of monoterpene speciation from forests in the United States, Atmos. Environ., 34(11), 1761–1781, doi:10.1016/S1352-2310(99)00364-7, 2000.

Ghirardo, A., Xie, J., Zheng, X., Wang, Y., Grote, R., Block, K., Wildt, J., Mentel, T., Kiendler-Scharr, A., Hallquist, M., Butterbach-Bahl, K. and Schnitzler, J.-P.: Urban stress-induced biogenic VOC emissions and SOA-forming potentials in Beijing, Atmospheric Chem. Phys., 16(5), 2901–2920, doi: https://doi.org/10.5194/acp-16-2901-2016 , 2016.

Giakoumi, A., Maggos, T., Michopoulos, J., Helmis, C., and Vasilakos, C.: PM2:5 and volatile organic compounds (VOCs) in ambient air: a focus on the effect of meteorology, Environ. Monit. Assess., 152, 83, https://doi.org/10.1007/s10661-008-0298-2 , 2009.

Gilman, J. B., Lerner, B. M., Kuster, W. C. and de Gouw, J. A.: Source Signature of Volatile Organic Compounds from Oil and Natural Gas Operations in Northeastern Colorado, Environ. Sci. Technol., 47(3), 1297–1305, doi:10.1021/es304119a , 2013.

Gilman, J. B., Lerner, B. M., Kuster, W. C., Goldan, P. D., Warneke, C., Veres, P. R., Roberts, J. M., Gouw, J. A. de, Burling, I. R. and Yokelson, R. J.: Biomass burning emissions and potential air quality impacts of volatile organic compounds and other trace gases from fuels common in the US, Atmospheric Chem. Phys., 15(24), 13915–13938, doi:https://doi.org/10.5194/acp-15-13915-2015, 2015.

Giorgi, F. and Lionello, P.: Climate change projections for the Mediterranean region, Glob. Planet. Change, 63(2), 90–104, 2008.

Giorio, C., J. Campbell, S., Bruschi, M., T. Archibald, A. and Kalberer, M.: Detection and identification of Criegee intermediates from the ozonolysis of biogenic and anthropogenic VOCs: comparison between experimental measurements and theoretical calculations, Faraday Discuss., 200(0), 559–578, doi:10.1039/C7FD00025A, 2017.

Glavas, S. and Moschonas, N.: Determination of PAN, PPN, PnBN and selected pentyl nitrates in Athens, Greece, Atmos. Environ., 35(32), 5467–5475, doi:10.1016/S1352-2310(01)00283-7, 2001.

Gong, X., Wex, H., Müller, T., Wiedensohler, A., Höhler, K., Kandler, K., Ma, N., Dietel, B., Schiebel, T., Möhler, O. and Stratmann, F.: Characterization of aerosol properties at Cyprus, focusing on cloud condensation nuclei and ice-nucleating particles, Atmospheric Chem. Phys., 19(16), 10883–10900, doi:https://doi.org/10.5194/acp-19-10883-2019, 2019.

Gouw, J. A. de, Middlebrook, A. M., Warneke, C., Ahmadov, R., Atlas, E. L., Bahreini, R., Blake, D. R., Brock, C. A., Brioude, J., Fahey, D. W., Fehsenfeld, F. C., Holloway, J. S., Henaff, M. L., Lueb, R. A., McKeen, S. A., Meagher, J. F., Murphy, D. M., Paris, C., Parrish, D. D., Perring, A. E., Pollack, I. B., Ravishankara, A. R., Robinson, A. L., Ryerson, T. B., Schwarz, J. P., Spackman, J. R., Srinivasan, A. and Watts, L. A.: Organic Aerosol Formation Downwind from the Deepwater Horizon Oil Spill, Science, 331(6022), 1295–1299, doi:10.1126/science.1200320, 2011.

Graham, B., Falkovich, A. H., Rudich, Y., Maenhaut, W., Guyon, P. and Andreae, M. O.: Local and regional contributions to the atmospheric aerosol over Tel Aviv, Israel: a case study using elemental, ionic and organic tracers, Atmos. Environ., 38(11), 1593–1604, doi:10.1016/j.atmosenv.2003.12.015, 2004.

Gratsea, M., Liakakou, E., Mihalopoulos, N., Adamopoulos, A., Tsilibari, E., and Gerasopoulos, E.: The combined effectof reduced fossil fuel consumption and increasing biomass combustion on Athens' air quality, as inferred from long term CO measurements, Sci. Total Environ., 592, 115–123, https://doi.org/10.1016/j.scitotenv.2017.03.045 , 2017.

Grivas, G., Chaloulakou, A., Samara, C. and Spyrellis, N.: Spatial and Temporal Variation of PM10 Mass Concentrations within the Greater Area of Athens, Greece, Water. Air. Soil Pollut., 158(1), 357–371, doi:10.1023/B:WATE.0000044859.84066.09, 2004.

Grivas, G., Cheristanidis, S. and Chaloulakou, A.: Elemental and organic carbon in the urban environment of Athens. Seasonal and diurnal variations and estimates of secondary organic carbon, Sci. Total Environ., 414, 535–545, 2012.

Gros, V., Gaimoz, C., Herrmann, F., Custer, T., Williams, J., Bonsang, B., Sauvage, S., Locoge, N., d'Argouges, O., Sarda-Estève, R., and Sciare, J.: Volatile organic compounds sources in Paris in spring 2007, Part I: qualitative analysis, Environ. Chem., 8, 74–90, https://doi.org/10.1071/EN10068 , 2011.

Guenther, A., Hewitt, C. N., Erickson, D., Fall, R., Geron, C., Graedel, T., Harley, P., Klinger, L., Lerdau, M., Mckay, W. A., Pierce, T., Scholes, B., Steinbrecher, R., Tallamraju, R., Taylor, J., and Zimmerman, P.: A global model of natural volatile organic compound emissions, J. Geophys. Res.-Atmos., 100, 8873–8892, https://doi.org/10.1029/94JD02950 , 1995.

Guha, A., Gentner, D. R., Weber, R. J., Provencal, R. and Goldstein, A. H.: Source apportionment of methane and nitrous oxide in California's San Joaquin Valley at CalNex 2010 via positive matrix factorization, Atmospheric Chem. Phys., 15(20), 12043–12063, doi: https://doi.org/10.5194/acp-15-12043-2015 , 2015.

Guo, H., So, K. L., Simpson, I. J., Barletta, B., Meinardi, S. and Blake, D. R.: C1–C8 volatile organic compounds in the atmosphere of Hong Kong: Overview of atmospheric processing and source apportionment, Atmos. Environ., 41(7), 1456–1472, doi:10.1016/j.atmosenv.2006.10.011, 2007.

Guo, H., Wang, T. and Louie, P. K. K.: Source apportionment of ambient non-methane hydrocarbons in Hong Kong: Application of a principal component analysis/absolute principal component scores (PCA/APCS) receptor model, Environ. Pollut., 129(3), 489–498, doi:10.1016/j.envpol.2003.11.006, 2004.

Gustafson, P., Barregard, L., Strandberg, B., and Sällsten, G.: The impact of domestic wood burning on personal, indoor and outdoor levels of 1,3-butadiene, benzene, formaldehyde and acetaldehyde, J. Environ. Monit., 9, 23–32, https://doi.org/10.1039/B614142K , 2007.

Gutbrod, R., Schindler, R. N., Kraka, E. and Cremer, D.: Formation of OH radicals in the gas phase ozonolysis of alkenes: the unexpected role of carbonyl oxides, Chem. Phys. Lett., 252(3), 221–229, doi:10.1016/0009-2614(96)00126-1, 1996.

Hakola, H., Hellén, H., Tarvainen, V., Bäck, J., Patokoski, J. and Rinne, J.: Annual variations of atmospheric VOC concentrations in a boreal forest, 2009.

Harrison, D., Hunter, M. C., Lewis, A. C., Seakins, P. W., Nunes, T. V. and Pio, C. A.: Isoprene and monoterpene emission from the coniferous species Abies Borisii-regis—implications for regional air chemistry in Greece, Atmos. Environ., 35(27), 4687–4698, doi:10.1016/S1352-2310(01)00092-9, 2001.

Hassan, S. K. and Khoder, M. I.: Chemical characteristics of atmospheric PM2.5 loads during air pollution episodes in Giza, Egypt, Atmos. Environ., 150, 346–355, doi:10.1016/j.atmosenv.2016.11.026, 2017.

Hasson, A. S., Ho, A. W., Kuwata, K. T. and Paulson, S. E.: Production of stabilized Criegee intermediates and peroxides in the gas phase ozonolysis of alkenes: 2. Asymmetric and biogenic alkenes, J. Geophys. Res. Atmospheres, 106(D24), 34143–34153, doi:10.1029/2001JD000598, 2001.

Hatfield, J. L., Boote, K. J., Kimball, B. A., Ziska, L. H., Izaurralde, R. C., Ort, D., Thomson, A. M. and Wolfe, D.: Climate Impacts on Agriculture: Implications for Crop Production, Agron. J., 103(2), 351–370, doi:10.2134/agronj2010.0303, 2011.

Hatzianastassiou, N., Gkikas, A., Mihalopoulos, N., Torres, O. and Katsoulis, B.: Natural versus anthropogenic aerosols in the eastern Mediterranean basin derived from multiyear TOMS and MODIS satellite data, J. Geophys. Res. Atmospheres, 114(D24), 2009.

Held, T., Ying, Q., Kleeman, M. J., Schauer, J. J. and Fraser, M. P.: A comparison of the UCD/CIT air quality model and the CMB source–receptor model for primary airborne particulate matter, Atmos. Environ., 39(12), 2281–2297, doi:10.1016/j.atmosenv.2004.12.034, 2005.

Hellén, H., Hakola, H. and Laurila, T.: Determination of source contributions of NMHCs in Helsinki (60°N, 25°E) using chemical mass balance and the Unmix multivariate receptor models, Atmos. Environ., 37(11), 1413–1424, doi:10.1016/S1352-2310(02)01049-X, 2003.

Hellén, H., Hakola, H., Haaparanta, S., Pietarila, H. and Kauhaniemi, M.: Influence of residential wood combustion on local air quality, Sci. Total Environ., 393(2), 283–290, doi:10.1016/j.scitotenv.2008.01.019, 2008.

Hellén, H., Hakola, H., Pirjola, L., Laurila, T. and Pystynen, K.: Ambient Air Concentrations, Source Profiles, and Source Apportionment of 71 Different C2−C10 Volatile Organic Compounds in Urban and Residential Areas of Finland, Environ. Sci. Technol., 40(1), 103–108, doi:10.1021/es051659d, 2006.

Hellén, H., Tykkä, T. and Hakola, H.: Importance of monoterpenes and isoprene in urban air in northern Europe, Atmos. Environ., 59, 59–66, doi:10.1016/j.atmosenv.2012.04.049, 2012.

Hellenic Statistical Authority: https://www.statistics.gr/en/statistics/-/publication/SME18/- , 2018

Helmig, D.: Ozone removal techniques in the sampling of atmospheric volatile organic trace gases, Atmos. Environ., 31(21), 3635–3651, doi:10.1016/S1352-2310(97)00144-1, 1997.

Henry, R. C.: Multivariate receptor modeling by N-dimensional edge detection, Chemom. Intell. Lab. Syst., 65(2), 179–189, doi:10.1016/S0169-7439(02)00108-9, 2003.

Henry, R., Norris, G. A., Vedantham, R. and Turner, J. R.: Source Region Identification Using Kernel Smoothing, Environ. Sci. Technol., 43(11), 4090–4097, doi:10.1021/es8011723, 2009.

Heo, J., Wu, B., Abdeen, Z., Qasrawi, R., Sarnat, J. A., Sharf, G., Shpund, K. and Schauer, J. J.: Source apportionments of ambient fine particulate matter in Israeli, Jordanian, and Palestinian cities, Environ. Pollut., 225, 1–11, doi:10.1016/j.envpol.2017.01.081, 2017.

Hong-li, W., Sheng-ao, J., Sheng-rong, L., Qing-yao, H., Li, L., Shi-kang, T., Cheng, H., Li-ping, Q. and Chang-hong, C.: Volatile organic compounds (VOCs) source profiles of on-road vehicle emissions in China, Sci. Total Environ., 607–608, 253–261, doi:10.1016/j.scitotenv.2017.07.001, 2017.

Hopke, P. K.: An introduction to receptor modeling, Chemom. Intell. Lab. Syst., 10(1), 21–43, doi:10.1016/0169-7439(91)80032-L, 1991.

Hopke, P. K.: Review of receptor modeling methods for source apportionment, J. Air Waste Manag. Assoc., 66(3), 237–259, doi:10.1080/10962247.2016.1140693, 2016.

Hopkins, J. R., Jones, I. D., Lewis, A. C., McQuaid, J. B. and Seakins, P. W.: Non-methane hydrocarbons in the Arctic boundary layer, Atmos. Environ., 36(20), 3217–3229, doi:10.1016/S1352-2310(02)00324-2, 2002.

Huang, G., Brook, R., Crippa, M., Janssens-Maenhout, G., Schieberle, C., Dore, C., Guizzardi, D., Muntean, M., Schaaf, E. and Friedrich, R.: Speciation of anthropogenic emissions of non-methane volatile organic compounds: a global gridded data set for 1970–2012, Atmospheric Chem. Phys., 17(12), 7683–7701, doi:https://doi.org/10.5194/acp-17-7683-2017, 2017.

IARC: Chemical Agents and Related Occupations, Monographs on the Evaluation of Carcinogenic Risks to Humans, 100, 249–285, 309–333, available at: http://monographs.iarc.fr/ENG/Monographs/vol100F/mono100F.pdf (last access: 5 October 2017), 2012.

IARC: Outdoor air pollution a leading environmental cause of cancer deaths, Press Release no. 221, 2013.

Ibarra-Berastegi, G., Elias, A., Barona, A., Saenz, J., Ezcurra, A., and Diaz de Argandoña, J.: From diagnosis to prognosis for forecasting air pollution using neural networks: Air pollution monitoring in Bilbao, Environ. Model. Softw., 23, 622–637, https://doi.org/10.1016/j.envsoft.2007.09.003, 2008.

Im, U. and Kanakidou, M.: Impacts of East Mediterranean megacity emissions on air quality, Atmospheric Chem. Phys., 12(14), 6335–6355, 2012.

Im, U., Incecik, S., Guler, M., Tek, A., Topcu, S., Unal, Y. S., Yenigun, O., Kindap, T., Odman, M. T. and Tayanc, M.: Analysis of surface ozone and nitrogen oxides at urban, semi-rural and rural sites in Istanbul, Turkey, Sci. Total Environ., 443(Supplement C), 920–931, doi:10.1016/j.scitotenv.2012.11.048, 2013.

International Energy Agency (IEA) report: Energy policies of IEA countries – Greece 2017 Review, IEA Policies and Measures Database © OECD/IEA, 2017; Download: 21-09-2018 from: https://www.iea.org/publications/freepublications/publication/EnergyPoliciesofIEACountriesGreeceReview2017.pdf

J. Crutzen, P.: Introductory lecture. Overview of tropospheric chemistry: developments during the past quarter century and a look ahead, Faraday Discuss., 100(0), 1–21, doi:10.1039/FD9950000001, 1995.

Jaimes-Palomera, M., Retama, A., Elias-Castro, G., Neria-Hernández, A., Rivera-Hernández, O., and Velasco, E.: Nonmethane hydrocarbons in the atmosphere of Mexico City: Results of the 2012 ozone-season campaign, Atmos. Environ., 132, 258–275, https://doi.org/10.1016/j.atmosenv.2016.02.047, 2016.

Jobson, B., Berkowitz, C. M., Kuster, W., Goldan, P., Williams, E., Fesenfeld, F., Apel, E., Karl, T., Lonneman, W. A. and Riemer, D.: Hydrocarbon source signatures in Houston, Texas: Influence of the petrochemical industry, J. Geophys. Res. Atmospheres, 109(D24), 2004.

Johnson, D. and Marston, G.: The gas-phase ozonolysis of unsaturated volatile organic compounds in the troposphere, Chem. Soc. Rev., 37(4), 699–716, doi:10.1039/B704260B, 2008.

Jorquera, H. and Rappenglück, B.: Receptor modeling of ambient VOC at Santiago, Chile, Atmos. Environ., 38(25), 4243–4263, doi:10.1016/j.atmosenv.2004.04.030, 2004.

Kalabokas, P. and Repapis, C.: A Review of Surface and Lower Troposphere Ozone Concentration Characteristics Around the Urban Area of Athens, the Aegean Sea and at the Central and Eastern Mediterranean, in Perspectives on Atmospheric Sciences, pp. 995–1000, Springer., 2017.

Kalabokas, P., Viras, L., and Repapis, C.: Analysis of the 11-year record (1987–1997) of air pollution measurements in Athens, Greece, Part I: Primary air pollutants, Glob. Nest Int. J., 1, 157–168, 1999.

Kalabokas, P.D., Hatzianestis, J., Bartzis, J.G., Papagiannakopoulos, P.,: Atmospheric concentrations of saturated and aromatic hydrocarbons around a Greek oil refinery. Atmos. Environ. 35, 2545–2555. doi:10.1016/S1352-2310(00)00423-4, 2001.

Kallos, G., Kassomenos, P. and Pielke, R. A.: Synoptic and Mesoscale Weather Conditions During Air Pollution Episodes in Athens, Greece, in Transport and Diffusion in Turbulent Fields, pp. 163–184, Springer, Dordrecht., 1993.

Kaltsonoudis, C., Kostenidou, E., Florou, K., Psichoudaki, M., and Pandis, S. N.: Temporal variability and sources of VOCs in urban areas of the eastern Mediterranean, Atmos. Chem. Phys., 16, 14825–14842, https://doi.org/10.5194/acp-16-14825-2016 , 2016.

Kanakidou, M., Mihalopoulos, N., Kindap, T., Im, U., Vrekoussis, M., Gerasopoulos, E., Dermitzaki, E., Unal, A., Koçak, M., Markakis, K., Melas, D., Kouvarakis, G., Youssef, A. F., Richter, A., Hatzianastassiou, N., Hilboll, A., Ebojie, F., Wittrock, F., von Savigny, C., Burrows, J. P., Ladstaetter-Weissenmayer, A., and Moubasher, H.: Megacities as hot spots of air pollution in the East Mediterranean, Atmos. Environ., 45, 1223–1235, https://doi.org/10.1016/j.atmosenv.2010.11.048 , 2011.

Kansal, A.: Sources and reactivity of NMHCs and VOCs in the atmosphere: A review, J. Hazard. Mater., 166, 17–26, https://doi.org/10.1016/j.jhazmat.2008.11.048 , 2009.

Karanasiou, A. and Mihalopoulos, N.: Air Quality in Urban Environments in the Eastern Mediterranean, in Urban Air Quality in Europe, pp. 219–238, Springer., 2013.

Kassomenos, P. A., Sindosi, O. A., Lolis, C. J. and Chaloulakou, A.: On the relation between seasonal synoptic circulation types and spatial air quality characteristics in Athens, Greece, J. Air Waste Manag. Assoc., 53(3), 309–324, 2003.

Kassomenos, P., Kotroni, V., and Kallos, G.: Analysis of climatological 710 and air quality observations from Greater Athens Area, Atmos. Environ., 29, 3671–3688, https://doi.org/10.1016/1352-2310(94)00358-R , 1995.

Katsoulis, B. D.: Aspects of the occurrence of persistent surface inversions over Athens basin, Greece, Theor. Appl. Climatol., 39(2), 98–107, doi:10.1007/BF00866395, 1988a.

Katsoulis, B. D.: Some meteorological aspects of air pollution in Athens, Greece, Meteorol. Atmospheric Phys., 39(3), 203–212, doi:10.1007/BF01030298, 1988b.

Katsoulis, B. D.: The relationship between synoptic, mesoscale and microscale meteorological parameters during poor air quality events in Athens, Greece, Sci. Total Environ., 181(1), 13–24, doi:10.1016/0048-9697(95)04953-3, 1996.

Kegge, W. and Pierik, R.: Biogenic volatile organic compounds and plant competition, Trends Plant Sci., 15(3), 126–132, doi:10.1016/j.tplants.2009.11.007, 2010.

Kesselmeier, J. and Staudt, M.: Biogenic Volatile Organic Compounds (VOC): An Overview on Emission, Physiology and Ecology, J. Atmospheric Chem., 33(1), 23–88, doi:10.1023/A:1006127516791, 1999.

Khoder, M. I.: Ambient levels of volatile organic compounds in the atmosphere of Greater Cairo, Atmos. Environ., 41(3), 554–566, doi:10.1016/j.atmosenv.2006.08.051, 2007.

Kleanthous, S., Vrekoussis, M., Mihalopoulos, N., Kalabokas, P. and Lelieveld, J.: On the temporal and spatial variation of ozone in Cyprus, Sci. Total Environ., 476–477(Supplement C), 677–687, doi:10.1016/j.scitotenv.2013.12.101, 2014.

Kleeman, M. J. and Cass, G. R.: A 3D Eulerian Source-Oriented Model for an Externally Mixed Aerosol, Environ. Sci. Technol., 35(24), 4834–4848, doi:10.1021/es010886m, 2001.

Kleindienst, T. E., Corse, E. W., Blanchard, F. T. and Lonneman, W. A.: Evaluation of the Performance of DNPH-Coated Silica Gel and C18 Cartridges in the Measurement of Formaldehyde in the Presence and Absence of Ozone, Environ. Sci. Technol., 32(1), 124–130, doi:10.1021/es970205g, 1998.

Klemm, O., Ziomas, I. C., Balis, D., Suppan, P., Slemr, J., Romero, R., and Vyras, L. G.: A summer air-pollution study in Athens, Greece, Atmos. Environ., 32, 2071–2087, https://doi.org/10.1016/S1352-2310(97)00424-X , 1998.

Koçak, M., Theodosi, C., Zarmpas, P., Im, U., Bougiatioti, A., Yenigun, O. and Mihalopoulos, N.: Particulate matter (PM10) in Istanbul: Origin, source areas and potential impact on surrounding regions, Atmos. Environ., 45(38), 6891–6900, doi:10.1016/j.atmosenv.2010.10.007, 2011.

Koch, S., Winterhalter, R., Uherek, E., Kolloff, A., Neeb, P. and Moortgat, G. K.: Formation of new particles in the gas-phase ozonolysis of monoterpenes, Atmos. Environ., 34(23), 4031–4042, doi:10.1016/S1352-2310(00)00133-3, 2000.

Koppmann, R.: Volatile Organic Compounds in the Atmosphere, John Wiley & Sons., 2008.

Kourtidis, K. A., Ziomas, I. C., Rappenglueck, B., Proyou, A., and Balis, D.: Evaporative traffic hydrocarbon emissions, traffic CO and speciated HC traffic emissions from the city of Athens, Atmos. Environ., 33, 3831–3842, https://doi.org/10.1016/S1352-2310(98)00395-1 , 1999.

Kroll, J. H. and Seinfeld, J. H.: Chemistry of secondary organic aerosol: Formation and evolution of low-volatility organics in the atmosphere, Atmos. Environ., 42(16), 3593–3624, doi:10.1016/j.atmosenv.2008.01.003, 2008.

Kuntasal, Ö. O., Kılavuz, S. A., Karman, D., Wang, D. and Tuncel, G.: C5–C12 volatile organic compounds at roadside, residential, and background locations in Ankara, Turkey: Temporal and spatial variations and sources, J. Air Waste Manag. Assoc., 63(10), 1148–1162, 2013.

Lai, C.-H., Chang, C.-C., Wang, C.-H., Shao, M., Zhang, Y. and Wang, J.-L.: Emissions of liquefied petroleum gas (LPG) from motor vehicles, Atmos. Environ., 43(7), 1456–1463, doi:10.1016/j.atmosenv.2008.11.045, 2009.

Lalas, D. P., Asimakopoulos, D. N., Deligiorgi, D. G., and Helmis, C. G.: Sea-breeze circulation and photochemical pollution in Athens, Greece, Atmos. Environ., 17, 1621–1632, https://doi.org/10.1016/0004-6981(83)90171-3 ,1983 .

Lalas, D. P., Tombrou-Tsella, M., Petrakis, M., Asimakopoulos,D. N., and Helmis, C.: An experimental study of the horizontaland vertical distribution of ozone over Athens, Atmos/ Environ., 21, 2681–2693, https://doi.org/10.1016/0004-6981(87)90200-9, 1987.

Lalas, D. P., Veirs, V. R., Karras, G., and Kallos, G.: An analysis of the SO2 concentration levels in Athens, Greece, Atmos. Environ., 16, 531–544, https://doi.org/10.1016/0004-6981(82)90162-7 , 1982.

Lam, S. H. M., Saunders, S. M., Cheng, H. R. and Guo, H.: Examination of regional ozone formation: POCPs for Western Australia and comparisons to other continents, Environ. Model. Softw., 74, 194–200, doi:10.1016/j.envsoft.2014.12.025, 2015.

Lamb, B., Westberg, H., Allwine, G. and Quarles, T.: Biogenic hydrocarbon emissions from deciduous and coniferous trees in the United States, J. Geophys. Res. Atmospheres, 90(D1), 2380–2390, doi:10.1029/JD090iD01p02380, 1985.

Laothawornkitkul, J., Taylor, J. E., Paul, N. D. and Hewitt, C. N.: Biogenic volatile organic compounds in the Earth system, New Phytol., 183(1), 27–51, 2009.

Larsen, B., Bomboi-Mingarro, T., Brancaleoni, E., Calogirou, A., Cecinato, A., Coeur, C., Chatzinestis, I., Duane, M., Frattoni, M., Fugit, J.-L., Hansen, U., Jacob, V., Mimikos, N., Hoffmann, T., Owen, S., Perez-Pastor, R., Reichmann, A., Seufert, G., Staudt, M. and Steinbrecher, R.: Sampling and analysis of terpenes in air. An interlaboratory comparison, Atmos. Environ., 31, 35–49, doi:10.1016/S1352-2310(97)00072-1, 1997.

Lascaratos, A., Roether, W., Nittis, K. and Klein, B.: Recent changes in deep water formation and spreading in the eastern Mediterranean Sea: a review, Prog. Oceanogr., 44(1), 5–36, 1999.

Legreid, G., Lööv, J. B., Staehelin, J., Hueglin, C., Hill, M., Buchmann, B., Prevot, A. S. H. and Reimann, S.: Oxygenated volatile organic compounds (OVOCs) at an urban background site in Zürich (Europe): Seasonal variation and source allocation, Atmos. Environ., 41(38), 8409–8423, doi:10.1016/j.atmosenv.2007.07.026, 2007.

Lelieveld, J., Berresheim, H., Borrmann, S., Crutzen, P. J., Dentener, F. J., Fischer, H., Feichter, J., Flatau, P. J., Heland, J., Holzinger, R., Korrmann, R., Lawrence, M. G., Levin, Z., Markowicz, K. M., Mihalopoulos, N., Minikin, A., Ramanathan, V., Reus, M. de, Roelofs, G. J., Scheeren, H. A., Sciare, J., Schlager, H., Schultz, M., Siegmund, P., Steil, B., Stephanou, E. G., Stier, P., Traub, M., Warneke, C., Williams, J. and Ziereis, H.: Global Air Pollution Crossroads over the Mediterranean, Science, 298(5594), 794–799, doi:10.1126/science.1075457, 2002.

Lelieveld, J., Evans, J. S., Fnais, M., Giannadaki, D. and Pozzer, A.: The contribution of outdoor air pollution sources to premature mortality on a global scale, Nature, 525(7569), 367–371, doi:10.1038/nature15371, 2015.

Lelieveld, J., Gromov, S., Pozzer, A. and Taraborrelli, D.: Global tropospheric hydroxyl distribution, budget and reactivity, Atmospheric Chem. Phys., 16(19), 12477–12493, doi: https://doi.org/10.5194/acp-16-12477-2016 , 2016.

Lelieveld, J., Hadjinicolaou, P., Kostopoulou, E., Chenoweth, J., El Maayar, M., Giannakopoulos, C., Hannides, C., Lange, M., Tanarhte, M. and Tyrlis, E.: Climate change and impacts in the Eastern Mediterranean and the Middle East, Clim. Change, 114(3–4), 667–687, 2012.

Li, Y., Ren, B., Qiao, Z., Zhu, J., Wang, H., Zhou, M., Qiao, L., Lou, S., Jing, S., Huang, C., Tao, S., Rao, P. and Li, J.: Characteristics of atmospheric intermediate volatility organic compounds (IVOCs) in winter and summer under different air pollution levels, Atmos. Environ., 210, 58–65, doi:10.1016/j.atmosenv.2019.04.041, 2019.

Liakakou, E., Vrekoussis, M., Bonsang, B., Donousis, Ch., Kanakidou, M. and Mihalopoulos, N.: Isoprene above the Eastern Mediterranean: Seasonal variation and contribution to the oxidation capacity of the atmosphere, Atmos. Environ., 41(5), 1002–1010, doi:10.1016/j.atmosenv.2006.09.034, 2007.

Liu, B., Liang, D., Yang, J., Dai, Q., Bi, X., Feng, Y., Yuan, J., Xiao, Z., Zhang, Y. and Xu, H.: Characterization and source apportionment of volatile organic compounds based on 1-year of observational data in Tianjin, China, Environ. Pollut., 218, 757–769, doi:10.1016/j.envpol.2016.07.072, 2016.

Liu, Y., Shao, M., Fu, L., Lu, S., Zeng, L. and Tang, D.: Source profiles of volatile organic compounds (VOCs) measured in China: Part I, Atmos. Environ., 42(25), 6247–6260, doi:10.1016/j.atmosenv.2008.01.070, 2008.

Liu, Y., Shao, M., Lu, S., Chang, C.-C., Wang, J.-L., and Chen, G.: Volatile Organic Compound (VOC) measurements in the Pearl River Delta (PRD) region, China, Atmos. Chem. Phys., 8, 1531–1545, https://doi.org/10.5194/acp-8-1531-2008 , 2008.

Lu, Q., Zhao, Y. and Robinson, A. L.: Comprehensive organic emission profiles for gasoline, diesel, and gas-turbine engines including intermediate and semi-volatile organic compound emissions, Atmospheric Chem. Phys., 18(23), 17637–17654, doi: https://doi.org/10.5194/acp-18-17637-2018 , 2018.

Luria, M., Weisinger, R. and Peleg, M.: CO and NOx levels at the center of city roads in Jerusalem, Atmospheric Environ. Part B Urban Atmosphere, 24(1), 93–99, doi:10.1016/0957-1272(90)90014-L, 1990.

Mahmoud, K. F., Alfaro, S. C., Favez, O., Abdel Wahab, M. M. and Sciare, J.: Origin of black carbon concentration peaks in Cairo (Egypt), Atmospheric Res., 89(1), 161–169, doi:10.1016/j.atmosres.2008.01.004, 2008.

Mantis, H. T., Repapis, C. C., Zerefos, C. S., and Ziomas, J. C.: Assessment of the Potential for Photochemical Air Pollution in Athens: A Comparison of Emissions and Air-Pollutant Levels in Athens with Those in Los Angeles, J. Appl. Meteorol., 31, 1467–1476, https://doi.org/10.1175/1520-0450(1992)031<1467:AOTPFP>2.0.CO;2 , 1992.

Marchwinska-Wyrwal, E., Dziubanek, G., Hajok, I., Rusin, M., K.Oleksiuk and M.Kubasiak: Impact of Air Pollution on Public Health, , doi:10.5772/17906, 2011.

Markakis, K., Poupkou, A., Melas, D., Tzoumaka, P. and Petrakakis, M.: A computational approach based on GIS technology for the development of an anthropogenic emission inventory of gaseous pollutants in Greece, Water. Air. Soil Pollut., 207(1–4), 157–180, 2010.

Massoud, R., Shihadeh, Alan. L., Roumié, M., Youness, M., Gerard, J., Saliba, N., Zaarour, R., Abboud, M., Farah, W. and Saliba, N. A.: Intraurban variability of PM10 and PM2.5 in an Eastern Mediterranean city, Atmospheric Res., 101(4), 893–901, doi:10.1016/j.atmosres.2011.05.019, 2011.

McGraw, G. W., Hemingway, R. W., Ingram, Leonard L., Canady, C. S. and McGraw, W. B.: Thermal Degradation of Terpenes: Camphene, Δ3-Carene, Limonene, and α-Terpinene, Environ. Sci. Technol., 33(22), 4029–4033, doi:10.1021/es9810641, 1999.

Melas, D., Ziomas, I., Klemm, O., and Zerefos, C. S.: Anatomy of the sea-breeze circulation in Athens area under weak large-scale ambient winds, Atmos. Environ., 32, 2223–2237, https://doi.org/10.1016/S1352-2310(97)00420-2, 1998.

Mellouki, A., Wallington, T. J. and Chen, J.: Atmospheric Chemistry of Oxygenated Volatile Organic Compounds: Impacts on Air Quality and Climate, Chem. Rev., 115(10), 3984–4014, doi:10.1021/cr500549n, 2015

Millet, D. B., Donahue, N. M., Pandis, S. N., Polidori, A., Stanier, C. O., Turpin, B. J. and Goldstein, A. H.: Atmospheric volatile organic compound measurements during the Pittsburgh Air Quality Study: Results, interpretation, and quantification of primary and secondary contributions, J. Geophys. Res. Atmospheres, 110(D7), D07S07, doi:10.1029/2004JD004601, 2005.

Molina, L. T., Madronich, S., Gaffney, J., Apel, E., Foy, B. de, Fast, J., Ferrare, R., Herndon, S., Jimenez, J. L. and Lamb, B.: An overview of the MILAGRO 2006 Campaign: Mexico City emissions and their transport and transformation, Atmospheric Chem. Phys., 10(18), 8697–8760, 2010.

Molina, M. J. and Molina, L. T.: Megacities and Atmospheric Pollution, J. Air Waste Manag. Assoc., 54(6), 644–680, doi:10.1080/10473289.2004.10470936, 2004.

Monks, P., Granier, C., Fuzzi, S., Stohl, A., Williams, M., Akimoto, H., Amann, M., Baklanov, A., Baltensperger, U. and Bey, I.: Atmospheric composition change–global and regional air quality, Atmos. Environ., 43(33), 5268–5350, 2009.

Montero, L., Duane, M., Manfredi, U., Astorga, C., Martini, G., Carriero, M., Krasenbrink, A. and Larsen, B. R.: Hydrocarbon emission fingerprints from contemporary vehicle/engine technologies with conventional and new fuels, Atmos. Environ., 44(18), 2167–2175, doi:10.1016/j.atmosenv.2010.03.027, 2010.

Moschonas, N. and Glavas, S.: C3-C10 hydrocarbons in the atmosphere of Athens, Greece, Atmos. Environ., 30, 2769–2772, https://doi.org/10.1016/1352-2310(95)00488-2 , 1996.

Moschonas, N. and Glavas, S.: Non-methane hydrocarbons at a high-altitude rural site in the Mediterranean (Greece), Atmos. Environ., 34(6), 973–984, doi:10.1016/S1352-2310(99)00205-8, 2000.

Moschonas, N., Glavas, S., and Kouimtzis, T.: C3 to C9 hydrocarbon measurements in the two largest cities of Greece, Athens and Thessaloniki, Calculation of hydrocarbon emissions by species, Derivation of hydroxyl radical concentrations, Sci.Total Environ., 271, 117–133, https://doi.org/10.1016/S0048-9697(00)00838-X , 2001.

Muezzinoglu, A., Odabasi, M. and Onat, L.: Volatile organic compounds in the air of Izmir, Turkey, Atmos. Environ., 35(4), 753–760, doi:10.1016/S1352-2310(00)00420-9, 2001.

Na, K. and Kim, Y. P.: Seasonal characteristics of ambient volatile organic compounds in Seoul, Korea, Atmos. Environ., 35(15), 2603–2614, 2001.

Na, K. and Pyo Kim, Y.: Chemical mass balance receptor model applied to ambient C2–C9 VOC concentration in Seoul, Korea: Effect of chemical reaction losses, Atmos. Environ., 41(32), 6715–6728, doi:10.1016/j.atmosenv.2007.04.054, 2007.

Nan, J., Wang, S., Guo, Y., Xiang, Y. and Zhou, B.: Study on the daytime OH radical and implication for its relationship with fine particles over megacity of Shanghai, China, Atmos. Environ., 154(Supplement C), 167–178, doi:10.1016/j.atmosenv.2017.01.046, 2017.

Neophytou, A. M., Yiallouros, P., Coull, B. A., Kleanthous, S., Pavlou, P., Pashiardis, S., Dockery, D. W., Koutrakis, P. and Laden, F.: Particulate matter concentrations during desert dust outbreaks and daily mortality in Nicosia, Cyprus, J. Expo. Sci. Environ. Epidemiol., 23(3), 275–280, doi:10.1038/jes.2013.10, 2013.

Nester, K.: Influence of sea breeze flows on air pollution over the attica peninsula, Atmos. Environ., 29, 3655–3670, https://doi.org/10.1016/1352-2310(95)98468-N , 1995.

Norris, G., Duvall, R., Brown, S. and Bai, S.: Epa positive matrix factorization (pmf) 5.0 fundamentals and user guide prepared for the us environmental protection agency office of research and development, washington, dc, Wash. DC, 2014.

Ozdemir, H., Pozzoli, L., Kindap, T., Demir, G., Mertoglu, B., Mihalopoulos, N., Theodosi, C., Kanakidou, M., Im, U. and Unal, A.: Spatial and temporal analysis of black carbon aerosols in Istanbul megacity, Sci. Total Environ., 473–474, 451–458, doi:10.1016/j.scitotenv.2013.11.102, 2014.

Paatero, P. and Hopke, P. K.: Discarding or downweighting high-noise variables in factor analytic models, Anal. Chim. Acta, 490(1), 277–289, doi:10.1016/S0003-2670(02)01643-4, 2003.

Paatero, P. and Tapper, U.: Analysis of different modes of factor analysis as least squares fit problems, Chemom. Intell. Lab. Syst., 18(2), 183–194, doi:10.1016/0169-7439(93)80055-M, 1993.

Paatero, P. and Tapper, U.: Positive matrix factorization: A non-negative factor model with optimal utilization of error estimates of data values, Environmetrics, 5(2), 111–126, doi:10.1002/env.3170050203, 1994.

Paatero, P., Eberly, S., Brown, S. G. and Norris, G. A.: Methods for estimating uncertainty in factor analytic solutions, Atmospheric Meas. Tech., 7(3), 781–797, doi:https://doi.org/10.5194/amt-7-781-2014, 2014.

Paatero, P.: Least squares formulation of robust non-negative factor analysis, Chemom. Intell. Lab. Syst., 37(1), 23–35, doi:10.1016/S0169-7439(96)00044-5, 1997.

Pallozzi, E., Lusini, I., Cherubini, L., Hajiaghayeva, R. A., Ciccioli, P. and Calfapietra, C.: Differences between a deciduous and a conifer tree species in gaseous and particulate emissions from biomass burning, Environ. Pollut., 234, 457–467, doi:10.1016/j.envpol.2017.11.080, 2018.

Panopoulou, A., Liakakou, E., Gros, V., Sauvage, S., Locoge, N., Bonsang, B., Psiloglou, B. E., Gerasopoulos, E. and Mihalopoulos, N.: Non-methane hydrocarbon variability in Athens during wintertime: the role of traffic and heating, Atmospheric Chem. Phys., 18(21), 16139–16154, doi:https://doi.org/10.5194/acp-18-16139-2018, 2018.

Paraskevopoulou, D., Liakakou, E., Gerasopoulos, E., and Mihalopoulos, N.: Sources of atmospheric aerosol from long-term measurements (5 years) of chemical composition in Athens, Greece, Sci. Total Environ., 527 (Supplement C), 165–178, https://doi.org/10.1016/j.scitotenv.2015.04.022 , 2015.

Paraskevopoulou, D., Liakakou, E., Gerasopoulos, E., Theodosi, C. and Mihalopoulos, N.: Long-term characterization of organic and elemental carbon in the PM 2.5 fraction: the case of Athens, Greece, Atmospheric Chem. Phys., 14(23), 13313–13325, 2014.

Pateraki, St., Maggos, Th., Michopoulos, J., Flocas, H. A., Asimakopoulos, D. N. and Vasilakos, Ch.: Ions species size distribution in particulate matter associated with VOCs and meteorological conditions over an urban region, Chemosphere, 72(3), 496–503, doi:10.1016/j.chemosphere.2008.02.061, 2008.

Pechtl, S. and von Glasow, R.: Reactive chlorine in the marine boundary layer in the outflow of polluted continental air: A model study, Geophys. Res. Lett., 34(11), L11813, doi:10.1029/2007GL029761, 2007.

Peñuelas, J. and Llusià, J.: Plant VOC emissions: making use of the unavoidable, Trends Ecol. Evol., 19(8), 402–404, doi:10.1016/j.tree.2004.06.002, 2004.

Petit, J.-E., Favez, O., Albinet, A. and Canonaco, F.: A user-friendly tool for comprehensive evaluation of the geographical origins of atmospheric pollution: Wind and trajectory analyses, Environ. Model. Softw., 88, 183–187, doi:10.1016/j.envsoft.2016.11.022, 2017.

Petrakis, M., Psiloglou, B., Kassomenos, P. A. and Cartalis, C.: Summertime Measurements of Benzene and Toluene in Athens Using a Differential Optical Absorption Spectroscopy System, J. Air Waste Manag. Assoc., 53(9), 1052–1064, doi:10.1080/10473289.2003.10466266, 2003.

Pikridas, M., Vrekoussis, M., Sciare, J., Kleanthous, S., Vasiliadou, E., Kizas, C., Savvides, C. and Mihalopoulos, N.: Spatial and temporal (short and long-term) variability of submicron, fine and sub-10 μm particulate matter (PM1, PM2.5, PM10) in Cyprus, Atmos. Environ., 191, 79–93, doi:10.1016/j.atmosenv.2018.07.048, 2018.

Platt, S. M., Haddad, I. E., Pieber, S. M., Huang, R.-J., Zardini, A. A., Clairotte, M., Suarez-Bertoa, R., Barmet, P., Pfaffenberger, L., Wolf, R., Slowik, J. G., Fuller, S. J., Kalberer, M., Chirico, R., Dommen, J., Astorga, C., Zimmermann, R., Marchand, N., Hellebust, S., Temime-Roussel, B., Baltensperger, U. and Prévôt, A. S. H.: Two-stroke scooters are a dominant source of air pollution in many cities, Nat. Commun., 5, 3749, 2014.

Polissar, A. V., Hopke, P. K., Paatero, P., Malm, W. C. and Sisler, J. F.: Atmospheric aerosol over Alaska: 2. Elemental composition and sources, J. Geophys. Res. Atmospheres, 103(D15), 19045–19057, doi:10.1029/98JD01212, 1998.

Politis, D. N. and White, H.: Automatic Block-Length Selection for the Dependent Bootstrap, Econom. Rev., 23(1), 53–70, doi:10.1081/ETC-120028836, 2004.

Pöschl, U. and Shiraiwa, M.: Multiphase Chemistry at the Atmosphere–Biosphere Interface Influencing Climate and Public Health in the Anthropocene, Chem. Rev., 115(10), 4440–4475, doi:10.1021/cr500487s, 2015.

Psiloglou, B., Mihalopoulos, N. and Paliatsos, Athanasios. G.: Benzene and Toluene Levels in the Atmosphere of Athens During Wintertime: Influence of Financial Crisis on Traffic and Biomass Burning Emissions, in Perspectives on Atmospheric Sciences, edited by T. Karacostas, A. Bais, and P. T. Nastos, pp. 1141–1147, Springer International Publishing., 2017.

Purvis, R. M., Lewis, A. C., Carney, R. A., McQuaid, J. B., Arnold, S. R., Methven, J., Barjat, H., Dewey, K., Kent, J., Monks, P. S., Carpenter, L. J., Brough, N., Penkett, S. A. and Reeves, C. E.: Rapid uplift of nonmethane hydrocarbons in a cold front over central Europe, J. Geophys. Res. Atmospheres, 108(D7), doi:10.1029/2002JD002521, 2003.

Puxbaum, H.: Biogenic emissions of alcohols, ester, ether and higher aldehydes, Biog. Volatile Org. Compd. Atmosphere–Summary Present Knowl. SPB Acad. Publ. Amst. Neth., 79–99, 1997.

Qiao, X., Ying, Q., Li, X., Zhang, H., Hu, J., Tang, Y. and Chen, X.: Source apportionment of PM2.5 for 25 Chinese provincial capitals and municipalities using a source-oriented Community Multiscale Air Quality model, Sci. Total Environ., 612, 462–471, doi:10.1016/j.scitotenv.2017.08.272, 2018.

Raja, N. B., Aydin, O., Türkoğlu, N. and Çiçek, İ.: Characterising the Seasonal Variations and Spatial Distribution of Ambient PM<Subscript>10</Subscript> in Urban Ankara, Turkey, Environ. Process., 5(2), 349–362, doi:10.1007/s40710-018-0305-8, 2018.

Rappenglück, B., Fabian, P., Kalabokas, P., Viras, L. G., and Ziomas, I. C.: Quasi-continuous measurements of nonmethane hydrocarbons (NMHC) in the Greater Athens area during medcaphot-trace, Atmos. Environ., 32, 2103–2121, https://doi.org/10.1016/S1352-2310(97)00430-5 , 1998.

Rappenglück, B., Kourtidis, K., Melas, D., and Fabian, P.: Observations of biogenic and anthropogenic NMHC in the greater Athens area during the PAUR campaign, Phys. Chem. Earth Pt.B, 24, 717–724, https://doi.org/10.1016/S1464-1909(99)00071-4 , 1999.

Rappenglück, B., Melas, D. and Fabian, P.: Evidence of the impact of urban plumes on remote sites in the Eastern Mediterranean, Atmos. Environ., 37(13), 1853–1864, doi:10.1016/S1352-2310(03)00065-7, 2003.

Ras, M. R., Borrull, F. and Marcé, R. M.: Sampling and preconcentration techniques for determination of volatile organic compounds in air samples, TrAC Trends Anal. Chem., 28(3), 347–361, doi:10.1016/j.trac.2008.10.009, 2009.

Robinson, A. L., Donahue, N. M., Shrivastava, M. K., Weitkamp, E. A., Sage, A. M., Grieshop, A. P., Lane, T. E., Pierce, J. R. and Pandis, S. N.: Rethinking Organic Aerosols: Semivolatile Emissions and Photochemical Aging, Science, 315(5816), 1259, doi:10.1126/science.1133061, 2007.

Rouvière, A., Brulfert, G., Baussand, P. and Chollet, J.-P.: Monoterpene source emissions from Chamonix in the Alpine Valleys, Atmos. Environ., 40(19), 3613–3620, doi:10.1016/j.atmosenv.2005.09.058, 2006.

Rudolph, J., Ramacher, B., Plass-Dülmer, C., Müller, K.-P. and Koppmann, R.: The indirect determination of chlorine atom concentration in the troposphere from changes in the patterns of non-methane hydrocarbons, Tellus B Chem. Phys. Meteorol., 49(5), 592–601, doi:10.3402/tellusb.v49i5.16016, 1997.

Saffari, A., Daher, N., Samara, C., Voutsa, D., Kouras, A., Manoli, E., Karagkiozidou, O., Vlachokostas, C., Moussiopoulos, N. and Shafer, M. M.: Increased biomass burning due to the economic crisis in Greece and its adverse impact on wintertime air quality in Thessaloniki, Environ. Sci. Technol., 47(23), 13313–13320, 2013.

Saffari, A., Daher, N., Samara, C., Voutsa, D., Kouras, A., Manoli, E., Karagkiozidou, O., Vlachokostas, C., Moussiopoulos, N., Shafer, M. M., Schauer, J. J., and Sioutas, C.: Increased Biomass Burning Due to the Economic Crisis in Greece and Its Adverse Impact on Wintertime Air Quality in Thessaloniki, Environ. Sci.Technol., 47, 13313–13320, https://doi.org/10.1021/es403847h, 2013.

Salameh, T., Afif, C., Sauvage, S., Borbon, A. and Locoge, N.: Speciation of non-methane hydrocarbons (NMHCs) from anthropogenic sources in Beirut, Lebanon, Environ. Sci. Pollut. Res., 21(18), 10867–10877, 2014.

Salameh, T., Borbon, A., Afif, C., Sauvage, S., Leonardis, T., Gaimoz, C. and Locoge, N.: Composition of gaseous organic carbon during ECOCEM in Beirut, Lebanon: new observational constraints for VOC anthropogenic emission evaluation in the Middle East, Atmos Chem Phys, 17(1), 193–209, doi:10.5194/acp-17-193-2017, 2017.

Salameh, T., Sauvage, S., Afif, C., Borbon, A. and Locoge, N.: Source apportionment vs. emission inventories of non-methane hydrocarbons (NMHC) in an urban area of the Middle East: local and global perspectives, Atmos Chem Phys, 16, 3595–3607, 2016.

Salameh, T., Sauvage, S., Afif, C., Borbon, A., Léonardis, T., Brioude, J., Waked, A., and Locoge, N.: Exploring the seasonal NMHC distribution in an urban area of the Middle East during ECOCEM campaigns: very high loadings dominated by local emissions and dynamics, Environ. Chem., 12, 316–328, https://doi.org/10.1071/EN14154 , 2015.

Salameh, T., Sauvage, S., Locoge, N., Gauduin, J., Perrussel, O. and Borbon, A.: Spatial and temporal variability of BTEX in Paris megacity: Two-wheelers as a major driver, Atmospheric Environ. X, 1, 100003, doi:10.1016/j.aeaoa.2018.100003, 2019.

Sarnat, J. A., Moise, T., Shpund, J., Liu, Y., Pachon, J. E., Qasrawi, R., Abdeen, Z., Brenner, S., Nassar, K. and Saleh, R.: Assessing the spatial and temporal variability of fine particulate matter components in Israeli, Jordanian, and Palestinian cities, Atmos. Environ., 44(20), 2383–2392, 2010.

Sauvage, S., Plaisance, H., Locoge, N., Wroblewski, A., Coddeville,P., and Galloo, J. C.: Long term measurement and source apportionment of non-methane hydrocarbons in three French rural areas, Atmos. Environ., 43, 2430–2441, https://doi.org/10.1016/j.atmosenv.2009.02.001 , 2009.

Schade, G. W. and Goldstein, A. H.: Fluxes of oxygenated volatile organic compounds from a ponderosa pine plantation, J. Geophys. Res. Atmospheres, 106(D3), 3111–3123, doi:10.1029/2000JD900592, 2001.

Schauer, J. J., Kleeman, M. J., Cass, G. R., and Simoneit, B. R. T.: Measurement of Emissions from Air Pollution Sources. 3. C1-C29 Organic Compounds from Fireplace Combustion of Wood, Environ. Sci. Technol., 35, 1716–1728, https://doi.org/10.1021/es001331e , 2001.

Seco, R., Peñuelas, J., Filella, I., Llusià, J., Molowny-Horas, R., Schallhart, S., Metzger, A., Müller, M. and Hansel, A.: Contrasting winter and summer VOC mixing ratios at a forest site in the Western Mediterranean Basin: the effect of local biogenic emissions, Atmospheric Chem. Phys., 11(24), 13161–13179, doi:https://doi.org/10.5194/acp-11-13161-2011, 2011.

Seco, R., Peñuelas, J., Filella, I., Llusia, J., Schallhart, S., Metzger, A., Müller, M. and Hansel, A.: Volatile organic compounds in the western Mediterranean basin: urban and rural winter measurements during the DAURE campaign, Atmospheric Chem. Phys., 13(8), 4291–4306, 2013.

Seinfeld, J. H. and Pandis, S. N.: Atmospheric Chemistry and Physics: From Air Pollution to Climate Change, John Wiley & Sons, Hoboken, New Jersey, 2016.

Shaltout, A. A., Hassan, S. K., Karydas, A. G., Zaki, Z. I., Mostafa, N. Y., Kregsamer, P., Wobrauschek, P. and Streli, C.: Comparative elemental analysis of fine particulate matter (PM2.5) from industrial and residential areas in Greater Cairo-Egypt by means of a multi-secondary target energy dispersive X-ray fluorescence spectrometer, Spectrochim. Acta Part B At. Spectrosc., 145, 29–35, doi:10.1016/j.sab.2018.04.003, 2018.

Shiraiwa, M. and Seinfeld, J. H.: Equilibration timescale of atmospheric secondary organic aerosol partitioning, Geophys. Res. Lett., 39(24), L24801, doi:10.1029/2012GL054008, 2012.

Sillmann, J., Kharin, V. V., Zwiers, F. W., Zhang, X. and Bronaugh, D.: Climate extremes indices in the CMIP5 multimodel ensemble: Part 2. Future climate projections, J. Geophys. Res. Atmospheres, 118(6), 2473–2493, doi:10.1002/jgrd.50188, 2013.

Simpson, I. J., Blake, N. J., Barletta, B., Diskin, G. S., Fuelberg, H. E., Gorham, K., Huey, L. G., Meinardi, S., Rowland, F. S., Vay, S. A., Weinheimer, A. J., Yang, M. and Blake, D. R.: Characterization of trace gases measured over Alberta oil

sands mining operations: 76 speciated C2–C10 volatile organic compounds (VOCs), CO2, CH4, CO, NO, NO2, NOy, O3 and SO2, Atmospheric Chem. Phys., 10(23), 11931–11954, doi: https://doi.org/10.5194/acp-10-11931-2010 , 2010.

Solomou, E., Poupkou, A., Bolis, S., Zanis, P., Lazaridis, M. and Melas, D.: Evaluating near-surface ozone levels simulated from MACC global and regional modelling systems in Eastern Mediterranean under the influence of Etesian winds, Atmospheric Res., 208, 191–200, doi:10.1016/j.atmosres.2017.09.010, 2018.

Song, C., Liu, B., Dai, Q., Li, H. and Mao, H.: Temperature dependence and source apportionment of volatile organic compounds (VOCs) at an urban site on the north China plain, Atmos. Environ., 207, 167–181, doi:10.1016/j.atmosenv.2019.03.030, 2019.

Song, Y., Dai, W., Shao, M., Liu, Y., Lu, S., Kuster, W. and Goldan, P.: Comparison of receptor models for source apportionment of volatile organic compounds in Beijing, China, Environ. Pollut., 156(1), 174–183, doi:10.1016/j.envpol.2007.12.014, 2008.

State of the Environment Report 2018: http://ekpaa.ypeka.gr/index.php/soer-2018

Stavroulas, I., Bougiatioti, A., Grivas, G., Paraskevopoulou, D., Tsagkaraki, M., Zarmpas, P., Liakakou, E., Gerasopoulos, E. and Mihalopoulos, N.: Sources and processes that control the submicron organic aerosol composition in an urban Mediterranean environment (Athens): a high temporal-resolution chemical composition measurement study, Atmospheric Chem. Phys., 19(2), 901–919, doi: https://doi.org/10.5194/acp-19-901-2019 , 2019.

Streets, D. G., Bond, T. C., Carmichael, G. R., Fernandes, S. D., Fu, Q., He, D., Klimont, Z., Nelson, S. M., Tsai, N. Y., Wang, M. Q., Woo, J.-H. and Yarber, K. F.: An inventory of gaseous and primary aerosol emissions in Asia in the year 2000, J. Geophys. Res. Atmospheres, doi:10.1029/2002JD003093@10.1002/(ISSN)2169-8996.TRACEP1, 2018.

Stull, R. B.: An Introduction to Boundary Layer Meteorology, Springer Science & Business Media., 2012.

Theodosi, C., Grivas, G., Zarmpas, P., Chaloulakou, A. and Mihalopoulos, N.: Mass and chemical composition of size-segregated aerosols (PM 1, PM 2.5, PM 10) over Athens, Greece: local versus regional sources, Atmospheric Chem. Phys., 11(22), 11895–11911, 2011.

Theodosi, C., Tsagkaraki, M., Zarmpas, P., Grivas, G., Liakakou, E., Paraskevopoulou, D., Lianou, M., Gerasopoulos, E. and Mihalopoulos, N.: Multi-year chemical composition of the fine-aerosol fraction in Athens, Greece, with emphasis on the contribution of residential heating in wintertime, Atmospheric Chem. Phys., 18(19), 14371–14391, doi: https://doi.org/10.5194/acp-18-14371-2018 , 2018.

Thurston, G. D. and Spengler, J. D.: A quantitative assessment of source contributions to inhalable particulate matter pollution in metropolitan Boston, Atmospheric Environ. 1967, 19(1), 9–25, doi:10.1016/0004-6981(85)90132-5, 1985.

Tiiva, P., Tang, J., Michelsen, A. and Rinnan, R.: Monoterpene emissions in response to long-term night-time warming, elevated CO2 and extended summer drought in a temperate heath ecosystem, Sci. Total Environ., 580, 1056–1067, doi:10.1016/j.scitotenv.2016.12.060, 2017.

Tkacik, D. S., Presto, A. A., Donahue, N. M. and Robinson, A. L.: Secondary Organic Aerosol Formation from Intermediate-Volatility Organic Compounds: Cyclic, Linear, and Branched Alkanes, Environ. Sci. Technol., 46(16), 8773–8781, doi:10.1021/es301112c, 2012.

Tohid, L., Sabeti, Z., Sarbakhsh, P., Zoroufchi Benis, K., Shakerkhatibi, M., Rasoulzadeh, Y., Rahimian, R. and Darvishali, S.: Spatiotemporal variation, ozone formation potential and health risk assessment of ambient air VOCs in an industrialized city in Iran, Atmospheric Pollut. Res., 10(2), 556–563, doi:10.1016/j.apr.2018.10.007, 2019.

Tominaga, Y. and Stathopoulos, T.: CFD simulation of near-field pollutant dispersion in the urban environment: A review of current modeling techniques, Atmos. Environ., 79, 716–730, doi:10.1016/j.atmosenv.2013.07.028, 2013.

Tsai, J.-H., Huang, P.-H. and Chiang, H.-L.: Air pollutants and toxic emissions of various mileage motorcycles for ECE driving cycles, Atmos. Environ., 153, 126–134, doi:10.1016/j.atmosenv.2017.01.019, 2017.

Tsigaridis, K. and Kanakidou, M.: Global modelling of secondary organic aerosol in the troposphere: a sensitivity analysis, Atmos. Chem. Phys., 3, 1849–1869, https://doi.org/10.5194/acp-3-1849-2003 , 2003.

Tsigaridis, K. and Kanakidou, M.: Secondary organic aerosol importance in the future atmosphere, Atmos. Environ., 41(22), 4682–4692, doi:10.1016/j.atmosenv.2007.03.045, 2007.

Turner, M. C., Jerrett, M., Pope, C. A., Krewski, D., Gapstur, S. M., Diver, W. R., Beckerman, B. S., Marshall, J. D., Su, J., Crouse, D. L. and Burnett, R. T.: Long-Term Ozone Exposure and Mortality in a Large Prospective Study, Am. J. Respir. Crit. Care Med., 193(10), 1134–1142, doi:10.1164/rccm.201508-1633OC, 2015.

Ulbrich, I. M., Canagaratna, M. R., Zhang, Q., Worsnop, D. R. and Jimenez, J. L.: Interpretation of organic components from Positive Matrix Factorization of aerosol mass spectrometric data, Atmospheric Chem. Phys., 9(9), 2891–2918, doi:https://doi.org/10.5194/acp-9-2891-2009, 2009.

United Nations, Department of Economic and Social Affairs, Population Division (2014). World Urbanization Prospects: The 2014 Revision, Highlights (ST/ESA/SER.A/352).

Vardoulakis, S., Fisher, B. E. A., Pericleous, K. and Gonzalez-Flesca, N.: Modelling air quality in street canyons: a review, Atmos. Environ., 37(2), 155–182, doi:10.1016/S1352-2310(02)00857-9, 2003.

Vasilakos, C., Pateraki, S., Veros, D., Maggos, T., Michopoulos, J., Saraga, D. and Helmis, C. G.: Temporal determination of heavy metals in PM2. 5 aerosols in a suburban site of Athens, Greece, J. Atmospheric Chem., 57(1), 1–17, 2007.

Vautard, R., Beekmann, M., Desplat, J., Hodzic, A. and Morel, S.: Air quality in Europe during the summer of 2003 as a prototype of air quality in a warmer climate, Comptes Rendus Geosci., 339(11), 747–763, doi:10.1016/j.crte.2007.08.003, 2007.

Viana, M., Kuhlbusch, T. A. J., Querol, X., Alastuey, A., Harrison, R. M., Hopke, P. K., Winiwarter, W., Vallius, M., Szidat, S., Prévôt, A. S. H., Hueglin, C., Bloemen, H., Wåhlin, P., Vecchi, R., Miranda, A. I., Kasper-Giebl, A., Maenhaut, W. and Hitzenberger, R.: Source apportionment of particulate matter in Europe: A review of methods and results, J. Aerosol Sci., 39(10), 827–849, doi:10.1016/j.jaerosci.2008.05.007, 2008.

Vrekoussis, M., Richter, A., Hilboll, A., Burrows, J. P., Gerasopoulos, E., Lelieveld, J., Barrie, L., Zerefos, C., and Mihalopoulos, N.: Economic crisis detected from space: Air quality observations over Athens/Greece, Geophys. Res. Lett., 40, 458–463, https://doi.org/10.1002/grl.50118 , 2013.

Wagner, P. and Kuttler, W.: Biogenic and anthropogenic isoprene in the near-surface urban atmosphere — A case study in Essen, Germany, Sci. Total Environ., 475, 104–115, doi:10.1016/j.scitotenv.2013.12.026, 2014.

Waked, A. and Afif, C.: Emissions of air pollutants from road transport in Lebanon and other countries in the Middle East region, Atmos. Environ., 61, 446–452, doi:10.1016/j.atmosenv.2012.07.064, 2012.

Waked, A., Afif, C. and Seigneur, C.: An atmospheric emission inventory of anthropogenic and biogenic sources for Lebanon, Atmos. Environ., 50, 88–96, doi:10.1016/j.atmosenv.2011.12.058, 2012.

Wang, H. and L., Shengrong and Huang, Cheng and Qiao, Liping and Tang, Xibin and Chen, Changhong and Zeng, Limin and Wang, Qian and Zhou, Min and Lu, Sihua and Yu, Xuena: Source Profiles of Volatile Organic Compounds from Biomass Burning in Yangtze River Delta, China, Aerosol Air Qual. Res., 14(3), 818–828, doi:10.4209/aaqr.2013.05.0174, 2014.

Wang, S., Wu, D., Wang, X.-M., Fung, J. C.-H. and Yu, J. Z.: Relative contributions of secondary organic aerosol formation from toluene, xylenes, isoprene, and monoterpenes in Hong Kong and Guangzhou in the Pearl River Delta, China: an emission-based box modeling study, J. Geophys. Res. Atmospheres, 118(2), 507–519, doi:10.1029/2012JD017985, 2013.

Watson, J. G., Chow, J. C. and Fujita, E. M.: Review of volatile organic compound source apportionment by chemical mass balance, Atmos. Environ., 35(9), 1567–1584, doi:10.1016/S1352-2310(00)00461-1, 2001.

Wayne, R. P., Barnes, I., Biggs, P., Burrows, J. P., Canosa-Mas, C. E., Hjorth, J., Le Bras, G., Moortgat, G. K., Perner, D., Poulet, G., Restelli, G. and Sidebottom, H.: The nitrate radical: Physics, chemistry, and the atmosphere, Atmospheric Environ. Part Gen. Top., 25(1), 1–203, doi:10.1016/0960-1686(91)90192-A, 1991.

Weinroth, E., Luria, M., Ben-Nun, A., Kaplan, J., Peleg, M. and Mahrer, I.: Air Pollution Emission Inventory Survey for Israel, Isr. J. Chem., 46(1), 59–68, doi:10.1560/5E7C-QEK0-YV0J-N0E2, 2006.

WHO - IARC: Outdoor air pollution a leading environmental cause of cancer deaths, Press Release no221, 2013

WHO, Regional Committee 61, 2014: http://www.emro.who.int/about-who/rc61/impact-air-pollution.html

Wu, W., Zhao, B., Wang, S. and Hao, J.: Ozone and secondary organic aerosol formation potential from anthropogenic volatile organic compounds emissions in China, J. Environ. Sci., 53, 224–237, doi:10.1016/j.jes.2016.03.025, 2017.

Xiang, Y., Delbarre, H., Sauvage, S., Léonardis, T., Fourmentin, M., Augustin, P. and Locoge, N.: Development of a methodology examining the behaviours of VOCs source apportionment with micro-meteorology analysis in an urban and industrial area, Environ. Pollut., 162, 15–28, doi:10.1016/j.envpol.2011.10.012, 2012.

Yang, H.-H., Chien, S.-M., Cheng, M.-T. and Peng, C.-Y.: Comparative Study of Regulated and Unregulated Air Pollutant Emissions before and after Conversion of Automobiles from Gasoline Power to Liquefied Petroleum Gas/Gasoline Dual-Fuel Retrofits, Environ. Sci. Technol., 41(24), 8471–8476, doi:10.1021/es0706495, 2007.

Yang, K.-L., Ting, C.-C., Wang, J.-L., Wingenter, O. W. and Chan, C.-C.: Diurnal and seasonal cycles of ozone precursors observed from continuous measurement at an urban site in Taiwan, Atmos. Environ., 39(18), 3221–3230, doi:10.1016/j.atmosenv.2005.02.003, 2005.

Yang, W., Zhang, Y., Wang, X., Li, S., Zhu, M., Yu, Q., Li, G., Huang, Z., Zhang, H., Wu, Z., Song, W., Tan, J. and Shao, M.: Volatile organic compounds at a rural site in Beijing: influence of temporary emission control and wintertime heating, Atmospheric Chem. Phys., 18(17), 12663–12682, doi:https://doi.org/10.5194/acp-18-12663-2018, 2018.

Yao, D., Lyu, X., Murray, F., Morawska, L., Yu, W., Wang, J. and Guo, H.: Continuous effectiveness of replacing catalytic converters on liquified petroleum gas-fueled vehicles in Hong Kong, Sci. Total Environ., 648, 830–838, doi:10.1016/j.scitotenv.2018.08.191, 2019.

Ying, Q. and Kleeman, M. J.: Source contributions to the regional distribution of secondary particulate matter in California, Atmos. Environ., 40(4), 736–752, doi:10.1016/j.atmosenv.2005.10.007, 2006.

Ying, Q., Lu, J., Allen, P., Livingstone, P., Kaduwela, A. and Kleeman, M.: Modeling air quality during the California Regional PM10/PM2.5 Air Quality Study (CRPAQS) using the UCD/CIT source-oriented air quality model – Part I. Base case model results, Atmos. Environ., 42(39), 8954–8966, doi:10.1016/j.atmosenv.2008.05.064, 2008.

Yoshino, A., Nakashima, Y., Miyazaki, K., Kato, S., Suthawaree, J., Shimo, N., Matsunaga, S., Chatani, S., Apel, E., Greenberg, J., Guenther, A., Ueno, H., Sasaki, H., Hoshi, J., Yokota, H., Ishii, K. and Kajii, Y.: Air quality diagnosis from comprehensive observations of total OH reactivity and reactive trace species in urban central Tokyo, Atmos. Environ., 49, 51–59, doi:10.1016/j.atmosenv.2011.12.029, 2012.

Young, C. J., Washenfelder, R. A., Edwards, P. M., Parrish, D. D., Gilman, J. B., Kuster, W. C., Mielke, L. H., Osthoff, H. D., Tsai, C., Pikelnaya, O., Stutz, J., Veres, P. R., Roberts, J. M., Griffith, S., Dusanter, S., Stevens, P. S., Flynn, J., Grossberg, N., Lefer, B., Holloway, J. S., Peischl, J., Ryerson, T. B., Atlas, E. L., Blake, D. R. and Brown, S. S.: Chlorine as a primary radical: evaluation of methods to understand its role in initiation of oxidative cycles, Atmospheric Chem. Phys., 14(7), 3427–3440, doi:https://doi.org/10.5194/acp-14-3427-2014, 2014.

Yuan, B., Hu, W. W., Shao, M., Wang, M., Chen, W. T., Lu, S. H., Zeng, L. M. and Hu, M.: VOC emissions, evolutions and contributions to SOA formation at a receptor site in eastern China, Atmos Chem Phys, 13(17), 8815–8832, doi:10.5194/acp-13-8815-2013, 2013.

Yuan, Z., Zhong, L., Lau, A. K. H., Yu, J. Z. and Louie, P. K. K.: Volatile organic compounds in the Pearl River Delta: Identification of source regions and recommendations for emission-oriented monitoring strategies, Atmos. Environ., 76, 162–172, doi:10.1016/j.atmosenv.2012.11.034, 2013.

Yurdakul, S., Civan, M. and Tuncel, G.: Volatile organic compounds in suburban Ankara atmosphere, Turkey: Sources and variability, Atmospheric Res., 120–121(Supplement C), 298–311, doi:10.1016/j.atmosres.2012.09.015, 2013.

Yurdakul, S., Civan, M., Kuntasal, Ö., Doğan, G., Pekey, H. and Tuncel, G.: Temporal variations of VOC concentrations in Bursa atmosphere, Atmospheric Pollut. Res., doi:10.1016/j.apr.2017.09.004, 2017.

Zerefos, C., Kourtidis, K., Balis, D., Bais, A. and Calpini, B.: Photochemical activity over the Eastern Mediterranean under variable environmental conditions, Phys. Chem. Earth Part C Sol. Terr. Planet. Sci., 26(7), 549–554, 2001.

Zhang, H., Yee, L. D., Lee, B. H., Curtis, M. P., Worton, D. R., Isaacman-VanWertz, G., Offenberg, J. H., Lewandowski, M., Kleindienst, T. E., Beaver, M. R., Holder, A. L., Lonneman, W. A., Docherty, K. S., Jaoui, M., Pye, H. O. T., Hu, W., Day, D. A., Campuzano-Jost, P., Jimenez, J. L., Guo, H., Weber, R. J., Gouw, J. de, Koss, A. R., Edgerton, E. S., Brune, W., Mohr, C., Lopez-Hilfiker, F. D., Lutz, A., Kreisberg, N. M., Spielman, S. R., Hering, S. V., Wilson, K. R., Thornton, J. A. and Goldstein, A. H.: Monoterpenes are the largest source of summertime organic aerosol in the southeastern United States, Proc. Natl. Acad. Sci., 115(9), 2038–2043, doi:10.1073/pnas.1717513115, 2018.

Zhang, Q., Wu, L., Fang, X., Liu, M., Zhang, J., Shao, M., Lu, S., and Mao, H.: Emission factors of volatile organic compounds (VOCs) based on the detailed vehicle classification in a tunnel study, Sci. Total Environ., 624, 878–886, https://doi.org/10.1016/j.scitotenv.2017.12.171 , 2018.

Zhang, Y., Yang, W., Simpson, I., Huang, X., Yu, J., Huang, Z., Wang, Z., Zhang, Z., Liu, D., Huang, Z., Wang, Y., Pei, C., Shao, M., Blake, D. R., Zheng, J., Huang, Z., and Wang, X.: Decadal changes in emissions of volatile organic compounds (VOCs) from on-road vehicles with intensified automobile pollution control: Case study in a busy urban tunnel in south China, Environ. Pollut., 233, 806–819, https://doi.org/10.1016/j.envpol.2017.10.133 , 2018.

Zhao, Y., Hennigan, C. J., May, A. A., Tkacik, D. S., de Gouw, J. A., Gilman, J. B., Kuster, W. C., Borbon, A. and Robinson, A. L.: Intermediate-Volatility Organic Compounds: A Large Source of Secondary Organic Aerosol, Environ. Sci. Technol., 48(23), 13743–13750, doi:10.1021/es5035188, 2014.

Zheng, J., Yu, Y., Mo, Z., Zhang, Z., Wang, X., Yin, S., Peng, K., Yang, Y., Feng, X. and Cai, H.: Industrial sector-based volatile organic compound (VOC) source profiles measured in manufacturing facilities in the Pearl River Delta, China, Sci. Total Environ., 456–457, 127–136, doi:10.1016/j.scitotenv.2013.03.055, 2013.

Zheng, J., Zhang, L., Che, W., Zheng, Z. and Yin, S.: A highly resolved temporal and spatial air pollutant emission inventory for the Pearl River Delta region, China and its uncertainty assessment, Atmos. Environ., 43(32), 5112–5122, doi:10.1016/j.atmosenv.2009.04.060, 2009.

Zhu, B., Han, Y., Wang, C., Huang, X., Xia, S., Niu, Y., Yin, Z. and He, L.: Understanding primary and secondary sources of ambient oxygenated volatile organic compounds (OVOCs) in Shenzhen utilizing photochemical age-based parameterization method, J. Environ. Sci., doi:10.1016/j.jes.2018.03.008, 2018

Ziomas, I. C., Gryning, S.-E. and Bornstein, R. D.: The Mediterranean campaign of photochemical tracers - Transport and chemical evolution (MEDCAPHOT-TRACE). Athens, Greece 1994-1995, Pergamon Press., 1998.

Ziomas, I. C., Suppan, P., Rappengluck, B., Balis, D., Tzoumaka,P., Melas, D., Papayiannis, D., Fabian, P., and Zerefos, C. S.: A contribution to the study of photochemical smog in the greater Athens area, Beitr. Phys. Atmosph., 68, 191–204 , 1995.

Ziomas, I. C.: The mediterranean campaign of photochemical tracers—transport and chemical evolution (MEDCAPHOT-TRACE): an outline, Atmos. Environ., 32(12), 2045–2053, 1998.

Ziomas, I., Suppan, P., Rappengluck, B., Balis, D., Tzoumaka, P., Melas, D., Papayannis, A., Fabian, P. and Zerefos, C.: A contribution to the study of photochemical smog in the greater Athens area, Beitrage Zur Phys. Atmosphare-Contrib. Atmospheric Phys., 68(3), 191–204, 1995.

Emission Inventories

AIRPARIF : https://www.airparif.asso.fr/

APEI: http://open.canada.ca/data/en/dataset/fa1c88a8-bf78-4fcb-9c1e-2a5534b92131

Canadian Environmental Protection Act (CEPA), "Guide for Reporting to the National Pollutant Release Inventory (NPRI), 2016 and 2017", https://www.ec.gc.ca/inrp-npri/default.asp?lang=En&n=1FAA2366-1

CITEPA : https://www.citepa.org/fr/

CMAQ – EPA : https://www.epa.gov/cmaq/cmaq-fact-sheet

EDGAR: http://edgar.jrc.ec.europa.eu/overview.php?v=432&SECURE=123

EMEP: http://www.emep.int/

FEI-GREGAA : The new open Flexible Emission Inventory for Greece and the Greater Athens Area (FEI-GREGAA): Account of pollutant sources and their importance from 2006 to 2012, 2016. . Atmos. Environ. 137, 17–37. doi:10.1016/j.atmosenv.2016.04.004

GEIA : http://www.geiacenter.org/

L-14 Africa: http://eccad.aeris-data.fr/

MACCity: http://accent.aero.jussieu.fr/MACC_metadata.php

MEGAN-MACC: Sindelarova, K., Granier, C., Bouarar, I., Guenther, A., Tilmes, S., Stavrakou, T., Müller, J.-F., Kuhn, U., Stefani, P., Knorr, W., 2014. Global data set of biogenic VOC emissions calculated by the MEGAN model over the last 30 years. Atmos Chem Phys 14, 9317–9341. doi:10.5194/acp-14-9317-2014

MISTRAL project: http://www.mistrals-home.org/

POET: http://accent.aero.jussieu.fr/POET_metadata.php

REAS: https://www.nies.go.jp/REAS/

RETRO: http://accent.aero.jussieu.fr/RETRO_metadata.php

SPECIATE: https://www.epa.gov/air-emissions-modeling/speciate-version-45-through-40

SPECIATE4.5, Environmental Protection Agency of United States of America (EPA), 2016 : https://www.epa.gov/air-emissions-modeling/speciate-version-45-through-40

Figures

Mediterranean Basin (Figure I - 17): https://goo.gl/maps/K26ZFT2fB7

Mediterranean cities and Climate Change – MC3, 2016 (Figure I - 18): http://mc3.lped.fr/Les-caracteristiques-des-villes-Mediterraneennes?lang=en

Megacities EMB (Figure I - 19): https://www.google.fr/maps/@38.8906771,29.6549731,927626m/data=!3m1!1e3?hl=fr

AirmoVOC schemes (Fig. II – 6) : COPYRIGHT of CHROMATO-SUD, 2004, 15 Rue d'Artiguelongue, 33 240, Saint Antoine, France

Nafion dryer (Fig II – 7): http://www.nafionstore.com/pg/19-Nafion-_US.aspx

Nafion substance (Fig. II – 7) : https://www.inacom.nl/gasdrogers-nafion-permeabel.html

Websites

Population: http://appsso.eurostat.ec.europa.eu/nui/submitViewTableAction.do

Sea breeze and land breeze: Encyclopædia Britannica, Inc, 2014 (Figure I - 15) https://www.britannica.com/science/sea-and-land-breeze#/media/1/530591/161945

Sampling with DNPH cartridges (Fig. II –14) : COPYRIGHT of WATERS

TERM001: https://www.eea.europa.eu/data-and-maps/indicators/transport-final-energy-consumption-by-mode/assessment-6

https://www.eea.europa.eu/data-and-maps/dashboards/necd-directive-data-viewer-2 (last assessed 10/09/2019)

https://www.eea.europa.eu/publications/TOP08-98/page004.html

https://www.eea.europa.eu/publications/TOP08-98/page006.html

https://www.who.int/news-room/fact-sheets/detail/ambient-(outdoor)-air-quality-and-health

List of Figures

Chapter 1

Chapter 2

Chapter 4

Chapter 6

List of Tables

Chapter 1

Chapter 2

Chapter 4

Chapter 6

Annex I

Sect. I – A1: Source Apportionment (SA): how-to

For the performance of SA, the main requirement is the acquisition of a dataset of one or more pollutants/compounds. However, for the selection of the appropriate method are considered firstly the sampling location and secondly other parameters like the size and variability of the dataset, the climatology and topography of the sampling site, and information for the major pollutant sources in the immediate vicinity (detailed or not). Thus, in the following paragraphs are presented the main models and methods for SA.

A1.1 Source- and Receptor- oriented models

Starting from the location of the sampling station, there are two categories of SA models; **source-** and **receptor-** oriented models. **Source-oriented models (SM)** are useful for datasets obtained in a proximity to **one specific source**, with no influence from other sources at least for long or certain periods. On the contrary, **receptor-oriented models (RM)** use data from sites that are receptors of air pollution plumes corresponding to background conditions or data from emission inventories. The SM have been used for the direct allocation of aerosols and ozone since they consider various atmospheric processes like transport, chemical reactions, gas-to particle conversion (Kleeman and Cass, 2001; Qiao et al., 2018) (Held et al., 2005; Kleeman and Cass, 2001; Qiao et al., 2018; Ying et al., 2008; Ying and Kleeman, 2006); however they were never used for VOC. Only RM models have been used in the literature for the source allocation of VOC.

A1.2 Receptor-oriented models (RM)

The aim of the RMs is the **identification** of sources and the **quantification** of their emissions. This is achieved by solving a mass balance equation, based on the **fundamental assumption** that the mass is **conserved** during transport. This means that the sum of the emissions of each source is linearly linked to the observed concentrations. The general mass balance equation is described in Eq. I – A1 (Belis et al., 2014):

$$x_{ij} = \sum_{k=1}^{p} g_{ik} f_{kj} + e_{ij} \qquad \text{Eq. I -A 1}$$

where x_{ij} is the concentration of the j^{th} species in the i^{th} sample, g_{ik} the contribution of k^{th} source to the i^{th} sample, f_{kj} the concentration of the j^{th} species in the k^{th} source, and e_{ij} is the residual (i.e. the difference between the measured and modeled values).

It is apparent that to solve the above equation, information on the sources can be useful prior to the modelling, from simple knowledge of the number and type, to the chemical profile of their emissions (Zhang et al., 2018). Based on this information, the RM approaches are classified, as presented in **Fig. I – A1**, depending on the knowledge about sources. According to the figure, multivariate models, Principal Component Analysis (PCA), Positive Matrix Factorization (PMF) or UNMIX are suggested for **little** information on sources, whereas regression models and Chemical Mass Balance (CMB) for **complete** information on sources.

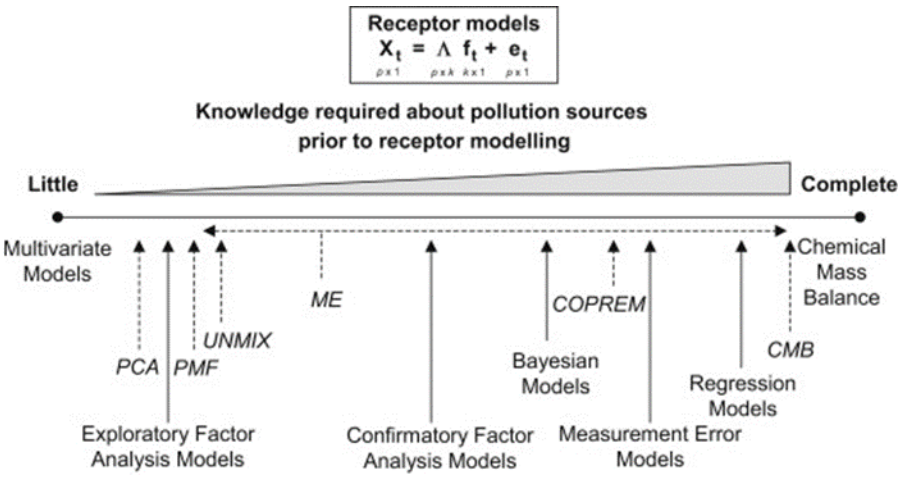

Fig. I - A1: Approaches to estimate pollution sources with RMs (Viana et al., 2008)

Principal component analysis (PCA)

PCA provides a first indication about the nature of the sources and their contribution on the pollutant concentrations, by correlating the variables with a smaller number of independent variables (or factors). The results are calculated using an eigenvector analysis of the correlation matrix (input data) (Hopke, 1991). This method identifies up to 8 sources (factors), but it requires a dataset larger than 50 samples including VOC markers. Important drawbacks of this approach are that the factors need further transformations (rotations) for their explanation, whereas there is no appropriate handling of missing and below-detection-limit data (Guo et al., 2004; Jorquera and Rappenglück, 2004). In addition, Paatero and Tapper (1993) showed that in PCA the scaling of the data can be by column or by row, resulting to distortions in the analysis, due to the bad reproducibility of the scaled data matrix.

The Thurston and Spengler, (1985) introduced the first ever PCA approach, the PCA/APCS method (principal component analysis/absolute principal component scores) to determine sources of particulate matter in Boston. The same method was later adapted by Guo et al., (2004, 2007) for source allocation of VOC in Hong Kong (China), revealing vehicle exhaust as the principal pollution source. Until 2003, PCA was the most frequently used method for source apportionment, however the aforementioned issues lead to its replacement from UNMIX and afterwards from PMF.

UNMIX

The UNMIX was developed as an answer to the limitations of PCA. The basic difference of the method compared to others is the assumption that the composition and contribution of the sources are all positive, which derives from the used geometrical approach and its edge-finding algorithm. In particular, the basic assumption is that there are some datapoints for which a source does not contribute at all or contributes insignificantly compared to the other sources. As a result, the model searches for these “edge points” and fits them in a hyperplane (Henry, 2003; Song et al., 2008). Moreover, the method is strictly non-negative, which may impose limitations for data-series that include negative values with a physical meaning.

Some examples of the application of UNMIX for ambient VOC analysis are given at Helsinki (Finland) by Hellén et al., (2003), Santiago (Chile) by Jorquera and Rappenglück, (2004) and at

Beijing (China) by Song et al., (2008). These previous works provide in addition an inter-comparison of UNMIX to other RM like PMF and CMB for the same data set. The observations indicated that UNMIX can successfully select a representative number of factors/sources in some cases, presenting similar results to PMF and CMB (Hellén et al., 2003; Song et al., 2008), however it couldn't provide a detailed source profile like PMF in the work of Jorquera and Rappenglück, (2004).

Positive Matrix Factorization (PMF)

PMF is another approach that was created to countermeasure the problem of the non-optimal scaling of PCA. In general, PMF estimates the mass contribution of each factor related to a source to VOC measurements (like every PCA and UNMIX method) and it provides the chemical profiles of these factors (Paatero and Tapper, 1994). For that, a large dataset is necessary, but prior knowledge of the sources profile is not needed. The proper scaling of the data is achieved by applying a least-squares formulation of the basic mass balance equation (Eq. I - A1) to the matrices (Paatero, 1997; Paatero and Tapper, 1994). Moreover, over the years the main model was optimized by adding extra features, resulted in the "expanded" and "constrained" PMF. Thus, it is possible to distinguish between sources with very good collinearity by inserting, for example, chemical information on sources, (Hopke, 2016).

In the literature exist many studies in which PMF was used for SA of VOCs. Gaimoz et al., (2011) used PMF on a VOC dataset from Paris (France), resulting in the identification and quantification of 7 factors for the studied period of spring 2007. In this case, traffic-related sources accounted for the majority of the observations. Similarly, the latest PMF source apportionment for VOC in Paris is done by Baudic et al., (2016), which report differences compared to the previous work of Gaimoz et al. Furthermore, Yurdakul et al., (2013) applied PMF for VOC in Ankara (Turkey), with an extending dataset of 6 months and almost 200 samples for every VOC. They revealed 4 factors, with gasoline exhaust having the major contribution. The same source was dominant also in Santiago (Chile) and Beijing (China), as it was reported from Jorquera and Rappenglück (2004) and Song et al., (2008) respectively, who both used PMF and UNMIX for source apportionment. PMF was also used for VOC datasets obtained in heavily industrialized regions like in Dumanoglu et al., (2014) for Aliaga industrial region (Turkey) and for remote sites like in Debevec et al. (2017) in Cyprus (Eastern Mediterranean), where it was shown the effect of geographic location (local and distant). In Eastern Mediterranean, Salameh et al. (2016) reports the first VOC source apportionment in a capital of this region, with traffic-related sources to dominate. Finally, Kaltsonoudis et al. (2016) applied PMF on a VOC dataset obtained in Athens from one-month campaigns in summer 2012 and winter 2013 (PTR-MS measurements) that included aromatics, OVOCs and BVOCs; it gave 5 factors/sources for the two studied seasons, but with different identification in every season.

Chemical Mass Balance (CMB)

For this type of model is required complete prior knowledge of the sources like their chemical profile (**Fig. I – A1**). The number of samples is not important for this method, since it is possible to perform CMB with only one sample. For the application of CMB, a number of assumptions is made (Seinfeld and Pandis 2016):

1. The composition of the source's profile remains constant during the transportation of the plume from the source to the receptor site.

2. The very reactive species are excluded (this assumption is often not followed).

3. The number of sources is less than or equal to the number of species.

Existing CMB models include SPECIATE (EPA, 2016) for VOCs and EPA-CMB v8.2 (EPA, 2005) for particulate matter. Hellén et al., (2006) applied the model to groups of VOC (e.g alkanes, alkenes, aromatics etc) in Helsinki (Finland) using emission profiles deriving from local sources. This work proved that CMB can be used for a large number of different compounds with different properties, although caution is needed for the reactive compounds (e.g. carbonyls and terpenes). In Seoul (Korea), Na and Pyo Kim, (2007) used CMB for the estimation of the diurnal contribution of the sources to VOC concentrations. In addition, they applied a chemical reaction loss effect for the CMB calculation into the standard CMB model to investigate the importance of reaction losses in the CMB calculations. In France, CMB was applied for source apportionment in Dunkerque (France), an urban location influenced by industrial emissions (Badol et al., 2008), since the emission profiles of the sources were already available. Likewise, CMB was used for Pearl River Delta (China), taking into account 12 VOC sources and their emission profile (Liu et al., 2008). The model was able to apportion VOC observations to sources, but it failed to separate sources with similar chemical compositions and to distinct between fresh and aged local air masses.

A1.3 Source allocation from concentration ratios

VOC levels in the atmosphere are affected by the emissions from sources, air mass dilution (horizontal and vertical) and chemical transformation. Moreover, the oldest means of SA was the examination of concentration ratios due to the following reasons:

a) They minimize the effect of atmospheric dilution.
b) Depending on the lifetime of the chosen compounds, the ratio can reflect either the emission from sources or the age of the air mass (due to photochemical depletion).
c) They can be used as tracers of sources when they are determined from measurements close to specific sources. In this context, they can be used for the comparison to observations from other type of sites (e.g. urban background stations). For this case, the reactivity of the compounds should be considered, which is achieved by selecting a study period with reduced or absent photochemistry (night, winter).

For the use of VOC-to-VOC ratios for SA, one compound of the ratio should be used as tracer. In the literature are found many examples of such ratios. Starting with Na and Kim, (2001), they studied the seasonal variation of the four major VOC sources in Seoul, Korea (vehicle exhaust, gasoline evaporation, solvent use and natural gas emissions) through specific VOC-to-sum-of-VOCs ratios (acetylene, i-pentane, TEX – toluene, ethylbenzene, m-p xylenes, and ethane as markers). Likewise, Jobson et al., (2004) compared the source ratio obtained from a tunnel in Houston (U.S.A), to the C1-C10 hydrocarbon data of an urban site outside Houston impacted by a combination of air plumes from major sources of the area. Their objective was to understand the impact of the industrial emissions to the observations, and their findings suggest that light alkanes and alkenes are mainly affected by the natural gas and petrochemical facilities of the area. Similarly, Gilman et al., (2013)

used the i-pentane-to-n-pentane ratio from three representative sources of a Northeastern site in Colorado to examine the influence of oil and natural gas emissions from industrial facilities of the area. The same ratio and the ratio of NMHCs to propane was also used recently by Bourtsoukidis et al. (2019) for the source identification of NMHCs in the Arabian Peninsula.

Benzene has been often used as a marker of sources. Until 1998, it was considered among the main tracers of vehicular exhaust (i. e. Rappenglück et al., 1998; Yurdakul et al., 2013). However, since 1998, regulations were imposed by the European Union (Directive 98/70/EC) for its concentration in fuels, leading to a dramatic decrease of its mixing ratios in ambient air. Thus, nowadays the major emission source of benzene is biomass burning for which it can be considered a good tracer (Baudic et al., 2016; Borbon et al., 2018; Hellén et al., 2008). Besides, toluene has many sources including traffic emissions, evaporation and solvent usage (Borbon et al., 2018; Yurdakul et al., 2013). As a result, a frequently used ratio is the toluene-to-benzene ratio (or the reverse), because it provides information to differentiate traffic and non-traffic sources, although for the interpretation of the results their photochemistry should be considered (toluene is more reactive compared to benzene).

For the estimation of the contribution of one source, an equation is given by Borbon et al. (2018) (derived from an approach developed by Borbon et al., 2003) and is expressed in Eq. I – A2:

$$[X]_a = ([tracer]_a - [tracer]_{bckgd})\ x\ ER_a \qquad \text{Eq. I -A 2}$$

Where $[tracer]_a$ is the concentration of a tracer of the source "a" subtracted by its regional background concentration $[tracer]_{bckgd}$ and ER_a is the urban enhancement emission ratio between the compound X and the tracer of the source "a".

The contribution of more than one sources can be examined by multivariate analysis. For instance, Millet et al., (2005) developed a source-tracer-ratio method for the estimation of the contribution of the different sources on OVOC concentrations in Pittsburg (U.S.A). This method was later adapted in a simpler form, by Legreid et al., (2007) and was applied for OVOC and NMHCs in Zurich (Switzerland). The basic equation is the following (Eq. I - A3):

$$[X]_i = [X]_{i,0} + [X]_{i,comb} + [X]_{i,other} \qquad \text{Eq. I -A 3}$$

Where $[X]_{i,0}$ is the background mixing ratio, $[X]_{i,comb}$ the contribution of the combustion sources and $[X]_{i,other}$ the other sources (for example industrial emissions). The contribution of each source is calculated for every compound based on the characteristic emission ratio X-to-CO (as a marker of vehicle exhaust) that is derived from a second method described in Millet et al., (2005).

A similar equation was used by Gilman et al., (2013), for the estimation of the contribution of combustion and oil - natural gas processes on the observed concentrations (Eq. I - A4). For the analysis, propane was used as a marker of oil and natural gas production, and ethylene as a marker of combustion processes.

$$[VOC] = Bckgd_{VOC} + \{ER'_{propane}\ x\ [propane_o]\} + \{ER'_{ethylene}\ x\ [ethylene_o]\} \qquad \text{Eq. I -A 4}$$

Where $[VOC]$ is the observed mixing ratio of the VOC to be fitted, $Bckgd_{VOC}$ is equal to the minimum observed values, $[propane_o]$ and $[ethylene_o]$ are the observed propane and ethylene

mixing ratios by subtracting their minimum observed, and $ER'_{propane}$ and $ER'_{ethylene}$ are the derived values for VOC emissions ratio relative to propane and ethylene respectively.

Sect. I – A2: Emission inventories: Another tool for VOC sources

For the better understanding of emission inventories, a small summary of their built up and the estimation of their uncertainty is presented in this section. The first steps for the compilation of an emission inventory are to decide the area of investigation, the time of interest and the spatial resolution, which stands for the number of grid cells. Next follows the classification of sources based on the activities of the area and the standard nomenclatures of existing emission inventories. Finally, the studied chemical compounds that occur from the data availability, are grouped into large aggregations.

For the calculation of the emissions, two approaches can be followed, the **bottom-up** and **top-down** approach. For the **top-down** approach, general data obtained from local, regional or global datasets are used and they need further distribution in more details to estimate the emissions of the source category to the relevant grid cells and the desired resolution. The **bottom-up** approach uses the most detailed data series to estimate the emissions for individual sources, then sums them all and calculates the estimations for every grid cell. The latter approach is useful for point sources (stationary). In most studies, both approaches are used for the compilation of an emission inventory (Borbon et al., 2003; François et al., 2005; Waked et al., 2012; Zheng et al., 2009). The emissions of air pollutants from individual sources can be directly computed by equations, like the following (Eq. I – A5):

$$E_{i,s,t} = A_{s,t} \times EF_{i,s} \qquad \text{Eq. I -A 5}$$

where $E_{i,s,t}$ is the quantity of the air pollutant *i* emitted in the air by a particular source *s* at a certain time *t*, $A_{s,t}$ is the activity of the source *s* in the time *t*, and $EF_{i,s}$ is the emission factor of the source s for the air pollutant i. However, for more complex emissions, different equations are proposed based on the complexity (EMEP/EEA report, 2016).

The compilation of an inventory is accompanied by the **uncertainty** of the results. There are various approaches to estimate them which could be **qualitative** or **quantitative** (EMEP/EEA report, 2016; Frey et al., 2007). An example of a quantitative approach is Monte Carlo simulation (Frey et al., 2007). Qualitative approaches (i. e. Monte Carlo simulation) are useful for source categories or pollutants with an adequate number of available data (for example when the bottom-up method is used), while quantitative approaches correspond to cases when quantitative uncertainty analysis cannot be conducted (for example when the top-down method is used) by assessing, for instance, the uncertainty in emission factors (Waked 2012 and references therein).

After the quality control/assurance (QC/QA), the final step is the **verification** of the inventory. This can be achieved by their comparison to other national estimates or independent inventory data. However, ideally, their observations would be directly compared to results from field atmospheric measurements that represent real atmospheric conditions.

Annex II

Table II – A1. Target compounds of sampling campaigns

MOP (C2 – C6 NMHCs)	**Target compounds:** ethane, ethylene, propane, propene, isobutane, n-butane, acetylene, trans-2-butene, 1-butene, isopentane, n-pentane, 1.3-butadiene, 1-pentene, isoprene
MOP (C6 – C12 NMHCs)	**Target compounds:** 2-me-pentane, n-hexane, benzene, isooctane, n-heptane, toluene, n-octane, ethylbenzene, m/p-xylenes, o-xylene, styrene, nonane, α-pinene, β-pinene, propyl-benzene, 1.3.5/1.2.4/1.2.3 Tri-me-benzene, limonene
Winter IOP	**Target compounds:** pentane, isoprene, 2methylpentane, 3methylpentane, hexene, hexane, 22dimethylpentane, 24dimethylpentane, 223trimethylbutane, benzene, 33dimethylpentane, cyclohexane, 2methylhexane, 23dimethylpentane, isooctane, heptane, toluene, hexanal, octane, ethylbenzene, m-xylene, p-xylene, styrene, o-xylene, heptanal, nonane, α-pinene, benzaldehyde, camphene, 3ethyltoluene, 4ethyltoluene, 1.3.5/1.2.4/1.2.3 Tri-ME-benzene, 2ethyltoluene, β-pinene, octanal, decane, limonene, g-terpinene, nonanal, nC11, decanal, nC12, undecanal, nC13, nC14, nC15, nC16
Summer IOP	**Target compounds:** **Charcoal cartridges –** pentane, isoprene, 2methylpentane, 3methylpentane, hexene, hexane, 22dimethylpentane, 24dimethylpentane, 223trimethylbutane, benzene, 33dimethylpentane, cyclohexane, 2methylhexane, 23dimethylpentane, isooctane, heptane, toluene, hexanal, octane, ethylbenzene, m-xylene, p-xylene, styrene, o-xylene, heptanal, nonane, α-pinene, benzaldehyde, camphene, 3ethyltoluene, 4ethyltoluene, 1.3.5/1.2.4/1.2.3 Tri-me-benzene, 2ethyltoluene, β-pinene, octanal, decane, limonene, g-terpinene, nonanal, nC11, decanal, nC12, undecanal, nC13, nC14, nC15, nC16 **DNPH cartridges -** formaldehyde, acetaldehyde, acetone, acroleine, propanal, methylvinylcetone, butenal, 2-butanone, methacroleine, butanal, benzaldehyde, glyoxal, isopentanal, pentanal, m+p-tolualdehyde, methylglyoxal, hexaldehyde
Near-source campaign 1: Attiki Odos Tunnel, Athens	**Target compounds:** **Canisters -** ethane, ethylene, propane, propene, isobutane, n-butane, acetylene, trans-2-butene, 1-butene, isopentane, n-pentane, 1.3-butadiene, 1-pentene, isoprene, 2-me-pentane, n-hexane, benzene, isooctane, n-heptane, toluene, n-octane, ethylbenzene, m/p-xylenes, o-xylene, styrene, nonane, α-pinene, β-pinene, propyl-benzene, 1.3.5/1.2.4/1.2.3 Tri-me-benzene, limonene **Charcoal cartridges –** pentane, isoprene, 2methylpentane, 3methylpentane, hexene, hexane, 22dimethylpentane, 24dimethylpentane, 223trimethylbutane, benzene, 33dimethylpentane, cyclohexane, 2methylhexane, 23dimethylpentane, isooctane, heptane, toluene, hexanal, octane, ethylbenzene, m-xylene, p-xylene, styrene, o-xylene, heptanal, nonane, α-pinene, benzaldehyde, camphene, 3ethyltoluene, 4ethyltoluene, 1.3.5/1.2.4/1.2.3 Tri-me-benzene, 2ethyltoluene, β-pinene, octanal, decane, limonene, g-terpinene, nonanal, nC11, decanal, nC12, undecanal, nC13, nC14, nC15, nC16 **DNPH cartridges -** formaldehyde, acetaldehyde, acetone, acroleine, propanal, methylvinylcetone, butenal, 2-butanone, methacroleine, butanal, benzaldehyde, glyoxal, isopentanal, pentanal, m+p-tolualdehyde, methylglyoxal, hexaldehyde

Near-source campaign 2: Patission traffic station, Athens	**Target compounds:** **Canisters -** ethane, ethylene, propane, propene, isobutane, n-butane, acetylene, trans-2-butene, 1-butene, isopentane, n-pentane, 1.3-butadiene, 1-pentene, isoprene, 2-me-pentane, n-hexane, benzene, isooctane, n-heptane, toluene, n-octane, ethylbenzene, m/p-xylenes, o-xylene, styrene, nonane, α-pinene, β-pinene, propyl-benzene, 1.3.5/1.2.4/1.2.3 Tri-me-benzene, limonene **Charcoal cartridges –** pentane, isoprene, 2methylpentane, 3methylpentane, hexene, hexane, 22dimethylpentane, 24dimethylpentane, 223trimethylbutane, benzene, 33dimethylpentane, cyclohexane, 2methylhexane, 23dimethylpentane, isooctane, heptane, toluene, hexanal, octane, ethylbenzene, m-xylene, p-xylene, styrene, o-xylene, heptanal, nonane, α-pinene, benzaldehyde, camphene, 3ethyltoluene, 4ethyltoluene, 1.3.5/1.2.4/1.2.3 Tri-me-benzene, 2ethyltoluene, β-pinene, octanal, decane, limonene, g-terpinene, nonanal, nC11, decanal, nC12, undecanal, nC13, nC14, nC15, nC16 **DNPH cartridges -** formaldehyde, acetaldehyde, acetone, acroleine, propanal, methylvinylcetone, butenal, 2-butanone, methacroleine, butanal, benzaldehyde, glyoxal, isopentanal, pentanal, m+p-tolualdehyde, methylglyoxal, hexaldehyde

Table II – A2. Composition of the NPL N° D64 1636 (left) and the N° D09 0597 (right).

NPL #D64 1636	PPB	+/-
ethane	4.11	*0.08*
ethylene	4.08	*0.08*
propane	4.07	*0.08*
propene	4.02	*0.08*
i-butane	4.08	*0.08*
n-butane	3.96	*0.08*
acetylene	4.08	*0.08*
trans-2-butene	3.96	*0.08*
1-butene	3.90	*0.08*
cis-2-butene	3.91	*0.08*
i-pentane	3.96	*0.08*
n-pentane	4.02	*0.08*
1,3 butadiene	4.01	*0.08*
trans-2-pentane	3.82	*0.08*
1-pentene	3.89	*0.08*
2-me-pentane	3.96	*0.08*
n-hexane	3.97	*0.08*
isoprene	3.97	*0.08*
n-heptane	3.92	*0.08*
benzene	3.99	*0.08*
i-octane	3.99	*0.08*
n-octane	3.95	*0.08*
toluène	3.94	*0.08*
ethylbenzène	3.89	*0.08*
m-xylene	3.89	*0.08*
p-xylene	3.84	*0.08*
o-xylene	4.00	*0.08*
1,3,5-TMB	4.00	*0.08*
1,2,4-TMB	4.15	*0.08*
1,2,3-TMB	3.89	*0.08*

NPL #D09 0597	PPB	+/-
ethane	2.08	*0.04*
ethylene	2.00	*0.04*
propane	2.10	*0.04*
propene	2.06	*0.04*
i-butane	2.16	*0.06*
n-butane	2.04	*0.04*
acetylene	2.14	*0.11*
trans-2-butene	2.03	*0.04*
1-butene	2.04	*0.04*
cis-2-butene	2.06	*0.04*
i-pentane	2.07	*0.04*
n-pentane	2.07	*0.04*
1,3 butadiene	2.03	*0.04*
trans-2-pentane	2.04	*0.04*
1-pentene	2.04	*0.04*
2-me-pentane	2.08	*0.04*
n-hexane	2.05	*0.04*
isoprene	2.06	*0.05*
n-heptane	2.06	*0.04*
benzene	1.97	*0.04*
i-octane	2.04	*0.04*
n-octane	2.07	*0.04*
toluène	1.97	*0.05*
ethylbenzène	1.97	*0.05*
m/p-xylene	3.95	*0.10*
o-xylene	1.97	*0.05*
1,3,5-TMB	2.01	*0.06*
1,2,4-TMB	1.99	*0.05*
1,2,3-TMB	2.05	*0.06*
(+/-) a-pinene	1.98	*0.10*
(+/-) b-pinene	2.01	*0.10*
limonene	2.03	*0.10*

Sect. II- A1: Analysis of blanks

For the quality control of the sampling and analysis methods of the GCs, blank samples were analyzed from May 2016 and afterwards, although not systematically due to the experimental set up. Furthermore, **one** or **two sampling cycles** of **zero-air** were conducted in parallel for the two instruments, by connecting to the sample port of the instruments either a zero-air bottle (May 2016) or a canister filled with zero-air (after May 2016). This resulted in 18 blank samples for the C6 – C12 GC – FID analyzer and 7 interpretable blanks for the C2 – C6 GC – FID analyzer, the latter due to the identification problems of the C2 – C6 analyzer (Sect. 2.2.1 of chapter 2). **Ethylene**, **acetylene** and **i – pentane** were detected in almost every blank of the GC C2 – C6, whereas **toluene**, **m/p – xylenes** and **o-xylene** were mostly present in the blanks of the GC C6 – C12. In **Table II – A3** the mean concentrations of the compounds in the blanks, as well as their mean values for the whole MOP are given. It is apparent that only for 1.3.5 TMB, 1.2.3 TMB and limonene the detected levels are similar to the mean concentration for the MOP. Unfortunately, considering the unsystematic acquisition of these blanks and the fact that some compounds are not detected in all blank samples, the blank is not subtracted from the standard or the air samples. Nevertheless, the blank is integrated in the calculations for the uncertainty of the concentrations (later in the chapter, **Sect. 2.2.6**)

Table II – A3: Mean concentrations ±STD of the identified C2 – C12 NMHCs in the blanks and in the MOP (February 2016 to February 2017). In the brackets the numbers indicate the representativity of each compound to the blank samples.

NMHCs (ppb)	Mean ±STD in the blanks	Mean ±STD in the MOP
Ethylene	0.07 ±0.02 (2 of 7 BL)	3.12 ±3.88
Acetylene	0.71 ±0.11 (6 of 7 BL)	5.41 ±4.82
i - Pentane	0.09 ±0.05 (6 of 7 BL)	3.08 ±3.59
n - Pentane	0.02 (1 of 7 BL)	0.74 ±0.93
2-me-pentane	0.05 ±0.004 (2 of 18 BL)	1.06 ±1.26
Benzene	0.02 ±0.001 (2 of 18 BL)	0.59 ±0.72
n-Heptane	0.02 (1 of 18 BL)	0.11 ±0.16
Toluene	0.11 ±0.09 (14 of 18 BL)	1.82 ±2.37
n - Octane	0.02 ±0.01 (4 of 18 BL)	0.10 ±0.15
Ethylbenzene	0.04 ±0.04 (8 of 18 BL)	0.30 ±0.40
m- /p-Xylenes	0.08 ±0.06 (15 of 18 BL)	0.95 ±1.27
o-Xylene	0.04 ±0.03 (11 of 18 BL)	0.31 ±0.45
Nonane	0.01 (1 of 18 BL)	0.06 ±0.07
α-Pinene	0.02 ±0.01 (9 of 18 BL)	0.12 ±0.15
1.3.5 TMB	0.07 ±0.03 (5 of 18 BL)	0.06 ±0.12
1.2.4 TMB	0.07 ±0.05 (9 of 18 BL)	0.28 ±0.43
1.2.3 TMB	0.07 ±0.05 (5 of 18 BL)	0.05 ±0.10
Limonene	0.05 ±0.04 (5 of 18 BL)	0.06 ±0.14

Sect. II – A2 Uncertainty of the concentration

Uncertainty due to the integration of the peak in the chromatogram

For the integration of one peak, the user of Vistachrom (**Sect. 2.3** of **this chapter**) has to set some parameters for the establishment of the baseline, thus the peaks could sometimes be integrated lower or higher than normal. Therefore, the uncertainty associated to the integration of the peak has to be considered for every type of sample (ambient air, standard and blank). Following the ACTRIS guidelines (ACTRIS, 2014), this uncertainty is calculated with respect to the Eq. II – A1:

$$u_{int}(A_{ij}) = \frac{\sigma_{i\,j\,int}}{\sqrt{3}} \qquad \text{Eq. II -A1}$$

where $u_{int}(A_{ij})$ is the absolute uncertainty of integration of a compound *i* in the sample *j*, and $\sigma_{i\,j\,int}$ the standard deviation of the 3 different areas obtained for the same peak ($A_{i\,min}$ for higher than normal baseline, $A_{i\,norm}$ for the area of the sample *j* and $A_{i\,max}$ for lower baseline than normal (the area units are UA). In our case we used as reference the chromatograms of the standards.

Uncertainty in the reproducibility of the calibrations

The calibration control charts (**Sect. 2.2.1** of **this chapter**), showed a variation of the relative difference (%) depending mainly on the stability of the instrument. Consequently, an uncertainty of reproducibility should be considered for different periods of stability. For example, for the GC – FID C6 – C12, two periods can be distinguished (**Fig. II – 9**, **Sect. 2.2.1**) associated to two uncertainties of reproducibility. The absolute uncertainty of reproducibility of the area of a compound *i* in the series of NPL samples corresponding to the stability period *k* is calculated following the Eq. II – A2:

$$u_{i\,k\,repro}(A_{i\,k\,NPL}) = \sigma_{i\,k\,NPL} \qquad \text{Eq. II – A2}$$

where $\sigma_{i\,k\,NPL}$ is the standard deviation of the area of the detected peaks of the compound *i* in the series of NPL samples corresponding to the stability period *k* (in UA).

Moreover, for the compounds of the GC C2 – C6, since 2 or 3 stability periods have been identified depending on the compound (**Sect. 2.2.1** of this chapter), 2 or 3 uncertainties of reproducibility have been calculated.

Uncertainty of the VOC concentrations in the NPL standards

The NPL standards are provided with certified mixing ratios and uncertainties for each VOC (**Table II – A2** in Annex II). The uncertainty that will be used is calculated by Eq. II – A3:

$$u\,(C_i)_{NPL} = \frac{U_{i\,NPL}}{2} \qquad \text{Eq. II – A3}$$

Where $u\,(C_i)_{NPL}$ is the absolute uncertainty of the compound *i* in the NPL and $U_{i\,NPL}$ is the extended (K=2) uncertainty of the compound *i* as given by the manufacturer (both in ppb).

Figure II – A1. Regression analysis of the NMHCs determined by the GC – FID C6 - C12 and the off-line method using charcoal cartridges, for the period of the winter IOP 2016 (28/01 – 10/02/2016).

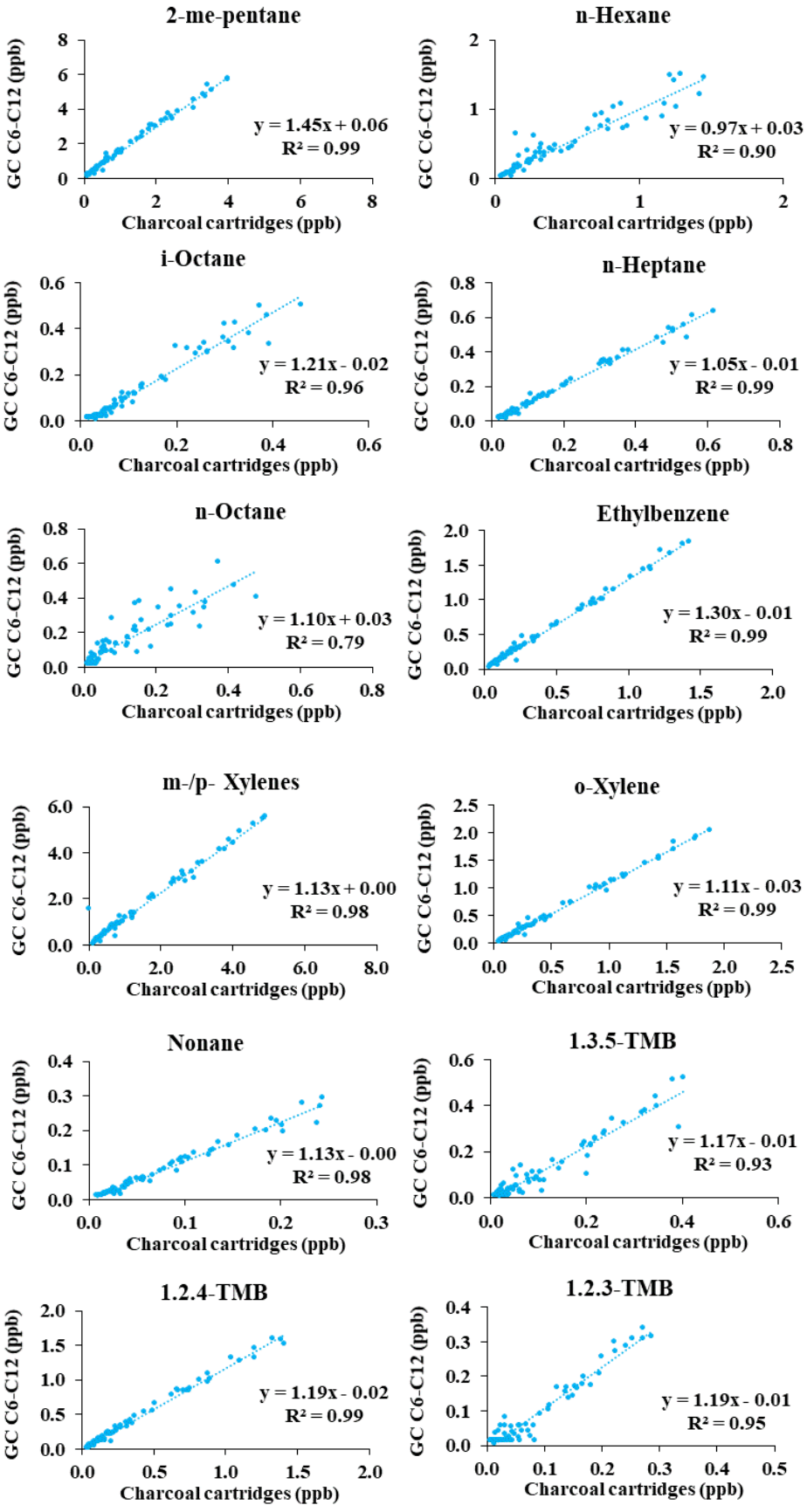

Figure II – A2. Regression analysis of the NMHCs determined by the GC – FID C6 - C12 and the off-line method using charcoal cartridges, for the period of the summer IOP 2016 (02/09 – 23/09/2016).

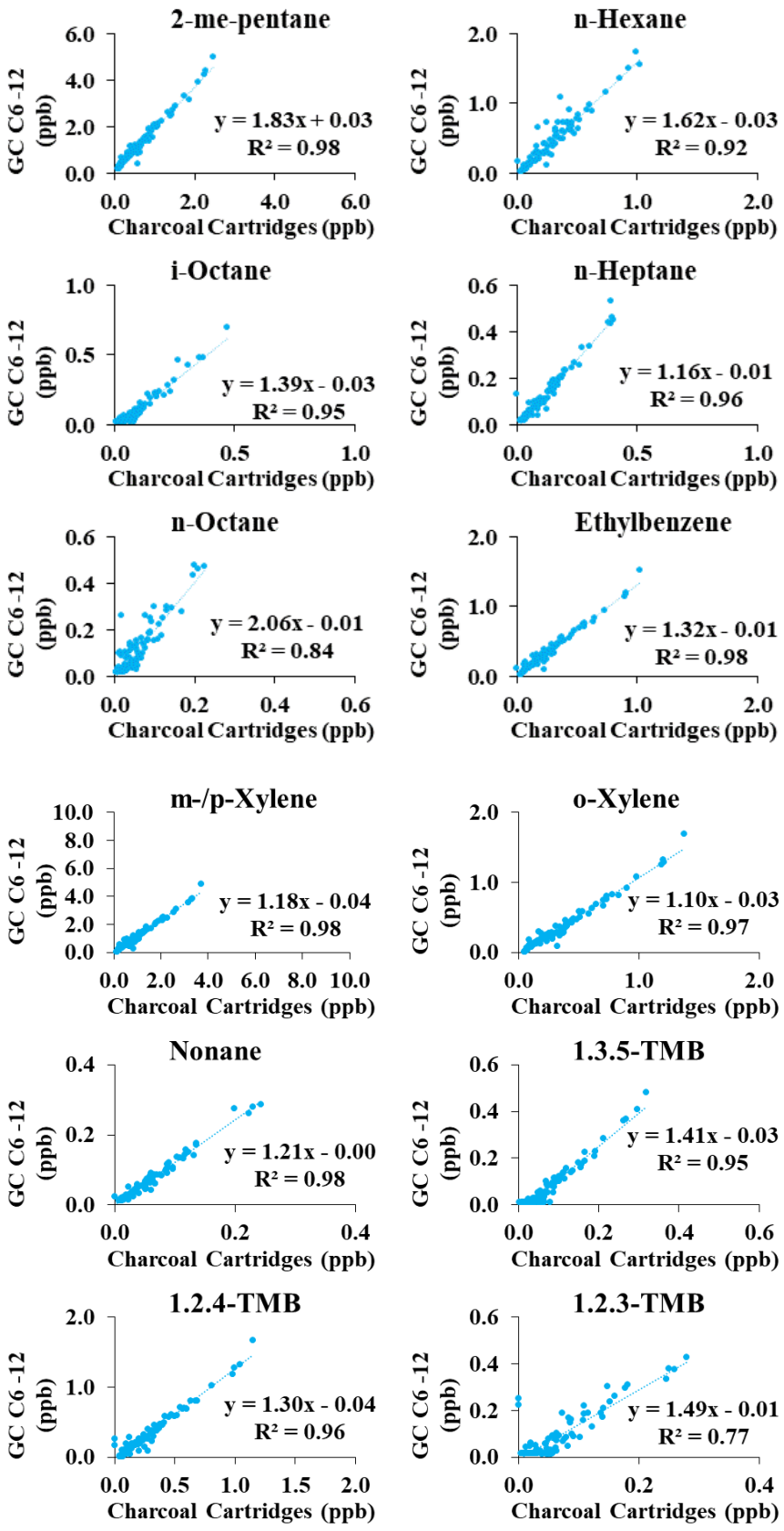

Figure II – A3. Regression analysis of the NMHCs determined by canisters and charcoal cartridges, for the near-source campaign in Patission station in 2017 (22/02 – 24/02/2017).

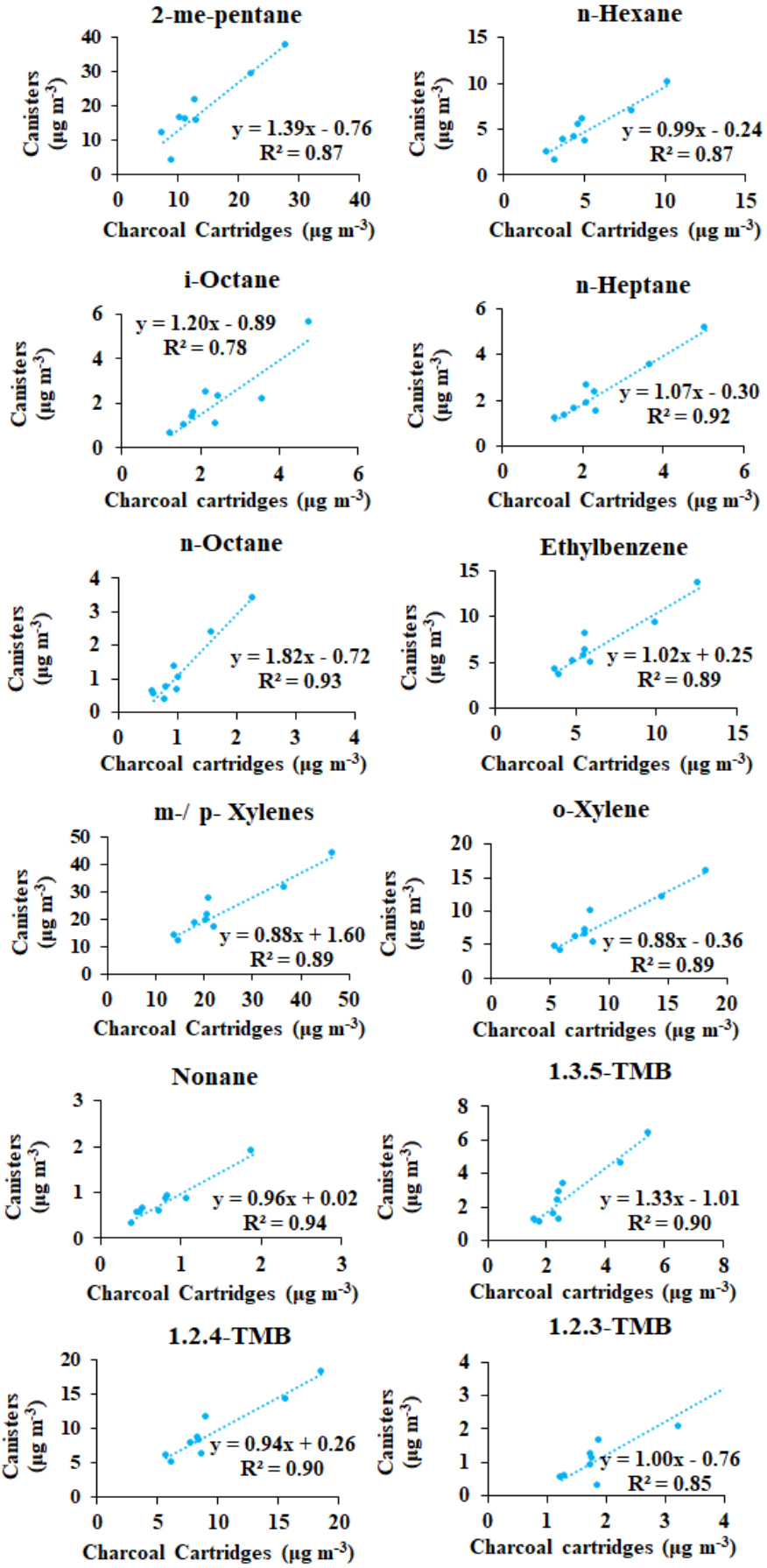

Annex III - Supplementary material of: Non Methane Hydrocarbons variability in Athens during winter-time: The role of traffic and heating

Supplementary material of:

Non Methane Hydrocarbons variability in Athens during winter-time: The role of traffic and heating

Anastasia Panopoulou[1,2,4], Eleni Liakakou[2], Valérie Gros[3], Stéphane Sauvage[4], Nadine Locoge[4], Bernard Bonsang[3], Basil E. Psiloglou[2], Evangelos Gerasopoulos[2], Nikolaos Mihalopoulos[1,2]

[1]Chemistry Department, University of Crete, 71003 Heraklion, Crete, Greece
[2]National Observatory of Athens, Institute for Environmental Research and Sustainable Development, 15236 PaleaPenteli, Greece.
[3]LSCE, Laboratoire des Sciences du Climat et de l'Environnement, Unité mixte CNRS-CEA-UVSQ, CEA/Orme des Merisiers, 91191 Gif sur Yvette Cedex, France.
[4]IMT Lille Douai, Univ. Lille, SAGE - Département Sciences de l'Atmosphère et Génie de l'Environnement, 59000 Lille, France

Correspondence to: Dr. Eleni Liakakou (liakakou@noa.gr)

Section S.1. Complementary figures.

Figure S1. Temporal variability of (a) propane and i-butane; and (b) i- and n - pentane based on hourly averaged levels for the period 16 October 2015 - 15 February 2016, at NOA's urban background site in Thissio, downtown Athens.

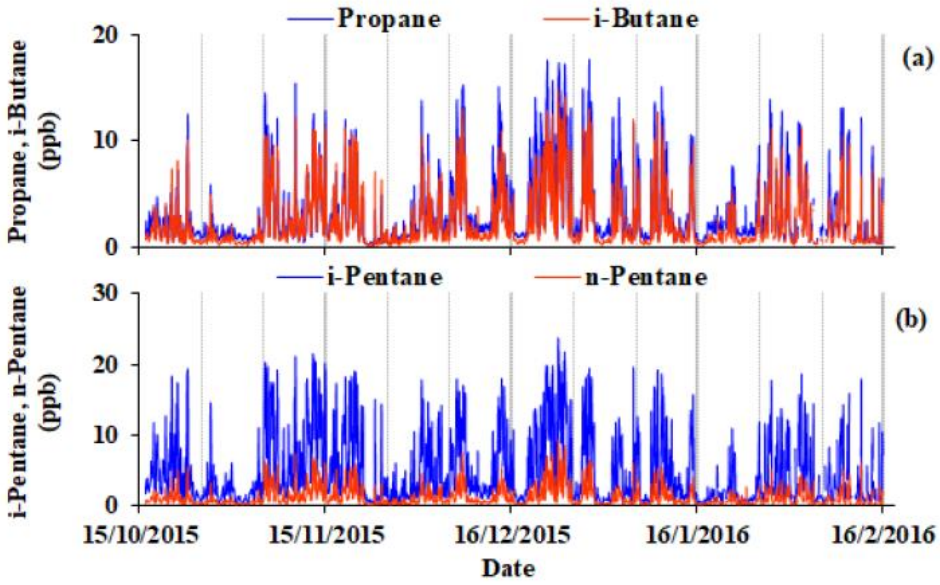

Figure S2. Monthly diurnal variability of (a) ethylene, (b) propane, (c) i-butane, (d) i-pentane and (e) n-pentane based on hourly averaged levels.

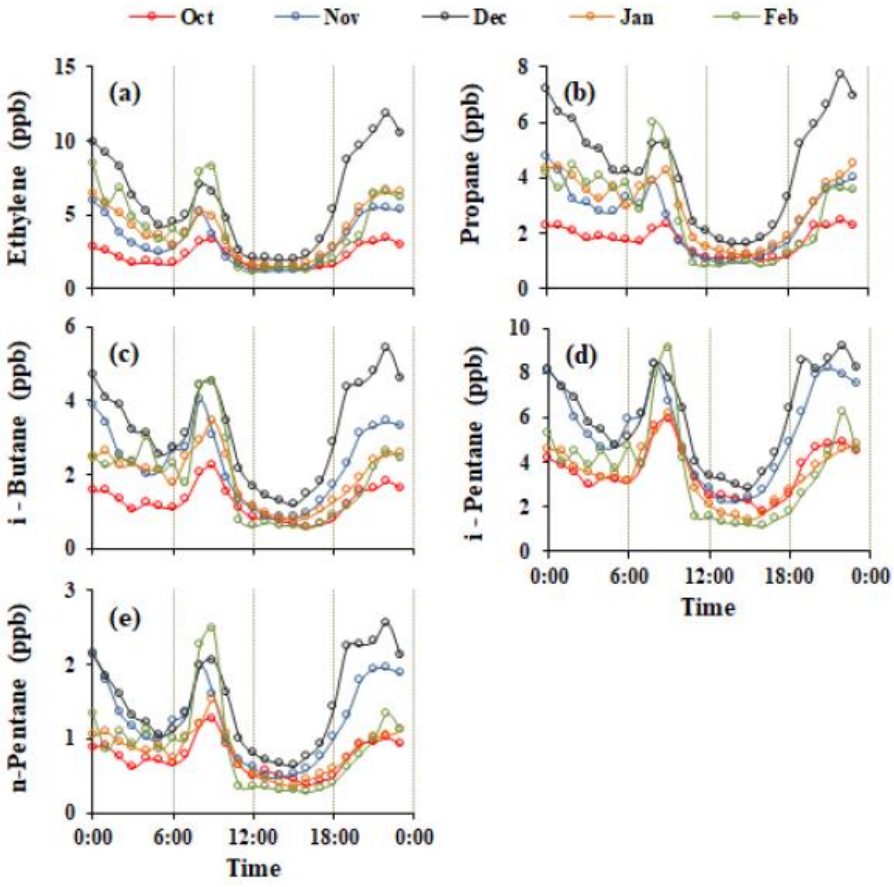

Figure S3. Correlation of (a) ethane, (b) ethylene, (c) propane, (d) propene, (e) i-butane, (f) i-pentane, (g) n-pentane, (h) isoprene, (i) CO, (j) BC, (k) BC_{wb} and (i) BC_{ff} relatively to wind speed for the period 16 October 2015 - 15 February 2016 at the Thissio urban background site.

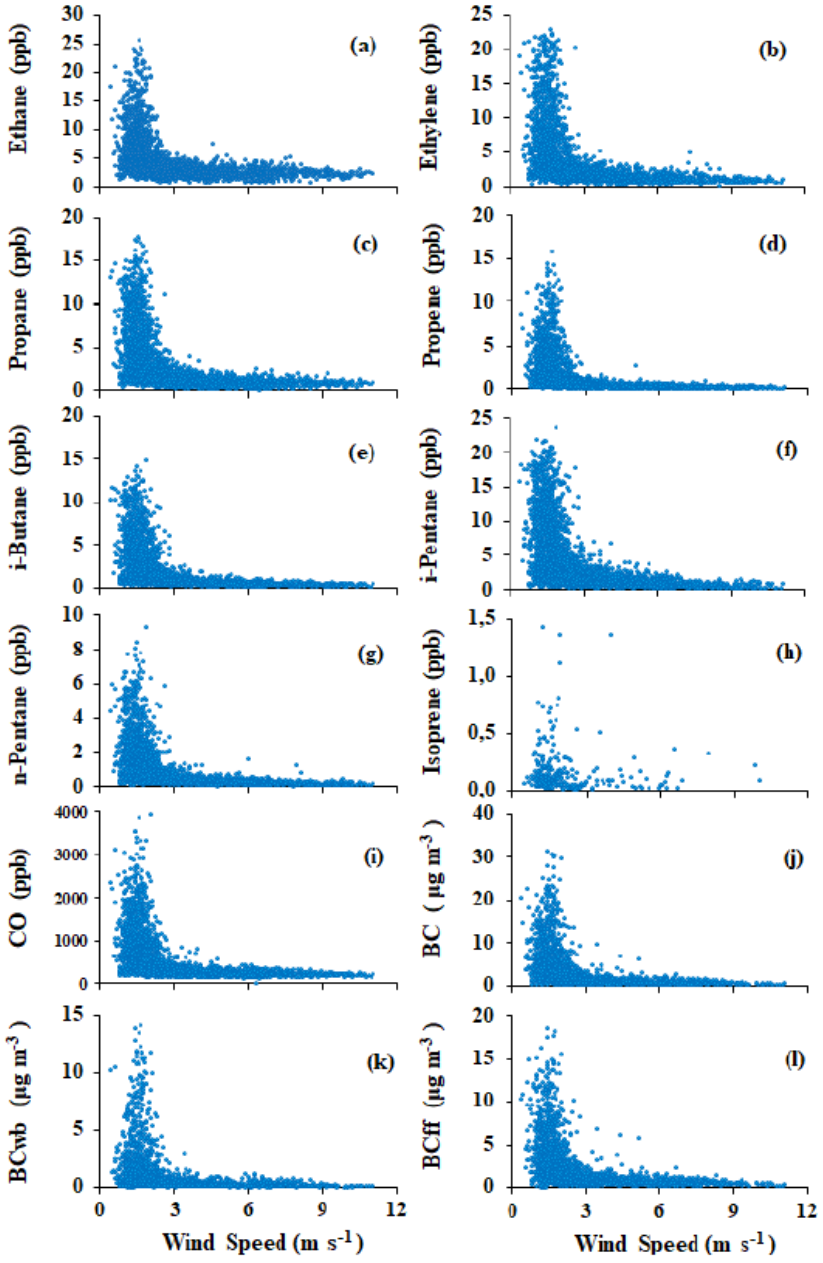

4

Figure S4. Wind rose (a) and concentration roses of (b) ethane, (c) ethylene, (d) propane, (e) propene, (f) i-butane, (g) i-pentane, (h) n-pentane, (i) isoprene, (j) toluene, (k) BC, (l) BC_{ff}, (m) BC_{wb}, (n) CO for the period 16 October 2015 - 15 February 2016 at the Thissio urban background site.

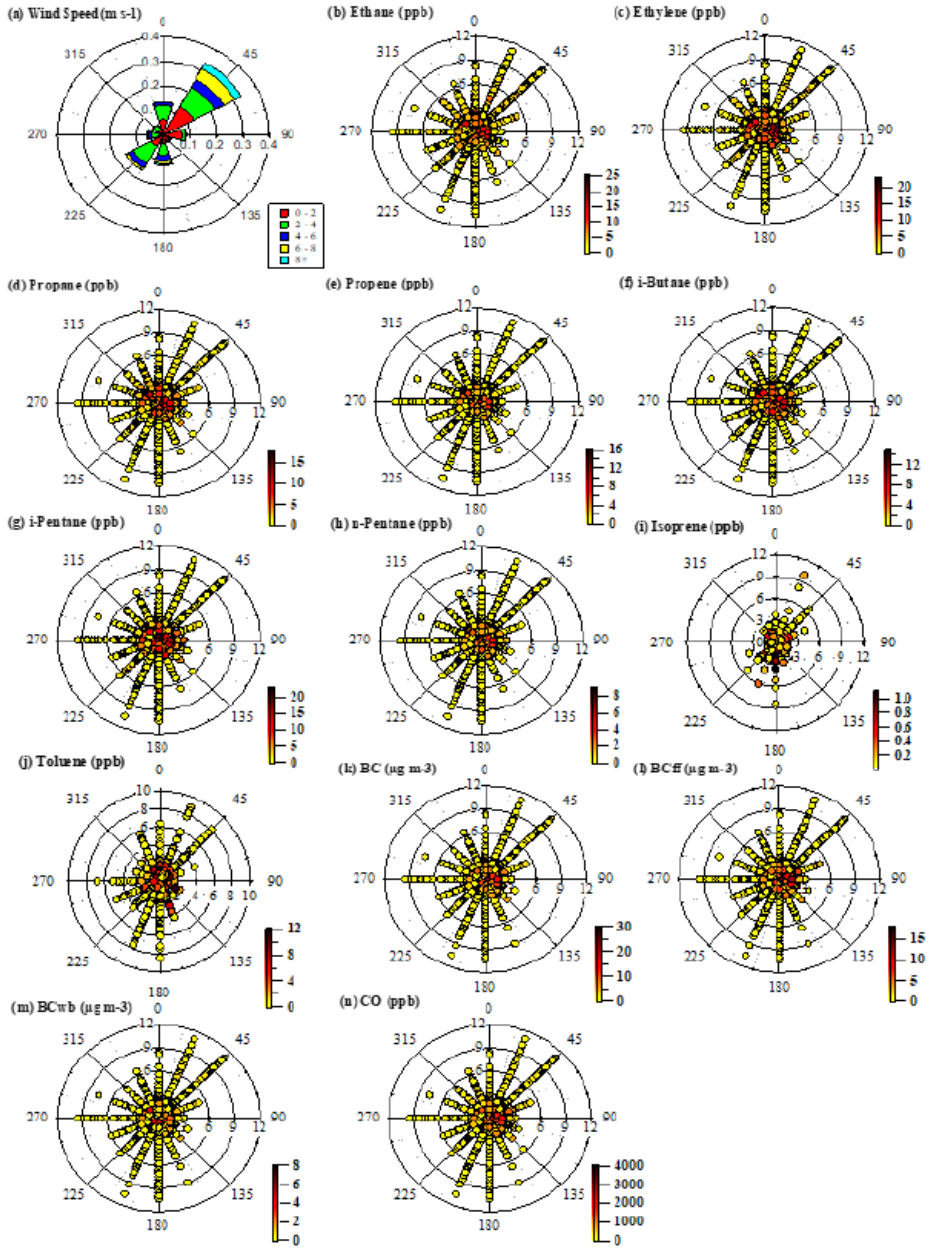

Figure S5. Monthly variability of n-butane, acetylene and benzene relatively to wind speed.

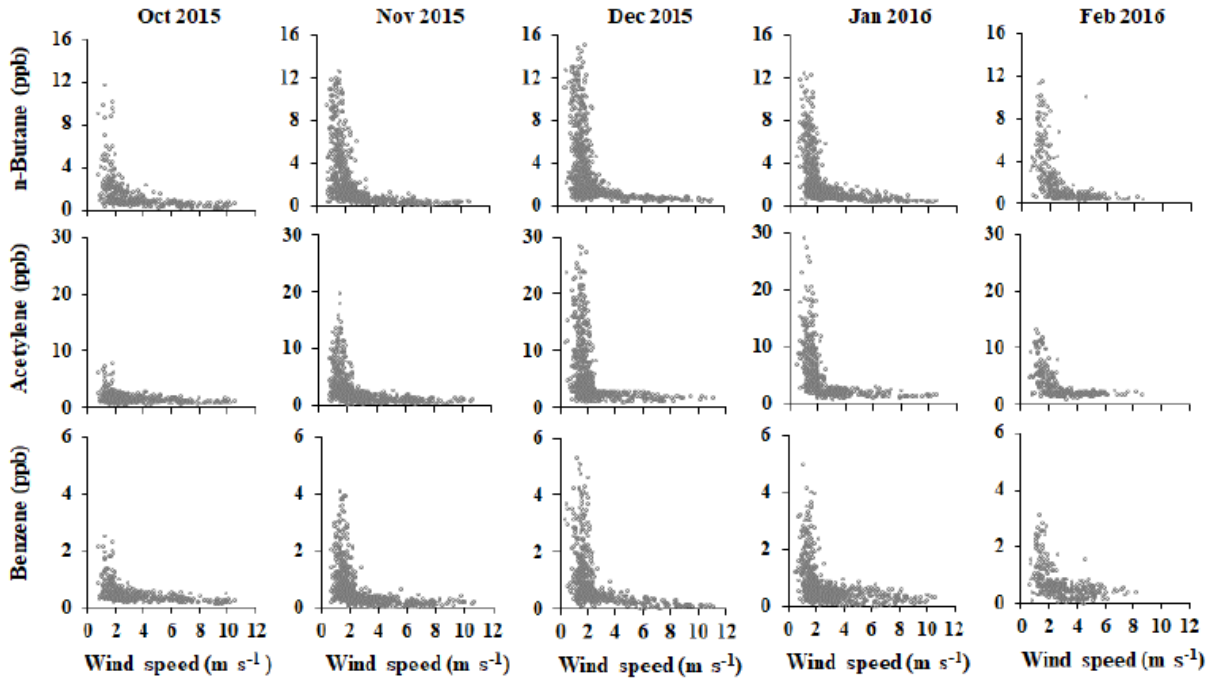

Figure S6. Wind roses for Thissio station for the morning hours (07:00 – 09:00) and night hours (21:00 – 23:00) of October (a-b) and December (c-d); concentration roses of n-butane and acetylene for October morning (07:00 – 09:00) (e-f), October night (21:00 – 23:00) (i-j), December morning (07:00 – 09:00) (g-h) and December night (21:00 – 23:00) (k-l) respectively.

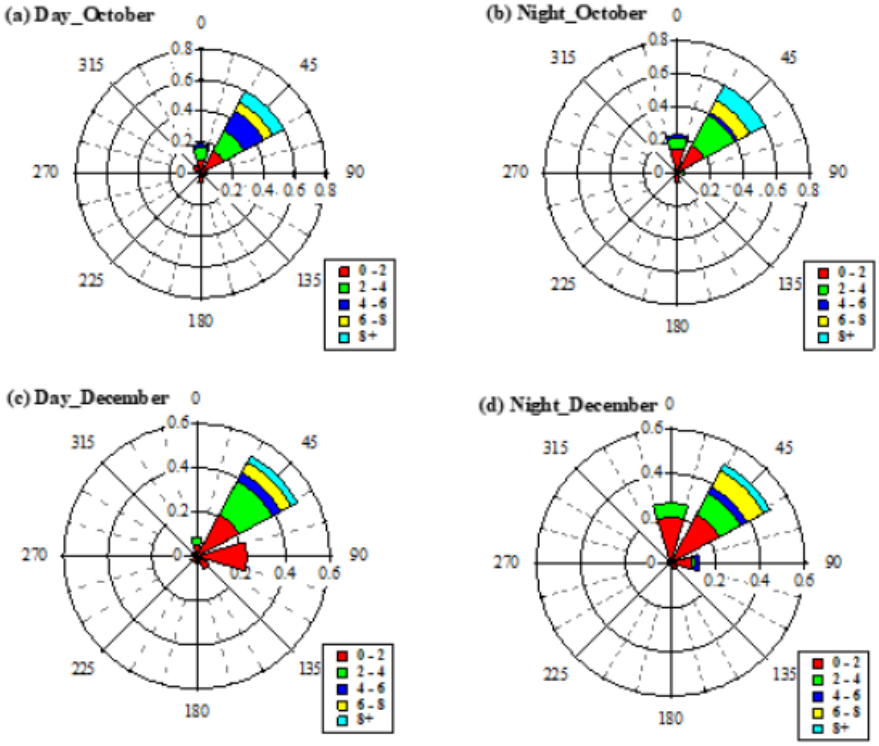

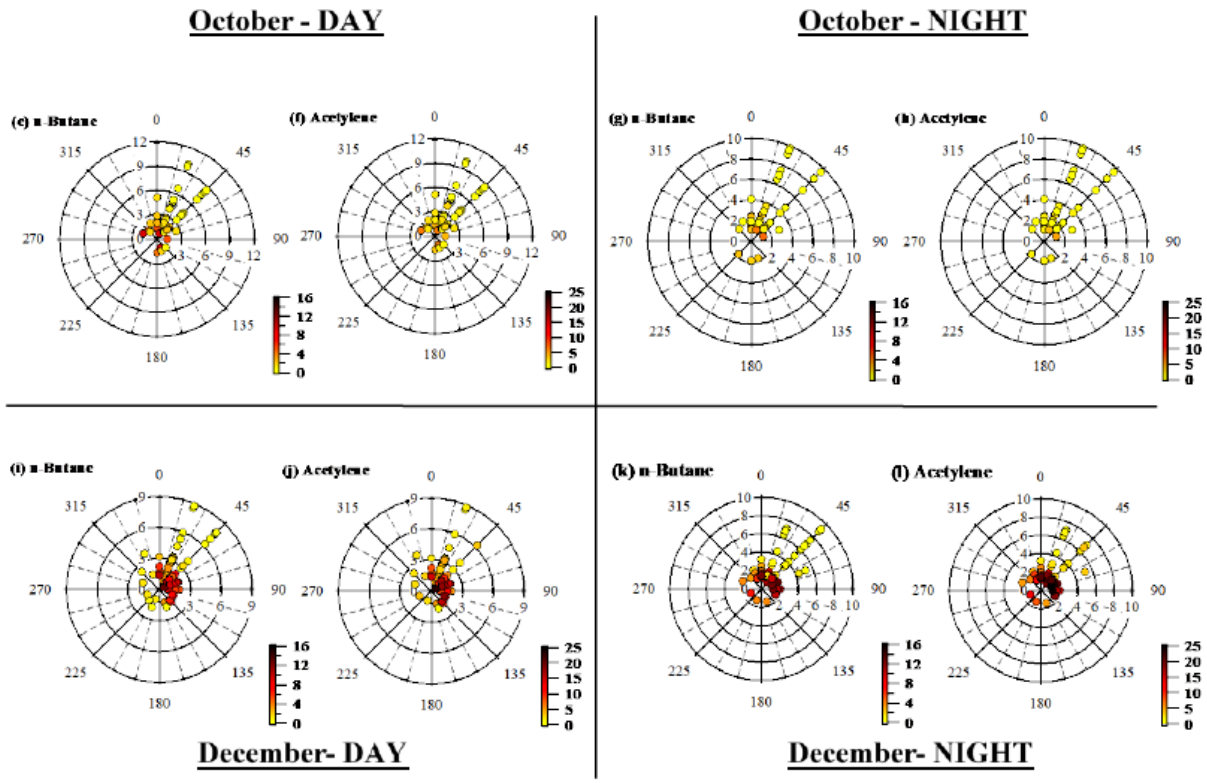
October - DAY
October - NIGHT
(e) n-Butane
(f) Acetylene
(g) n-Butane
(h) Acetylene
(i) n-Butane
(j) Acetylene
(k) n-Butane
(l) Acetylene
December- DAY
December- NIGHT

Figure S7. Monthly variability of (a) n-butane, (b) acetylene,(c) BC_{wb} and (d) BC_{ff} against temperature for the period 16 October 2015 - 15 February 2016 at Thissio urban background site.

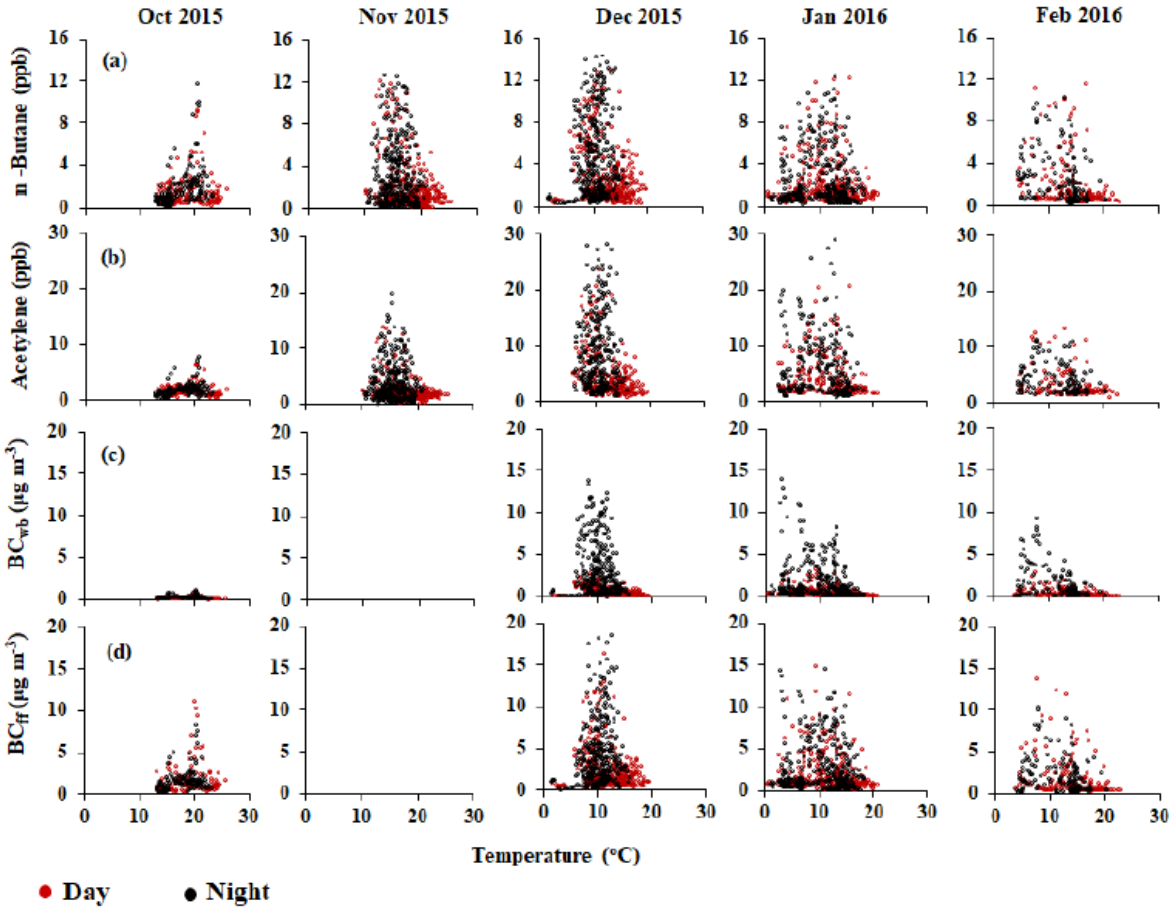

Figure S8. Diurnal patterns of (a) ethane, (b) propane, (c) propene, (d) i-butane, (e) acetylene, (f) n-pentane, (g) BC and (h) BC_{ff} during the SP (left column) and the nSP (right column) periods identified during October 2015 (red) and December 2015 (black) respectively. Note: SP periods are defined by wind-speed lower than 3 ms^{-1} and absence of rainfall, while nSP periods are defined by winds-speeds higher than 3 m s^{-1}.

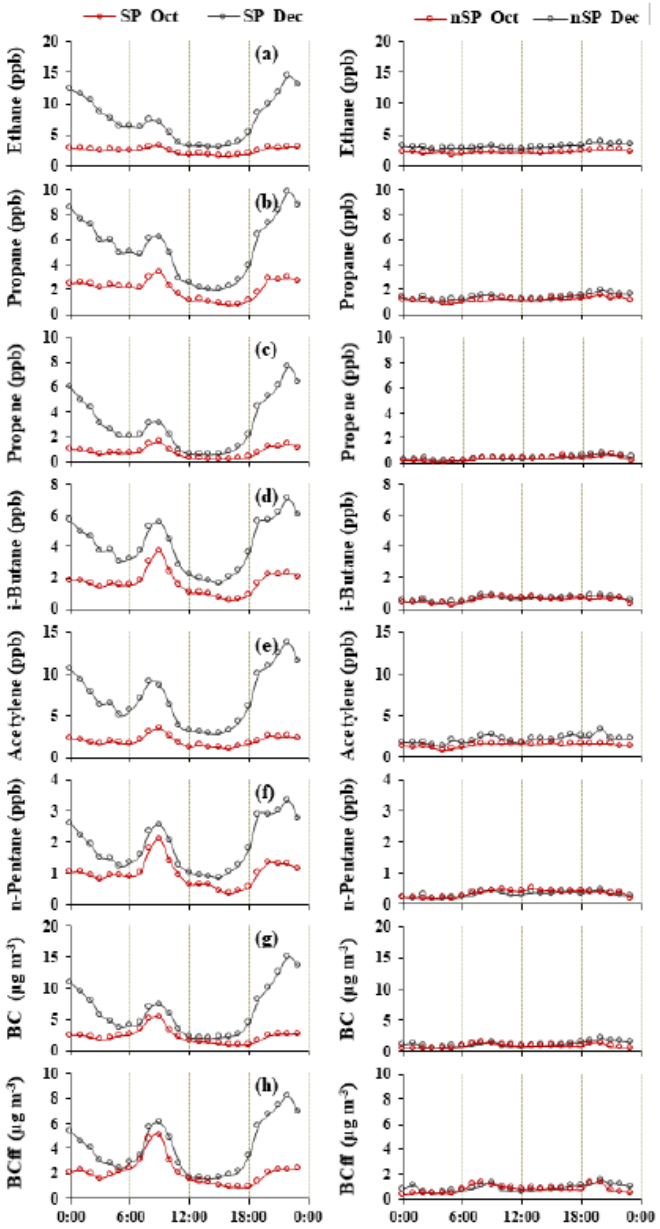

Section S.2.% Mass contribution of the measured NMHCs in the morning peak (Sect. 3.4.3, Fig. 9).

The morning profile of NMHCs at Thissio station was obtained from the measurements of specific SP days of January and February 2016, due to TEX availability. **The first step of the procedure is the conversion of the NMHC concentrations from ppb to μg m^{-3}**, based on Eq. (S1):

$$C_i(\mu g\ m^{-3}) = C_i(ppb)\ x\ \frac{M_i}{24}, \quad \text{(S1)}$$

where $C_i(\mu g\ m^{-3})$ is the calculated concentration of the compound i in μg m^{-3}, $C_i(ppb)$is the concentration of the compound i in ppb, M_i is the molar mass of the compound in g mol^{-1} and the number 24 is the molecular volume of the ideal gas in 1atm and ambient temperature 25°C.

The next step is the calculation of the baseline level that will be subtracted by the morning maximum value in order to minimize the contribution of other sources besides traffic. This is important because the shape of the morning peak is not very clear, as it is depicted in Fig. S9 for i-pentane (motor vehicle exhaust marker, Baudic et al., 2016) for a representative day from the studied period.

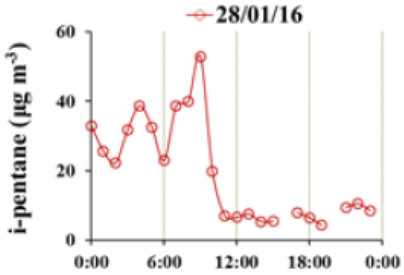

Figure S9. Daily variability of i-pentane for the 28/01/2016.

As a result, the baseline level is given from Eq. (S2), as the average of the measured concentrations at the beginning and the end of the morning peak:

$$C_{baseline,i} = \frac{C_{6,i}+C_{11,i}}{2}, \quad \text{(S2)}$$

where $C_{baseline,i}$ is the calculated baseline level for the compound i in μg m^{-3},$C_{6,i}$ is the concentration of the compound i at 06:00LT and $C_{11,i}$ is the concentration of the compound i at 11:00LT.

Subsequently, the mass contribution of each NMHC for the morning peak is calculated from Eq. (S3):

$$MassContribution_i = \frac{C_{morning,i} - C_{baseline,i}}{\sum_{i=1}^{n} C_i^*}, \quad \text{(S3)}$$

where $MassContribution_i$ is the calculated contribution of the compound i to the total mass of compounds, $C_{morning,i}$ is the maximum morning concentration of the compound i between 07:00 - 10:00LT, $C_{baseline,i}$ is the baseline level of the compound i calculated by the Eq. (S2) and C_i^* is the result of the subtraction of the $C_{baseline,i}$ from the $C_{morning,i}$ for a compound i.

For the morning profile of NMHCs at Patission station the same approach was adapted for the subtraction of the baseline, however, due to the small number of samples, the concentrations of the 06:55 sample were taken as the baseline level. Consequently, the mass contribution of each NMHC for the morning peak of Patission is calculated from Eq. (S4):

$$MassContribution_i = \frac{C_{morning,i} - C_{baseline,i}}{\sum_{i=1}^{n} C_i^*}, \quad \text{(S4)}$$

where $MassContribution_i$ is the calculated contribution of the compound i to the total mass of compounds, $C_{morning,i}$ is the maximum morning concentration of the compound i (in μg m^{-3}) between 08:00 - 10:00LT, $C_{baseline,i}$ is concentration of the compound i of the 06:55 sample (in μg m^{-3}) and C_i^* is the result of the subtraction of the $C_{baseline,i}$ from the $C_{morning,i}$ for a compound i.

Section S.2.a. Tunnel measurements (Sect. 3.4.3, Fig. 9).

Apart from the street canyon measurements described in Sect. 2.4 and Sect. 3.4.3, NMHCs measurements were also conducted in a tunnel at the peripheral highway of Athens, (Attiki Odos), on 12 May 2016 from 12:00 LT to 12:45 LT (LT = UTC+2), to identify the NMHCs fingerprint of traffic emissions. The tunnel's length is 200 m with 3 lanes at each direction and no specific restrictions for heavy duty vehicles. Each driving direction consists of a separated compartment and a ventilation system was installed but not operated. The measurements are performed at the middle of the tunnel length to avoid as much as possible the influence of ambient air from outside. For the sampling 6L stainless steel – silonite canisters were used and the sampling time ranged between 2 and 10 minutes. The sampling method for ambient air is described in details elsewhere (Sauvage et al., 2009). Before the analysis, the cylinders were pressurized by adding a known amount of zero-air resulting in a sample dilution by a factor of two. Afterwards each canister was connected to the GC-FID system using a Teflon (PTFE) sampling line and analyzed by the method described in Sect. 2.2. Before sampling, the canisters were cleaned by filling them up with zero air and re-evacuated, at least three times. The content of the cylinders was then analyzed by the GC-FID system to verify the efficiency of the cleaning procedure. The canisters were evacuated a few days prior to the use and they were analyzed maximum 1 day after the sampling.

To complement the analysis and explanation of the morning peak observed in Thissio and Patission measurements, in Sect. 3.4.3 we compare the mass contribution (%) of NMHCs in the mentioned morning profiles (Sect. 3.4.3, Fig. 9), with the profile derived from the tunnel measurements in Athens (Highway Tunnel - Athens), as well as the profile derived from tunnel measurements conducted 20 Km southern of the center of Paris (France) in autumn 2012 (Highway Tunnel – Paris) (Fig. S10).

The profile of the tunnel measurements of Athens derives as follows: First of all, the NMHC concentrations are converted from ppb to μg m^{-3}, based on Eq. (S1). Secondly, the mass contribution of each NMHC for the Athens Tunnel Profile of is calculated from Eq. (S5):

$$Mass\ Contribution_i = \frac{C_i}{\sum_{i=1}^{n} C_i}, \quad \text{(S5)}$$

where $Mass\ Contribution_i$ is the calculated contribution of the compound i to the total mass of compounds, and C_i is the mean concentration of the compound i (in μg m^{-3}) in the samples of 12:05 & 12:40 LT. Due to the small number of samples a baseline subtraction from the tunnel data was not possible.

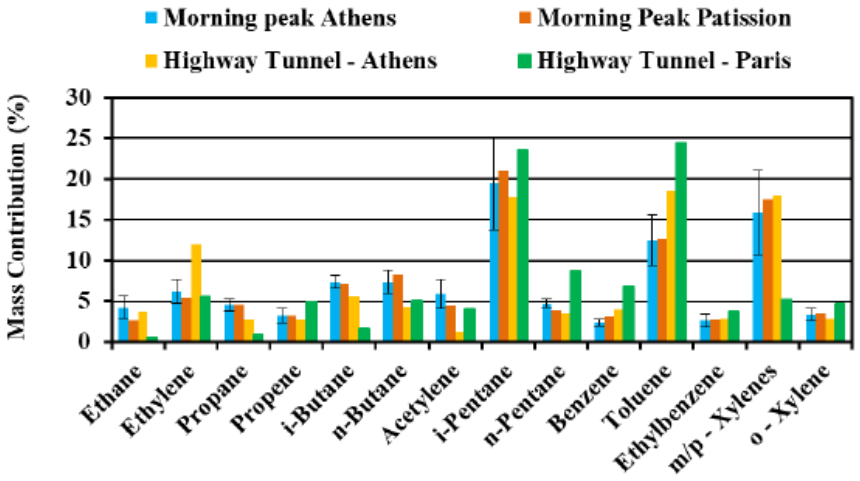

Figure S10. % Mass contribution of the measured NMHCs during the morning peak (07:00 – 10:00 LT), median values in Thissio, mean values in Patission Monitoring Station, in a highway tunnel in GAA and a highway tunnel close to Paris.

The tunnel profiles present a lot of common features as well as a few large discrepancies (R^2 = 0.53), despite the different conditions associated with their profiles (Paris versus Athens, tunnel length, season etc). Again i-pentane and toluene are the two main compounds of the profiles at least in Athens accounting for about 54% of the total measured NMHCs, followed by

n -butane, ethylene and benzene accounting for almost 20% at both sites. The most striking difference between the two tunnels concerns ethylene (factor of 2 higher in Athens compared to Paris), acetylene (factor of 3 lower in Athens compared to Paris), i-butane (factor of 3 lower in Paris than Athens), n-pentane (almost a factor of two higher in Paris compared to Athens) and m-/p- xylenes (almost a factor of 3 lower in Paris compared to Athens). The biggest difference between the two Athens morning peaks and Athens tunnels concerns acetylene and toluene (factor of 4 and 1.5 respectively). The above similarities and differences can be attributed to the car-fleet and the type of fuel used, as it is described in Sect. 3.4.3 of the manuscript.

Section S.3. Investigation of the evaporation losses (Sect. 3.4.3, Fig. 9).

In Sect. 3.4.3, the increased mass contribution of butanes and propane to the morning profiles of Thissio and Patission was attributed to LPG fuels, thus to fuel evaporation. To better investigate this possibility, we followed a similar approach as Na and Kim (2001) for Seoul (South Korea), in order to examine the relationship of the ratio Butanes-to-(C2 – C5)Alkanes (%) and temperature for every month (Fig. S11). More specifically, the ratio of the sum of i-butane and n-butane versus the sum of ethane, propane, i-butane, n-butane, i-pentane and n-pentane for every sample was calculated. Ethylene, propene and acetylene are excluded from this ratio due to their reactivity. The mean and standard deviation values of the ratio were derived for the temperatures between 1°C to 25°C (minimum and maximum of the period respectively). These values were plotted against the temperature for each month. The highest values of the ratio are observed for high temperatures and the lowest for low ambient temperature, although the standard deviation is considerable. It is interesting to note that the same pattern occurs when the ratio Pentanes-to-(C2 – C5)Alkanes (%) versus the temperature is examined (Fig. S12). Taking into account the positive dependence of the two ratios to temperature, we can assume that fuel evaporation losses are also an important source of NMHCs. In addition, the above results could indicate why the Athens tunnel results performed in May differ from Patission and Thissio winter morning profiles.

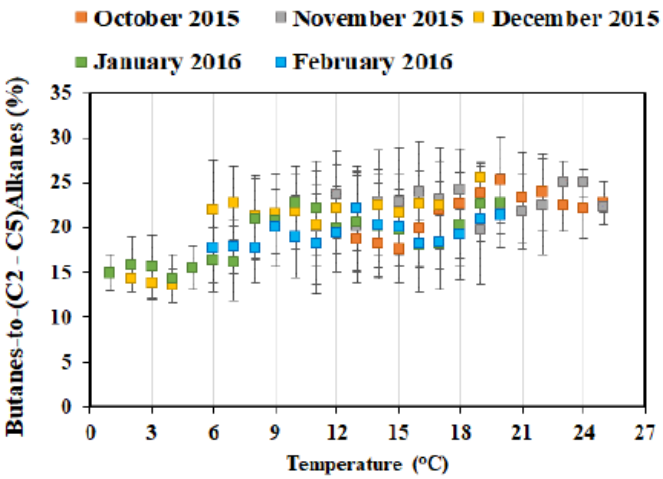

Figure S11. Scatter plots of the ratio Butanes-to-(C2 – C5)Alkanes (%) to temperature for October 2015, November 2015, December 2015, January 2016 and February 2016.

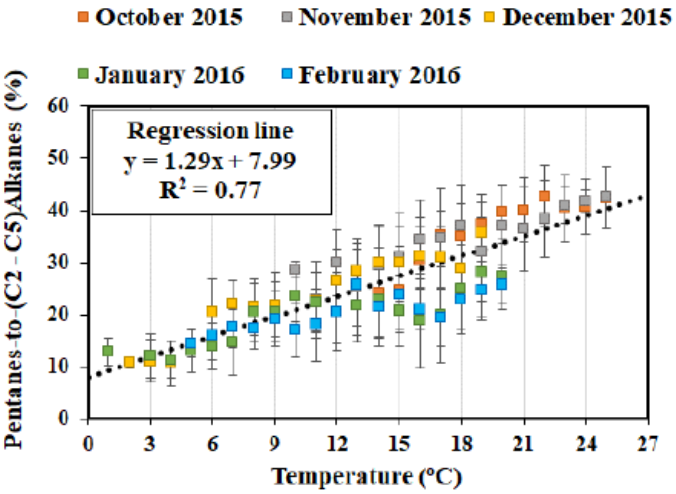

Figure S12. Scatter plots of the ratio Pentanes-to-(C2 – C5)Alkanes (%) to temperature for October 2015, November 2015, December 2015, January 2016 and February 2016.

Furthermore, it is important to mention that Kourtidis et al., (1999) also performed an investigation of the evaporative emissions for Athens with data obtained at a street canyon location (Patission station) in September 1994. To compare our observations from Thissio station with those reported by Kourtidis et al., (1999), the ratio of NMHC/benzene at 15:00 and 07:00 (normalized to the OH reactions) versus the boiling point of selected NMHC was examined, using our data from Thissio station (Fig. S.14). To include more common NMHC with Kourtidis et al., (1999), we used data from 21 January to 15 February 2016, when toluene, ethylbenzene and o-xylene are additionally available. The selected data had wind speed less than 2.8 m s^{-1} to maximize impact from local sources, while at 07:00 and 15:00 LT the mean temperature was approximately 8°C and 12.5°C respectively. Although the examined periods have discrepancies in ambient temperature (winter is colder than autumn), the exponential curve fitting of our data (y = 0.3533e-0.0129x, where x is the boiling point in °C) is very close to the one reported in Kourtidis et al., (1999) (y = 0.44e- 0.0118212T, where T is the boiling point in °C).

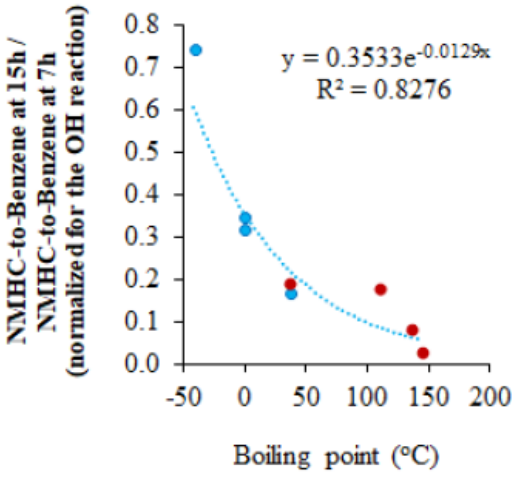

Figure S13. Ratios of the NMHC/benzene ratio for 15:00 and 07:00 to the boiling points of the selected NMHC, divided by the reaction rate constant of each species with OH. The plotted NMHC are propane, i-/n- butane,i-/n-pentane, toluene, ethylbenzene and o-xylene. The red cycles indicate compounds (not values) in common with the work of Kourtidis et al., (1999).

Finally, we examine the monthly variation of i-butane relatively to n-butane (Fig. S13). The two compounds have linear relationship with no significant temporal differences on the slopes (only October and December equations are presented). In addition, the regression is similar to the one derived from the Patission measurements (depicted on Fig. S13), thus supporting our assumption that the observations are traffic related.

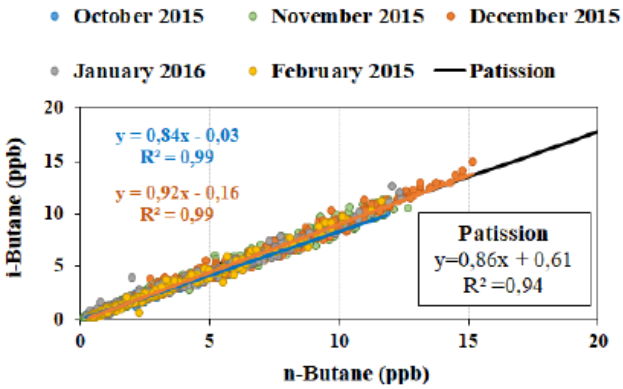

Figure S14. Scatter plots between i-butane relatively to n-butane for October 2015, November 2015, December 2015, January 2016 and February 2016 for the Thissio site. The black line corresponds to the Patission data regression.

Section S.4. %Mass contribution of the measured NMHCs in the night-time enhancement period (Sect. 3.4.3, Fig. 11).

The night profile of NMHCs at Thissio station was obtained from the measurements of specific SP nights of October and December 2015, due to their different temperature condition (October is warmer than December) that influence the need for residential heating. **The first step of the procedure is the conversion of the NMHC concentrations from ppb to μg m^{-3}**, based on Eq. (S1).

The next step is the determination of the baseline level that will be subtracted by the night maximum value (between 22:00 and 23:00 LT) as it is also seen in Fig. 4 and Fig. 8. For that purpose, the minimum concentration of each compound between 12:00 LT – 17:00 LT is used.

Subsequently, the mass contribution of each NMHC for the night peak is calculated from Eq. (S6):

$$MassContribution_i = \frac{C_{night,i} - C_{baseline,i}}{\sum_{i=1}^{n} C_i^*}, \quad \text{(S6)}$$

where $MassContribution_i$ is the calculated contribution of the compound i to the total mass of compounds, $C_{night,i}$ is the maximum night concentration of the compound i between 22:00 - 23:00LT, $C_{baseline,i}$ is the minimum concentration of the compound i for the same date between 12:00 – 17:00 LT and C_i^* is the result of the subtraction of the $C_{baseline,i}$ from the $C_{night,i}$ for a compound i.

References

Baudic, A., Gros, V., Sauvage, S., Locoge, N., Sanchez, O., Sarda-Estève, R., Kalogridis, C., Petit, J.-E., Bonnaire, N., Baisnée, D., Favez, O., Albinet, A., Sciare, J. and Bonsang, B.: Seasonal variability and source apportionment of volatile organic compounds (VOCs) in the Paris megacity (France), AtmosChem Phys, 16(18), 11961–11989, doi:10.5194/acp-16-11961-2016, 2016.

Kourtidis, K. A., Ziomas, I. C., Rappenglueck, B., Proyou, A. and Balis, D.: Evaporative traffic hydrocarbon emissions, traffic CO and speciated HC traffic emissions from the city of Athens, Atmos. Environ., 33(23), 3831–3842, doi:10.1016/S1352-2310(98)00395-1, 1999.

Na, K. and Kim, Y. P.: Seasonal characteristics of ambient volatile organic compounds in Seoul, Korea, Atmos. Environ., 35(15), 2603–2614, 2001.

Annex IV

Table IV - A1: Correlation coefficients (R^2) for the NMHC of the main campaign for the period 16 October 2015 to 28 February 2017. The bold and italics indicate very good relationships ($R^2 > 0.69$). All the relationships are statistically significant at the 95% confidence level.

	Ethane	Ethylene	Propane	Propene	i-Butane	n-Butane	Acetylene	Trans-2-butene	1-Butene	i-Pentane	n-Pentane	Isoprene	Benzene	2-me-Pentane	n-Hexane	i-Octane	n-Heptane	Toluene	n-Octane	Ethylbenzene	m-/p-Xylenes	o - Xylene	Nonane	1.3.5-TMB	1.2.4-TMB	1.2.3-TMB	a-Pinene
Ethane	1.00																										
Ethylene	***0.81***	1.00																									
Propane	***0.76***	***0.85***	1.00																								
Propene	***0.75***	***0.88***	***0.89***	1.00																							
i-Butane	0.64	***0.81***	***0.91***	***0.83***	1.00																						
n-Butane	0.64	***0.81***	***0.93***	***0.82***	***0.97***	1.00																					
Acetylene	0.66	***0.71***	***0.70***	***0.74***	0.69	0.66	1.00																				
Trans-2-butene	0.62	***0.79***	***0.84***	***0.84***	***0.91***	***0.86***	0.68	1.00																			
1-Butene	0.69	***0.84***	***0.87***	***0.91***	***0.93***	***0.88***	***0.75***	***0.94***	1.00																		
i-Pentane	0.49	***0.71***	***0.78***	***0.71***	***0.91***	***0.89***	0.60	***0.83***	***0.82***	1.00																	
n-Pentane	0.50	***0.71***	***0.79***	***0.72***	***0.92***	***0.89***	0.63	***0.86***	***0.86***	***0.93***	1.00																
Isoprene	0.00	0.00	0.00	0.00	0.00	0.00	0.03	0.00	0.00	0.00	0.01	1.00															
Benzene	0.53	***0.75***	***0.78***	***0.71***	***0.89***	***0.88***	0.65	***0.80***	***0.82***	***0.92***	***0.92***	0.01	1.00														
2-me-Pentane	0.44	0.64	***0.71***	0.61	***0.81***	***0.82***	0.55	0.66	0.70	***0.84***	***0.87***	0.00	***0.90***	1.00													
n-Hexane	0.69	***0.85***	***0.82***	***0.88***	***0.81***	***0.82***	0.64	***0.75***	***0.83***	***0.70***	0.69	0.00	***0.81***	0.70	1.00												
i-Octane	0.51	***0.71***	***0.75***	***0.75***	***0.84***	***0.84***	0.65	***0.78***	***0.81***	***0.81***	***0.81***	0.00	***0.91***	***0.80***	***0.84***	1.00											
n-Heptane	0.58	***0.75***	***0.83***	***0.75***	***0.90***	***0.90***	0.66	***0.81***	***0.84***	***0.87***	***0.89***	0.00	***0.95***	***0.89***	***0.83***	***0.92***	1.00										
Toluene	0.51	***0.73***	***0.79***	***0.71***	***0.87***	***0.87***	0.61	***0.77***	***0.80***	***0.87***	***0.86***	0.00	***0.94***	***0.88***	***0.81***	***0.89***	***0.93***	1.00									
n-Octane	0.46	0.65	***0.72***	0.63	***0.81***	***0.81***	0.56	0.69	***0.73***	***0.81***	***0.82***	0.00	***0.87***	***0.87***	***0.72***	***0.82***	***0.89***	***0.89***	1.00								
Ethylbenzene	0.55	***0.77***	***0.81***	***0.75***	***0.90***	***0.90***	0.66	***0.82***	***0.84***	***0.90***	***0.90***	0.00	***0.98***	***0.88***	***0.84***	***0.93***	***0.95***	***0.96***	***0.89***	1.00							
m-/p- Xylenes	0.55	***0.77***	***0.81***	***0.75***	***0.90***	***0.89***	0.66	***0.82***	***0.84***	***0.89***	***0.88***	0.00	***0.97***	***0.87***	***0.85***	***0.93***	***0.95***	***0.96***	***0.88***	0.99	1.00						
o - Xylene	0.55	***0.77***	***0.80***	***0.75***	***0.90***	***0.89***	0.67	***0.82***	***0.84***	***0.89***	***0.88***	0.00	***0.97***	***0.86***	***0.85***	***0.94***	***0.95***	***0.95***	***0.86***	***0.99***	0.99	1.00					
Nonane	0.49	0.61	***0.77***	0.60	***0.79***	***0.83***	0.53	0.66	0.68	***0.80***	***0.81***	0.00	***0.84***	***0.84***	0.66	***0.77***	***0.89***	***0.86***	***0.83***	***0.84***	***0.83***	***0.82***	1.00				
1.3.5-TMB	0.54	***0.73***	***0.79***	***0.74***	***0.86***	***0.87***	0.64	***0.81***	***0.82***	***0.83***	***0.83***	0.00	***0.91***	***0.81***	***0.82***	***0.93***	***0.92***	***0.91***	***0.83***	***0.93***	***0.94***	***0.94***	***0.82***	1.00			
1.2.4-TMB	0.55	***0.76***	***0.82***	***0.79***	***0.89***	***0.90***	0.67	***0.81***	***0.85***	***0.87***	***0.85***	0.00	***0.95***	***0.84***	***0.88***	***0.93***	***0.94***	***0.95***	***0.85***	***0.97***	***0.97***	***0.97***	***0.84***	***0.94***	1.00		
1.2.3-TMB	0.43	0.62	0.70	0.64	***0.76***	***0.78***	0.59	***0.71***	***0.71***	***0.73***	***0.76***	0.00	***0.82***	***0.73***	0.69	***0.84***	***0.82***	***0.81***	***0.74***	***0.83***	***0.83***	***0.83***	***0.77***	***0.87***	***0.83***	1.00	
a-Pinene	0.29	0.41	0.47	0.43	0.49	0.51	0.42	0.45	0.45	0.46	0.45	0.02	0.46	0.42	0.41	0.43	0.47	0.47	0.44	0.46	0.47	0.45	0.49	0.44	0.48	0.45	1.00
Limonene	0.60	***0.71***	***0.75***	***0.74***	***0.74***	***0.74***	0.61	***0.79***	***0.76***	0.62	0.64	0.01	***0.71***	0.58	***0.74***	***0.75***	***0.74***	0.68	0.63	***0.73***	***0.73***	***0.74***	0.65	***0.77***	***0.75***	***0.74***	0.48

Fig. IV - A1: Temporal variability of selected NMHCs from 16 October 2015 to 28 February 2017 for the C2 – C6 NMHCs and from 1 February 2016 to 28 February 2017 for the C6 – C12. The mean hourly values are utilized.

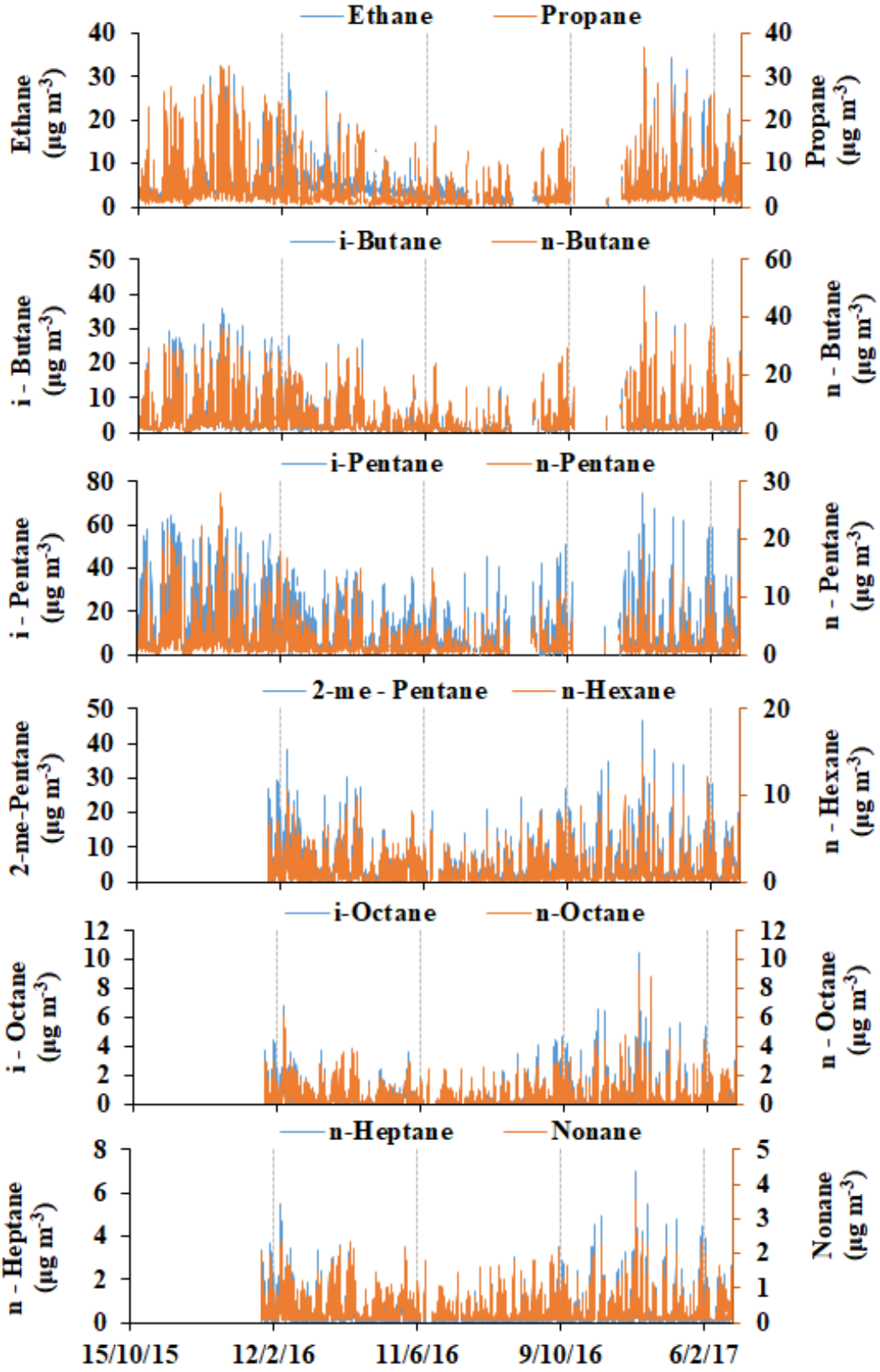

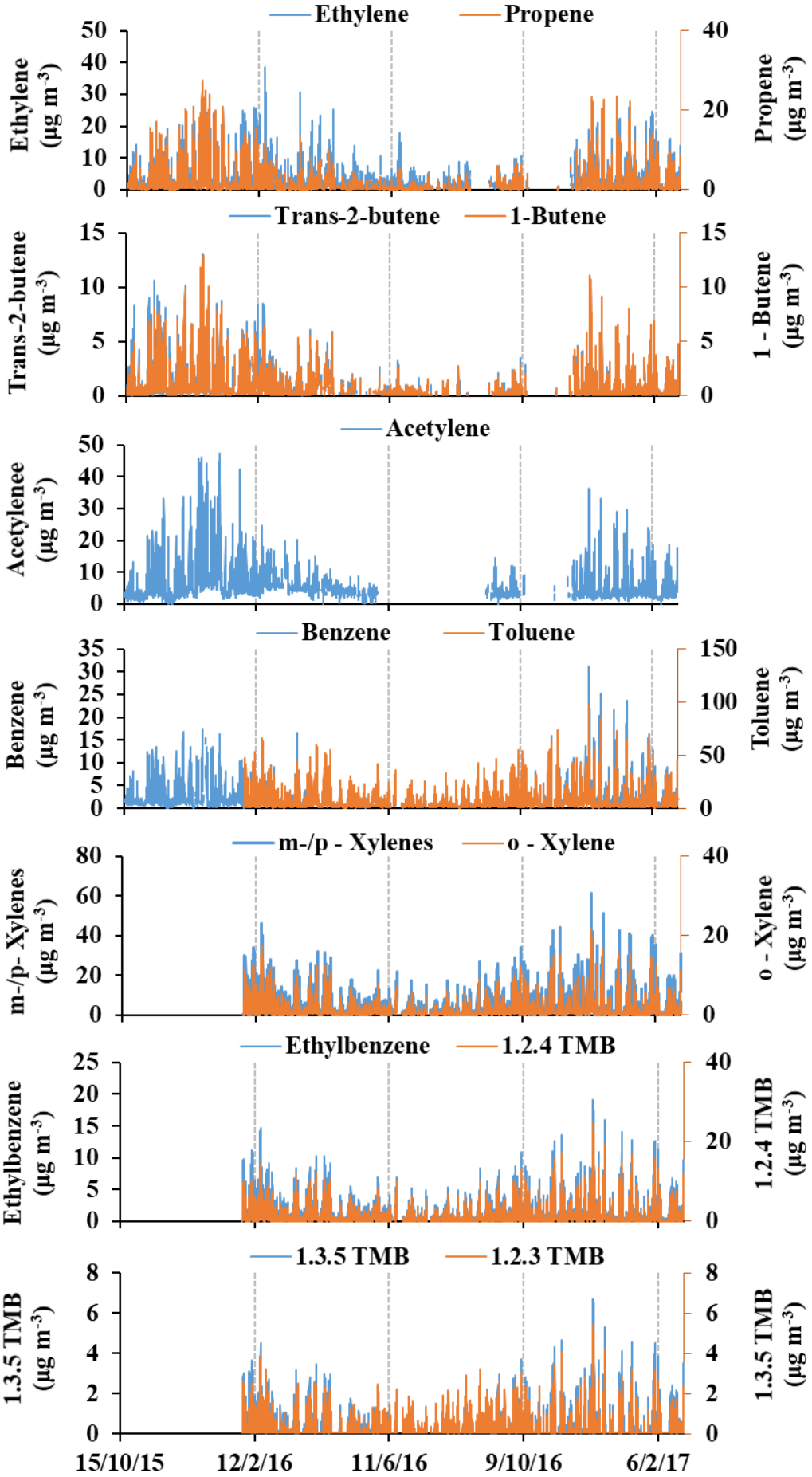
Ethylene
Propene
Ethylene (µg m-3)
Propene (µg m-3)
Trans-2-butene
1-Butene
Trans-2-butene (µg m-3)
1 - Butene (µg m-3)
Acetylene
Acetylenee (µg m-3)
Benzene
Toluene
Benzene (µg m-3)
Toluene (µg m-3)
m-/p - Xylenes
o - Xylene
m-/p- Xylenes (µg m-3)
o - Xylene (µg m-3)
Ethylbenzene
1.2.4 TMB
Ethylbenzene (µg m-3)
1.2.4 TMB (µg m-3)
1.3.5 TMB
1.2.3 TMB
1.3.5 TMB (µg m-3)
1.3.5 TMB (µg m-3)
15/10/15
12/2/16
11/6/16
9/10/16
6/2/17

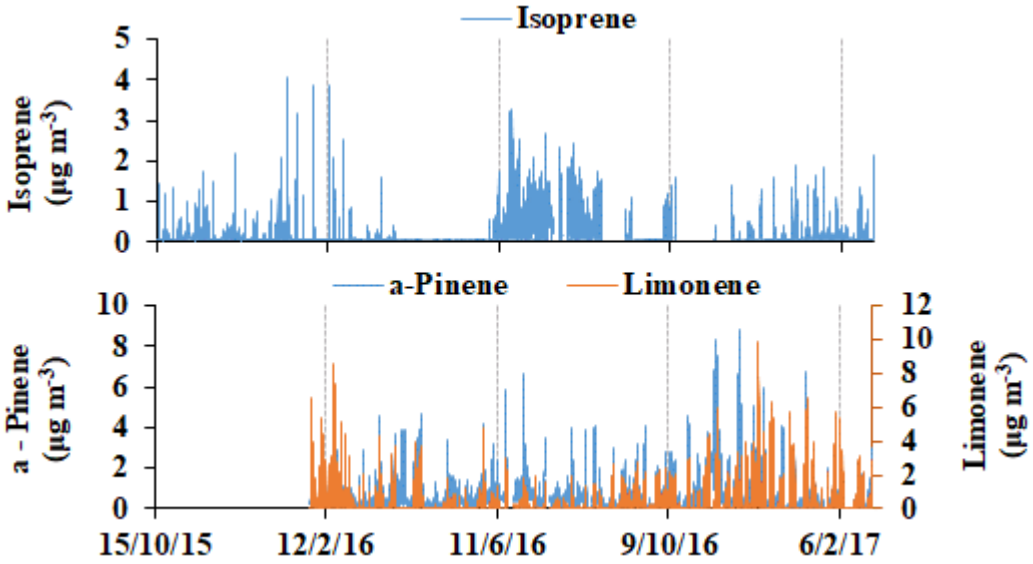
Isoprene
Isoprene (µg m-3)
5
4
3
2
1
0
a-Pinene
Limonene
a - Pinene (µg m-3)
10
8
6
4
2
0
12
10
8
6
4
2
0
Limonene (µg m-3)
15/10/15
12/2/16
11/6/16
9/10/16
6/2/17

Fig. IV - A2: Seasonal diurnal variability of C2 – C6 NMHCs for the period 16 October 2015 to 28 February 2017, and for C6 – C12 NMHCs from 1 March 2016 to 28 February 2017.

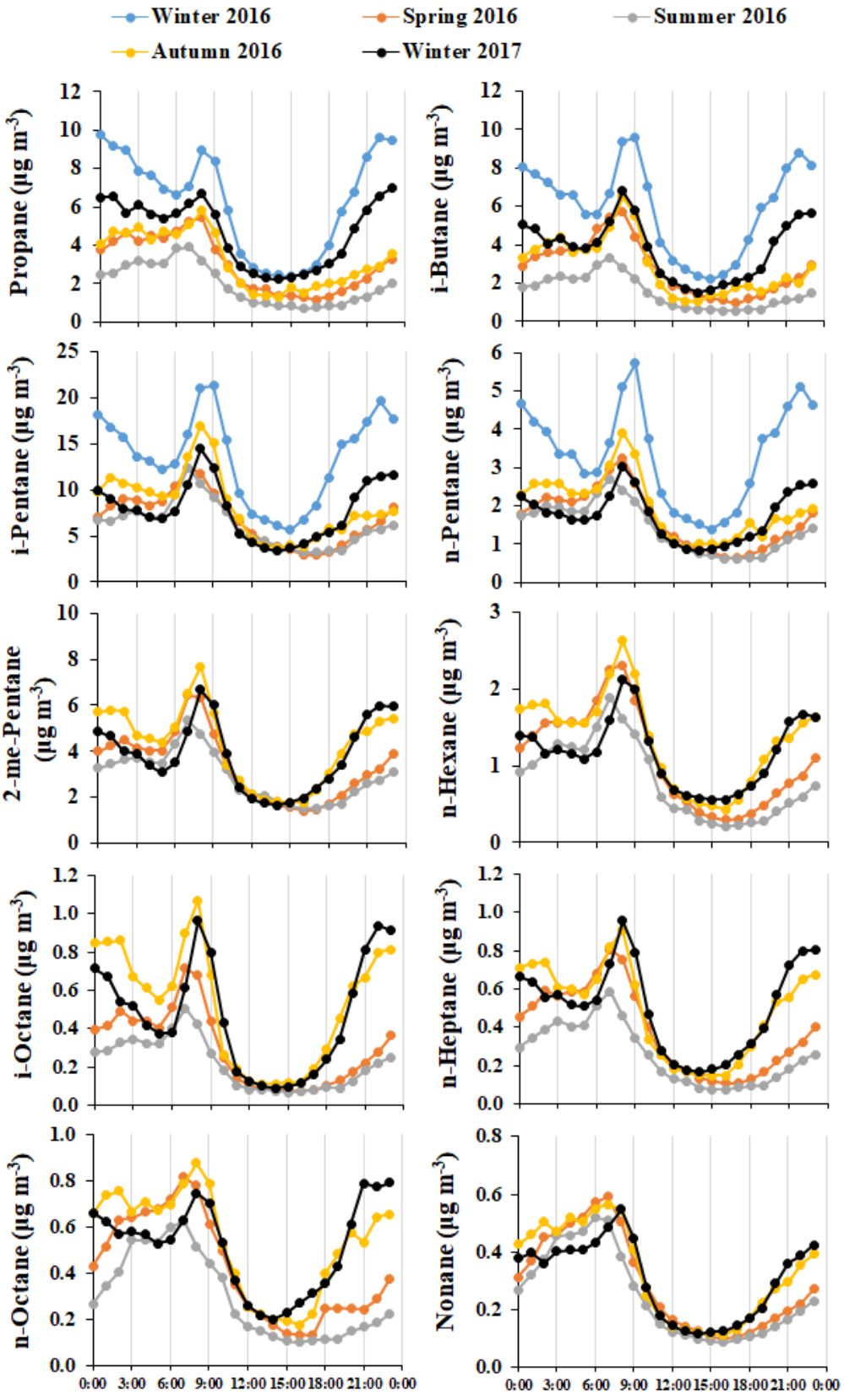

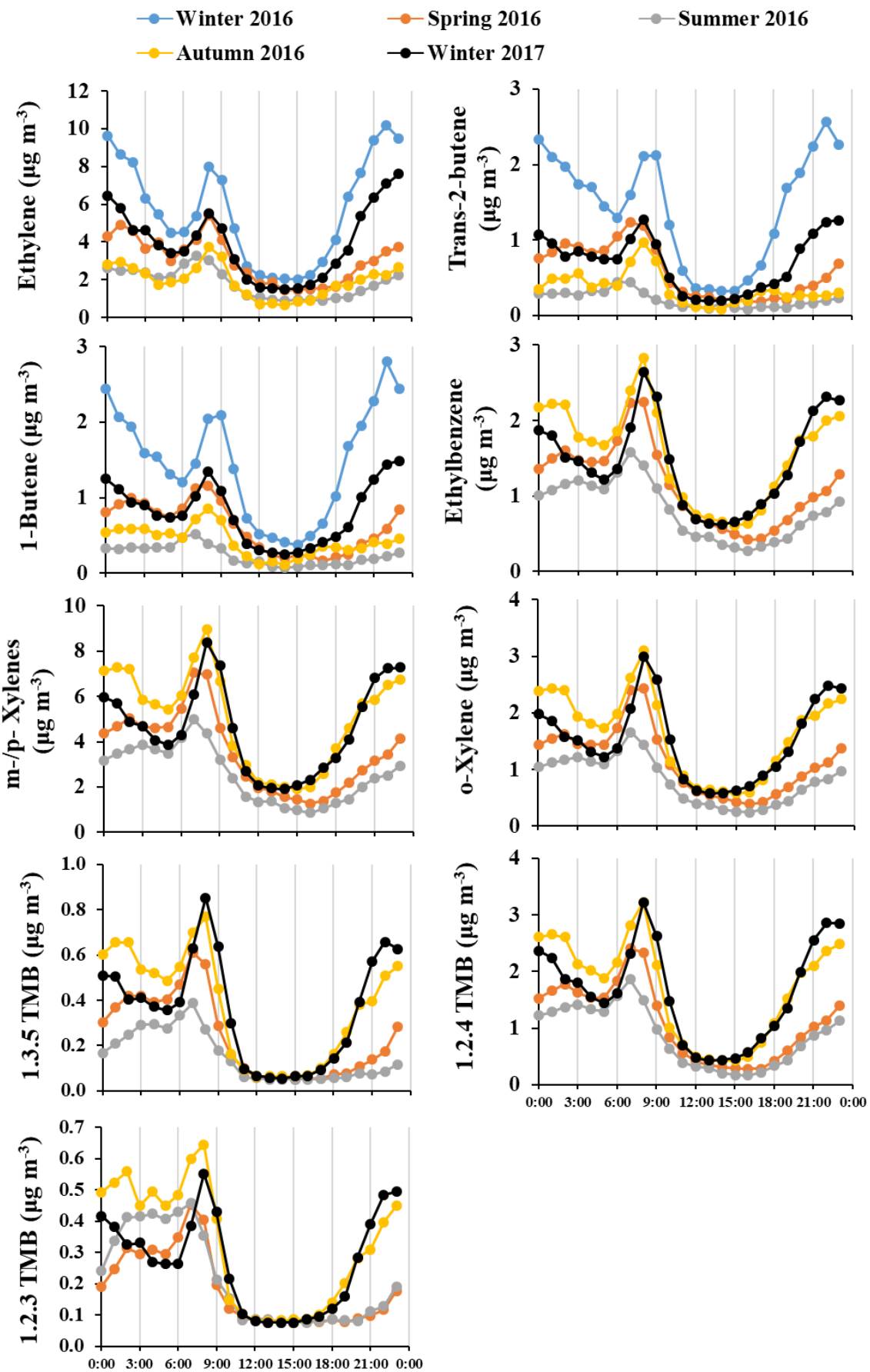
Winter 2016
Spring 2016
Summer 2016
Autumn 2016
Winter 2017
Ethylene (µg m-3)
Trans-2-butene (µg m-3)
1-Butene (µg m-3)
Ethylbenzene (µg m-3)
m-/p- Xylenes (µg m-3)
o-Xylene (µg m-3)
1.3.5 TMB (µg m-3)
1.2.4 TMB (µg m-3)
1.2.3 TMB (µg m-3)
0:00 3:00 6:00 9:00 12:00 15:00 18:00 21:00 0:00

Fig. IV - A3: Relationship of C2 – C12 NMHCs to wind speed from 1 December 2015 to 28 February 2017 for the C2 – C6 NMHCs and from 1 March 2016 to 28 February 2017 for the C6 – C12 NMHCs in seasonal basis.

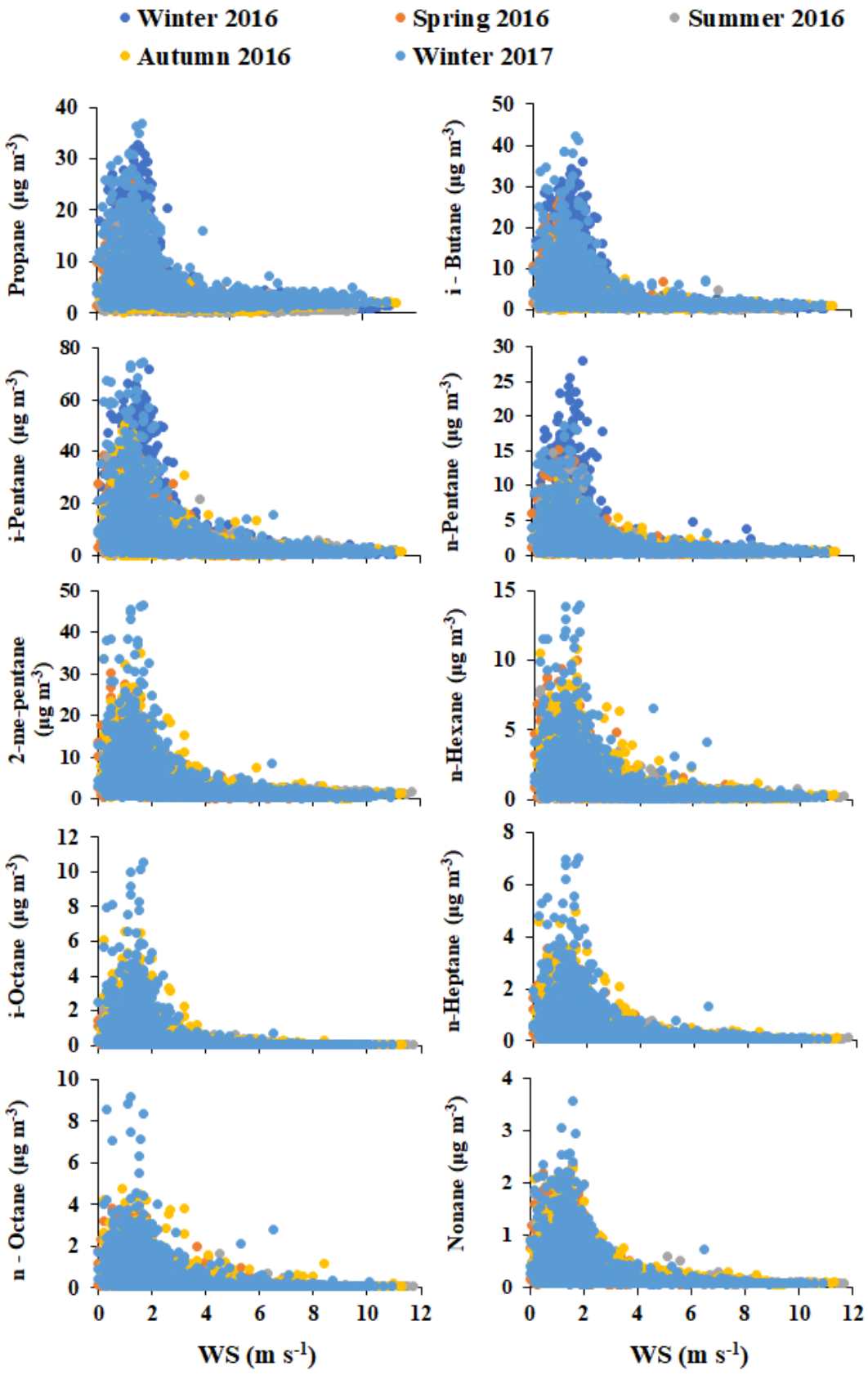

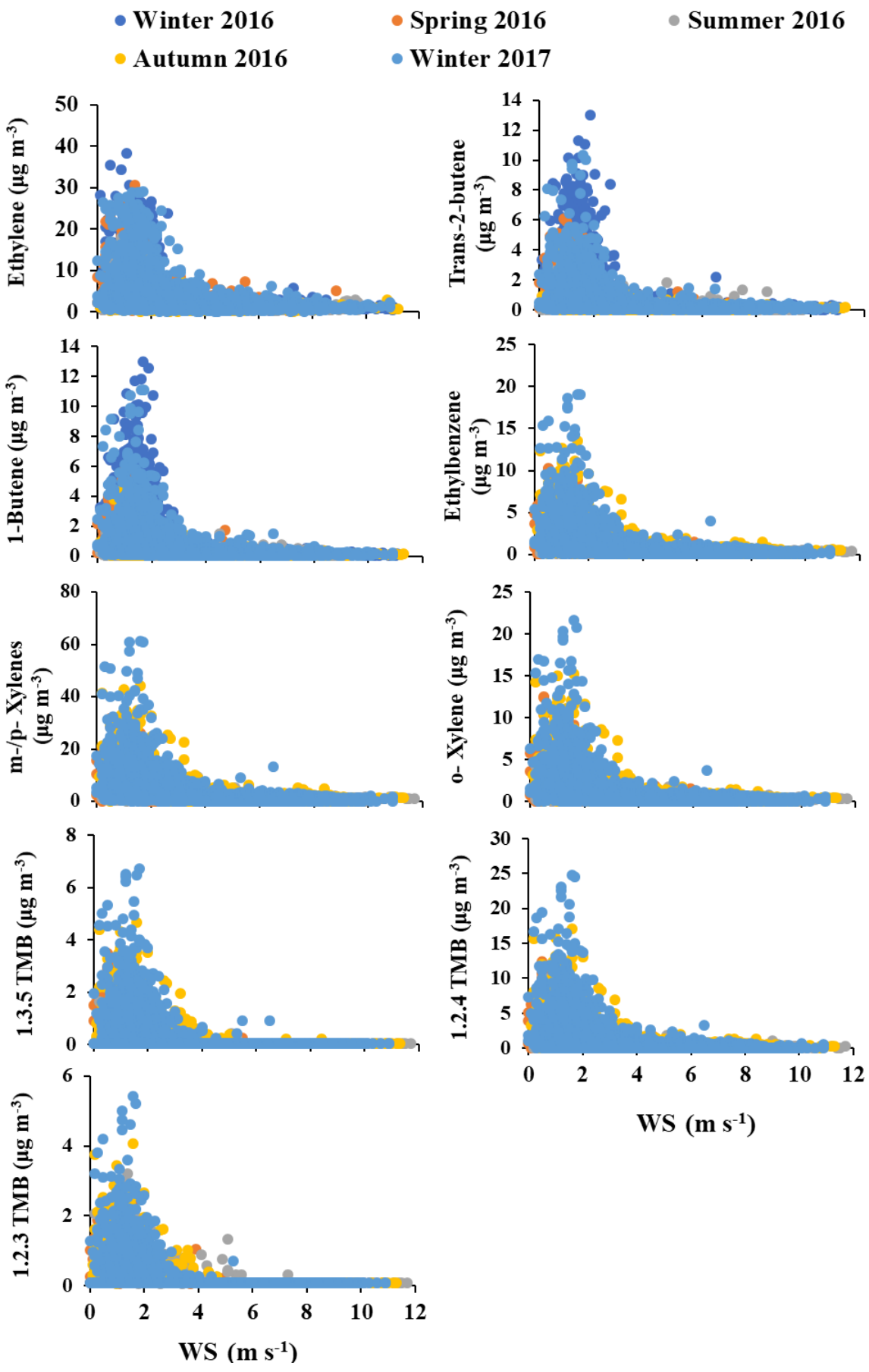
Winter 2016
Spring 2016
Summer 2016
Autumn 2016
Winter 2017
Ethylene (µg m-3)
Trans-2-butene (µg m-3)
1-Butene (µg m-3)
Ethylbenzene (µg m-3)
m-/p- Xylenes (µg m-3)
o- Xylene (µg m-3)
1.3.5 TMB (µg m-3)
1.2.4 TMB (µg m-3)
1.2.3 TMB (µg m-3)
WS (m s-1)
WS (m s-1)

Fig. IV - A4: Relationship of C2 – C12 NMHCs to ambient temperature from 1 December 2015 to 28 February 2017 for the C2 – C6 NMHCs and from 1 March 2016 to 28 February 2017 for the C6 – C12 NMHCs in seasonal basis.

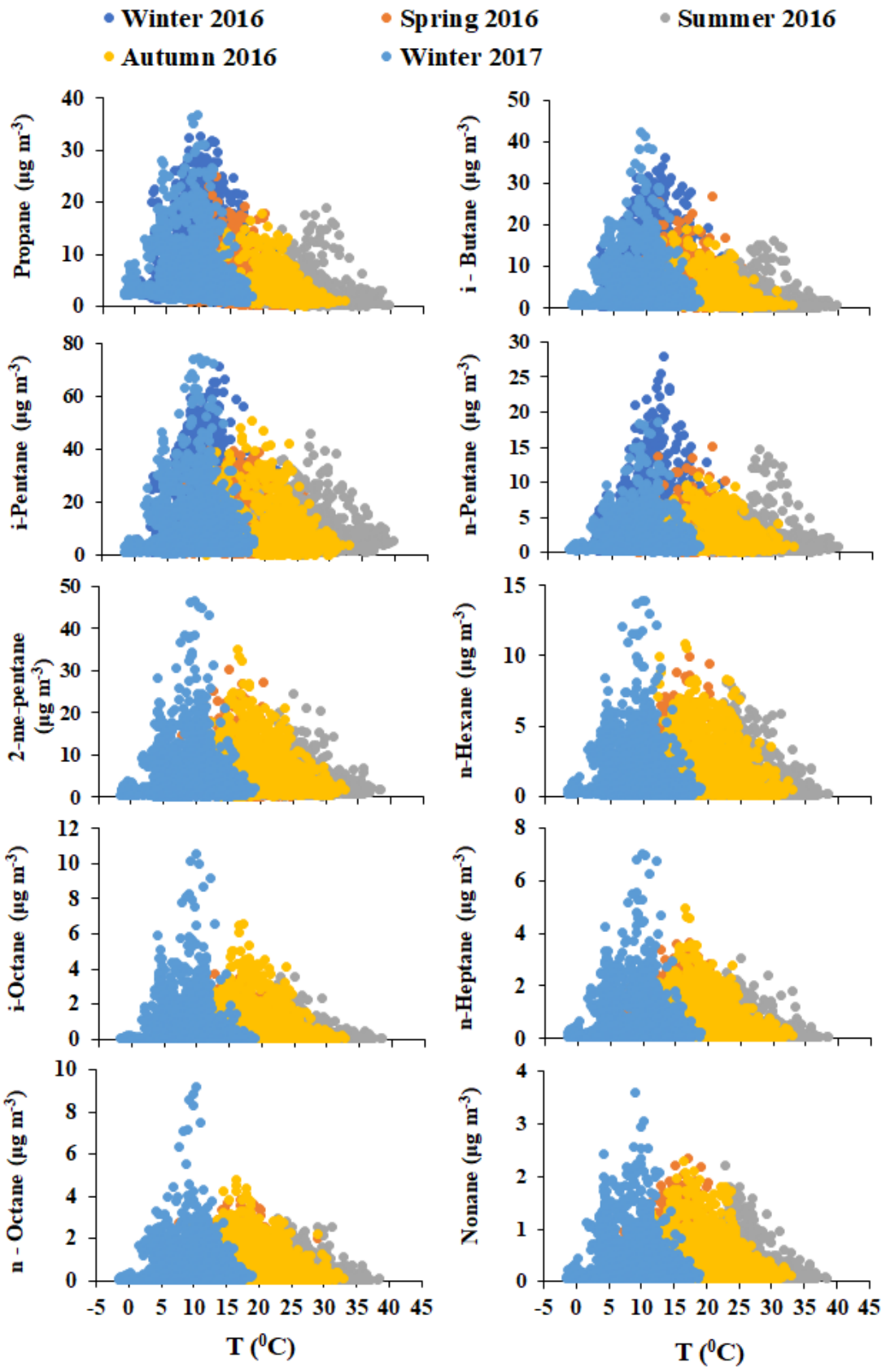

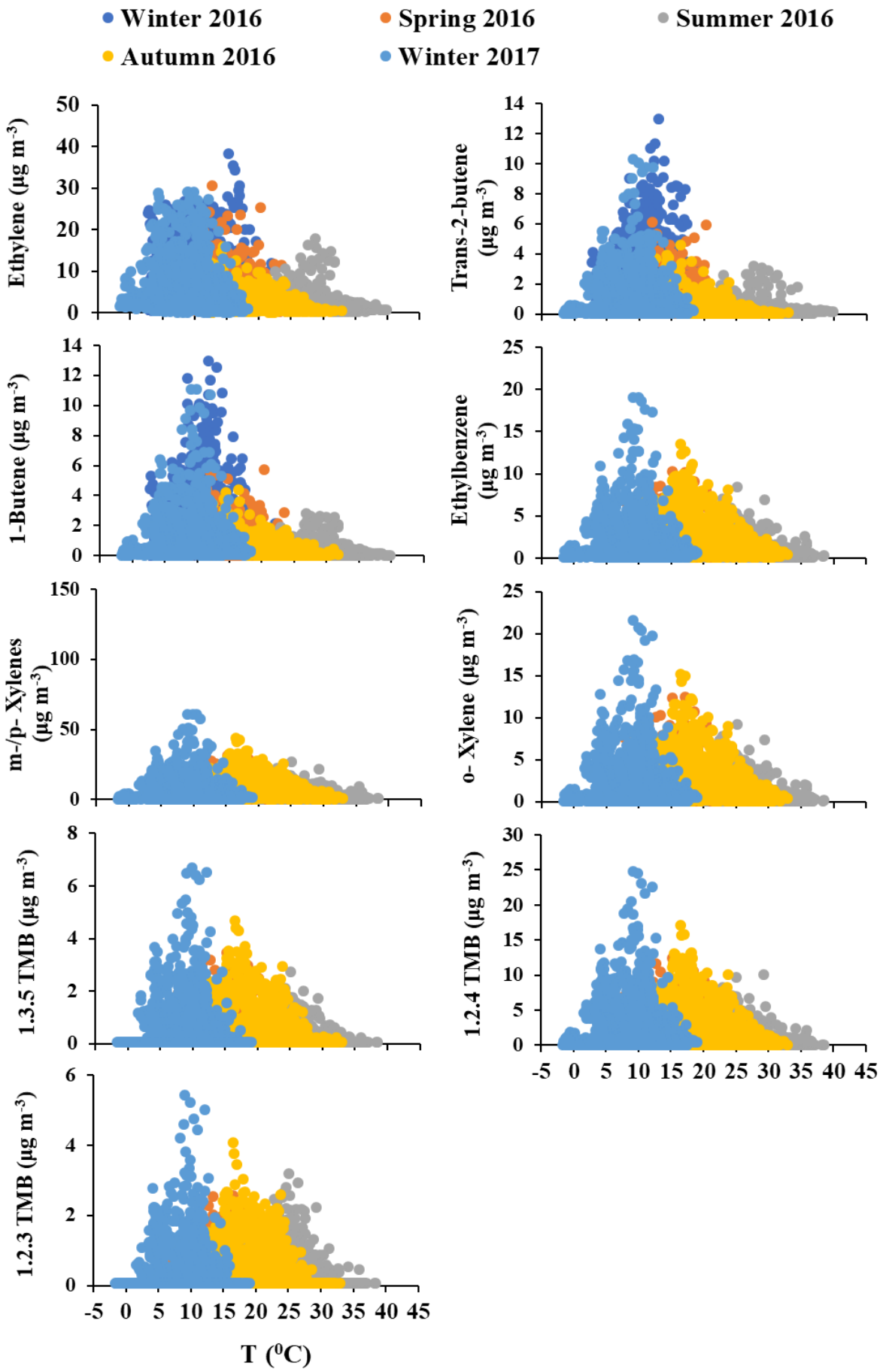
Winter 2016
Spring 2016
Summer 2016
Autumn 2016
Winter 2017
Ethylene (µg m-3)
Trans-2-butene (µg m-3)
1-Butene (µg m-3)
Ethylbenzene (µg m-3)
m-/p- Xylenes (µg m-3)
o- Xylene (µg m-3)
1.3.5 TMB (µg m-3)
1.2.4 TMB (µg m-3)
1.2.3 TMB (µg m-3)
T (0C)

Table IV - A2: Concentrations of NOx, CO, BC, BC_{wb} and BC_{ff} measured in the Athens urban background site from 1 February 2016 to 28 February 2017. For standard deviation of the seasonal mean values is given in the brackets.

	Mean	Median	STD	Min	Max	Spring 2016	Summer 2016	Autumn 2016	Winter 2017	NB	(%) Representativity
NO_x (ppb)	21.4	14.1	21.1	0.6	238.2	16.7 (17.9)	13.4 (13.3)	25.8 (25.2)	24.1 (19.5)	6714	71%
CO (ppb)	366.2	251.9	333.9	72.0	4250.2	313.4 (198.9)	225.4 (123.6)	383.1 (301.9)	501.6 (488.5)	9298	98%
BC ($\mu g\ m^{-3}$)	1.8	1.0	2.3	0.1	29.6	1.5 (1.7)	1.1 (0.9)	1.7 (1.7)	2.5 (3.4)	8485	90%
BC_{wb} ($\mu g\ m^{-3}$)	0.5	0.2	1.1	0.0	18.0	0.2 (0.4)	0.2 (0.2)	0.4 (0.6)	1.0 (1.9)	8485	90%
BC_{ff} ($\mu g\ m^{-3}$)	1.3	0.8	1.5	0.0	16.9	1.2 (1.4)	0.9 (0.7)	1.3 (1.3)	1.4 (1.7)	8485	90%

Table IV - A3: Correlation coefficients (R^2) for the NMHC of the main campaign for the period 16 October 2015 to 28 February 2017. The bold and italics indicate good relationships ($R^2 > 0.49$). All the relationships are statistically significant at the 95% confidence level.

	Ethane	*Ethylene*	*Propane*	*Propene*	*i-Butane*	*n-Butane*	*Trans-2-butene*	*1-Butene*	*i-Pentane*	*n-Pentane*	*2-me - Pentane*	*n-Hexane*	*Benzene*	*i-Octane*	*n-Heptane*	*Toluene*	*n-Octane*	*Ethyl benzene*	*m-/p - Xylenes*	*o-Xylene*	*Nonane*	*1.3.5 TMB*	*1.2.4 TMB*	*1.2.3 TMB*
Ethane	1.00																							
Ethylene	***0.81***	1.00																						
Propane	***0.76***	***0.85***	1.00																					
Propene	***0.75***	***0.88***	***0.89***	1.00																				
i-Butane	***0.64***	***0.81***	***0.91***	***0.83***	1.00																			
n-Butane	***0.64***	***0.81***	***0.93***	***0.82***	***0.97***	1.00																		
Trans-2-butene	***0.62***	***0.79***	***0.84***	***0.84***	***0.91***	***0.86***	1.00																	
1-Butene	***0.69***	***0.84***	***0.87***	***0.91***	***0.93***	***0.88***	***0.94***	1.00																
i-Pentane	0.50	***0.72***	***0.78***	***0.71***	***0.91***	***0.90***	***0.83***	***0.82***	1.00															
n-Pentane	***0.50***	***0.71***	***0.79***	***0.72***	***0.92***	***0.89***	***0.86***	***0.86***	***0.93***	1.00														
2-me - Pentane	***0.53***	***0.75***	***0.78***	***0.71***	***0.89***	***0.88***	***0.80***	***0.82***	***0.92***	***0.92***	1.00													
n-Hexane	0.44	***0.64***	***0.71***	***0.61***	***0.81***	***0.82***	***0.66***	***0.70***	***0.84***	***0.87***	***0.90***	1.00												
Benzene	***0.69***	***0.85***	***0.82***	***0.88***	***0.81***	***0.82***	***0.75***	***0.83***	***0.70***	***0.69***	***0.81***	***0.70***	1.00											
i-Octane	***0.51***	***0.71***	***0.75***	***0.75***	***0.84***	***0.84***	***0.78***	***0.81***	***0.81***	***0.81***	***0.91***	***0.80***	***0.84***	1.00										
n-Heptane	***0.58***	***0.75***	***0.83***	***0.75***	***0.90***	***0.90***	***0.81***	***0.84***	***0.87***	***0.89***	***0.95***	***0.89***	***0.83***	***0.92***	1.00									
Toluene	***0.51***	***0.73***	***0.79***	***0.71***	***0.87***	***0.87***	***0.77***	***0.80***	***0.87***	***0.86***	***0.94***	***0.88***	***0.81***	***0.89***	***0.93***	1.00								
n-Octane	0.46	***0.65***	***0.72***	***0.63***	***0.81***	***0.81***	***0.69***	***0.73***	***0.81***	***0.82***	***0.87***	***0.87***	***0.72***	***0.82***	***0.89***	***0.89***	1.00							
Ethylbenzene	***0.55***	***0.77***	***0.81***	***0.75***	***0.90***	***0.90***	***0.82***	***0.84***	***0.90***	***0.90***	***0.98***	***0.88***	***0.84***	***0.93***	***0.95***	***0.96***	***0.89***	1.00						
m-/p - Xylenes	***0.55***	***0.77***	***0.81***	***0.75***	***0.90***	***0.89***	***0.82***	***0.84***	***0.89***	***0.88***	***0.97***	***0.87***	***0.85***	***0.93***	***0.95***	***0.96***	***0.88***	0.99	1.00					
o - Xylene	***0.55***	***0.77***	***0.80***	***0.75***	***0.90***	***0.89***	***0.82***	***0.84***	***0.89***	***0.88***	***0.97***	***0.86***	***0.85***	***0.94***	***0.95***	***0.95***	***0.86***	***0.99***	0.99	1.00				
Nonane	0.49	***0.61***	***0.77***	***0.60***	***0.79***	***0.83***	***0.66***	***0.68***	***0.80***	***0.81***	***0.84***	***0.84***	***0.66***	***0.77***	***0.89***	***0.86***	***0.83***	***0.84***	***0.83***	***0.82***	1.00			
1.3.5 TMB	***0.54***	***0.73***	***0.79***	***0.74***	***0.86***	***0.87***	***0.81***	***0.82***	***0.83***	***0.83***	***0.91***	***0.81***	***0.82***	***0.93***	***0.92***	***0.91***	***0.83***	***0.93***	***0.94***	***0.94***	***0.82***	1.00		
1.2.4 TMB	***0.55***	***0.76***	***0.82***	***0.79***	***0.89***	***0.90***	***0.81***	***0.85***	***0.87***	***0.85***	***0.95***	***0.84***	***0.88***	***0.93***	***0.94***	***0.95***	***0.85***	***0.97***	***0.97***	***0.97***	***0.84***	***0.94***	1.00	
1.2.3 TMB	0.43	***0.62***	***0.70***	***0.64***	***0.76***	***0.78***	***0.71***	***0.71***	***0.73***	***0.76***	***0.82***	***0.73***	***0.69***	***0.84***	***0.82***	***0.81***	***0.74***	***0.83***	***0.83***	***0.83***	***0.77***	***0.87***	***0.83***	1.00
BC	***0.71***	***0.84***	***0.82***	***0.90***	***0.79***	***0.78***	***0.78***	***0.85***	***0.72***	***0.72***	***0.75***	***0.67***	***0.82***	***0.73***	***0.76***	***0.73***	***0.68***	***0.77***	***0.76***	***0.76***	***0.65***	***0.73***	***0.79***	***0.63***
BC_{wb}	***0.64***	***0.68***	***0.61***	***0.78***	0.50	***0.51***	***0.53***	***0.61***	0.41	0.38	0.38	0.33	***0.69***	0.44	0.42	0.38	0.35	0.41	0.41	0.41	0.33	0.42	0.48	0.34
BC_{ff}	***0.57***	***0.73***	***0.75***	***0.72***	***0.81***	***0.78***	***0.75***	***0.79***	***0.78***	***0.81***	***0.80***	***0.74***	***0.68***	***0.70***	***0.77***	***0.77***	***0.72***	***0.80***	***0.78***	***0.79***	***0.69***	***0.74***	***0.77***	***0.65***
NOx	0.36	***0.66***	***0.73***	***0.73***	***0.79***	***0.80***	***0.63***	***0.71***	***0.76***	***0.73***	***0.75***	***0.68***	***0.78***	***0.67***	***0.74***	***0.75***	***0.67***	***0.78***	***0.77***	***0.76***	***0.65***	***0.67***	***0.79***	***0.50***
CO	***0.72***	***0.86***	***0.85***	***0.90***	***0.83***	***0.82***	***0.78***	***0.87***	***0.73***	***0.71***	***0.73***	***0.62***	***0.88***	***0.75***	***0.75***	***0.72***	***0.64***	***0.77***	***0.77***	***0.77***	***0.60***	***0.74***	***0.80***	***0.61***

Table IV - A4: Concentrations of the additional C6 – C16 NMHCs measured in the winter and summer 2016 IOPs in the Athens urban background site.

µg m^{-3}	Mean		Median		STD		Min		Max		NB	
	Winter 2016	Summer 2016	Winter 2016	Summer 2016	Winter 2016	Summer 2016	Winter 2016	Summer 2016	Winter 2016	Summer 2016	Winter 2016	Summer 2016
3-me-pentane	2.43	1.22	1.36	0.91	2.28	1.05	0.22	0.08	8.40	5.11	106	112
Hexene	0.16	0.07	0.08	0.05	0.18	0.05	0.01	0.01	1.00	0.30	104	111
2,2-dimet-pentane	0.10	0.07	0.05	0.06	0.11	0.06	0.01	0.01	0.80	0.31	97	112
2,4-dimet-pentane	0.19	0.10	0.09	0.07	0.20	0.11	0.01	0.01	0.73	0.55	104	111
2,2,3-trimet-butane	0.05	0.02	0.03	0.01	0.03	0.02	0.01	0.01	0.13	0.12	77	108
3,3-dimet-pentane	0.38	0.07	0.10	0.06	2.20	0.05	0.01	0.01	22.49	0.23	103	112
Cyclohexane	0.49	0.14	0.36	0.12	0.39	0.09	0.05	0.01	1.79	0.52	105	112
2-me-hexane	0.76	0.48	0.43	0.34	0.72	0.45	0.07	0.06	2.66	2.23	106	112
2,3-dimet-pentane	0.27	0.19	0.15	0.14	0.26	0.18	0.02	0.01	0.98	0.82	105	110
Styrene	0.49	0.15	0.27	0.09	0.52	0.18	0.03	0.01	3.00	1.00	106	99
3-ethyl-toluene	1.16	0.61	0.64	0.46	1.12	0.56	0.09	0.03	4.17	2.87	106	112
4-ethyl-toluene	0.53	0.29	0.32	0.22	0.50	0.26	0.04	0.03	1.87	1.32	105	112
2-ethyl-toluene	0.64	0.35	0.37	0.26	0.60	0.31	0.07	0.02	2.20	1.57	106	112
Camphene	0.30	0.10	0.13	0.08	0.43	0.10	0.01	0.01	2.59	0.52	99	112
g-terpinene	0.06	0.06	0.04	0.05	0.05	0.06	0.01	0.01	0.26	0.31	73	112
Decane	0.65	0.29	0.43	0.23	0.55	0.28	0.07	0.03	2.10	1.40	106	112
nC11	0.39	0.30	0.26	0.20	0.33	0.28	0.01	0.04	1.20	1.47	106	112
nC12	0.20	0.15	0.15	0.11	0.15	0.13	0.02	0.01	0.58	0.69	105	112
nC13	0.13	0.11	0.10	0.09	0.09	0.08	0.01	0.01	0.41	0.45	106	112
nC14	0.10	0.09	0.09	0.08	0.06	0.05	0.01	0.02	0.25	0.33	106	112
nC15	0.08	0.07	0.07	0.06	0.05	0.04	0.01	0.01	0.22	0.25	102	112
nC16	0.02	0.04	0.02	0.04	0.02	0.02	0.01	0.01	0.08	0.11	85	111

Fig. IV - A5: Seasonal diurnal variability of C6 – C16 VOC from the IOP of winter and summer 2016.

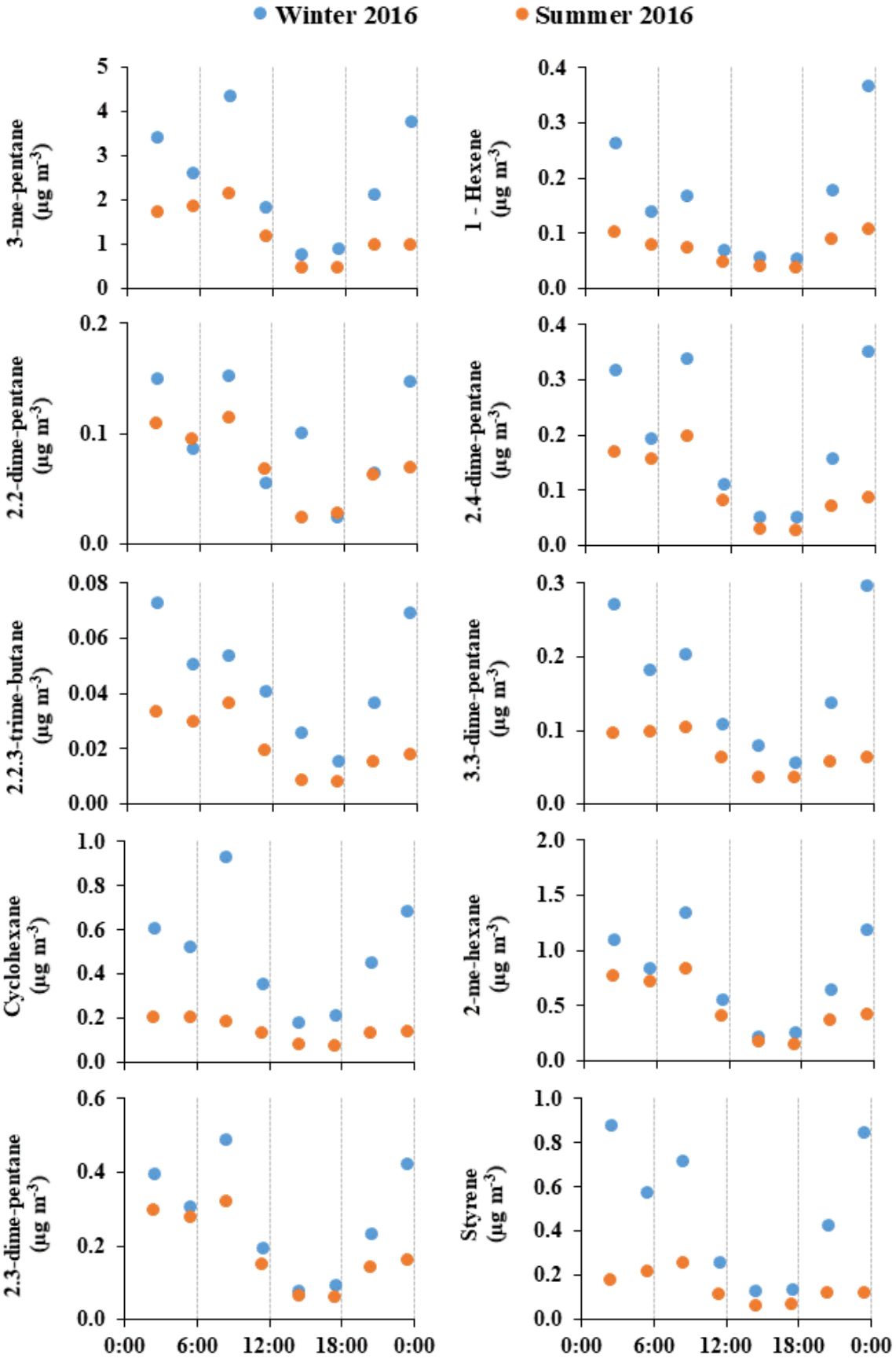

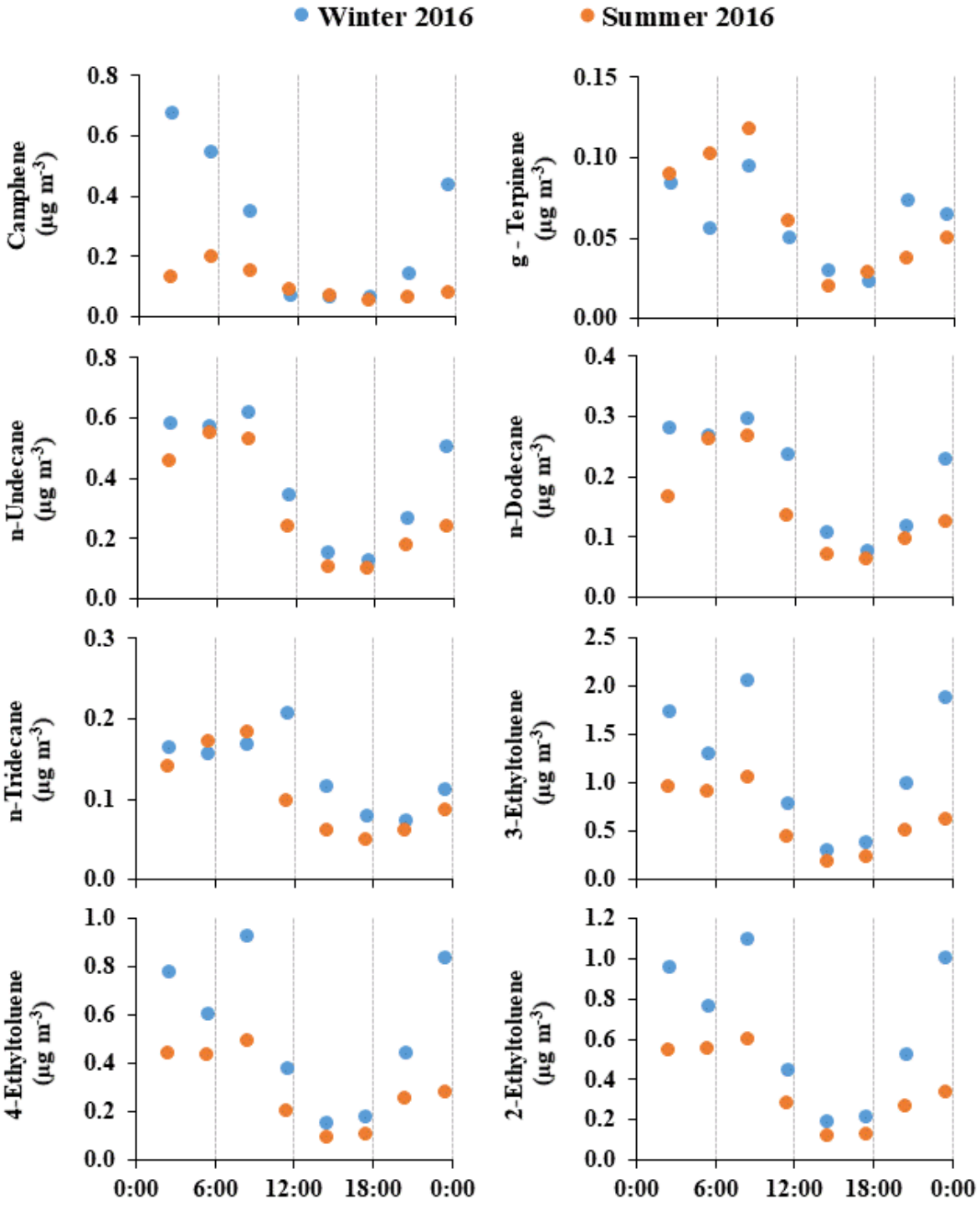
Winter 2016
Summer 2016
Camphene (µg m-3)
g - Terpinene (µg m-3)
n-Undecane (µg m-3)
n-Dodecane (µg m-3)
n-Tridecane (µg m-3)
3-Ethyltoluene (µg m-3)
4-Ethyltoluene (µg m-3)
2-Ethyltoluene (µg m-3)
0:00
6:00
12:00
18:00
0:00

Fig. IV - A6: Relationship to wind speed of IVOC from the IOP of winter and summer 2016

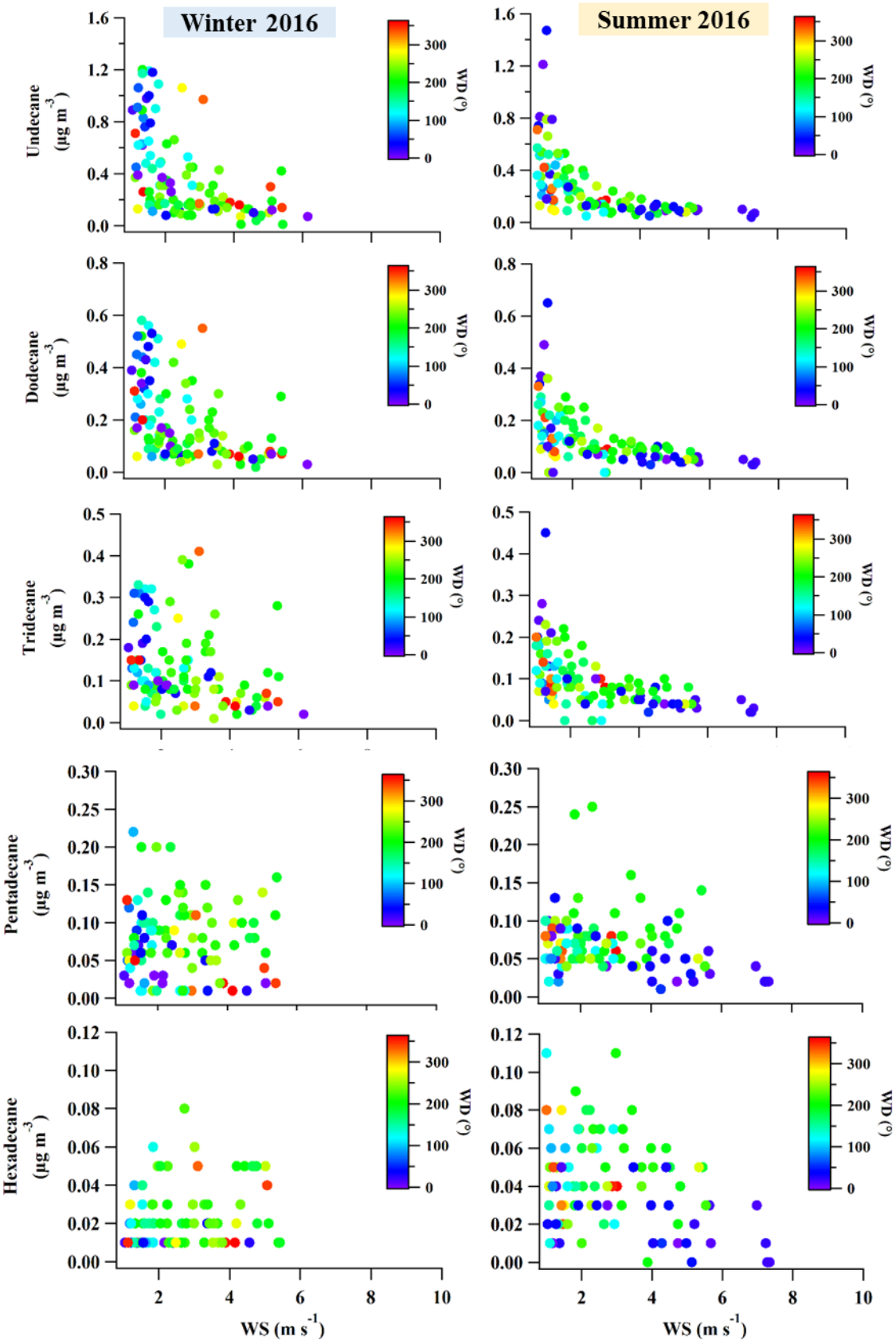

Figure IV – A7: Relationship of IVOC from the IOPs (winter and summer 2016) to temperature.

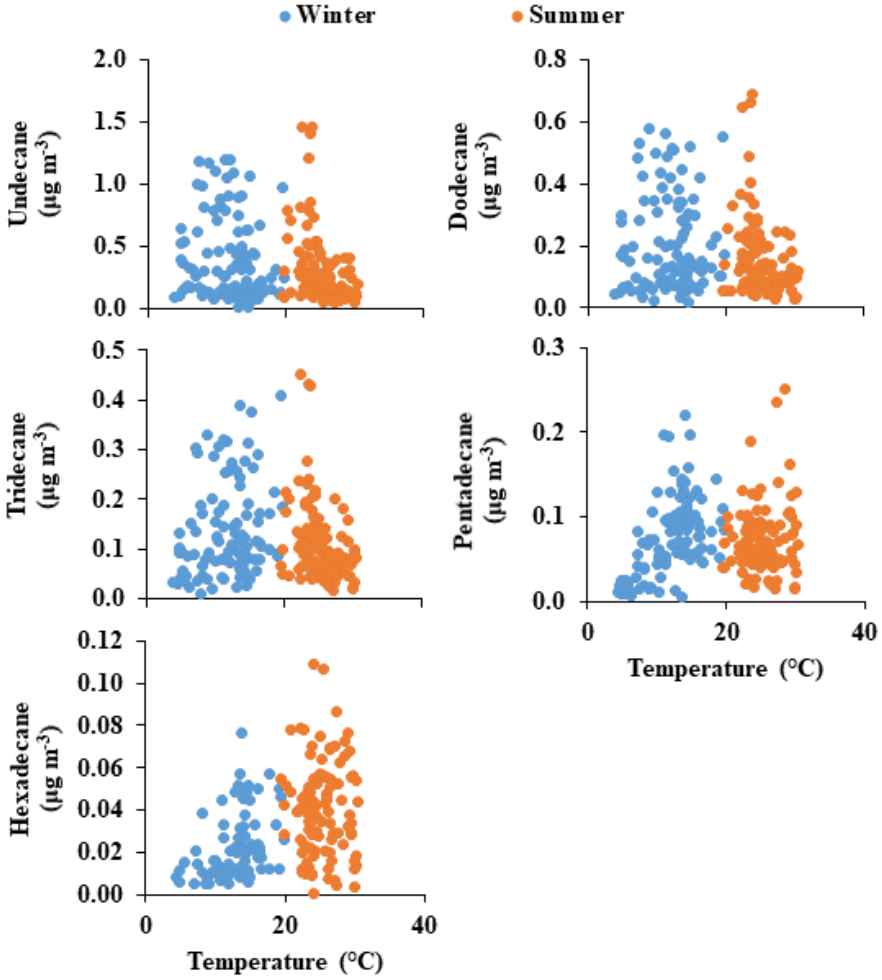

Annex V: Supplement of "Yearlong measurements of Monoterpenes and Isoprene in a Mediterranean city (Athens): Natural vs anthropogenic origin"

Tables

Table S1: Concentrations of VOCs and ancillary pollutants measured in the Athens urban background site from 01 February 2016 to 28 February 2017. The standard deviation of the seasonal mean values is given in the brackets.

	Median	Mean	STD	Min	Max	Spring 2016	Summer 2016	Autumn 2016	Winter 2017	Number of samples	Data coverage (%)
Isoprene (μg m^{-3})	0.06	0.19	0.35	0.06	3.88	0.07 (0.06)	0.48 (0.56)	0.12 (0.19)	0.12 (0.18)	7010	74
α-Pinene (μg m^{-3})	0.44	0.70	0.83	0.08	8.86	0.53 (0.57)	0.70 (0.66)	0.89 (1.08)	0.67 (0.91)	8312	88
Limonene (μg m^{-3})	0.07	0.33	0.78	0.07	9.86	0.18 (0.43)	0.15 (0.31)	0.35 (0.63)	0.48 (1.06)	8795	94
Toluene (μg m^{-3})	3.41	6.98	9.06	0.06	97.78	6.23 (7.88)	4.54 (5.08)	8.32 (9.65)	7.57 (10.78)	8791	93
NO (ppb)	2.7	15.6	35.3	0.2	209.6	9.0 (21.7)	2.2 (5.8)	14.2 (30.7)	24.1 (47.6)	8698	77
NO_2 (ppb)	11.1	13.7	9.5	0.01	65.2	10.4 (9.0)	11.2 (8.9)	16.8 (10.8)	15.5 (8.3)	7898	71
NO_x (ppb)	14.1	21.4	21.1	0.6	238.2	16.7 (17.9)	13.4 (13.3)	25.8 (25.2)	24.1 (19.5)	6714	71
CO (ppb)	251.9	366.2	333.9	72.0	4250.2	313.4 (198.9)	225.4 (123.6)	383.1 (301.9)	501.6 (488.5)	9298	98
BC (μg m^{-3})	1.0	1.8	2.3	0.1	29.6.5	1.5 (1.7)	1.1 (0.9)	1.7 (1.7)	2.4 (3.4)	8485	90
BC_{wb} (μg m^{-3})	0.2	0.5	1.1	0.0	18.0	0.2 (0.4)	0.2 (0.2)	0.4 (0.6)	1.0 (1.9)	8485	90
BC_{ff} (μg m^{-3})	0.8	1.3	1.5	0.0	16.9	1.2 (1.4)	0.9 (0.7)	1.3 (1.3)	1.4 (1.7)	8485	90

Table S2: Correlation coefficients (R^2) of the NMHCs (in μg m^{-3}) relative to the major anthropogenic pollutants (in μg m^{-3} for BC, BC_{wb} and BC_{ff}, and in ppb for NO and CO) for the period 01 February 2016 to 28 February 2017. All the correlations are statistically significant at the 95% confidence level. The bold and italics represent good relationships (R^2 > 0.49). Days with rain events are excluded.

Total	***Isoprene***	***a-Pinene***	***Limonene***	***Toluene***
Isoprene	1.00			
a-Pinene	1.93E-02	1.00		
Limonene	3.38E-04	***0.51***	1.00	
Toluene		0.48	***0.74***	1.00
BC	4.74E-03	0.48	***0.71***	***0.73***
BC_{wb}	3.20E-03	0.32	***0.62***	0.38
BC_{ff}	4.33E-03	0.45	***0.51***	***0.78***
NO	5.89E-02	0.19	0.23	0.42
CO		0.34	***0.51***	***0.73***

Summer	***Isoprene***	***a-Pinene***	***Limonene***	***Toluene***
Isoprene	1.00			
a-Pinene		1.00		
Limonene		0.46	1.00	
Toluene		0.39	***0.67***	1.00
BC		0.46	***0.51***	***0.72***
BC_{wb}		0.26	0.35	0.46
BC_{ff}		0.45	0.48	***0.69***
NO		0.45	***0.61***	0.47
CO	1.7E-02	0.35	***0.52***	***0.84***

Winter	***Isoprene***	***a-Pinene***	***Limonene***	***Toluene***
Isoprene	1.00			
a-Pinene	0.11	1.00		
Limonene	0.11	***0.81***	1.00	
Toluene	0.13	***0.75***	***0.80***	1.00
BC	0.12	***0.73***	***0.80***	***0.83***
BC_{wb}	0.09	***0.66***	***0.72***	***0.61***
BC_{ff}	0.12	***0.58***	***0.64***	***0.84***
NO	0.17	***0.71***	***0.76***	***0.81***
CO	0.13	***0.75***	***0.83***	***0.85***

Table S3: Molar mass, MIR, SOAP, and ER to toluene for isoprene, α-pinene and limonene. The ER are calculated for day (06:00 – 17:00 LT) and night (18:00 – 05:00 LT) concentrations.

	Molar Mass[1]	**MIR[1]**	**SOAP[2]**	**ER to toluene (±STD) (μg m^{-3}/ μg m^{-3})**							
				Spring		**Summer**		**Autumn**		**Winter 2017**	
				Day	Night	Day	Night	Day	Night	Day	Night
Isoprene	68.12	10.28	1.9								
α - Pinene	136.23	4.38	17.4	0.066 (±0.001)	0.073 (±0.001)	0.117 (±0.0027)	0.103 (±0.0030)	0.072 (±0.0019)	0.070 (±0.0018)	0.061 (±0.0010)	0.073 (±0.0011)
Limonene	136.23	4.40	18*			0.049 (±0.001)	0.036 (±0.0009)	0.043 (±0.0007)	0.053 (±0.0008)	0.062 (±0.0012)	0.089 (±0.0012)

[1] Carter, 2009; [2]Derwent et al., 2010; *Taken from Dominutti et al. (2018), which was estimated from analogous species

Figures

Figure S1. Mean hourly temporal variability of isoprene, α-pinene, limonene, temperature and solar radiation during the period of measurements.

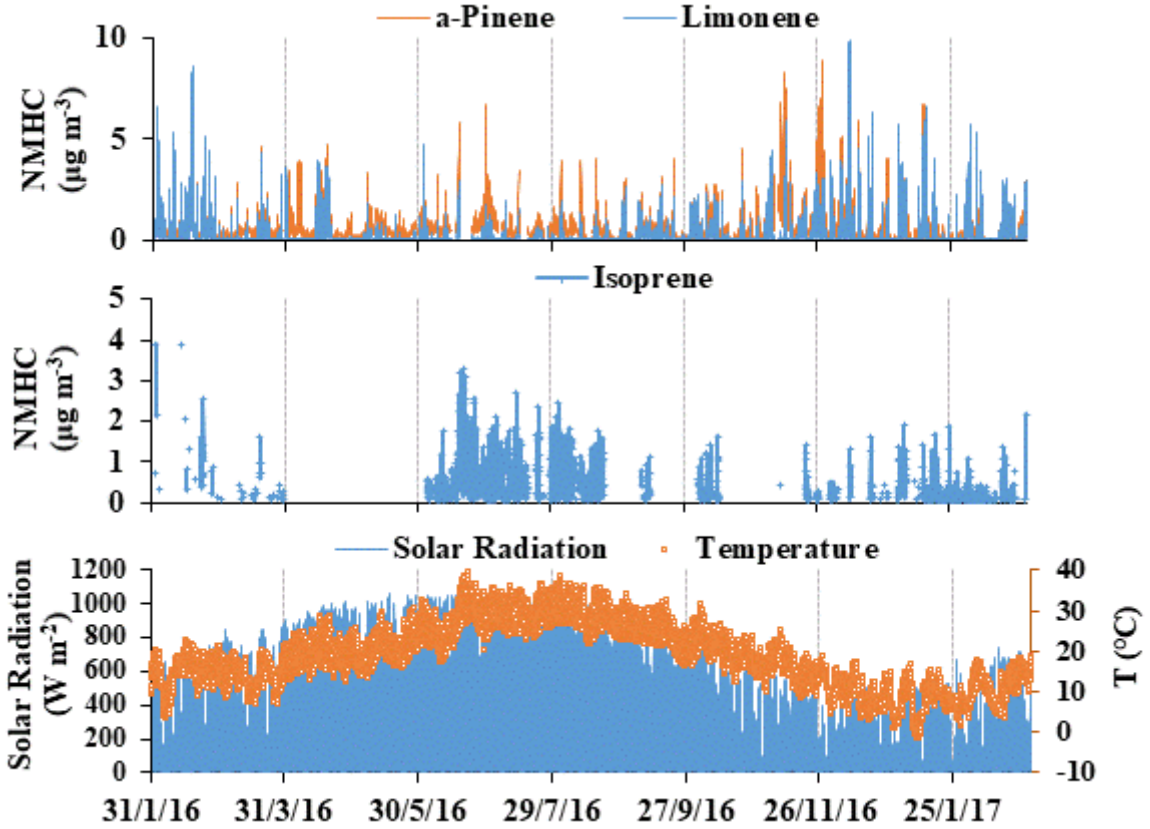

Figure S2. Diurnal variability of α-pinene and limonene for February 2016.

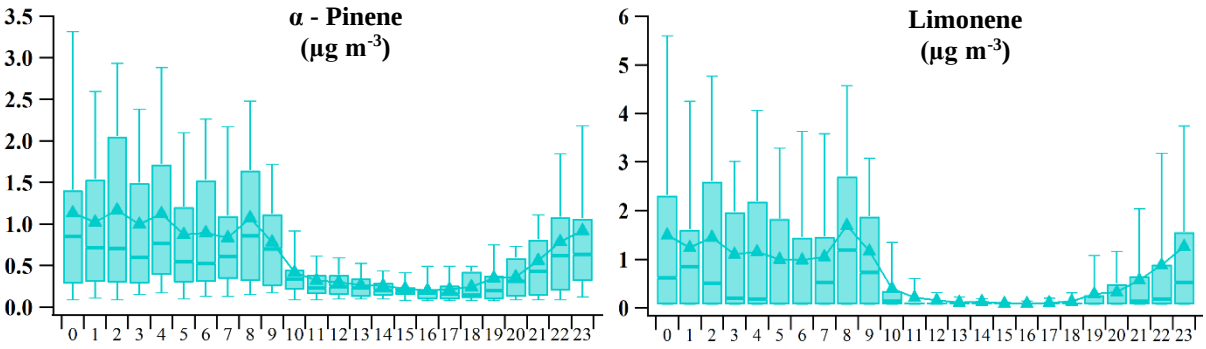

Figure S3. Seasonal diurnal variability of selected pollutants for the period 01 March 2016 to 28 February 2017.

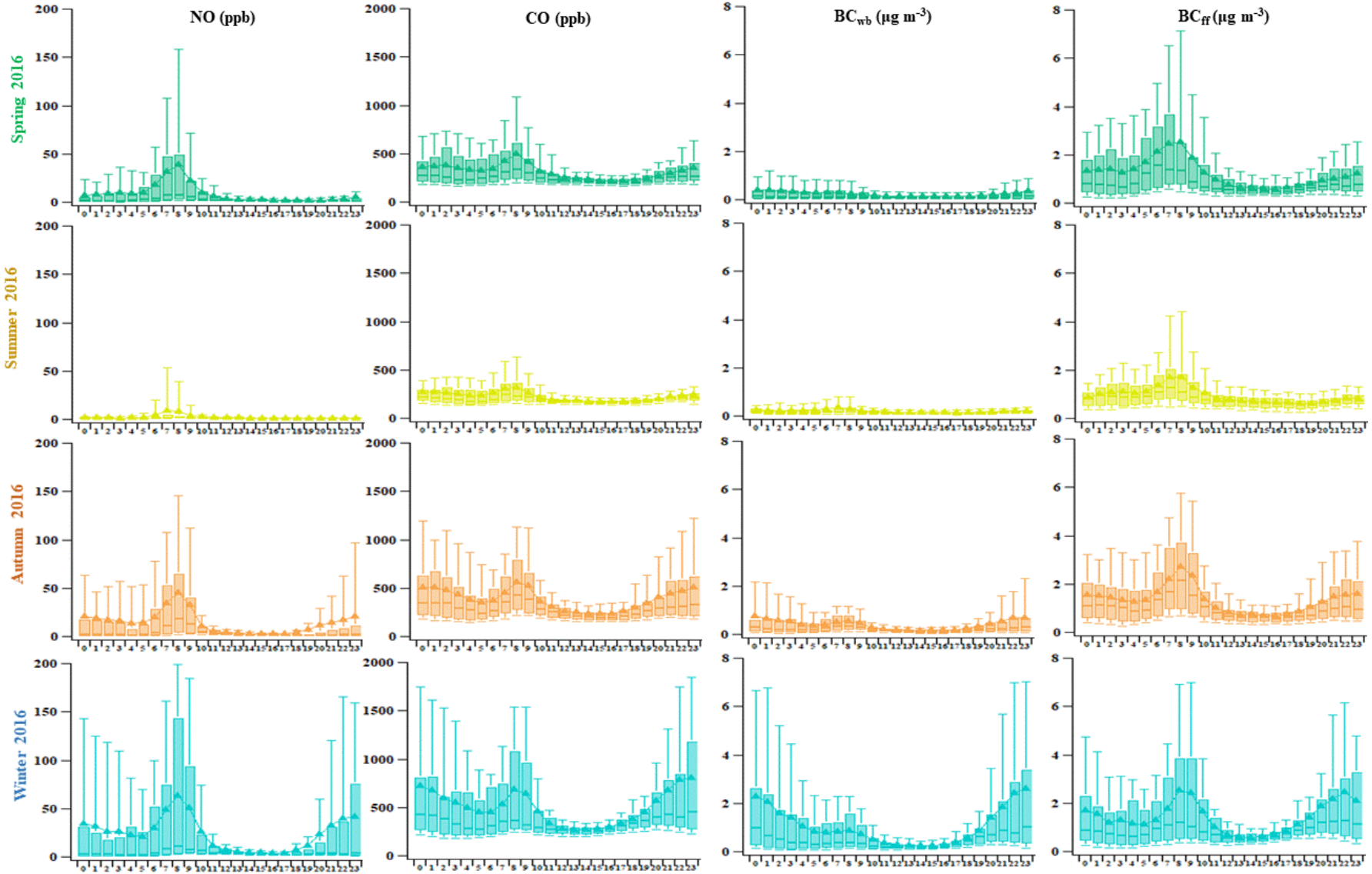

Figure S4. Mean diurnal variation of isoprene, α-pinene, limonene and BC, as well as their MLH-normalized values in spring, summer and autumn. Each figure includes the seasonal-mean diurnal cycle of the MLH (m) obtained from HYSPLIT.

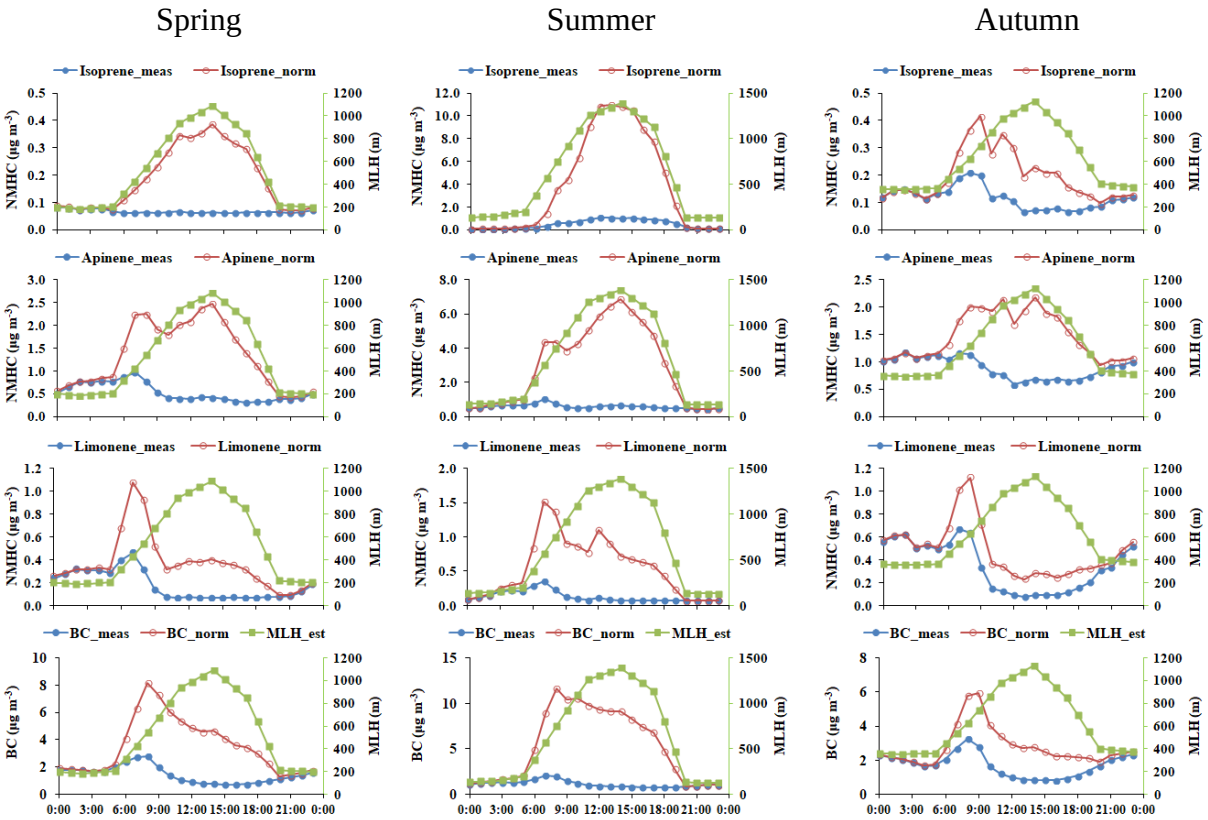

Figure S5. Monthly boxplots of meteorological parameters for March 2016 to February 2017.

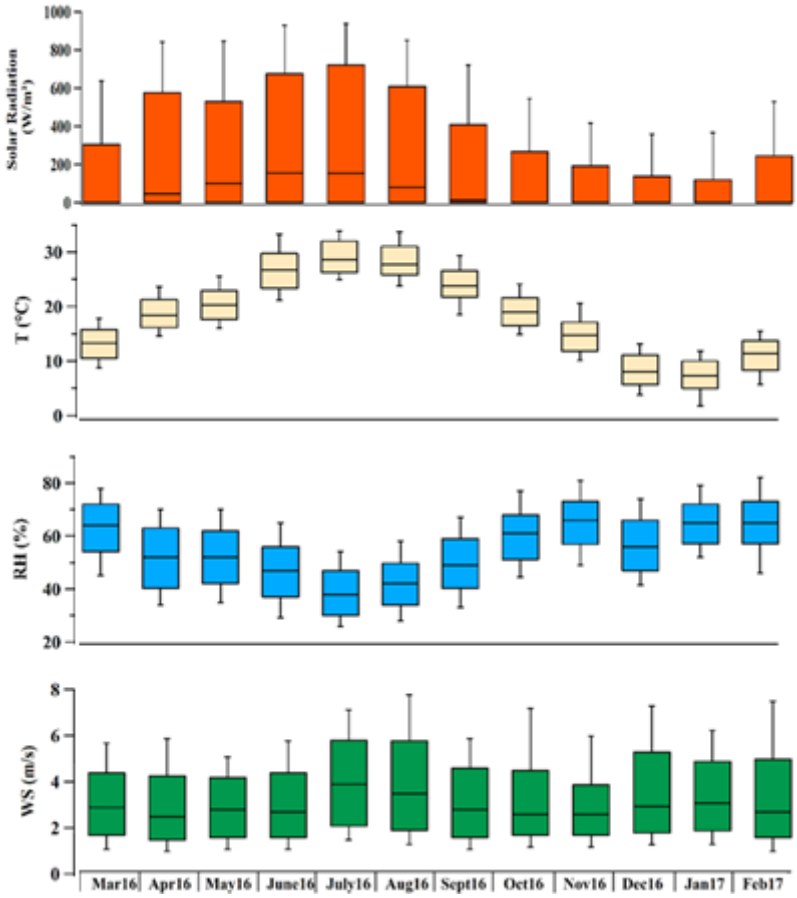

Figure S6. Scatterplots of the VOC diurnal cycles in seasonal basis.

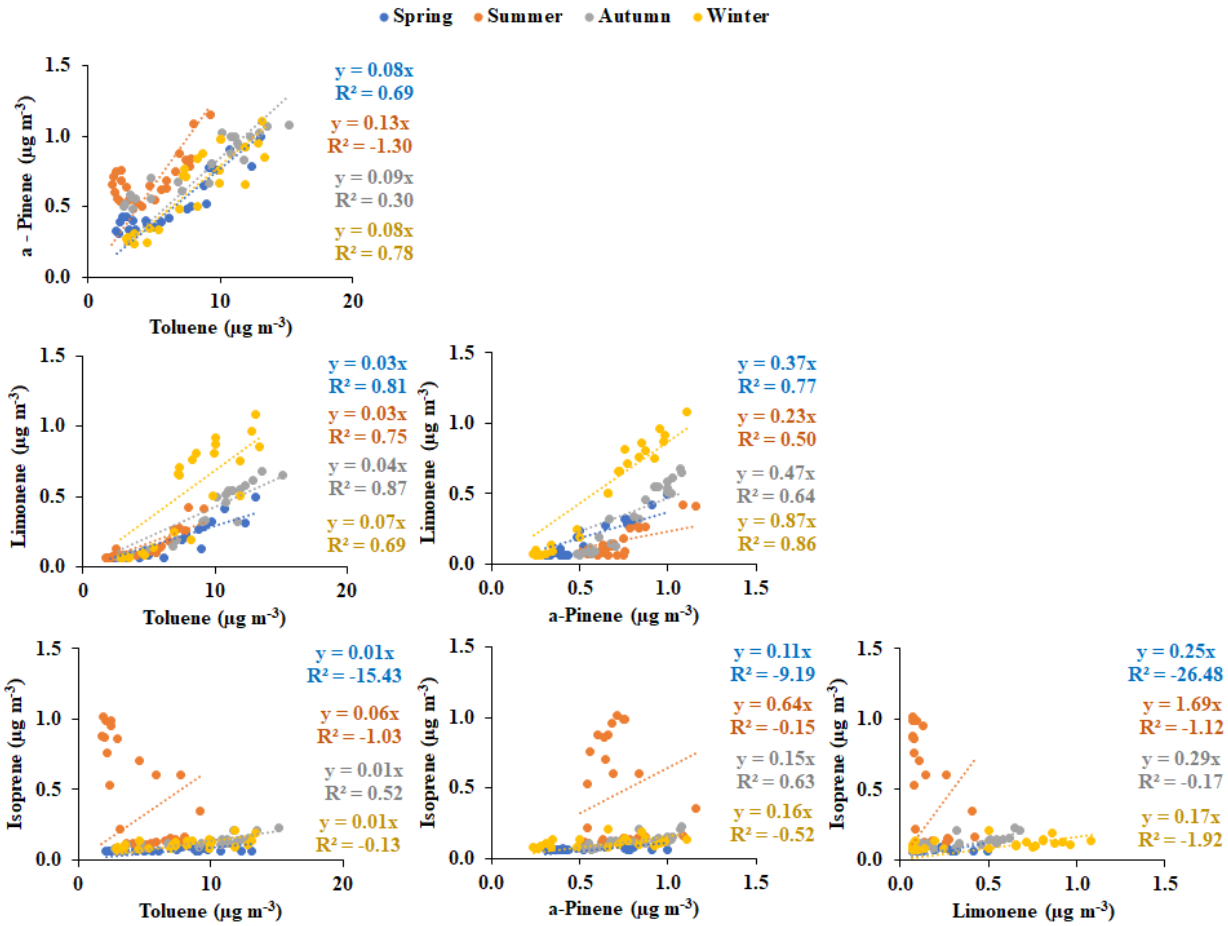

Figure S7: Seasonal Variability of monoterpenes (sum of α-pinene and limonene), SV-OOA+HOA and organics. Days with rain events are excluded.

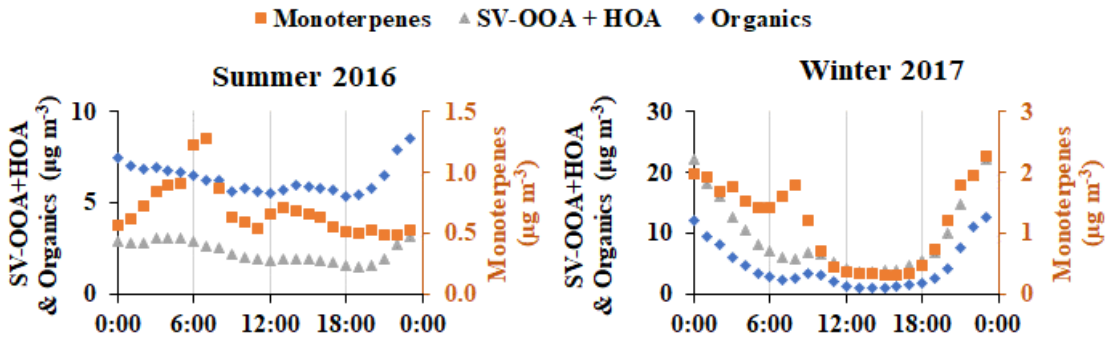

Annex VI

Table VI – A1: NMHCs of the Main Observation Campaign, their characterization and their S/N ratio. The SUM of VOC (last row) is calculated for every sample and it is used as the total variable (this parameter is used by the program in the post-processing of results, thus it has a high uncertainty in order to have a minimum influence on the sample)

NMHCs	Category	S/N
Ethane	Strong	2.0
Ethylene	Strong	5.9
Propane	Strong	9.3
Propene	Strong	5.6
i-Butane	Strong	9.6
n-Butane	Strong	9.0
Trans-2-butene	Bad	4.9
1-Butene	Bad	5.2
i-Pentane	Strong	9.7
n-Pentane	Strong	8.9
2-me-pentane	Strong	7.9
n-Hexane	Strong	4.5
Benzene	Strong	3.4
i-Octane	Strong	1.6
n-Heptane	Strong	2.0
Toluene	Strong	4.0
n-Octane	Strong	2.2
Ethylbenzene	Strong	3.3
m,p - Xylenes	Strong	3.5
o - Xylene	Strong	3.2
Nonane	Strong	2.0
1.3.5 TMB	Bad	1.0
1.2.4 TMB	Strong	1.8
1.2.3 TMB	Bad	0.4
SUM_VOC	Weak	4.5

Fig. VI – A1: Modelled contribution (µg m^{-3}) of each species to the Factors (light blue bars) and relative contribution of the factor to each species (red squares), for the MOP PMF 4-factor solution (left), 5-factor solution (center) and 6-factor solution (right). The deconvoluted factors are indicated with arrows.

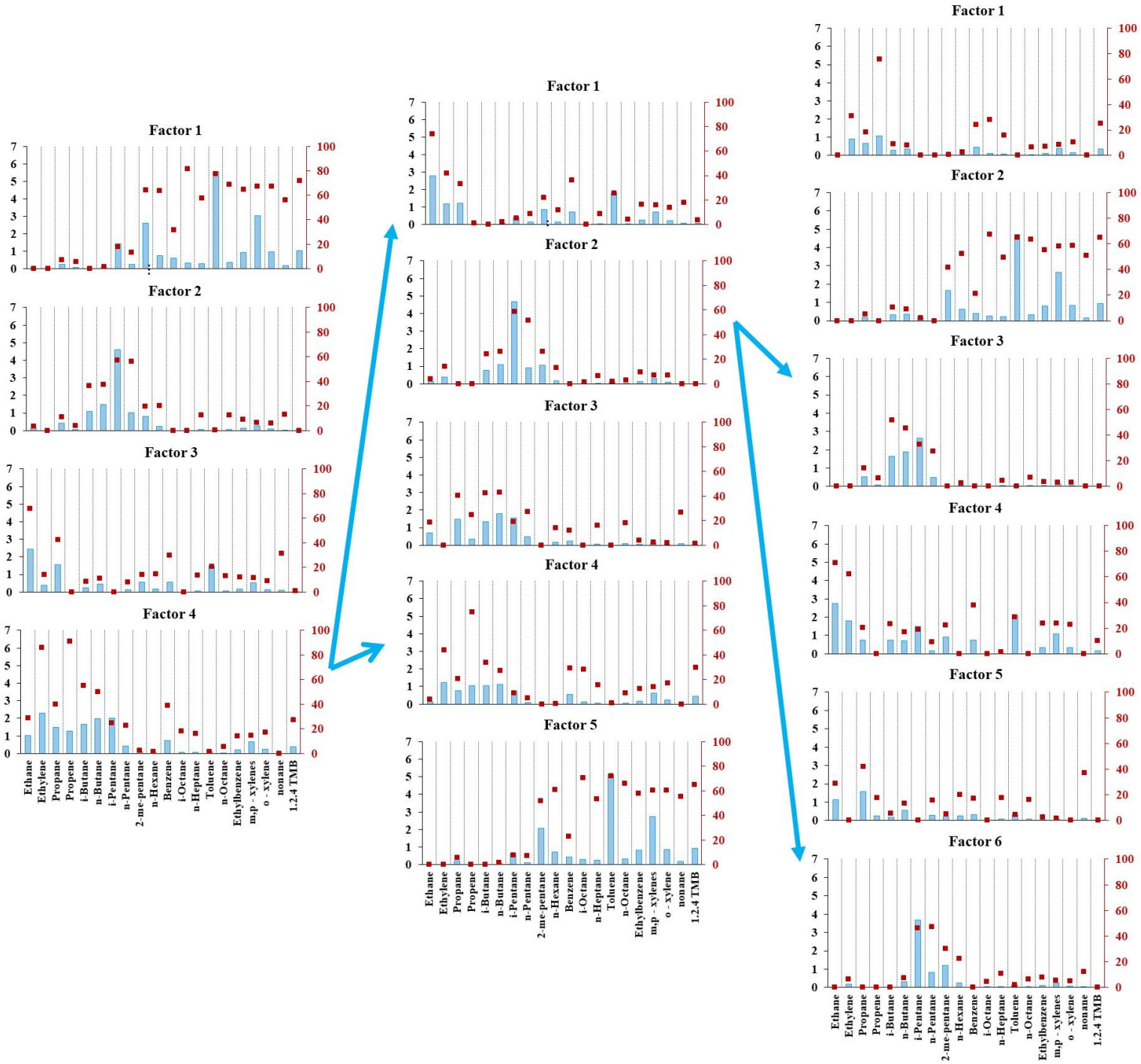

Fig. VI – A2: Diurnal variability in (a) spring and (b) summer of the ONG related short- and long-lived factors from the PMF simulations presented in Abeleira et al. (2015) (Adjusted figure).

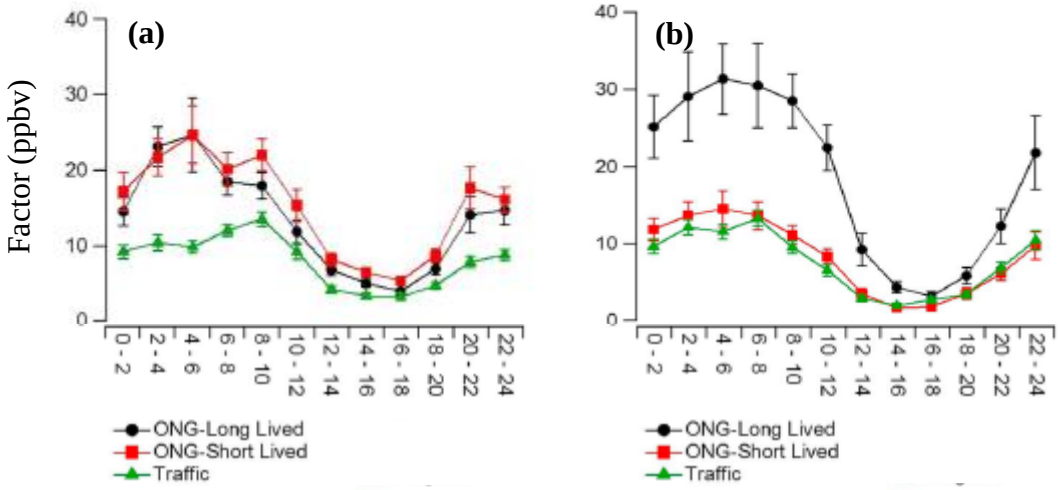

Sect. VI – A1: CPF graphs

The influence of the geographical location of the air masses can be investigated using a conditional probability function (CPF; Ashbaugh et al., 1985) and a threshold as criterion. The basic assumption for the interpretation of the results of the method is that the air arriving at a receptor site has traveled on a relatively straight path from the source. The latter does not apply to all sampling stations, however, it can true for our station since it is characterized as urban background and the observations in chapters 3 and 4 showed mainly the influence of local emissions to VOC levels. Nevertheless, this has already performed in studies (Debevec et al., 2018; Gaimoz et al., 2011; Xiang et al., 2012).

The CPF equation is the following (Eq. VI – A1):

$$CPF_i = \frac{m_{\Delta\theta}}{n_{\Delta\theta}} \qquad \text{Eq. VI - A1}$$

where $m_{\Delta\theta}$ is the number of samples in the wind sector *i* that exceeded the threshold criterion and $n_{\Delta\theta}$ the total number of samples in the wind sector *i*. In this study, wind directions were binned into eight sectors and the threshold was set at the upper 75th percentile of the contribution of each source for all the samples, in order to catch the frequency of extreme episodes. In addition, calm winds of wind speed <1 m s^{-1} were excluded from the calculations. For this work the data were separated according to wind speed (2.99 m s^{-1} the upper limit of low wind speed) and the corresponding CPF graphs are presented in Figure V1 – A3:

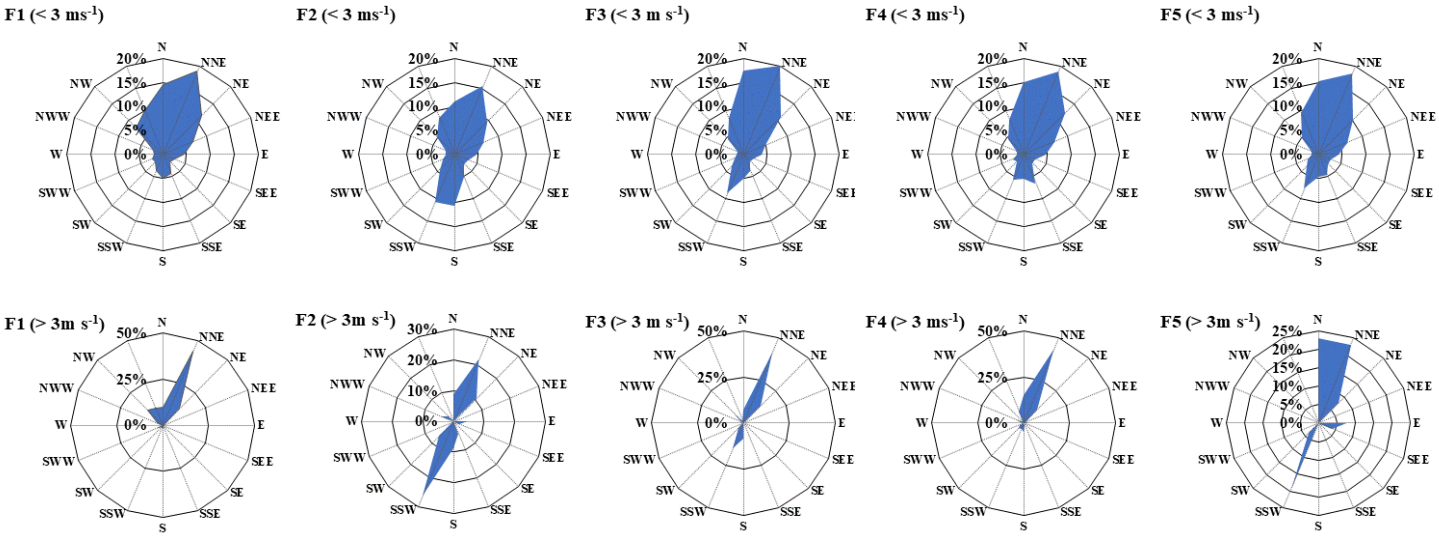

Fig. VI -A3 : 1st row: CPF graphs of the factors for wind speed < 3m s^{-1}.; 2nd row: CPF graphs of the factors for wind speed > 3m s^{-1}

Fig. VI – A4: a) Map of Greater Athens Area. The center of the rose indicates the location of Thissio monitoring station and the yellow circle the ONG facilities in Attica, b) Natural gas infrastructure close to Attica region. The pipelines are shown with purple, the 1st priority consumption centers are with blue circles and the LNG import terminal is shown with the red cycle (Adapted from IEA report of Greece, 2017)

Fig. VI – A5: Seasonal diurnal variability of Factor 5: Vehicle exhaust

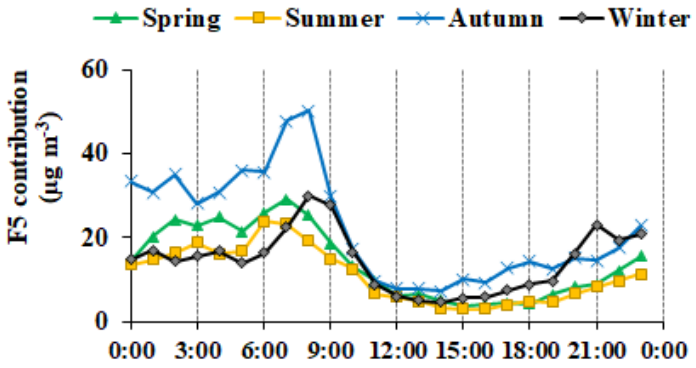

Fig. VI – A6: Diurnal variability of Factor 2: Fuel evaporation (related to traffic) and BC_{ff}

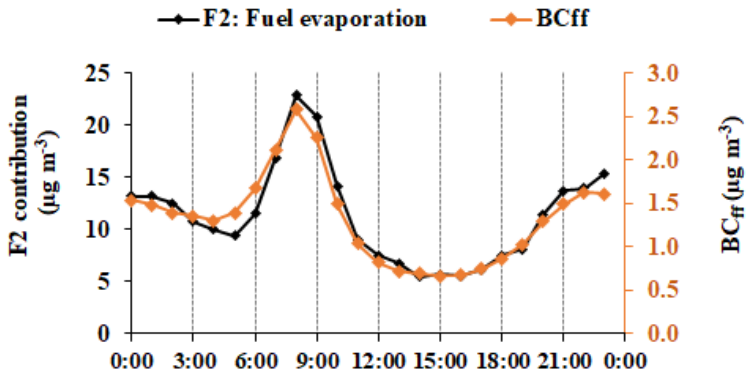

Sect. VI – A2: Traffic profiles in the literature

In **Sect. 2.1** of **Chapter 6**, the "Traffic emissions" mass contribution profile of Thissio is compared to the profiles of the PMF results for Paris and Beirut (Baudic et al., 2016; Salameh et al., 2016). The common species between our work and these studies are ethane, ethylene, propane, propene, isobutane, n-butane, isopentane, n-pentane, n-hexane, benzene and toluene, thus the mass contribution (%) of the NMHC in every profile is re-calculated taking into account only these common species.

Salameh et al. (2016) performed two separate PMF simulations, for their summer and winter datasets respectively. Both PMF approaches gave three factors related to traffic, however, their identification differs depending on the season. In particular for winter, the traffic related sources are identified as combustion mainly related to regional traffic, combustion related to local traffic and gasoline evaporation related to traffic, whereas in summer the factors were characterized as combustion related to diurnal traffic, combustion related to nocturnal traffic and gasoline evaporation related to traffic. Although similarities are observed between individual factors in the PMF results of Athens and Beirut (e.g. "Vehicle Exhaust" –Thissio and "Combustion related to diurnal traffic" – Beirut, in Fig. VI – A7), it would be better to use a combination of all the factors' contribution in the different seasons, in order to decrease as much as possible the discrepancies due to the sampling period, since the PMF results of Athens are based on a whole year of measurements. Consequently, the "traffic" profile of the 3 traffic factors for every season is calculated for Beirut as follows, resulting in a total "Traffic" profile that combines the seasonal traffic contribution:

1. The contribution of each species to each factor is summed for every season, resulting in the seasonal contribution of the species (Eq. VI – A2):

$$[X]_a = C_1 + C_2 + C_3$$

Where $[X]_i$ is the total contribution (in μg m^{-3}) of the compound X, a is the season (winter or summer), and C_1, C_2, C_3 are the contributions of the compound X to each of the 3 traffic factors for Beirut (in μg m^{-3}).

2. The mass contribution (%) of each compound to the seasonal traffic profile is then calculated from Eq. VI – A3:

$$Mass\ Contribution\ [X]_a(\%) = \frac{[X]_i}{\sum_{i=1}^{n}[X]_\mathrm{i}},$$

Where $Mass\ Contribution\ [X]_a$ (%) is the calculated contribution of the compound X to the total mass of compounds ($\sum_{i=1}^{n}[X]_\mathrm{i}$) for the season a (winter or summer), and $[X]_\mathrm{i}$ is the total contribution of the compound X (in μg m^{-3}) as it was calculated by Eq. VI – A2.

3. Finally, the mass contribution (%) to the "Traffic" profile for both seasons is calculated for every compound as the mean value of the mass contribution (%) of the compound for winter and summer traffic profile (Eq. VI – A4):

$$Mass\ Contribution\ [X]_{total} = \frac{Mass\ contribution\ [X]_{i,winter} + Mass\ contribution\ [X]_{i,summer}}{2}$$

Where $Mass\ Contribution\ [X]_{total}$ (%) is the mean value of the $Mass\ contribution\ [X]i$ (%) of the compound X to the winter and summer profile, as calculated from Eq. VI – A3.

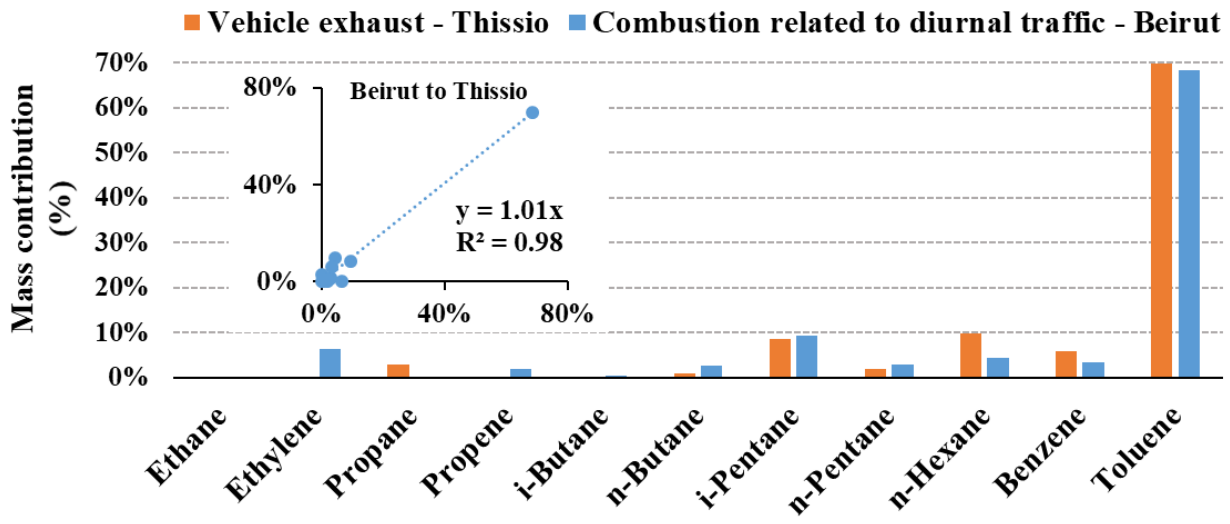

Figure VI -A7: Mass contribution (%) of NMHC in the factors: Vehicle Exhaust (Thissio) and Combustion related to diurnal traffic (Beirut). For Beirut, this factor was identified only in summer

It is important to examine whether the total "Traffic" profile of Beirut is representative of the seasonal traffic profiles (estimated by Eq. VI – A3). Figure VI – A8 presents the three traffic profiles: winter, summer and total "Traffic profile. It is apparent that the total "Traffic" profile agrees well with the seasonal profiles, whereas the few discrepancies can be attributed to small differences in the factor contributions as a result of the different seasonal PMF analysis. For example, propane is completely absent from the winter traffic profile, since 60% of it was attributed to a 6th factor identified as "Gas leakage".

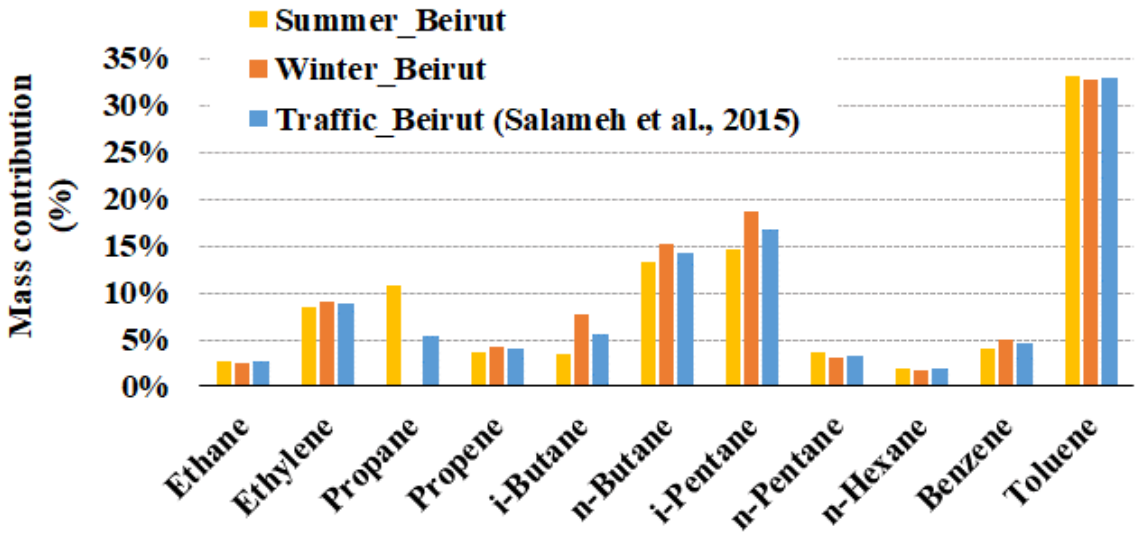

Figure VI – A8: Mass contribution (%) of NMHCs in the winter and summer traffic profiles of Beirut and the total "Traffic" profile.

Baudic et al. (2016) identified 6 VOC sources in Paris by using PMF analysis. From these, only two are connected to traffic, which are "Motor Vehicle Exhaust" and "Evaporative Sources" (Fig. VI –

A9). The latter is related to various fuel evaporation emissions (e.g. gasoline and/or LPG evaporation from storage, extraction and distribution), which explains the high apportion of propane and butanes.

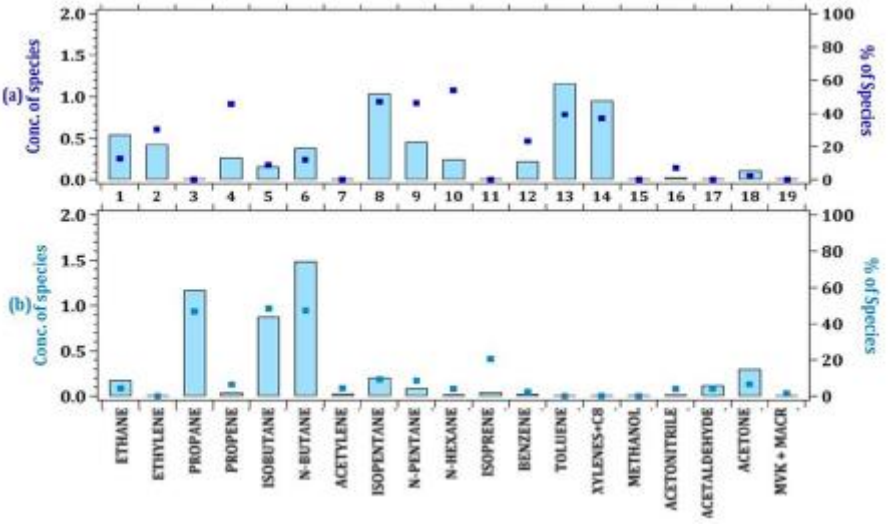

Figure VI – A9: "Motor Vehicle Exhaust" and "Evaporative Sources" factor profiles (Adapted from Baudic et al., 2016).

It is important to decide whether we will use the Paris traffic-related profiles separately or combine them to one "Traffic" profile. For that reason, in Figure VI – A10 are presented the two traffic-related profile of Paris, the total "Traffic" profile of Paris (calculated as the mean contribution of the "Motor Vehicle Exhaust" and "Evaporative Sources" factors to the common species), and the "Traffic emissions" profile of Athens. It is apparent that the total "Traffic" profile of Paris is representative of "Motor Vehicle Exhaust" and "Evaporative Sources", with the main compounds of the profile being propane, butanes, isopentane and toluene. Furthermore, butanes and propane present higher contribution than i-pentane and toluene, which indicates that the evaporative sources have a stronger impact to the total "Traffic" profile. This is not observed in the "Traffic emissions" profile of Athens. As we already mentioned before, the evaporative factor of Paris might include other fugitive emissions related to fuels but not to vehicles' movement (i. e. fuel storage). As a consequence, I decided to exclude the "Evaporative Sources" profile from the comparison and keep only the "Motor Vehicle Exhaust" profile, which agrees well with the Athens "Traffic Emissions" profile.

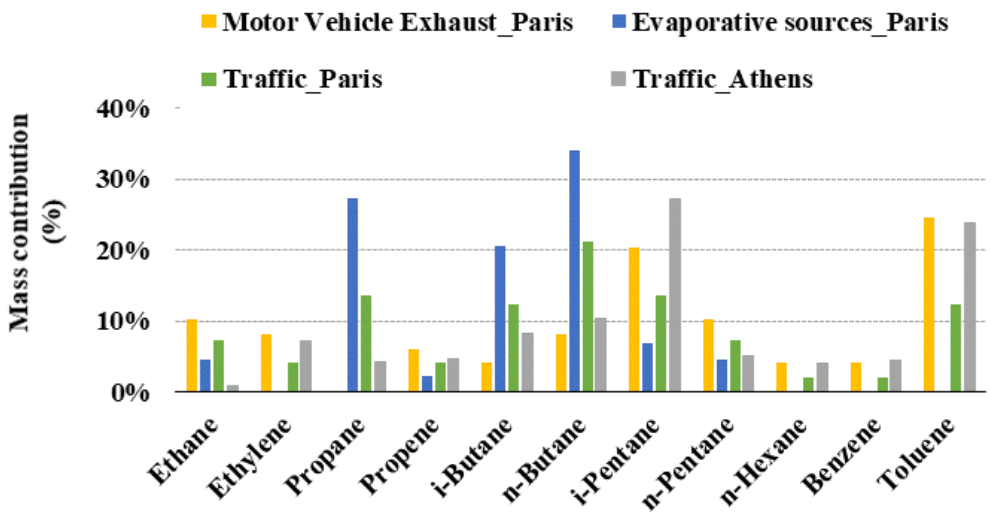

Figure VI – A10: Mass contribution (%) of NMHC in the "Motor Vehicle Exhaust" and "Evaporative Sources" of Paris (adapted from Baudic et al., 2016), the Traffic profile of Paris (estimation; "Traffic_Paris") and the Traffic profile of Athens ("Traffic_Athens").

Table VI – A2: VOCs of the Intensive Observation Campaigns, their characterization and their S/N ratio. The SUM of VOC (last row) is calculated for every sample and it is used as the total variable (this parameter is used by the program in the post-processing of results, thus it has a high uncertainty in order to have a minimum influence on the sample)

Species	Category	S/N
Ethane	Strong	4.8
Ethylene	Strong	5.4
Propane	Strong	7.3
Propene	Strong	4.4
i-Butane	Strong	6.8
n-Butane	Strong	7.2
Trans-2-butene	Strong	2.8
1-Butene	Strong	2.8
i-Pentane	Strong	8.1
n-Pentane	Strong	6.4
2-me-pentane	Strong	8.6
n-Hexane	Strong	5.4
Benzene	Strong	5.3
i-Octane	Strong	2.2
n-Heptane	Strong	2.4
Toluene	Strong	8.8
n-Octane	Strong	2.6
Ethylbenzene	Strong	5.3
m,p - xylenes	Strong	7.8
o - xylene	Strong	4.8
nonane	Weak	1.7
a-pinene	Strong	3.1
1.3.5 TMB	Bad	1.4
1.2.4 TMB	Strong	3.9
1.2.3 TMB	Bad	1.1
Limonene	Bad	1.1
3-me-Pentane	Strong	5.6
Hexene	Strong	4.9
Cyclohexane	Strong	5.4
2-me-hexane	Strong	5.5
2.3-dime-pentane	Strong	5.1
Styrene	Strong	5.2
Decane	Strong	5.5
nC11	Strong	5.4
nC12	Strong	5.2
nC13	Strong	5.1
nC14	Strong	5.2
nC15	Strong	4.7
nC16	Bad	3.3
22dimethylpentane	Strong	4.3
24dimethylpentane	Strong	4.8
223trimethylbutane	Strong	3.0
33dimethylpentane	Strong	4.9
3ethyltoluene	Strong	5.5
4ethyltoluene	Strong	5.4
2ethyltoluene	Strong	5.5
SUM_VOC	Weak	5.8

Sect. VI – A3: IOPs PMF simulation

Data preparation

During the intensive campaigns were deployed in parallel on-line and off-line sampling and analysis methods (Chapter 2). Because the sampling time of the cartridges is ~3h, the 30-min concentrations of the NMHC of the MOP were averaged to 3h. As a result, the input dataset for the PMF simulation contains VOC from 6 compound families: alkanes, alkenes, aromatics, IVOC and monoterpenes (in total 45 compounds). Furthermore, the data points were treated as follows:

- NMHCs from MOP: The 30-min concentrations of NMHCs from the MOP were averaged in 3 hours based on Eq. VI – A5:

$$C_{XX:40} = \frac{1}{6}\left(A_{YY:10} + B_{YY:40} + C_{WW:10} + D_{WW:40} + E_{ZZ:10} + F_{ZZ:40}\right) \qquad \text{Eq. VI – A5}$$

Were $C_{XX:40}$ is the averaged concentration to 3h (in μg m^{-3}), $A_{YY:10}$, $B_{YY:40}$ and $C_{WW:10}$ are the concentrations of the three samples before the mean sampling time of XX:40, and $D_{WW:40}$, $E_{ZZ:10}$, and $F_{ZZ:40}$ are the concentrations of the three samples after the mean sampling time of XX:40. For example the mean sampling time for one cartridge starting at 07:00 LT and ending at 10:00 LT is 08:30 LT. Thus, the corresponding NMHC samples (30-min) are from 07:10 LT to 09:40 LT, and the obtained levels are averaged to 3h, in order to get a mean sampling time at 08:40 LT.

- NMHCs of the IOPs: The data points were treated as follows :

$$x_{ij}\begin{cases} x_{ij} & , \; x_{ij} > LoD_{ij} \\ LoD_{ij} & , \; x_{ij} \leq LoD_{ij} \\ Median_i & , \; x_{ij} missing \end{cases}$$

Were x_{ij} and LoD_{ij} are the concentration and LoD of the compound *i* in the *j* sample respectively (in μg m^{-3}), and $Median_i$ is the median value of the compound *i* (in μg. m^{-3}).

Then, the two datasets were combined in the input matrix, which contained 47 compounds x 153 samples (6885 data), with equal number of samples for winter and summer. Two approaches were followed for the replacement of the missing values. More specifically, the reason for this is that the IOPs and the C6 – C12 MOP datasets have less than 5% missing values (only 1.3.5 TMB had 10% missing values), but for the C2 – C5 MOP dataset (GC – FID C2 – C6) the percentage varied from ~10% to ~20%. To avoid any bias by replacing with the median of the compound (option provided by the PMF tool), the two approaches were:

a) For the C6 – C12 NMHC of the MOP and the NMHCs of the IOPs, the missing values were replaced by the median concentration of the species over all measurements.

b) For the C2 – C5 NMHC of the MOP, the missing data were replaced by the median of the concentrations measured the previous and next days at the same hour, considering the variability of the other species. For instance, if the missing value occurred in a time-frame for which the concentrations of the other compounds were low, the estimated median will

not take into account samples with extremely high levels. However, there are exceptions to this approach: (a) some concentrations of propene and n-pentane from 08-09-2018 to 22-09-2018 had to be replaced by the median value over all measurements, since they presented the highest number of missing values and further substitution by the first approach could create a bias; (b) the missing values of 10-09 and 11-09 at 08:30LT of i-butane, n-butane and trans-2-butene, as well as all the NMHC C2 – C5 of the sample 19/9/2016 at 17:30LT, were also replaced by the median concentration of the compounds over all the measurements for the same reason as (a).

Estimation of the concentration uncertainty

The uncertainty matrix of this PMF simulation requires the combination of different approaches depending on the dataset. For the NMHCs of the IOP, the uncertainty of the concentrations was built upon the procedure described by Norris et al., (2014) (adapted from Polissar et al., 1998). In a summary, for the concentrations above LoD, the uncertainty can be roughly calculated using only an error fraction percentage and the detection limit (Eq. VI – A6), at the expense of losing specific errors associated to the samples. The error fraction in our case was 0.15 (or 15%):

$$Unc = \sqrt{(Error\ Fractions\ x\ concentration)^{2} + (\frac{LoD}{3})^{2}} \qquad \text{Eq. VI – A6}$$

Furthermore, the individual uncertainty applied in the IOP dataset is summarized as follows:

$$u_{ij}\begin{cases} u_{ij} & , \quad x_{ij} > LoD_j \\ {}^{5}/_{6}\, LoD_j & , \quad x_{ij} \le LoD_j \\ x_{ij} missing & , \quad 4 * Median_i \end{cases}$$

The uncertainty of concentrations of the NMHCs of the MOP is described in detail in Sect. 2.2.6 of Chapter 2. However, since the concentrations were averaged to 3h, a new uncertainty was estimated using error propagation, which takes into account the uncertainty of the 30-min concentrations (Eq. VI – A7):

$$u_{i\,XX:40} = \frac{\sqrt{(u\,A_{YY:10})^2 + (u\,B_{YY:40})^2 + (u\,C_{WW:10})^2 + (u\,D_{WW:40})^2 + (u\,E_{ZZ:10})^2 + (u\,F_{ZZ:40})^2}}{Nb_i}$$

Were $u_{i\,XX:40}$ is the uncertainty of the averaged-to-3h concentration of the compound *i* for sampling time XX:40, $u\,A_{YY:10}$, $u\,B_{YY:40}$ and $u\,C_{WW:10}$ are the concentration uncertainties of the three samples before the mean sampling time of XX:40, and $u\,D_{WW:40}$, $u\,E_{ZZ:10}$, and $u\,F_{ZZ:40}$ are the concentration uncertainties of the three samples after the mean sampling time of XX:40, and Nb_i is the number of concentrations (without missing values) that contribute to the calculation of the 3-hour averaged concentration of the compound *i* .

Concerning the replaced and missing values, their uncertainty was set as four times the species-specific median, which is suggested in Norris et al. (2014), an option also provided by the PMF tool.

For this simulation, compounds with S/N ratio less than 1.4are categorized as “bad” and they are excluded; for an S/N ratio between 1.5 and 2, the species are considered “weak”, thus their

uncertainty is tripled; finally, compounds with S/N greater than 2 are considered "strong" and their uncertainty remains unchanged. In our case, 3 compounds had S/N less than 1.5 (1.3.5 TMB, 1.2.3 TMB and limonene) and were characterized as "bad". nC16 was also excluded due its concentrations being close to the LoD (Chapter 4, Section 2.1). Nonane (S/N = 1.7) was the only compound characterized as "weak".

Determination of the optimal solution

For the determination of the optimal solution, PMF simulations were performed with 4 to 8 factors. For all the simulations were performed 100 runs. Similarly to the MOP PMF simulation (Sect. 1.1 of chapter 6), the diagnostic parameters R^2, IM, IS and $Q_{true}/Q_{expected}$ are plotted against the number of factors and they are presented in Figure VI – A11. IM and R^2 are stable regardless of the number of factors, while R^2 is already good ($R^2 > 0.993$), indicating good modelling of the input concentration matrix. IS decreases significantly from the 4- to the 6-factor solution and then increases again. Furthermore, $Q_{true}/Q_{expected}$ decreases also with increasing number of factors, however the most appropriate values are observed for the 7- and 8-factor solution. In particular, we need a $Q_{true}/Q_{expected}$ value close to 1 for a good estimation of the uncertainty, thus our values of 1.9 and 1.7 (7- and 8- factor respectively) indicate that there are modelled datapoints outside the estimated error value.

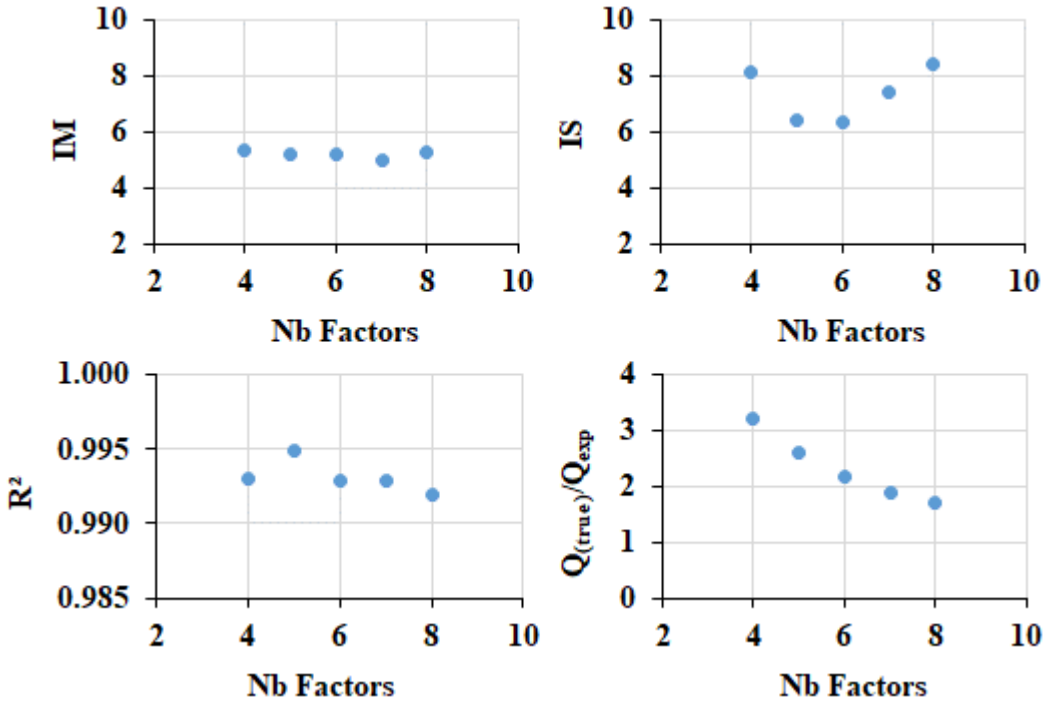

Figure VI - A11: Graphs of IM, IS and R^2 to the number of factors.

Based on the previous observations, the optimal solution includes 7 or 8 factors. However, by selecting 8 factors we risk to lose the physical meaningfulness of the profiles due to splitting (Ulbrich et al., 2009). For this reason, as final solution was chosen the one with 7 factors. This was further affirmed by the bootstrap error estimation that was performed for both the 7- and 8-factor solutions, giving 73% of good mapping for the 7-factor but only 46% for the 8-factor solution. In addition,

bootstrap error estimation was conducted also for the 5- and 6-factor solutions, giving less than 66% good mapping. All the above verify that the 7-factor solution is the optimal one.

Robustness of PMF results

The technical and mathematical indicators of the 7-factor solution for the assessment of its robustness and quality are presented in this section. Firstly, the ratio between Q_{robust} and Q_{true} is 0.94 which is close to 1.0, indicating that the modeled results were not biased by peak events. Furthermore, 97% of the scaled residuals were within ±3σ. In addition, the very good R^2 (0.993) shows that all variance in the total concentration of the 43 modelled VOCs can be explained by the PMF model. This is also reflected in the correlation coefficients (R^2) between predicted and observed concentrations which were > 0.75 for all the compounds except of a-pinene (0.72). The slopes between the modeled and measured NMHC concentrations varied from 0.69 (hexene) to 1.07 (4ethyltoluene), with 8 compounds having slopes lower than 0.85. This indicates an insufficient modelling of their maximum levels and/or their greater number of concentrations close to the LoD, which could affect the simulation of these compounds by the PMF. Overall, the statistical parameters indicate that the 7-factor PMF solution is robust enough for the explanation of the variation of the measured VOC concentrations. Finally, the mathematical diagnostics of the final PMF run are presented in Table VI – A3.

Table VI – A3: Mathematical diagnostics for the final PMF run

(m) species	47
(n) samples	153
(p) Factors	7
Runs	100
Number of species characterized as weak	1
Number of species characterized as bad	4
Number of random seed	3
$Q_{(robust)}$	8734
$Q_{(true)}$	9284
Q(T)/Qexp	1.89
$NMHC_{modeled}$ vs. $NMHC_{measured}$ (R^2)	0.993
Number of species with R^2 > 0.75 (modeled vs. measured)	42
Fpeak	-0.5
$dQ_{(robust)}$ of Fpeak	113.7 (1.28%)

Estimation of model prediction uncertainties

Starting from the DISP (base model displacement error estimation), the results showed no error and no drop of Q. Furthermore, the base model bootstrap method was carried out, executing 100 iterations, using a random seed (number 3), a block size of 13 samples (calculated according to the methodology of Politis and White, 2004) and a minimum Pearson correlation coefficient (R value) of 0.6. All factors were correctly mapped for 73%. Although this value is less than the satisfactory mapping of 80%, it can be attributed to the PMF model that might failed to fit the variability of one source or the variability of some compounds, which can be corroborated with the smaller slopes reported for some compounds (previous paragraph). Nevertheless, taking into account that the dataset consists in only 153 samples combining two seasons and that the block of the BS has a size of only 13 samples for the re-built of the BS boot factors, the mapping of the solution is considered satisfactory enough for the interpretation of the uncertainties.

Finally, the rotational ambiguity of this 7-factor PMF configuration was also investigated using the Fpeak parameter. Different Fpeak values from -05 to 1.5 were used to generate a more realistic PMF solution. The results from the non-zero Fpeak values were generally consistent with the runs associated with the zero Fpeak value (base model run), thus illustrating a low rotational ambiguity of the final PMF solution.

Sect. VI – A4: Common Factors between the IOPs and MOP PMF

VI - A4.1 Wood burning

The chemical profile of Factor I6 (**Fig. VI – A12**) is characterized by C2 – C3 alkanes and alkenes (48% to 21%), benzene (26%), hexene (36%) and cyclohexane (25%). This profile is similar to Factor 1 "Wood-burning / Background" of the MOP, thus it is temporally characterized as "Wood-Burning". To verify the identification, in the following paragraph is examined the temporal variability and the relationship to BC_{wb}.

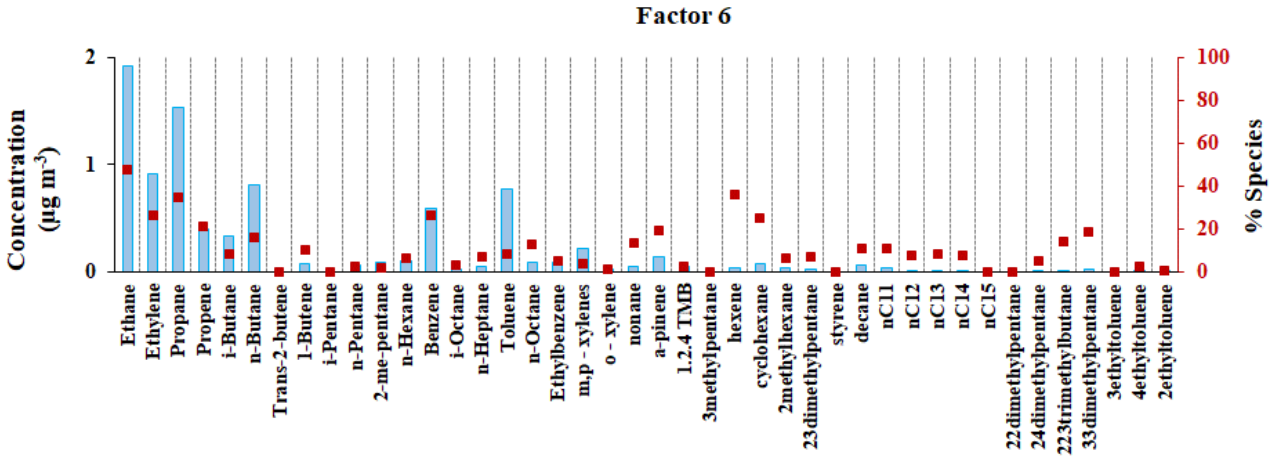

Figure VI -A12: Modelled contribution (µg m^{-3}) of each species to the Factor I6 (light blue bars) and relative contribution of the factor to each species (red squares).

Figure VI – A13a,b presents the temporal variability of Factor I6 and wind speed in February (winter) and September (summer). The factor contribution to VOCs is higher in February (13.1 ± 12.7 µg m^{-3}) and decreases more than a factor of 4 in September (3.7 ± 3.4 µg m^{-3}). In addition, low wind speeds (<3 m s^{-1}) favor the enhancement of the contribution in February, indicating the influence of local emissions. Furthermore, in February, the diurnal cycle is characterized by a night

maximum at midnight that decreases until morning, staying very low during day (**Fig. VI – A13c**). In summer, there is no diurnal variability (**Fig. VI – A13d**). The observed trend follows closely the one of BC_{wb}, which is more apparent in winter. All the above indicate that Factor I6 is indeed related to "Wood Burning". This is further affirmed by the dependence of the contribution from cold temperatures (**Fig VI – A14**) that triggers these emissions. No difference is observed in the contribution between weekends and workdays.

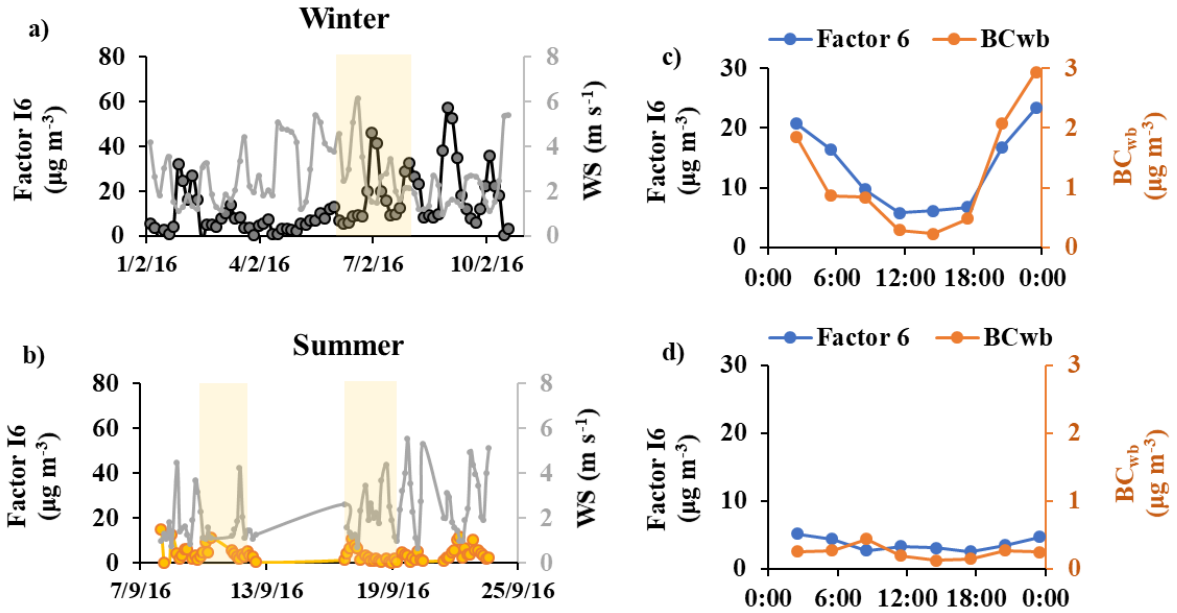

Figure VI -A13: Temporal variability of Factor I6 and wind speed in a) February (winter) and b) September (summer) 2016; c) Diurnal variability of Factor I6 and BC_{wb} for February (winter) and d) Diurnal variability of Factor 6 and BC_{wb} for September (summer). Yellow frames indicate weekends.

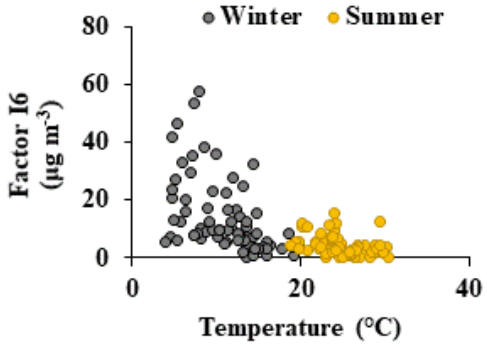

Figure VI - A14: Factor I6 contribution versus temperature for February (winter) and September (summer) 2016.

VI - A4.2 Fuel combustion (related to traffic and heating)

This factor profile is characterized by alkenes like trans-2-butene (76%), 1-butene (63%) and styrene (63%), however, the highest concentrations are observed for i-pentane, C2 – C4 alkanes and alkenes (**Fig. VI – A15**). Because the chemical profile explains an important percentage of unsaturated

compounds, it resembles the one of Factor 4 from the MOP, so it is identified as Fuel combustion related to traffic and heating. This will be verified in the following paragraph.

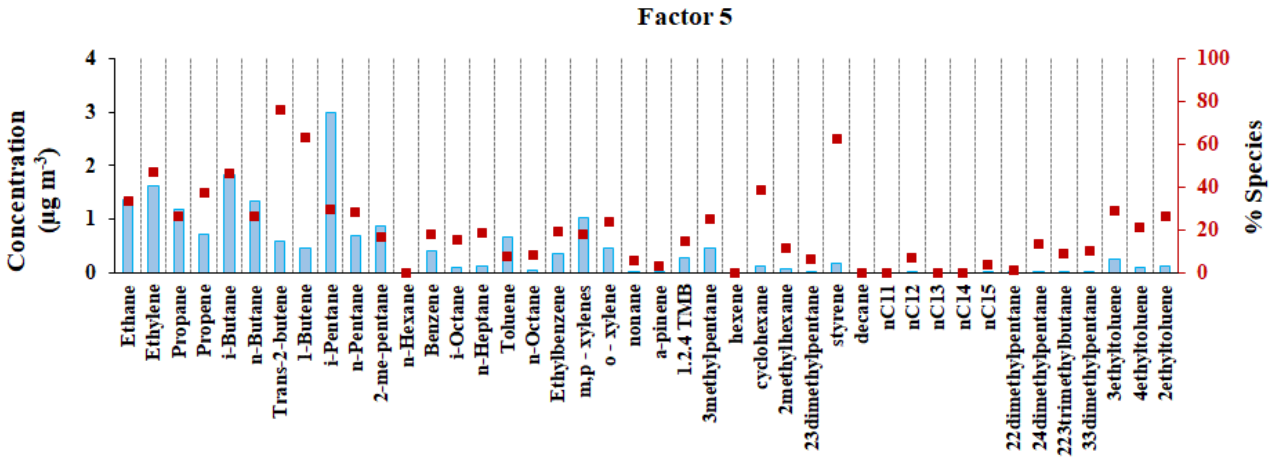

Figure VI -A15: Modelled contribution (μg m^{-3}) of each species to the Factor I5 (light blue bars) and relative contribution of the factor to each species (red squares).

The temporal variability of Factor I5 is presented in **Figure VI – A16a,b**. The contribution is the highest in February (36.6 ± 41.8 μg m^{-3}), whereas it drastically decreases in September (1.4 ± 4.2 μg m^{-3}). Furthermore, in February, the diurnal cycle exhibits a bimodal pattern with a morning (09:00 LT) and a night maximum (00:00 LT), with very low concentrations during the day (12:00 – 18:00 LT) (**Fig. VI – A16c**), in contrast to September that there is no apparent variability (**Fig. VI – A16d**). Remarkably, the diurnal cycle follows closely the one of BC_{ff} in February and NO in both months; the latter highlights the important decrease of their levels in September compared to February (factor of 6 and 15 for NO and Factor I5 respectively). Moreover, in addition to the excellent correlation to NO and BC_{ff} in winter (R^2 < 0.90 for both), Factor I5 correlates very well with CO and Factor I4, which is related to vehicle exhaust emissions as it is shown in the next Section (R^2 0.89 and 0.84 respectively). On the contrary, moderate correlation is observed with BC_{wb} indicating that the origin is not related to wood-burning and the observation is associated more to the co-existence of the emissions in the atmosphere. Moreover, low wind speed enhances the contribution of the factor in February and September, while it was higher in workdays than weekends in February (**Fig. VI – A16a,b**). All the above verify the identification of the factor, which reflects combustion of fuels, probably from vehicles, as well as fossil fuel burning for residential heating in winter. In addition, the same variability was also observed for Factor 4 of the MOP.

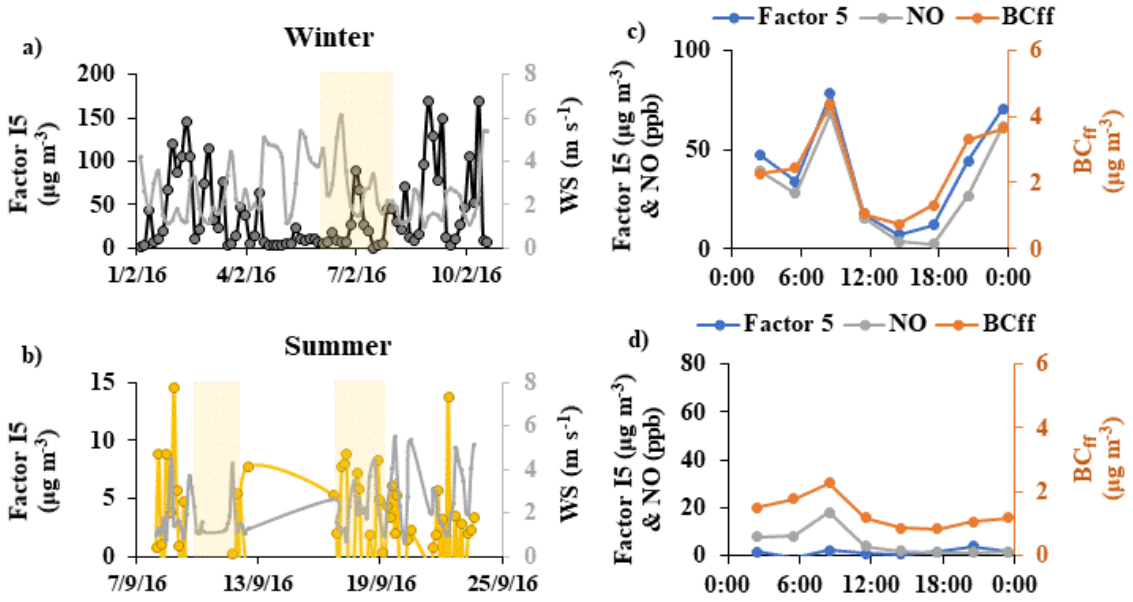

Figure VI -A16: Temporal variability of Factor I5 and wind speed in a) February (winter) and b) September (summer) 2016; c) Diurnal variability of Factor I5, NO and BC_{ff} for February (winter) and d) Diurnal variability of Factor 5, NOx and BC_{ff} for September (summer). Yellow frames indicate weekends. Please note the different y-axis for Factor I5 in Figure (b)

It is important to understand the reason behind the decrease of the contribution of the factor in September, because summer vacations are finished by the middle of the month, thus traffic circulation is increased compared to summer. As it was shown in **Table I – 1** of **Sect. 1.3.1 – 6** of **Chapter 1**, trans-2-butene, 1-butene and styrene (main compounds of the factor) have a lifetime of less than 3 hours in respect to the OH radical. Consequently, the decrease of the contribution of Factor I5 and NOx simultaneously to the increase of ozone that follows the increase of solar intensity (**Fig. VI – A17**) indicate that the main driving parameter of the variability of this factor in summer is photochemistry.

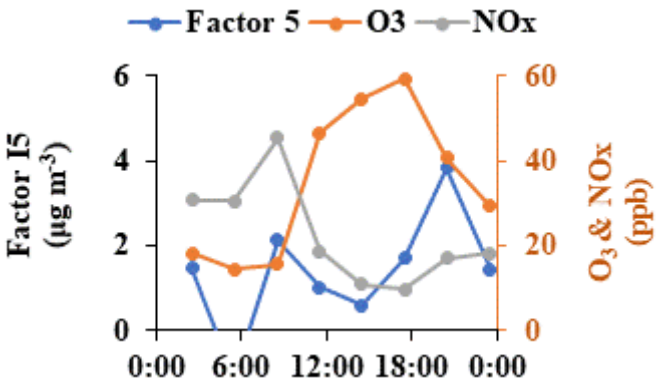

Figure VI -A17: Diurnal variability of Factor I5, O_3 and NO_x for September.

VI - A4.3 Vehicle exhaust

The chemical profile of this factor explains more than 20% aromatics and substituted alkanes, while the highest concentrations are observed for toluene, m-/p- xylenes, 2-me-pentane and i-pentane (**Fig. VI – A18**). As it was mentioned before, these compounds are found in the profiles of vehicle

exhausts, however, the important contribution of BTEX and aromatics is often associated to solvent usage also (Baudic et al., 2016; Liu et al., 2008; Song et al., 2019; Yao et al., 2019). Nevertheless, the presence of decane, undecane, alkenes and BTEX, indicates emissions from diesel and gasoline vehicle exhausts, as well as motorcycles (Guha et al., 2015; Hong-li et al., 2017; Liu et al., 2008; Salameh et al., 2019). Furthermore, as it was mentioned to the previous section, this factor correlates with Factor 5 "Fuel combustion related to traffic and heating" denoting their common origin, thus it is identified as "Vehicle exhausts".

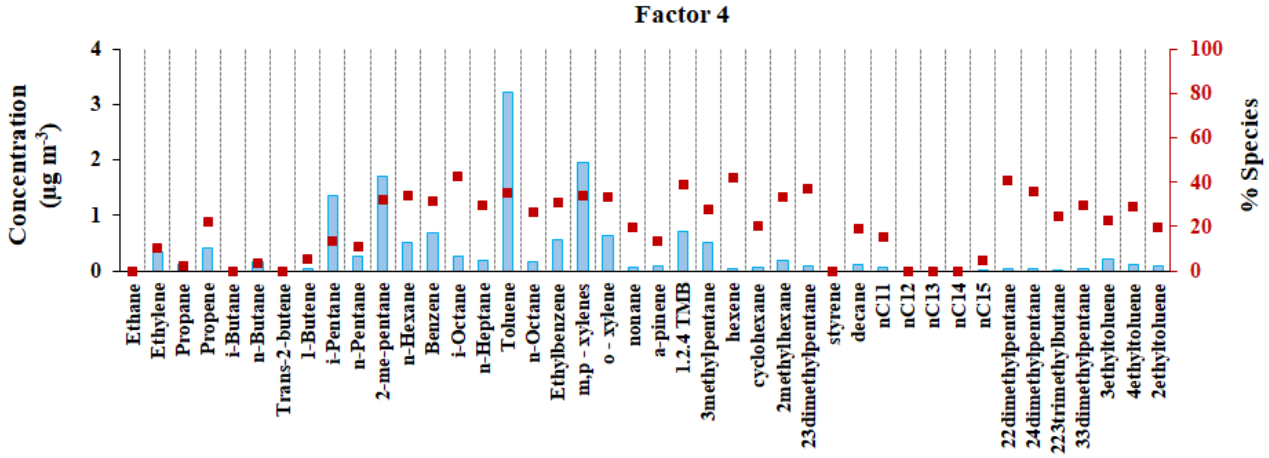

Figure VI -A18: Modelled contribution (μg m^{-3}) of each species to the Factor I4 (light blue bars) and relative contribution of the factor to each species (red squares).

In **Figure VI – A19a,b** is presented the diurnal variability of Factor I4. The highest contribution occurs in the cold season (February 20.7 ± 29.8 μg m^{-3}), while it is lower in the warm period (September 11.8 ± 12.8 μg m^{-3}). In both months, the contribution enhances under low wind speed, whereas it is not possible to distinguish an effect from workdays and weekends. Moreover, the diurnal variability exhibits a bimodal pattern in both months with a morning (09:00 LT) and a night maximum (00:00 LT), with a minimum during the day (12:00 – 18:00 LT) (**Fig. VI – A19c,d**). Furthermore, the above trend follows closely the one of CO and NO in both months. This indicates their common origin from traffic (Panopoulou et al., 2018). Moreover, Factor I4 presents a very good correlation to NO and CO for the IOP (R^2 0.74 and 0.76 respectively), as well as to BC_{ff} and Factor I5 (R^2 0.69 and 0.66 respectively).

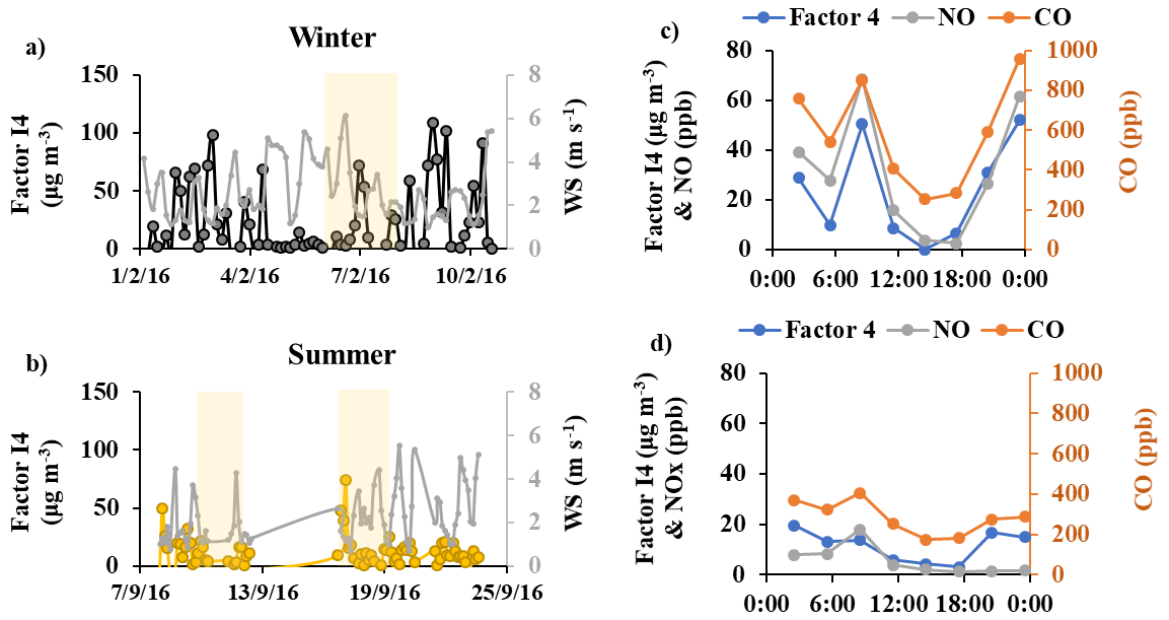

Figure VI -A19: Temporal variability of Factor I4 and wind speed in a) February (winter) and b) September (summer) 2016; c) Diurnal variability of Factor I4, NO and CO for February (winter) and d) Diurnal variability of Factor 4, NO and CO for September (summer). Yellow frames indicate weekends.

VI - A4.4 Fuel evaporation (related to traffic)

Pentanes (~40%), butanes (~30%), propane (~23%) and toluene (~18%) are the main species of the speciation profile of Factor I2 (**Fig. VI – A20**). These compounds are highly volatile, so they are found often in the profiles of fuel evaporation emissions (Liu et al., 2008; Salameh et al., 2015; Baudic et al., 2016). As a result, this factor is identified as fuel evaporation (related to traffic). Moreover, pentanes and butanes were also the principal compounds of the homonymous Factor I2 of the MOP PMF (**Sect. 1.2 – 5 of this Chapter**), which corroborates the identification.

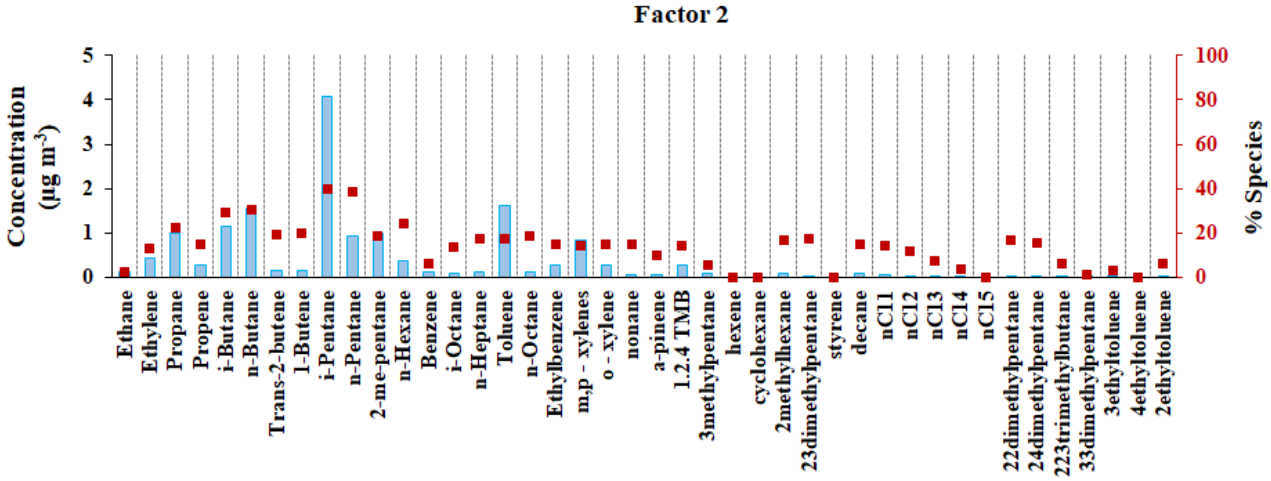

Figure VI -A20: Modelled contribution (µg m^{-3}) of each species to the Factor I2 (light blue bars) and relative contribution of the factor to each species (red squares).

The temporal and diurnal variability of Factor I2 is presented in **Figure VI – A21a,b**. For this Factor the highest contribution is in September (20.5 ± 22.9 µg m^{-3}) and the lowest in February (11.4 ±

14.8 μg m^{-3}). Furthermore, the diurnal cycle of both February and September (**Fig. VI – A21c,d**) presents a morning maximum (09:00 LT), in addition to a night maximum of low amplitude in February and a night-time enhancement period in September (**Fig. VI – A21d**). In **Figure VI – A21c** it is apparent that in winter Factor I2 follows the trend of BC_{ff}, verifying the association to traffic. The latter, however, is not observed in summer, since the contribution of Factor I2 increases significantly during night, whereas it rapidly decreases after the morning maximum. Similar temporal variability was also observed for the homonymous factor of the MOP (**Sect. 2.1 – 5 of this chapter**, **Fig. VI – 23a**). Finally, the contribution is higher for low wind speed, whereas in February is observed an enhancement in workdays.

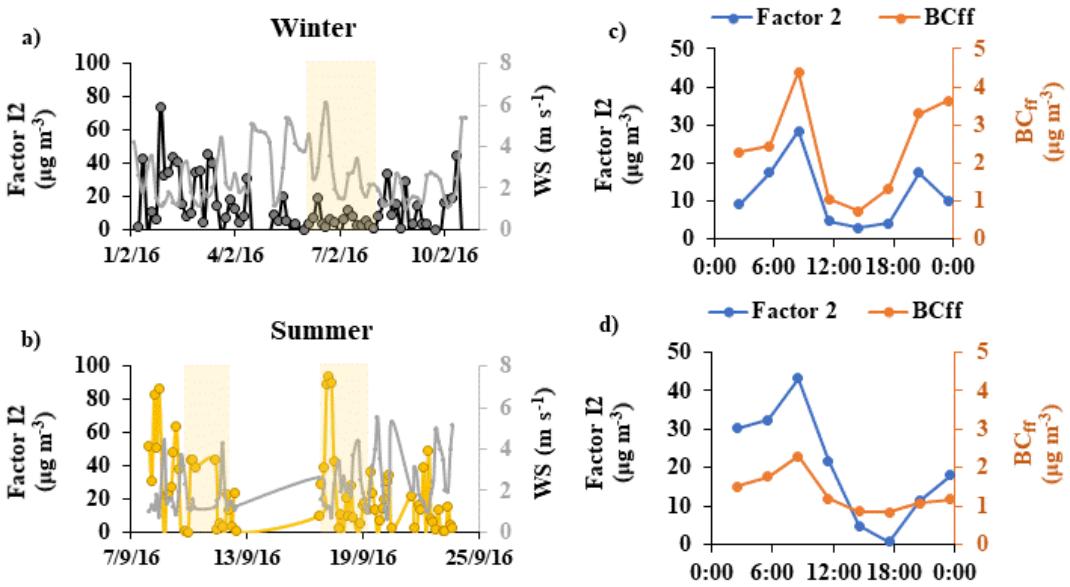

Figure VI -A21: Temporal variability of Factor I2 and wind speed in a) February (winter) and b) September (summer) 2016; Diurnal variability of Factor I2 and BC_{ff} for c) February (winter) and d) September (summer). Yellow frames indicate weekends.

VI - A4.4 Fugitive emissions of ONG exploitation

More than 20% of poly-substituted alkanes, aromatics and C10 – C13 IVOC (57% of dodecane) are explained in the chemical profile of Factor I3 (**Fig. VI – A22**). In addition, ethane, propane, n-butane and 3-me-pentane have the highest concentrations in the profile. This combination of compounds has been attributed to fugitive emissions from petroleum and ONG exploitation in facilities (Abeleira et al., 2017; Guha et al., 2015). Thus, the factor is identified as "Fugitive emissions of ONG exploitation".

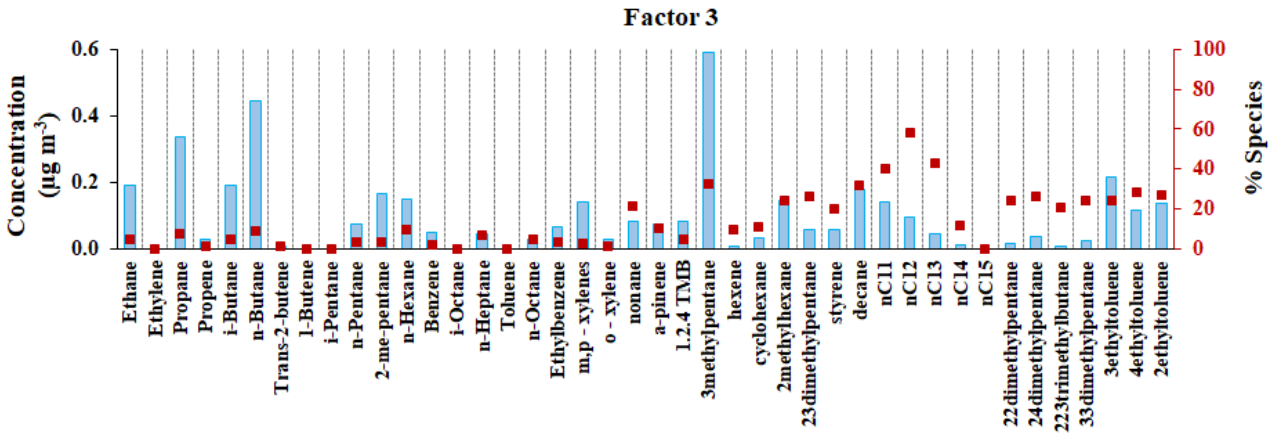

Figure VI – A22: Modelled contribution (µg m^{-3}) of each species to the Factor I3 (light blue bars) and relative contribution of the factor to each species (red squares).

Starting from the temporal variability, Factor I3 contributes similarly to VOC in both February and September (3.5 ± 3.9 µg m^{-3} and 3.0 ± 3.1 µg m^{-3} respectively; **Figs. VI – A23a,b**). The diurnal cycle presents a night-time enhancement period starting from 20:00 LT, with decreasing levels after 12:00 LT. Moreover, the similar contribution and diurnal variability in both months indicate a rather stable source. Finally, an enhancement of the contribution is observed for wind speed < 3 m s^{-1} .

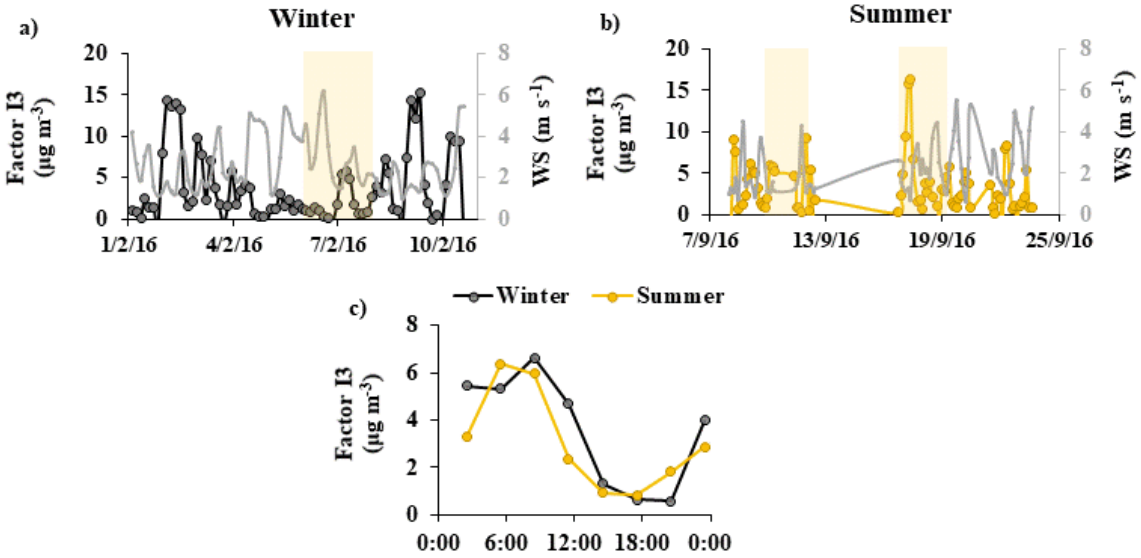

Figure VI -A23: Temporal variability of Factor I3 and wind speed in a) February (winter) and b) September (summer) 2016; c) Diurnal variability of Factor I3 for February (winter) and September (summer). The yellow frames indicate weekends.